X-RAY POWDER DIFFRACTION, SCANNING ELECTRON MICROSCOPY, AND ENERGY DISPERSIVE SPECTROSCOPY STUDIES OF SOIL CONTAINING CHROMIUM IMMOBILIZED BY MICROWAVE TREATMENT

by

Nagui Ibrahim

Thesis submitted to the Faculty of the Graduate School of the New Jersey Institute of Technology in partial fulfillment of the requirements for the degree of Master Science in Chemistry

1990

Approval of Thesis

X-ray Powder Diffraction, Scanning Electron
Microscopy, and Energy Dispersive
Spectroscopy Studies of Soil Containing
Chromium Immobilized by Microwave Treatment

BY

NAGUI I IBRAHIM

FOR

DEPARTMENT OF CHEMISTRY

NEW JERSEY INSTITUTE OF TECHNOLOGY

FACULTY COMMITEE APPROVAL :

NEWARK, NEW JERSEY

MAY 1990

VITA

Name: Nagui I Ibrahim

Permanent address:

Degree and date to be conferred: Master of Science, 1990

Date of birth:

Place of birth:

Secondary education: Abbasiah High School, 1966

Collegiate institutions attended	Date	Degree	Date of Degree
Ein Shams University	9/66 to 9/71	B.S.	1971
New Jersey Institute of Technology	1/86 to 5/90	M.S.	1990

Major: Polymer Chemistry.

ABSTRACT

Title of Thesis: X-ray Powder Diffraction, Scanning Electron
Microscopy, and Energy Dispersive
Spectroscopy Studies of Soil Containing
Chromium Immobilized by Microwave Treatment.

Nagui I Ibrahim, Master of Science, 1990

Thesis directed by: Leonard Dauerman, Associate Professor
of Chemical Engineering, Chemistry and
Enviromental Science

The orientation of soil contaminants such as chromium is altered during microwave heating. The SEM and EDS were utilized in the study. The nature of the orientation is related to the heating time. This results in immobilizing the contaminant in leaching tests. The non-leachibility was related to the reactivity of the chromium salt with the soil hematite phase (Fe_2O_3) during the microwaving. This was proved By the X-ray diffraction analysis. The spectrums obtained from 30 and 60 minutes microwaved samples were identical in the crystal phases and were significantly different from the contaminated unheated sample.

TABLE OF CONTENTS

	PAGE
ABSTRACT	ii
TABLE OF CONTENTS	iii
ACKNOWLEDGMENT	iv
LIST OF DIAGRAMS	v
LIST OF FIGURES	vi
INTRODUCTION	1
INSTRUMENTATION	5
EXPERIMENTS	19
RESULTS I	25
RESULTS II	33
CONCLUSION	35
REFERENCES	37

ACKNOWLEDGMENT

I express my deepest appreciation to Professor L. Dauerman for giving me the opportunity to work on such interesting and important topic and for his guidance. I sincerely thank Dr. DK Mehra for giving me the moral support while pursuing my degree. To my dearest friend E. Sedhom, I can not find the proper words to genuinely thank you for your support and advice to me through this study.

LIST OF DIAGRAMS

PAGE

I Schematic Drawing of the Electron and X-ray Optics of the SEM 7

II The electron Gun 9

III Illustration Showing the Depth of Signal Generation when the Primary Electron Beam Interacts with the Sample Surface 11

IV Optimum Positions of the Secondary and Backscattered Detectors 13

V Detector of an X-ray Energy Dispersive Spectrometer 15

vi Schematic of the Microwave 17

vii Vacuum Evaporator 23

LIST OF FIGURES

SEM Images, X-ray Image, X-ray Energy Spectra and X-ray Diffraction

PAGE

SEM ANALYSIS

Blank Soil

Powder Sample 38

Cross Section Sample 63

Impregnated Soil

Powder Sample 73

Cross Section Sample 87

Microwave 15 minutes

Powder Sample 109

Cross Section Sample 128

Microwave 30 minutes

Powder Sample 142

Cross Section Sample 162

Microwave 45 minutes

Powder Sample 178

Cross Section Sample 192

X-RAY DIFFRACTION ANALYSIS

Blank Soil 210

Impregnated Soil 212

Microwave 30 minutes 214

Microwave 60 minutes 215

INTRODUCTION

There is a critical need for new remediation technologies to treat hazardous wastes. This is evidenced by the EPA's Superfund Innovative Technology Evaluation (SITE) program the objective of which is to evaluate promising technologies ( ). The applications of microwave technology to treat hazardous wastes have been the subject of study in this laboratory. Mostly benchscale studies have been carried out, though we are presently installing a pilot plant in our facility in cooperation with Raytheon, Inc. Our investigations have covered a number of areas: removal of organic contaminants from soils and other substrates (volatiles, semi-volatiles and non-volatiles); destruction of organics in the gas phase; regeneration of granulated activated charcoal (GAC); immobilization of heavy metal ions in soil. This thesis deals with the immobilization of chromium in soil.

There is a need for new technologies to deal with the problem of remediating chromium-contaminated soil. The traditional approach of burying the excavated soil in a landfill is no longer acceptable. A range of new technologies is required because of the fact that each remediation task is unique and thus there is a need for the project engineer to have available a wide range of technologies from which to choose. It is the objective of this thesis to continue the study of the immobilization of chromium in soil started by Jou (1). That study showed that microwave treatment of the soil could lead to the immobilization of the chromium where immobilization is defined by the EPA Leachate test adopted to implement the United States Resource Conservation and Recovery Act (RCRA). There is a compelling need to determine how the chromium is immobilized to ensure that it does not become mobile as a result of foreseeable circumstances. The approach taken in this thesis to ascertain how the chromium is immobilized, is to study the soil spectroscopically after various periods of microwave treatment.

The spectroscopic techniques utilized and the corresponding information obtainable are as follows:

a) Powder X-ray Diffraction Spectroscopy:	to define the crystalline phase.
b) Scanning Electron Microscopy (SEM):	to view the morphology of the individual particles.
c) Energy Dispersion Spectroscopy (EDS):	to characterize the nature and relative amount of each element (that can emit X-rays) in each soil particle.

The production of chromium in the form of metal and its compounds is the highest among the enviromentally significant carcinogenic elements principally because chromium is used metallurgically in alloys. The realization that exposure to dusts and fumes of chromium compounds represents a substantial cancer hazard to human emerged in the period from 1937 to 1946.

Overwhelming epidemiological evidence shows a considerable excess of chromium compounds induced occupational cancers. Exposure to chromium, particularly in the chrome production and chrome pigment industries, is associated with cancer of the respiratory tract. As early as 1936, German health authorities recognized cancer of the lung among workers exposed to chromium dust. Baetjer described 109 cases of cancer in the chromate-producing industry. In a review of the histologic classification of 123 cases of lung cancer in chromate workers, Hueper found 46 squamous cell carcinomas, 66 anaplastic tumors and 11 adenocarcinomas. The greatest risk to cancer is attributed to exposure to acid-soluble hexavalentchromium as occurs in the roasting or refining processes <2>.

Of concern is how to dispose of soil contaminated with chromium compounds or to render the chromium in the soil non-hazardous. Such soil should not be buried because of the foreseeability of the leaching of the chromium compounds from the soil into aquifers.

Animal experiments confirm the carcinogenic activity of chromates on mice, rats and rabbits. Chromium may exist in the bi-, tri-, and hexavalent states. Of greatest interest from a toxicity point of view is the hexavalent state. The hexavalent is a stable form. The dichromate solubility varies with the elements involved and the temperature. At 20 C, the sodium salt solubility is 180 parts /100 parts water; the potassium salt solubility, 12.5 parts/100 parts water. The dichromate is an oxidizer. The chromate has a tendency to form hexacovalent complexes by coordination.

The overwhelming majority of epidemiological reports are based on data from workers in industries using soluble chromates. There is a belief that only hexavalent chromium compounds represent a cancer hazard to humans. Attempts to demonstrate the carcinogenicity of chromite ore or chromium (II) sulfate in the strain A mouse pulmonary tumorigenesis assay system were unsuccessful (Shimkin and Leiter, 1940/1941). Also, rats fed Cr2O3 at 1%, 2%, and 5% level for 2 years tolerated the compound well with no teterogenic effect in the offspring. The average daily chromium intake of individuals in the United States was estimated by Schroder (1970) to be 0.28, 4, and 280 microgram from air, water, and food, respectively <3>.

INSTRUMENTATION

Introduction

The scanning electron microscope (SEM) is one of the most versatile and widely used tools in modern science. The SEM when combined with the energy dispersion spectrometer (EDS) can yield a great deal of morphological, physical and chemical information about a specimen.

Theory of the Scanning Electron Microscope

A JEOL-JSM 35C model was employed. It utilizes a focused beam of high energy electrons that systematically scans across the surface of the specimen. The interaction of the beam with the specimen produces a large number of signals at or near the surface. These interactions include lower energy electrons, termed secondary electrons. The low energy of the secondary electrons makes them a conveniently collected signal for the SEM since they can be easily drawn to a positively biased detector system. The electron signal is eventually converted to an electronic signal which is imaged on a cathode ray tube. The scanning of the beam is synchronized with the scanning of the cathode ray tube, thus producing a one-to-one relation between points on the specimen and points on the CRT. Electrons emitted from a surface which faces away from the detector are partially blocked by the specimen and the image of such a surface is darker than that of a surface which faces toward the detector <4>.

The SEM in conjunction with the EDS can provide valuable information in sample analysis. The x-ray image can be obtained by selecting a specific window for a specific element. When the computer is commanded to run Fe, for example, Fe window will be opened. The results are presented with white spots. The magnitude of the white spots relates to the element concentration.

The area scan is obtained as a spectrum generated by the EDS. The elements in the SEM field are identified in the EDS print out. Usually, the area scan is taken from a low field magnification in order to have as best representation as possible. The area scan does not tell us where a particular element is in this field.

In the point scan the electron beam is focused on a specific point of interest. The elements present in such spot are displayed in the EDS print out, regardless of the surrounding. In the material we are testing, the chemical analysis is coming from a spot approximately 0.5 micron in diameter. Also, the electron beam in such material has a maximum penetration of 0.5 micron.

The line profile scan is a format which provides a graphic display of elemental distribution along a line on the specimen. The line (which appears in the picture) is modulated through the EDS ratemeter. The intensities of the elemental line profile scan represents the concentration.

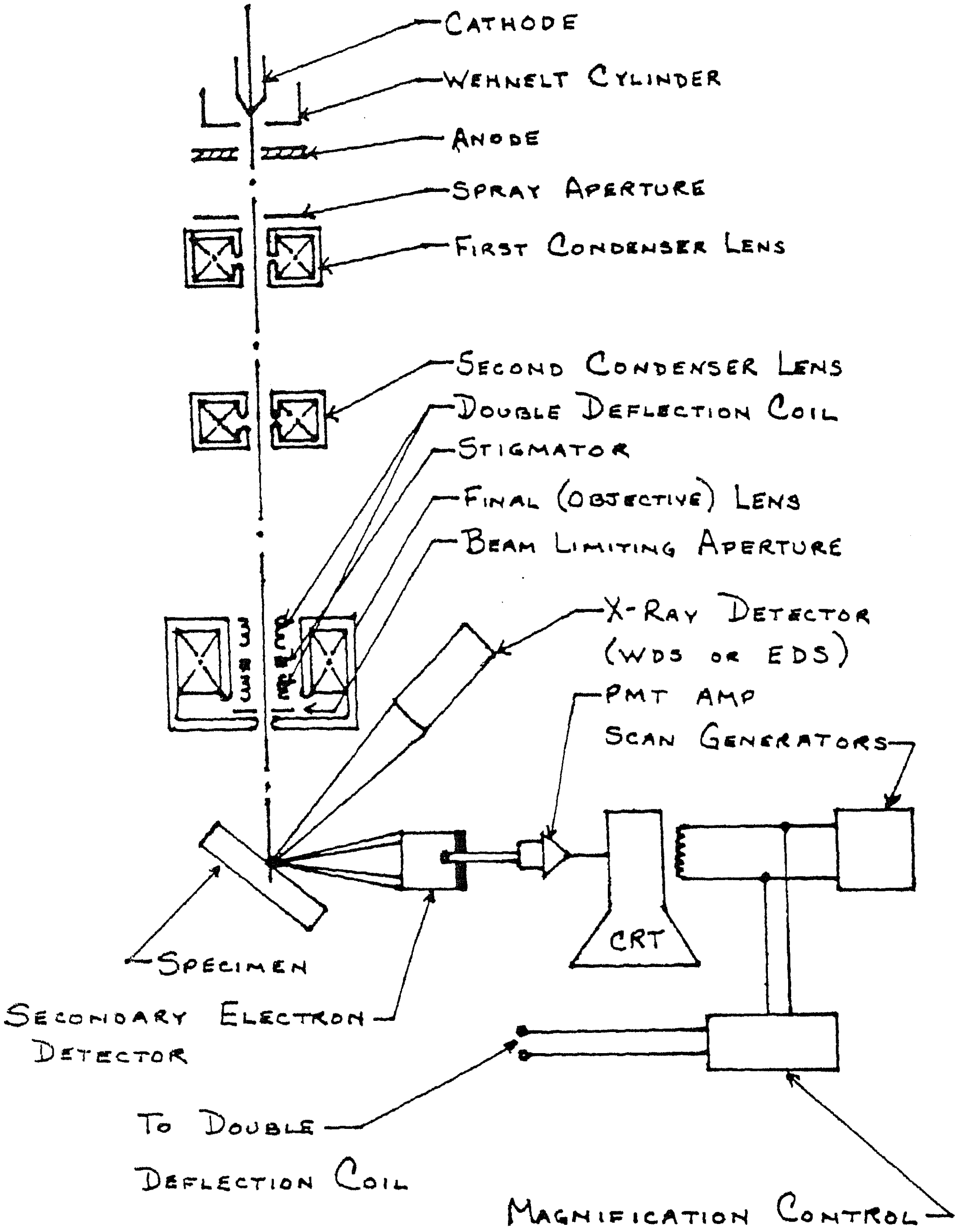

DIAGRAM I SCHEMATIC DRAWING OF THE ELECTRON AND X-RAY OPTICS OF THE SEM

Components of the Scanning Electron Microscope

The Electron Gun

The electron gun is composed of a hairpin-shaped tungsten filament (the cathode), Wehnelt cylinder, and an anode plate. The gun and the cylinder are connected to a negative pole of a high voltage source. The negatively charged electrons are accelerated toward the anode. The voltage difference between the cathode and the anode is referred to as the "accelerating voltage". The emission of the electrons from the filament due to heating is called thermionic emission. These electrons are contained and condensed between the filament tip and Wehnelt cylinder (called the gridcap) by a slightly greater negative charge on the cylinder than on the filament. This charge differential is called "bias". The positioning of the filament within the gridcap is important in creating a focused beam. The accelerated electrons pass through a hole in the anode which acts as a crude aperture and block the peripheral electrons and allows the more cohesive ones to pass through the column <4>.

Electromagnetic Lenses

An electromagnetic lens is essentially a length of wire coiled around a metal cylinder. Within the cylinder is found a soft iron pole piece. As currents applied to the wire is increased, the magnetic field in the bore of the pole piece also increases in strength. Altering the path of an electron through the pole is related to the strength of the field, the velocity of the electron, and the relative path between the

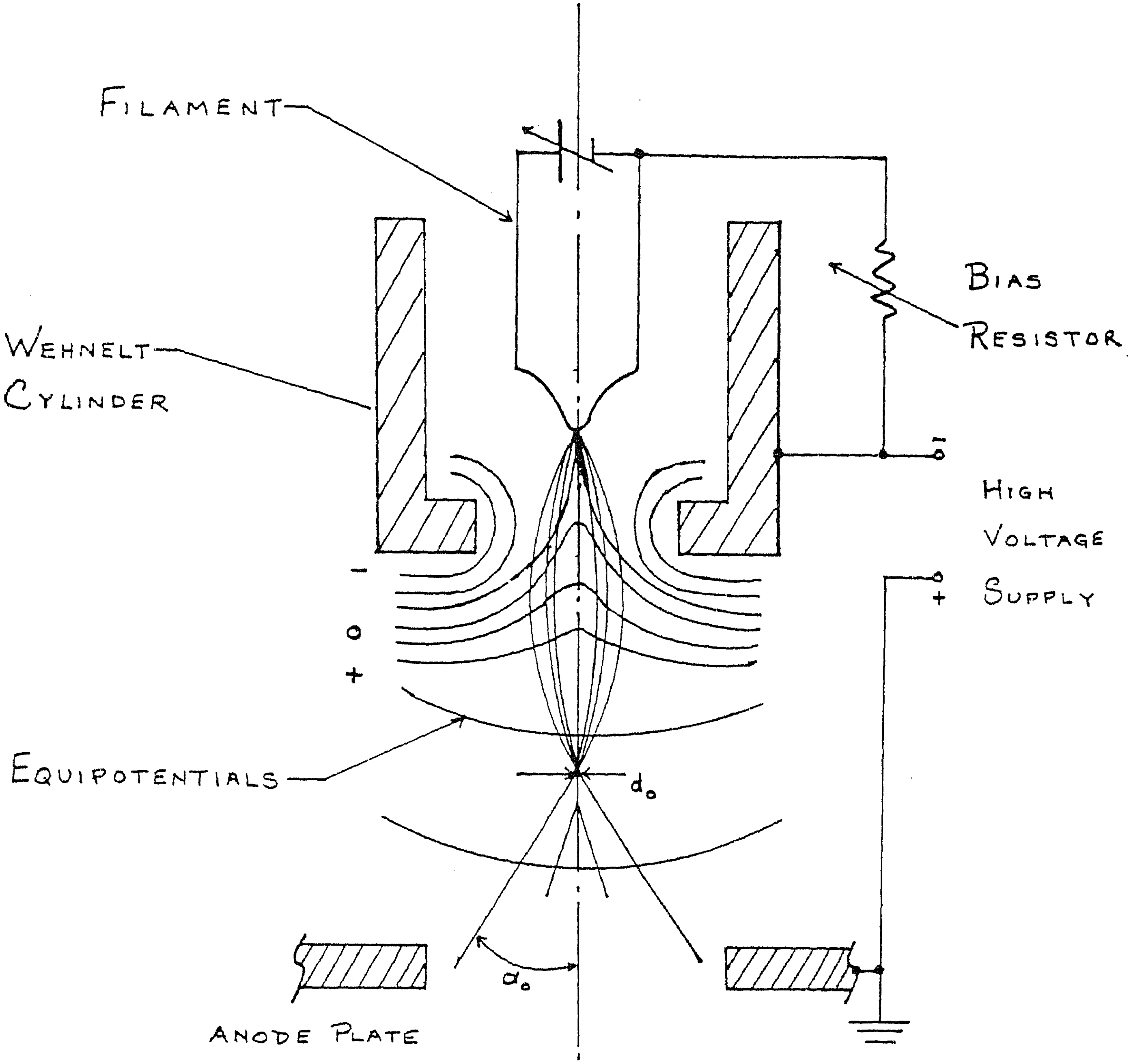

DIAGRAM II THE ELECTRON GUN

electron path and lines of force. The electrons assume a helical path under the magnetic field influence. The first lens that influences the electron beam is the condenser lens. The beam is demagnified on passing through condenser and objective lenses. A second condenser lens below the first one provides more control over the electron beam. The condenser lens in conjunction with the chosen accelerating voltage is responsible for determining the intensity of the electron beam when it strikes a specimen and consequently the image brightness. The beam will diverge below the condenser lens aperture. A final lens is used to bring the beam into focus at the specimen by demagnifying it to a focal point at the specimen surface <4>.

Apertures

Spray-type apertures are used to reduce and exclude extraneous electrons in the lenses. In addition it is used to reduce spherical aerrations in the final lens and also affects the depth of the field. Decreasing the aperture size increases the depth of field with a relative brightness loss.

Stigmation

A stigmator is a series of coils surrounding the beam below one of the lenses to insure that the electron beam will be circular in cross section when it reaches the specimen and results in high image resolution <4>.

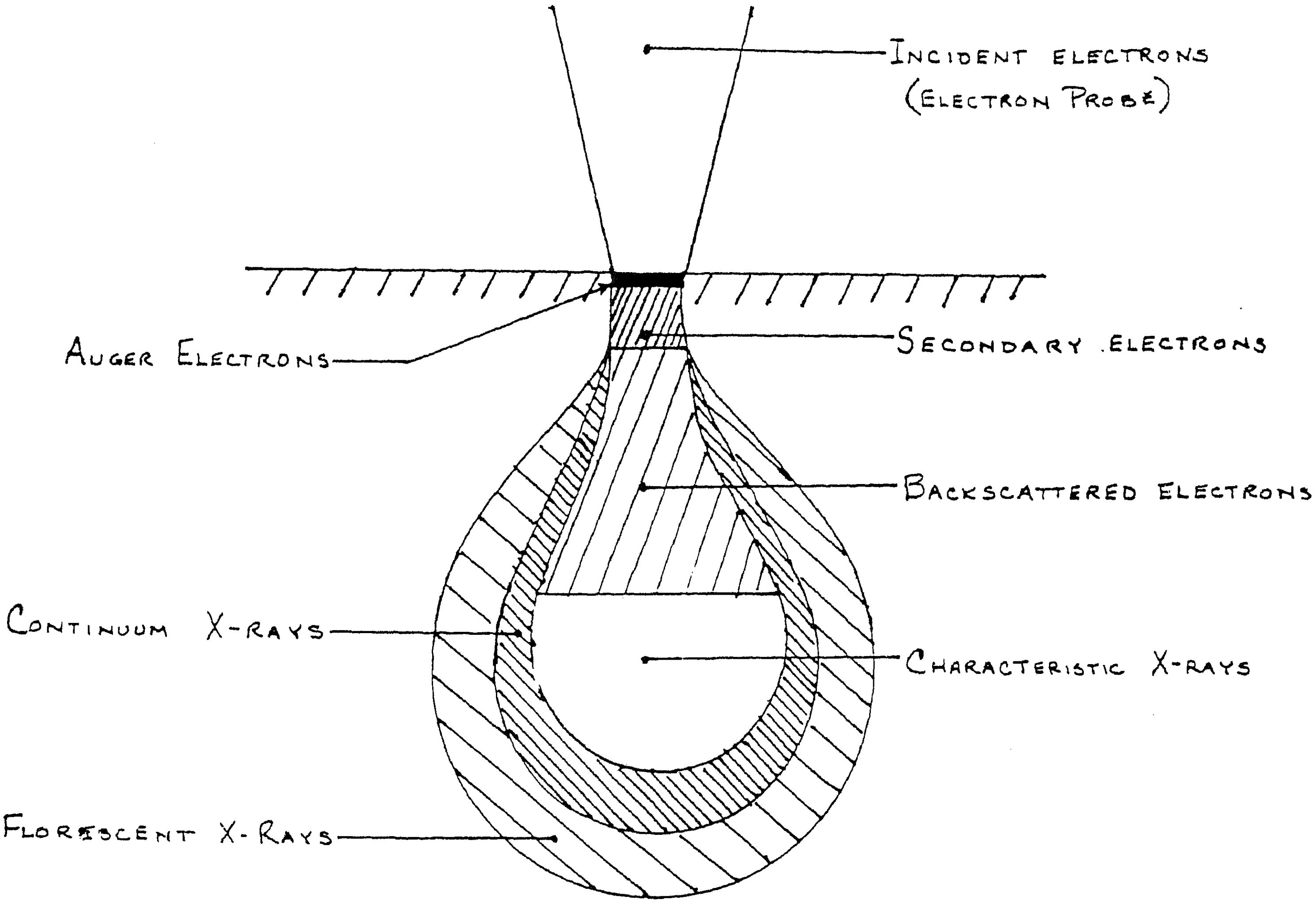

DIAGRAM III ILLUSTRATION SHOWING THE DEPTH OF SIGNAL GENERATION WHEN THE PRIMARY ELECTRON BEAM INTERACTS WITH THE SAMPLE SURFACE

Specimen Stage

The specimen stage is the platform upon which the specimen rests in the column.

Depth of Field

Depth of field is the extent of the zone on a specimen which appears acceptably in focus. This represents the zone above and below the sharpest focus. To increase the depth of field, the specimen can be lowered from the final lens to decrease the aperture angle or the size of the lens aperture can be reduced <4>.

Vacuum Systems

A mechanical and a diffusion pump are used to vacuum the air in the SEM column. This protects the hot filament from oxidation, keeps the column clean, the electron beam well focused, and prevents moisture corrosion. The air pressure inside the column is usually 5 x 10 ^-5 mm Hg.

Image Formation

Signal Generation

When the beam hit the specimen, elastic and inelastic electrons are generated. The elastic are of high energy and called back scattered electrons. The inelastic are weak, 50 ev or less, and are called secondary electrons. The emitted electrons are detected by system composed of a collector, scintillator, light pipe, and photomultiplier tube. The collector draws the electrons to the scintillator which transfer the energy of the electrons to the photons. The anode or collector around the scintillator accelerates

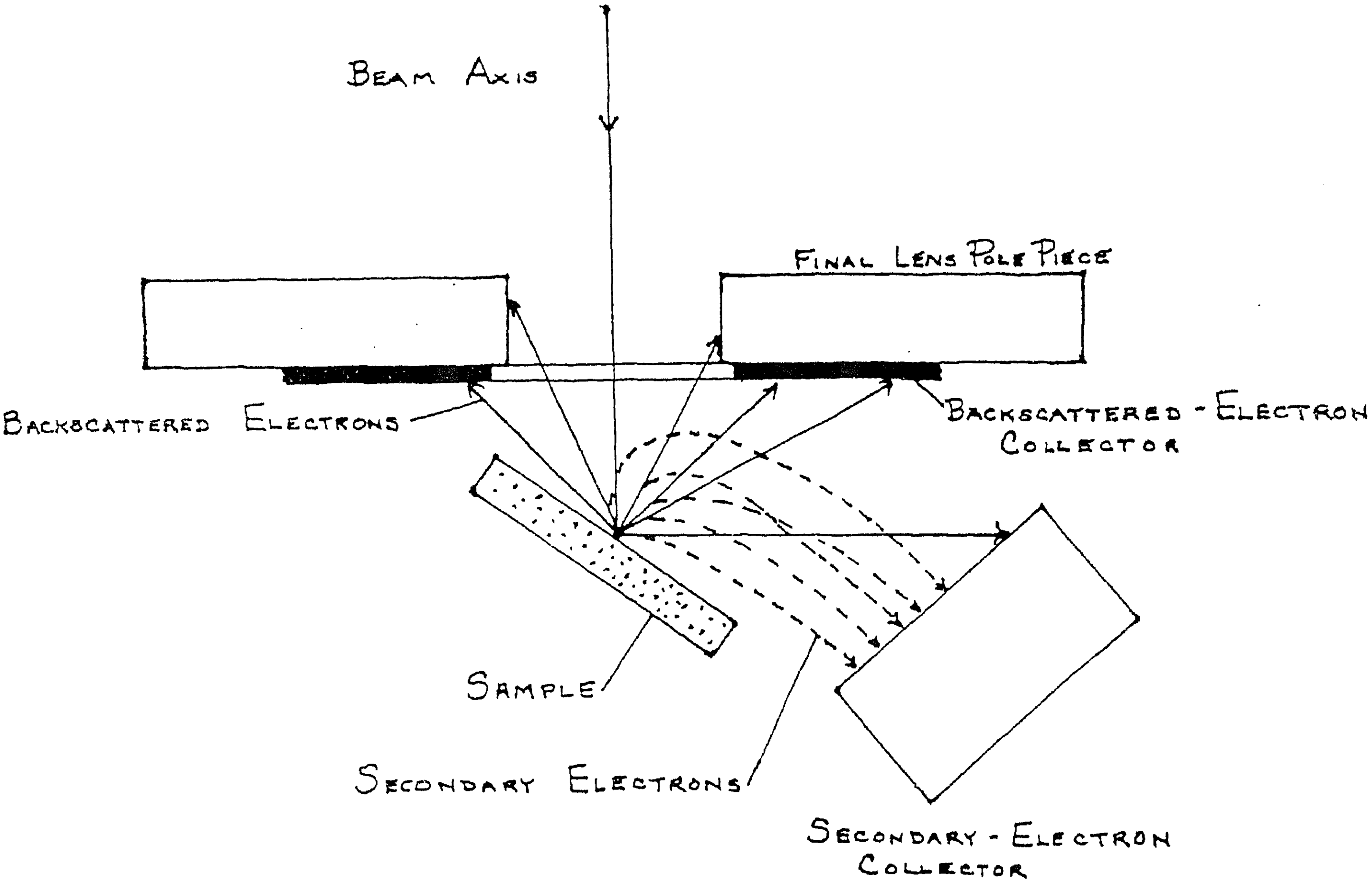

DIAGRAM IV OPTIMUM POSITIONS OF THE SECONDARY AND BACKSCATTERED DETECTORS the low energy secondary electrons toward the detector. The scintillator produces photons when struck by electrons. The light produced is transported through a light pipe and converted to an amplified electronic signal <4>.

Image Display

The SEM is equipped with two cathode ray tubes for the visualization and recording of the specimen image. One cathode ray tube is used for the display of the specimen image to the microscope operator and the second is used for photography only. The brightness of the image increases as the number of the secondary electrons reaching the detector increases. Also, the brightness will increase if the beam hits a tilted sample and faces the detector <4>.

The Energy Dispersive Spectrometer

The x-rays produced in an SEM include x-rays with energies characteristic of the elements in the specimen. Energy dispersion is the segregation of x-rays according to their energy. When an x-ray strikes a semiconductor crystal, electrons in the crystal each absorb a given amount of energy. The greater the energy of the x-ray, the greater the number of electrons excited. The energy absorbed by the electrons is then converted to an electrical signal which is emitted and amplified. The strength of the current from the crystal is proportional to the x-ray energy. The amplified electrical pulses from the semiconductor are converted to digital form and fed into a mechanical analyzer (MCA) which

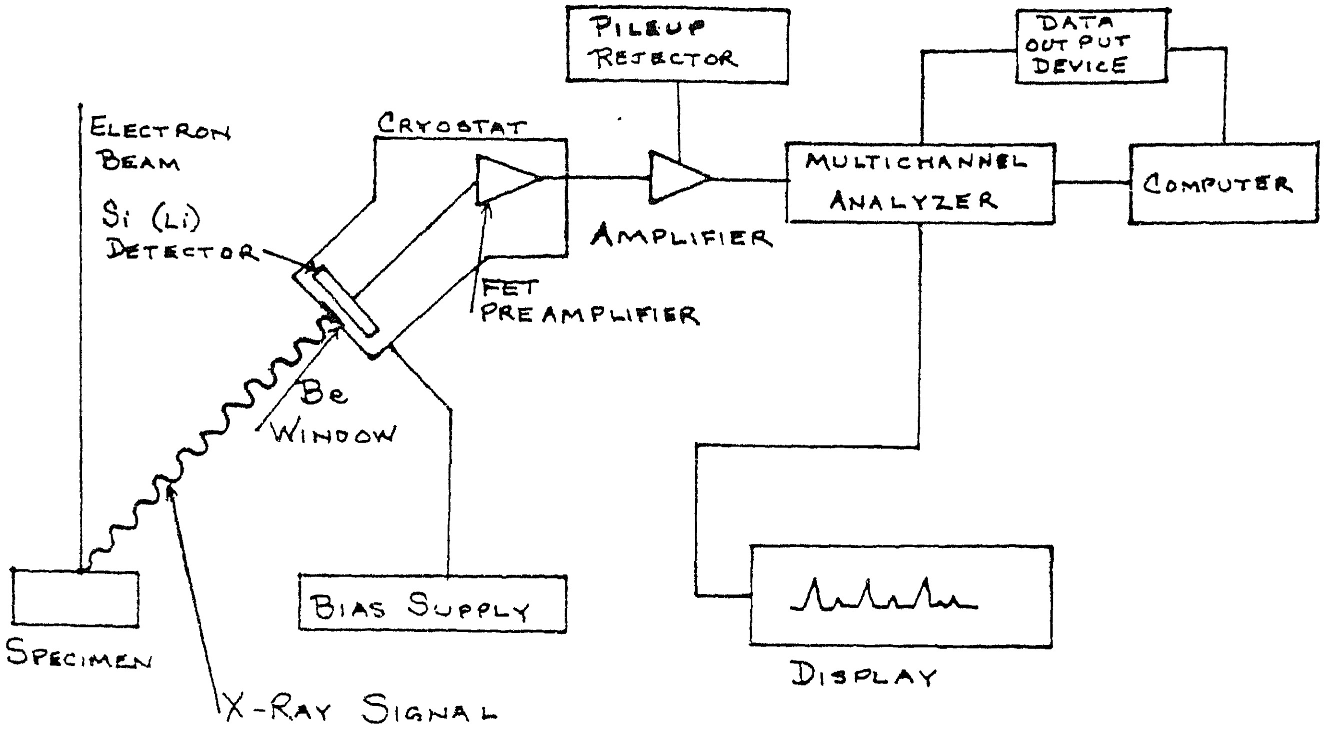

DIAGRAM V Si(Li) DETECTOR OF AN X-RAY ENERGY DISPERSIVE SPECTROMETER sorts these signals and, in effect, counts the number of x-rays at each energy level which strike the crystal. This information is then plotted to form a representative spectrum. The energy dispersive spectrometer (EDS) used in this experiment was model PGT system plus <5>.

Theory of the Microwave

Microwaves are a form of energy generated by a magnetron. The microwave radiation belongs to the electromagnetic radiation spectrum. The wave length utilized in this experiment was 12.25 cm, corresponding to 2450 MHZ frequency. The microwave consists of:

1) Magnetron tube
2) Wave guider
3) Mode stirrer
4) Cavity

The magnetron generates the microwaves. The collected energy is radiated from an antenna which is enclosed in the vacuum envelope of the tube. This energy is transmitted to the oven cavity through a wave guide. The reflection of a single wave from the cavity surfaces will generate a standing wave that will cause non-uniform radiation and subsequently uneven heating. To minimize such effect, the mode stirrer generates additional wavelengths and the sample is placed on a carousel.

A material in the cavity will absorb the microwave energy if it meets any of the following criterion:

1) The presence of a dipole ratating at 2450 MHZ (The

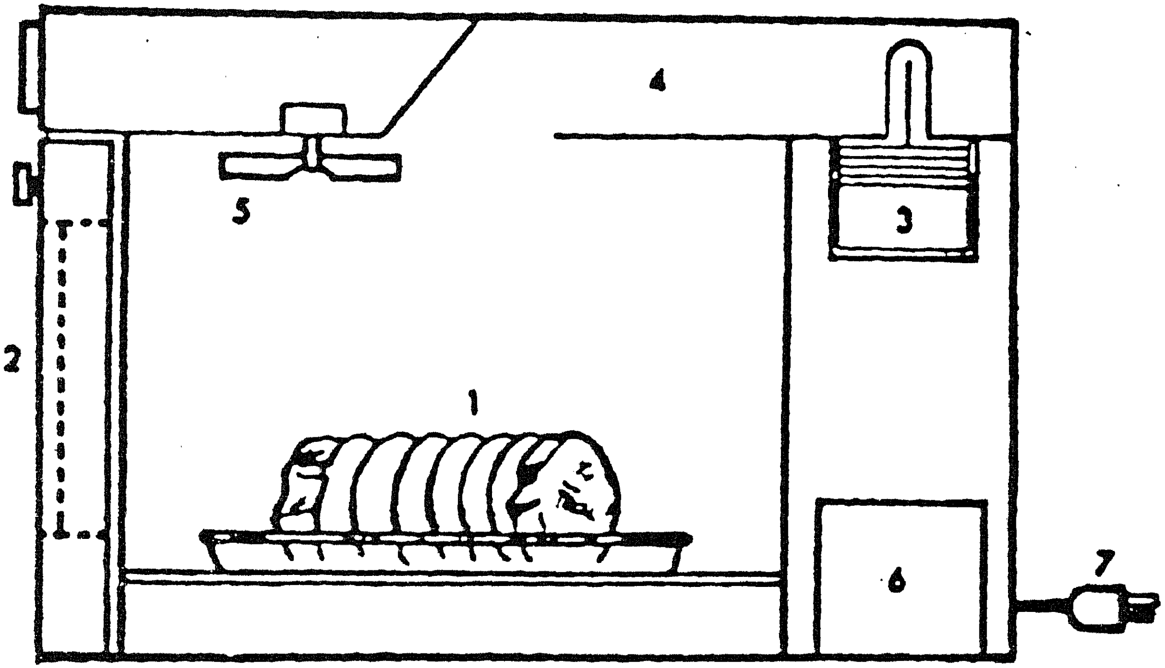

DIAGRAM VI SCHEMATIC OF THE MICROWAVE

1. Cavity	5. Mode Stirrer
2. Door	6. Power Supply
3. Magnetron	7. Power Cord
4. Waveguide	

frequency used in this experiment).

2) The presence of mobile electrostatic charges at the applied frequency.
3) Magnetic domains that rotates at the of the incident radiation.

When the electromagnetic field is applied, the electrical dipole in the material (e.g.water) orients to reduce the internal field. The molecules will return to the random state when the external field is disengaged. At this point, the molecules will collide and heat will be generated. Ice can not absorb microwave energy because the dipole rotate too slow. The temperature will rise faster in the microwave oven as compared to the convection type.

Electrostaticl charged fine particles are good microwave absorbers. Such materials are heated "skin deep", due to the large surface to volume ratio, causing high temperature rise. In large objects, the absorbed energy at the surface is conducted to the bulk of the substance <6,7>

EXPERIMENTS

Soil Preparation

Non-hazardous soil from the Brunswick formation was used. The soil was a situ and clay mixture obtained from a construction site at the Veteran Administration Hospital, Lyons NJ. The soil was provided by Professor John Schuring of the department of Civil and Enviromental Engineering of New Jersey Institute of Technology, Newark NJ.

The soil exhibited a broad particle size distribution. The soil was milled in a Brinkam ultra centrifugal mill model ZM1 fitted with 0.05 cm stainless steel screen opening. The milled soil was shaken for 20 minutes in the presence of ceramic grinding media (to prevent screens blinding) in a Ro-Tap and the 200/325 USS mesh cut was collected. SEM analysis necessitates fine soil particles to demonstrate sample homogenesity and to achieve uniform sample coating prior to picturing.

Part of this prepared soil was to be used as the blank and the other part to be impregnated.

Soil Impregnation for SEM Analysis

Six hundred grams of the above soil 200/325 mesh cut was slurried in solution of deionized water and 33.387 g of potassium dichromate salt (K2Cr2O7) using a Cowel dispersator to provide uniform soil wettability. The slurry was dried in a convection oven at 105 c for 24 hrs, stirred with a spatula, and dried for a further 48 hrs. The dry mass was placed in double plastic bags, crushed with a hammer (hammering the outside of the bag). The soil was then milled in a Micro hammer-cutter mill fitted with 0.05 cm stainless screen opening. The soil should contain theoretically 11.802 g chromium ion or 1.96654%. This high level of Cr impregnation is essential for easy detection with the SEM/EDS.

Soil Impregnation for X Ray Diffraction Analysis

Three hundred grams of the fine blank soil was slurried with 71.369 g of K2Cr2O7 and dried as above. Chromium ion theoretical concentration in the dry soil was 25.228 g or 7.20%. Below such concentration, chromium detectability with the X ray could be compromised.

The dry impregnated soil was also milled in the same Micro hammer mill as above.

Soil Microwaving

Portions of the dry impregnated soil with the two different K2Cr2O7 concentrations were microwaved for 15, 30, 45 and 60 minutes, respectively,in the following manner: The soil samples were placed in porcelain drying dishes; each dish was covered with a porcelain cover and placed in a sand bath. The surrounding sand bath reached up to the dish rim. Each drying dish contained 75 g of the soil prior to heating. Each dish was removed from the microwave after the designated heating period and was allowed to cool at 22 C. The soil became fused as the heating time progressed. The non-fused part was removed. The fused portion was milled in the Mikro

Hammer mill fitted with 0.05 cm screen opening. The milled portion was placed on a Ro-Tap for 20 minutes and the 200/325 USS mesh cut was collected for each heated sample. A small portion of the fused mass was left intact for further examination by SEM cross section method.

Sample Preparation for SEM Powder Soil Analysis

Aluminum stubs (1" dia. x 1" height) were used. The powder soil was sprinkled sparingly on a double sided adhesive tape placed on the stub. The word powder refers to the soil 200/325 mesh regardless of the heat treatment or whether it is impregnated with K2Cr2O7 or not. The stubs were tapped gently to ensure the adherence of the powder to the tape. The loose particles were removed with a microscopically clean compressed gas (Refrigerant 12-di-chlorofloromethane). Each stub was then coated with a very thin layer of carbon in a vacuum evaporator.

Sample Preparation for SEM Cross Section Analysis

Cross section refers to the fused non-ground soil due to microwaving: the blank and impregnated soil, respectively. The sample was prepared as follows:

Blank and Impregnated Samples

A small portion from each sample was placed in a vial. A few grams of ultra fine carbon powder was added to the sample to protect the cross section of the particles from the electron beam. A mixer mill (chatter box) was used for five minutes to mix the sample with the carbon. A small portion

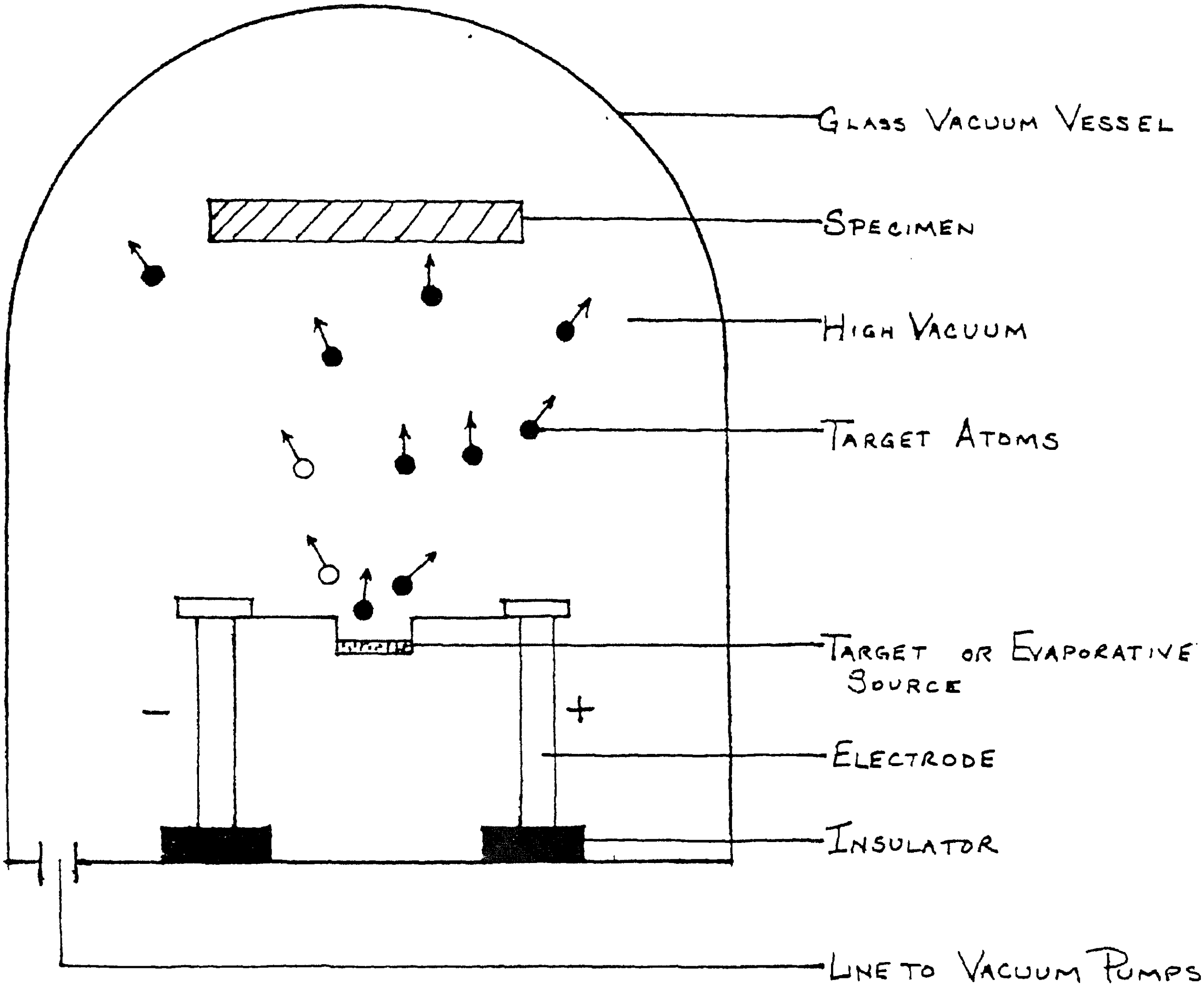

DIAGRAM VII VACUUM EVAPORATOR

There are two carbon rods (acting as a conductor). An arc is struck between the two rods and rapid evaporation of the conductor surface occurs. It is the practice to strike the arc several times in quick succession to avoid undue heating of the sample. The carbon may be evaporated by the arc or resistive method using spectroscopically pure carbon rods.

In the resistive method, two carbon rods 6 mm in diameter are ground at the edge to a 1.5 mm in diameter. The rods are held coaxically and kept in contact by springs. The carbon rods are heated gently to a dull red at high vacuum and before back filling with argon gas in order to remove any volatile substances. A few bursts of power are given at 10 seconds intervals while the sample is rotated until the desired thickness of coating is achieved. The carbon layer is typically 50-100 Angstroms thick.

RESULTS I

Blank Soil

X-Ray Image

All particles were irregular in shape, non-uniform in size and had very rough surface.

The X ray image of the blank soil (powder) in figure 1 (100x magnification) indicated that most particles contained a very high level of Si (figure 3), a low level of Al (figure 2), low level of K (figure 4),a very low level of Ti (figure 5) and a low level of Fe (figure 6). Few particles had high level of Ti (figure 5) and a number of particles had very level of Fe (figure 6).

At a higher magnification (1000 X) the x -ray image of the blank soil (powder) exhibited the same above results (figure 7). In addition some particles contained mainly Si only, bright spots (figure 9).

Another field 1000X magnification was pictured (Figure 13). The results here were similar to figure 7 except particles containing high Ti were not detected in the X-ray image analysis.

The cross section X ray image of the soil field shown in figure 18 (500X magnification) as well as the X ray image of the soil field in figure 24 (3000X magnification) were similar to those of figure 7.

Line Profile Scan

The line profile scan for a cross section of a blank soil particle magnified at 1000x and in the middle of figure 30, indicated the presence of high level of Si (figure 32) and low levels of Al (figure 31), K (figure 33) and Fe (figure 34) across the particle. The intensities of Al and K appear to be similar to Si because The latter was obtained at higher full scale than Al and K. The full scale is being adjusted automatically by the EDS computer so that every line scan will be contained within the boundaries of the image regardless to its concentration.

A high level of Fe was present at the right side edge of the particle due to the fact that a very small Fe particle attached or close to the side of that large particle was observed (figure34).

A different particle in figure 35 at a magnification of 3000x was found to contain very low levels of Al (figure 36), Si (figure 37), and K (figure 38). This particle was found to be mainly Fe (figure 39).

At a magnification of 6000x, for another particle in the middle of figure 40, the line scan profiles are similar to those found in the previously-discussed figure 30.

Area and Point Scan

Spectra B1-B3 were area scans obtained from 3 different fields (100X field magnification). This low field magnification contains more particles in the field than at higher magnification and consequently better elemental analysis representation in the EDS spectra results. Very high level of Si, low levels of Al, K, Fe, very low level of Ti and traces of Na and Mg were found.

Point scan analysis was conducted on a large number of particles to study the elemental composition of individual particles.

Spectra B4, B5, B16 and B17 exhibited very high level of Fe. A number of particles contained mainly Si (spectra B6, B8, B14 and B18). Very high level of Si and low level of Al, Fe and K were detected from particles in spectra B10, B13, B19 and B20. A number of particles contained mainly Si and Fe, Ti and Fe, Al and Si, Si, AL and K, or Ti alone.

Impregnated Soil

X Ray Image

The X-ray images analysis for the soil sample impregnated (powder sample) with K2Cr2O7 sample, non-microwaved, indicated the following:

At 100X magnification, the x ray images of figure 45 demonstrated that most particles contained Al, Si and K, low levels of Fe and Cr and very low level of Ti, (figures 46,47,48,49,50,&51). The presence of some aggregates was evident when compared to blank soil of same magnification. The main element, however, was Si.

The cross section of the impregnated soil in figure 66 (100X magnification) demonstrated the presence of large aggregates. Obviously these aggregates were generated by the process of wetting and drying during the impregnation step. It also demonstrates that the dry milling step after impregnation and drying was performed with a relatively large screen opening (.5 mm) to prevent micronizing the soil and potentially altering the elements distribution.

Line Profile Scan

The line profile scan in a cross section of an impregnated particle in figure 80 (1000X magnification), depicts the particle to contain mainly Si, AL and K, with some Fe and low Cr level across the particle. Ti was found in a trace and scattered distribution across that particle (Figures 81-86).

The line profile scan of figure 87 (1600x magnification) confirms the above results (figures 88-93).

Area and Point Scan

Area scan analysis of different fields at 100X magnification indicated the presence of : Si as a major element, Al & K & Fe as low elements, Cr as very low, and Ti as very low to trace element (EDS spectra SIMP1, SIMP2, &SIMP3).

In the point scan analysis, the particles demonstrating high level of K exhibited high levels of Cr (EDS spectra SIMP5, &6). This relationship is due to the use of K2Cr2O7 as the salt in impregnation. The particles exhibiting high level of Fe had low level of Cr (EDS spectra SIMP 10).

Area and Point Scan

Area and point scans were employed to study the elemental composition and distribution of the milled particles and, also, to find out the possible phases. The number of particles containing mainly Si or Fe were found to be less than in the blank sample. The particles detected with very high level of Fe also contained very high level of Cr; this was not observed in non-heated samples (EDS spectra, S15C2, S15C3,S15C4, S15H9, S15H10 & S15H12). The affinity of Cr to Fe suggests a reaction might be taking place between K2Cr2O7 added and Fe of the soil in the microwave.

Thirty Minutes Microwave

X-Ray Image

The x-ray image analysis of figure 157 (100x magnification) for the impregnated/ 30 minutes microwave followed by milling (powder sample), indicated the presence of Al,Si,K,Ti,Cr and Fe. A different field (300xmagnification), large number of holes appeared on the surfaces of the particles (Figure 164). The size of these holes were larger than the 15 minutes microwaved sample.

Figure 168 (300x magnification) exhibited few particles containing very high level of Ti.

Line Profile Scan

The line profile scan for an impregnated/30 minutes microwaved/non-milled cross section field for the figure 213 (3000x magnification), clearly demonstrates the presence of

Cr and Fe together as the electron beam travels across the particle (figures 218 and 219).

Area and Point Scan

Area scan analysis performed on many fields confirmed the elements distribution uniformity (EDS Spectra S30H1,S30H2, S30H3). The scan analysis exhibited numerous particles contained Al, Si, K ,Ti, Cr and Fe. Areas containing mainly Fe or Si were not detected.

The point scan analysis did not identify spots with Ti only. Ti was found to be associated with Fe (EDS S30H4). A number of Cr-Fe particles were detected (EDS S30H6). The Cr concentration varied from low to very high. It appeared that the level of Cr associated with Fe was higher than in the 15 minutes microwaved sample.

A large number of particles containing Al, Si and K were observed. Such particles contained trace of Ti, Cr and Fe. Particles containing mainly Si were not detected in this sample.

The point scan analysis performed on a cross section sample (non-milled) from many fields indicated the presence of low to very high concentrations of Cr where high Fe was detected (EDS S30C1,S30C3,S30C4). The level of K found in these same spots was low to normal. This indicates that K in K2Cr2O7, used for impregnation, reacted with or was dispersed into the particles containing high level of Al,Si and K. Therefore, we can conclude that K2Cr2O7 dissociated during the microwave process with K favoring the silicate and Cr favoring Fe.

Forty Five Minutes Microwaving

X-Ray Image

The morphology of the 45 minutes sample was similar to the 30 minutes microwaved sample. The x-ray image analysis identified most particles to contain Al, Si,K, Ti, Cr and Fe (figures 186-191). A very small number of particles contained higher levels than normal of Cr, Fig 218 (100xmagnification). The line profile scan was not determined for this sample.

Area and Point Scan

The area scan analysis performed on many fields indicated that the distribution of the elements was uniform (EDS S45C1, S45C2,S45C3,S45H1,S45H2,S45H3).

Point scan examination employed on many particles indicated: Large number of particles contained AL, Si, K, Ti, Cr, & Fe. Particles containing Ti only were not detected. Ti was distributed in the sample. Si particles were detected (EDS S45C4 & S45H8). A number of Fe-Cr particles were detected. The Cr concentration in such particles varied from low to very high,(EDS S45C10,S45H4,S45H5).

It appeared that the level of Cr associated with the Fe in the 45 minutes sample was higher than that in samples which were treated for 15 or 30 minutes. Also, spots with high level of Ti was found to contain high level of Fe as well (EDS S45C6, S45C7, S45C8).

RESULTS II

Blank Soil

X-Ray Diffraction

The X-ray diffraction reveals that the blank soil contains the following 4 crystal phases (figures 227 & 228):

Muscovite : $K AL_2 (Si_3 AL) O_{10} (OH, F)_2$
Quartz : $Si O_2$
Hematite : $Fe_2 O_3$
Iron fluoride hydrate : $Fe F_3 . H_2O$

Impregnated Soil

The X-ray diffraction identified the same phases in the blank plus the potassium dichromate added in the impregnation step (figures 229 and 230).

Microwaved Soil

The phases identified in 30 minutes and 60 minutes microwaved sample were identical (figures 231 & 232). Four crystal phases were present (figures 233 & 234), they were:

Silicon dioxide : $Si O_2$ (Quartz was not detected).
: $FE_2 Si O_4$
: $Cr_2 O_3$
: $Fe Cr_2 O_4$

It is clear that the heating process had changed the quartz structure to another $Si O_2$ crystal form. We expect also that some crystalline $Si O_2$ may have been converted to an amorphous form.

Some of the iron, from the hematite phase, reacted with the silicon dioxide and formed ferrous silicate.

A minor amount of the chromium from $K_2Cr_2O_7$ was converted to chromium oxide Cr_2O_3. A much larger chromium amount reacted with the hematite and formed $FeCr_2O_4$ phase. The SEM and EDS confirmed the presence of Cr jointly with Fe in the point scan analysis (Cr was never found alone). This statement applies to the microwaved sample only. What we don't know is if any chromium reacted with the silicate to form an amorphous structure. The X-ray diffraction does not identify the amorphous phase structure. The X-ray diffraction applies Braggs law in the identification of the D spacing in a crystal. The crystal phases are identified by matching the highest intensities of the D spacing in a crystal sample with those of the X-ray diffraction card. The computer performs that automatically.

Braggs law:

nY = 2d sin 0

where n = integer
Y = wave length of the x-ray tube
d = the d spacing in a crystal
0 = the diffraction angle.

CONCLUSION

The soil type used in this experiment was mainly muscovite (potassium aluminum silicate) with some hematite. Based on the SEM, EDS and X-ray diffraction results we can state with certainty that the microwave oven is a useful tool in immobilizing chromium in contaminated soil. The heating time was immaterial (30 versus 60 minutes) in this experiment; the yield of fused versus non-fused soil will vary with heating time. The soluble dichromate $K2Cr2O7$ used in this experiment became insoluble by mainly forming $Cr2O3$ and by reacting with the hematite phase in the soil to form a new phase of $FeCr2O4$.

$FeCr2O4$, also, called chromite and $Cr2O3$ were the two major ores from which chromium was extracted commercially in the United States. This process returns the dichromate to its nature state.

The transition elements present in the soil tend to be in the same areas as the heating progressed, for example, Ti and Fe after 45 minutes of microwave treatment. The degree of the soil crystallization and the type of crystal phases had changed due to the heating. The quartz and muscovite disappeared. The potassium from the dichromate favored the silicon and the aluminum.

Future Area of Research

1) To perform the same experiment in soil deficient in iron,i.e, sand or in sodium aluminum silicate (bauxite)

media to see if the presence of iron in the soil is crucial or not.

2) To test soils contaminated with other hazardous elements.

3) To scale up the process and determine its feasibility.

REFERENCES

1 Chih-Ju, J, 1989 Thesis. Application of Microwave to the Remediation of Soils Contaminated with Chromium.

2 Casarett and Doull's Toxicology. The Basic Science of Poisons, Third Edition.

3 Sontag, M.J. 1981. Carcinogens in Industry and the Enviroment. Marcel Dekker, Inc.

4 Posteck,T.M. and Ladd Reseach Industries, 1980. Scan Electron Microscopy.

5 Sedhom, A.E, 1981 Thesis. Scanning Electron Microscopy and X-ray Energy Dispersive Spectroscopic Analysis of Selected Sorbent Materials.

6 Osepchuk J.M. Basic Principles of Microwave Oven. Raytheon Research Division.

7 Mudgett, R.E. Microwave food processing. Food Technology. 43:117-126, January 1989.

8 Connerton, Susan L. and John J. Shuleva. How Fats, Oils and emulsifiers function in microwave Food Formulation. Microwave Foods conference. pp 1-15, March 1989.

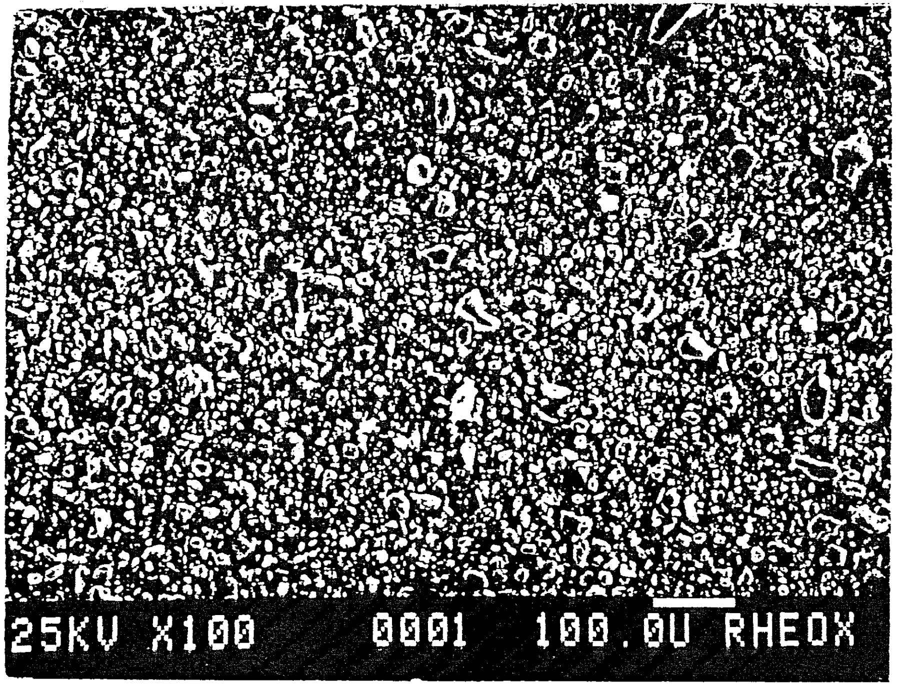

Figure 1

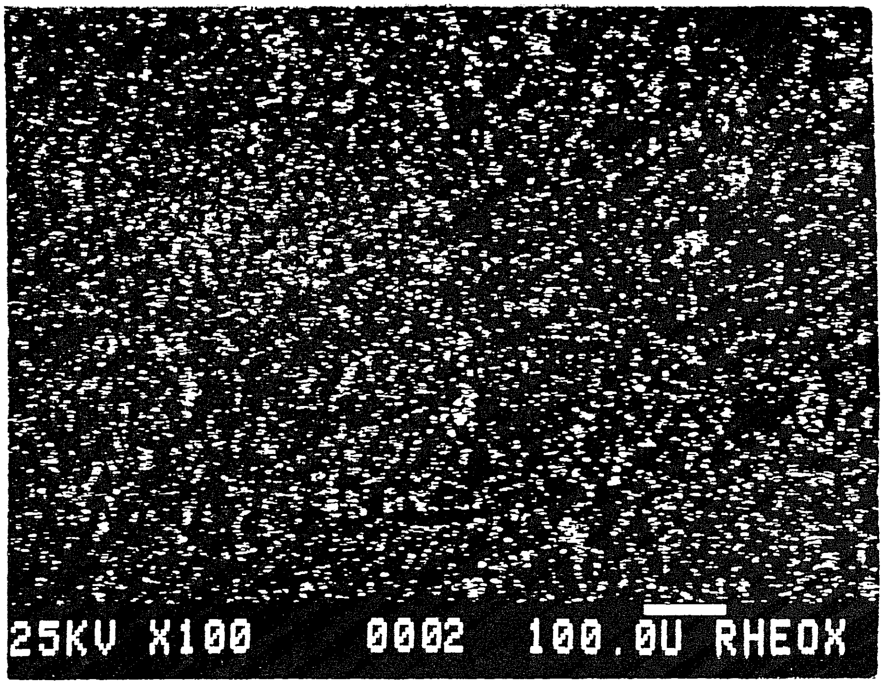

Figure 2 AL X-ray Image of Figure 1

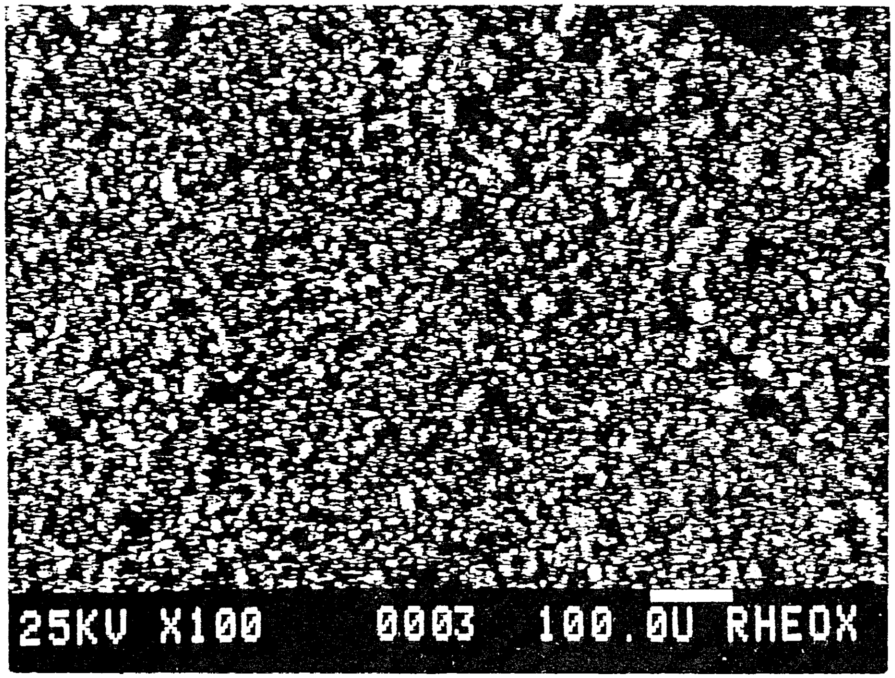

Figure 3 Si X-ray Image of Figure 1

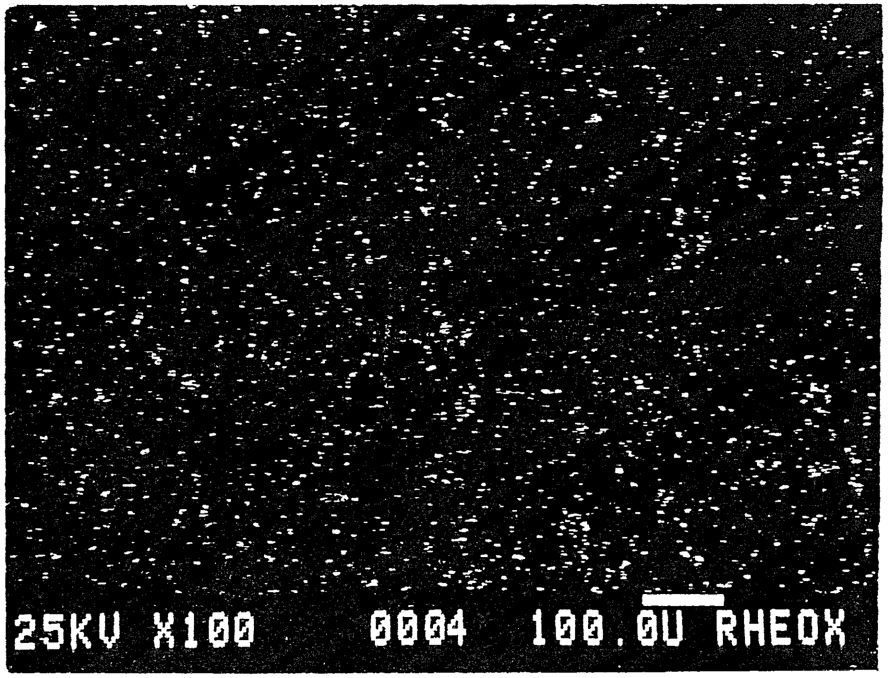

Figure 4 K X-ray Image of Figure 1

SEM IMAGES OF SAMPLE # 1 Blank Soil Powder

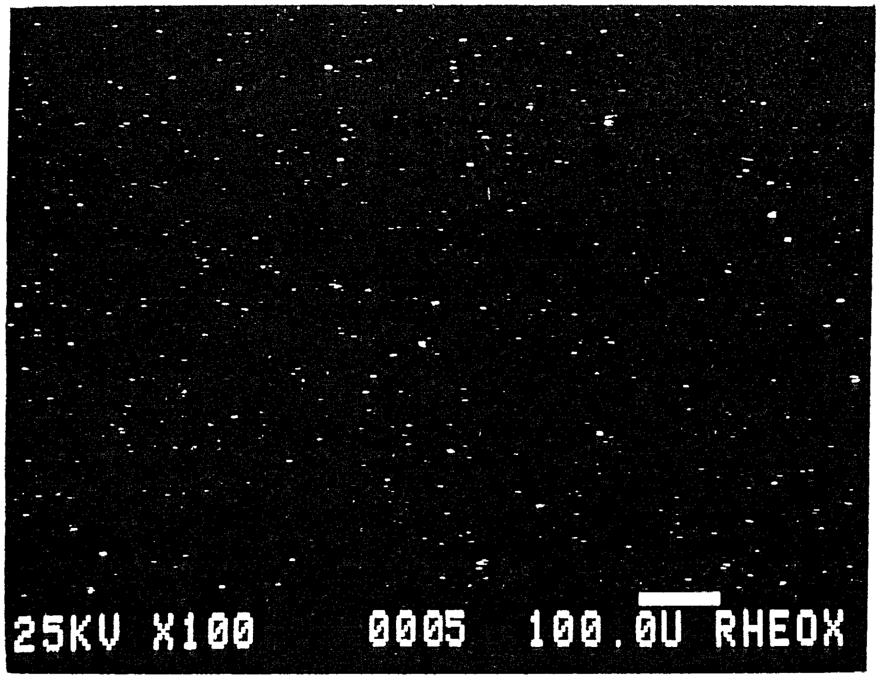

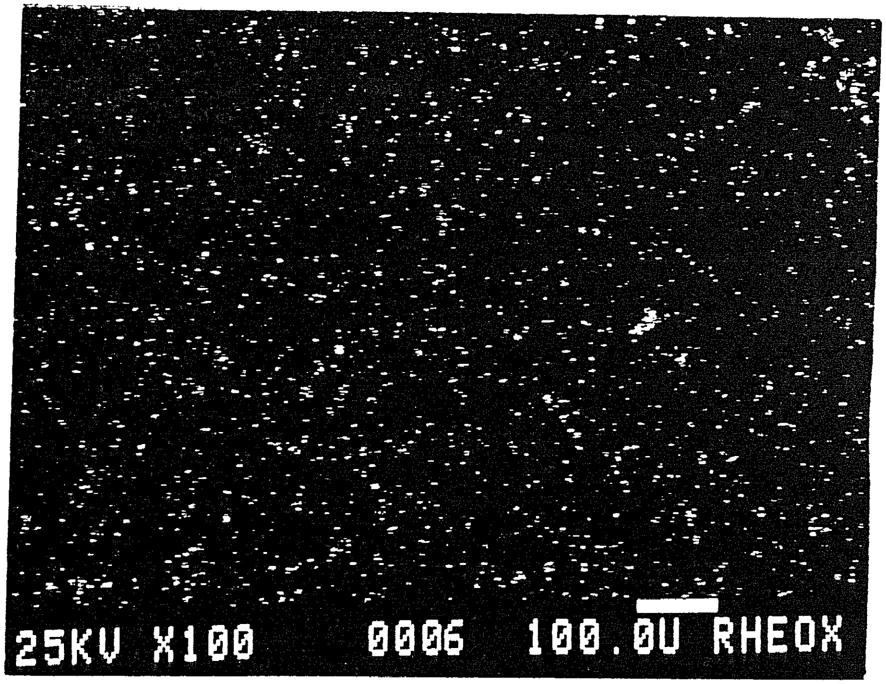

Figure 5 Ti X-Ray Image of Figure 1

Figure 6. Fe X-Ray Image of Figure 1

SEM IMAGES OF SAMPLE # 1 Blank Soil Powder

Figure 7

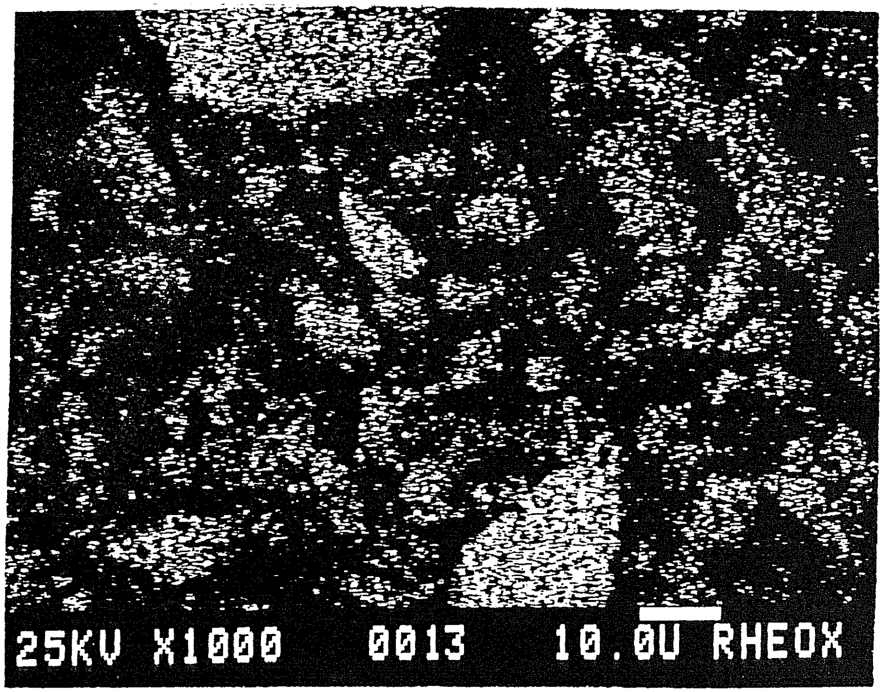

Figure 8 AL X-ray Image of Figure 7

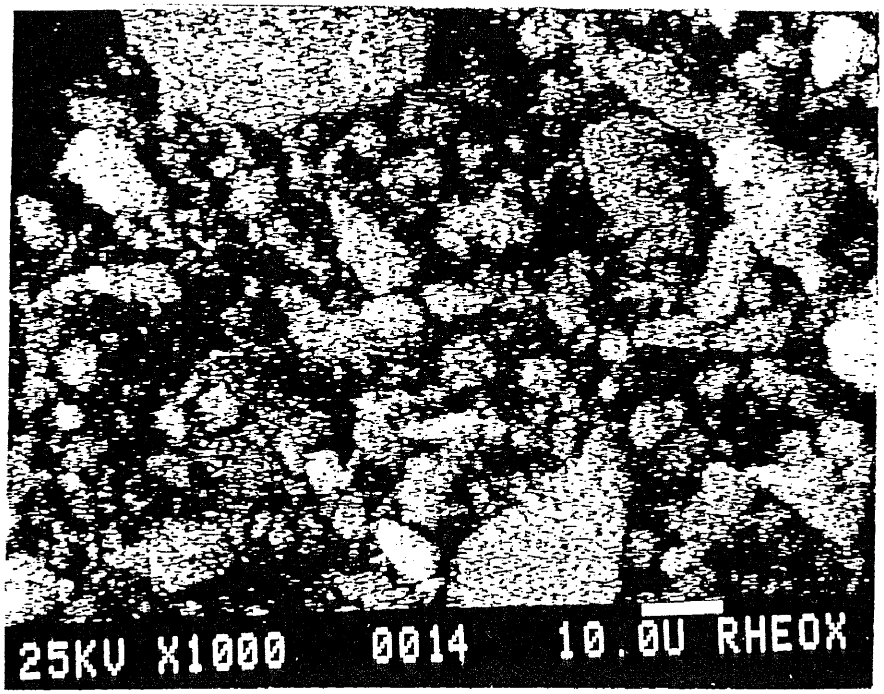

Si X-ray Image of Figure 7

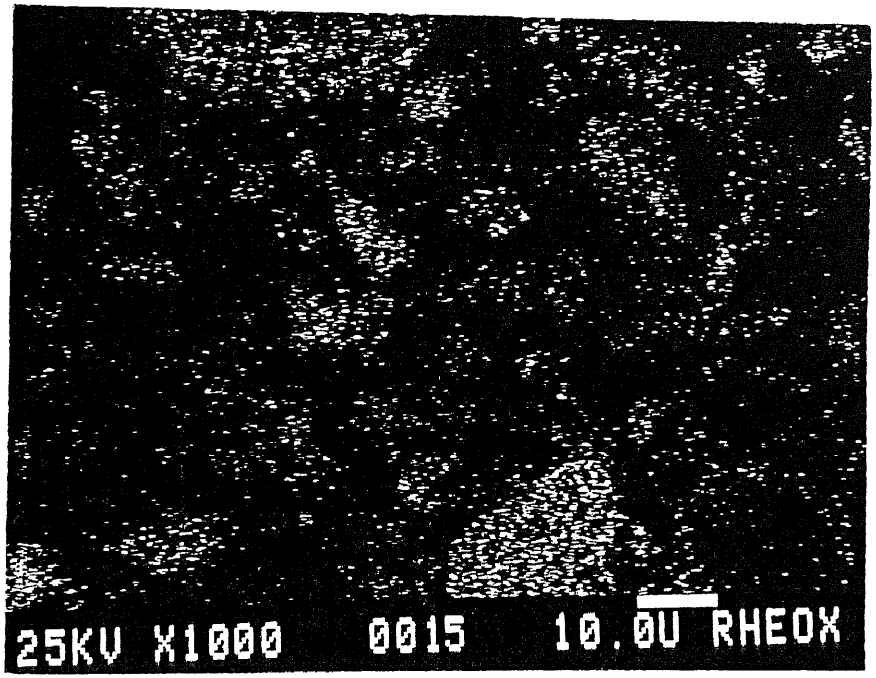

Figure 10 K X-ray Image of Figure 7

SEM IMAGES OF SAMPLE # 1 Blank soil Powder

Figure 11 Ti X-Ray Image of Figure 7

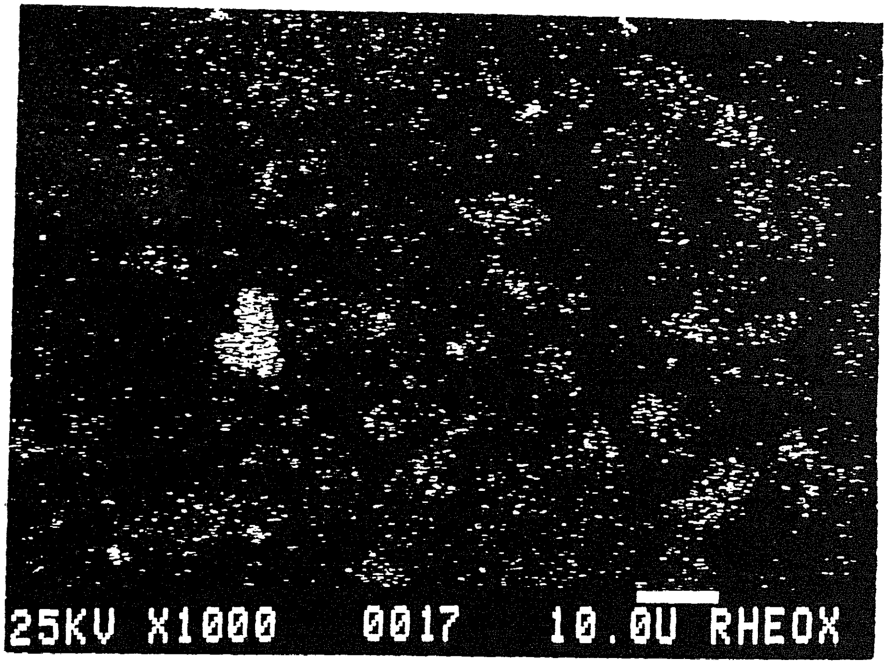

Figure 12 Fe X-Ray Image of Figure 7

F

SEM IMAGES OF SAMPLE # 1 Blank Soil Powder

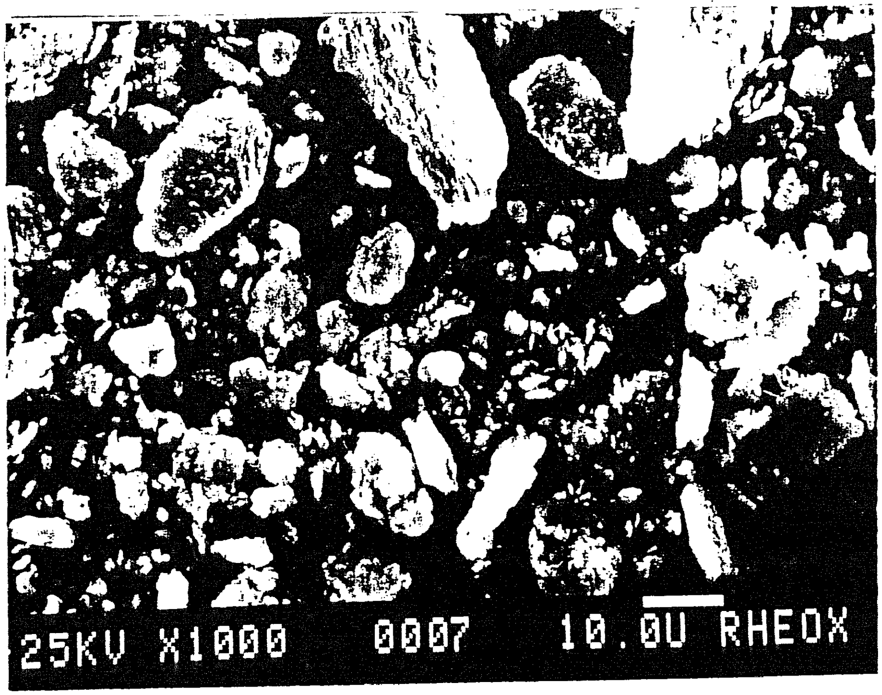

Figure 13

F2

SEM IMAGES OF SAMPLE # 1 Blank Soil Powder

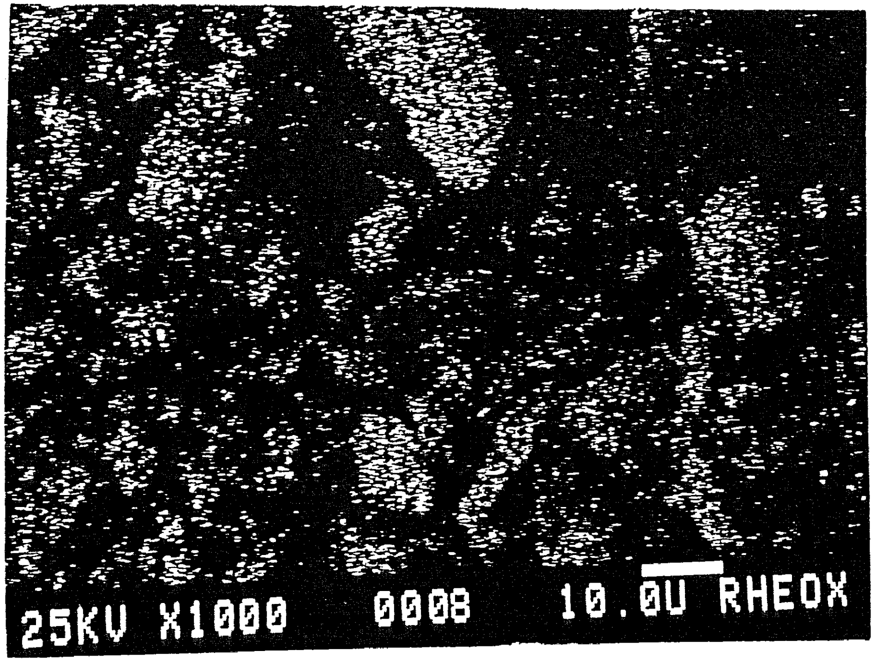

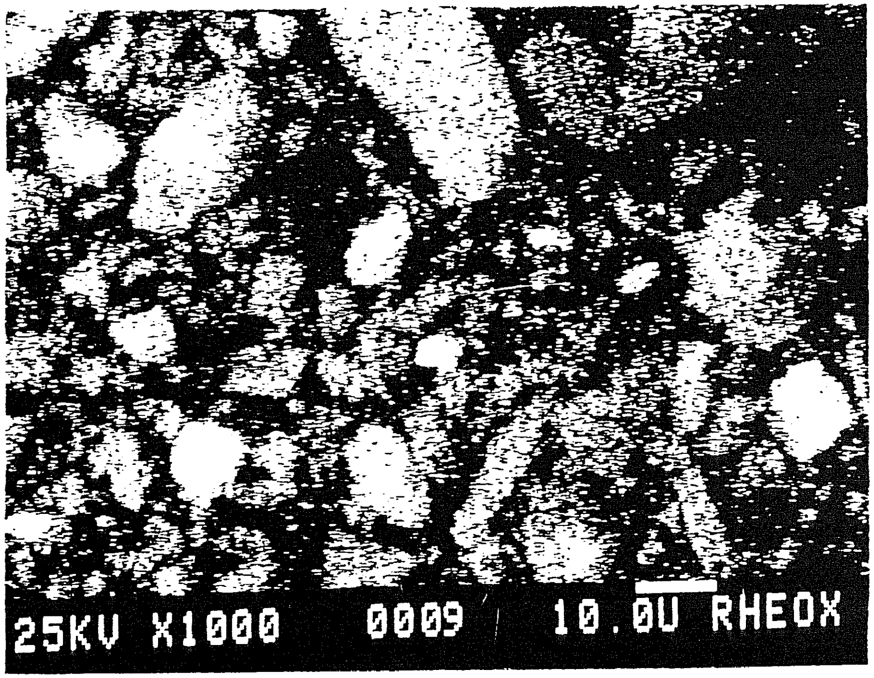

Figure 14 AL X-Ray Image of Figure 13

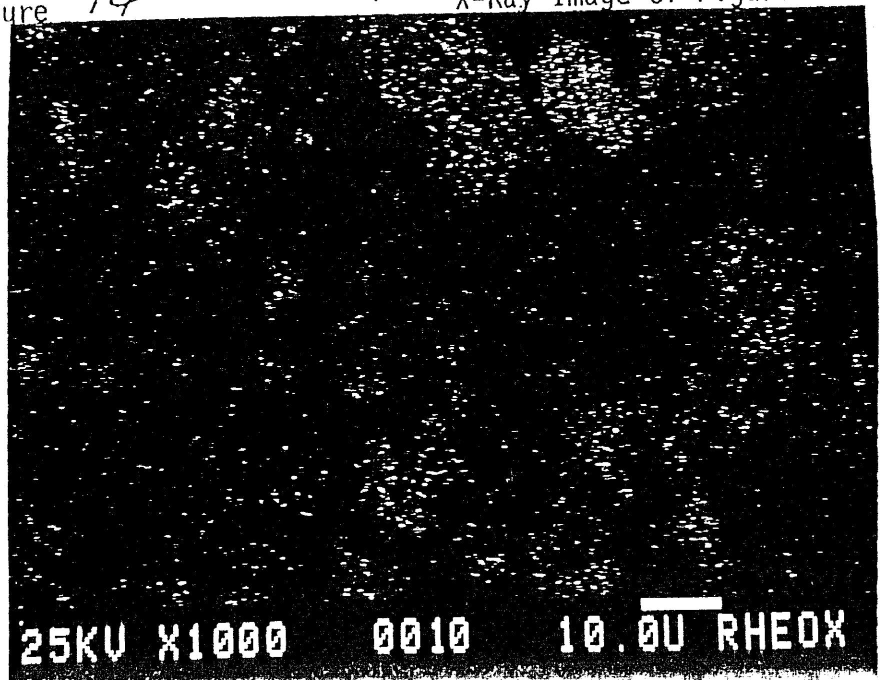

Figure 15 Si X-Ray Image of Figure 13

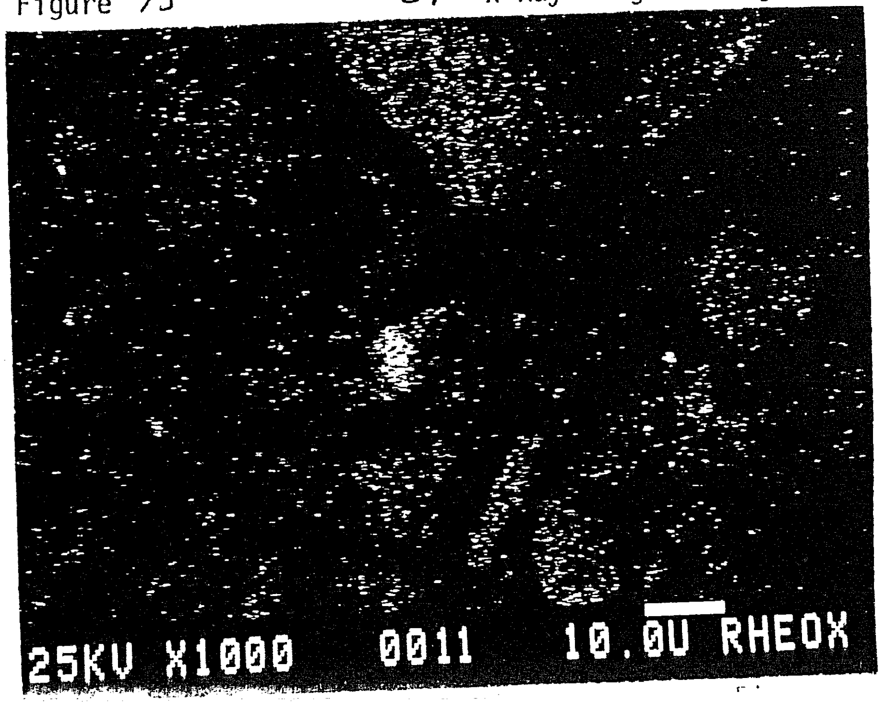

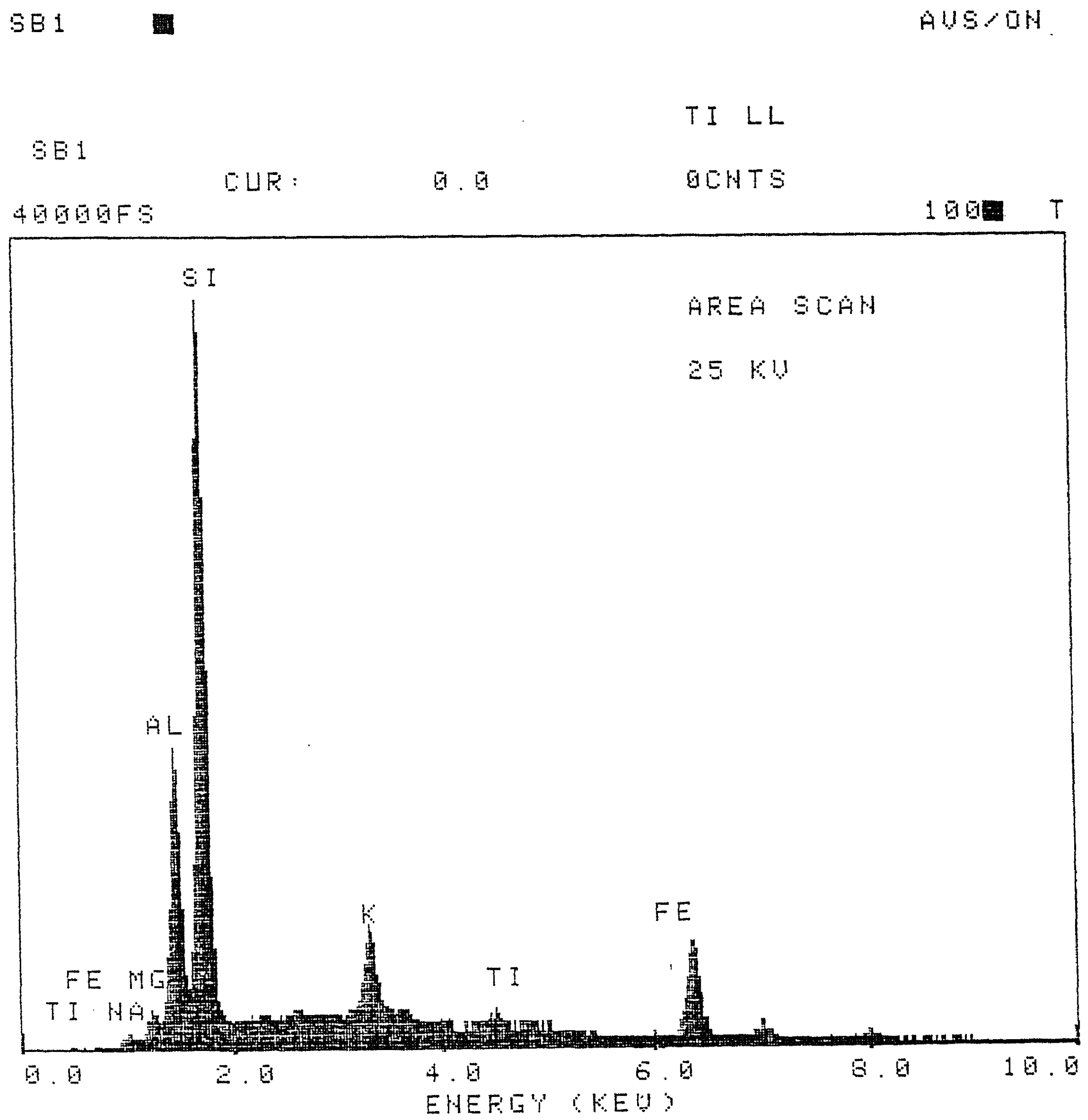

07-Oct-89 21:00

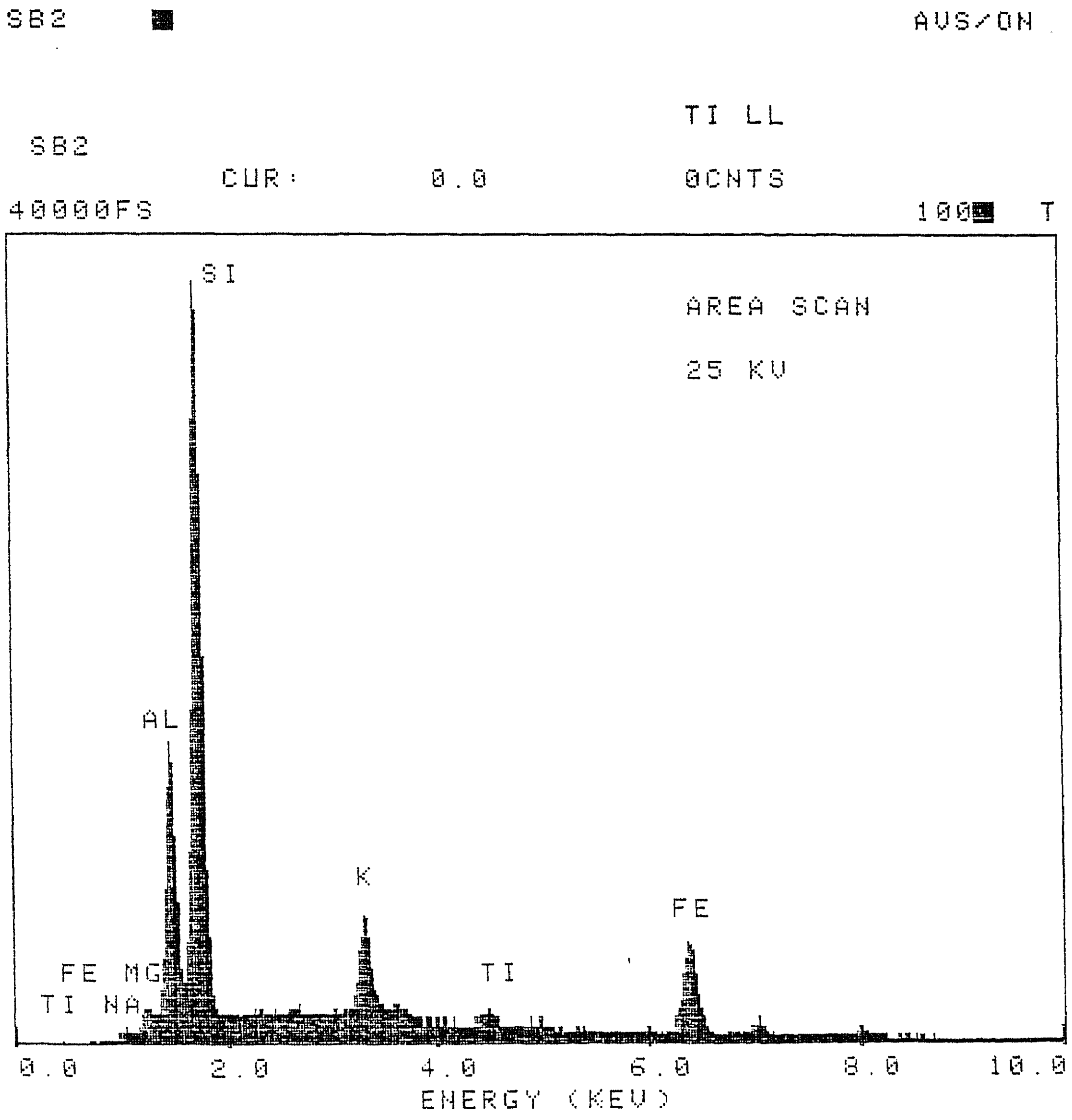

07-Oct-89 21:00

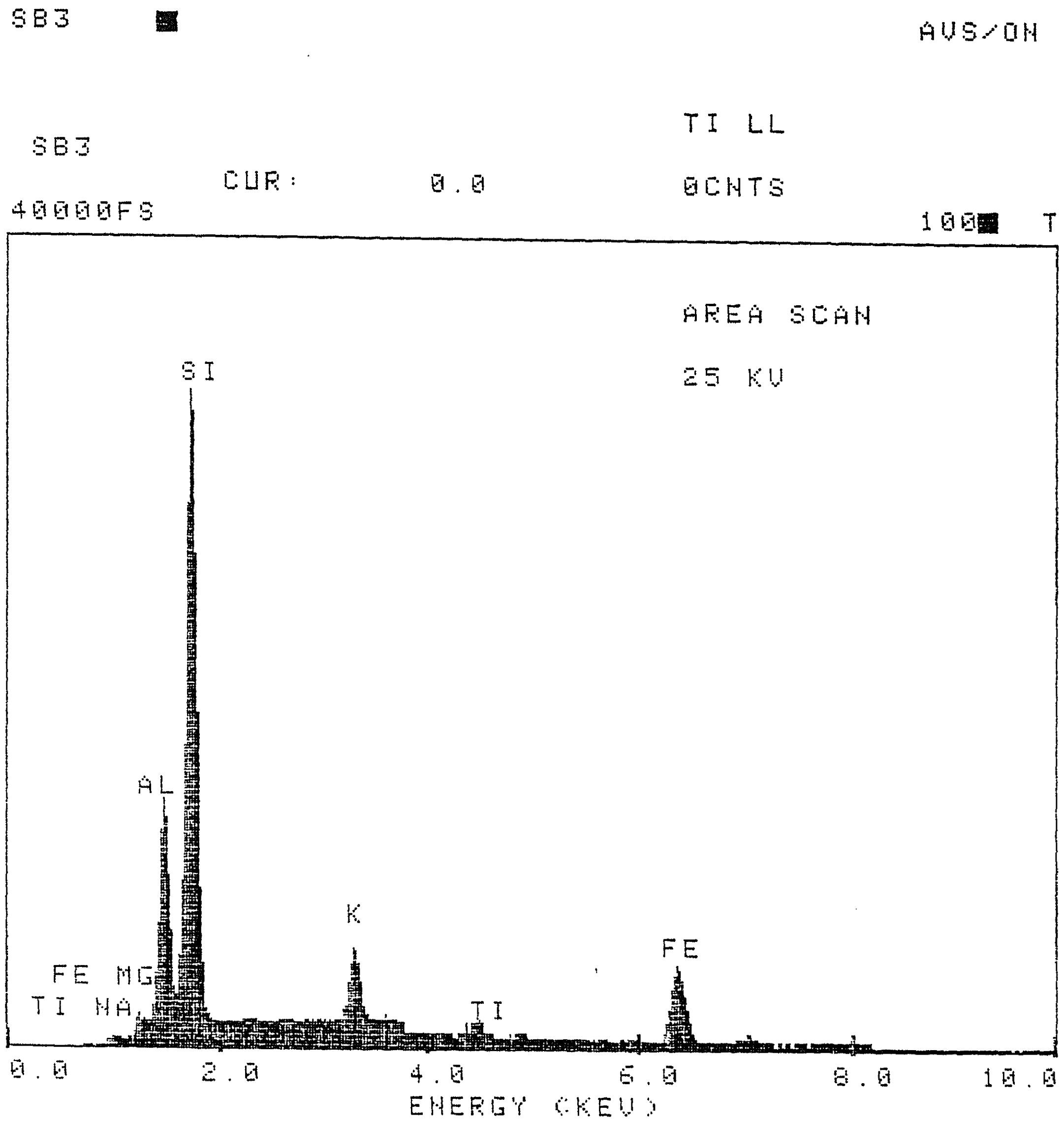

07-Oct-89 21:00

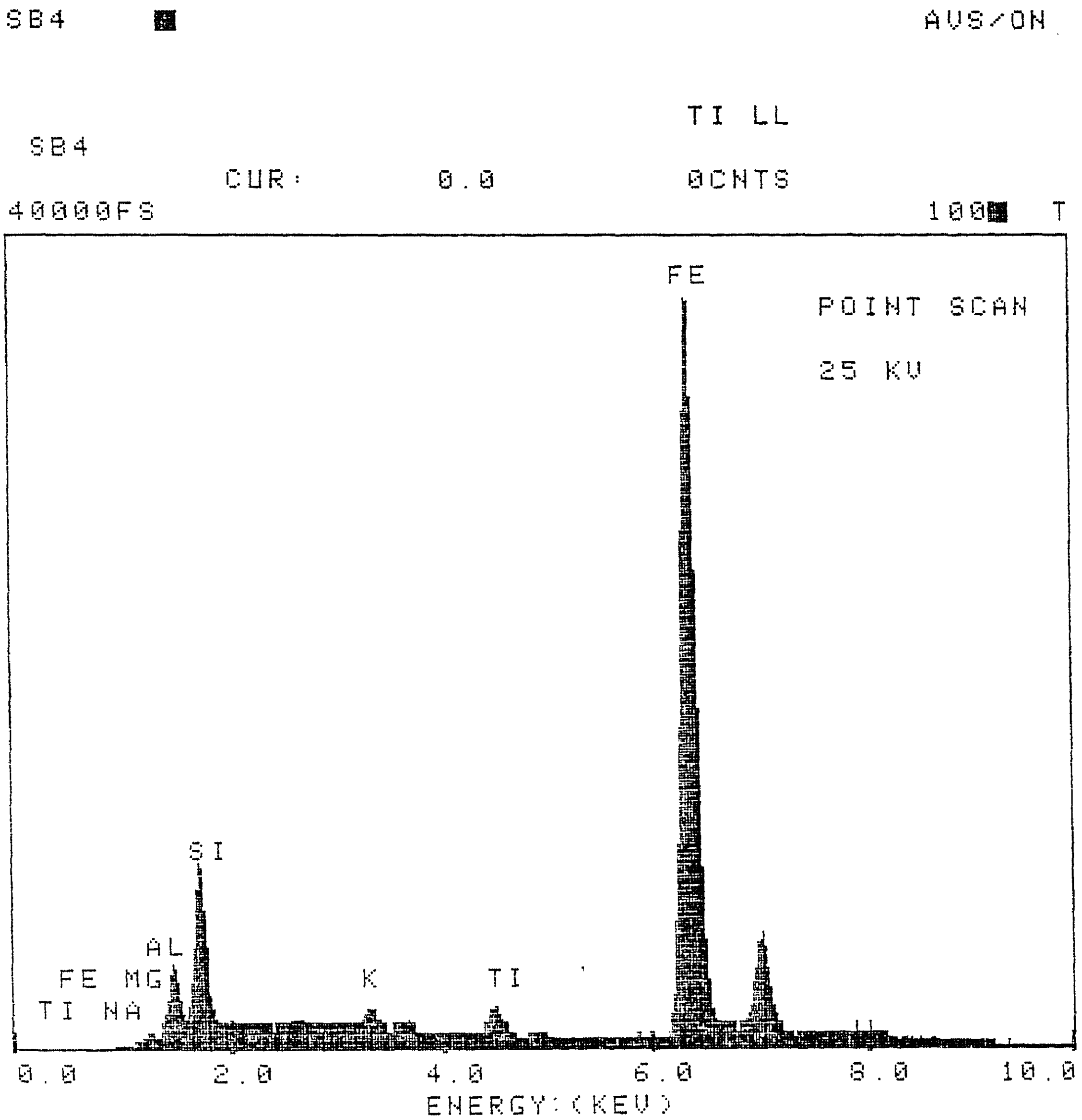

07-Oct-89 21:00

SB5 ■ AVS/ON

TI LL

SB5

CUR: 0.0 0CNTS

40000FS 100■ T

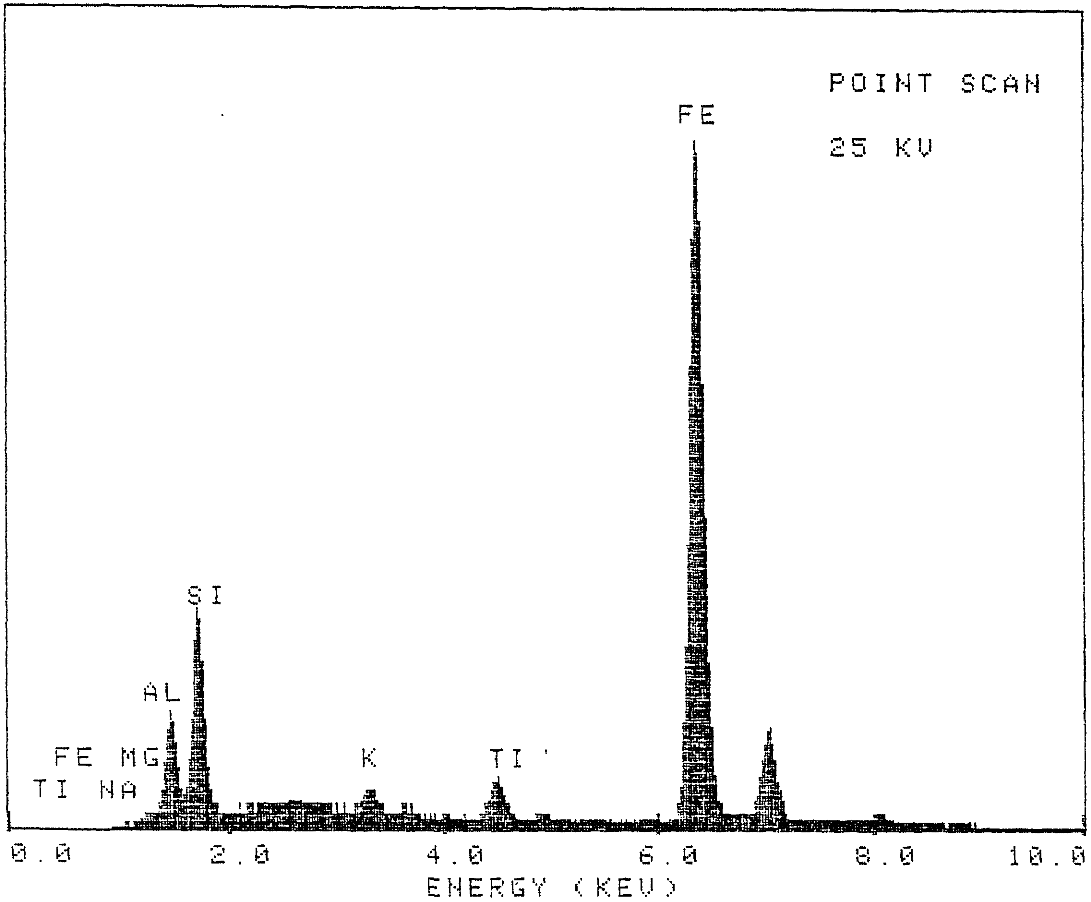

07-Oct-89 21:00

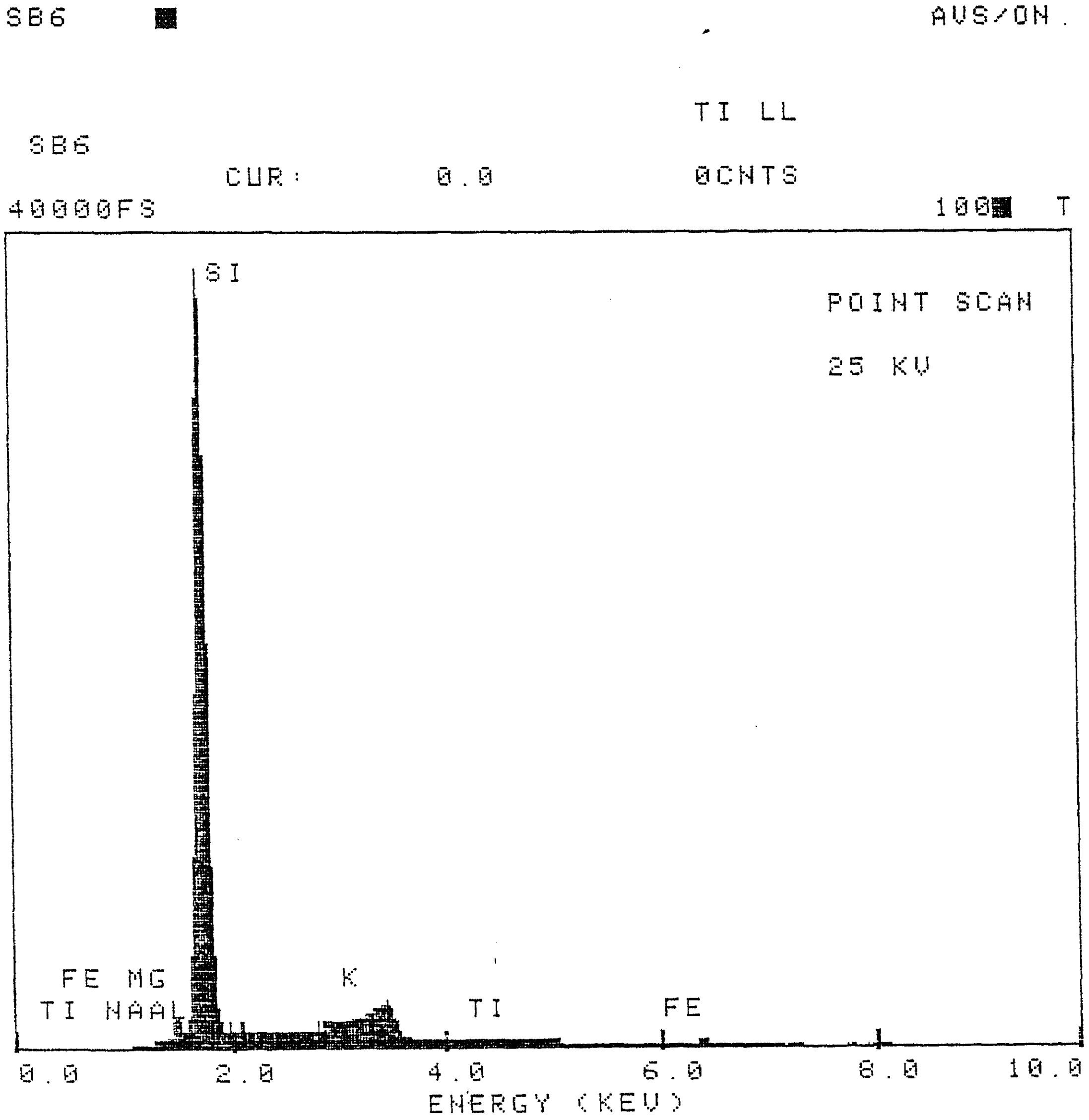

SB6 ■ AVS/ON.

TI LL

SB6

CUR: 0.0 0CNTS

40000FS 100■ T

POINT SCAN

25 KV

07-Oct-89 21:00

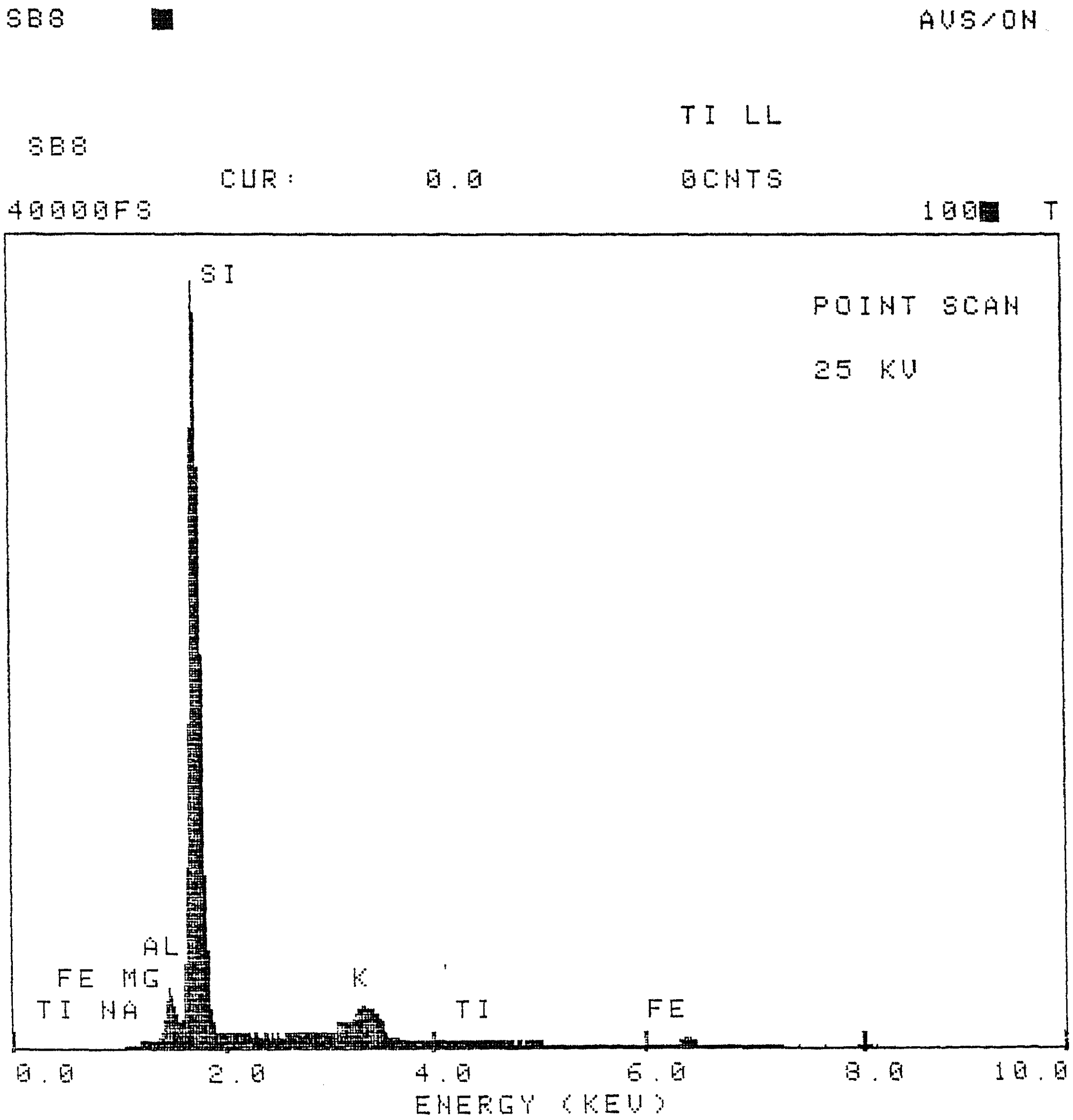

07-Oct-89 21:00

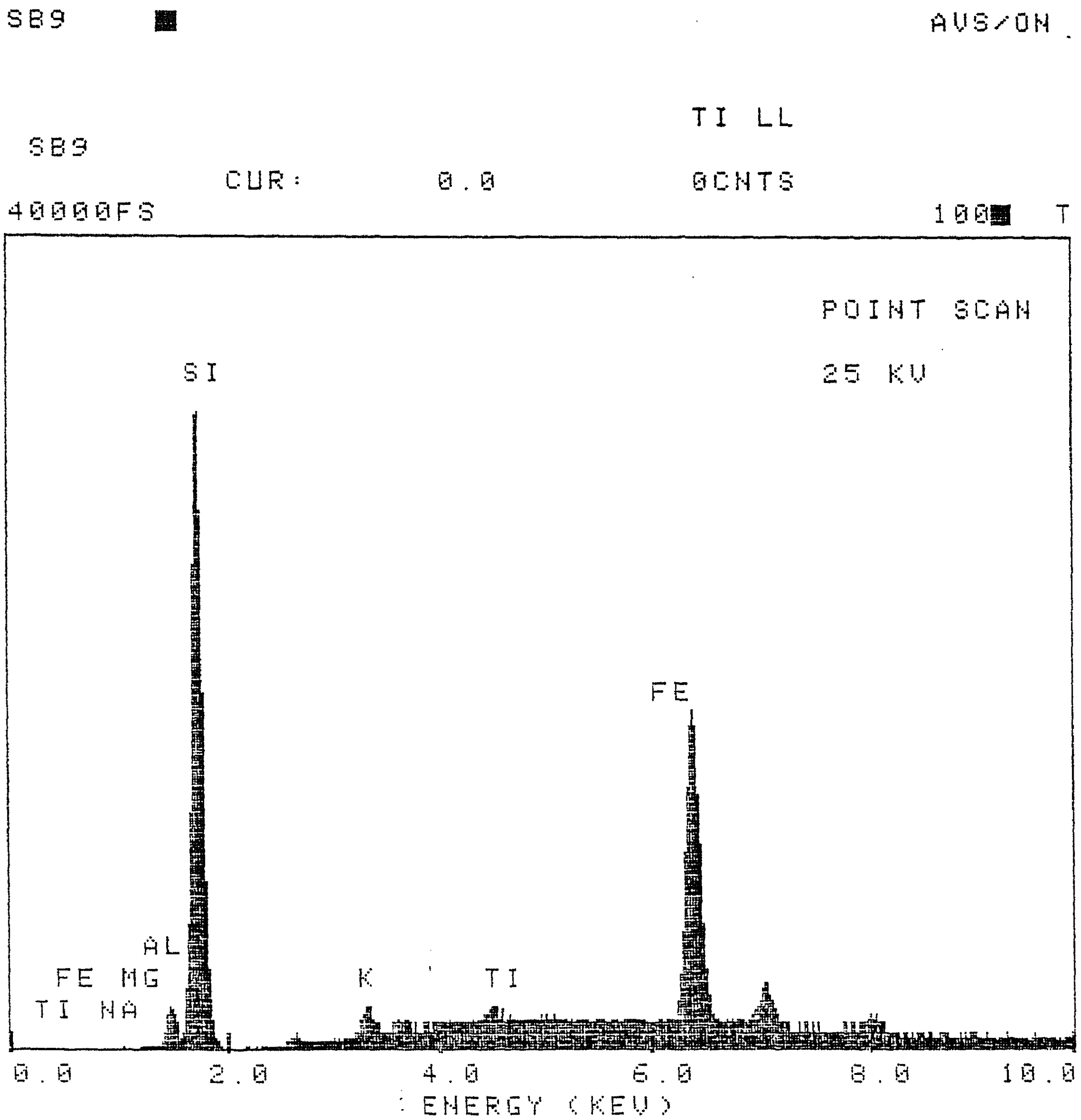

07-Oct-89 21:00

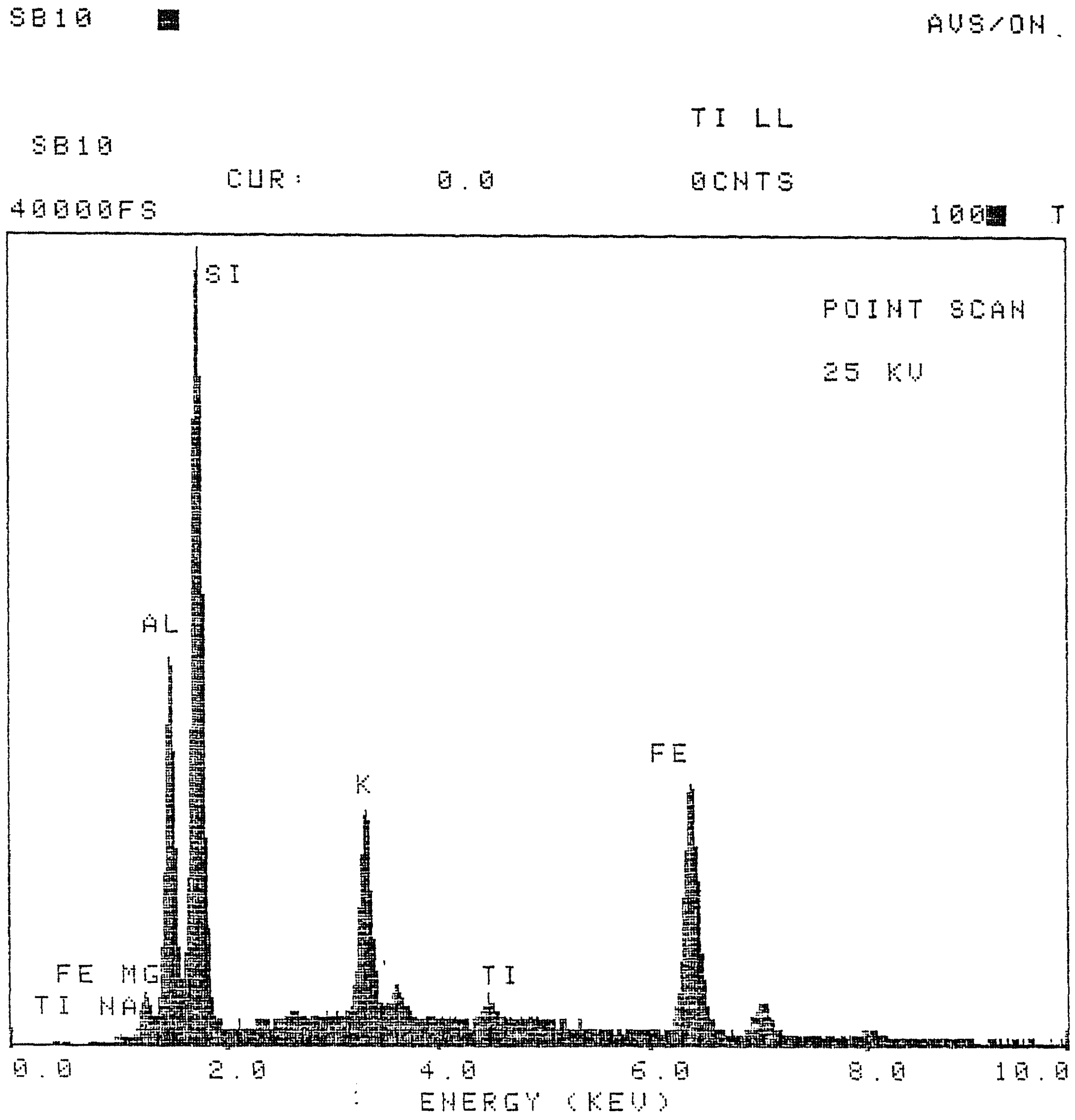

07-Oct-89 21:00

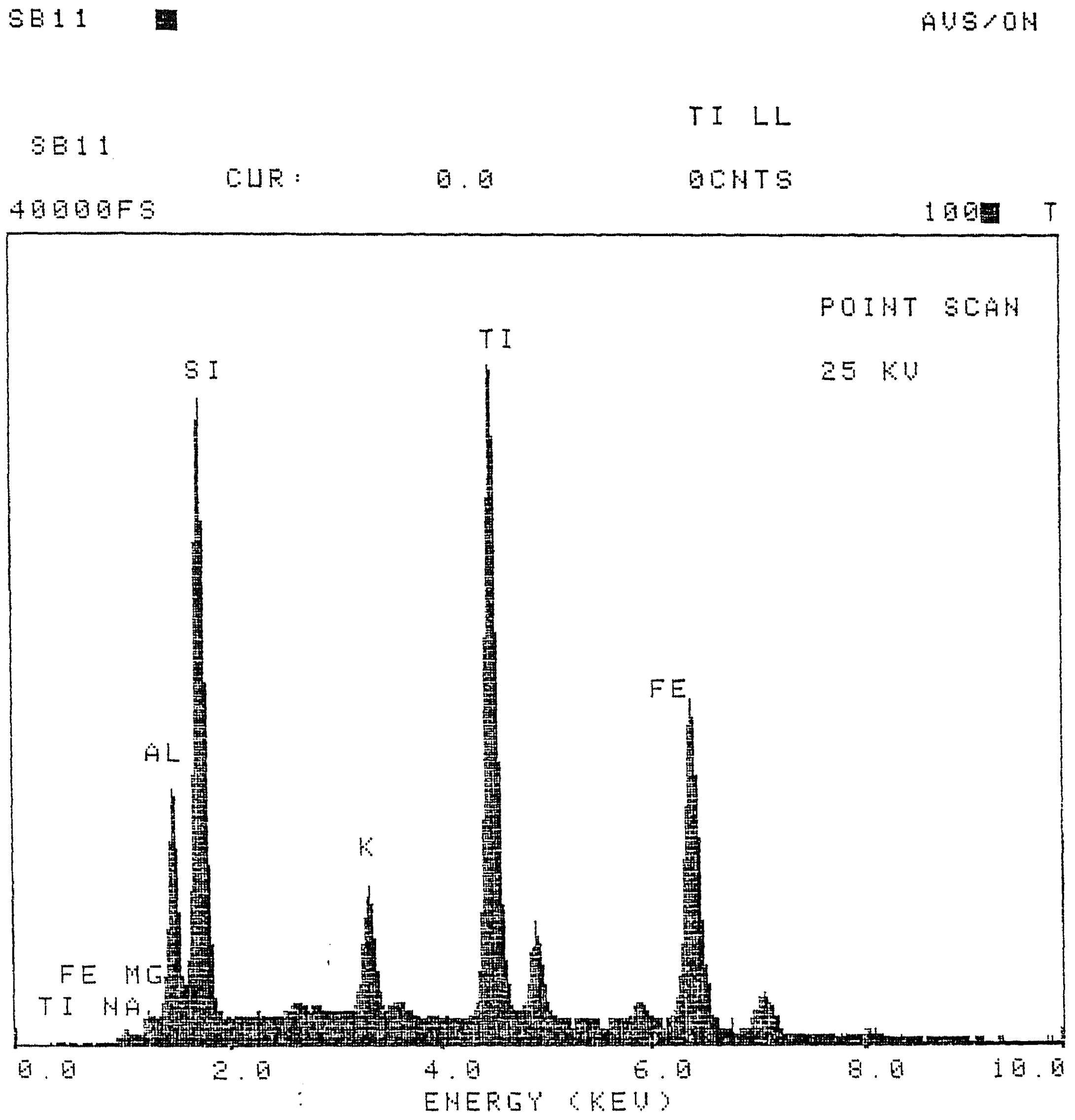

07-Oct-89 21:00

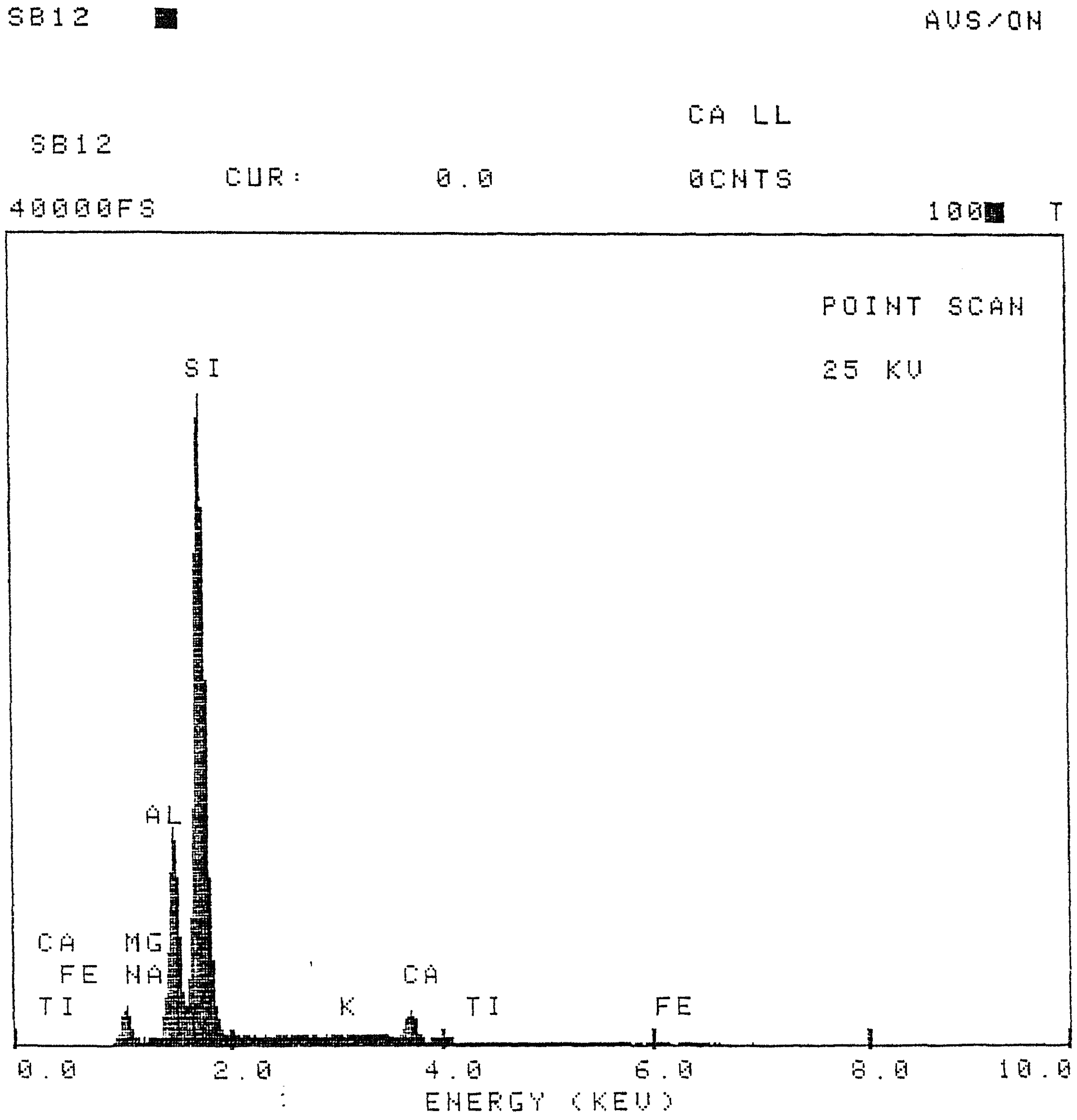

07-Oct-89 21:00

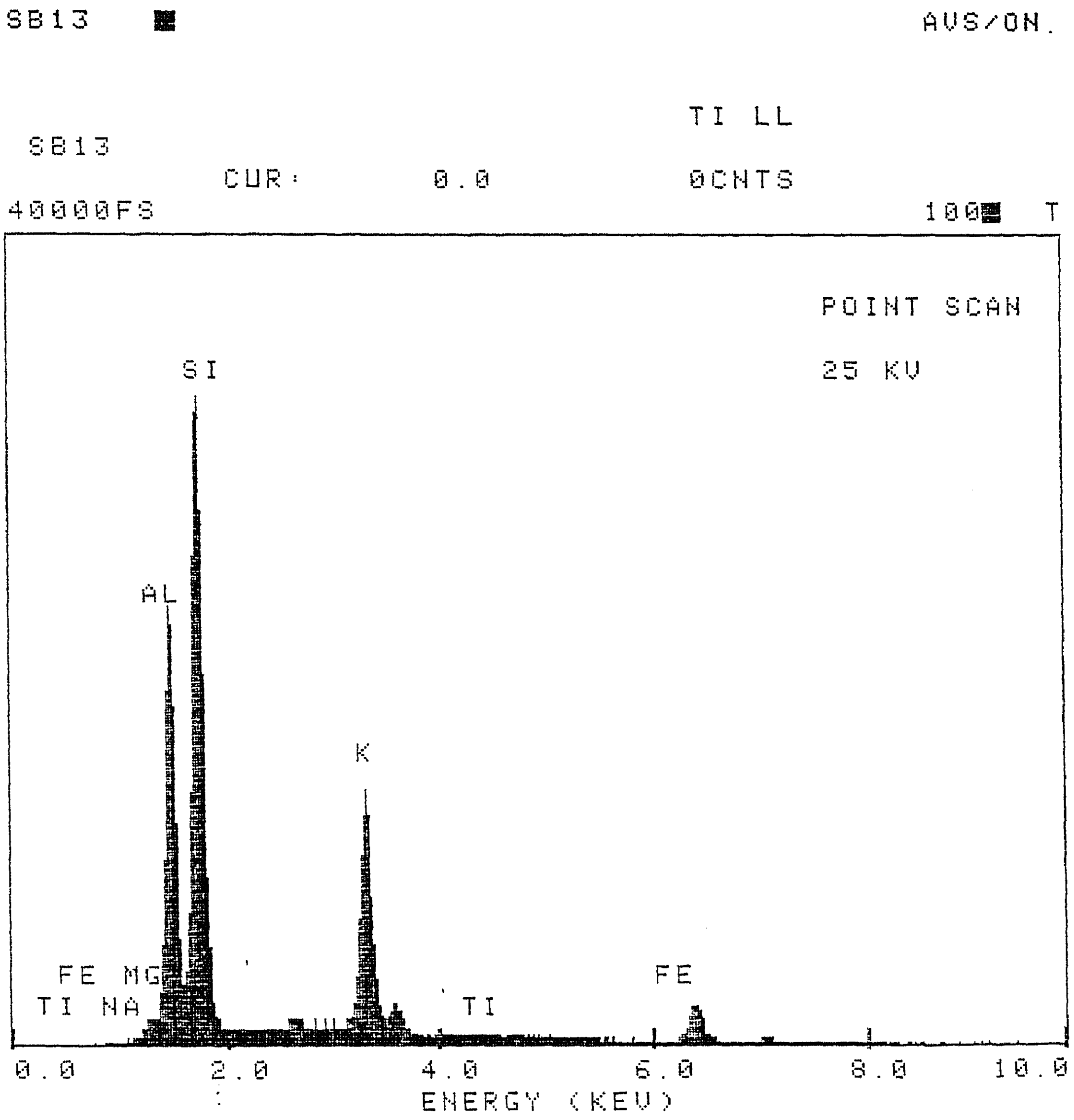

07-Oct-89 21:00

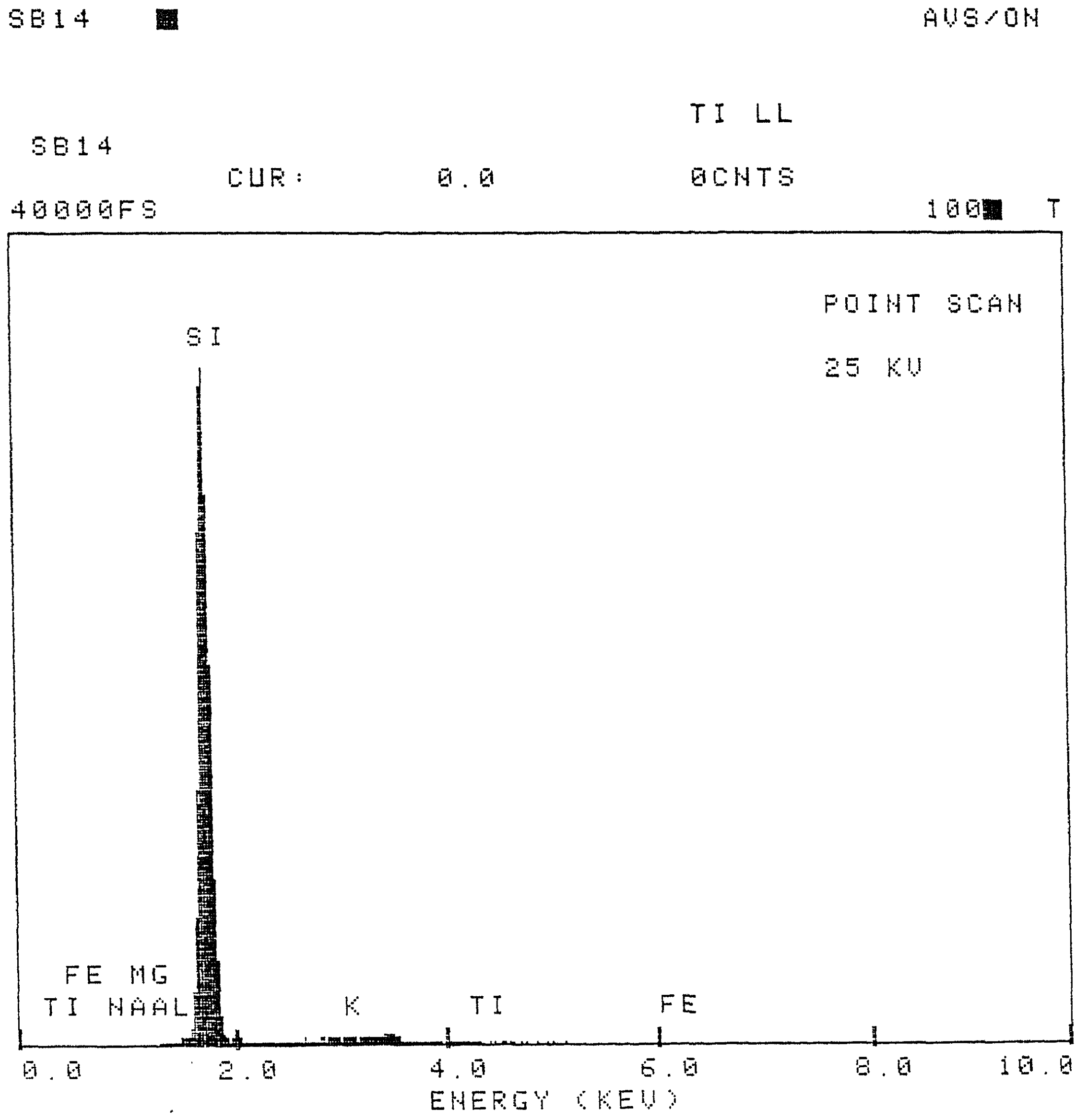

07-Oct-89 21:00

SB15 ■ AVS/ON

TI LL

SB15

CUR: 0.0 0CNTS

40000FS 100■ T

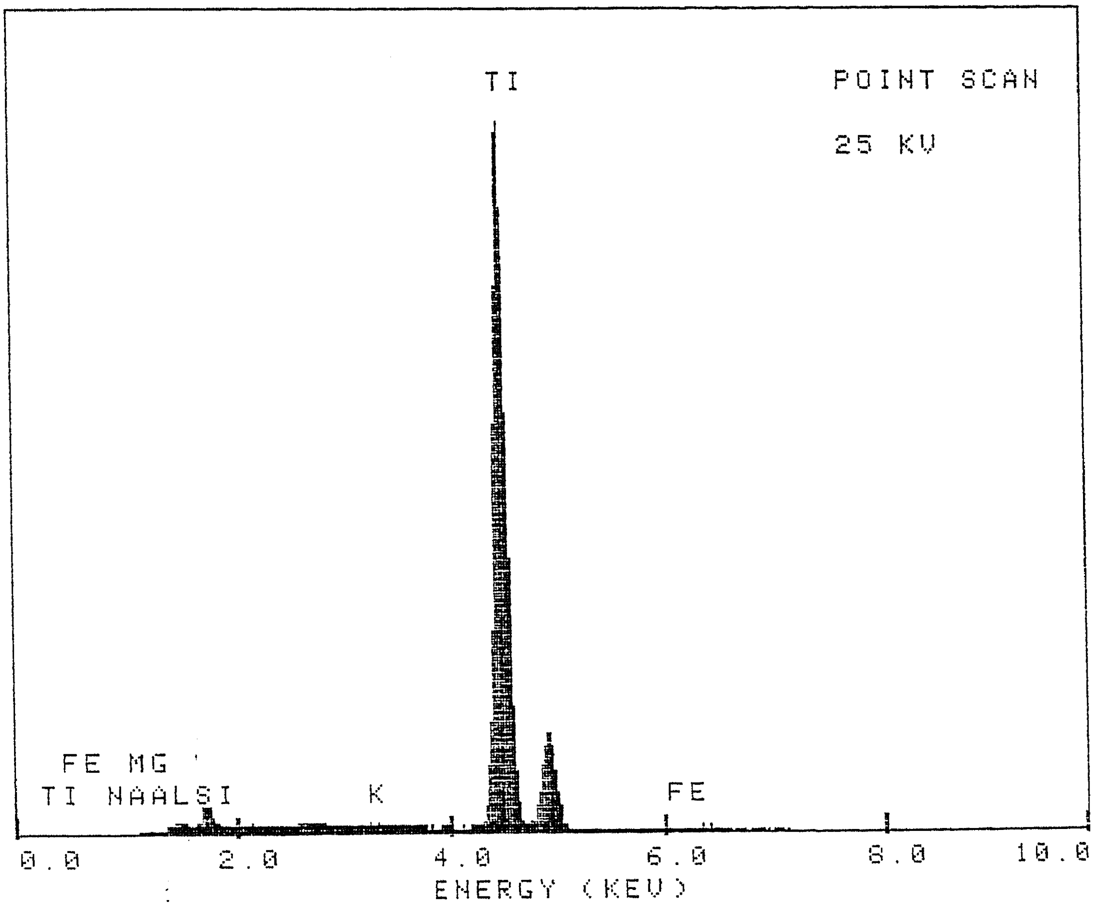

07-Oct-89 21:00

SB16 ■ AVS/ON

CA LL

SB16

CUR: 0.0 0CNTS

40000FS 100■ T

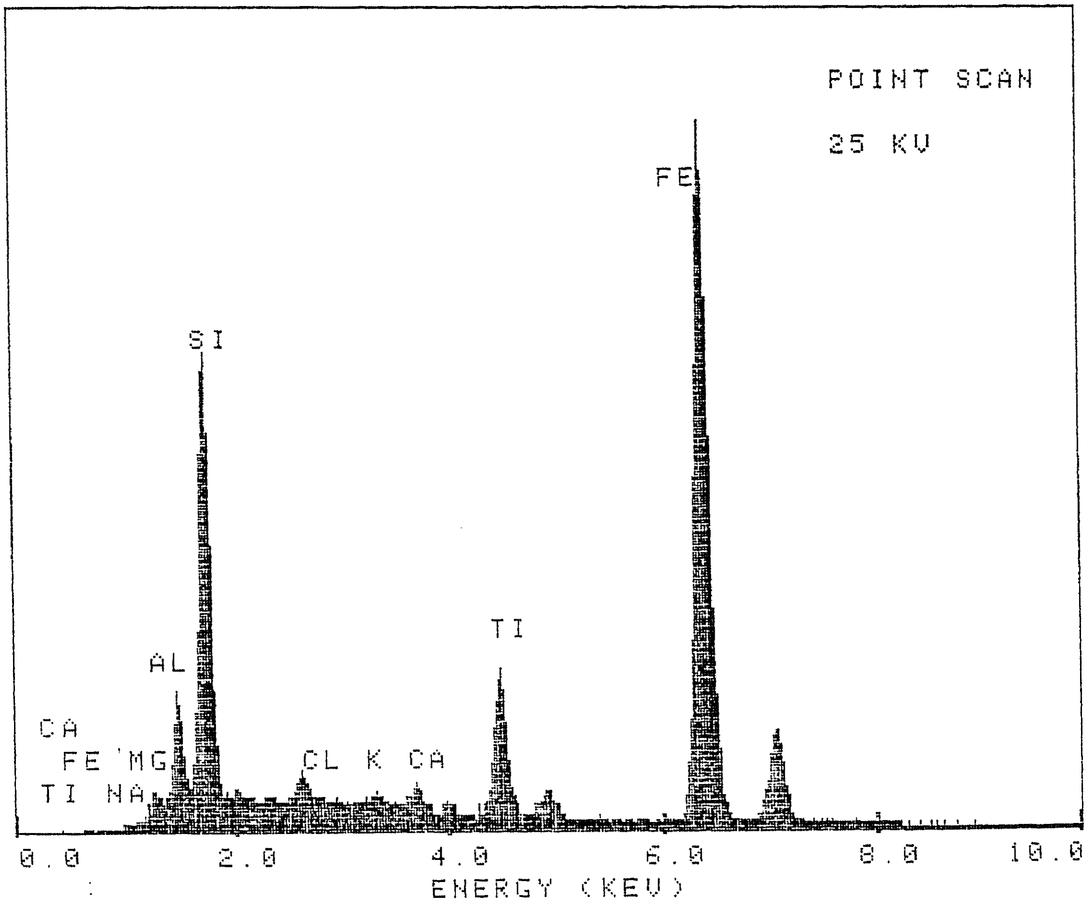

07-Oct-89 21:00

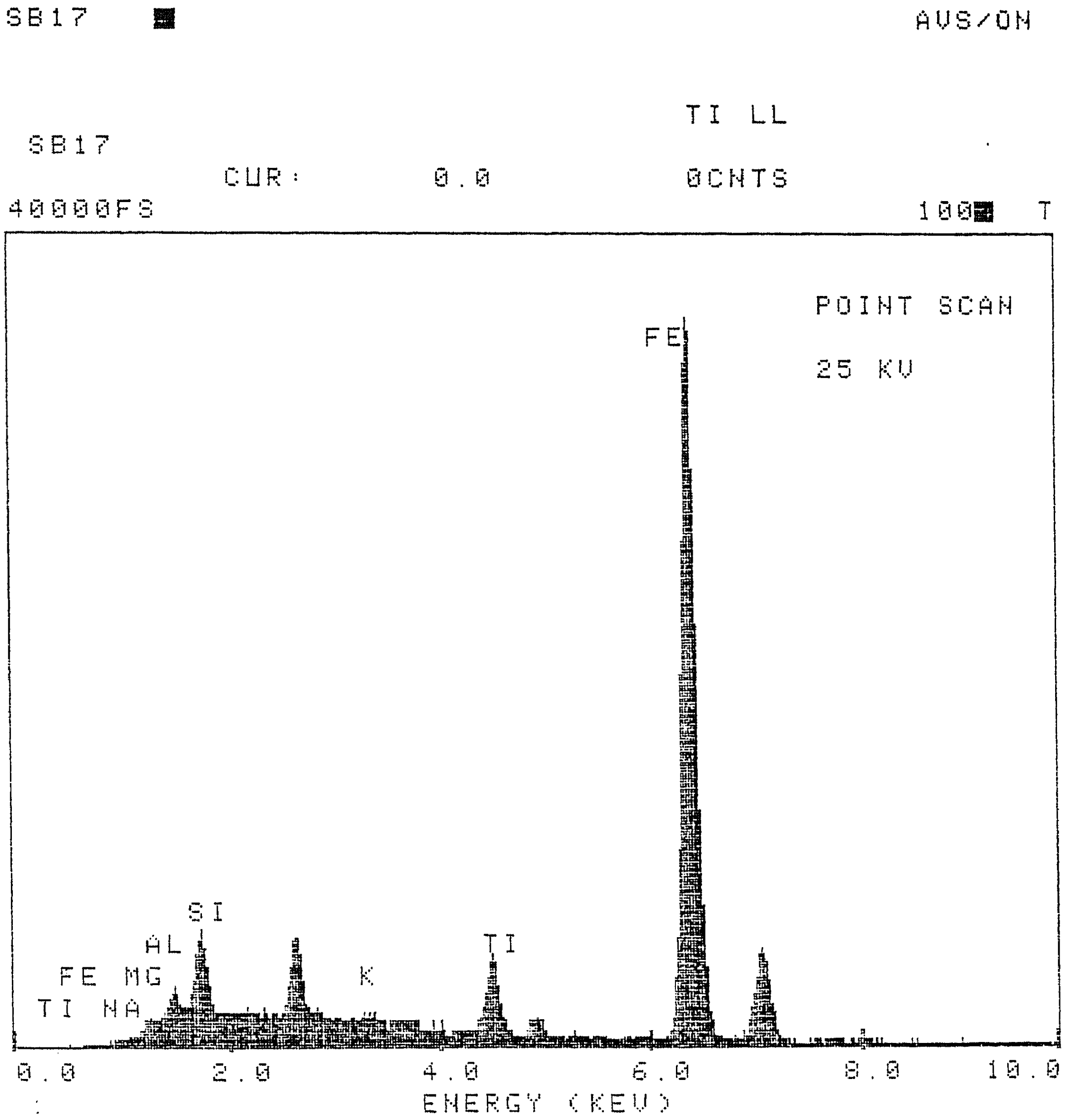

07-Oct-89 21:00

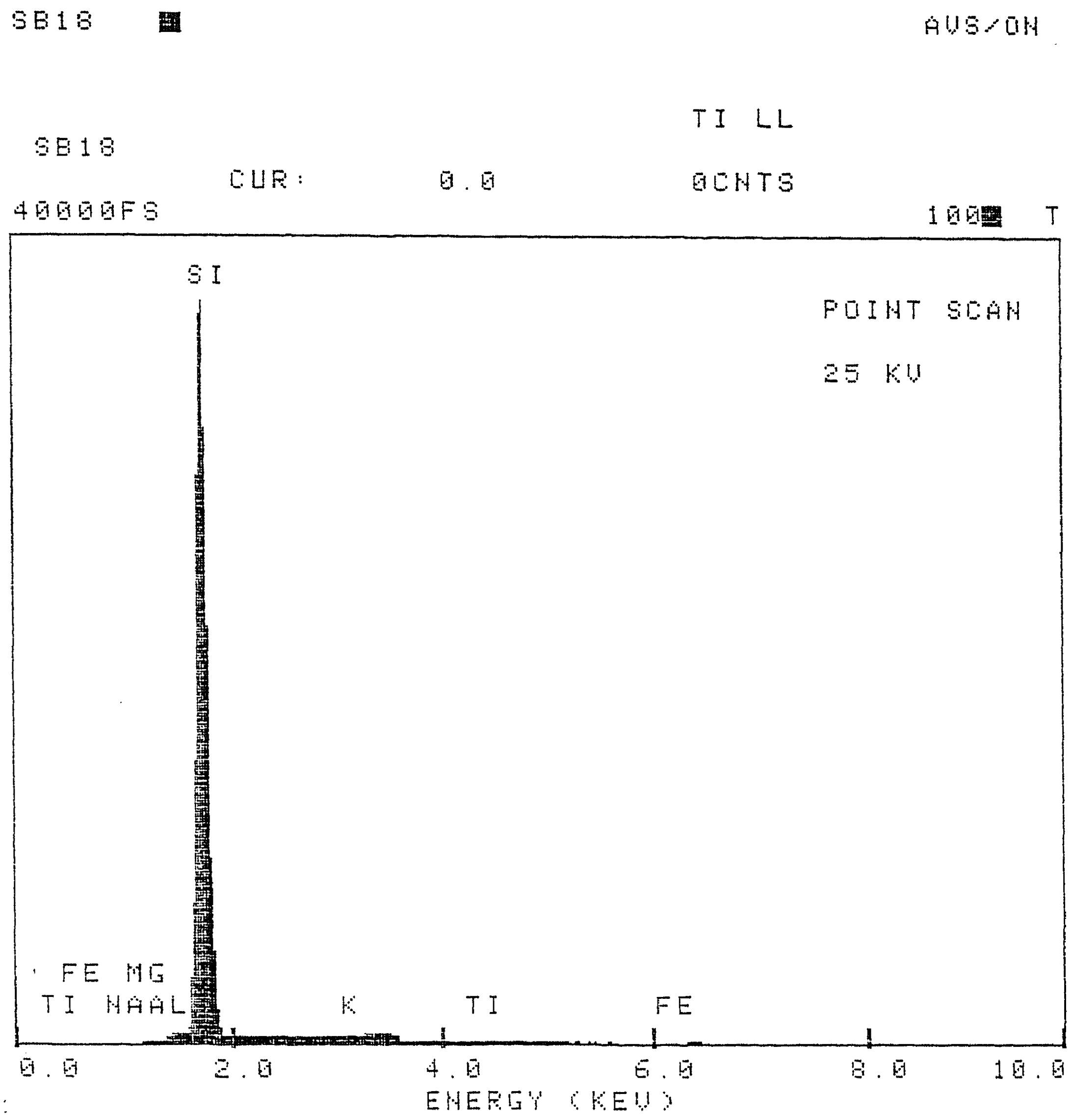

07-Oct-89 21:00

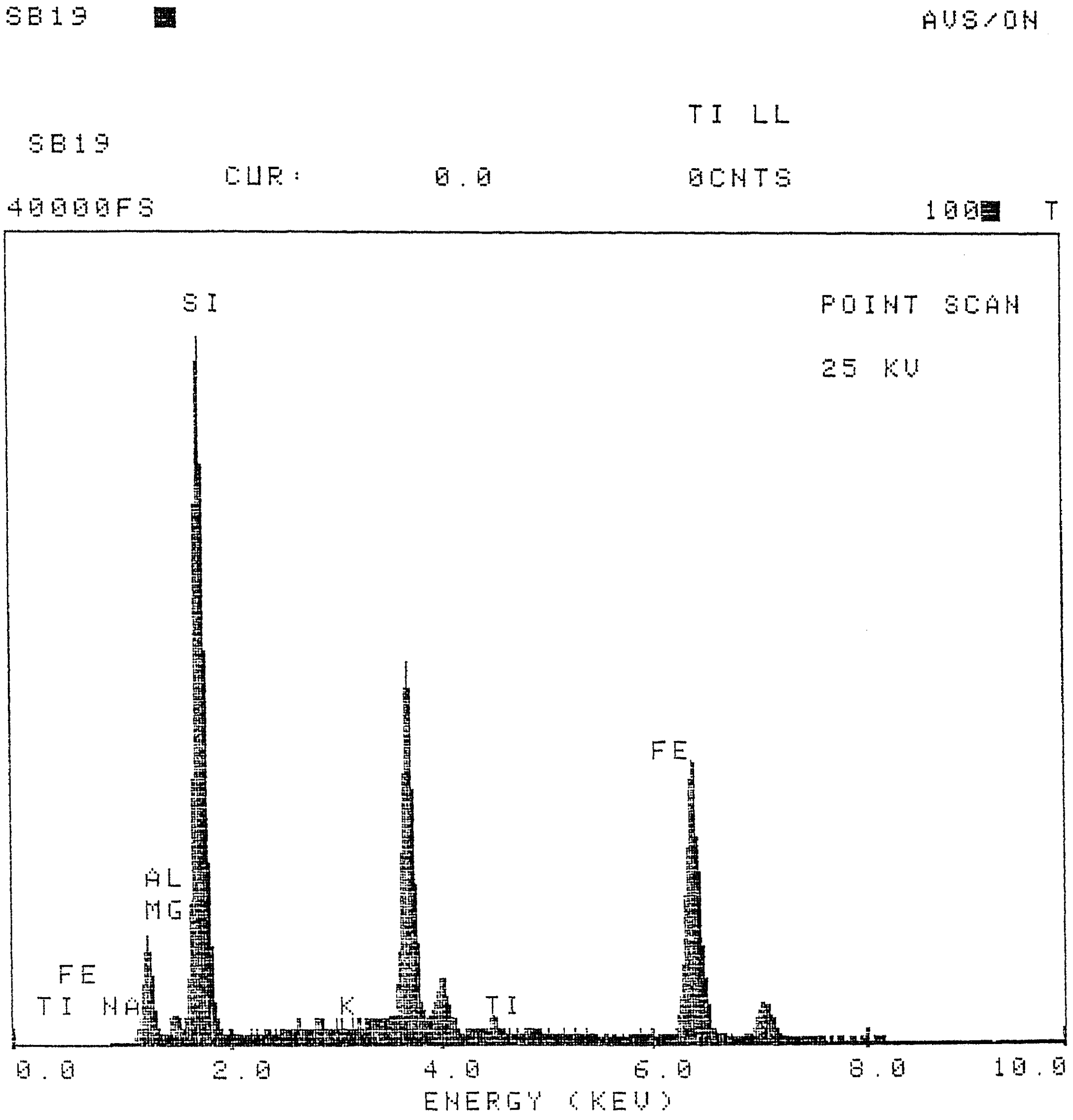

07-Oct-89 21:00

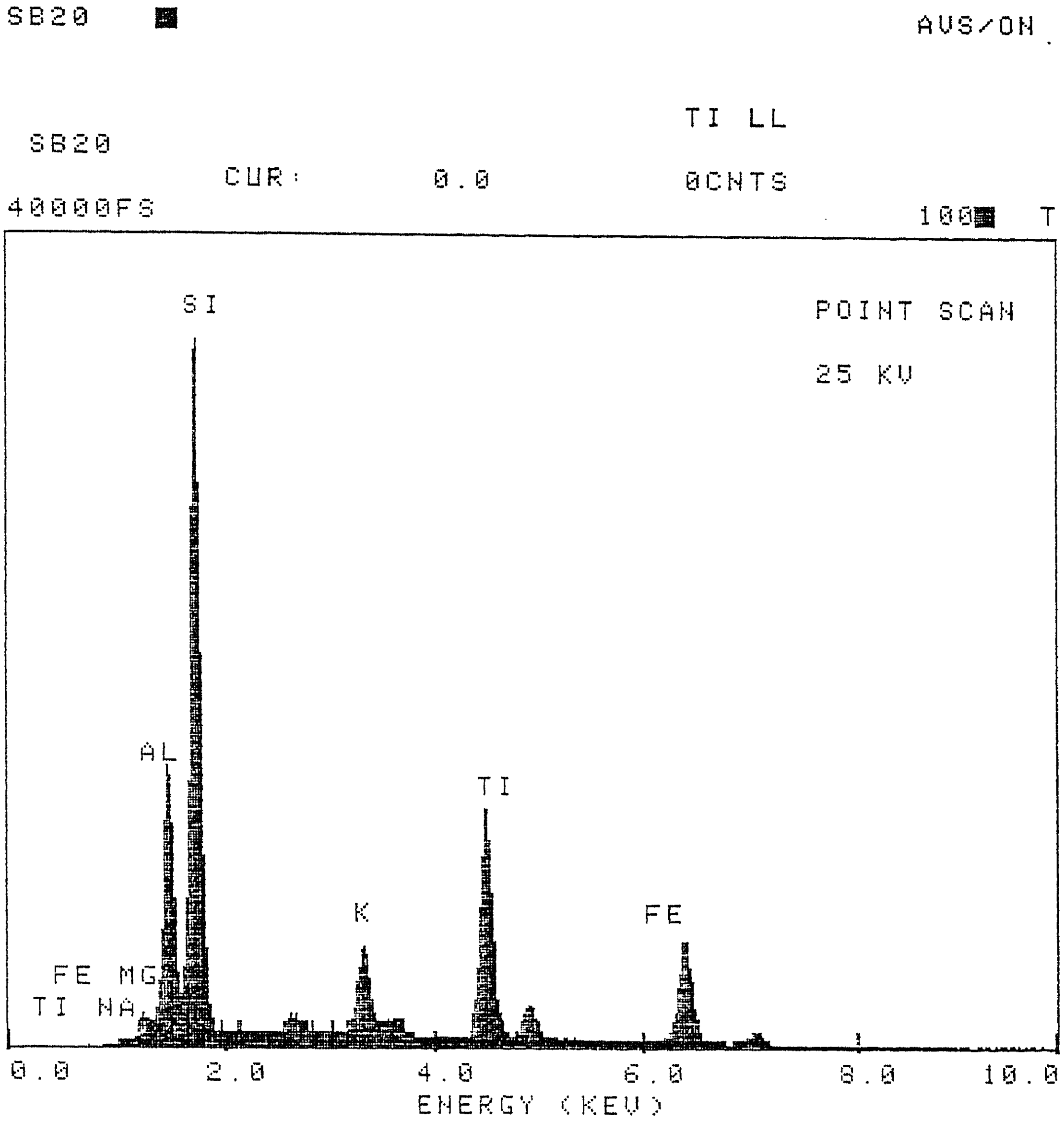

07-Oct-89 21:00

SEM IMAGES OF SAMPLE # Blank Cross Section of SOIL

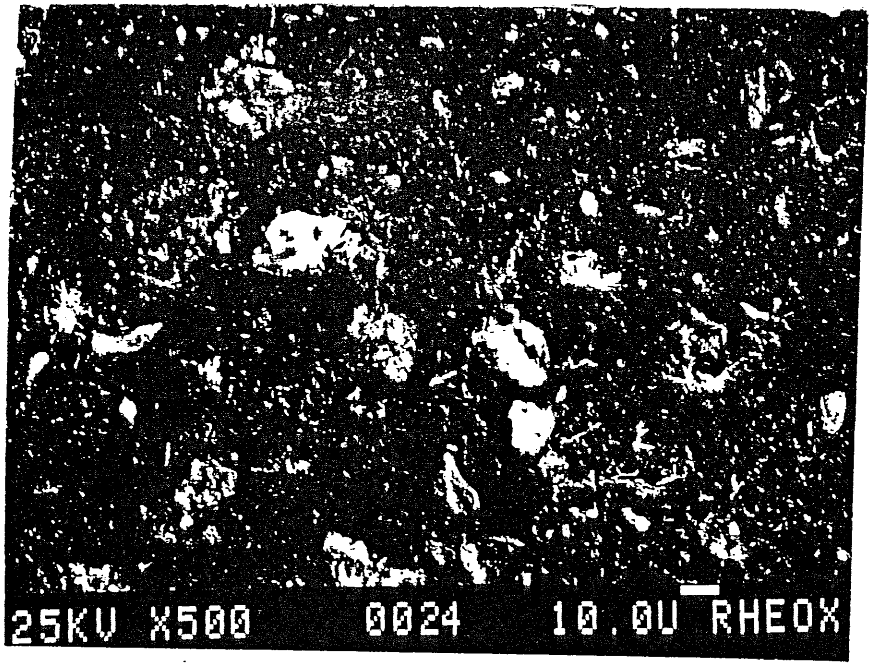

Figure 18

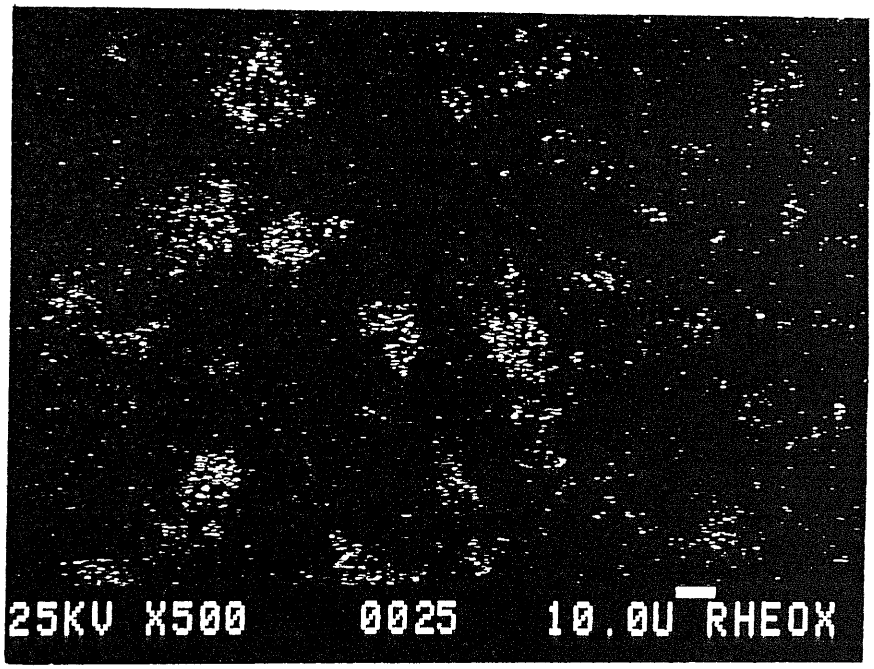

Figure 19 AL X-ray Image of Figure 18

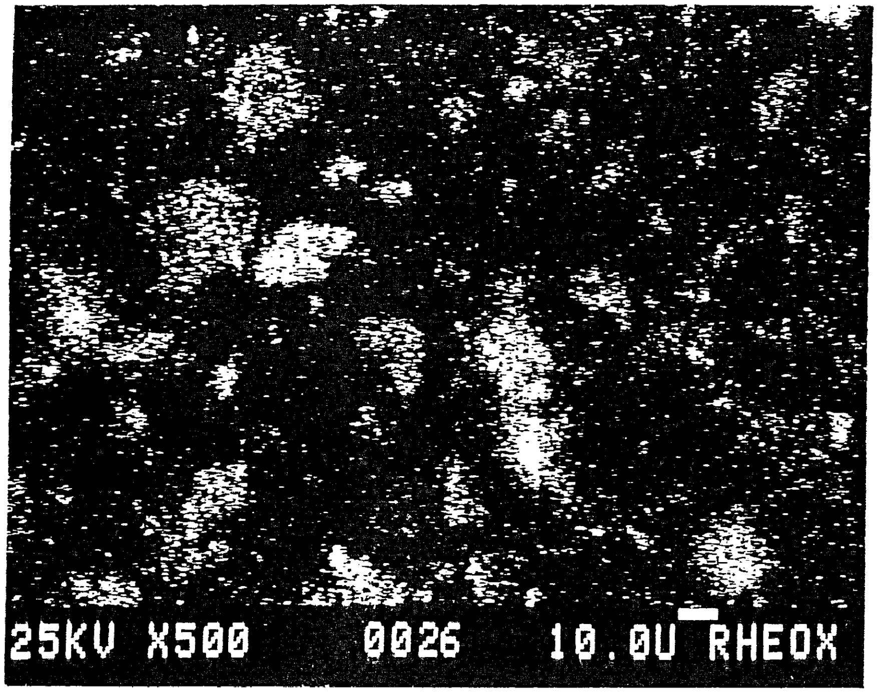

Figure 20 Si X-ray Image of Figure 18

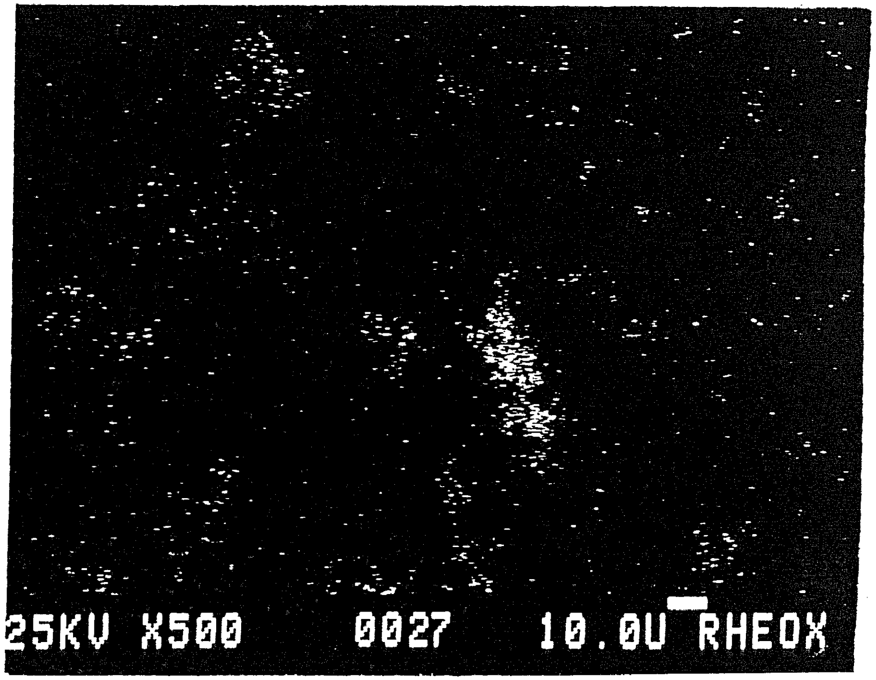

Figure 21 K X-ray Image of Figure 18

SEM IMAGES OF SAMPLE # Blank Cross Section of Soil

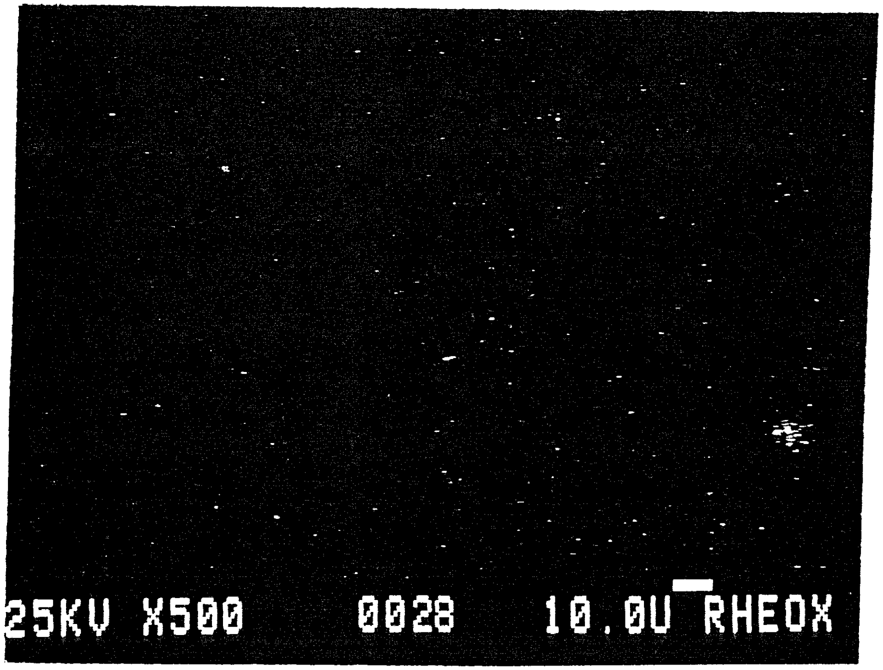

Figure 22 Ti X-Ray Image of Figure 18

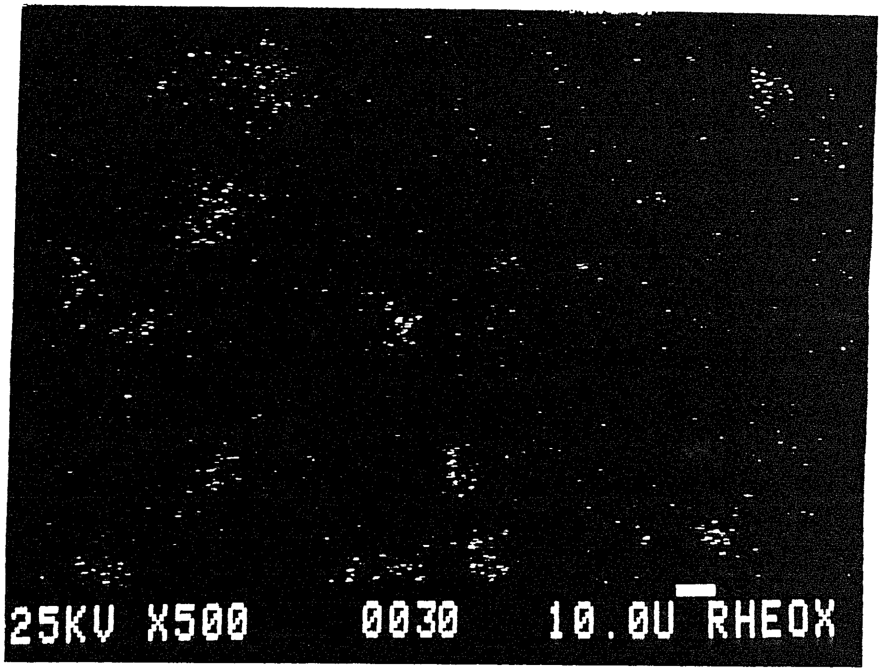

Figure 23. Fe X-Ray Image of Figure 18

SEM IMAGES OF SAMPLE # Blank Cross Section of Soil

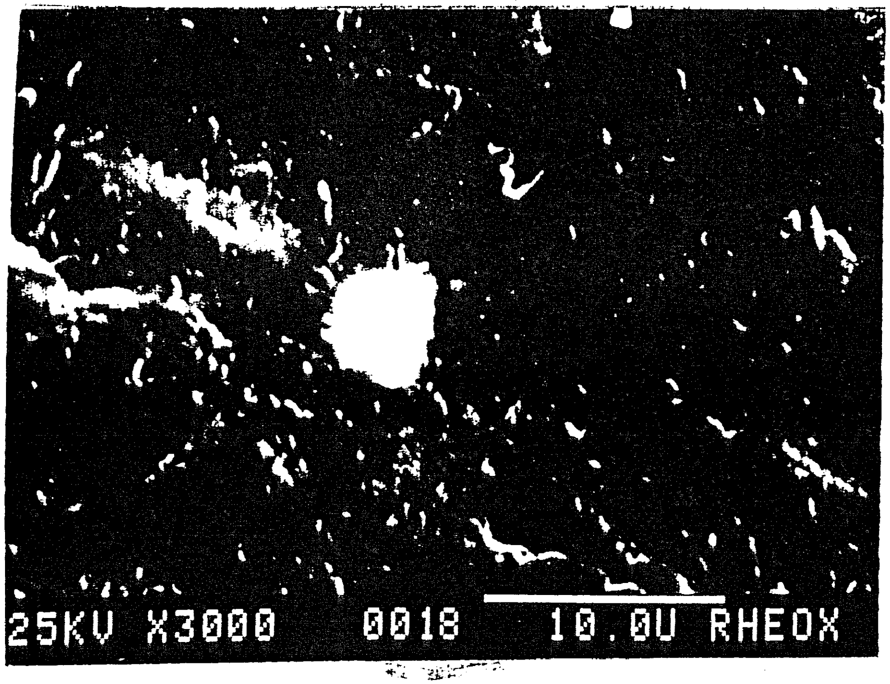

Figure 24

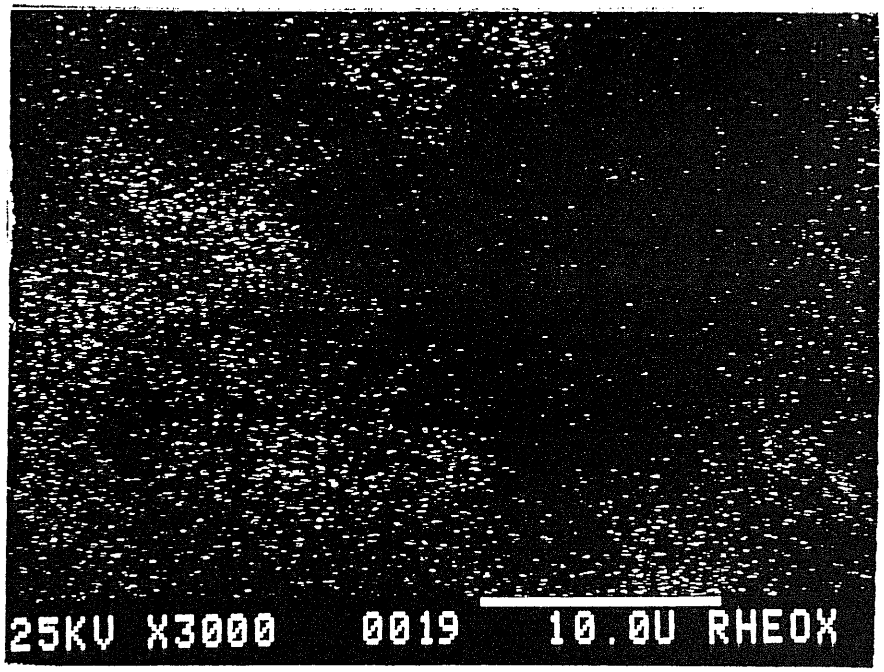

Figure 25 AL X-ray Image of Figure 24

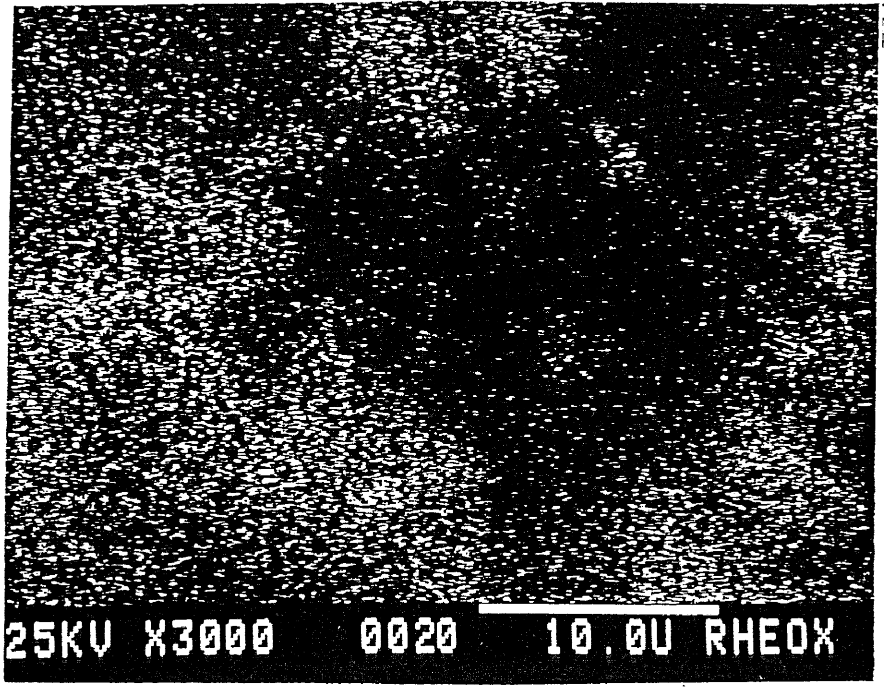

Figure 26 Si X-ray Image of Figure 24

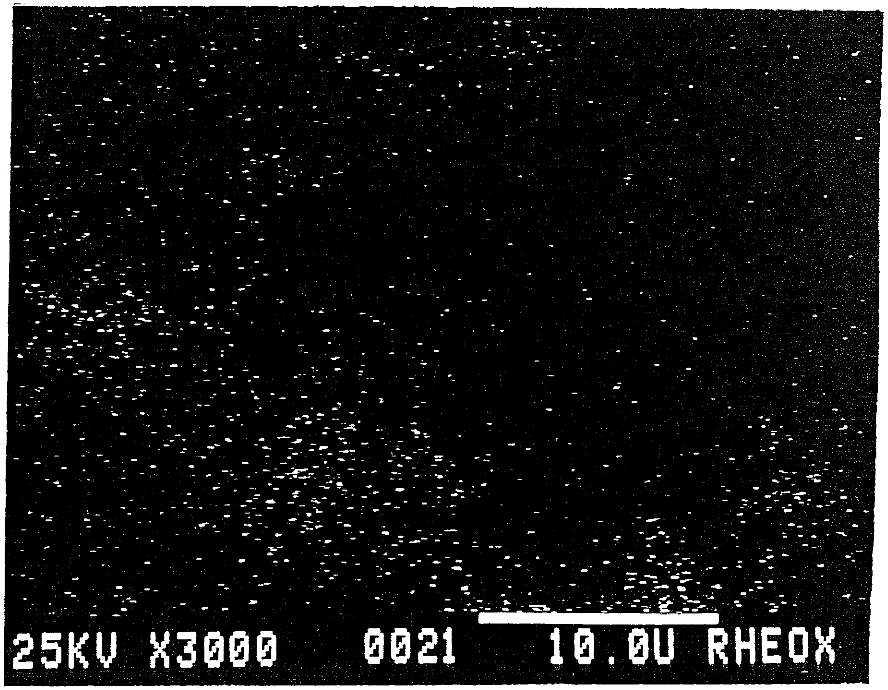

Figure 27 K X-ray Image of Figure 24

SEM IMAGES OF SAMPLE # Blank Cross Section of Soil

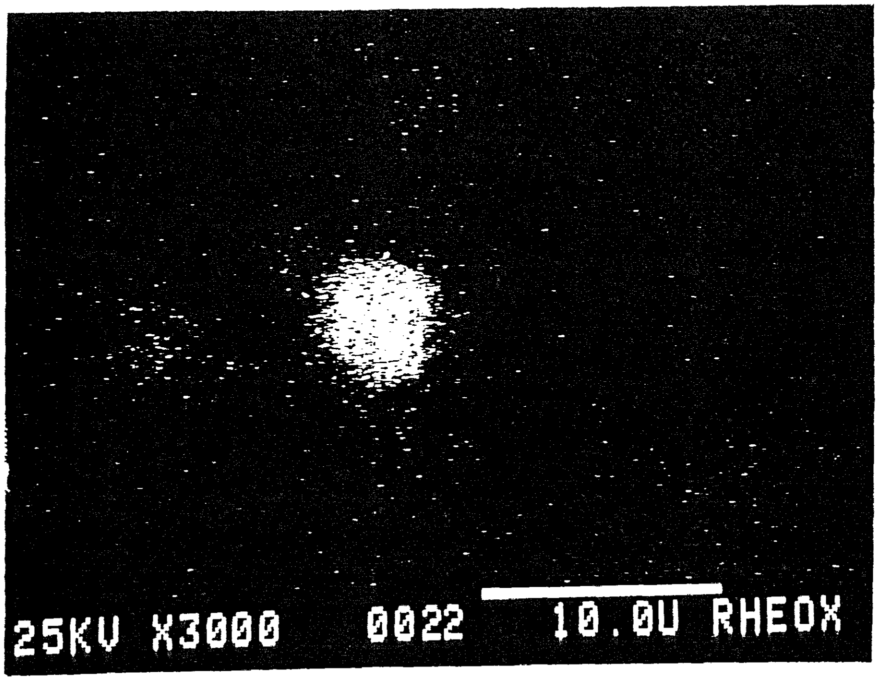

Figure 28 Ti X-Ray Image of Figure 24

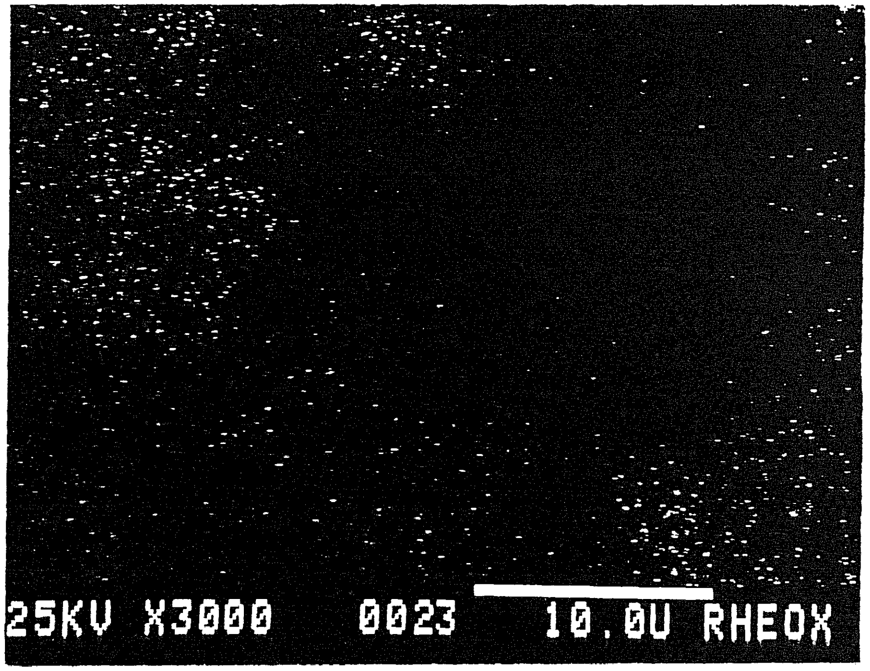

Figure 29 Fe X-Ray Image of Figure 24

SEM IMAGES OF SAMPLE # 1 [illegible] Cross Section of Soil

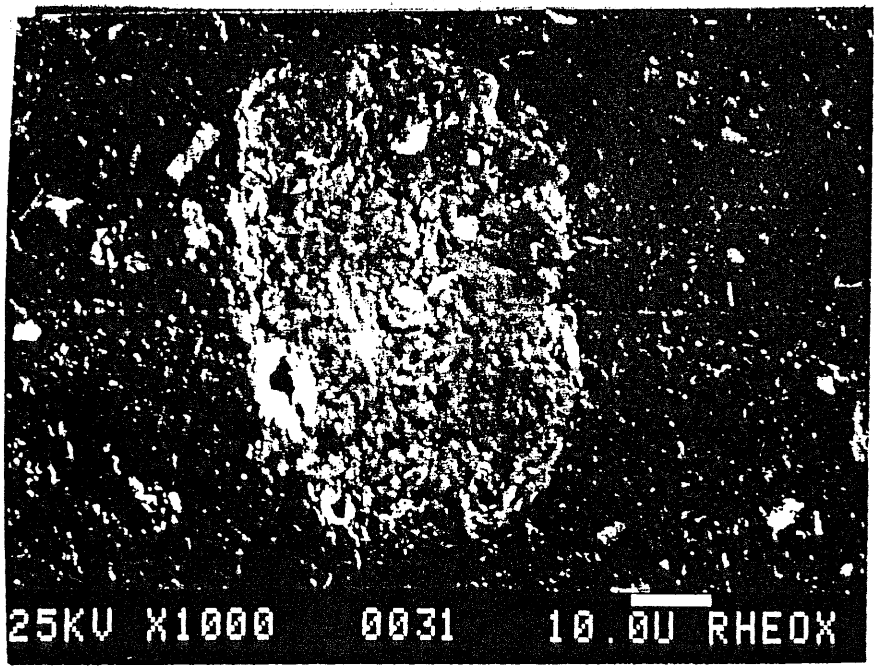

Figure 30

Al →

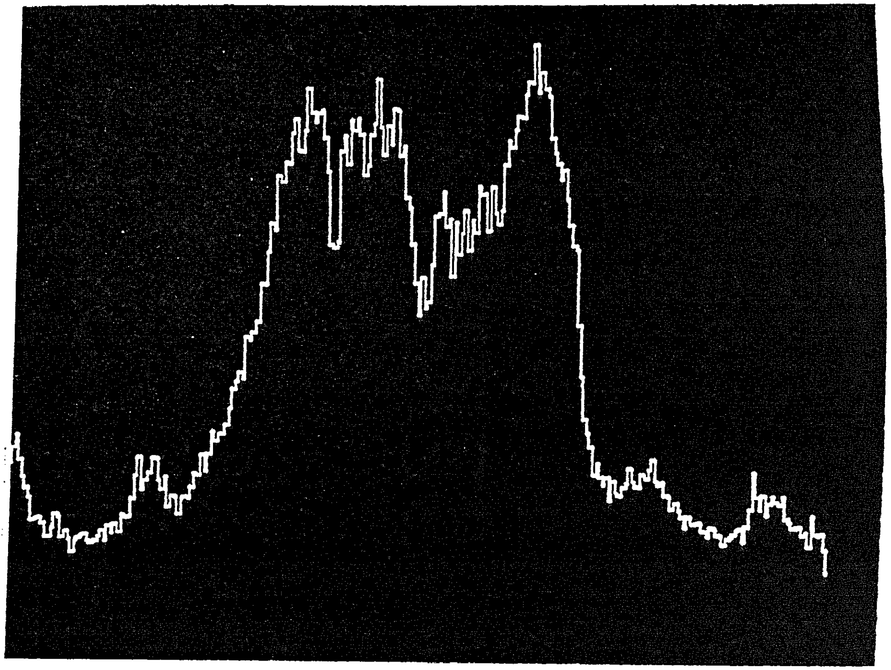

Figure 31

Line Profile Scan

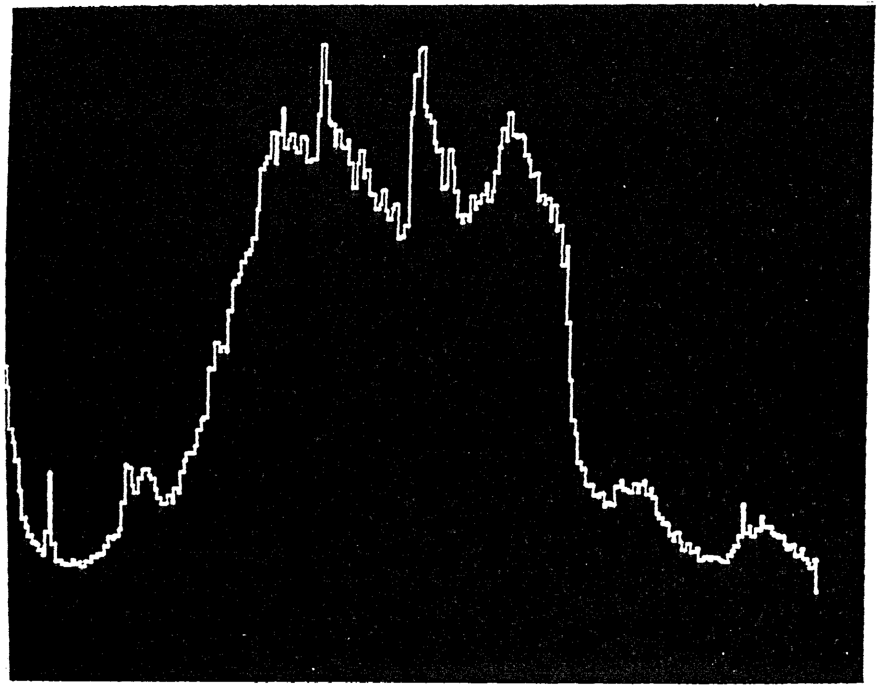

Figure 32

← Si

K →

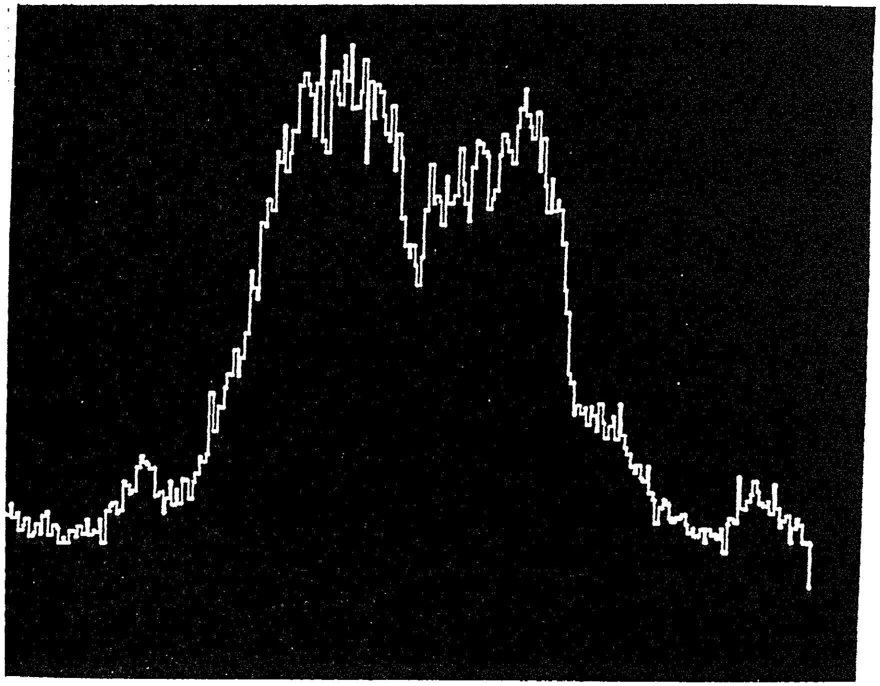

Figure 33

SEM IMAGES OF SAMPLE # 1 Blank Cross Section of Soil

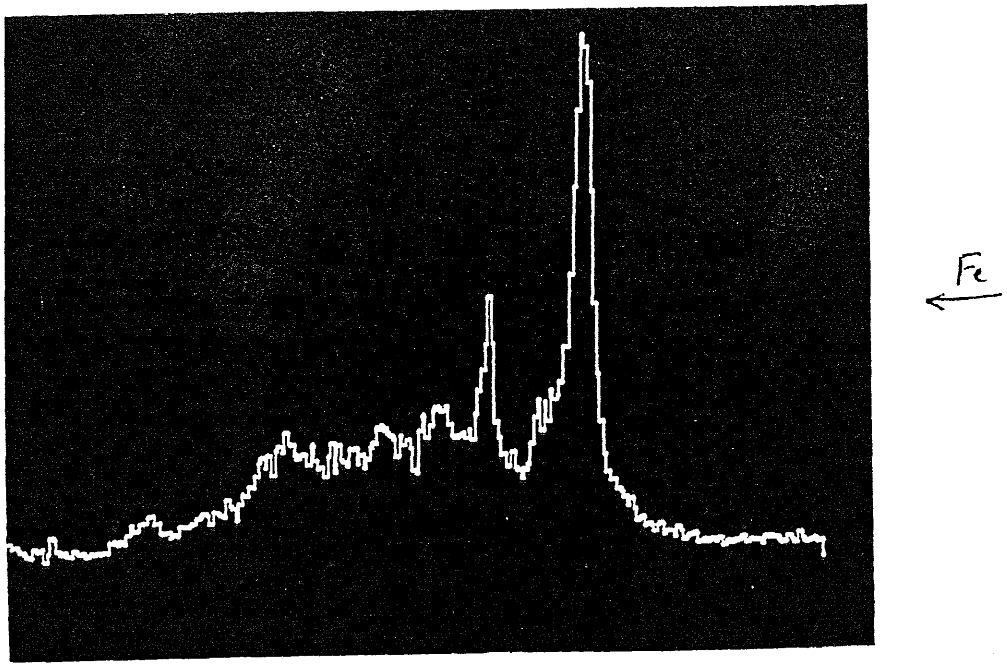

Figure 34

blank cross section of soil

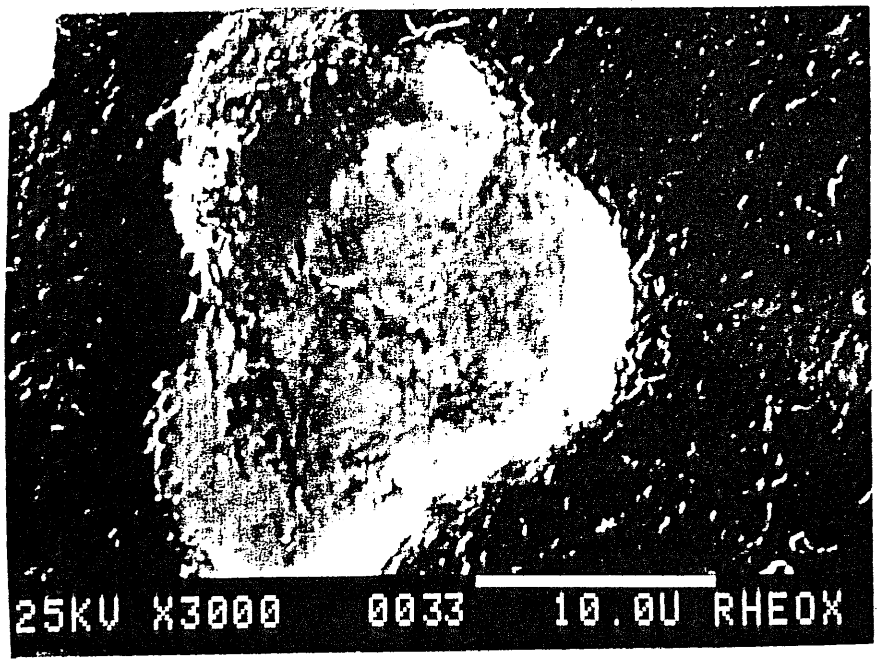

Figure 35

AL →

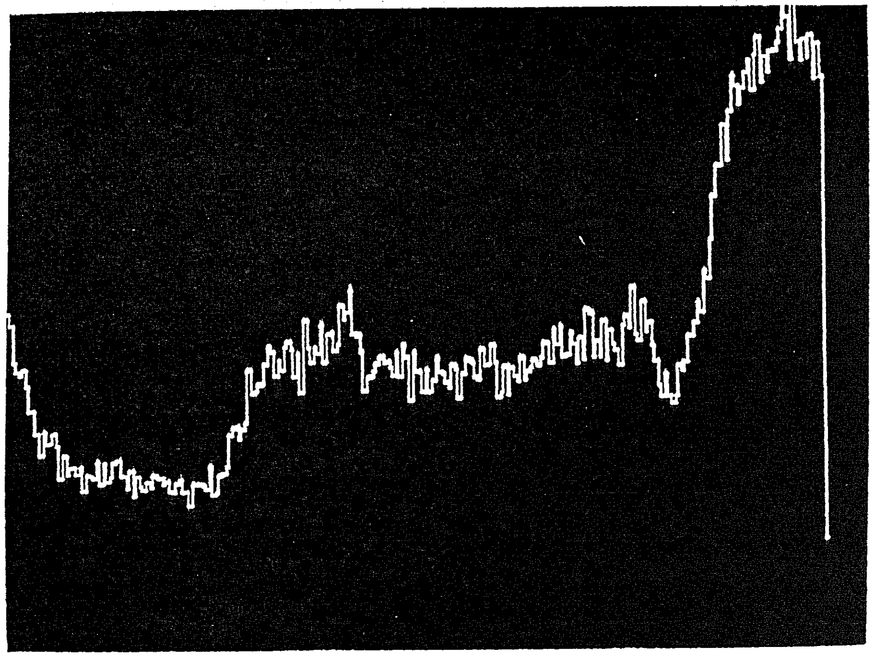

Figure 36

Line Profile Scan

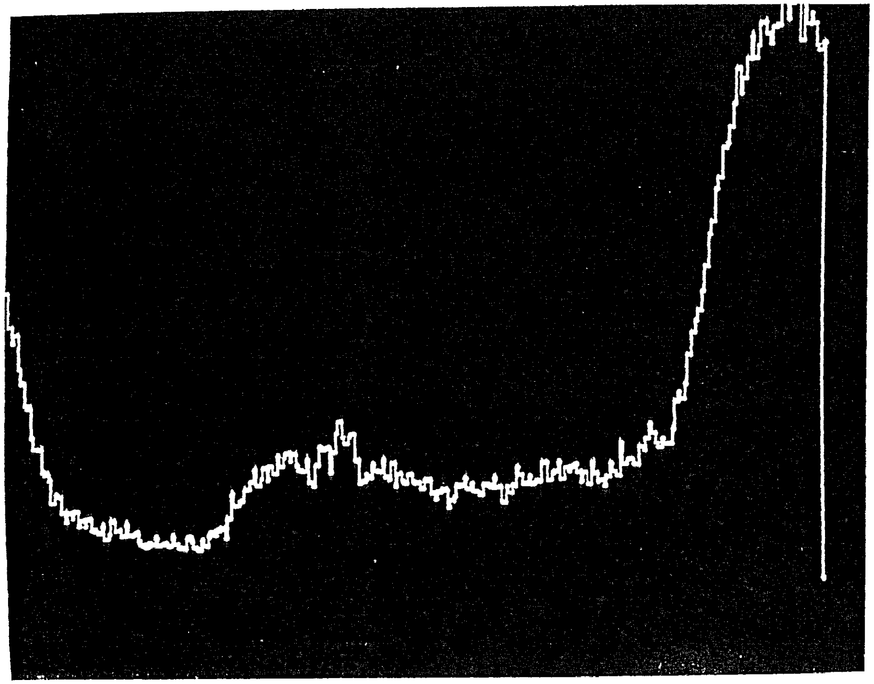

Figure 37

Si ←

K →

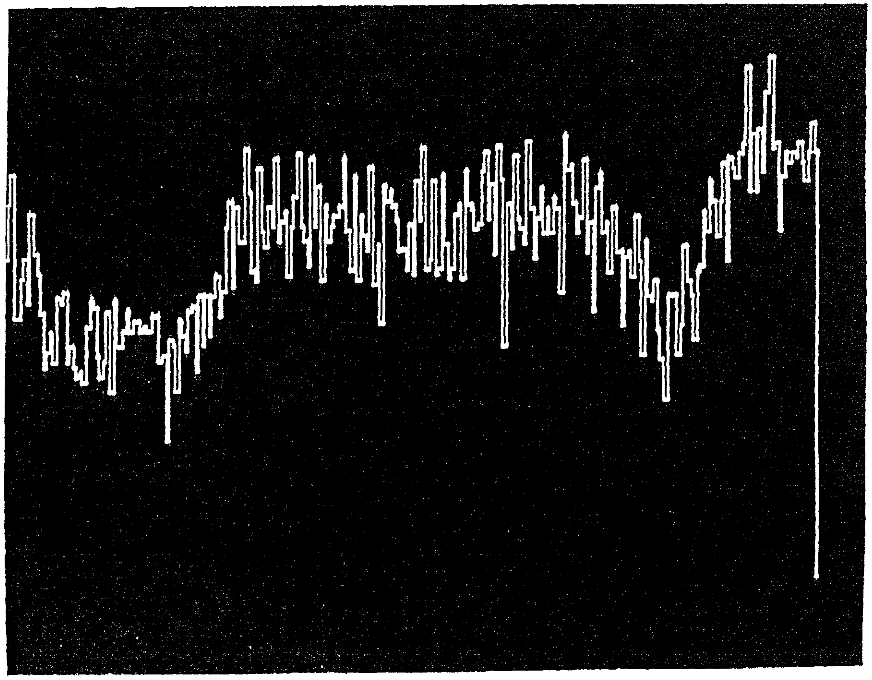

Figure 38

SEM IMAGES OF SAMPLE # 1 Blank Cross Section of Soil

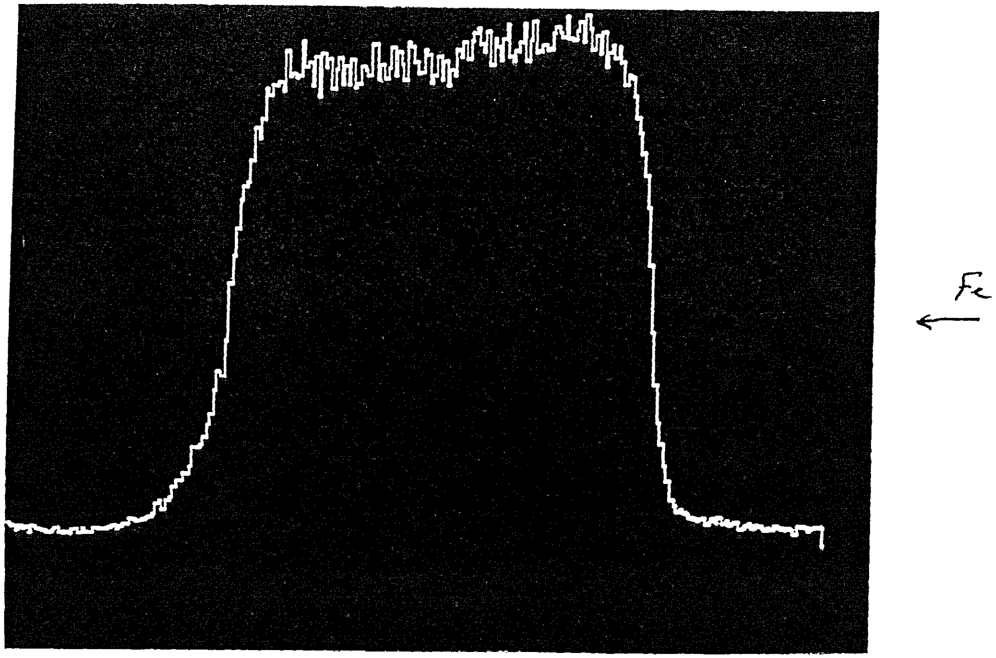

Figure 39

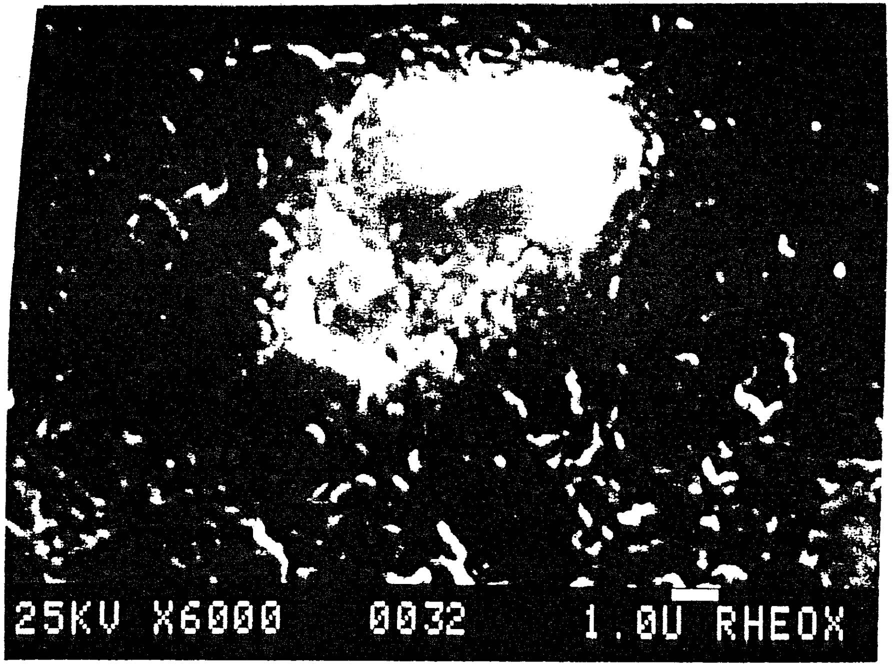

Figure 40

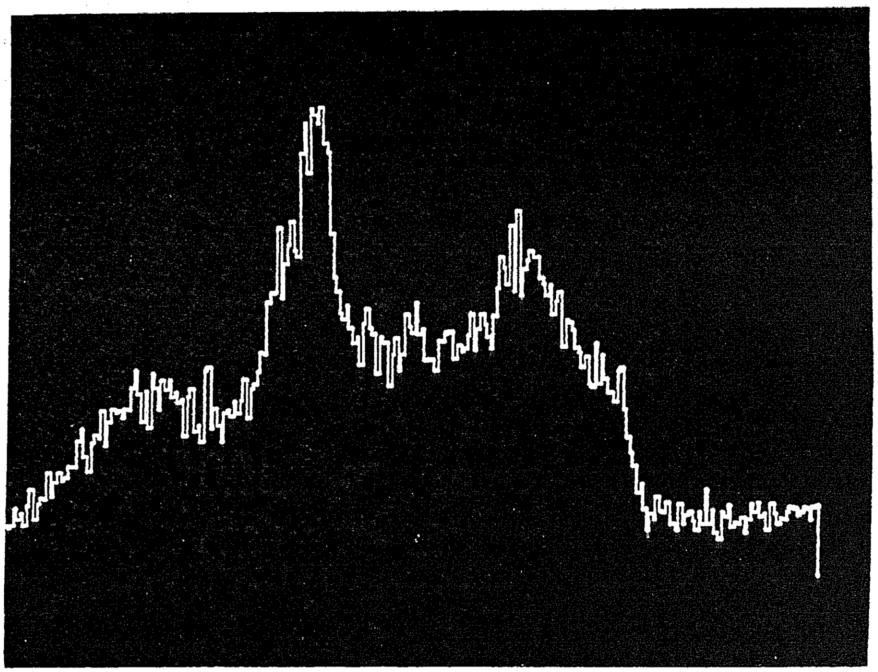

Figure 41

AL →

Line Profile Scan

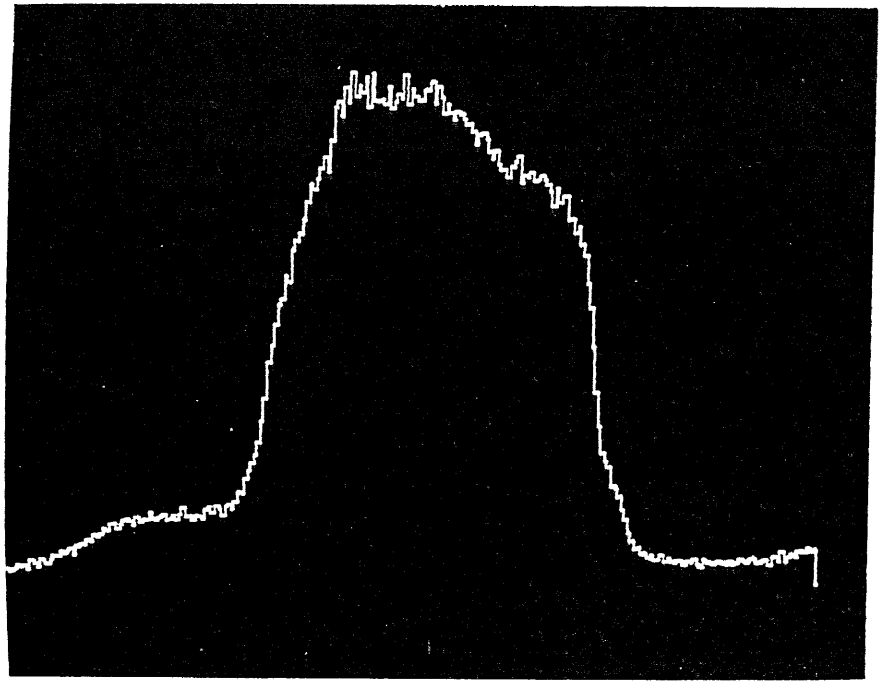

Figure 42

Si ←

K →

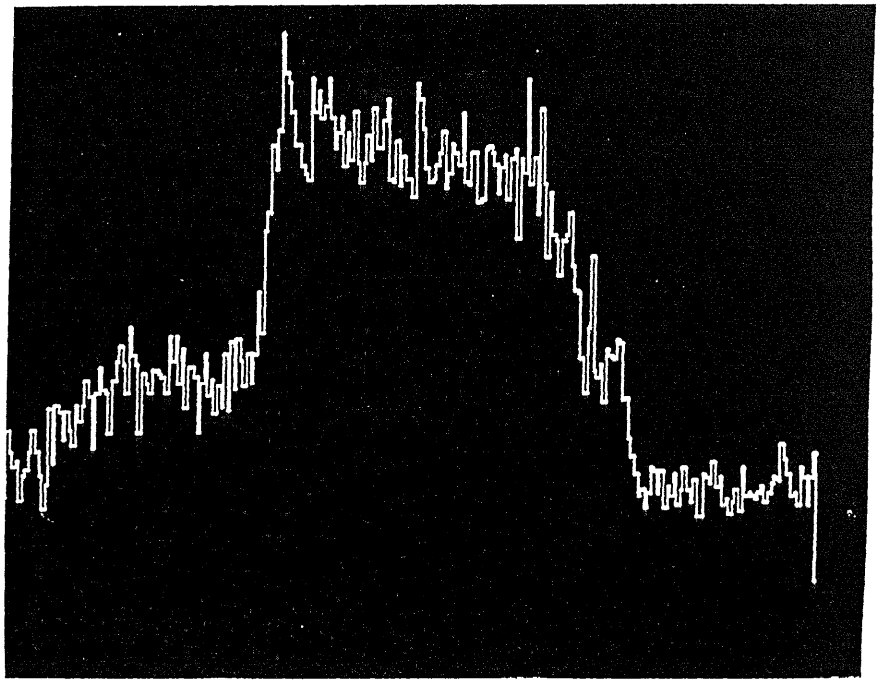

Figure 43

SEM IMAGES OF SAMPLE # 1 Blank Cross Section of Soil

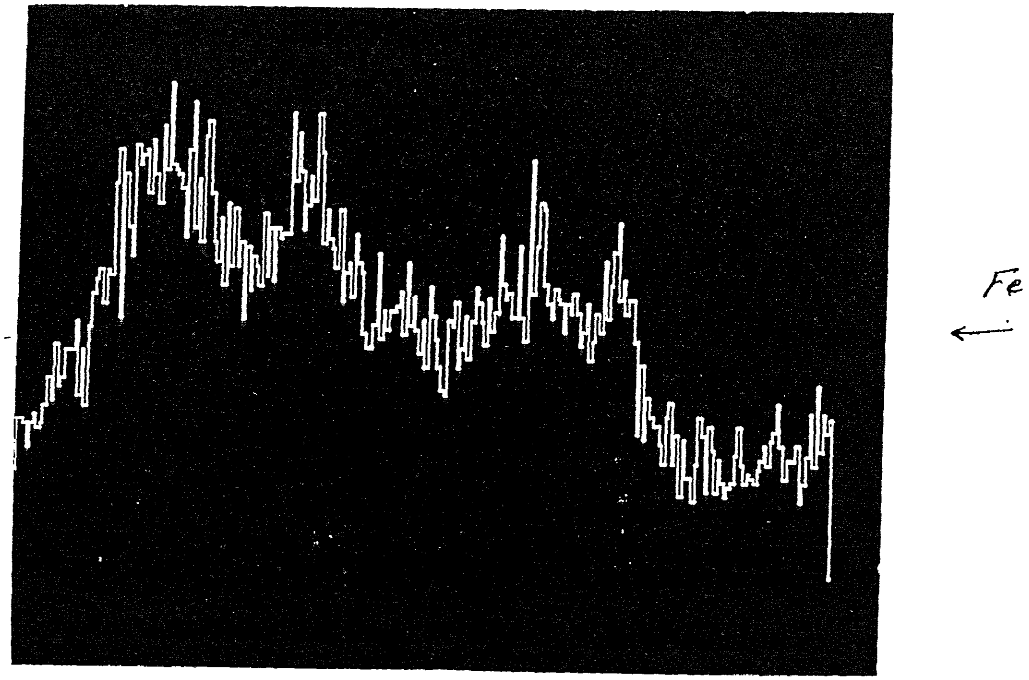

Figure 44

SEM IMAGES OF SAMPLE # Impregnated Soil powder

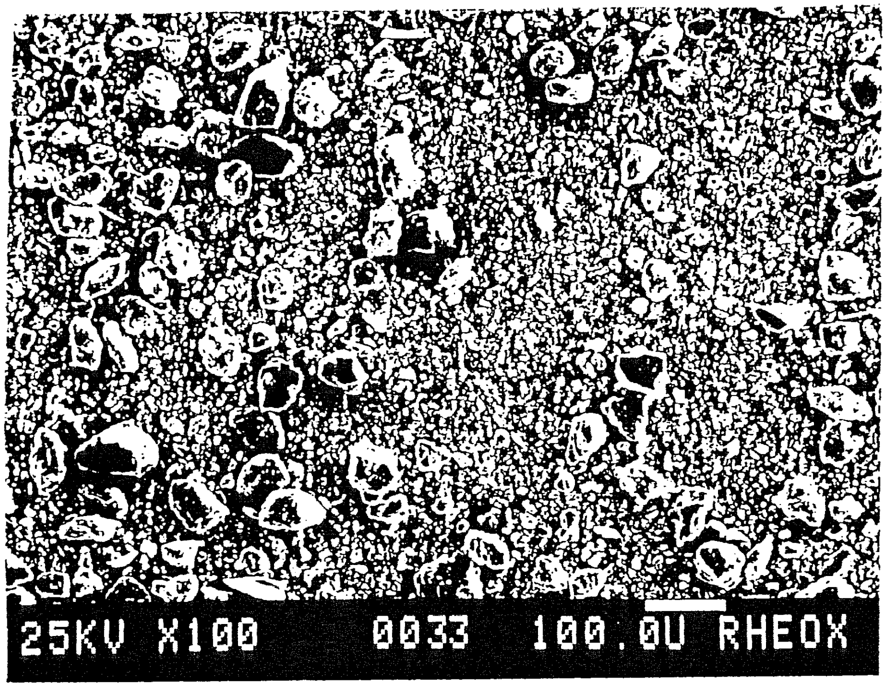

Figure 45

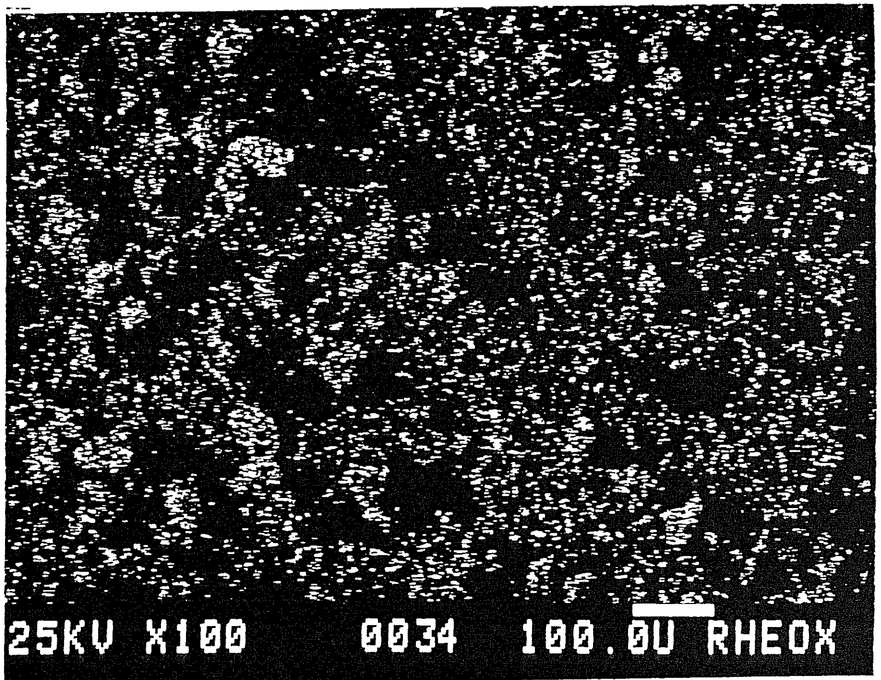

Figure 46 AL X-ray Image of Figure 45

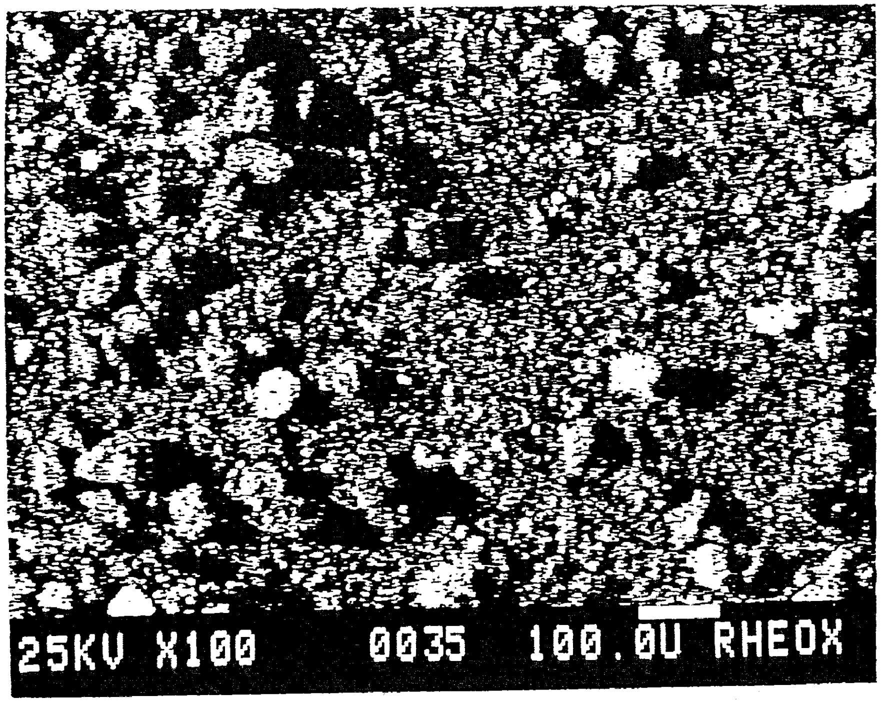

Figure 47 Si X-ray Image of Figure 45

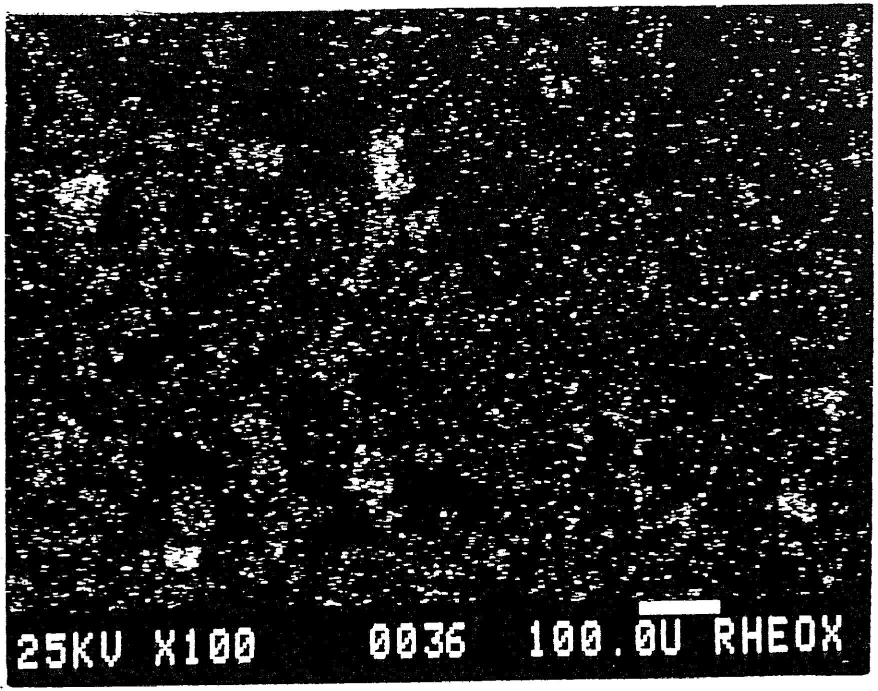

Figure 48 K X-ray Image of Figure 45

SEM IMAGES OF SAMPLE # Impregnated soil powder

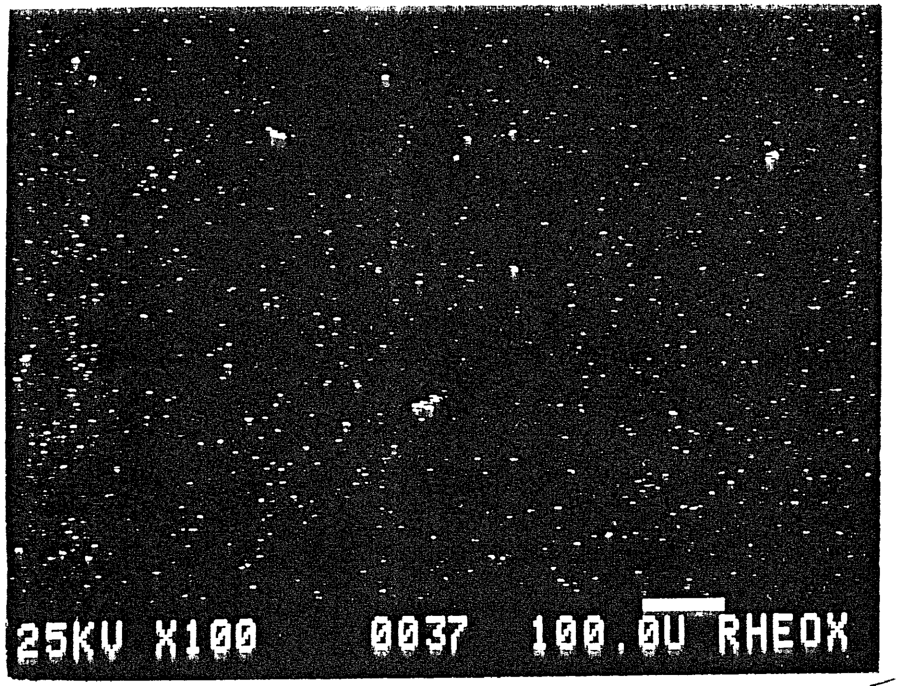

igure 49 Ti X-Ray Image of Figure 45

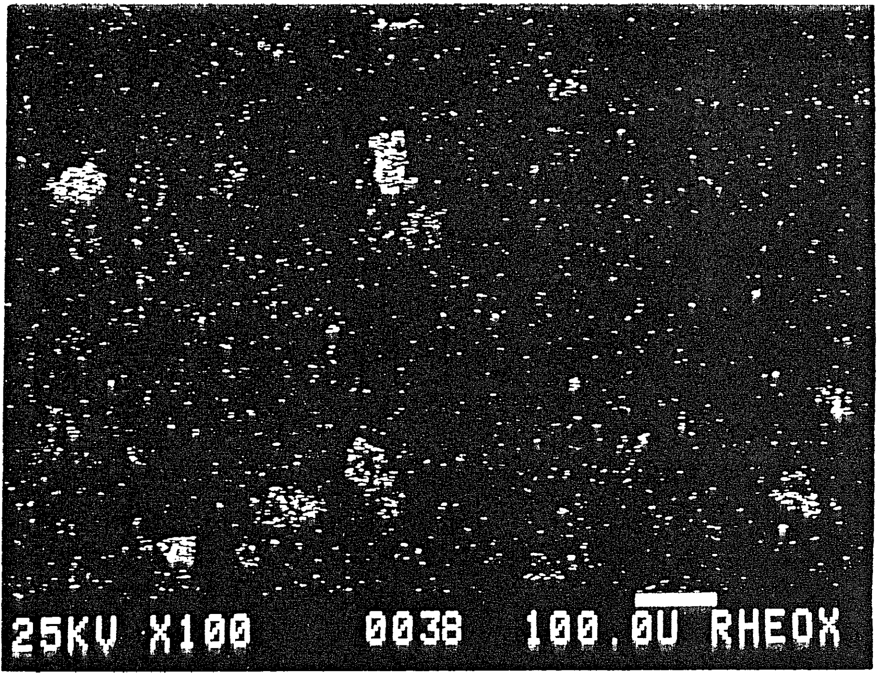

Figure 50 Cr X-Ray Image of Figure 45

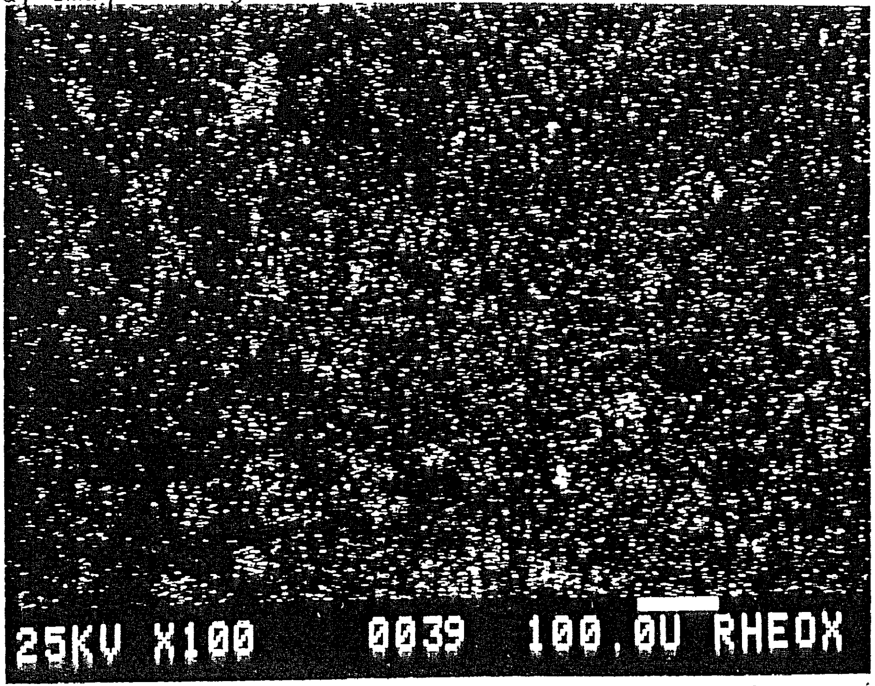

Figure 51 Fe X-Ray Image of Figure 45

SEM IMAGES OF SAMPLE # Impregnated Soil powder

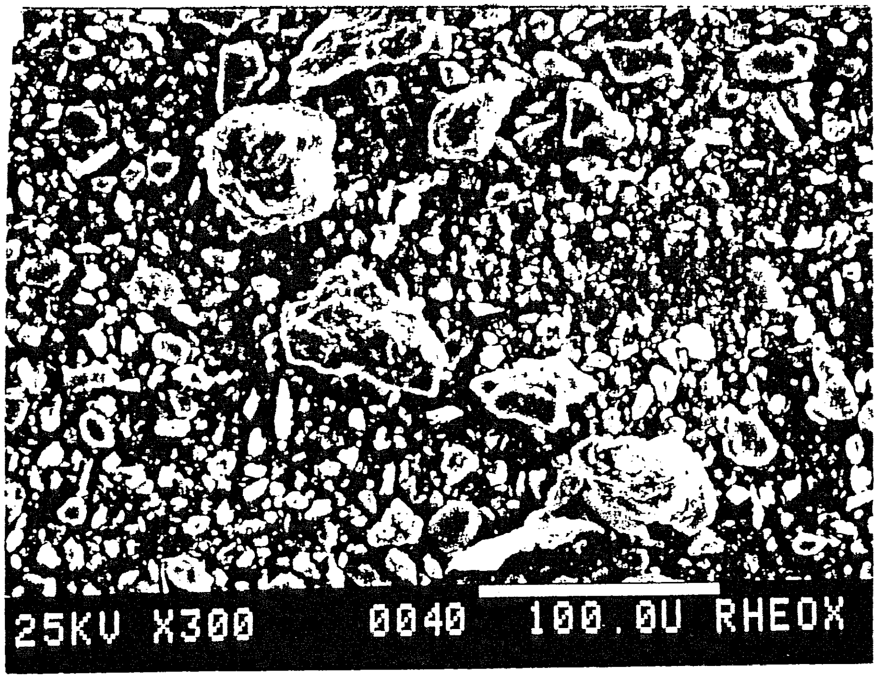

Figure 52

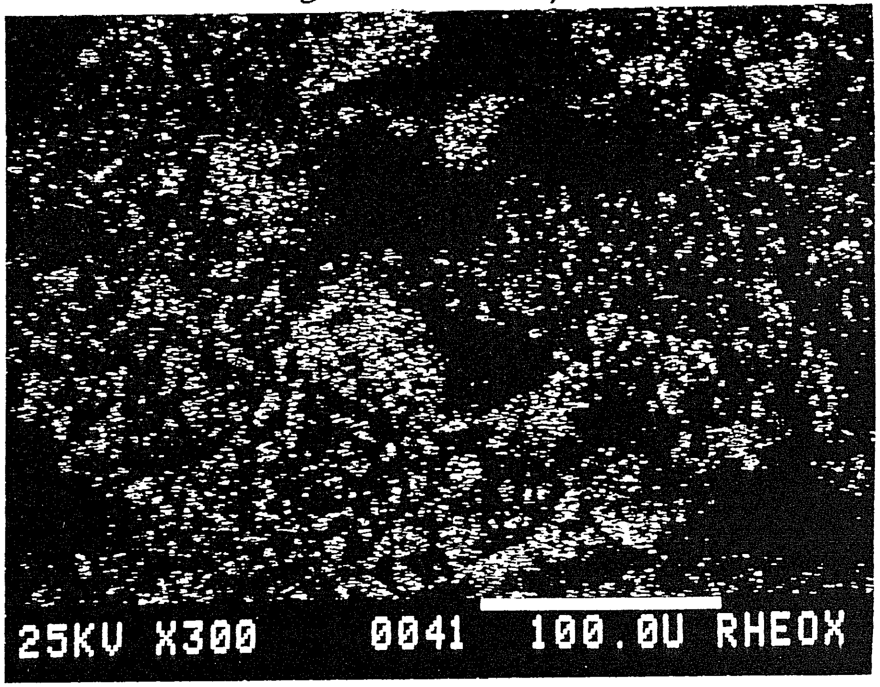

Figure 53 AL X-ray Image of Figure 52

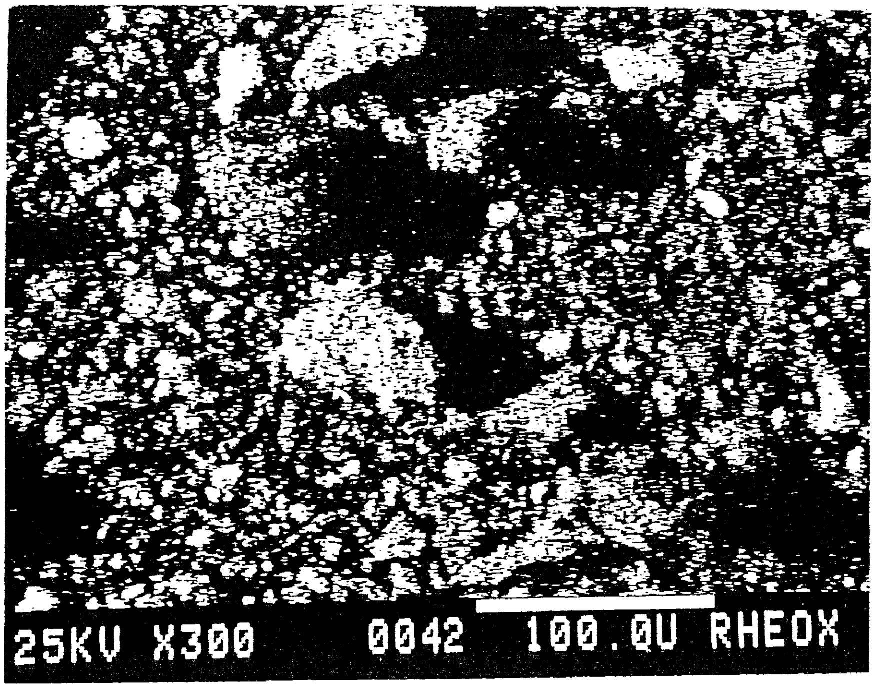

Figure 54 Si X-ray Image of Figure 52

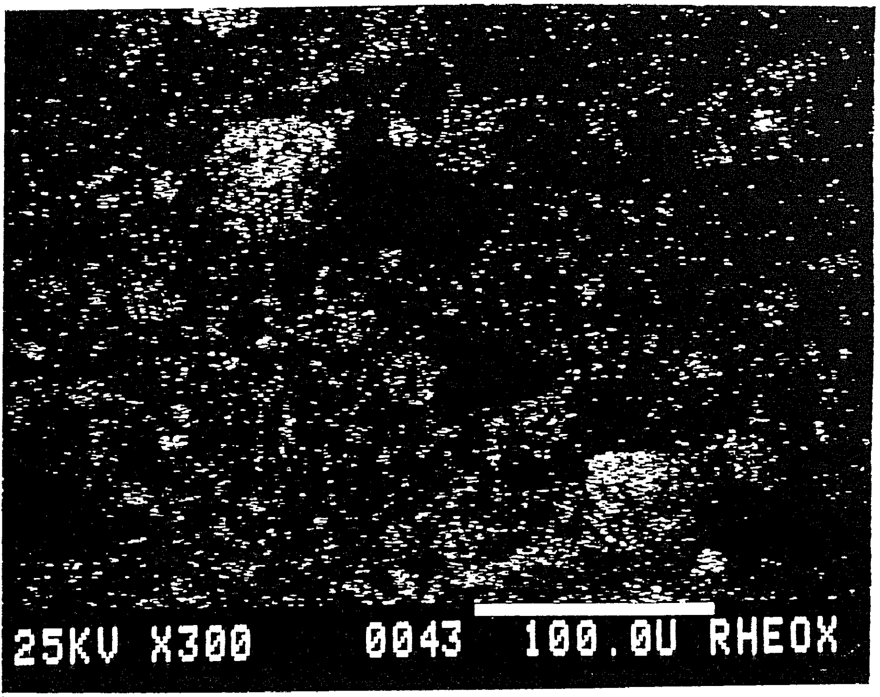

Figure 55 K X-ray Image of Figure 52

SEM IMAGES OF SAMPLE # Impregnated Soil Powder

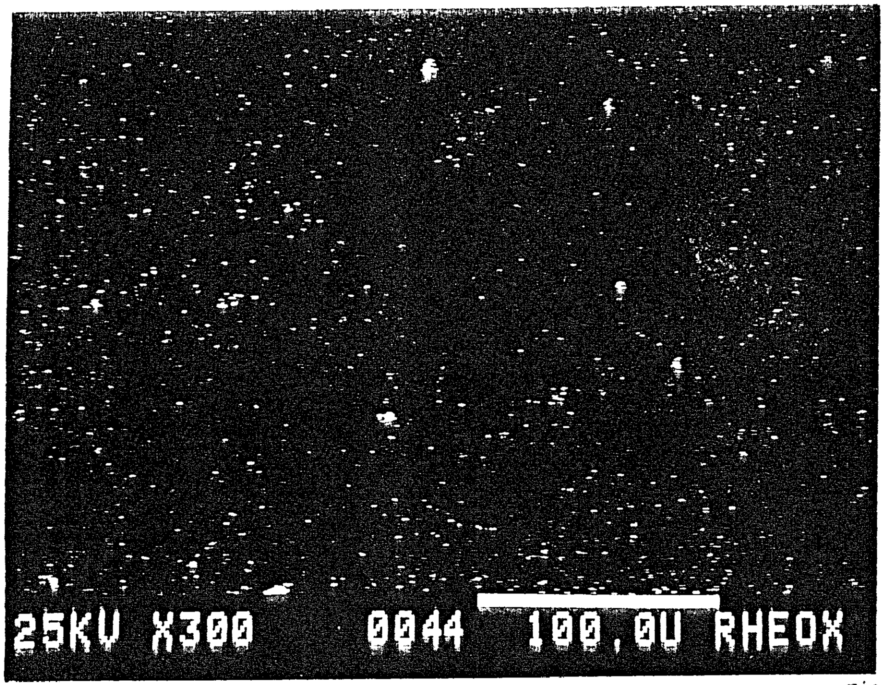

Figure 56 Ti X-Ray Image of Figure 52.

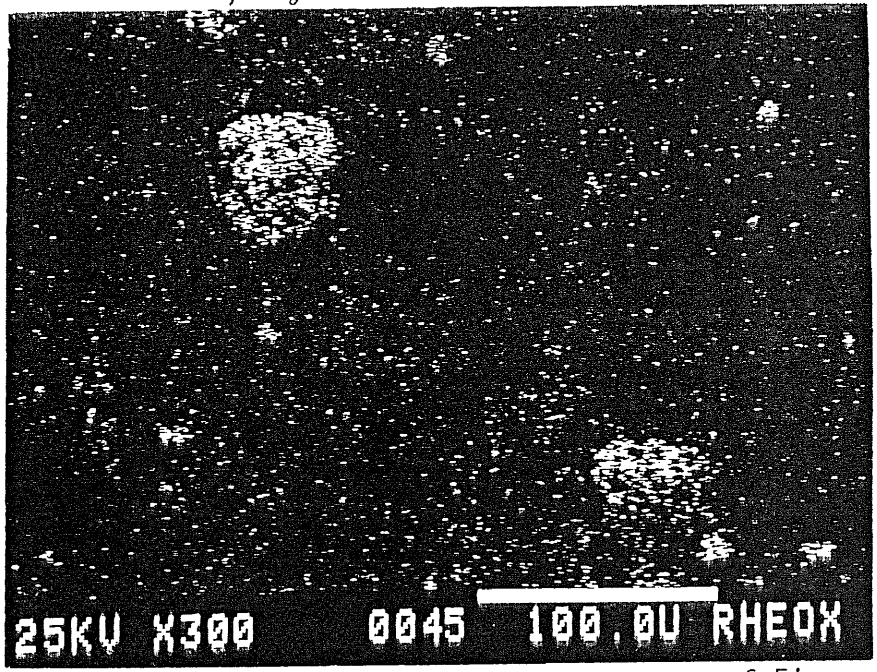

Figure 57 Cr X-Ray Image of Figure 52

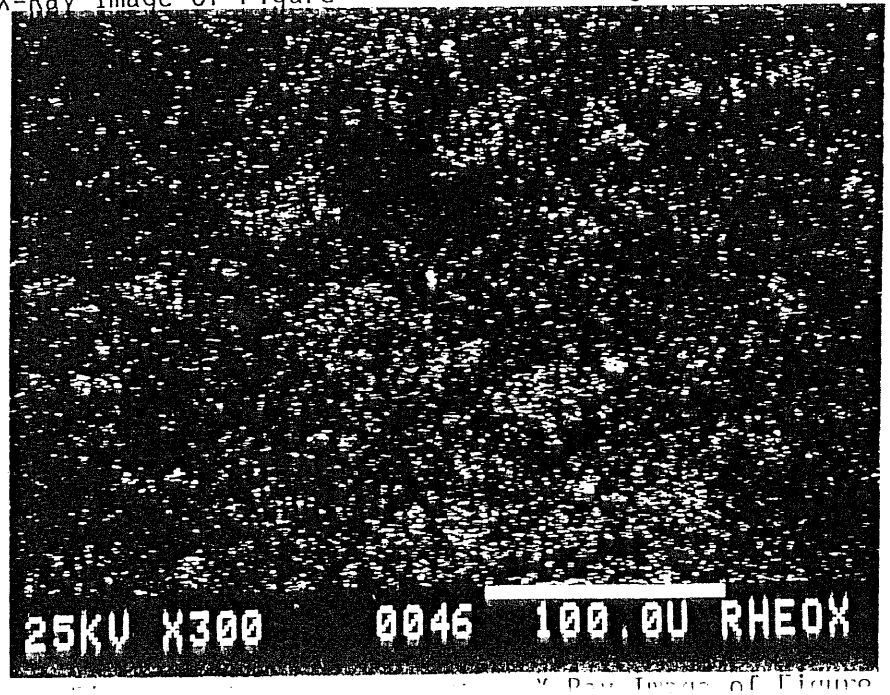

X-Ray Image of Figure 52

SEM IMAGES OF SAMPLE # Impregnated coal [illegible]

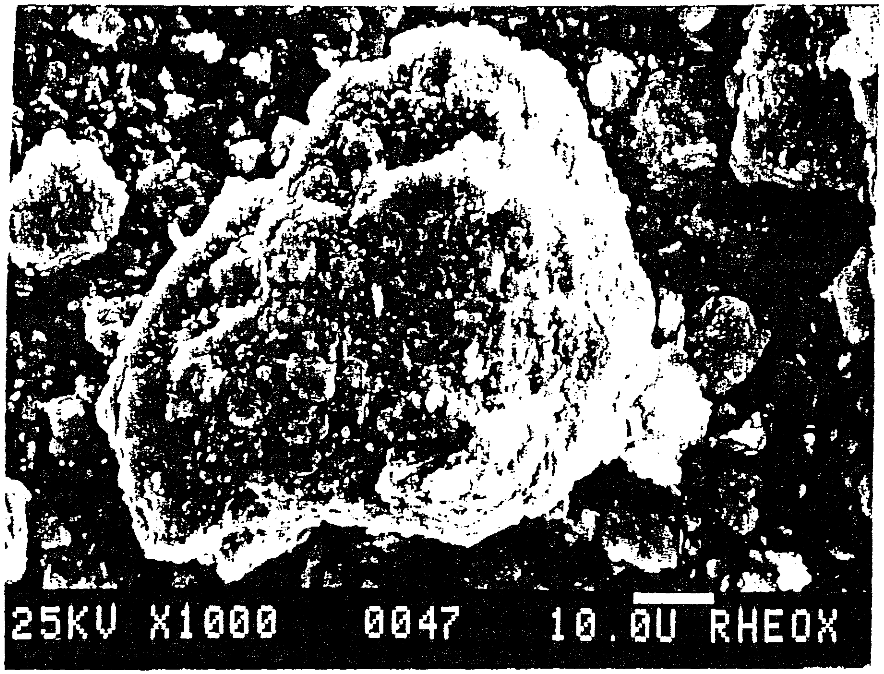

Figure 59

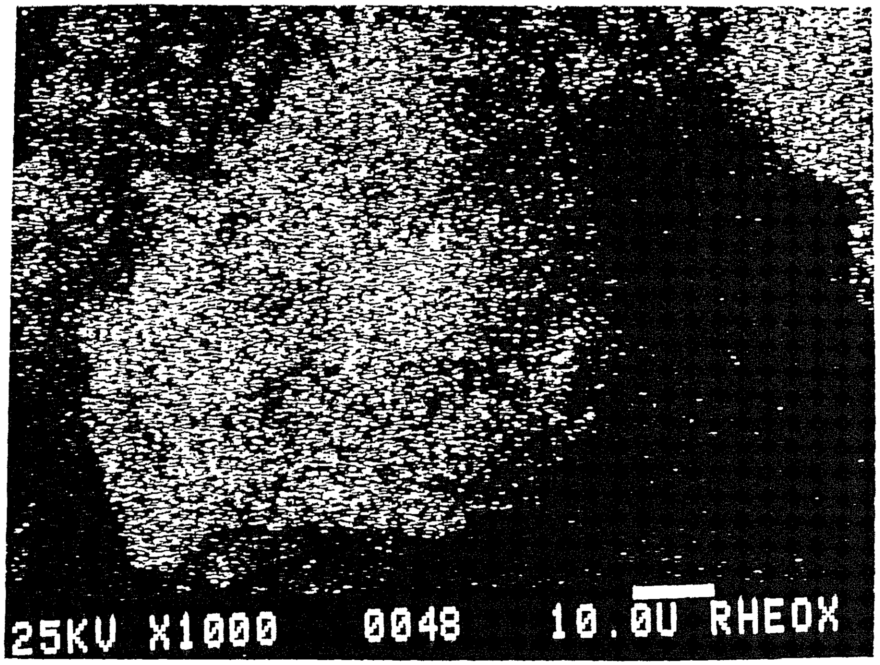

Figure 60 X-ray Image of Figure 59

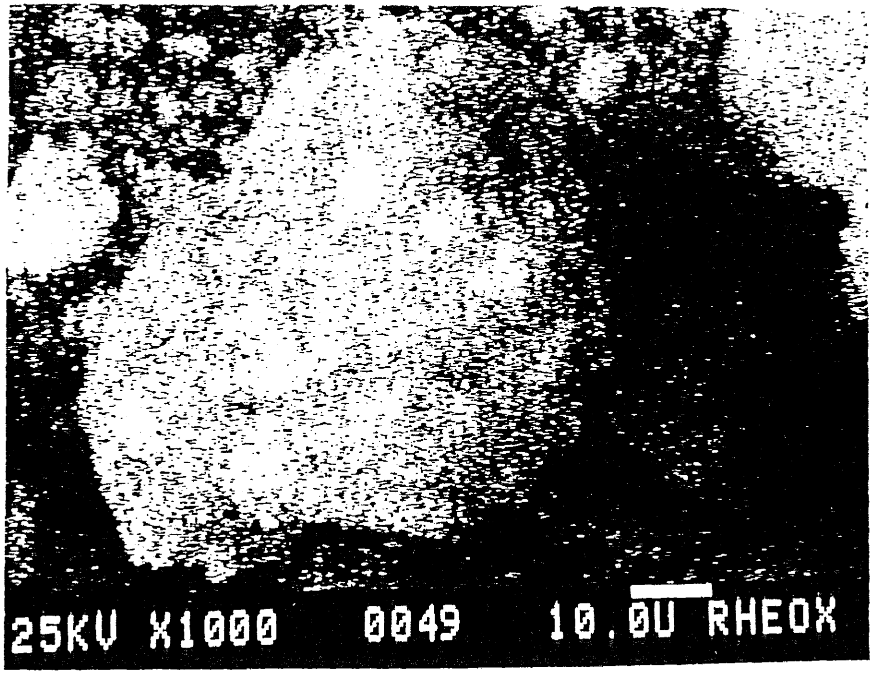

Figure 61 X-ray Image of Figure 59

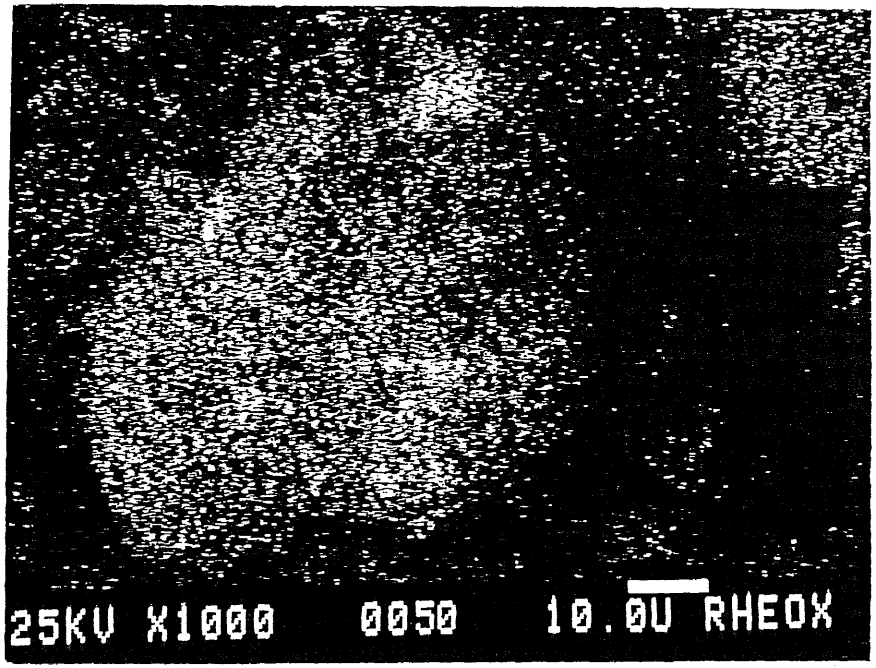

Figure 62 X-ray Image of Figure 59

SEM IMAGES OF SAMPLE # Impregnated Soil Powder

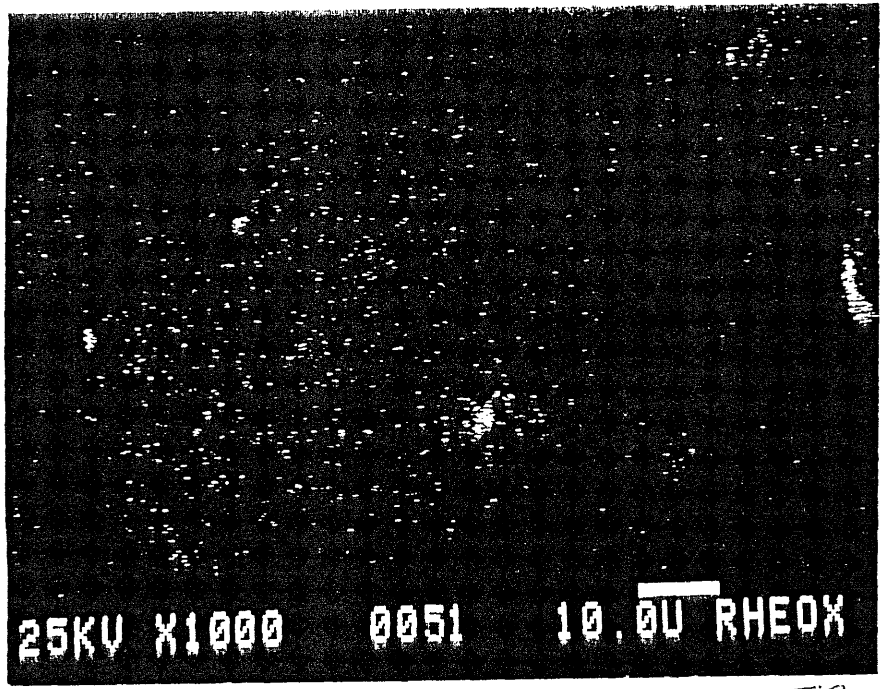

Figure 63 Ti X-Ray Image of Figure 59

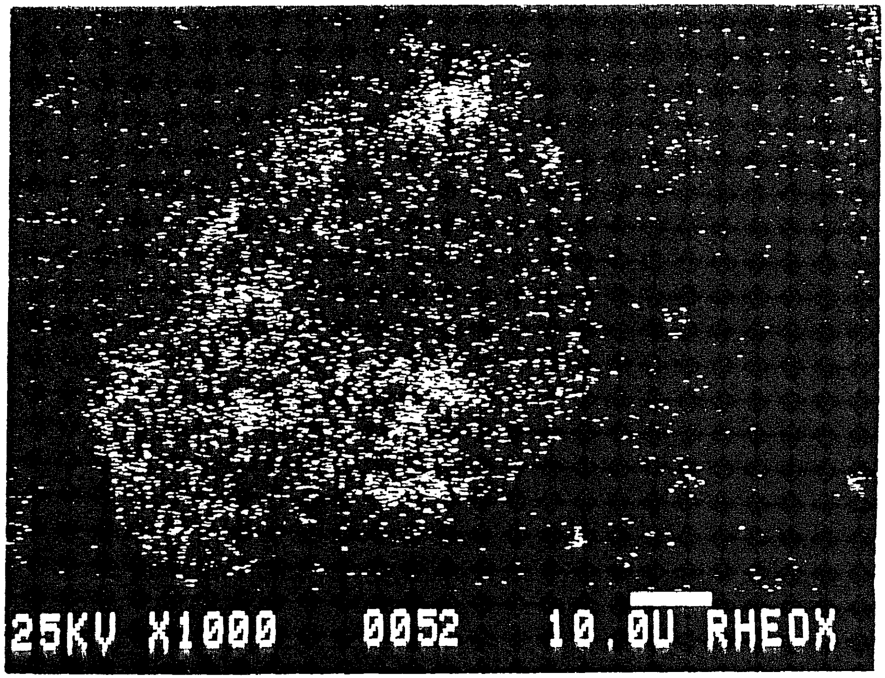

Figure 64 Cr X-Ray Image of Figure 59

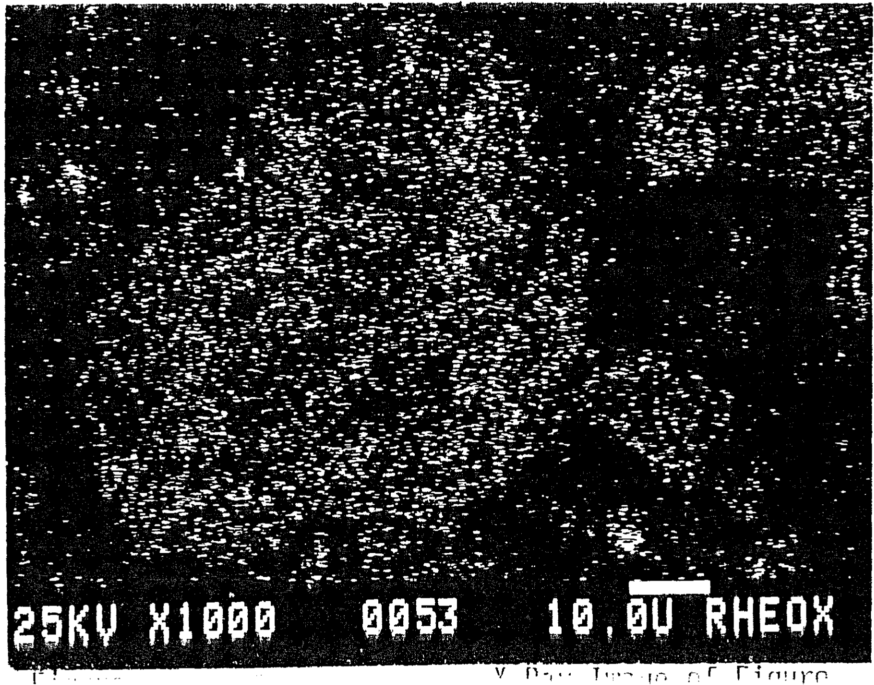

Figure X-Ray Image of Figure 59

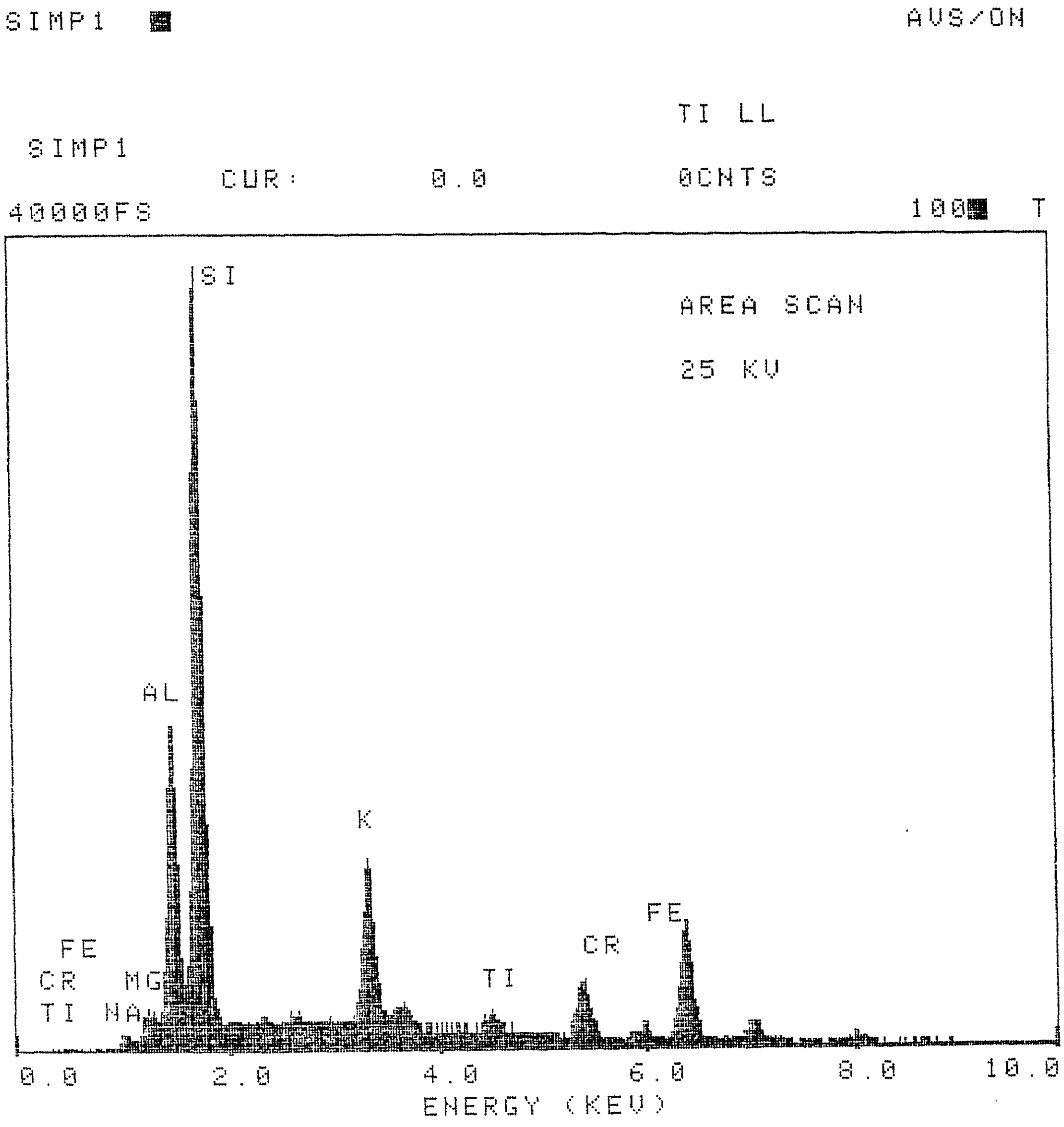

12-Oct-89 12:45

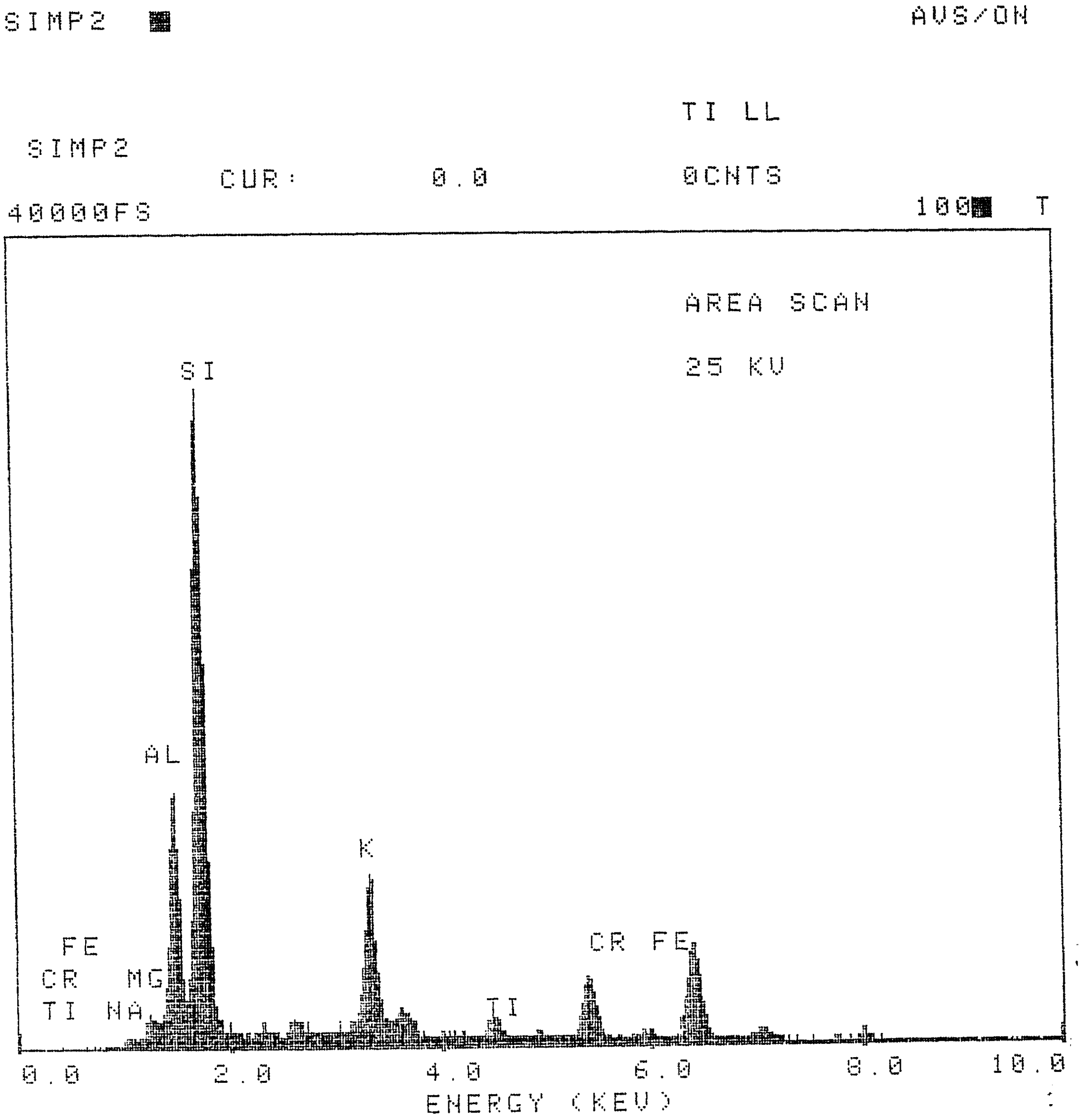

12-Oct-89 12:45

SIMP3 ■ AVS/ON

TI LL

SIMP3

CUR: 0.0 0CNTS

40000FS 100■ T

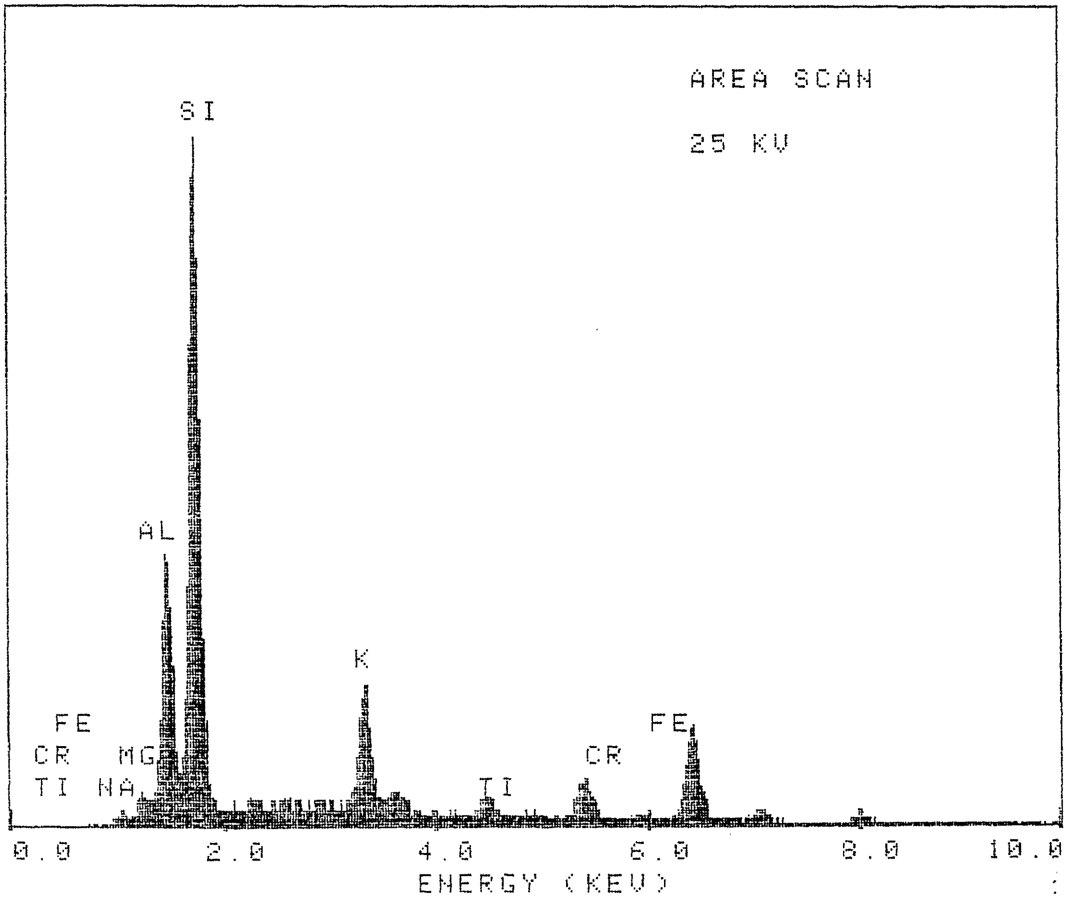

12-Oct-89 12:45

SIMP4 ■ AVS/ON

TI LL

SIMP4

CUR: 0.0 0CNTS

40000FS 100■ T

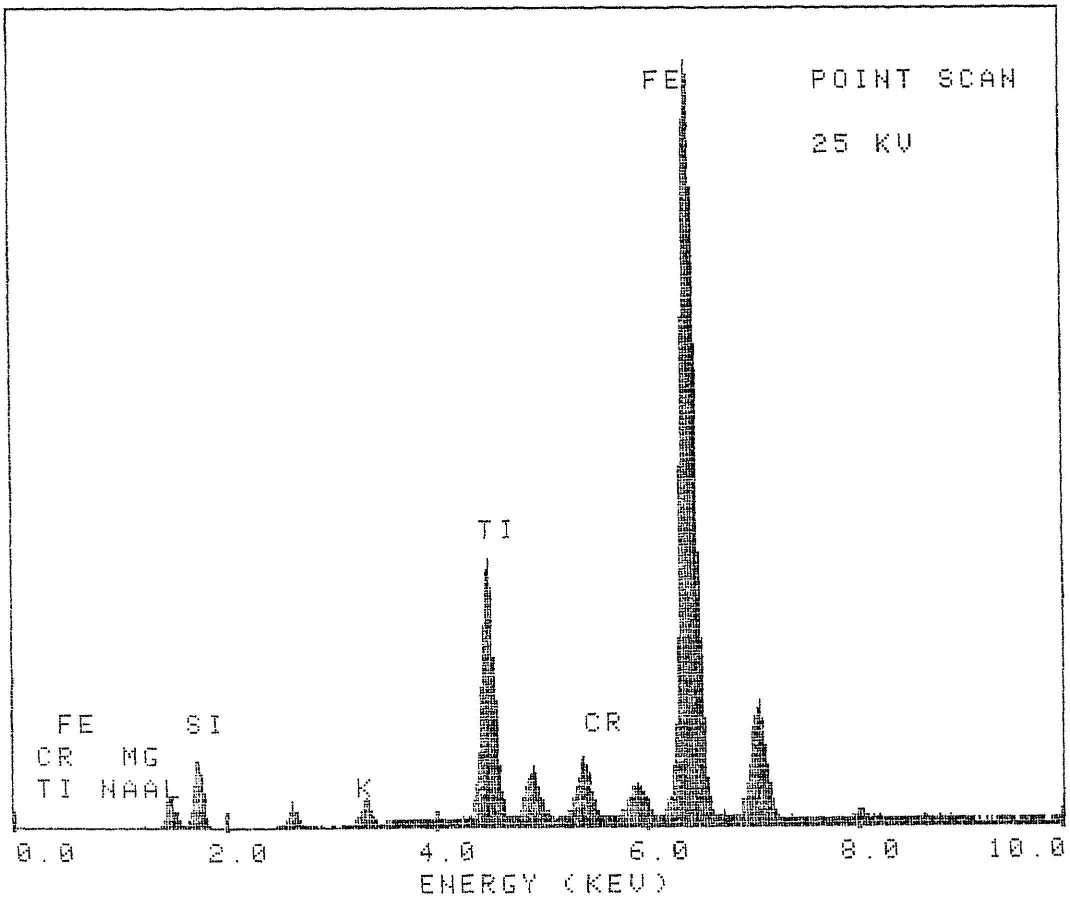

12-Oct-89 12:45

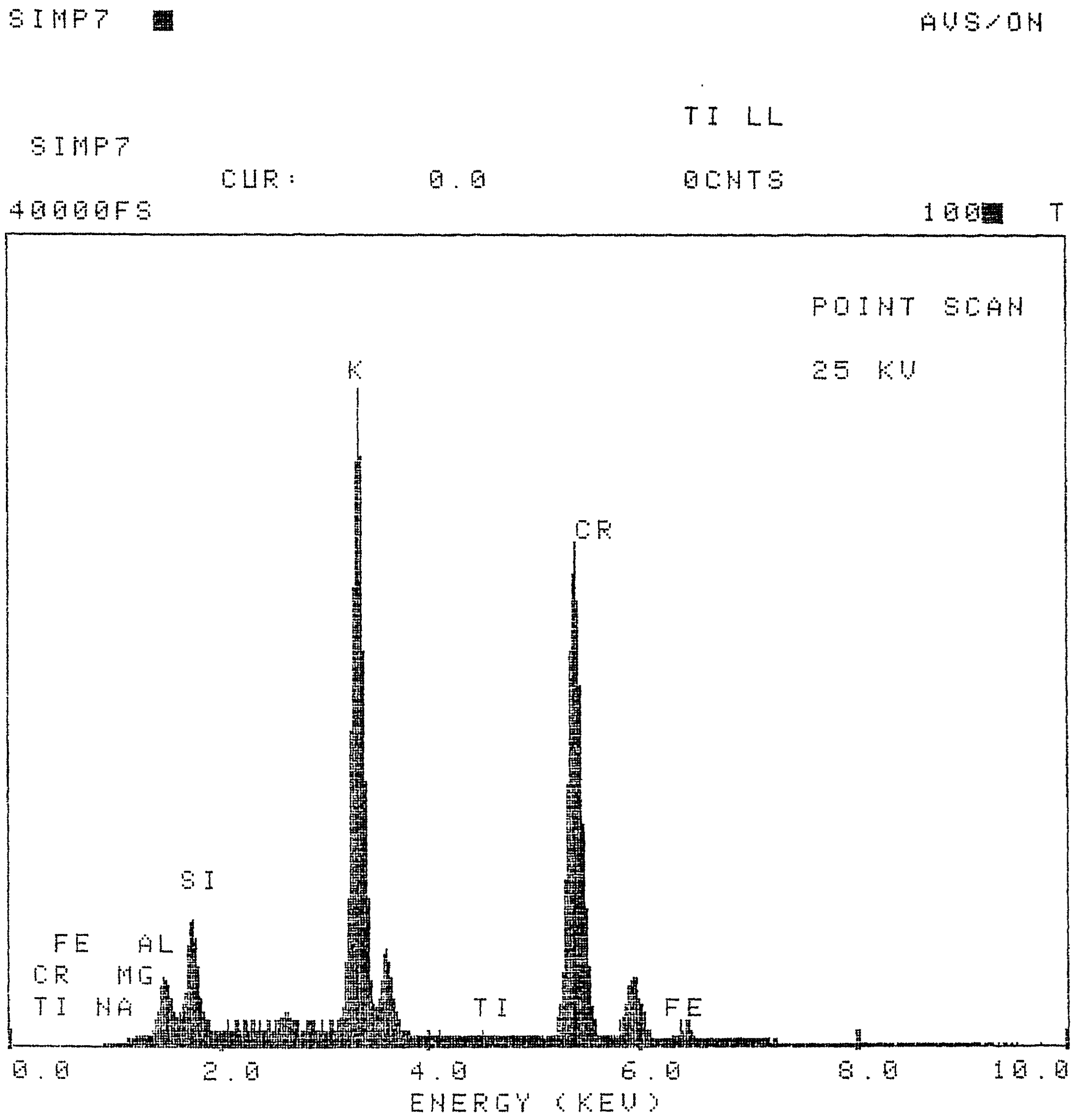

12-Oct-89 12:45

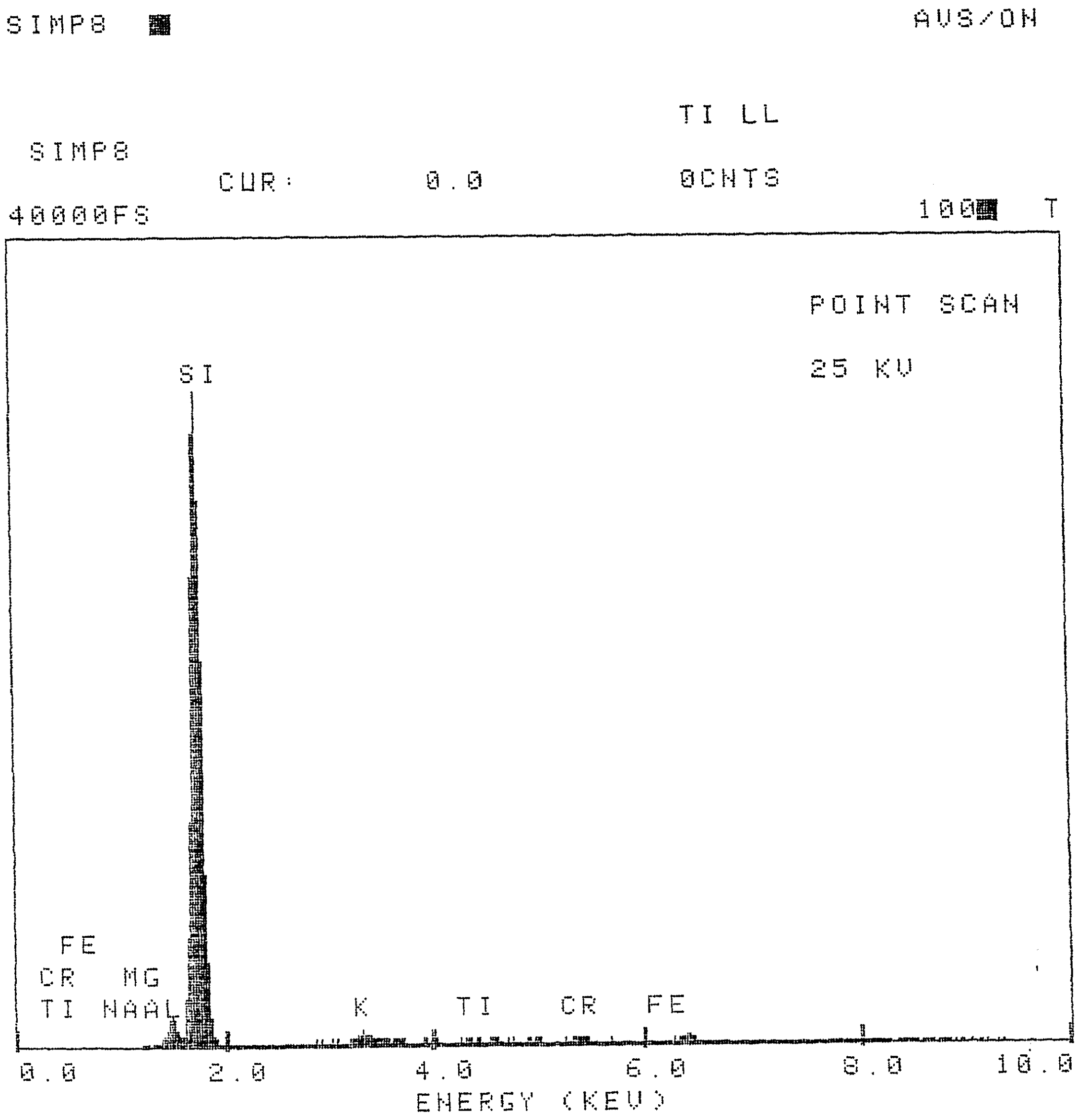

12-Oct-89 12:45

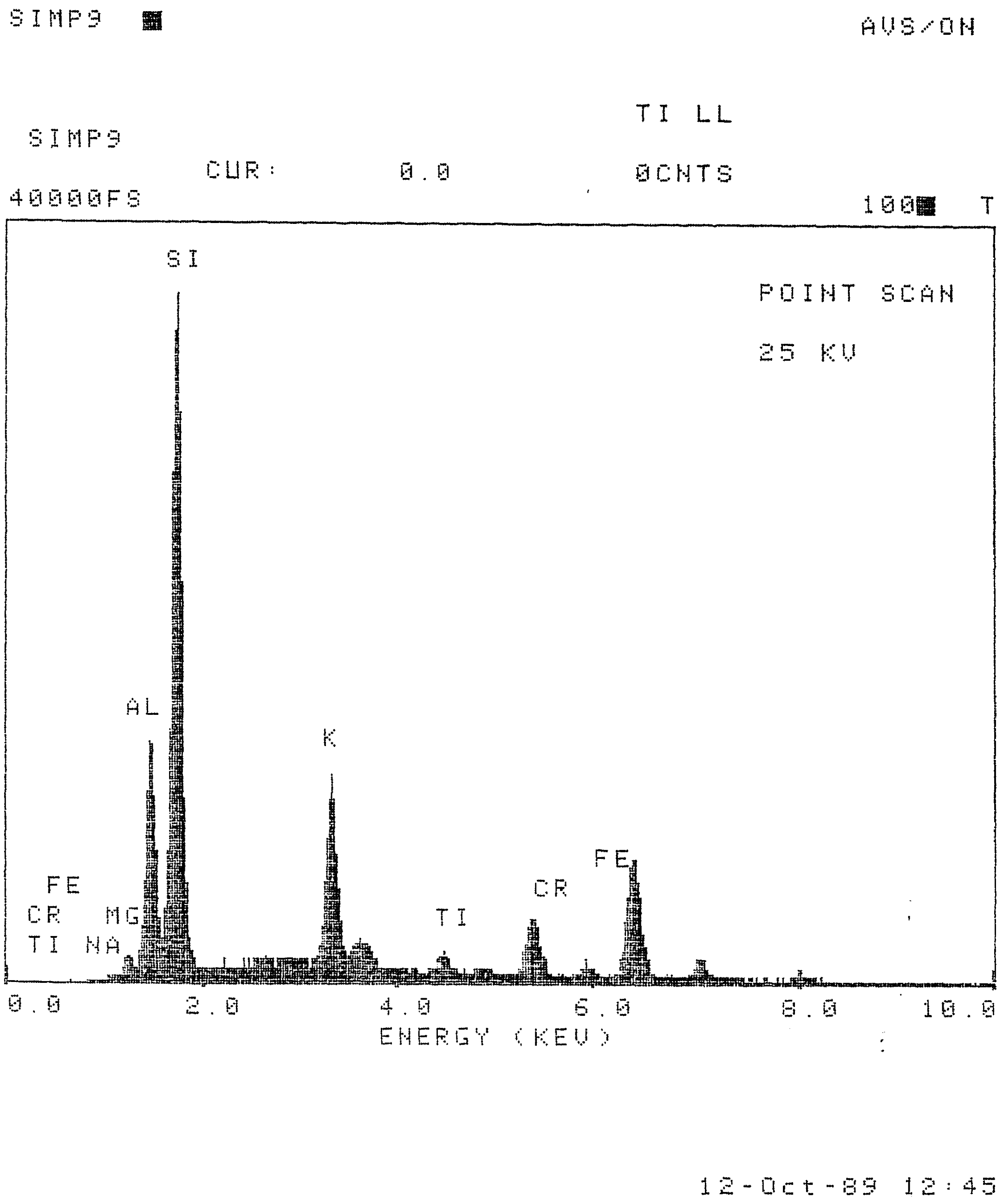
SIMP9
AVS/ON
TI LL
SIMP9
CUR: 0.0
0CNTS
40000FS
100 T
SI
POINT SCAN
25 KV
AL
K
FE
CR MG
TI NA
TI
CR
FE
0.0
2.0
4.0
6.0
8.0
10.0
ENERGY (KEV)
12-Oct-89 12:45

SIMP10 ■ AVS/ON

TI LL

SIMP10

CUR: 0.0 0CNTS

40000FS 100■ T

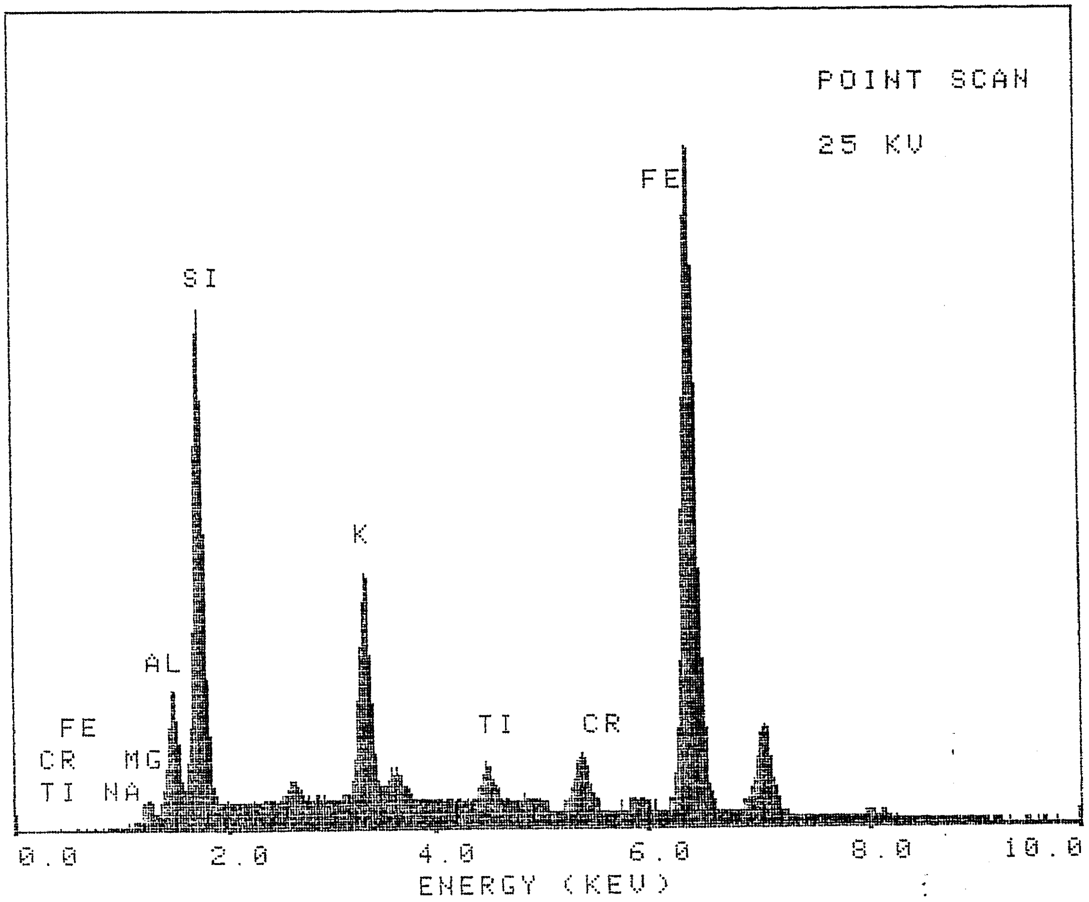

12-Oct-89 12:45

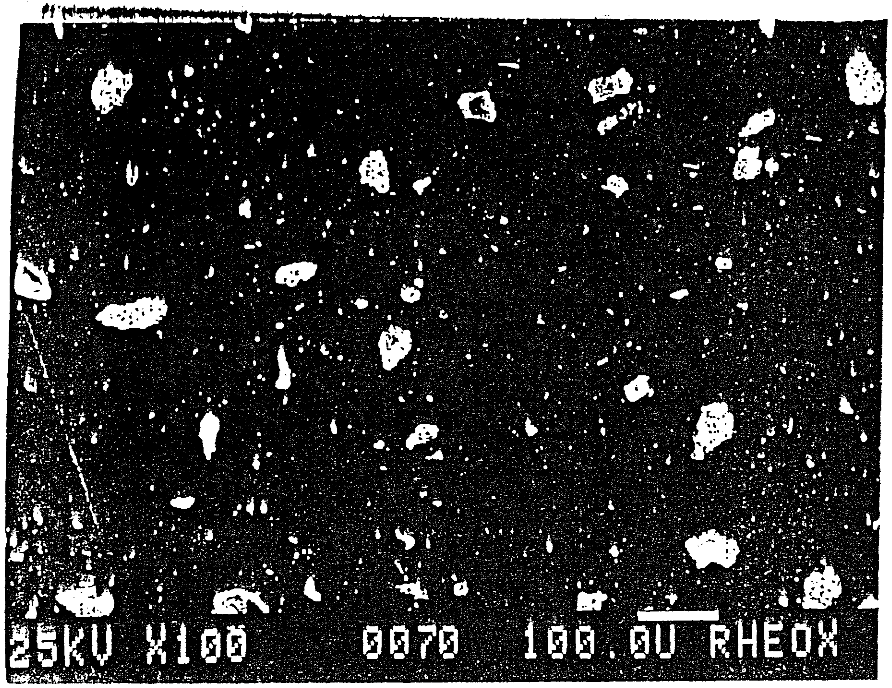

Figure 66

Figure 67 AL X-ray Image of Figure 66

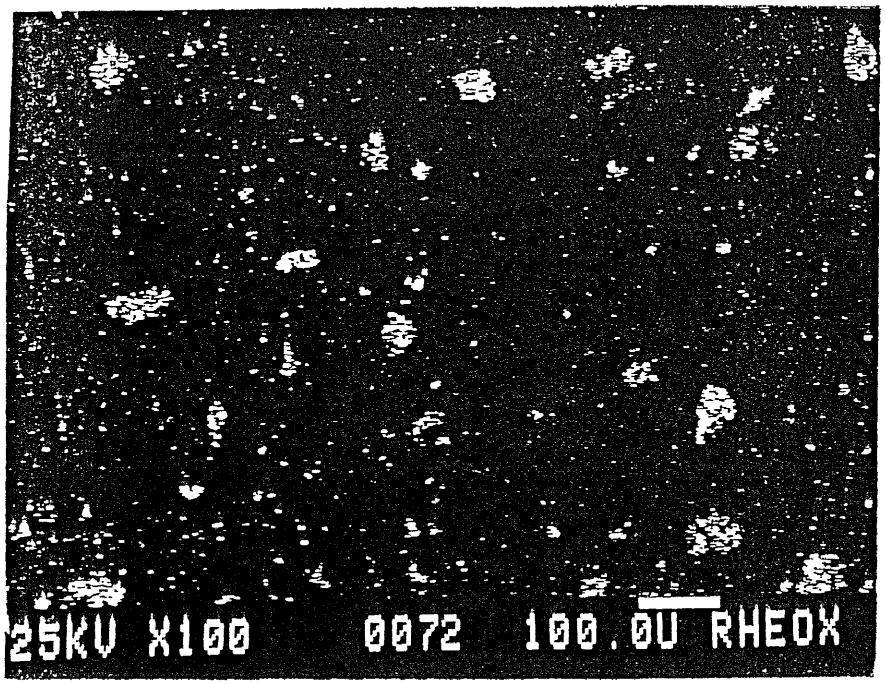

Figure 68 Si X-ray Image of Figure 66

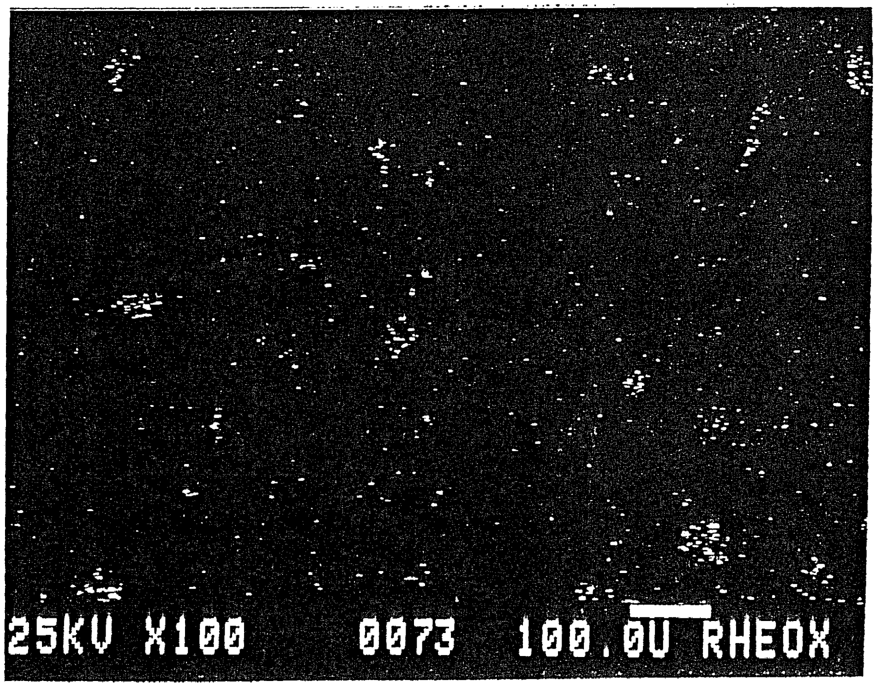

Figure 69 K X-ray Image of Figure 66

SEM IMAGES OF SAMPLE # Impregnated Cross Section

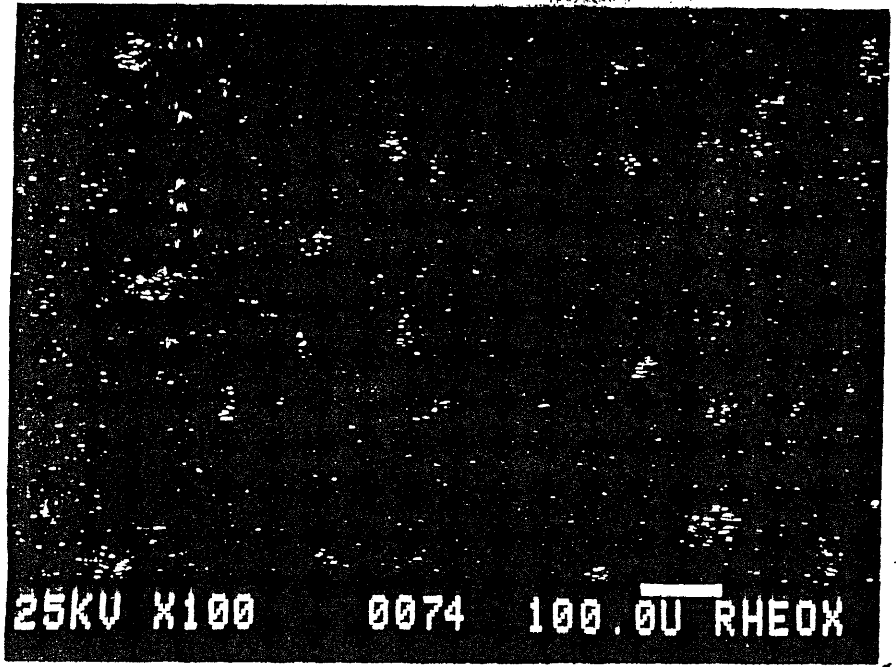

Figure 70 Ti X-Ray Image of Figure 66

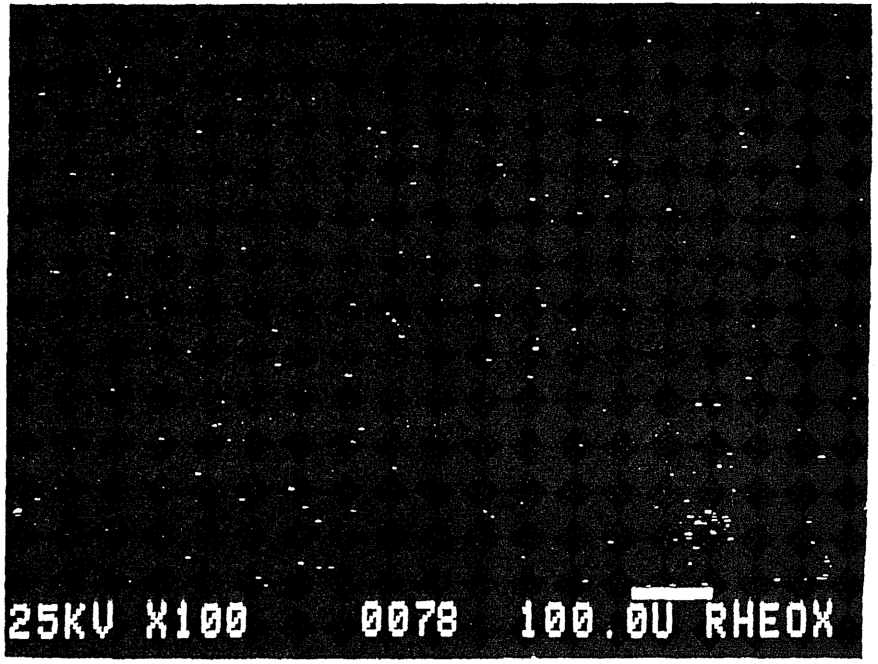

Figure 71 Cr X-Ray Image of Figure 66

Figure 72 Fe X-Ray Image of Figure 66

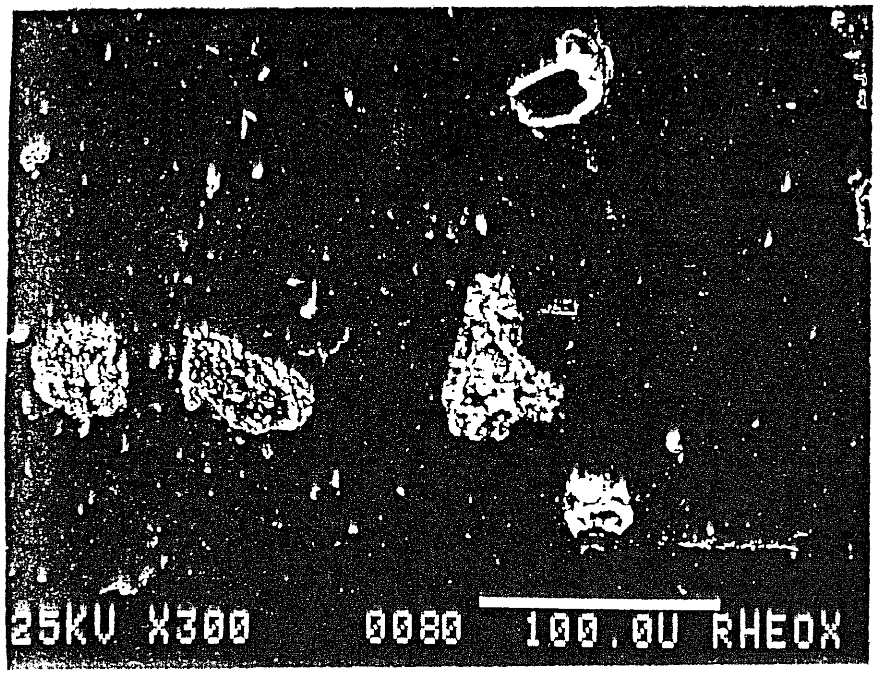

Figure 73

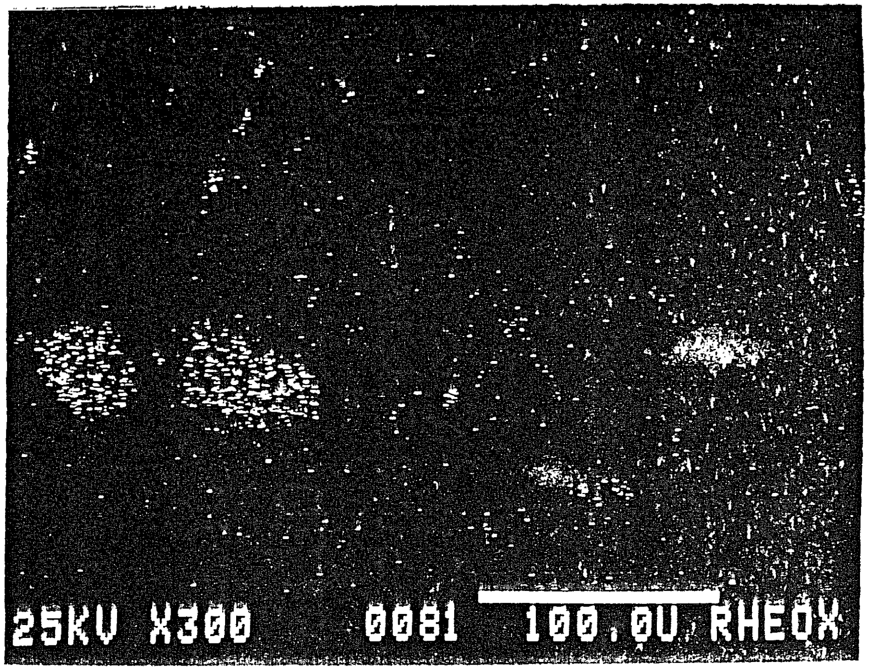

Figure 74 AL X-ray Image of Figure 73

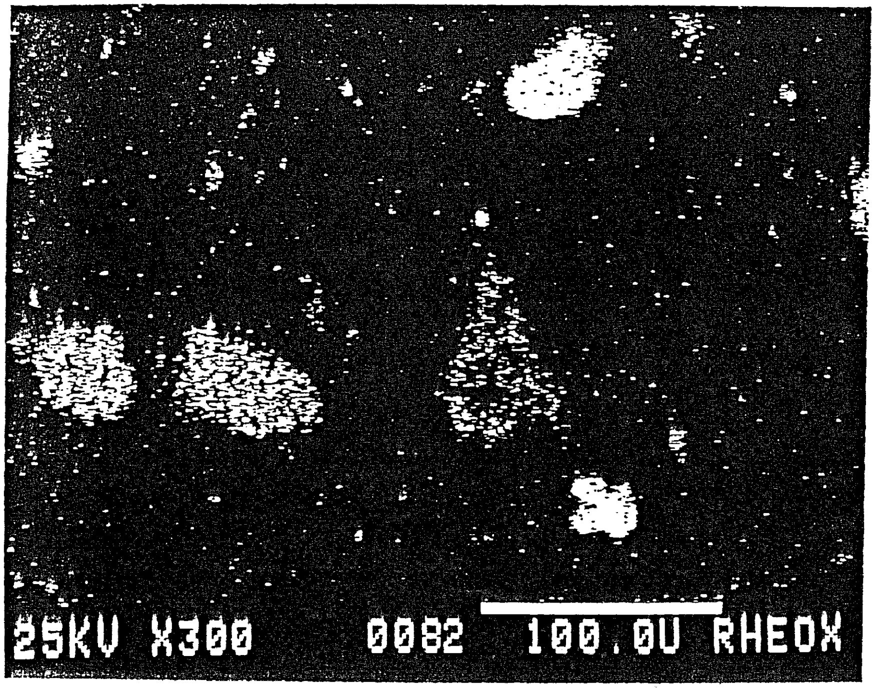

Figure 75 Si X-ray Image of Figure 73

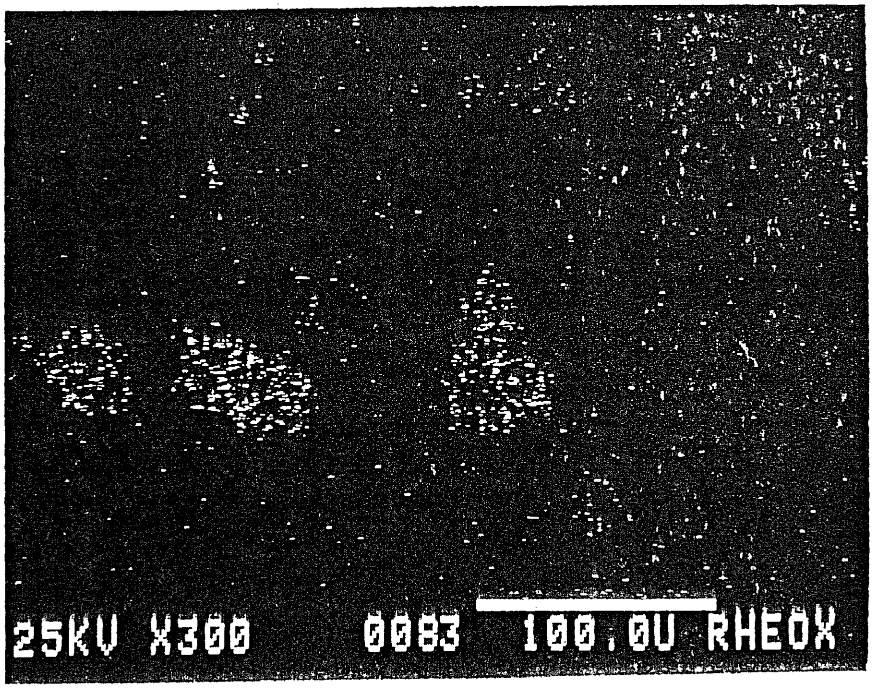

Figure 76 K X-ray Image of Figure 73

SEM IMAGES OF SAMPLE # Impregnated Cross Section

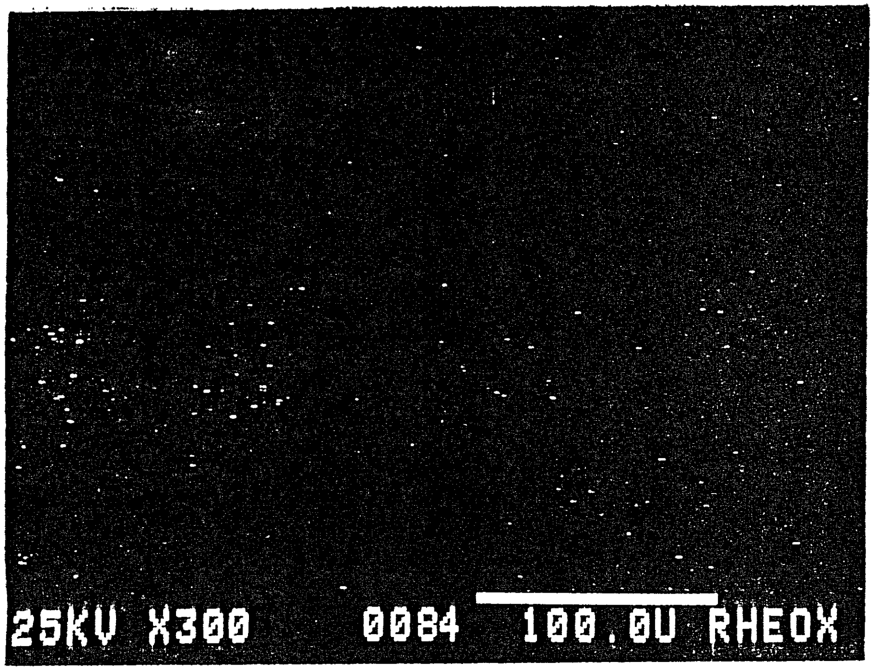

Figure 77 Ti X-Ray Image of Figure 73

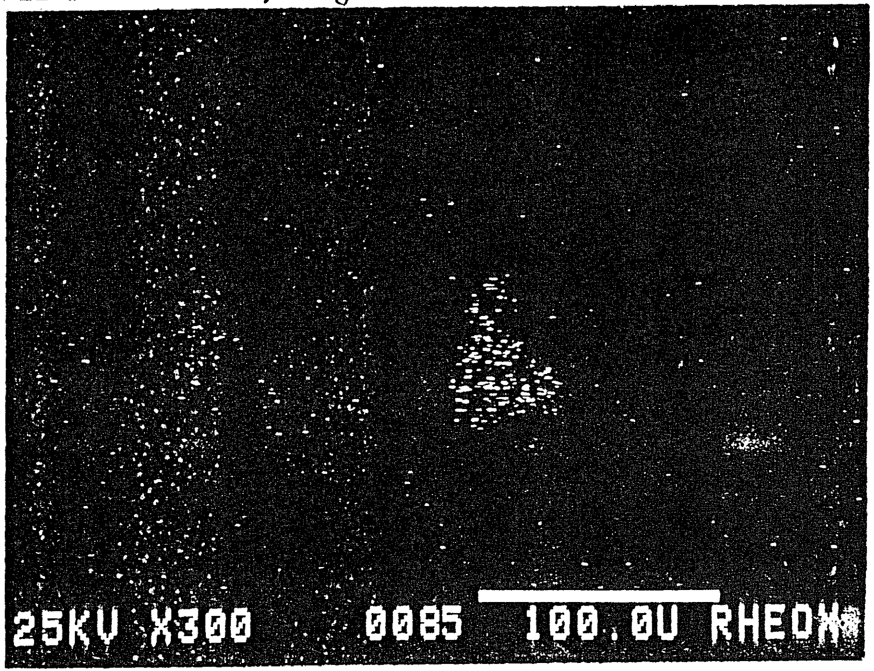

Figure 78 Cr X-Ray Image of Figure 73

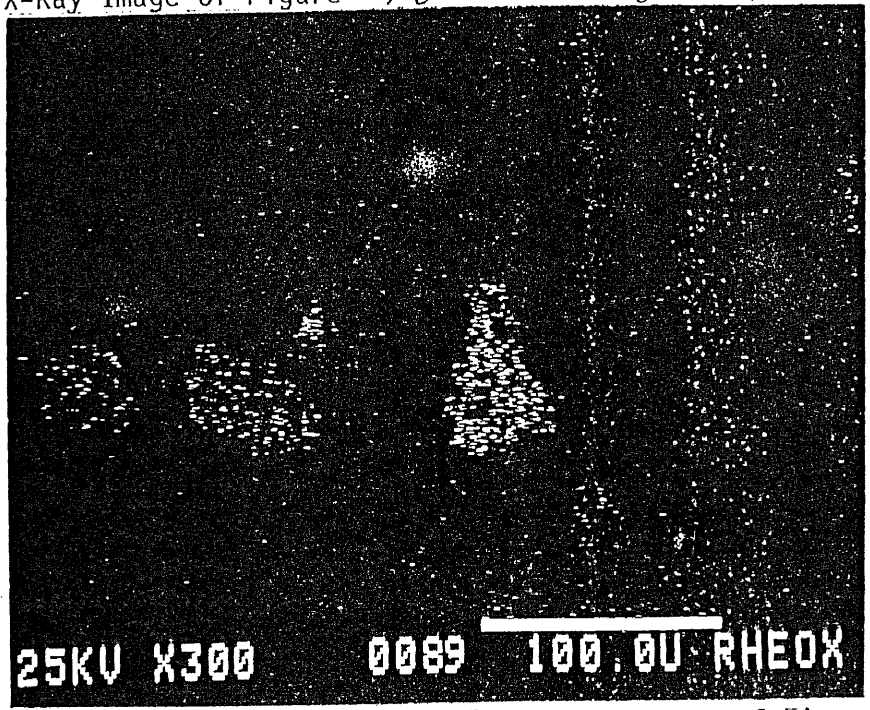

Figure 79 Fe X-Ray Image of Figure 73

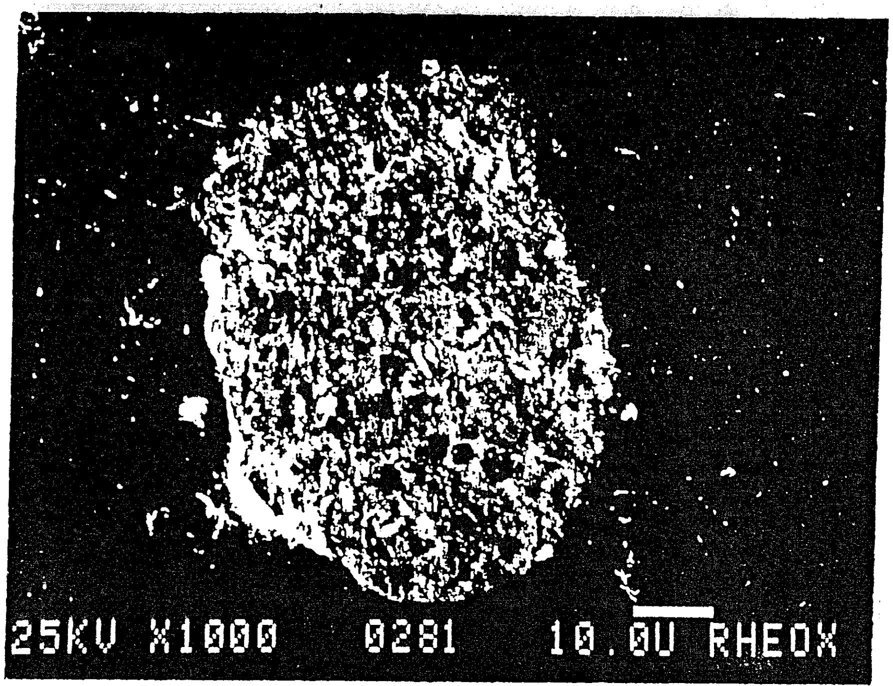

Figure 80

Line Profile Scan

AL

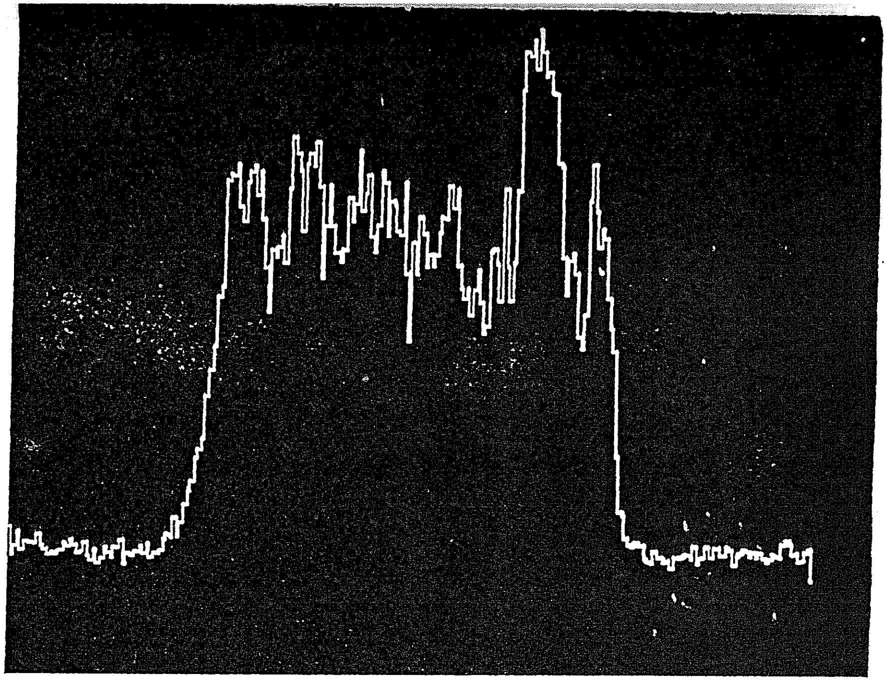

Figure 81

Si

K

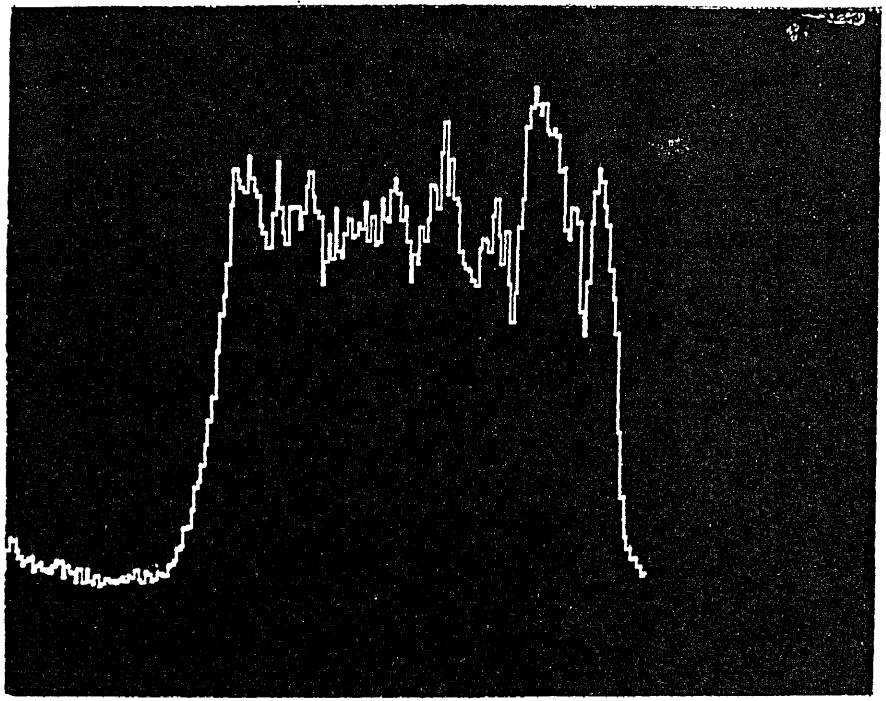

Figure 82

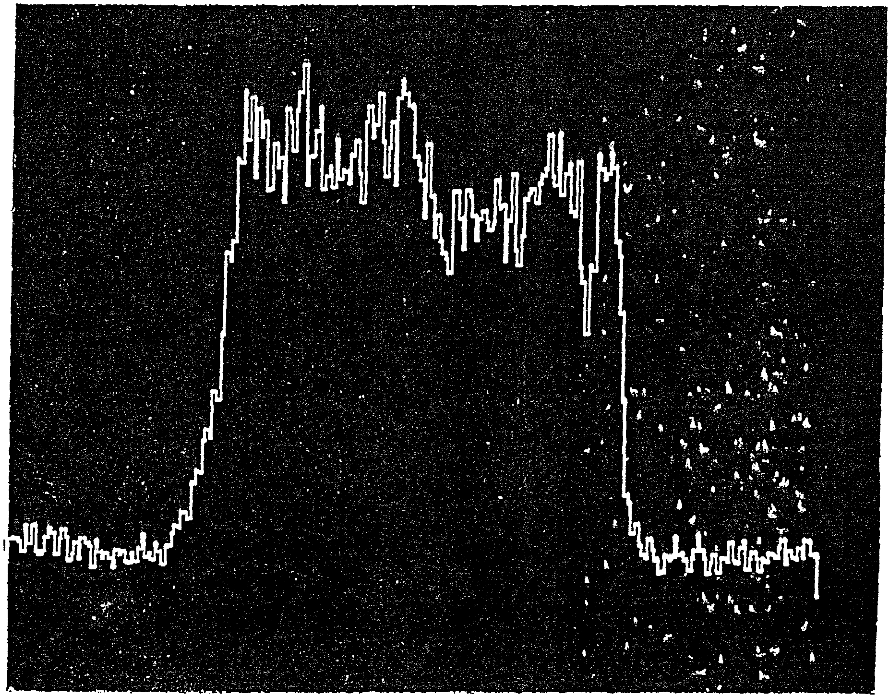

Figure 83

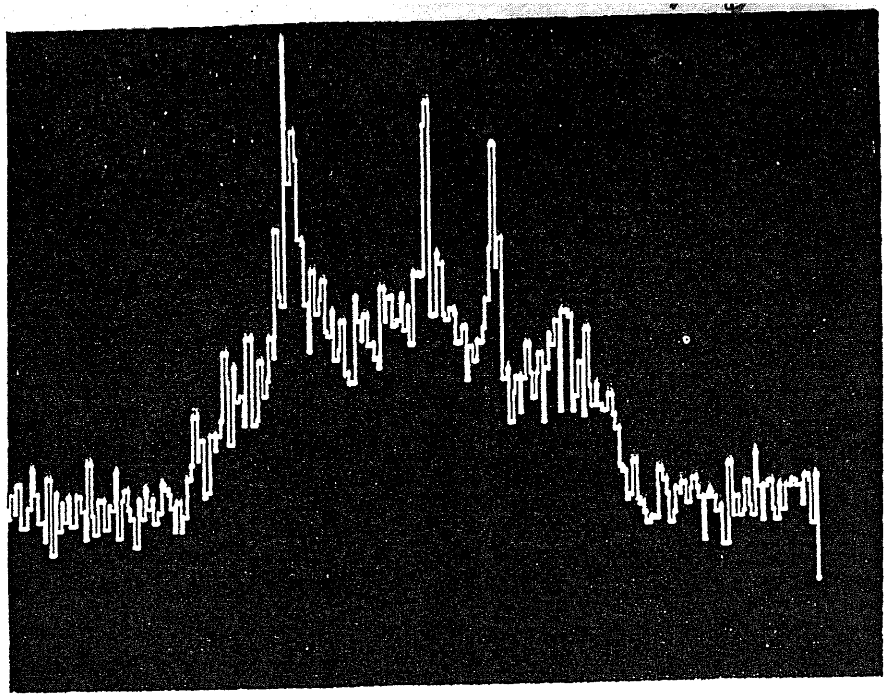

Figure 84 Line Profile Scan

Ti ←

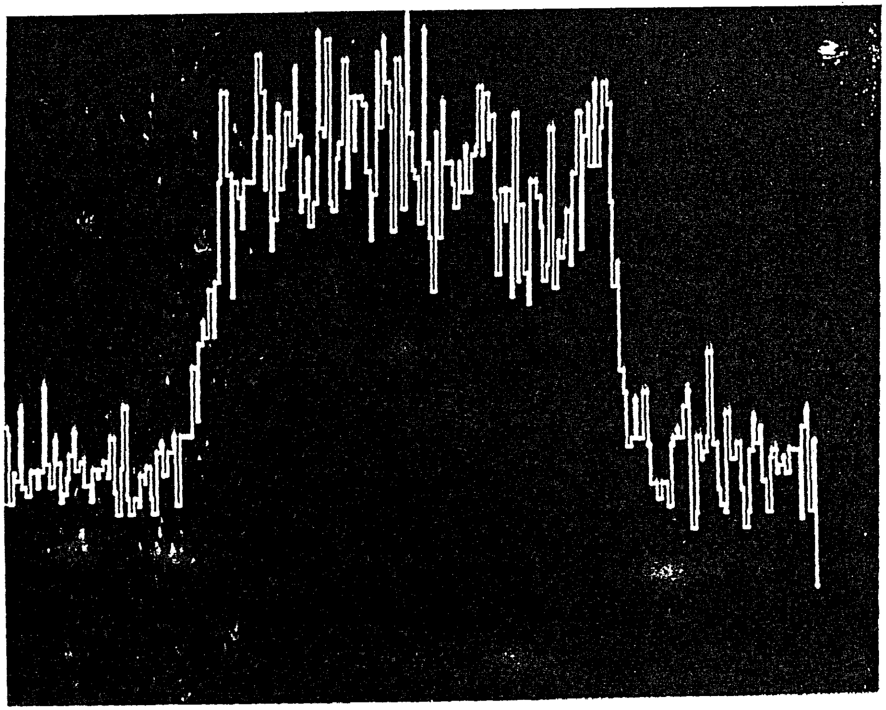

Figure 85

Cr ←

Fe →

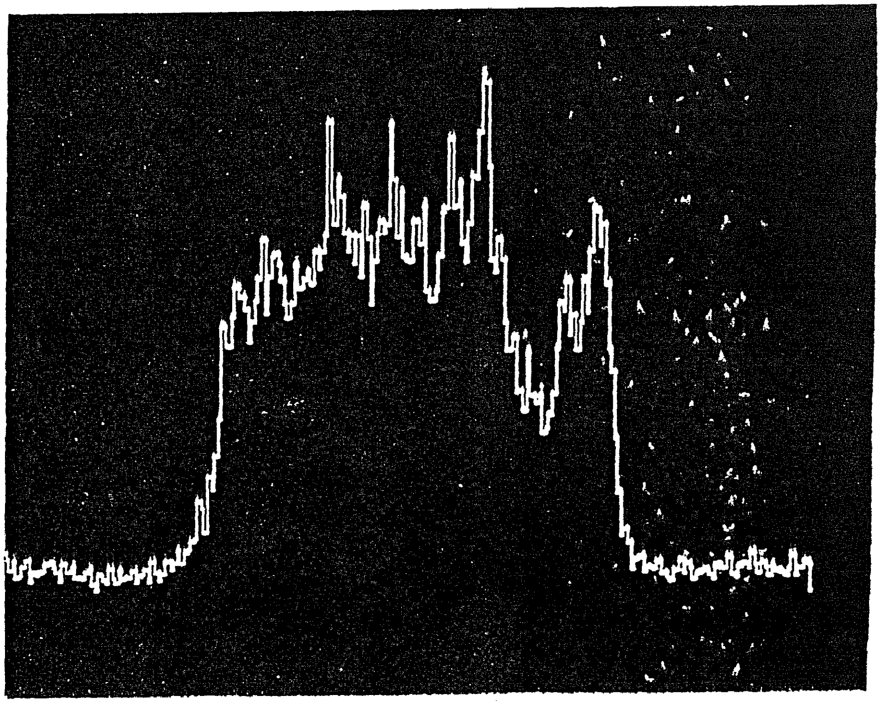

Figure 86

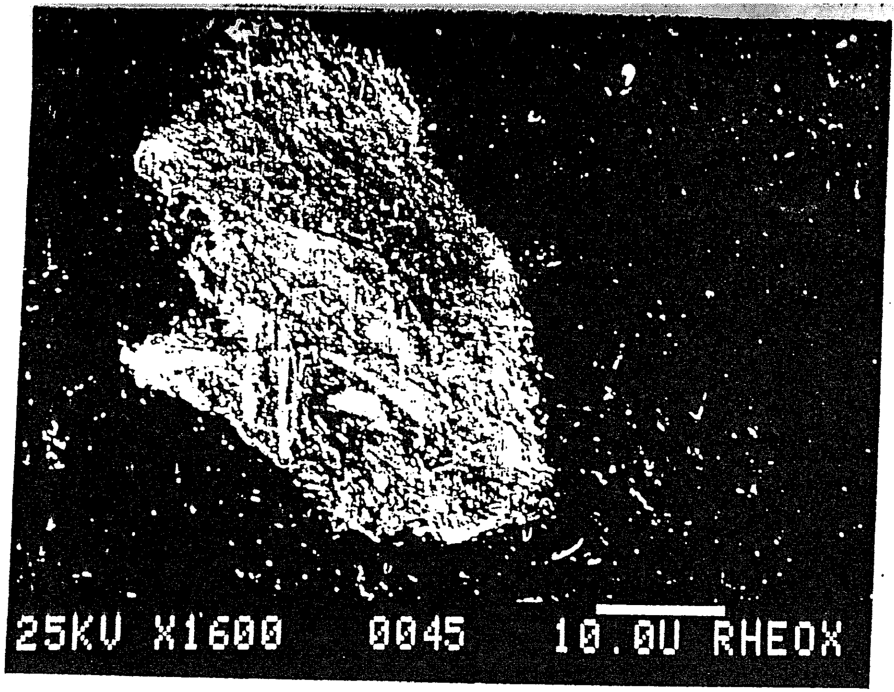

Figure 87

Line Profile Scans

AL →

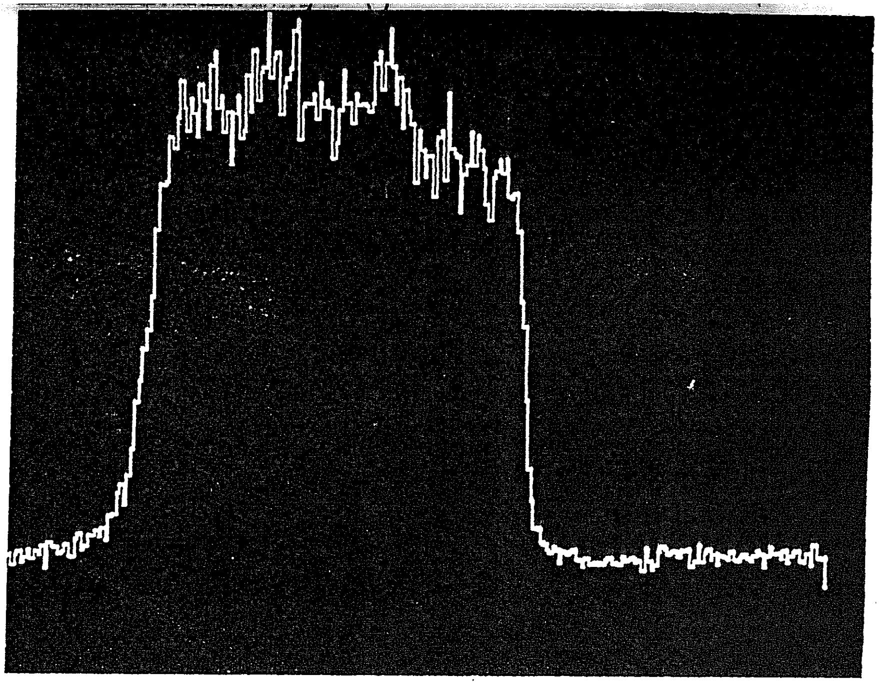

Figure 88

Si ←

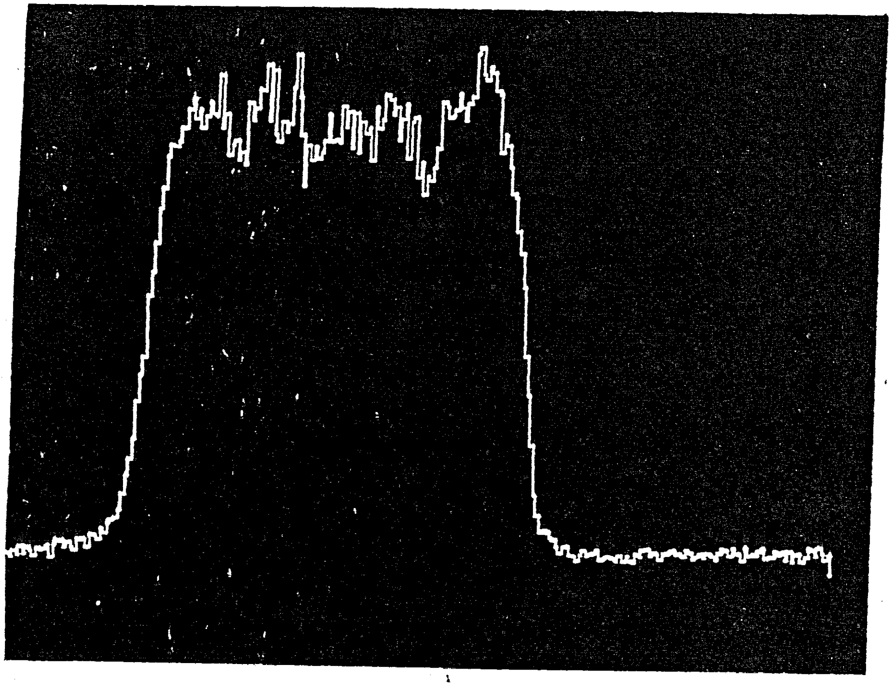

Figure 89

K →

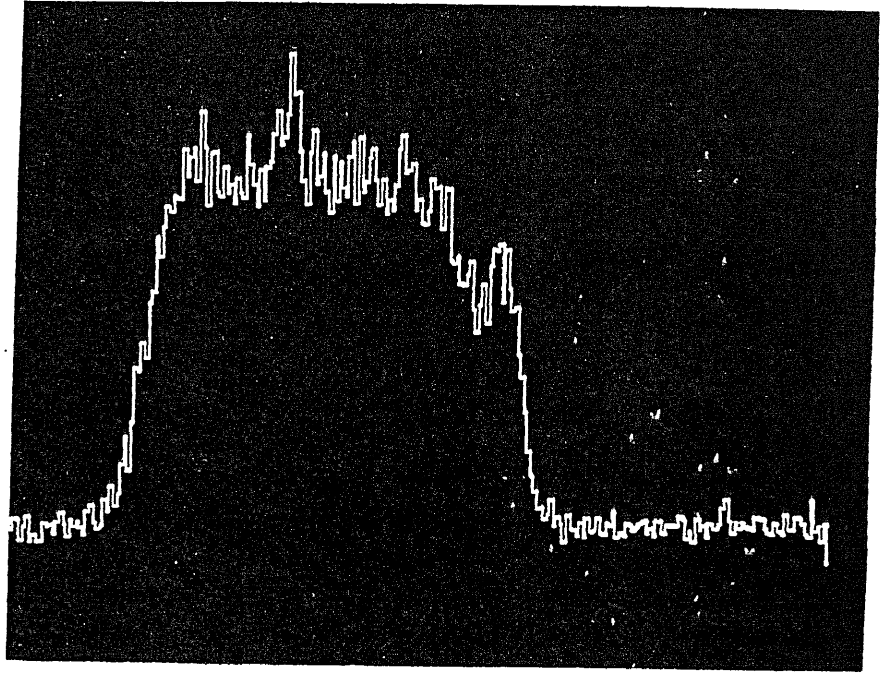

Figure 90

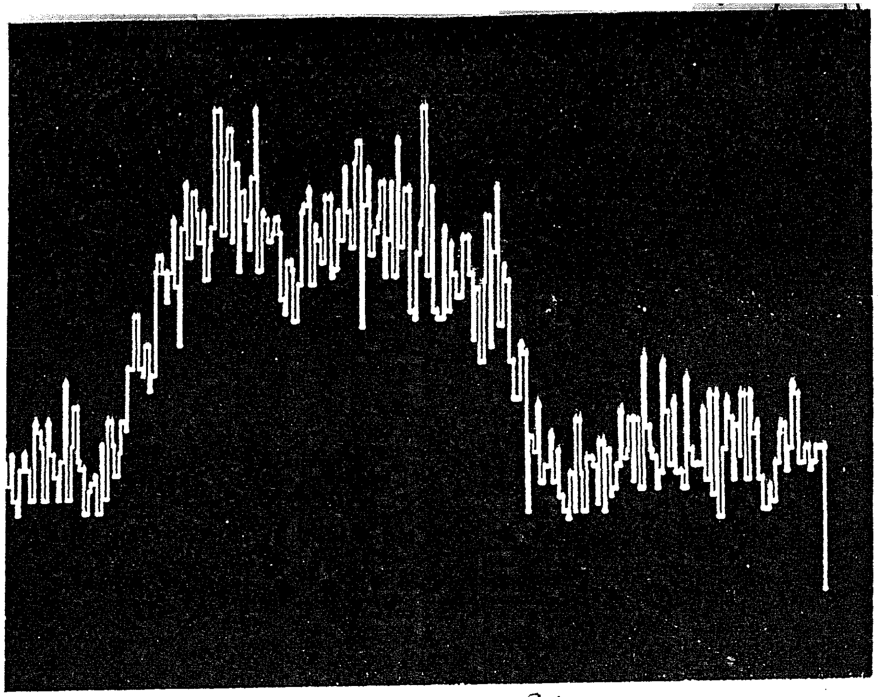

Figure 91
Line Profile Scans

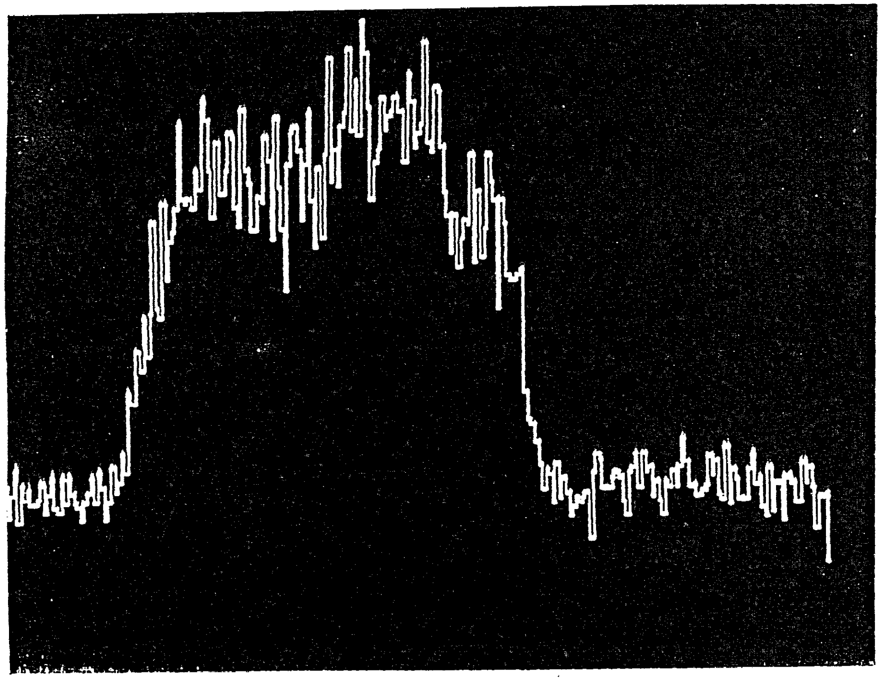

Figure 92

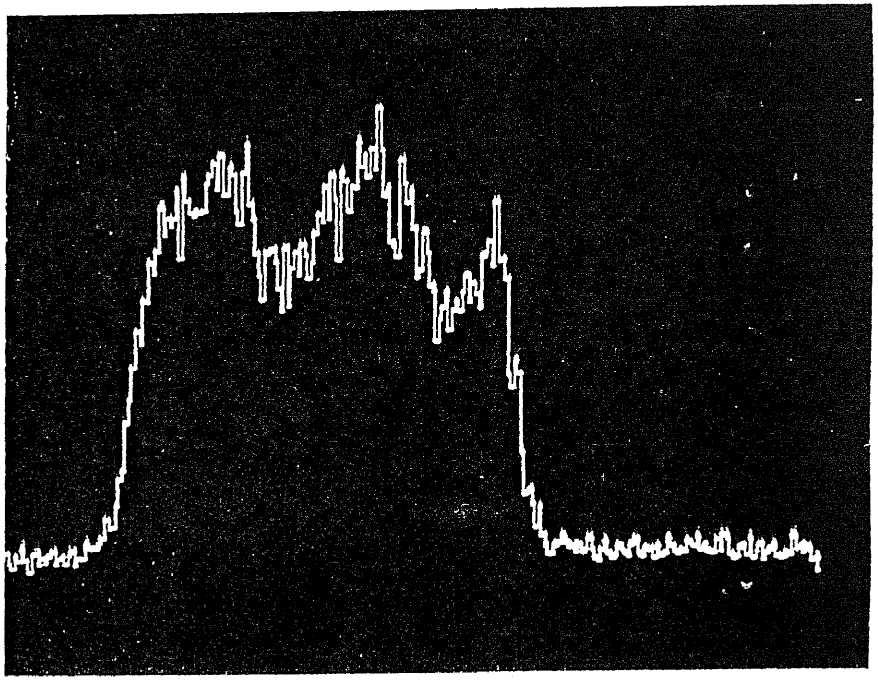

Figure 93

Figure 94

AL →

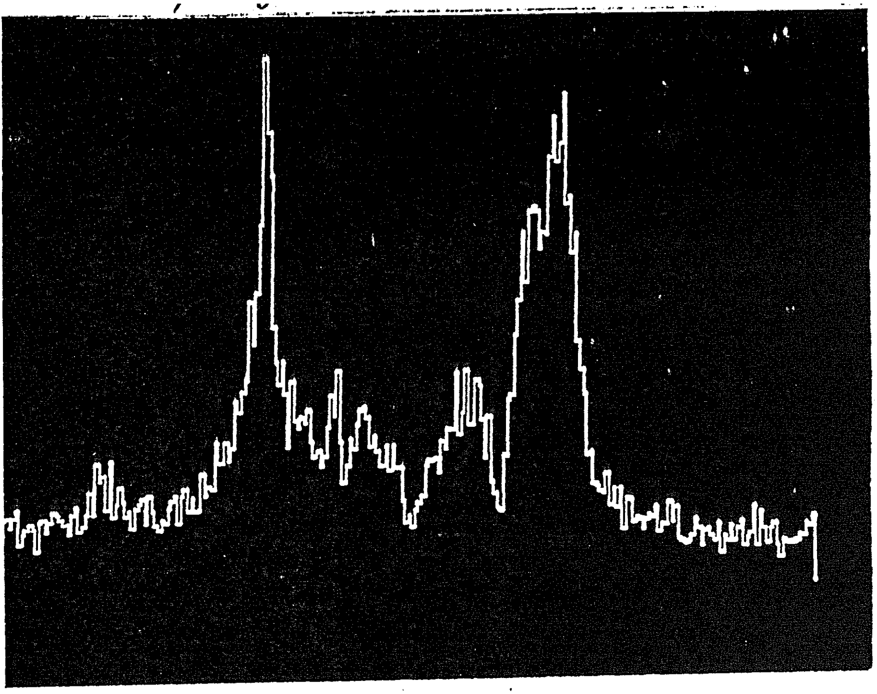

Figure 95

Line Profile Scan

Si ←

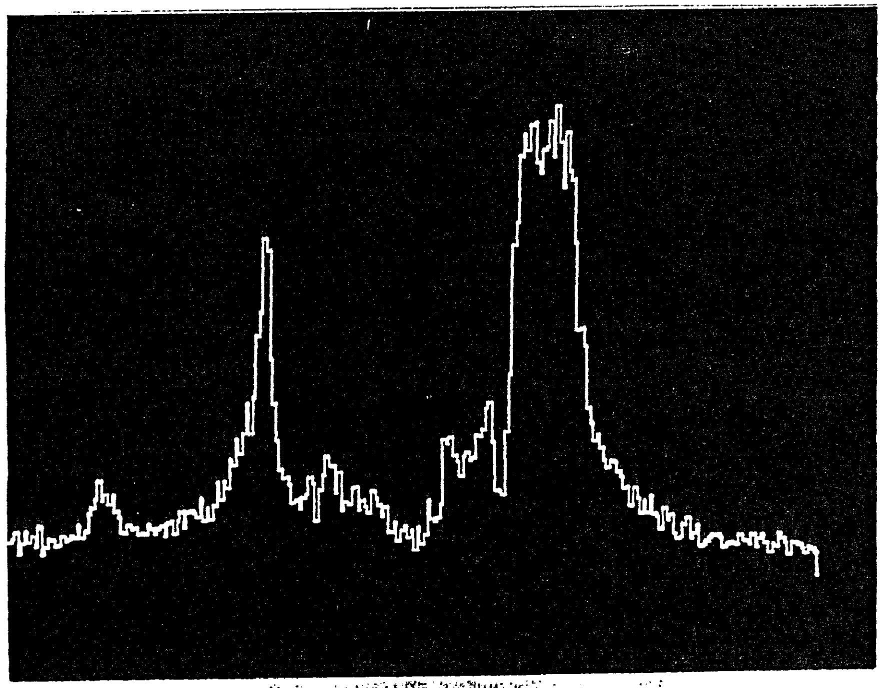

Figure 96

K →

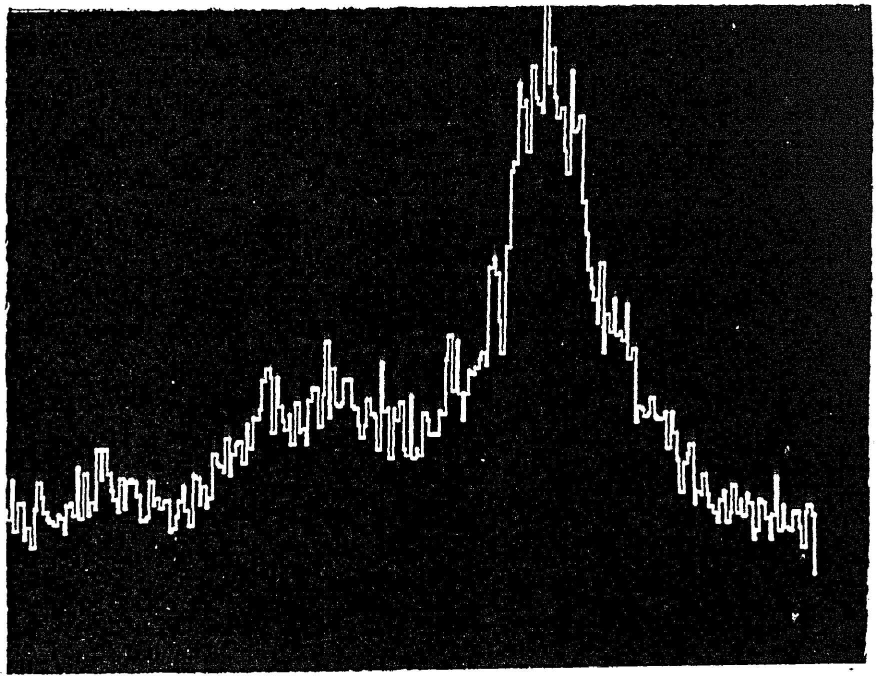

Figure 97

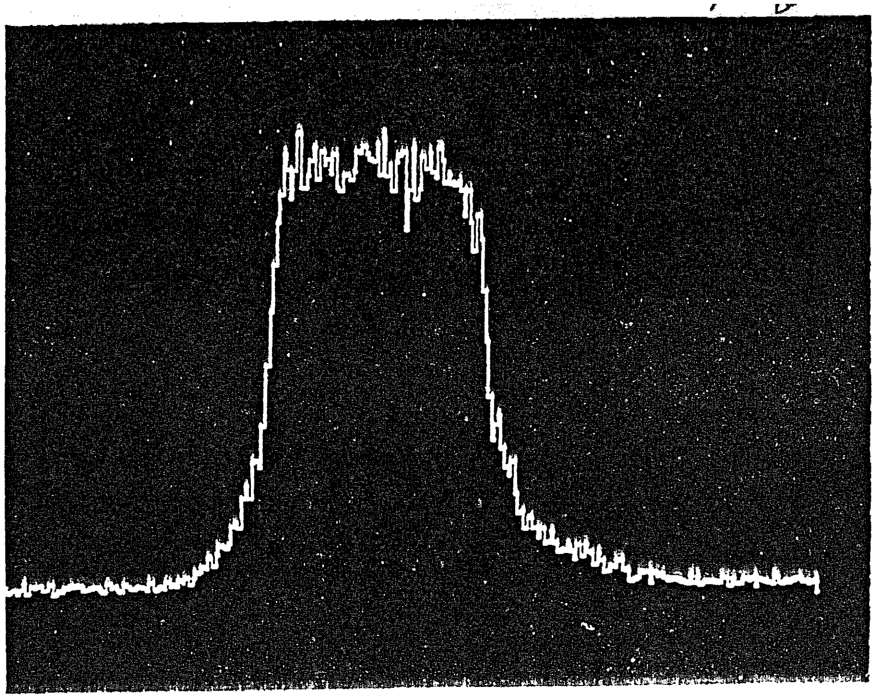

Ti ←

Figure 98 Line Profile Scan

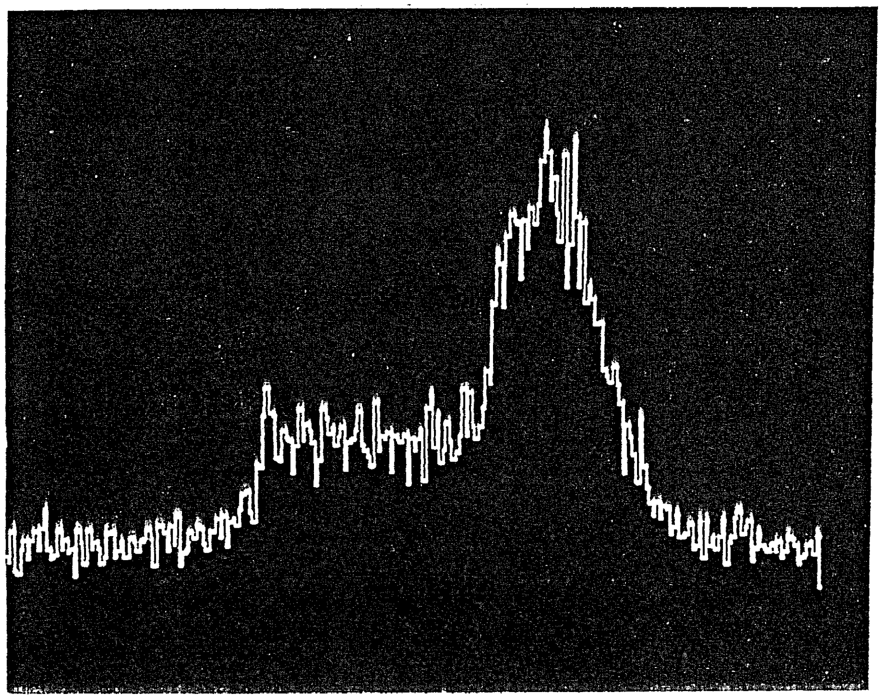

Cr ←

Fe →

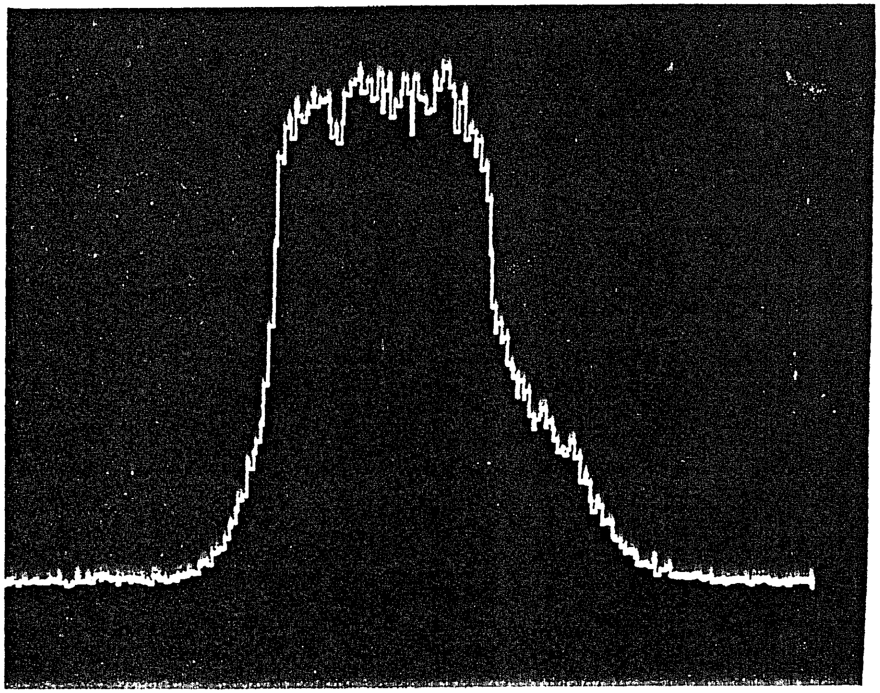

Figure 99

Figure 100

```
SIMP11 ■                                                AVS/ON .

                                          CA LL
 SIMP11
          CUR:          0.0               0CNTS
40000FS                                                  100■   T
```

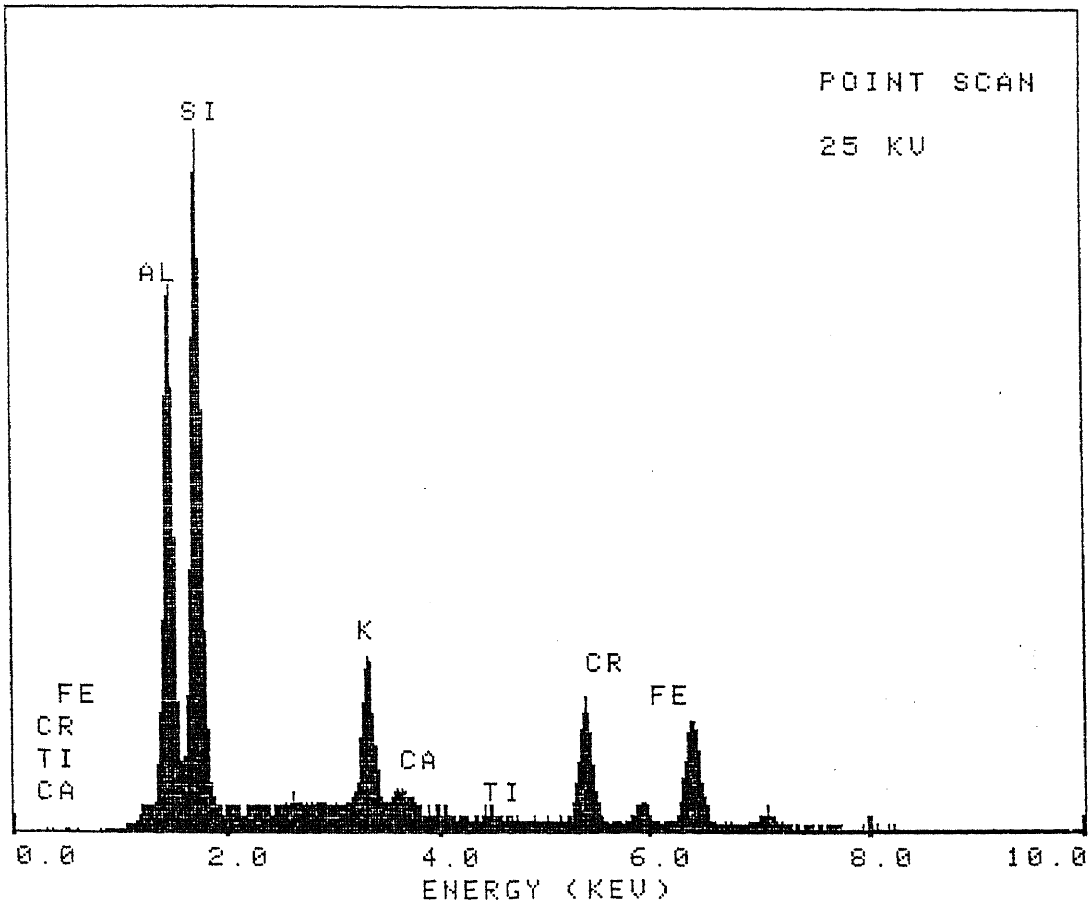

```
            SAVE THE STATE OF THE SYSTEM
ARE YOU SURE ? * Y

                                           20-Oct-89 11:35
```

SIMP12 ■ AVS/ON.

CA LL

SIMP12

CUR: 0.0 0CNTS

40000FS 100■ T

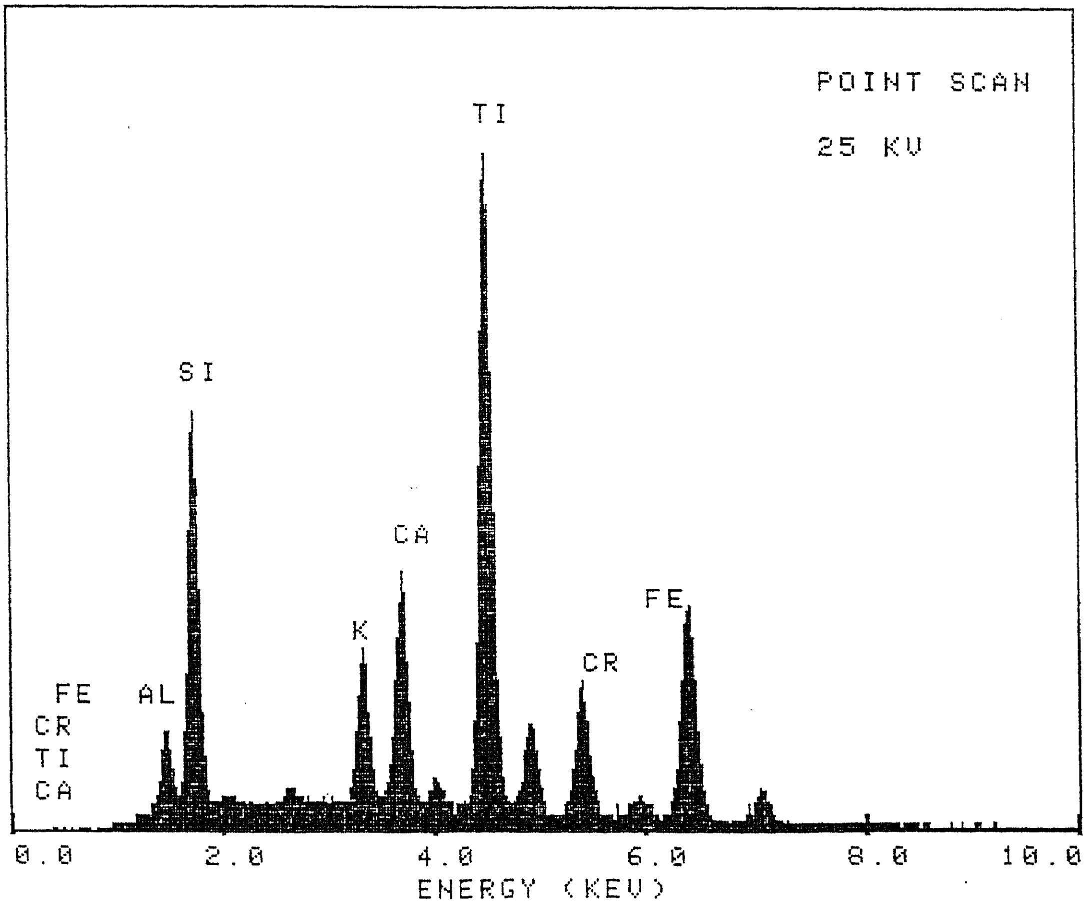

20-Oct-89 11:35

SIMP13 ▇ AVS/ON

CA LL

SIMP13

CUR: 0.0 0CNTS

40000FS 100▇ T

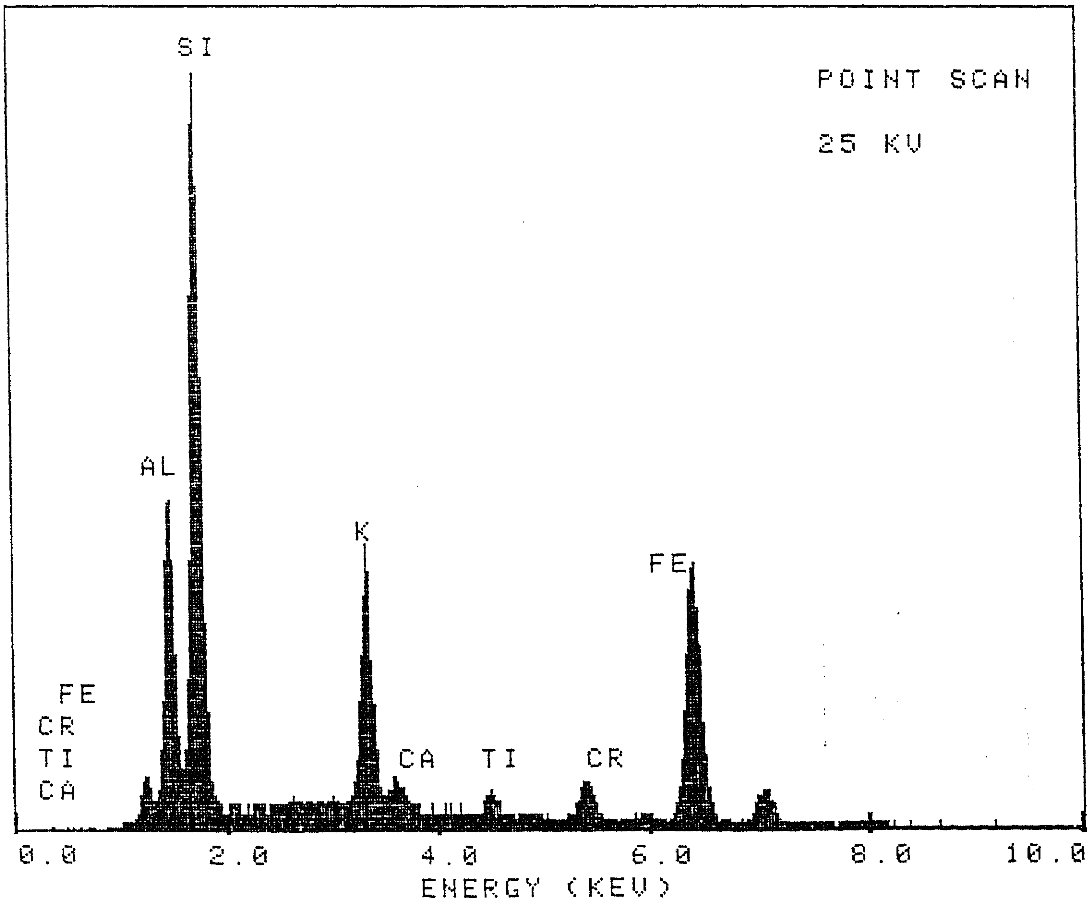

20-Oct-89 11:35

SIMP14 ■ AVS/ON

CA LL

SIMP14

CUR: 0.0 0CNTS

40000FS 100■ T

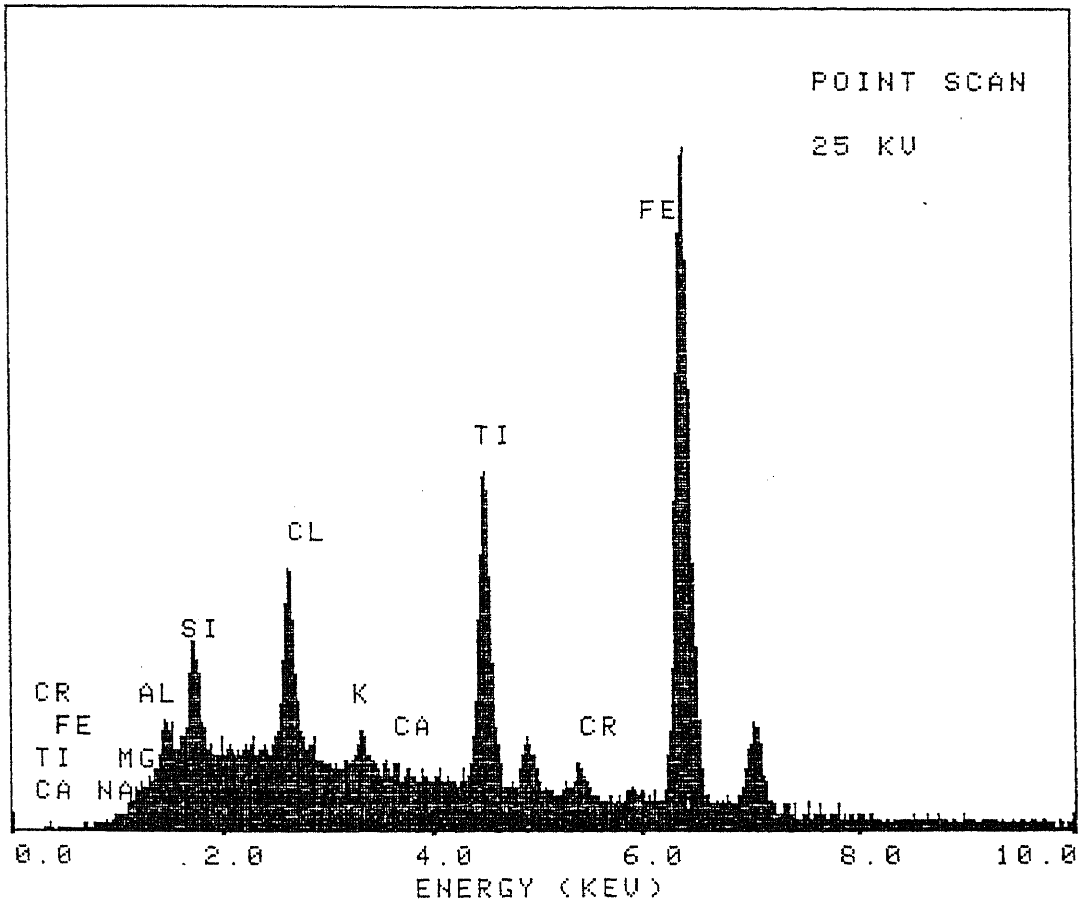

20-Oct-89 11:35

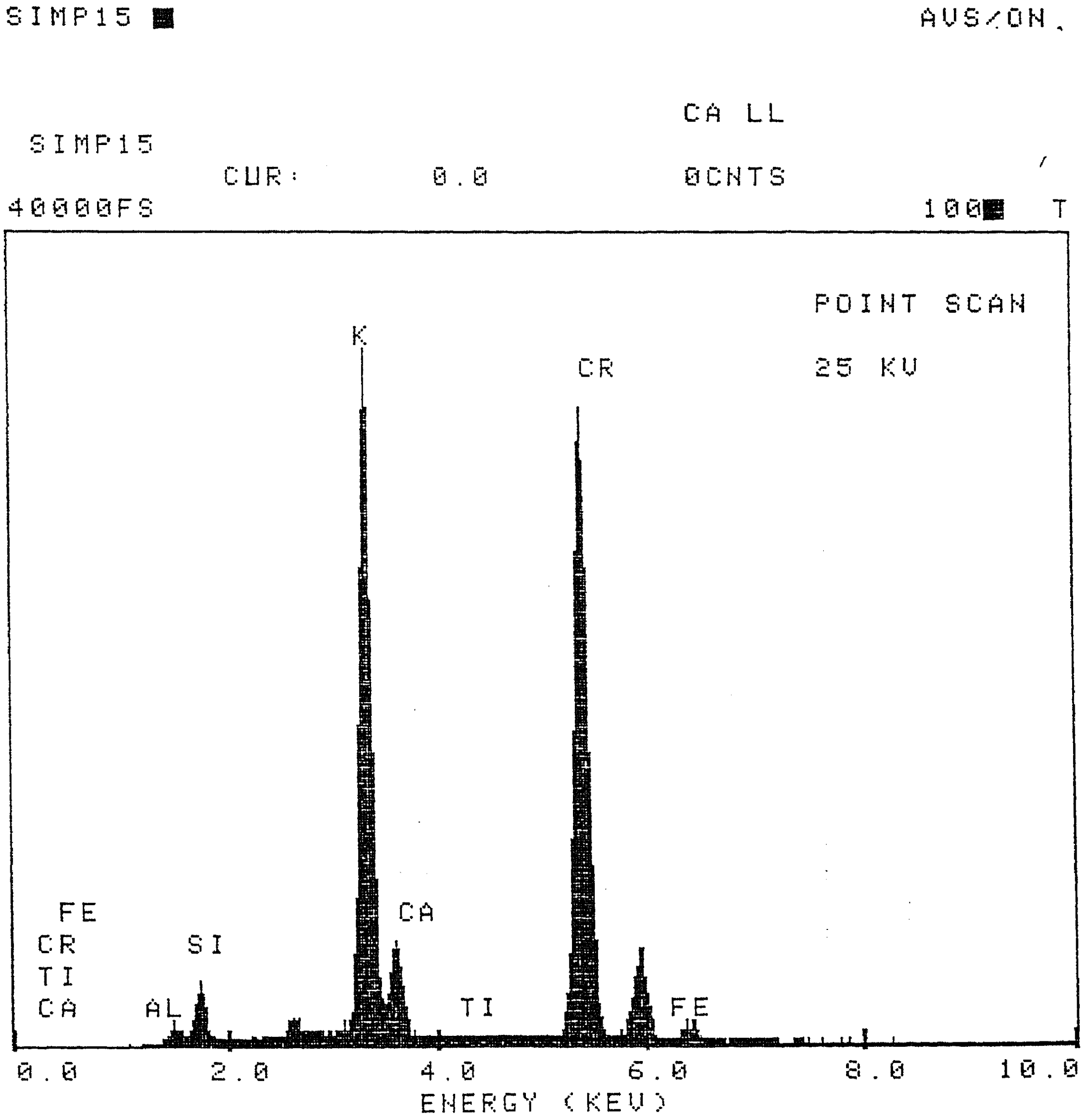

20-Oct-89 11:35

SIMP16 ▩ AVS/ON .

CA LL

SIMP16

CUR: 0.0 0CNTS

40000FS 100▩ T

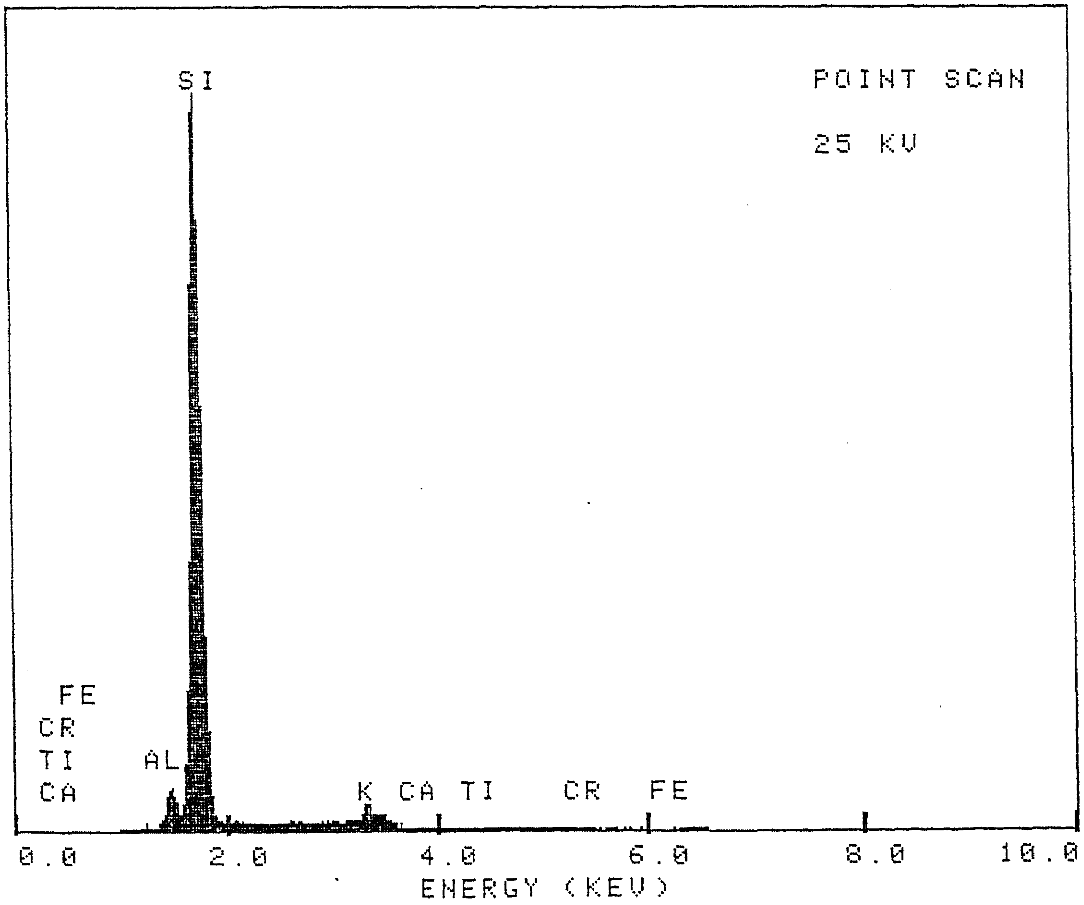

20-Oct-89 11:35

SIMP17 ■ AVS/ON

CA LL

SIMP17

CUR: 0.0 0CNTS

40000FS 100■ T

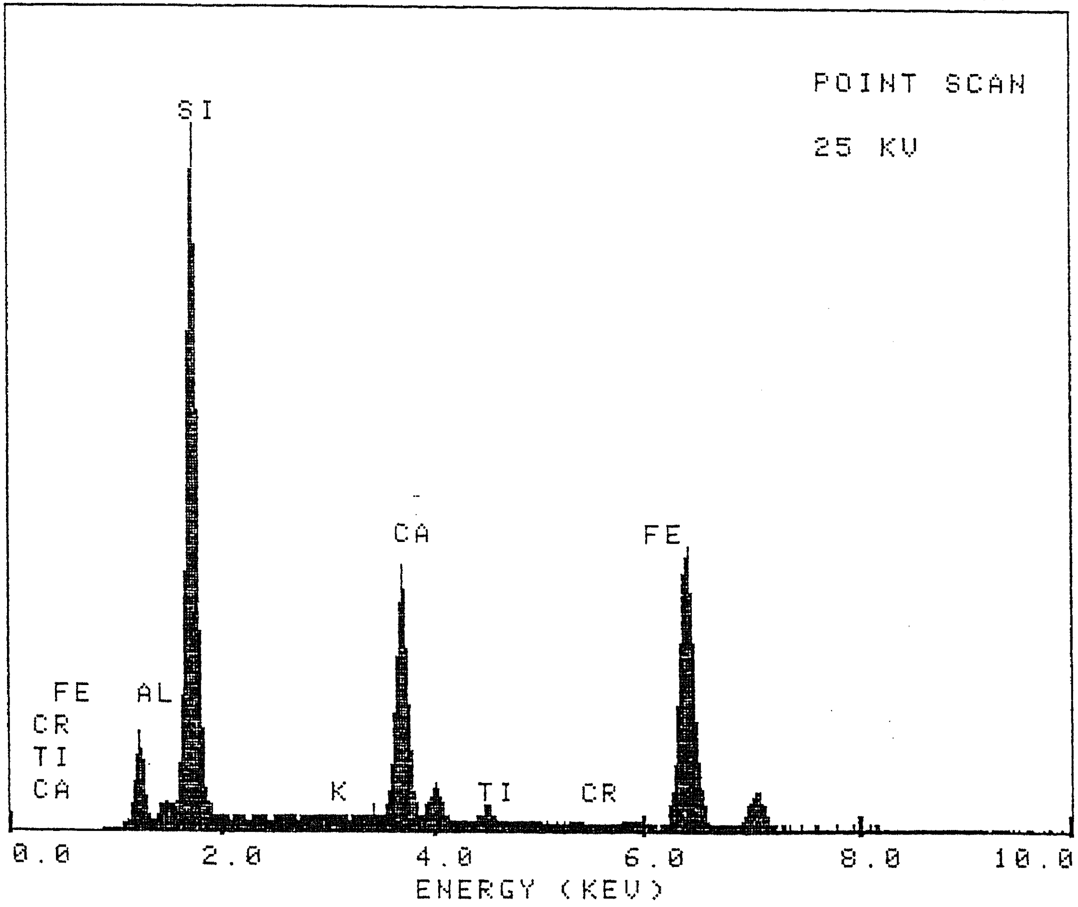

20-Oct-89 11:35

SIMP18 ■ AVS/ON.

CA LL

SIMP18

CUR: 0.0 0CNTS

40000FS 100■ T

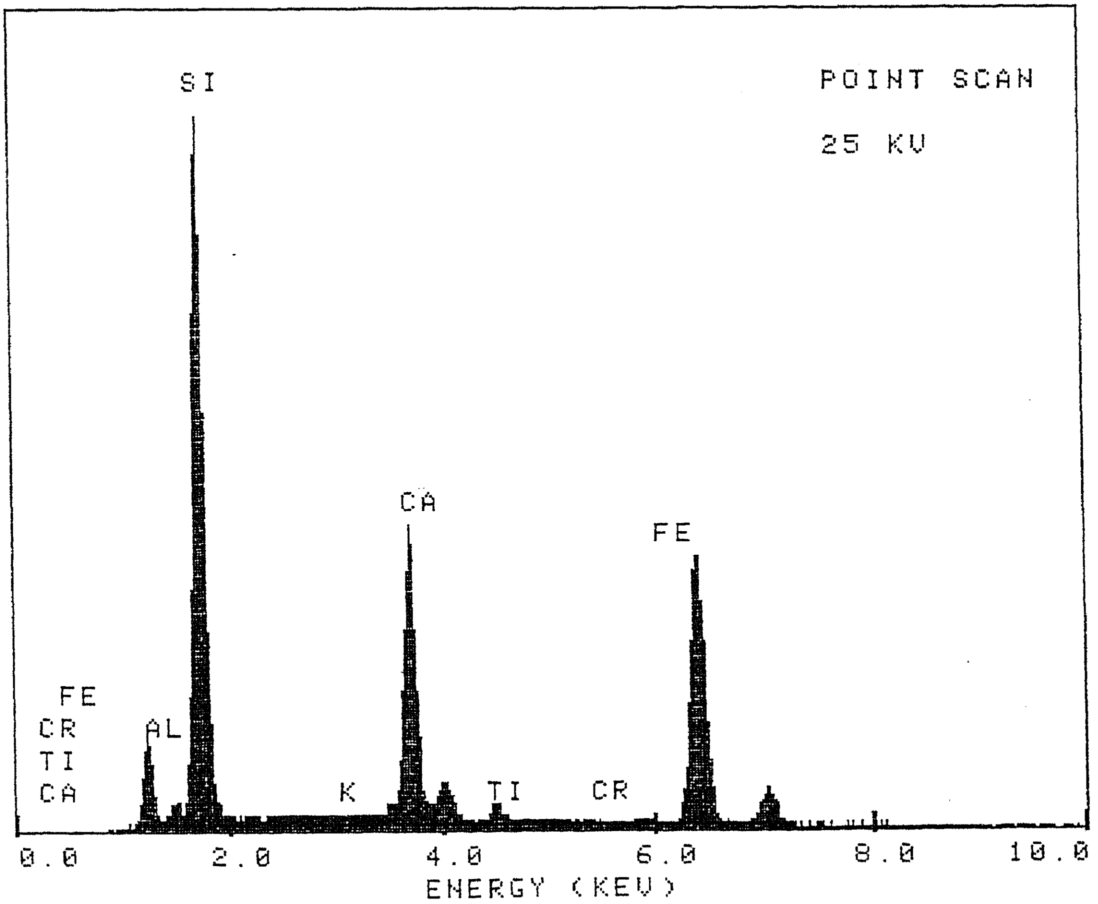

20-Oct-89 11:35

SIMP19 ■ AVS/ON

CA LL

SIMP19

CUR: 0.0 0CNTS

40000FS 100■ T

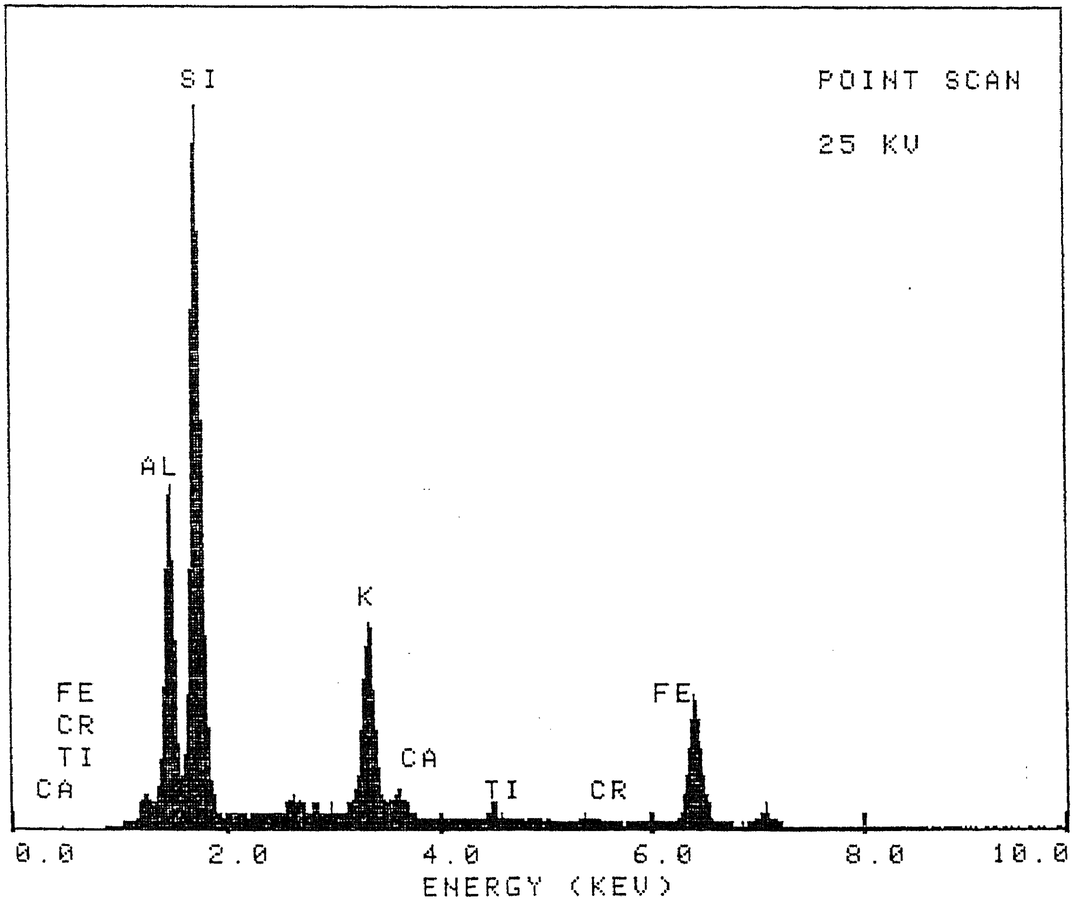

20-Oct-89 11:35

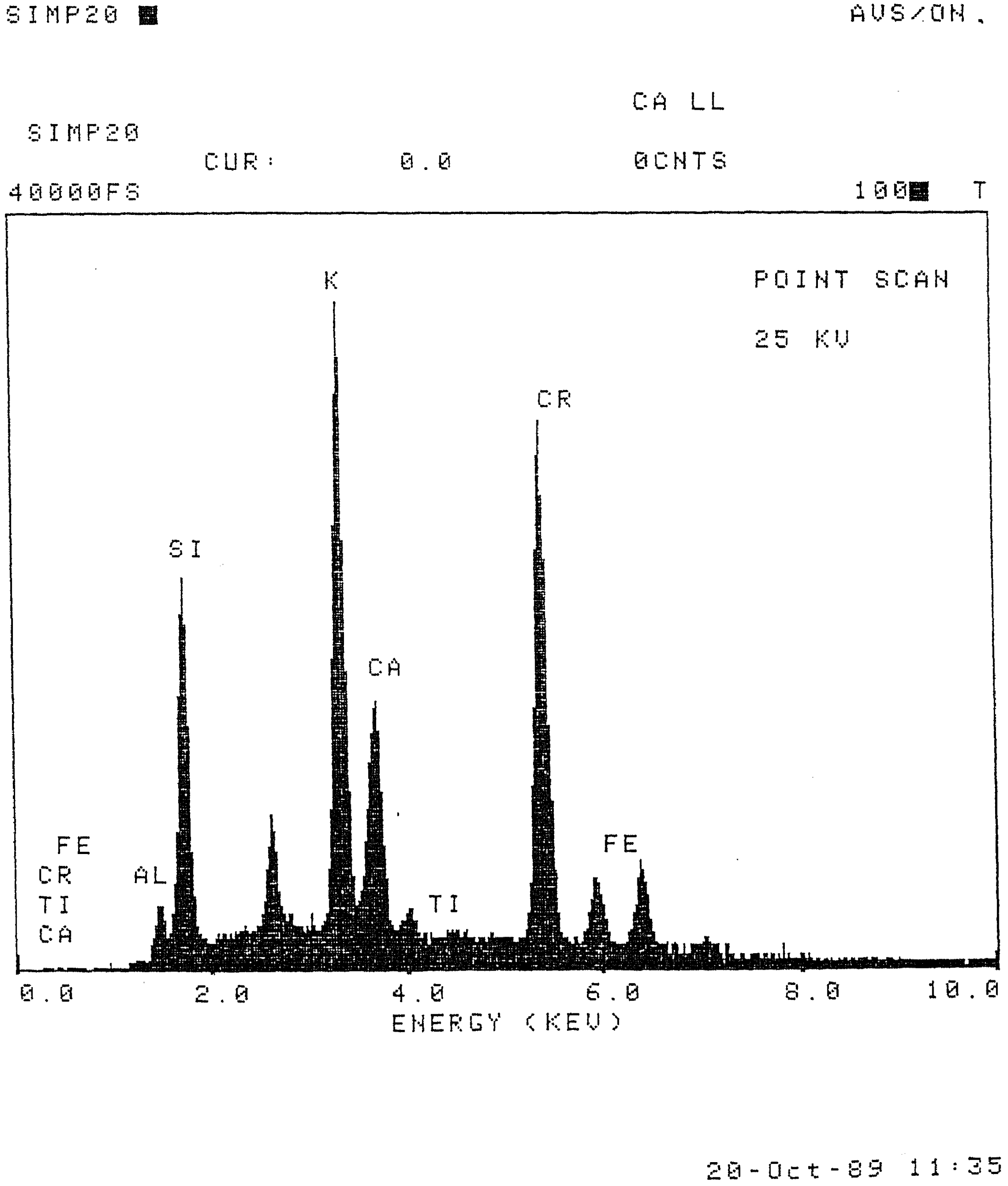
SIMP20 ■
AVS/ON.
CA LL
SIMP20
CUR: 0.0
0CNTS
40000FS
100■ T
POINT SCAN
25 KV
K
CR
SI
CA
FE
CR
TI
CA
AL
TI
FE
0.0
2.0
4.0
6.0
8.0
10.0
ENERGY (KEV)
20-Oct-89 11:35

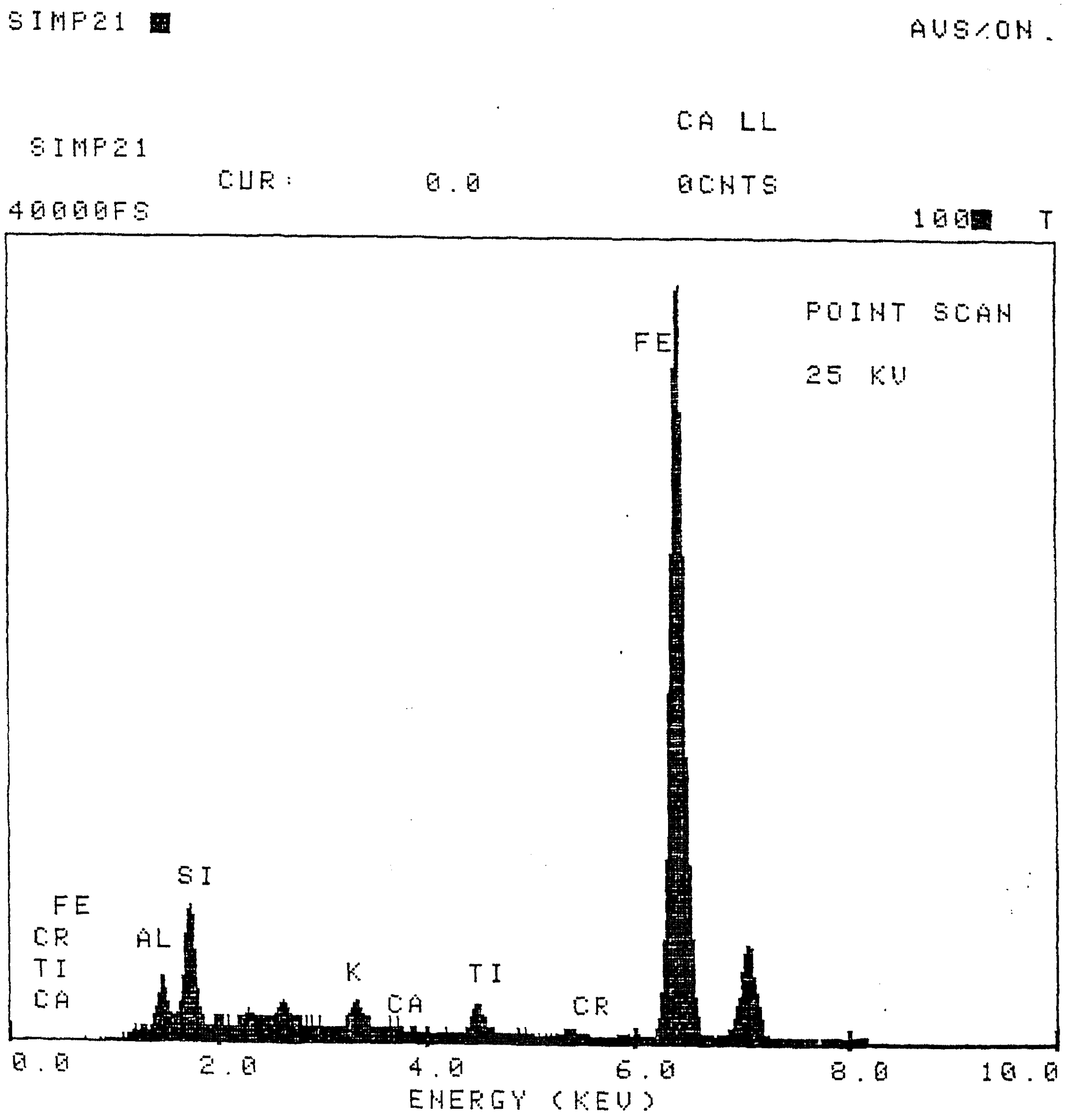

20-Oct-89 11:35

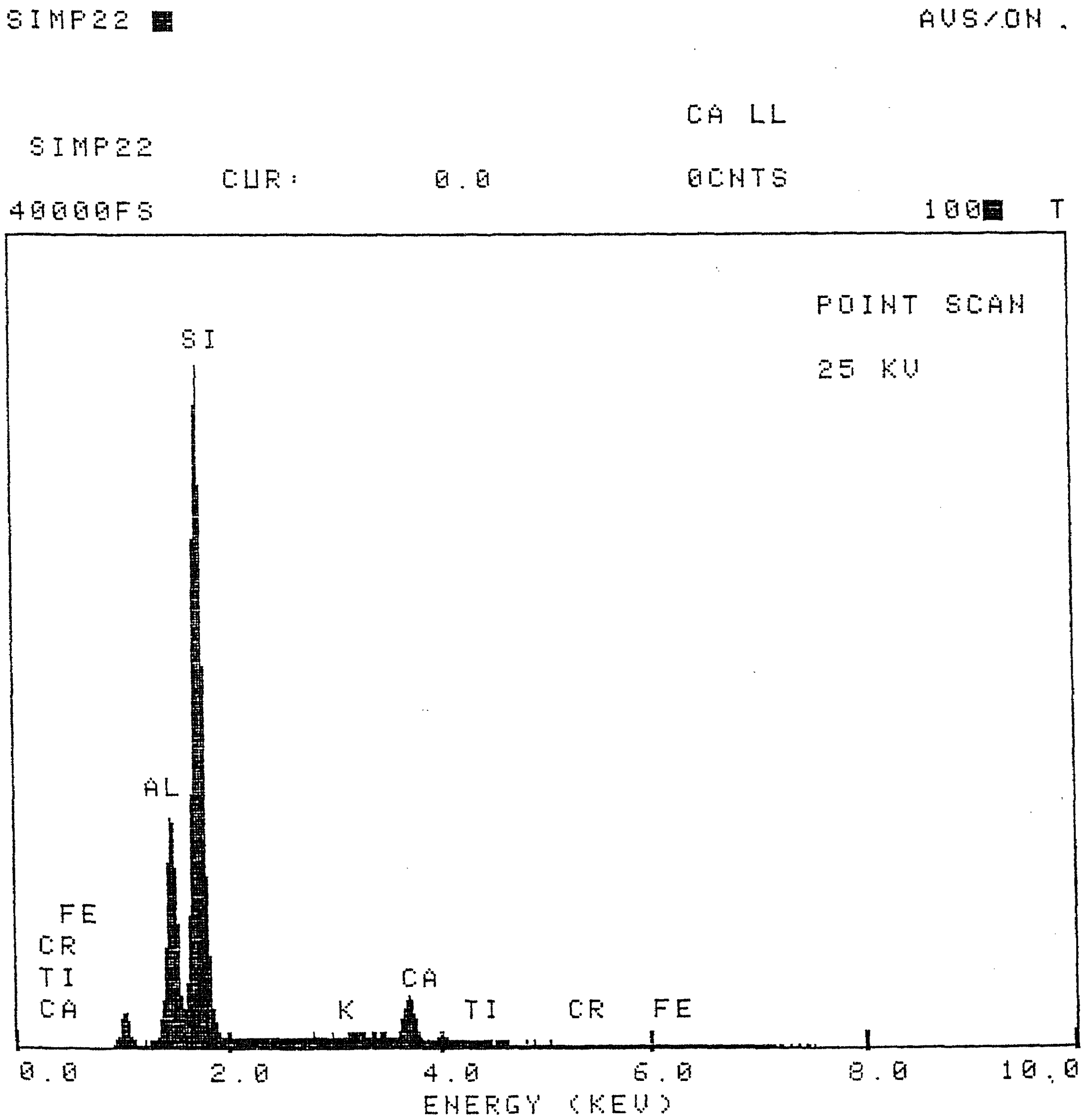

20-Oct-89 11:35

SEM IMAGES OF SAMPLE # Microwave 1.5 minutes powder

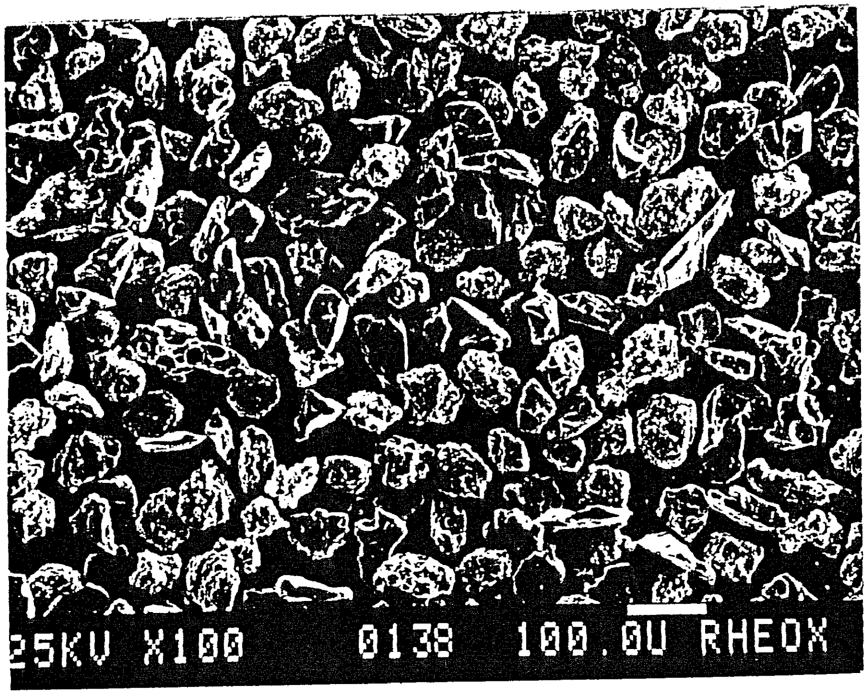

Figure 101

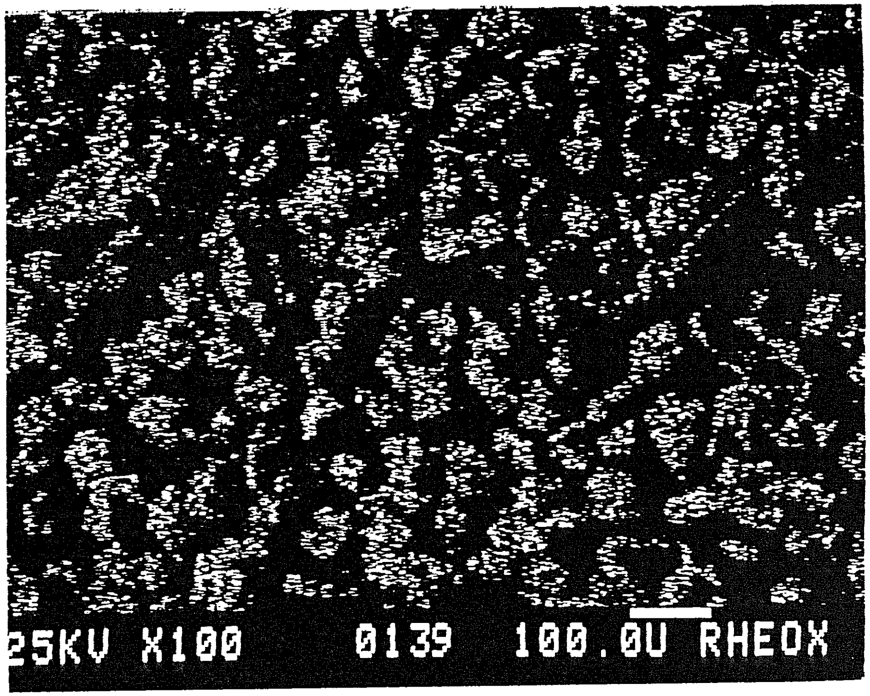

Figure 102 AL X-ray Image of Figure 101

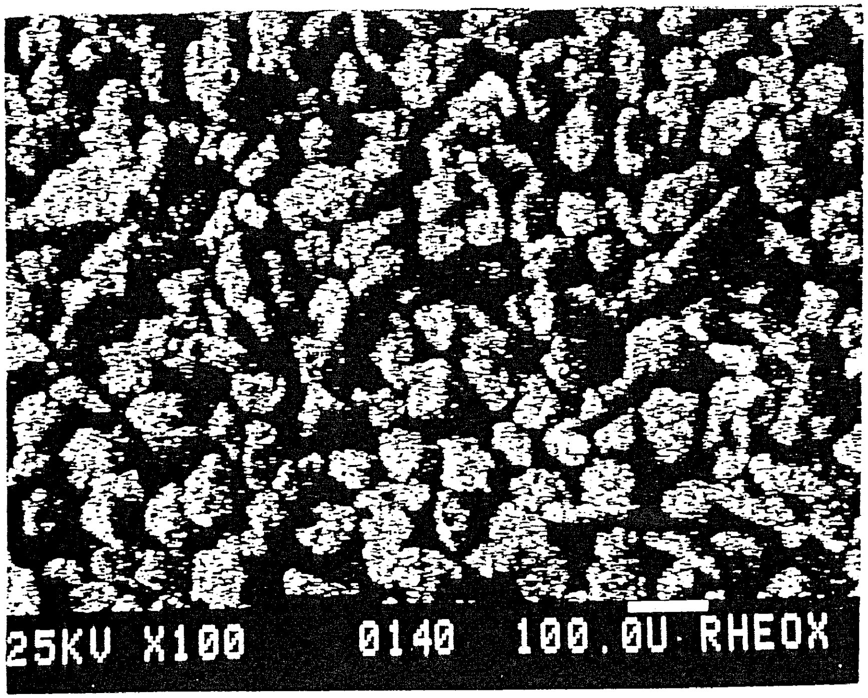

103 Si X-ray Image of Figure 101

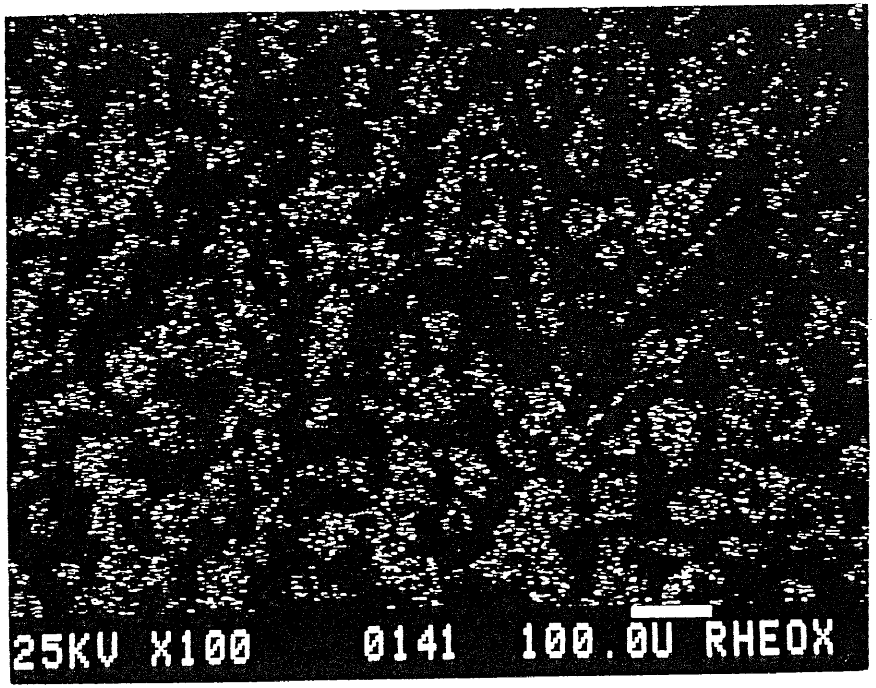

Figure 104 K X-ray Image of Figure 101

SEM IMAGES OF SAMPLE # Microwave 15 minutes Powder

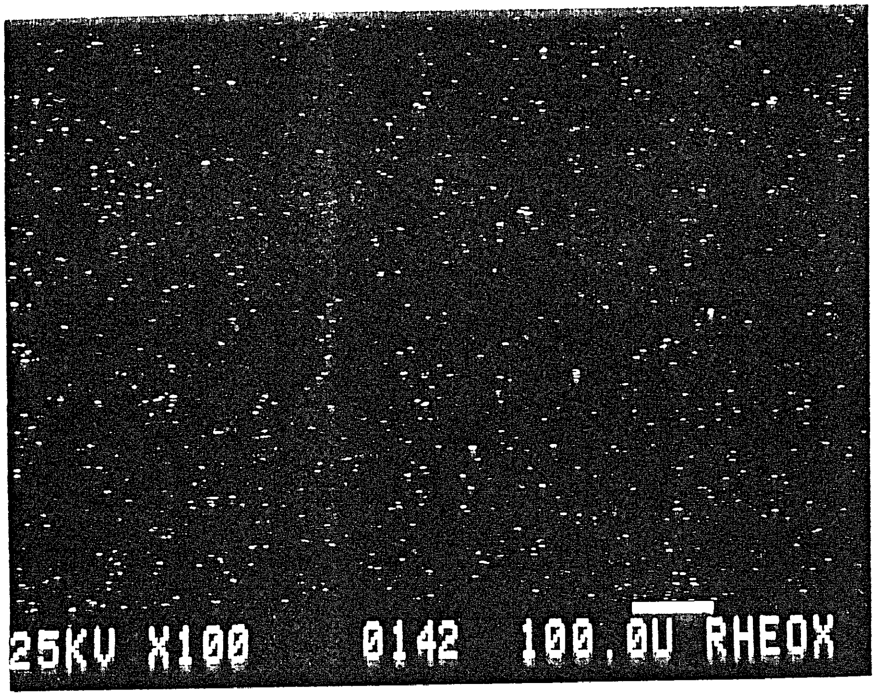

Figure 105 Ti X-Ray Image of Figure 101

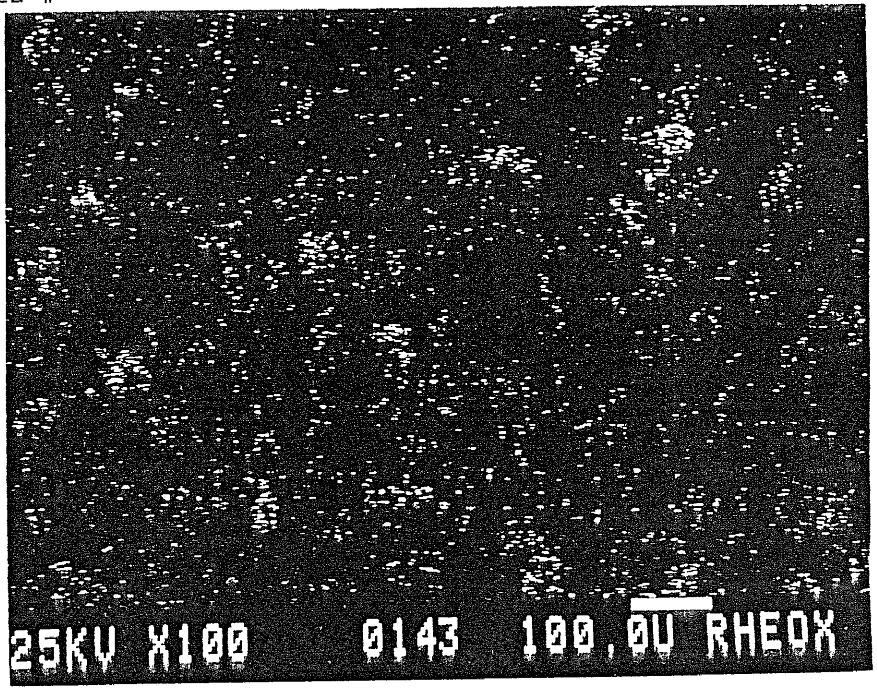

Figure 106 Cr X-Ray Image of Figure 101

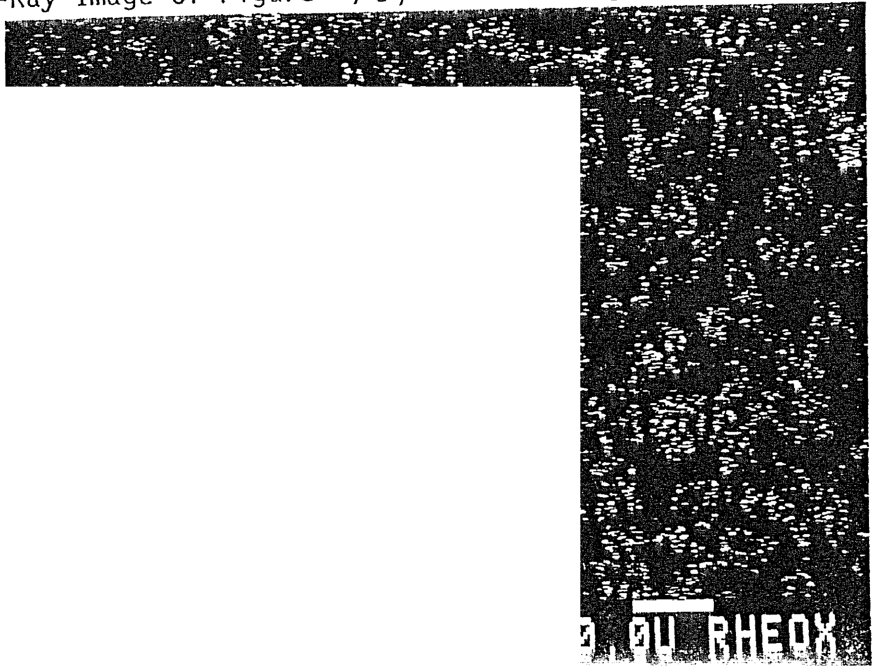

Fig. 107 Fe X-Ray Image of Figure 101

SEM IMAGES OF SAMPLE # *Microwave 15 minutes powder*

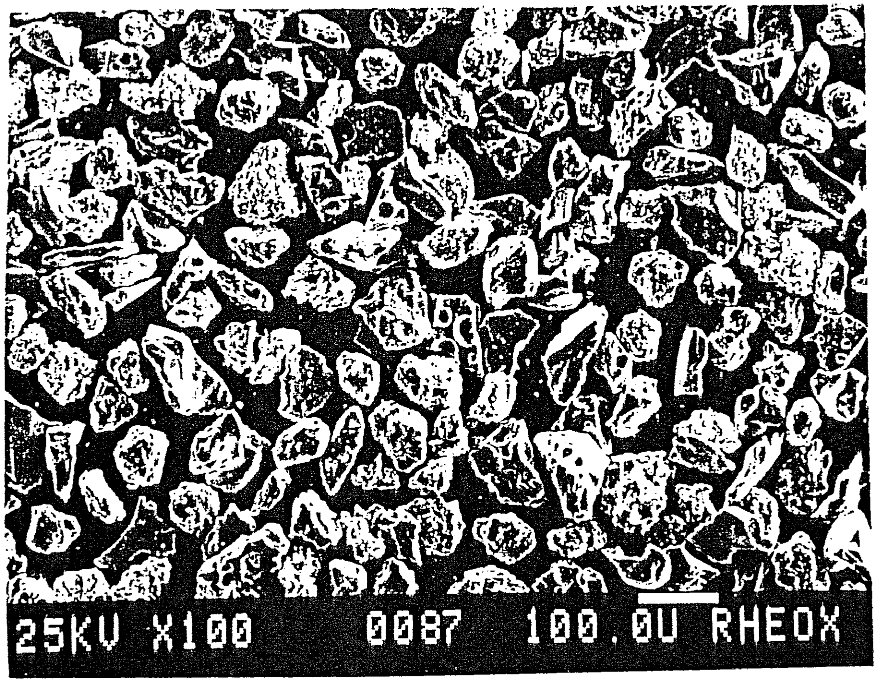

Figure *108*

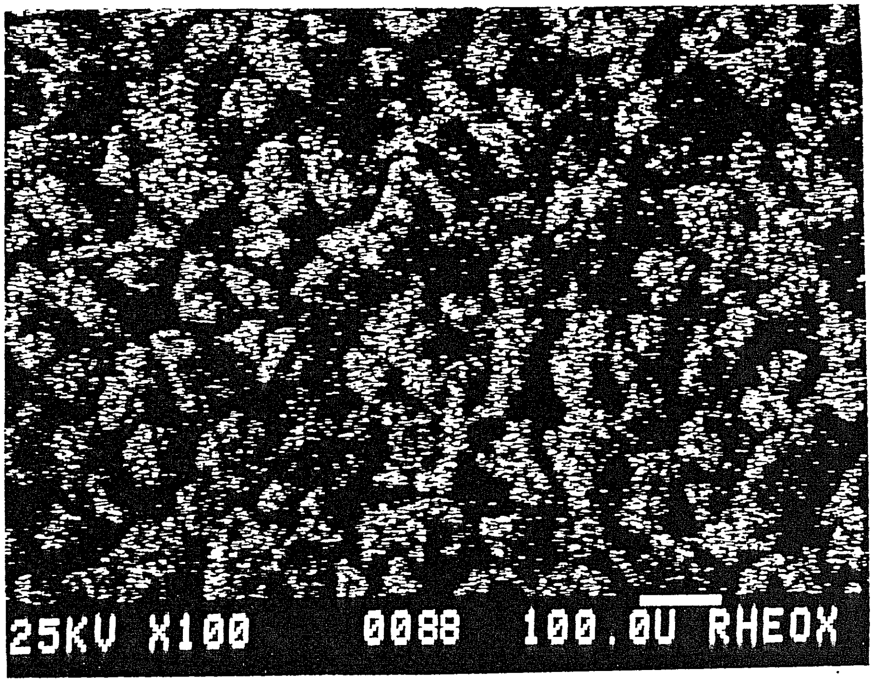

Figure *109* *AL* X-ray Image of Figure *108*

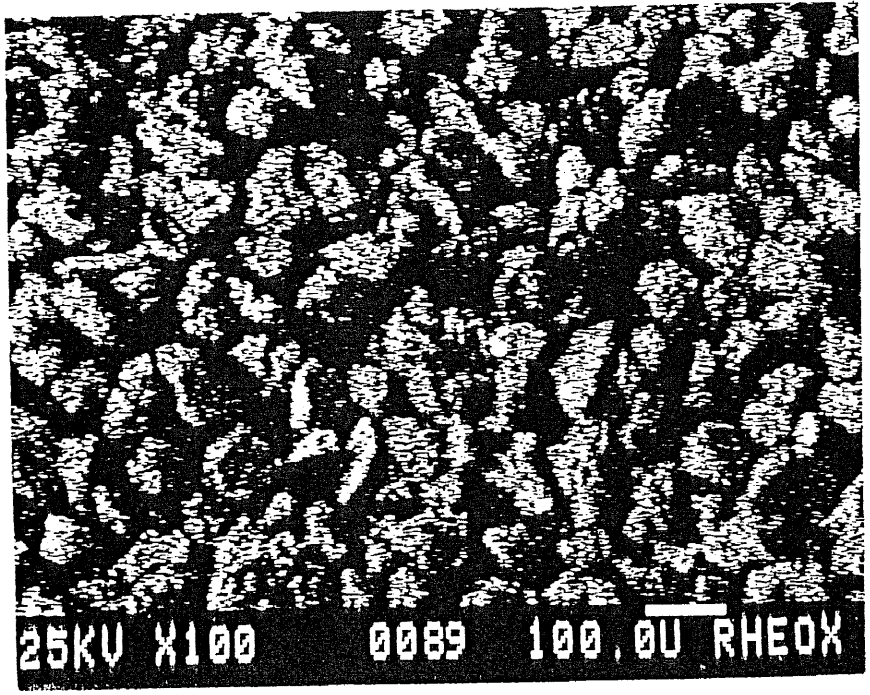

Figure 110 Si X-ray Image of Figure 108

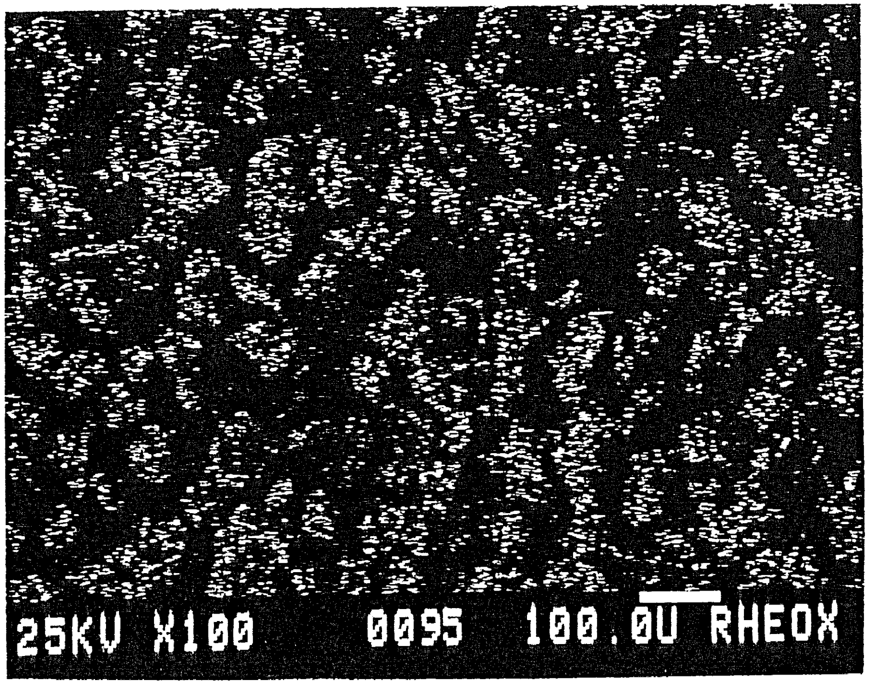

Figure 111 *K* X-ray Image of Figure *108*

SEM IMAGES OF SAMPLE # Microwave 15 minutes Powder

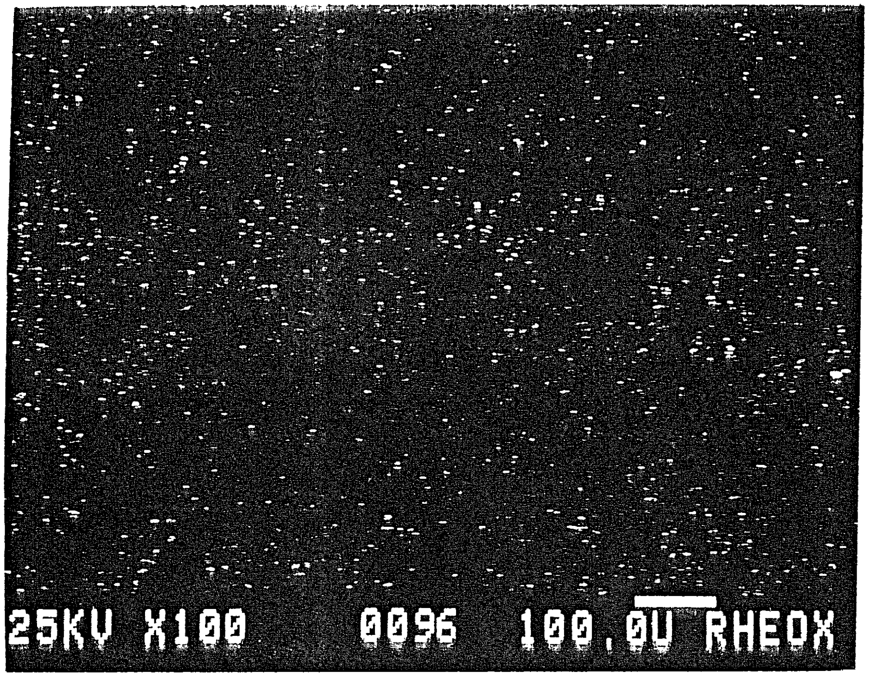

Figure 112 Ti X-Ray Image of Figure 108

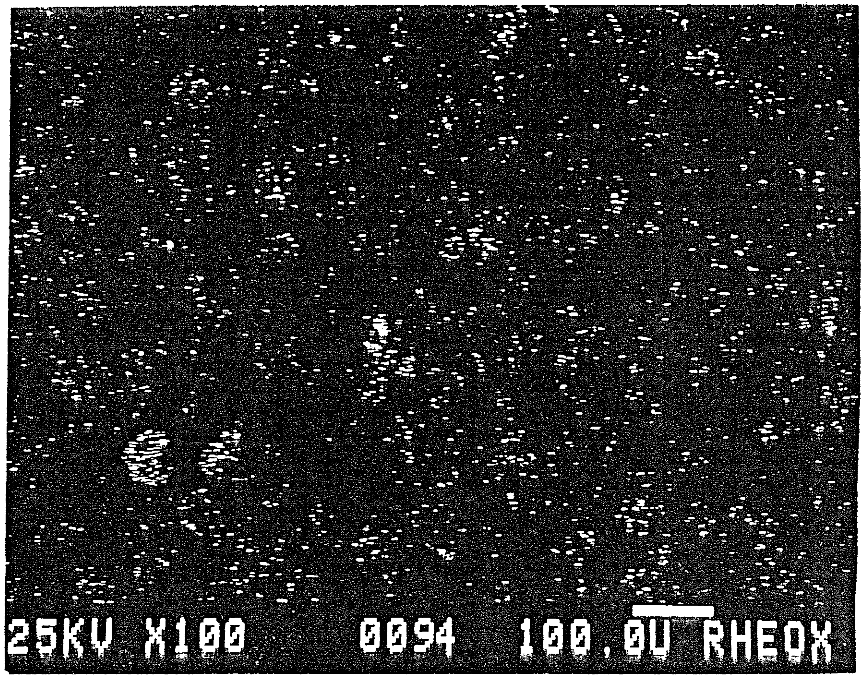

Figure 113 Cr X-Ray Image of Figure 108

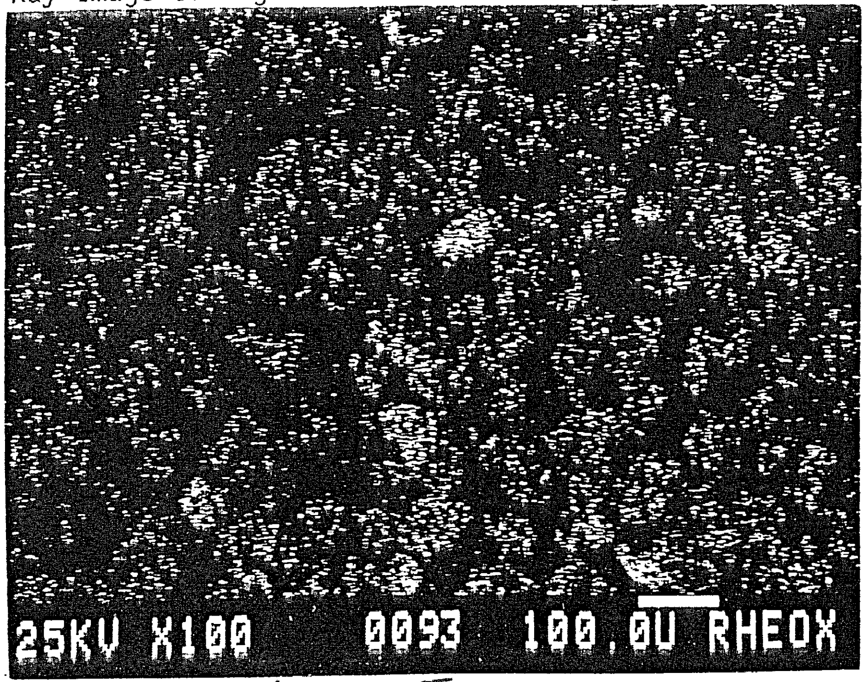

Figure 114 Fe X-Ray Image of Figure 108

SEM IMAGES OF SAMPLE # Microwave 15 minutes powder

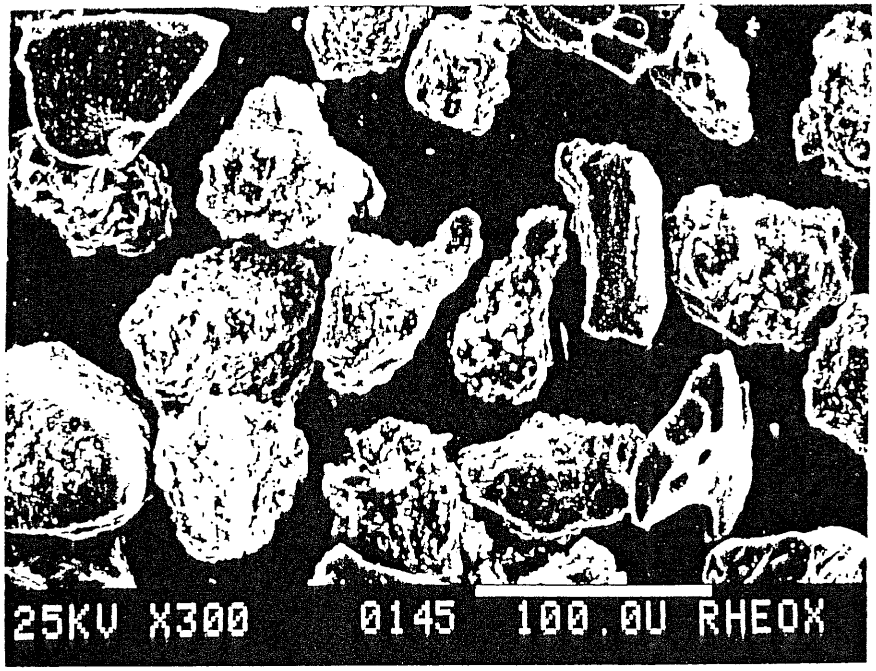

Figure 115

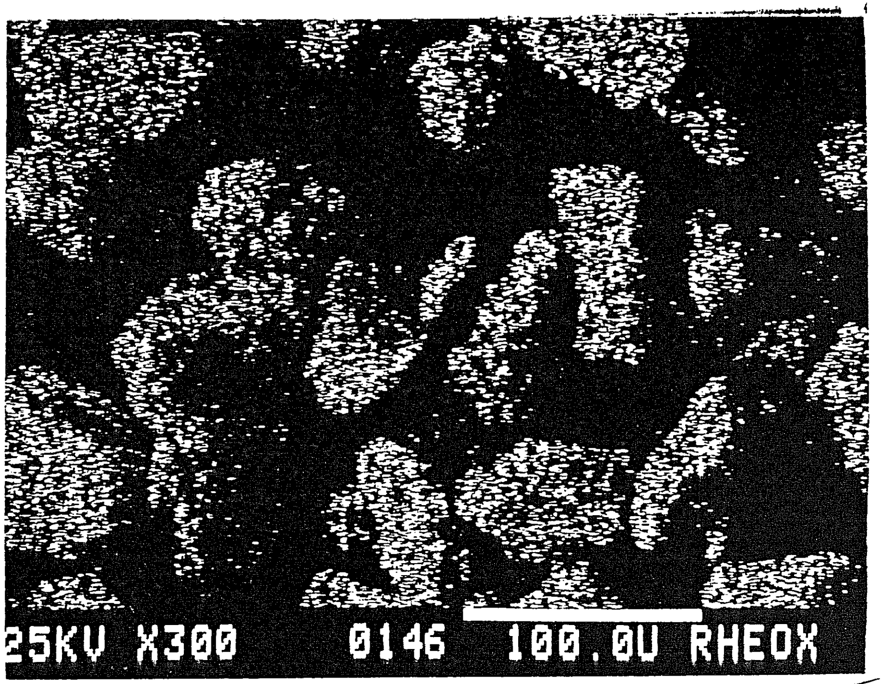

Figure 116 AL X-ray Image of Figure 115

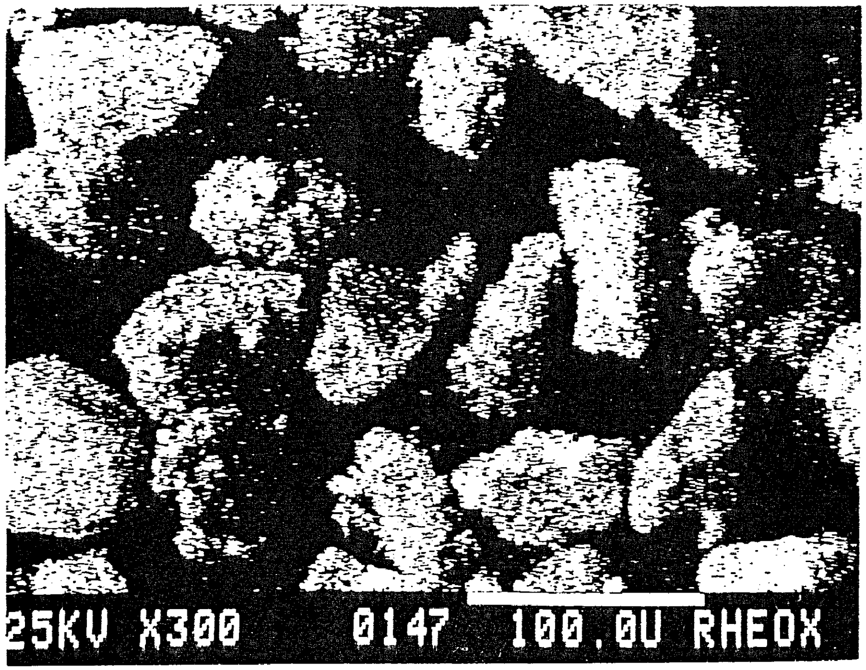

Figure 117 Si X-ray Image of figure 115

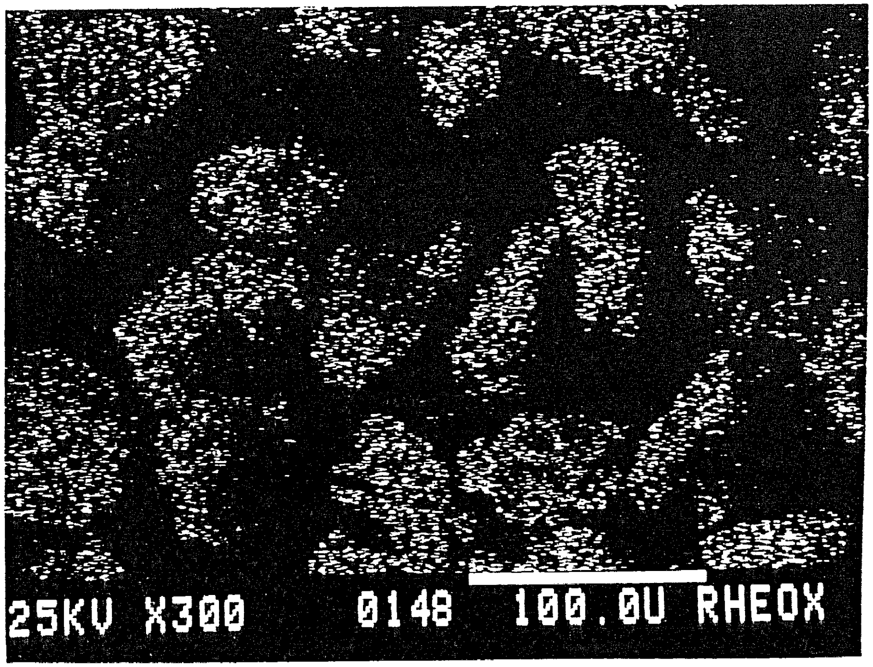

Figure 118 K X-ray Image of Figure 115

SEM IMAGES OF SAMPLE # Microwave 15 minutes Powder

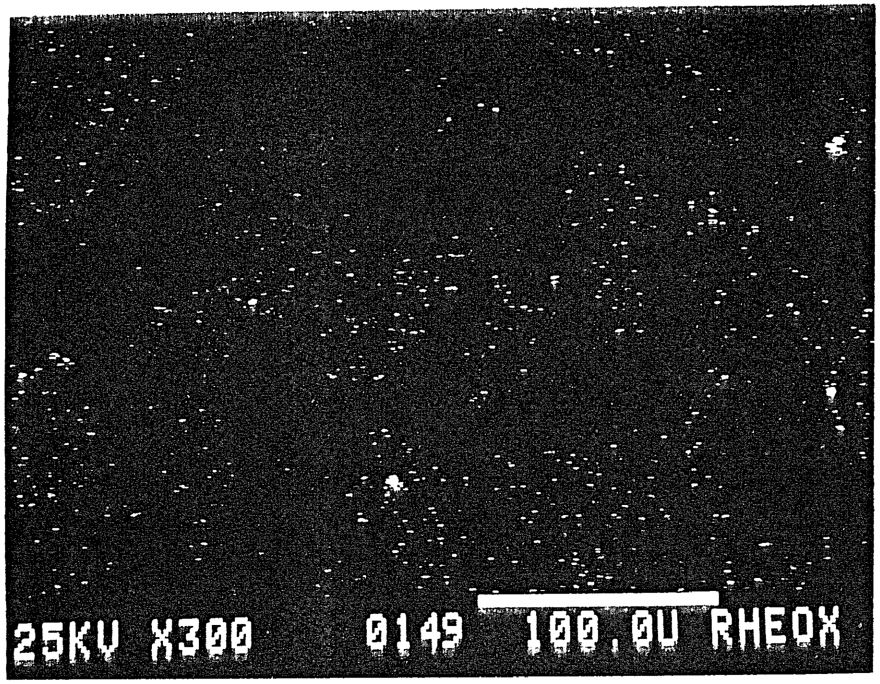

Figure 119 Ti X-Ray Image of Figure 115

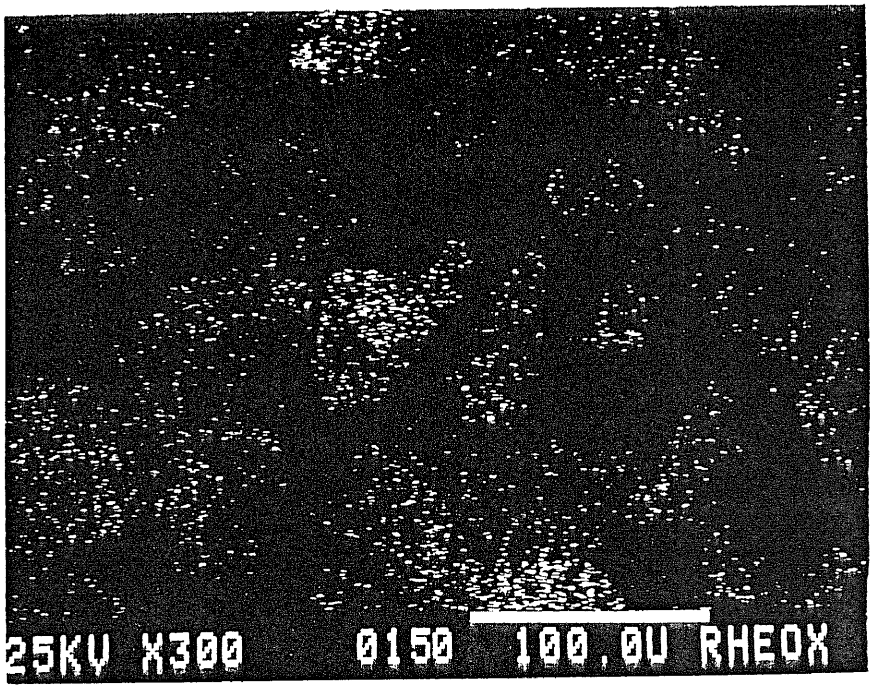

Figure 120 Cr X-Ray Image of Figure 11

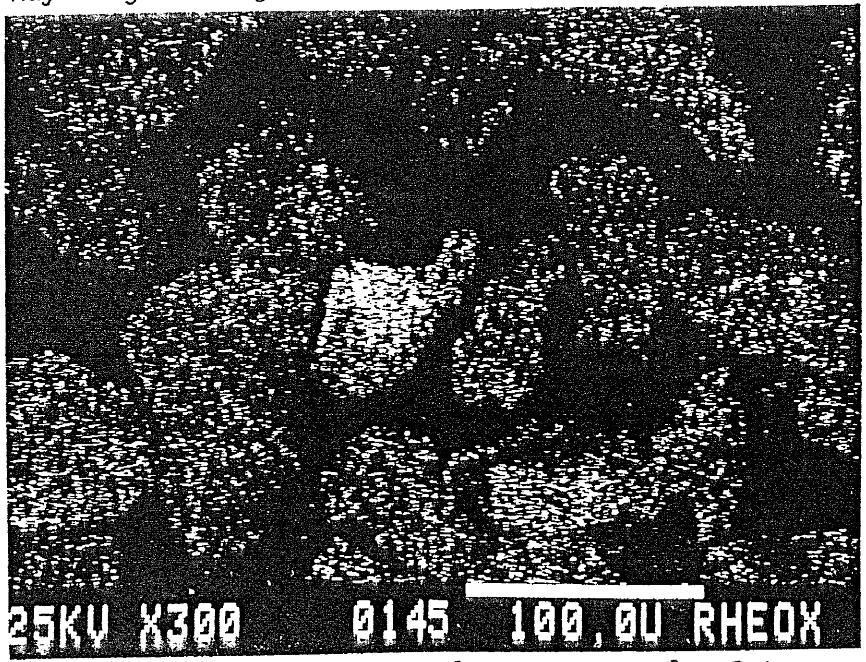

Figure 121 Fe X-Ray IMAGE of Figure 115

SEM IMAGES OF SAMPLE # Microwave 15 minutes Powder

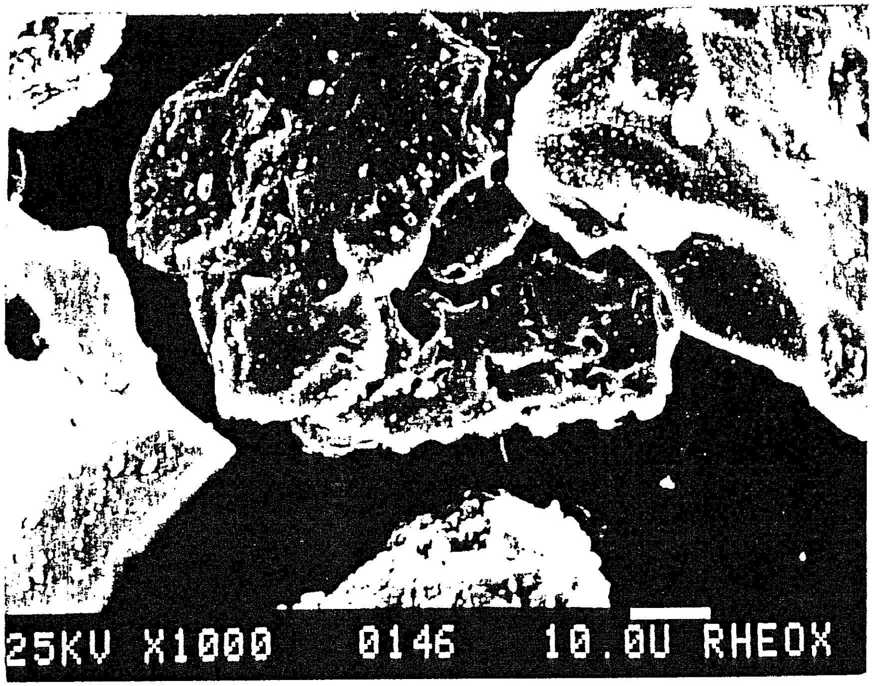

Figure 122

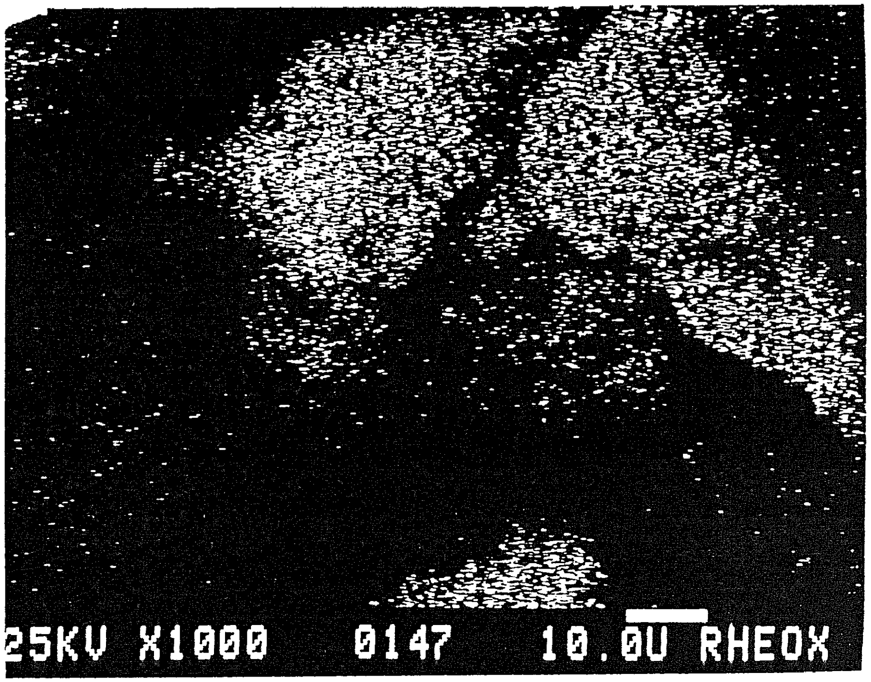

Figure 123 Al X-ray Image of Figure 122

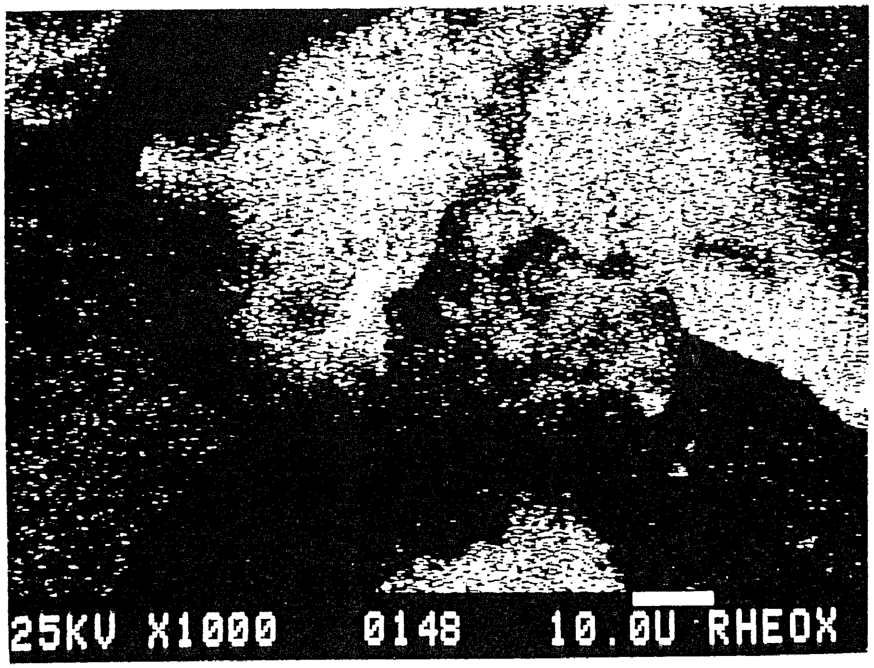

Figure 124 Si X-ray Image of Figure 122

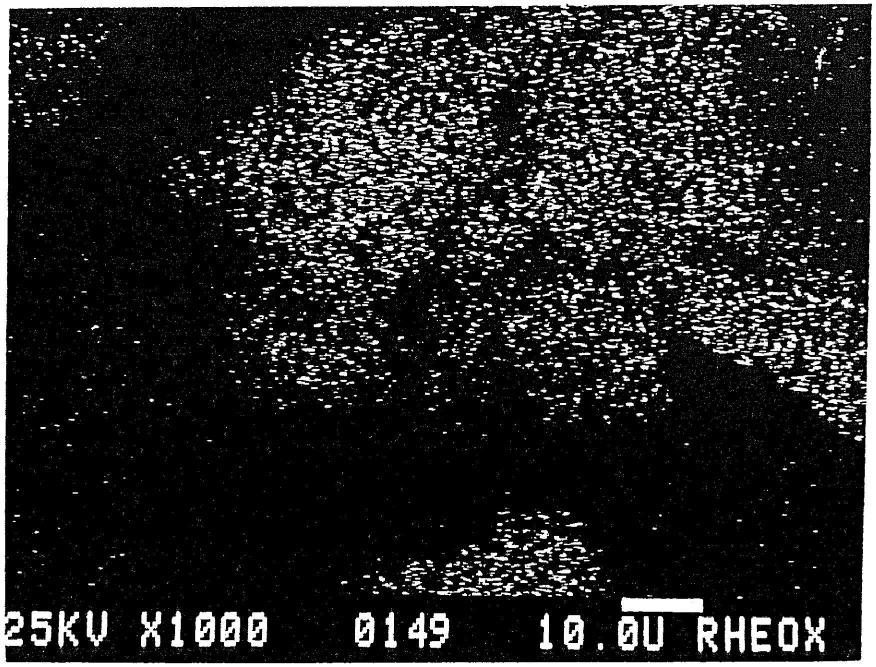

Figure 125 K X-ray Image of Figure 122

SEM IMAGES OF SAMPLE # Microwave 15 minutes Powder

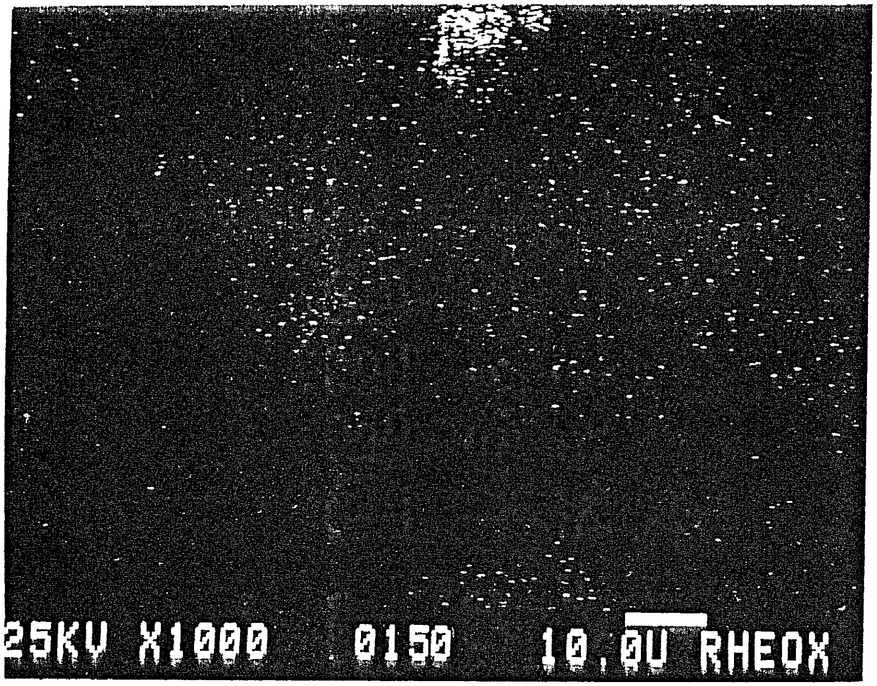

Figure 126 Ti X-Ray Image of Figure 122

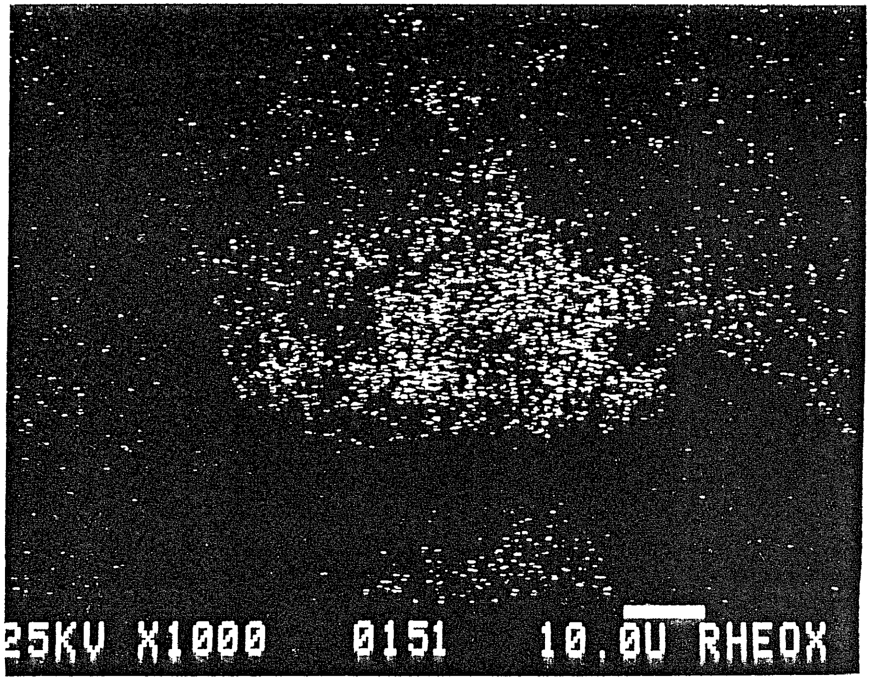

Figure 127 Cr X-Ray Image of Figure 122

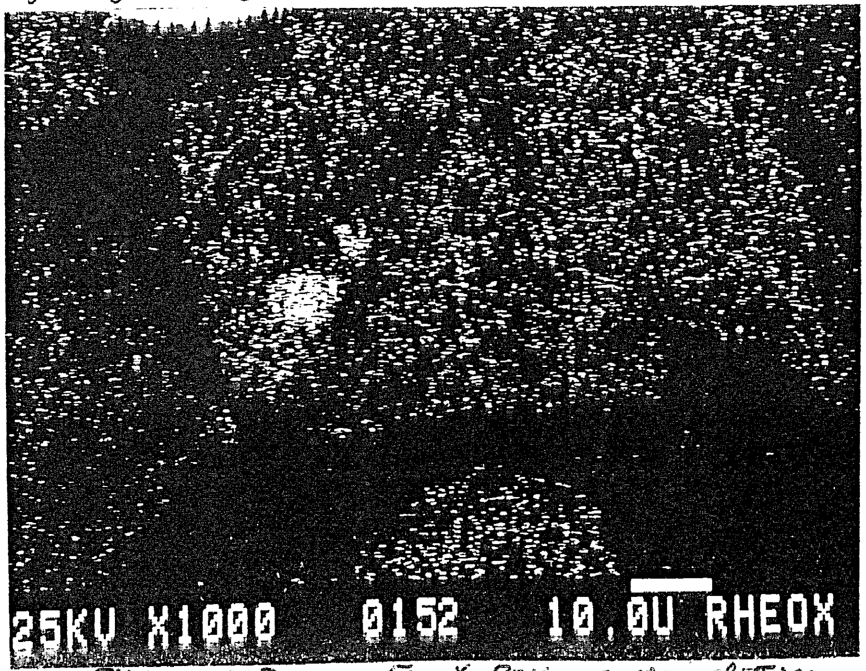

Figure 128 Fe X-Ray image of Figure 122

SEM IMAGES OF SAMPLE # Microwave 15 minutes Powder

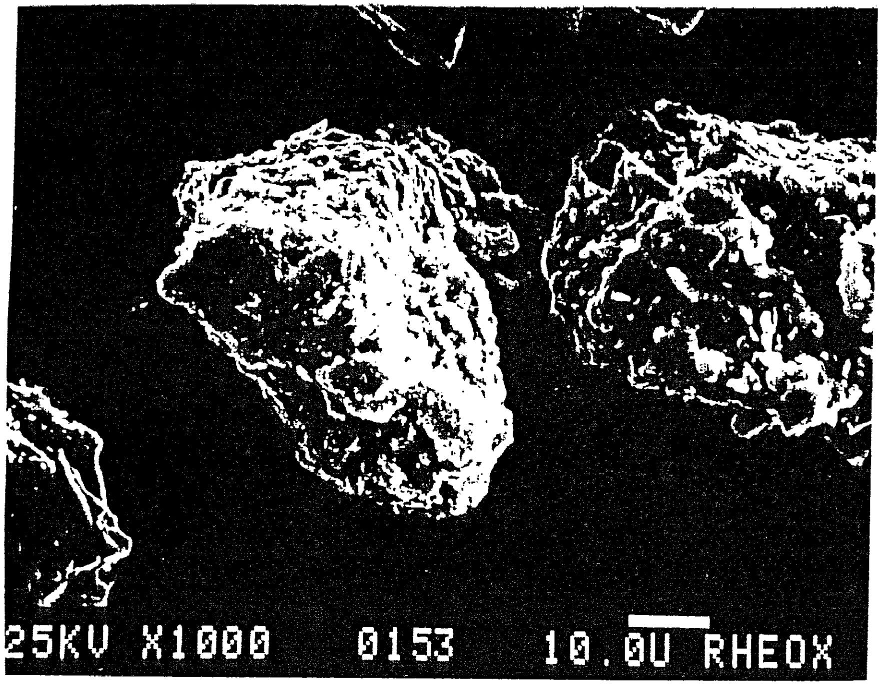

Figure 129

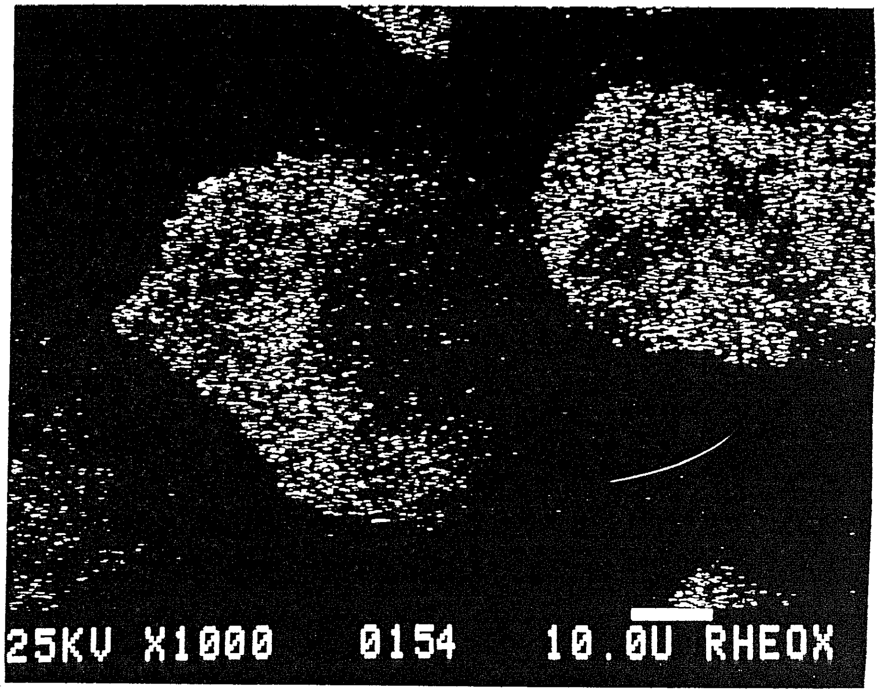

Figure 130 AL X-ray Image of Figure 129

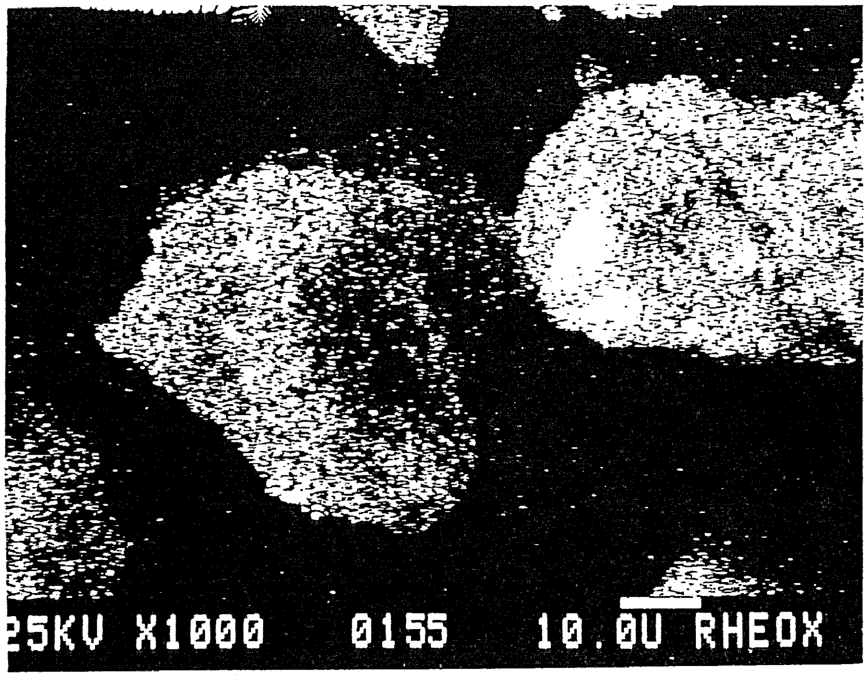

Figure 131 Si X-ray Image of Figure 129

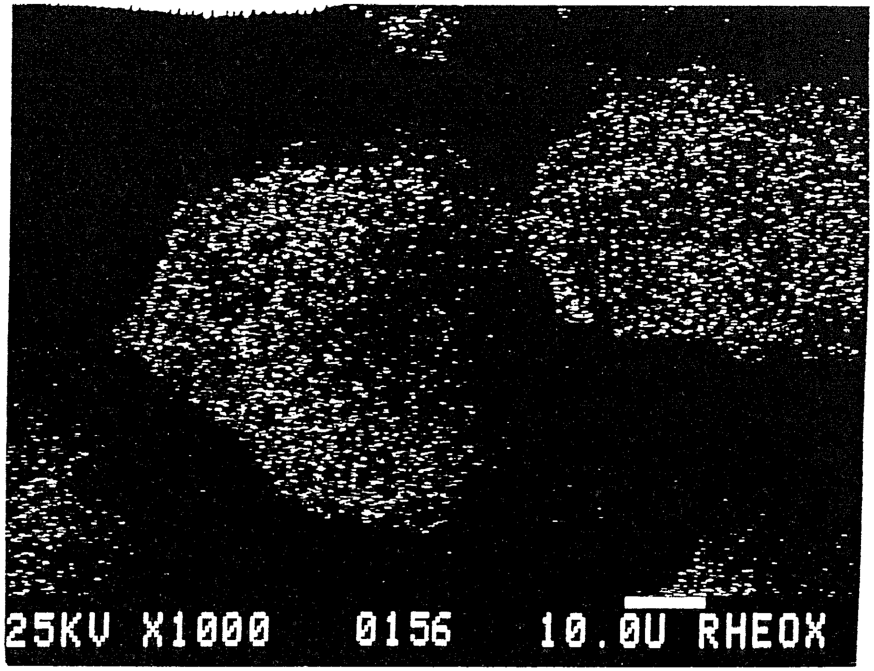

Figure 132 K X-ray Image of Figure 129

SEM IMAGES OF SAMPLE # Microwave 15 minutes Powder

Figure 133 Ti X-Ray Image of Figure 129

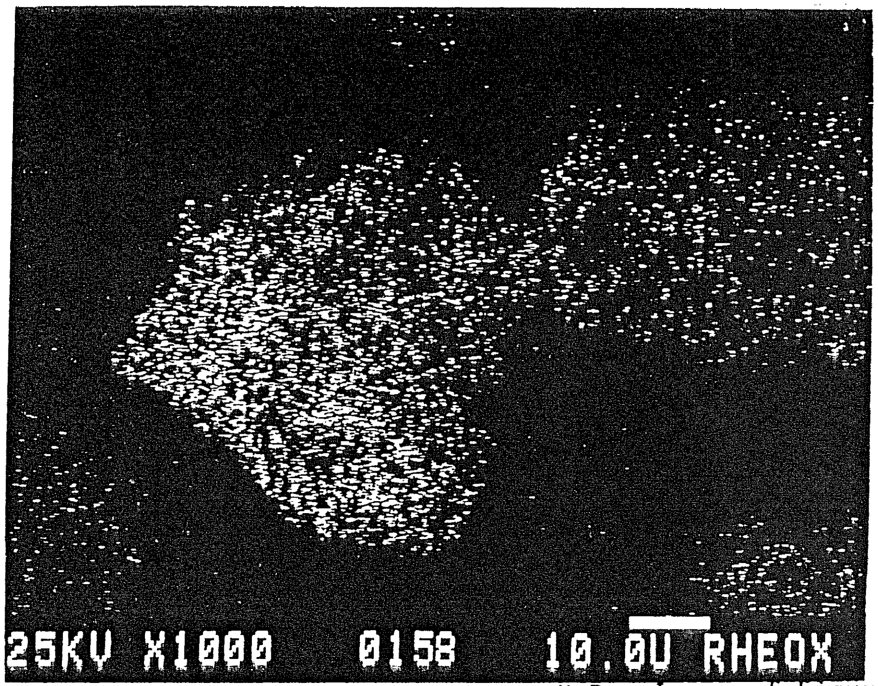

Figure 134 Cr X-Ray Image of Figure 129

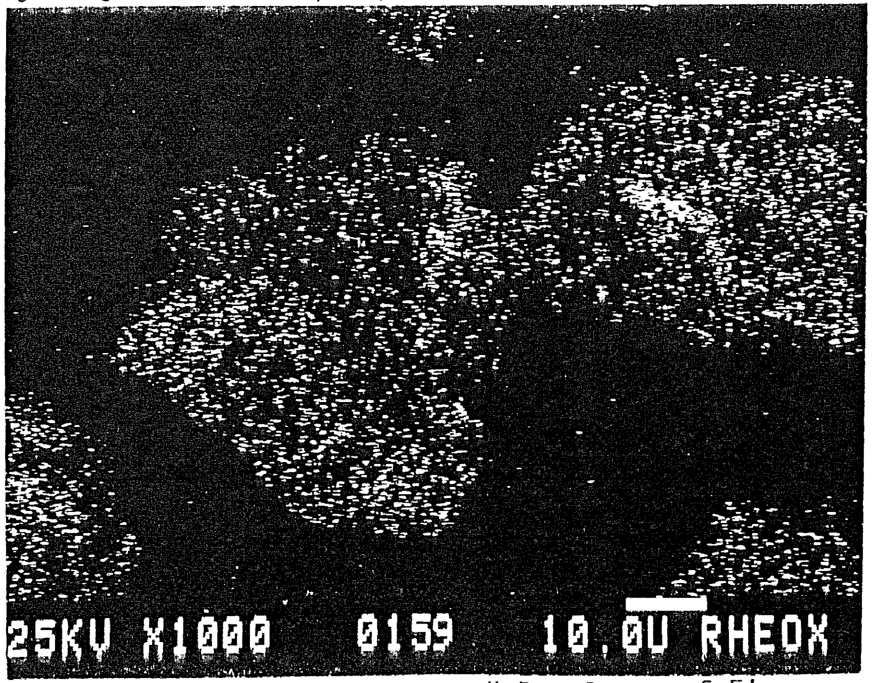

Figure 135 Fe X-Ray Image of Figure 129

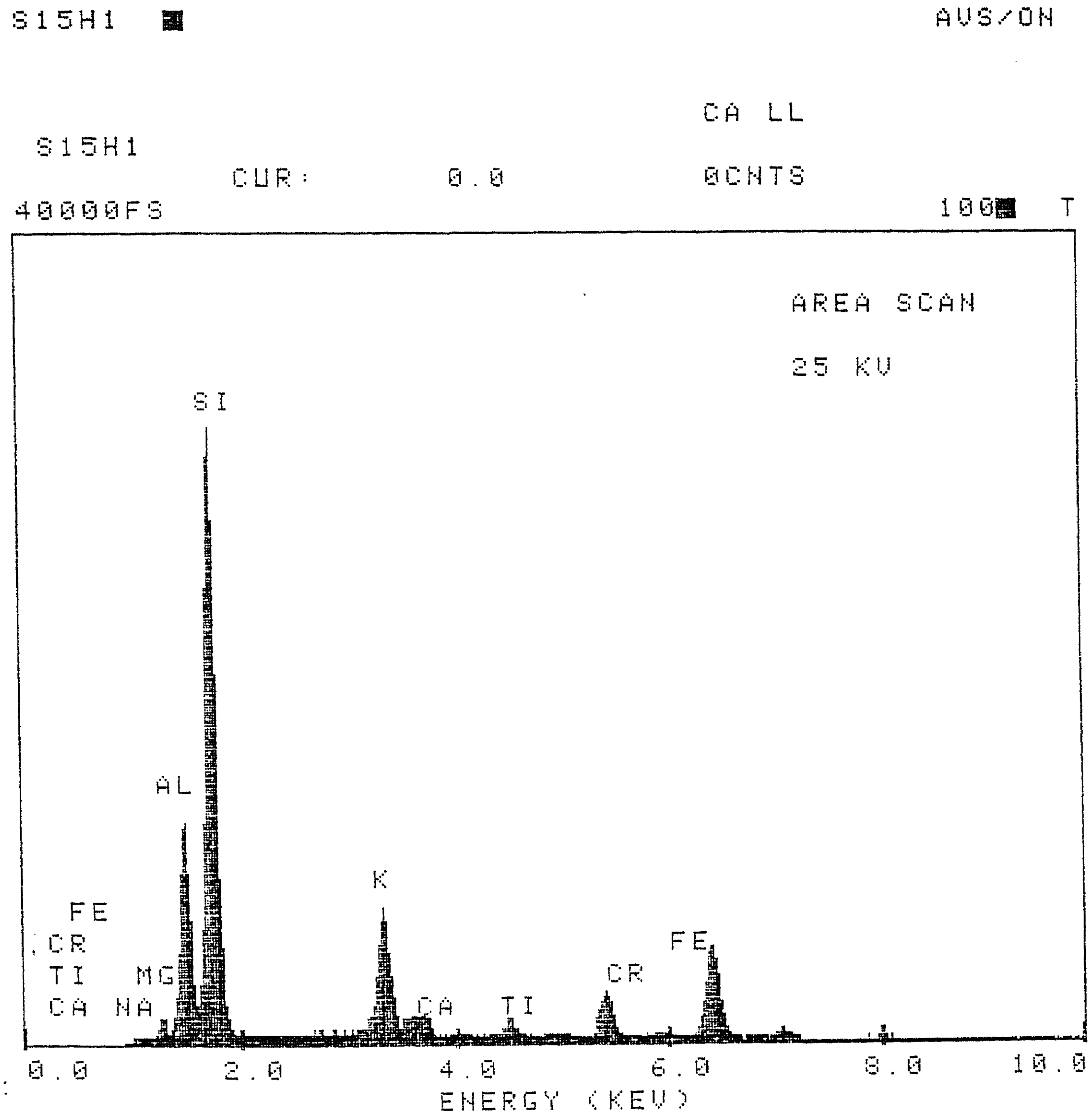

20-Oct-89 11:35

S15H2 ■ AVS/ON ·

CA LL

S15H2

CUR: 0.0 0CNTS

40000FS 100■ T

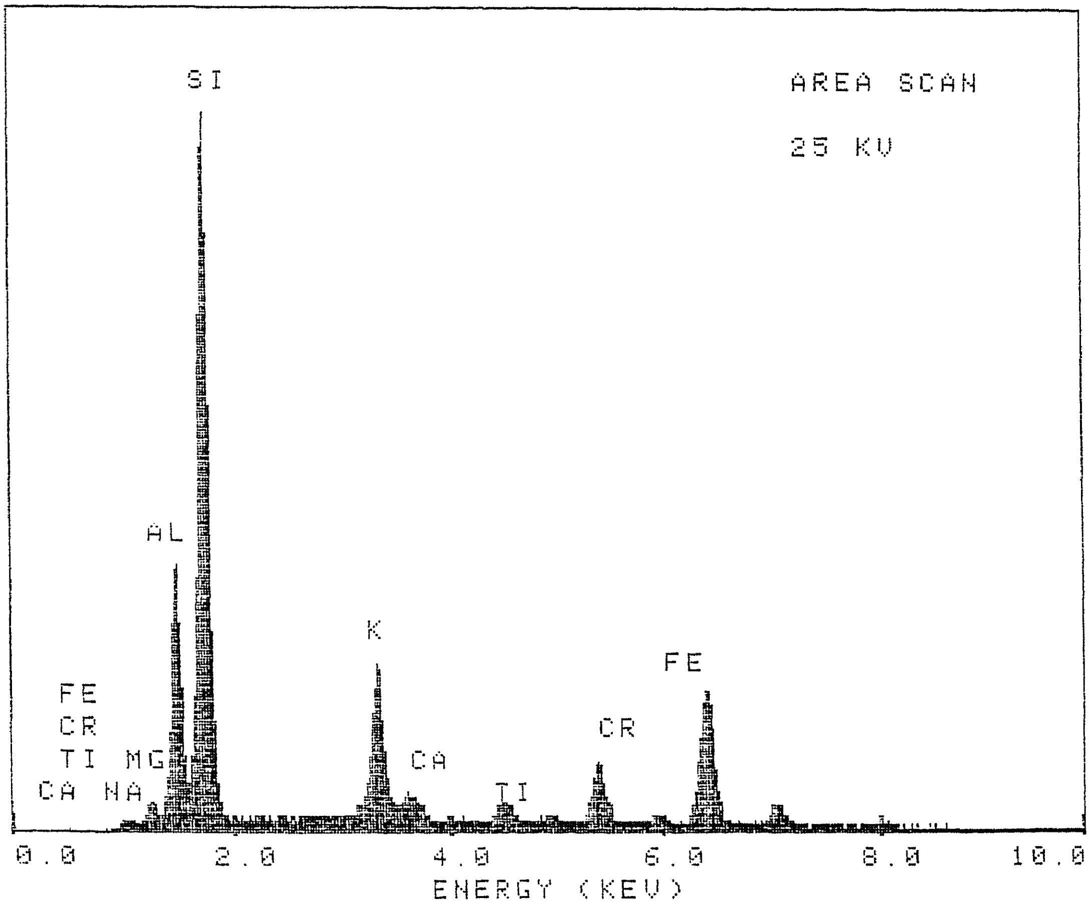

SAVE THE STATE OF THE SYSTEM

ARE YOU SURE ? * Y

20-Oct-89 11:35

S15H3 ▨ AVS/ON

CA LL

S15H3

CUR: 0.0 0CNTS

40000FS 100▨ T

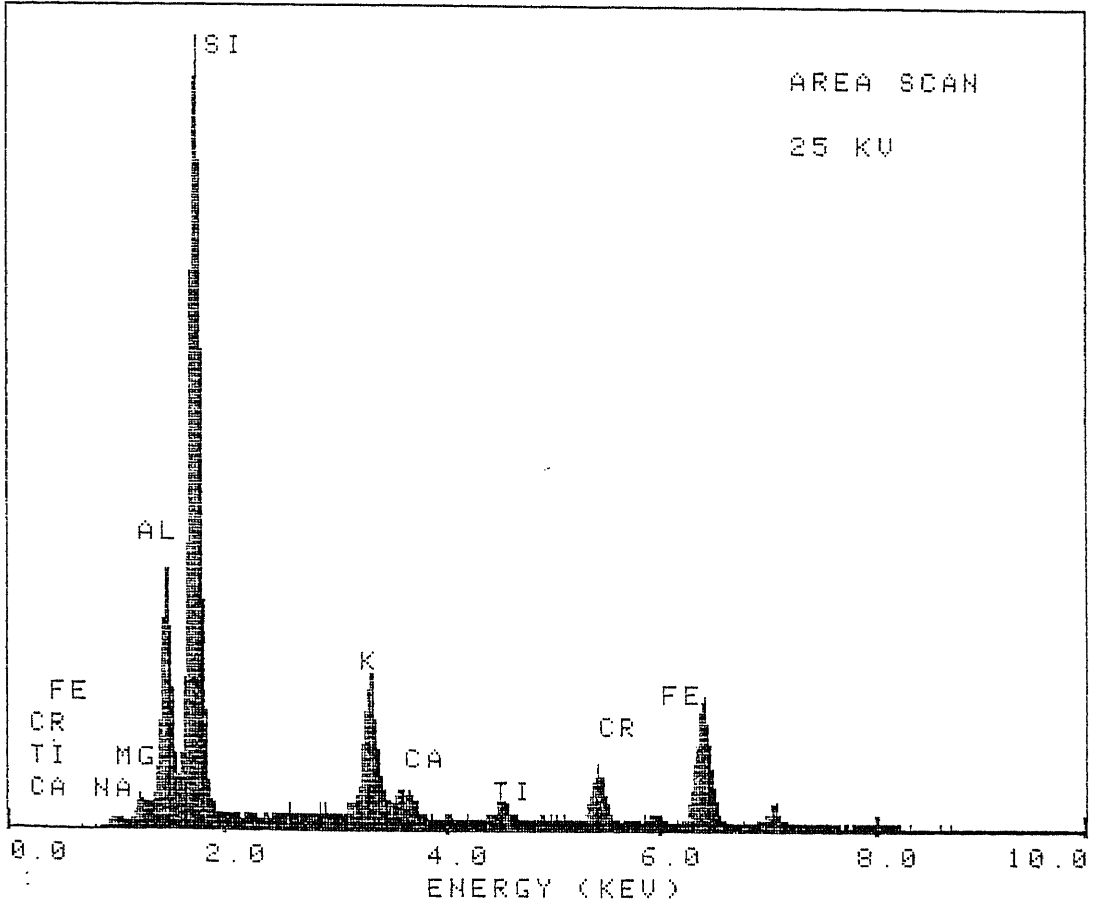

20-Oct-89 11:35

S15H8 ■ AVS/ON

CA LL

S15H8

CUR: 0.0 0CNTS

40000FS 100■ T

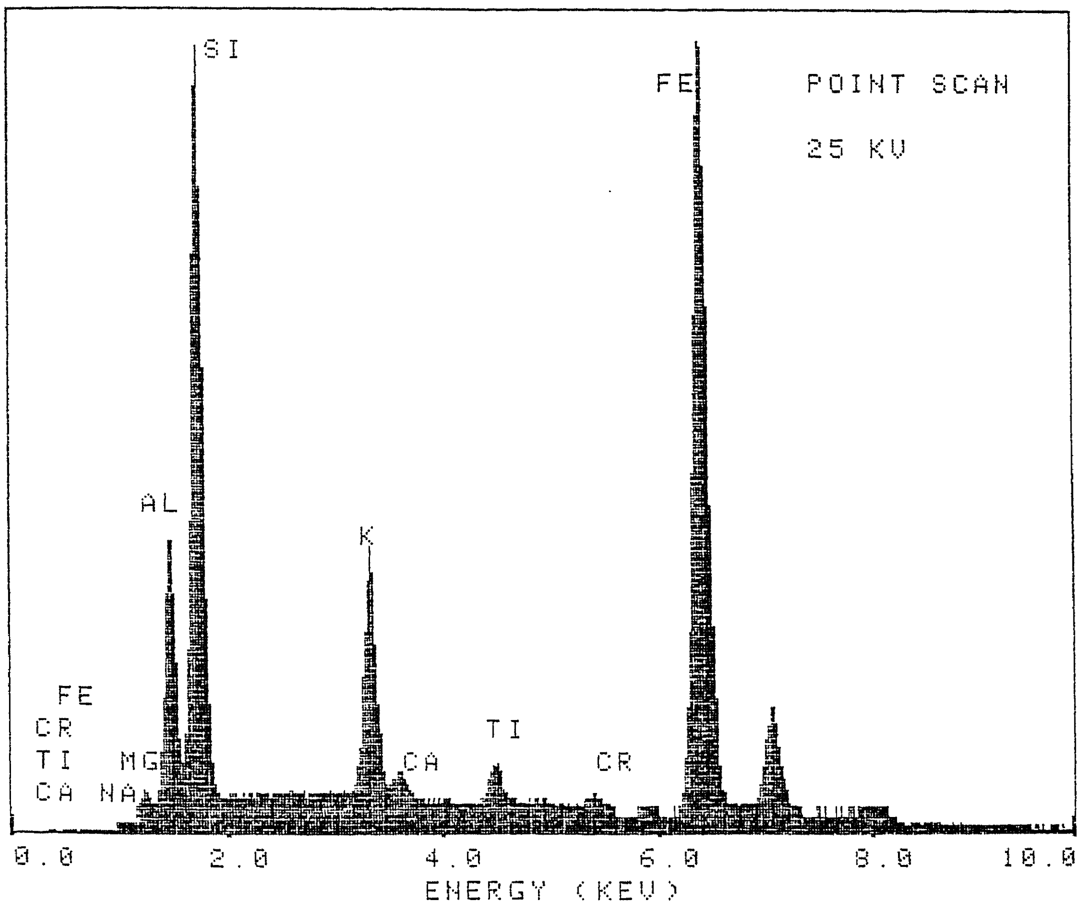

20-Oct-89 11:35

123

```
S15H9  ■                                                AVS/ON.

                                          CA LL
 S15H9
              CUR:          0.0           0CNTS
40000FS                                                100■  T
```

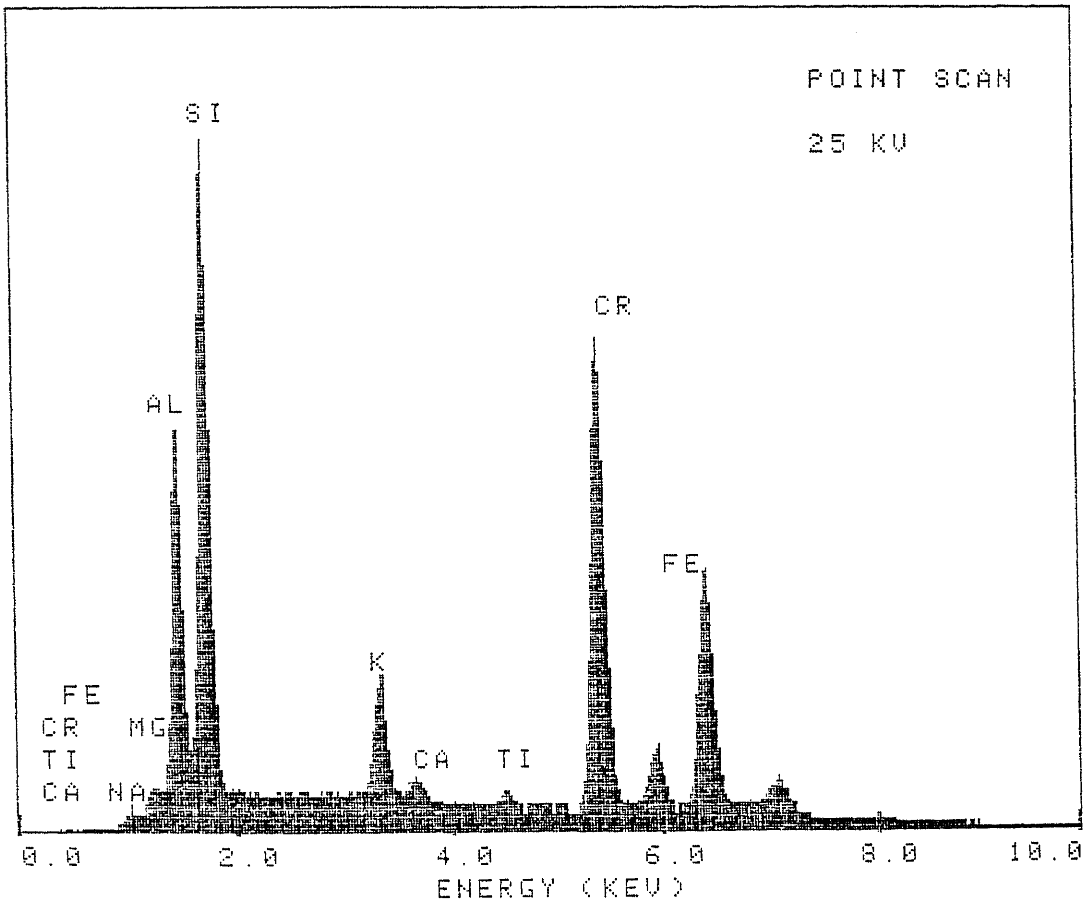

20-Oct-89 11:35

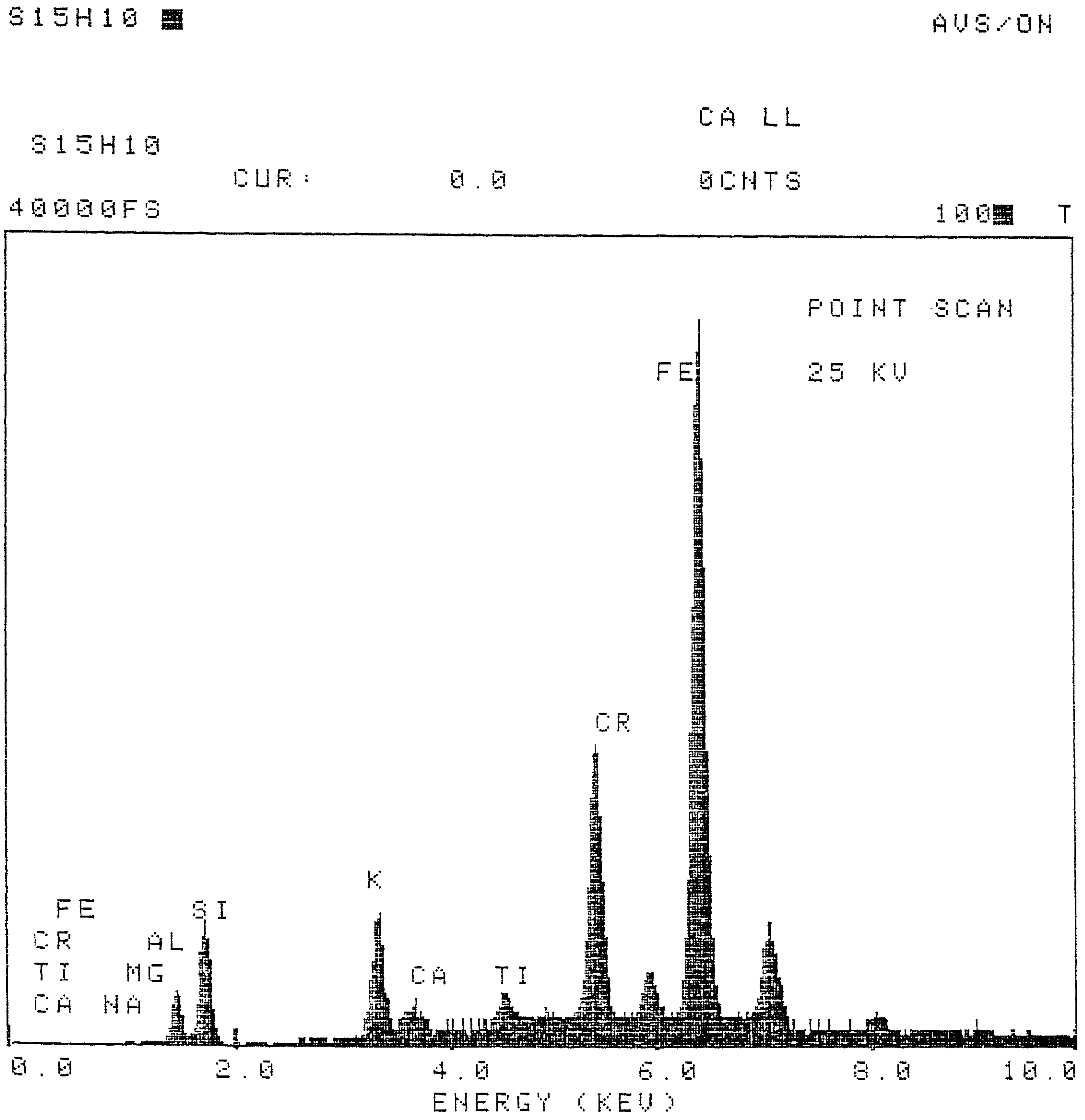

20-Oct-89 11:35

S15H12 AVS/ON.

CA LL

S15H12

CUR: 0.0 0CNTS

40000FS 100 T

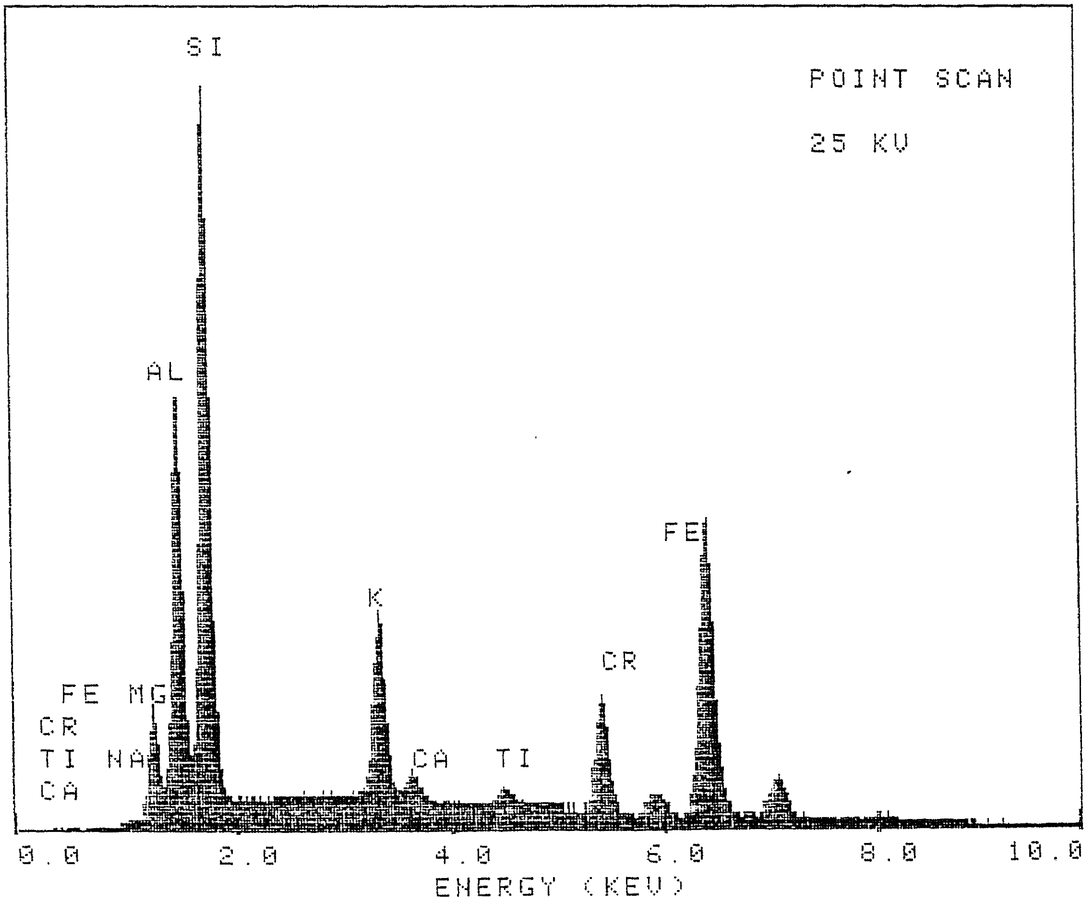

20-Oct-89 11:35

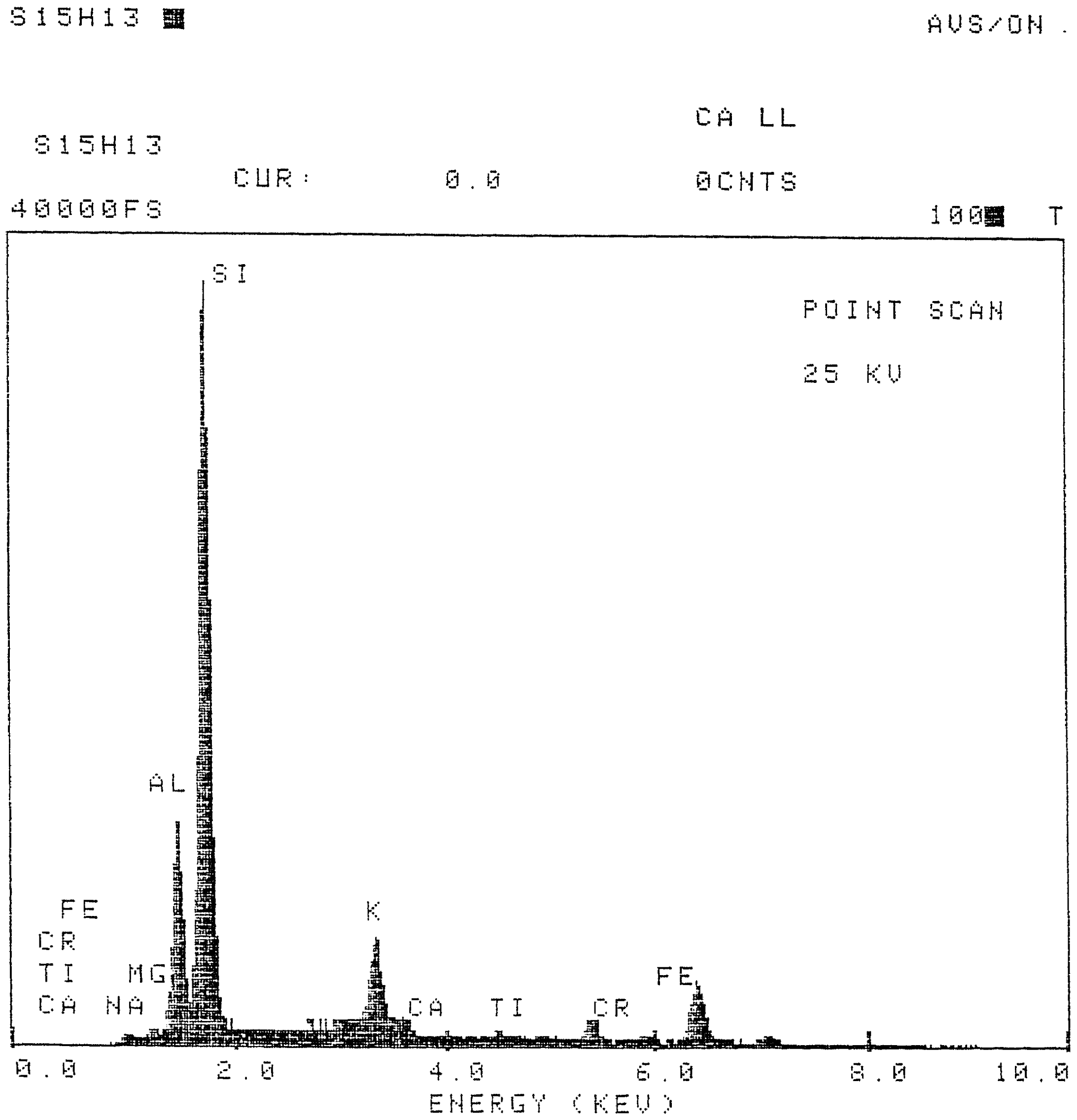

20-Oct-89 11:35

```
S15H14 ■                                              AVS/ON

                                            CA LL
 S15H14
         CUR:          0.0                  0CNTS
40000FS                                               100■  T
```

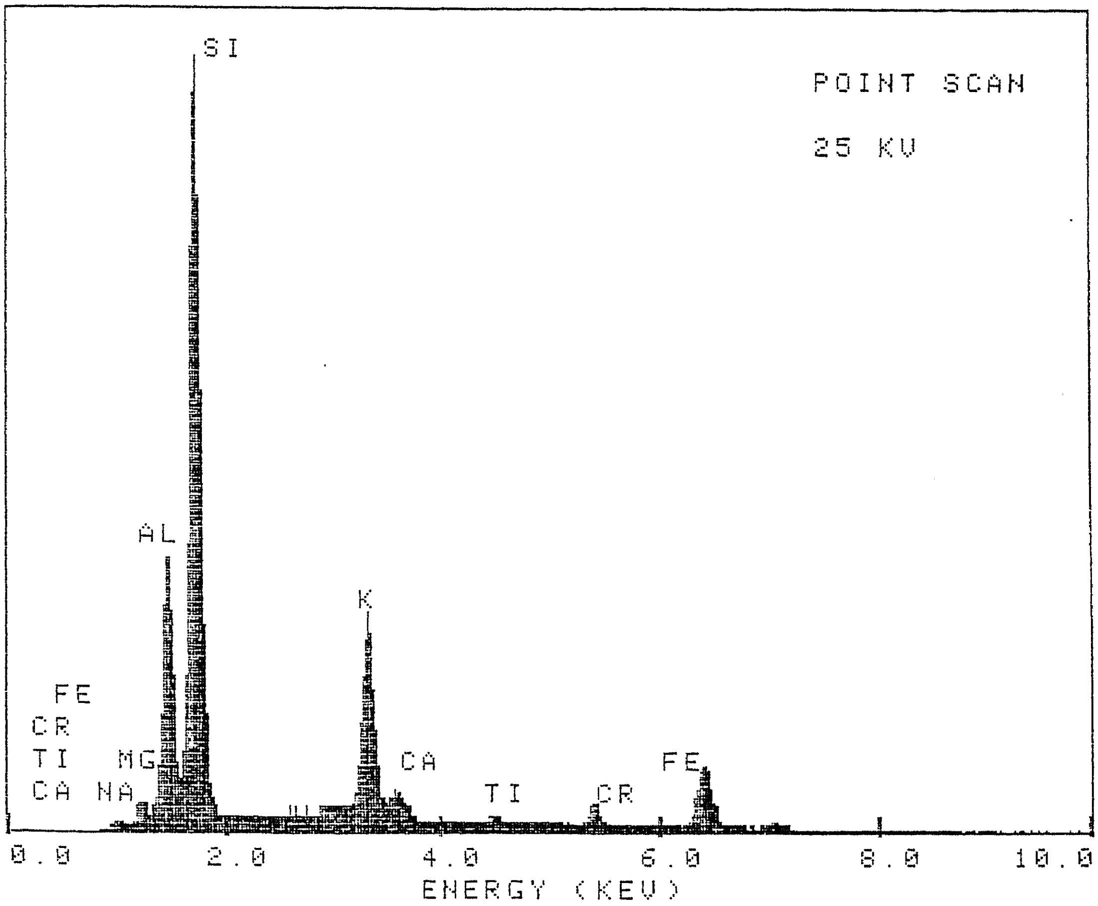

20-Oct-89 11:35

SEM IMAGES OF SAMPLE #

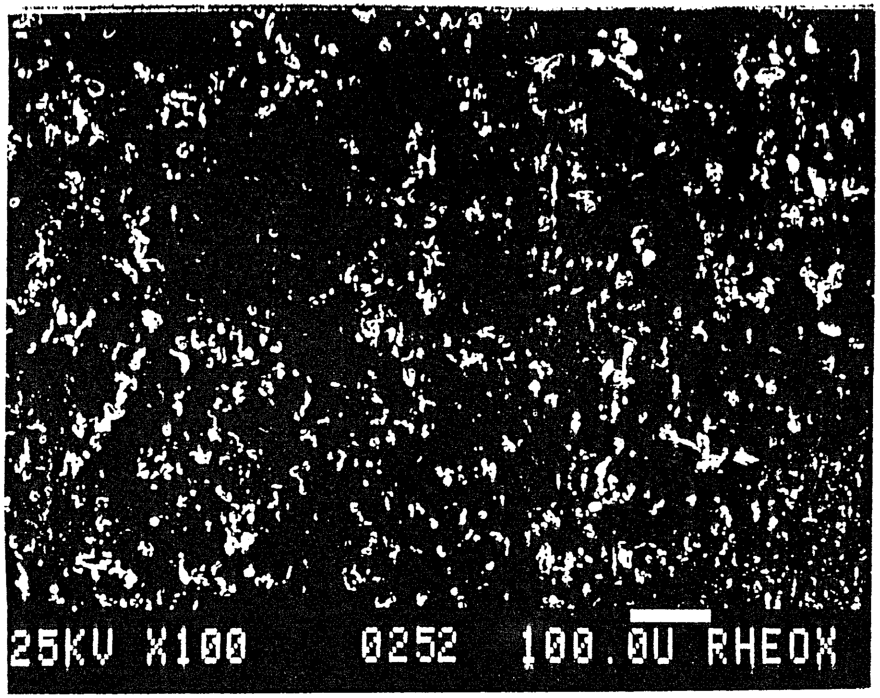

Figure 136

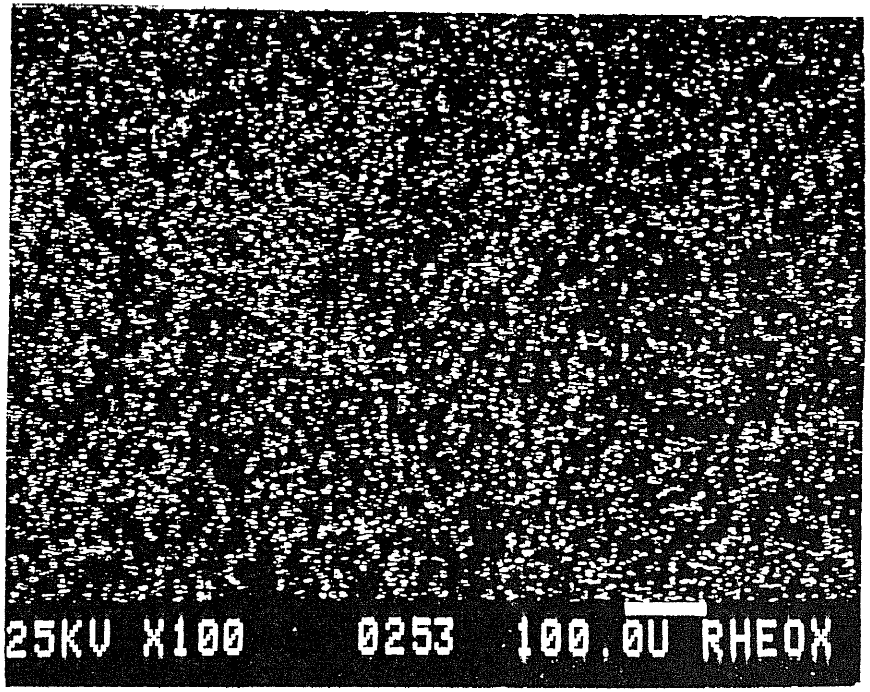

Figure 137 AL X-ray Image of Figure 136

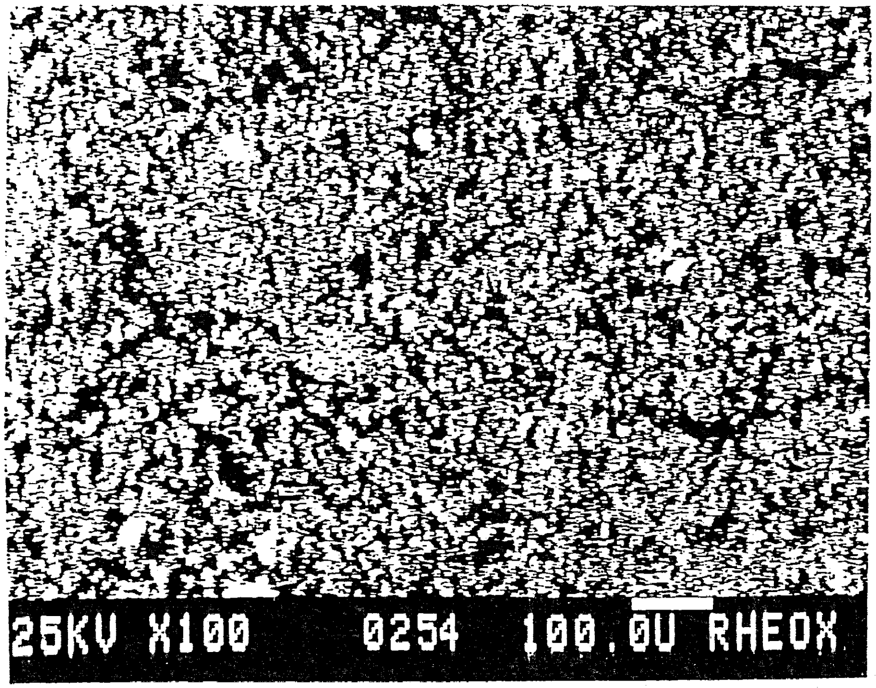

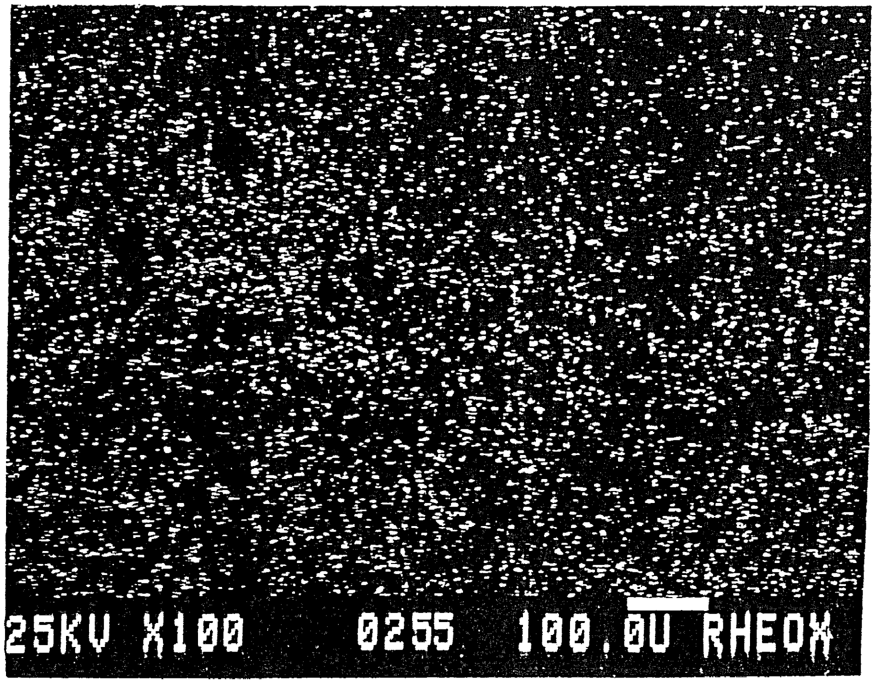

Microwave 15 minutes Cross Section

SEM IMAGES OF SAMPLE #

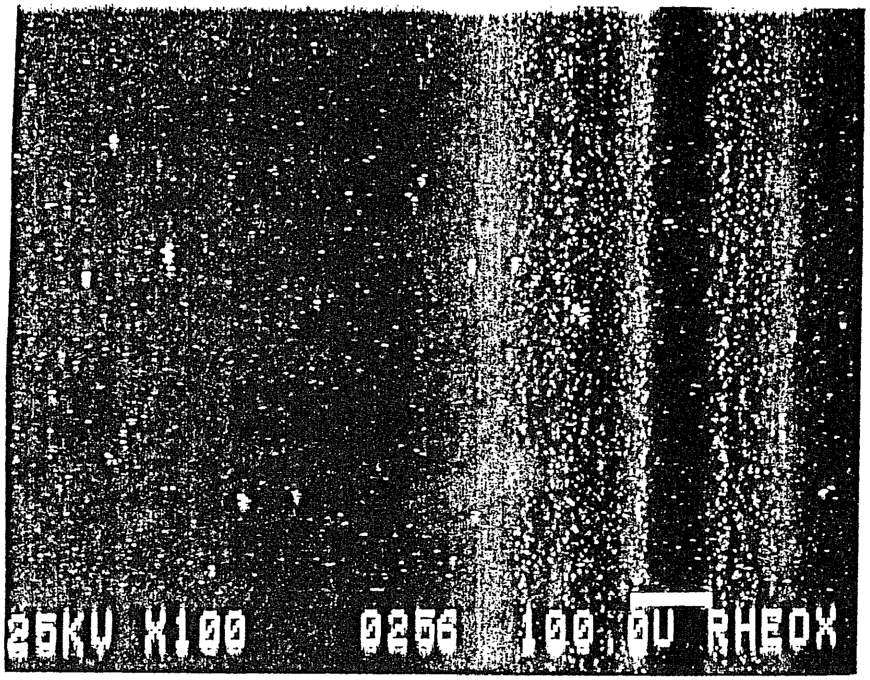

Figure 140 Ti X-Ray Image of Figure 136

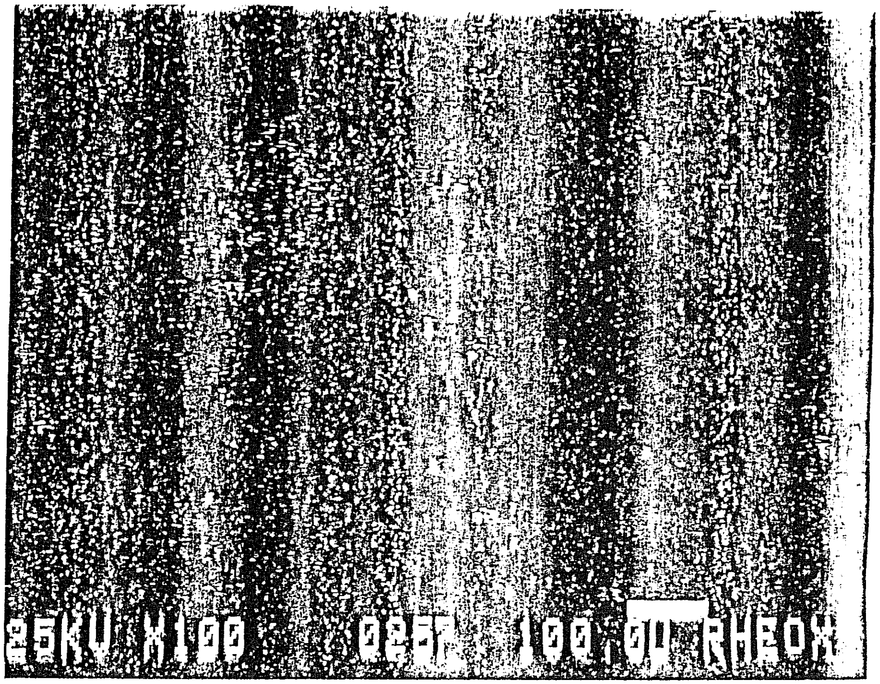

Figure 141 Cr X-Ray Image of Figure 13

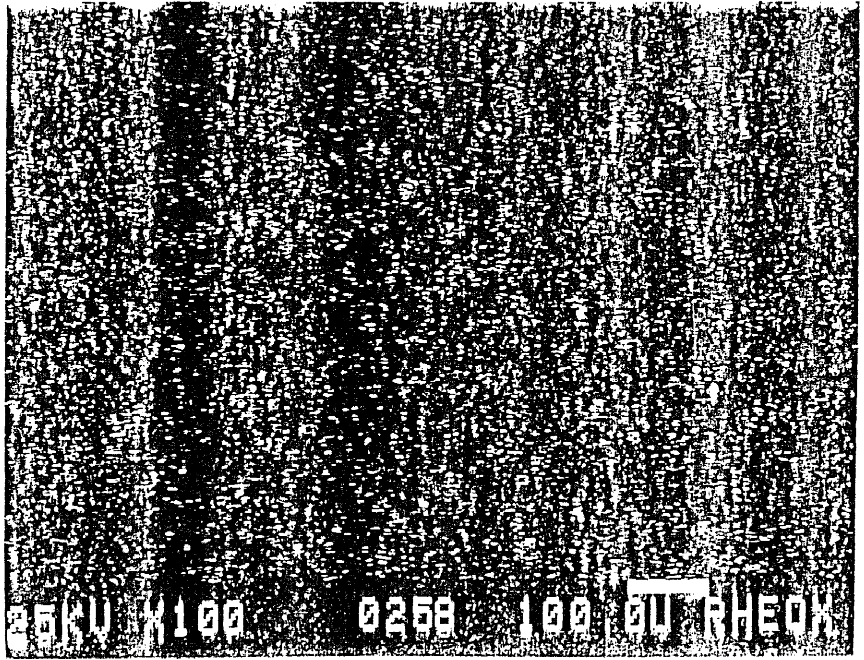

Figure 142 Fe X Ray Image of Figure 136

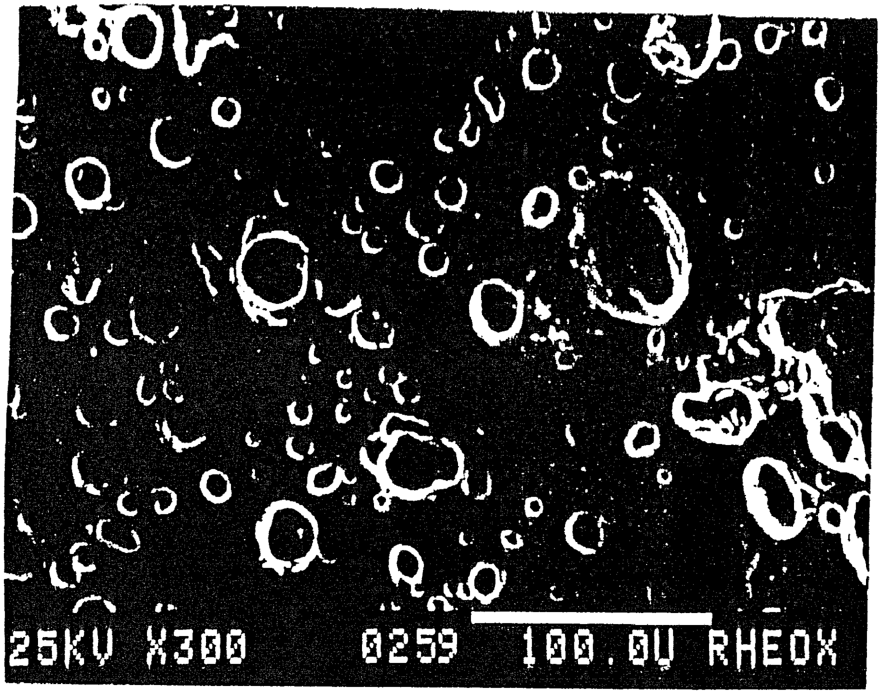

Figure 143

Line Profile Scan

AL →

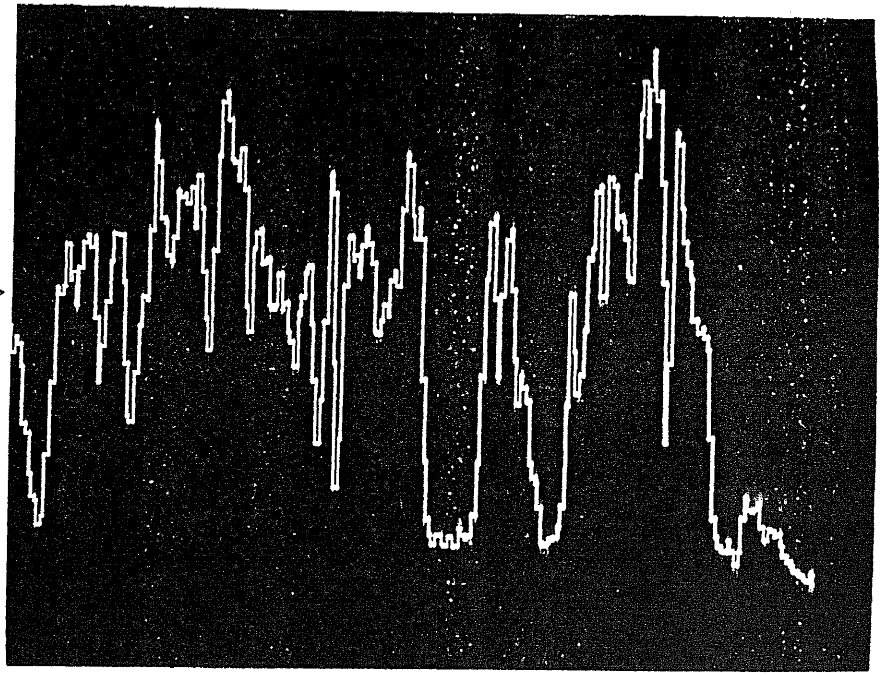

Figure 144

Si ←

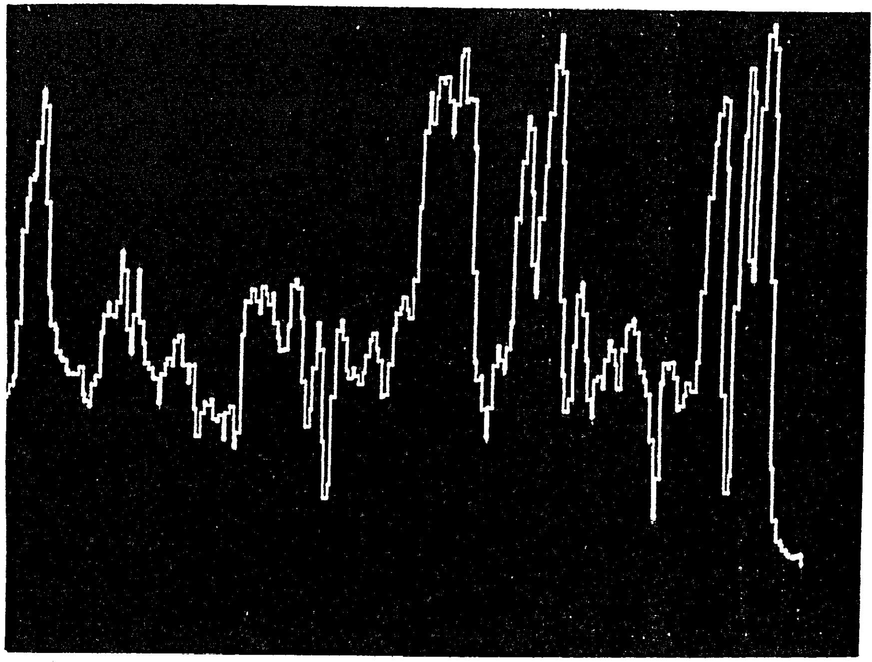

Figure 145

K →

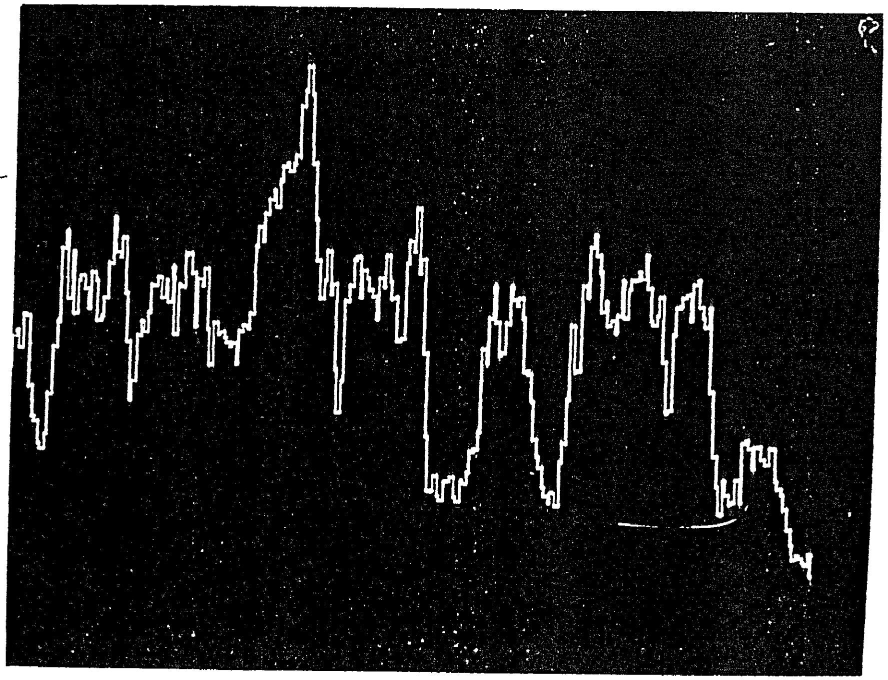

Figure 146

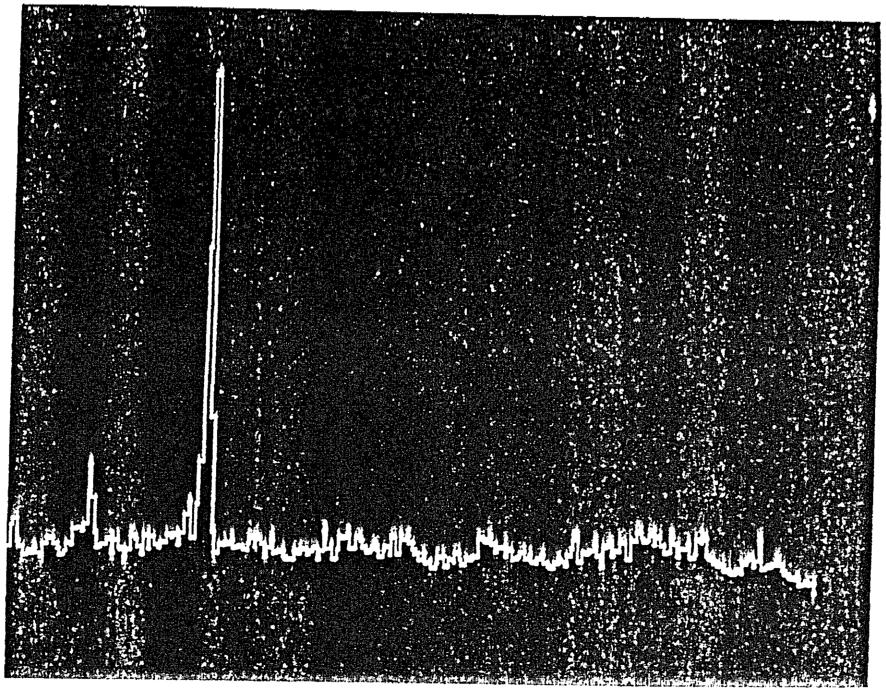

Ti

Figure 147 Line Profile Scan

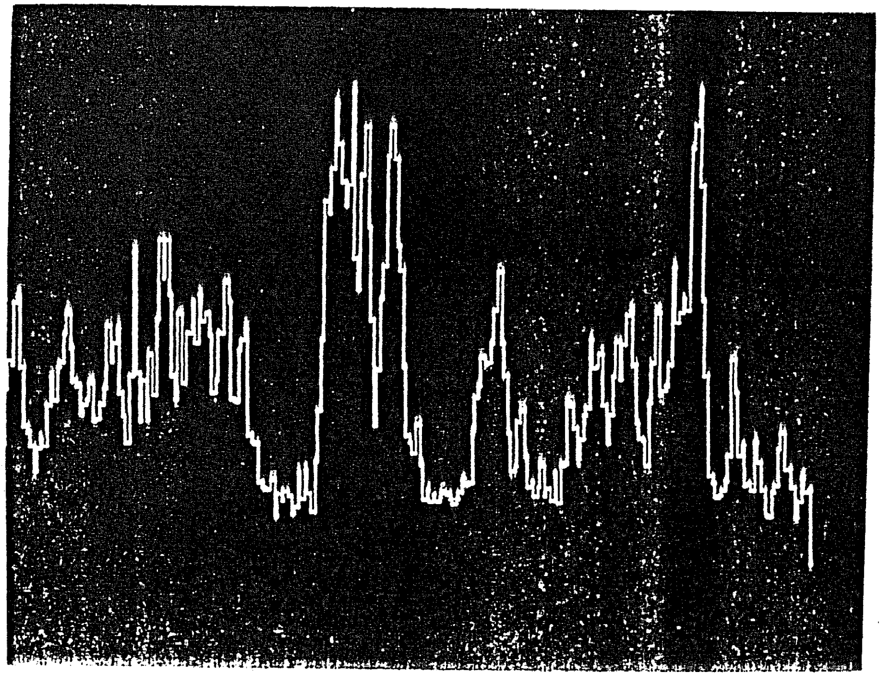

Cr

figure 148

Fe

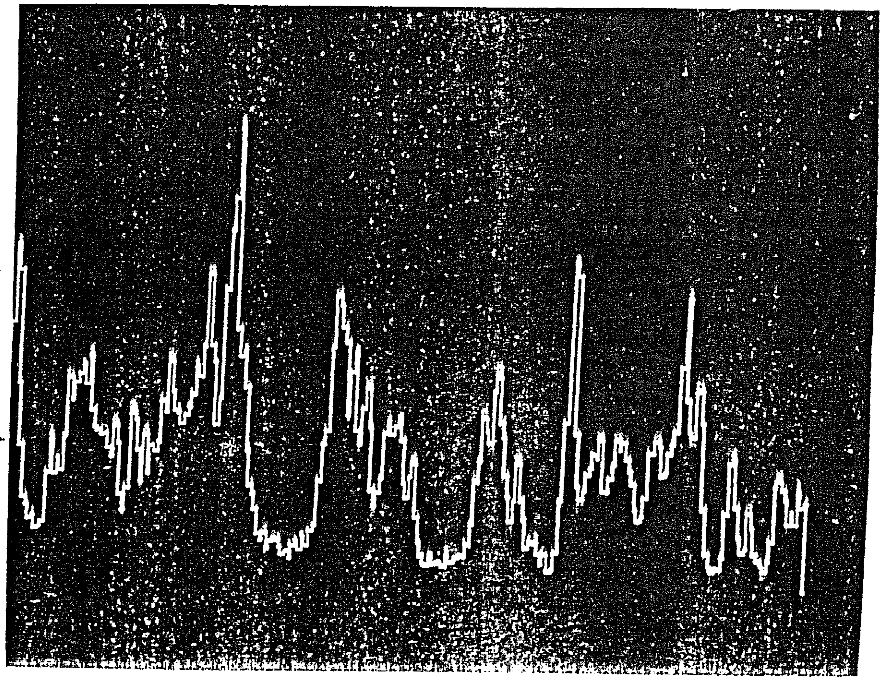

Figure 149

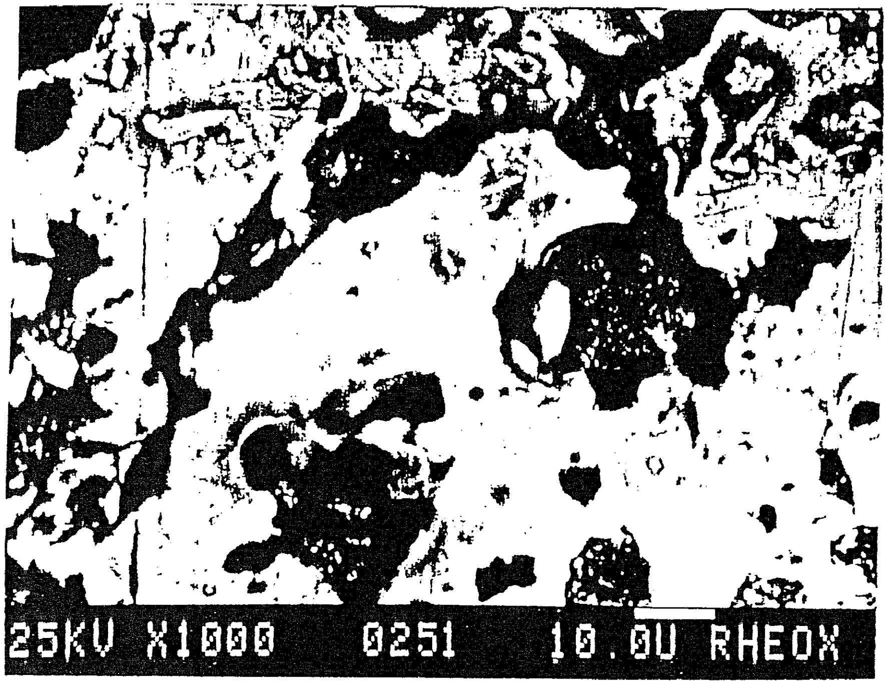

Figure 150

Line Profile Scan

AL →

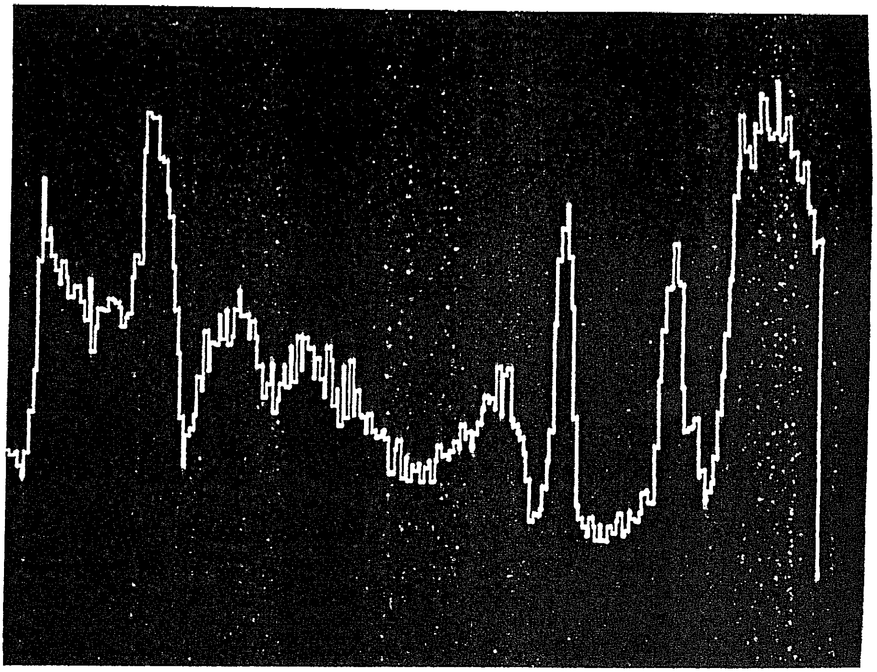

Figure 151

Si ←

K →

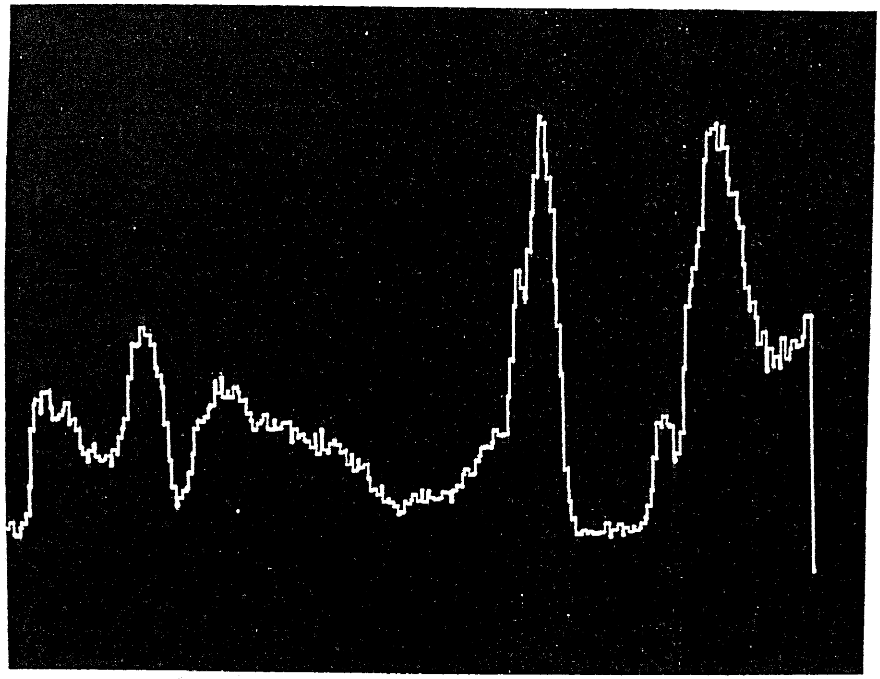

Figure 152

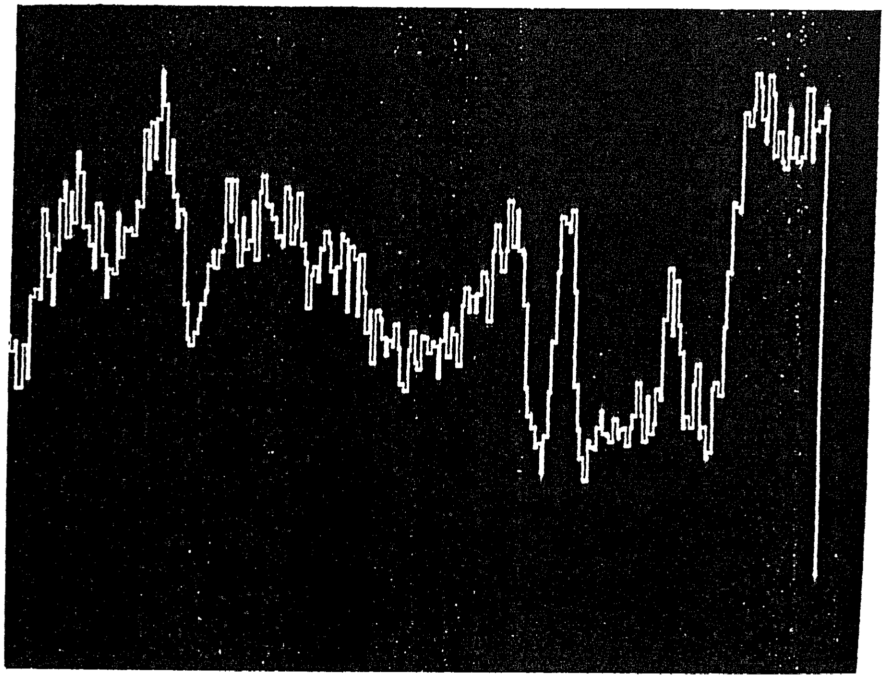

Figure 153

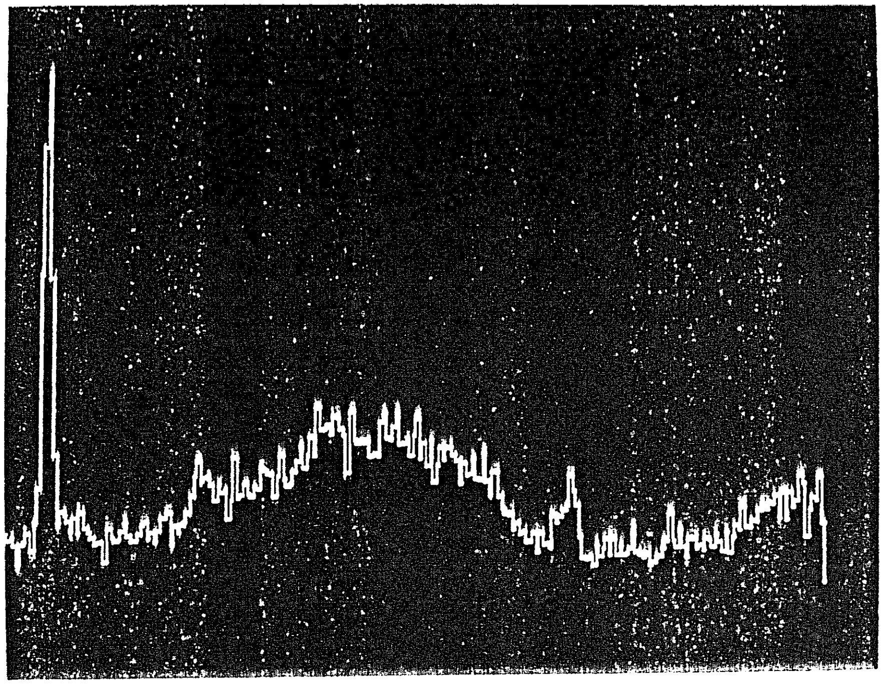

Figure 154 Line Profile Scan

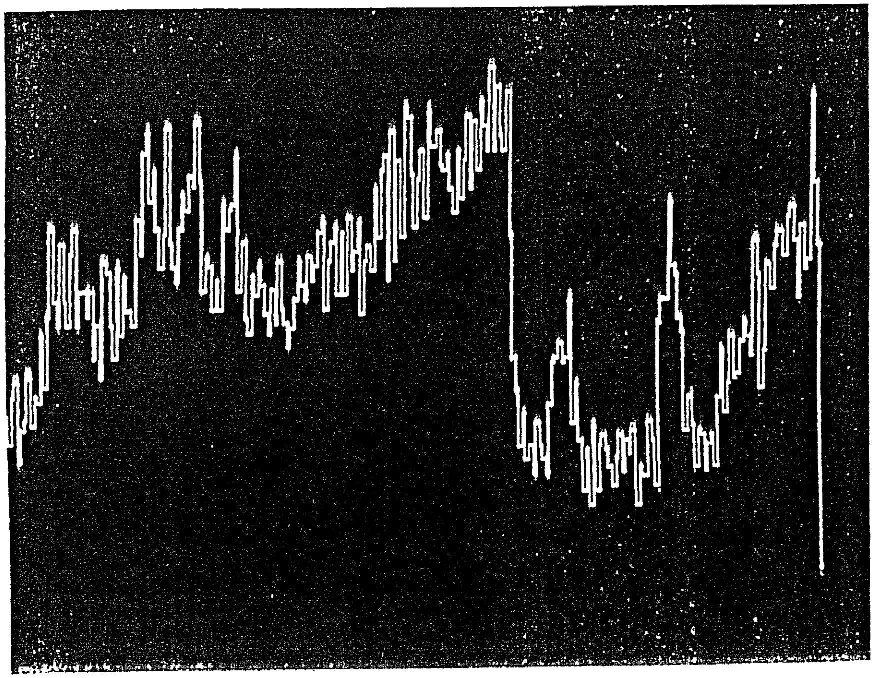

Figure 155

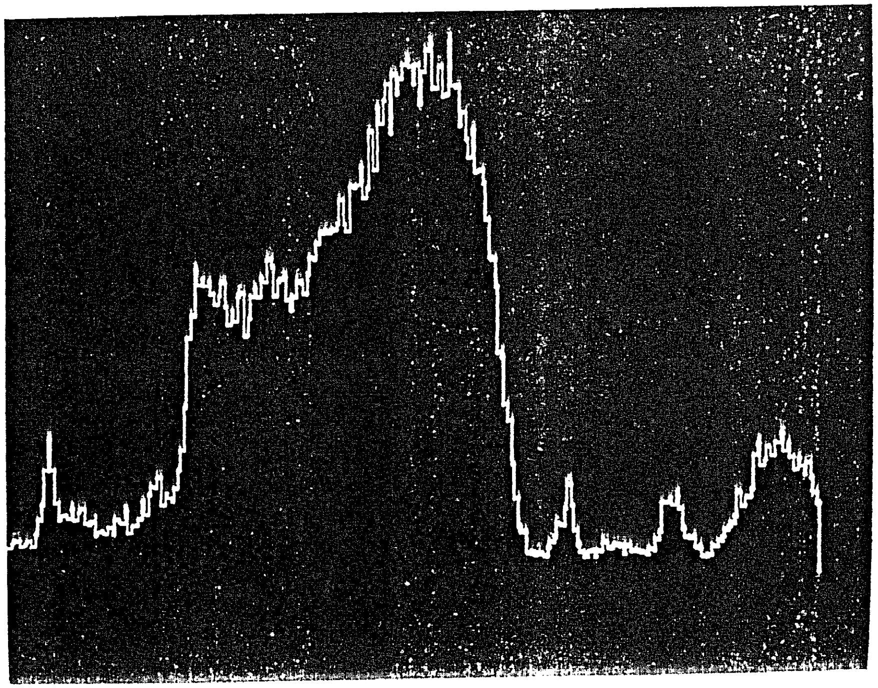

Figure 156

S15C1 ■ AVS/ON

CA LL

S15C1

CUR: 0.0 0CNTS

40000FS 100■ T

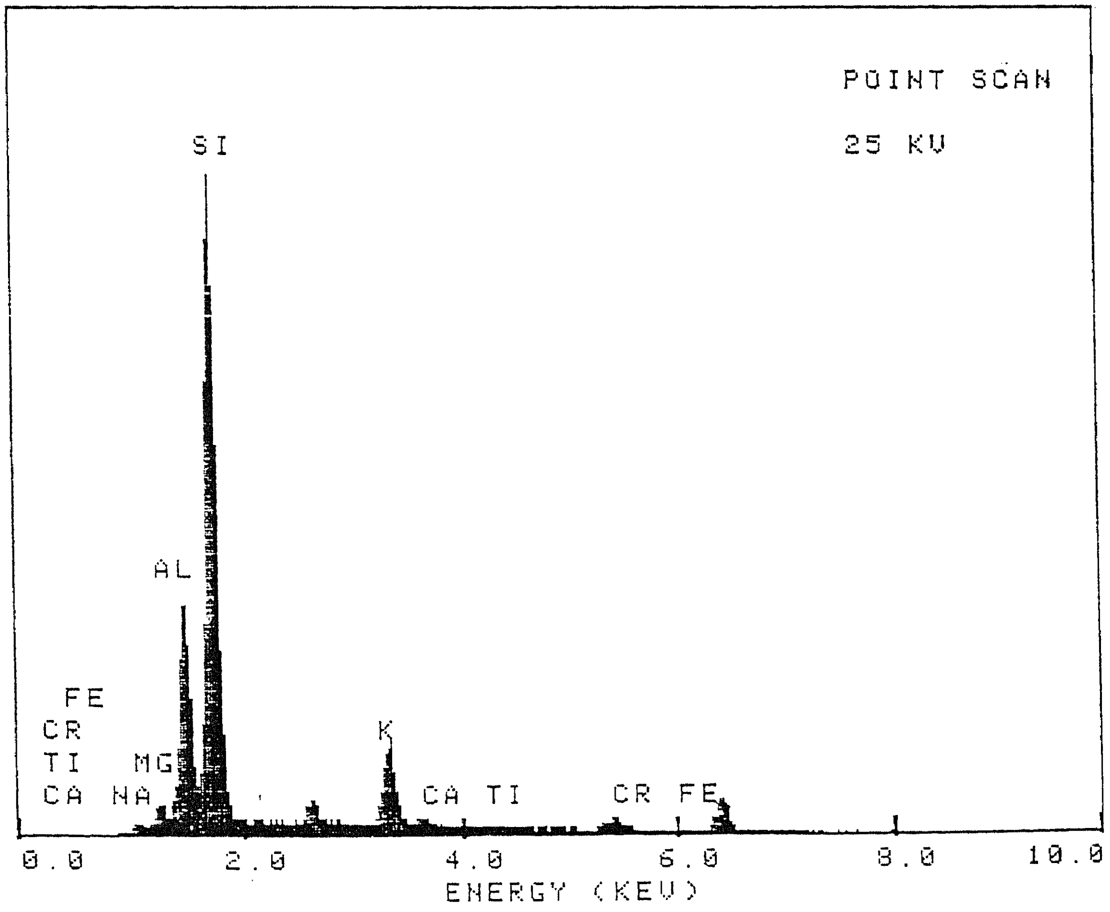

20-Oct-89 11:35

S15C2 ■ AVS/ON

CA LL

S15C2

CUR: 0.0 0CNTS

40000FS 100■ T

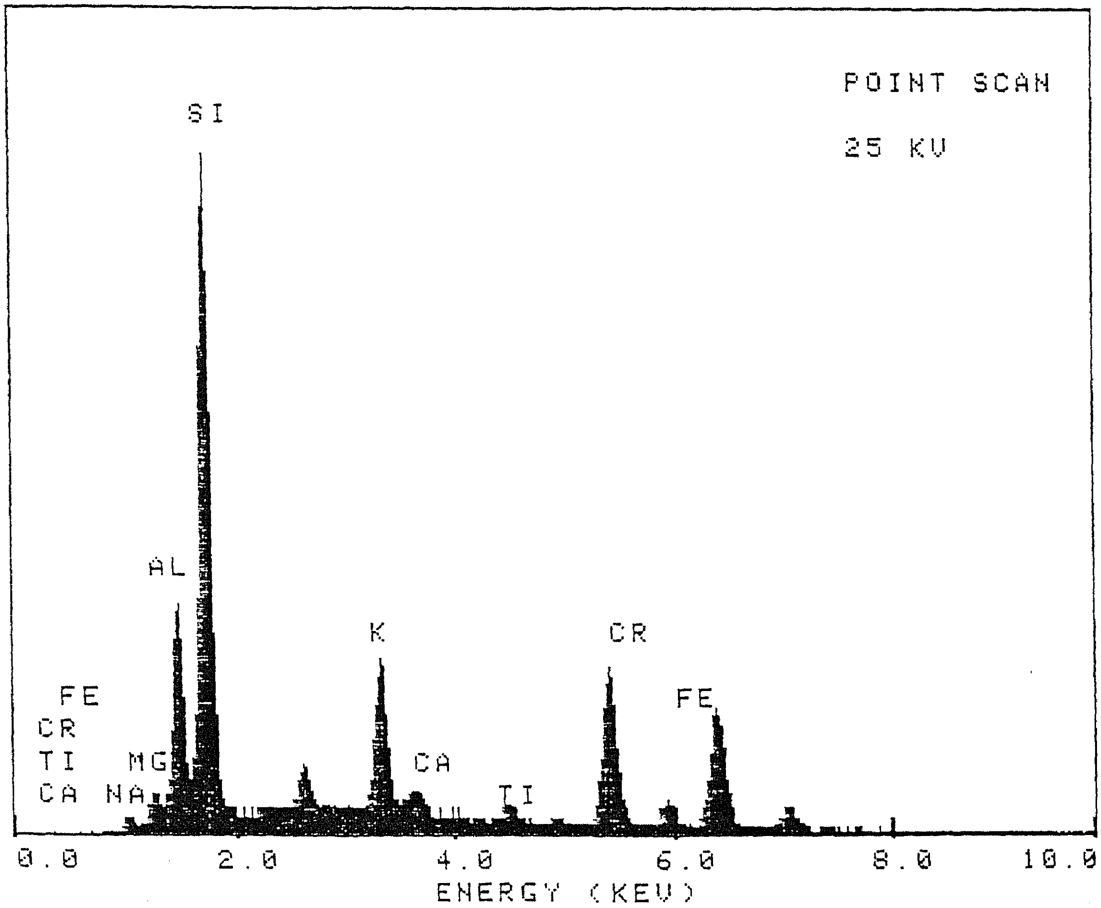

20-Oct-89 11:35

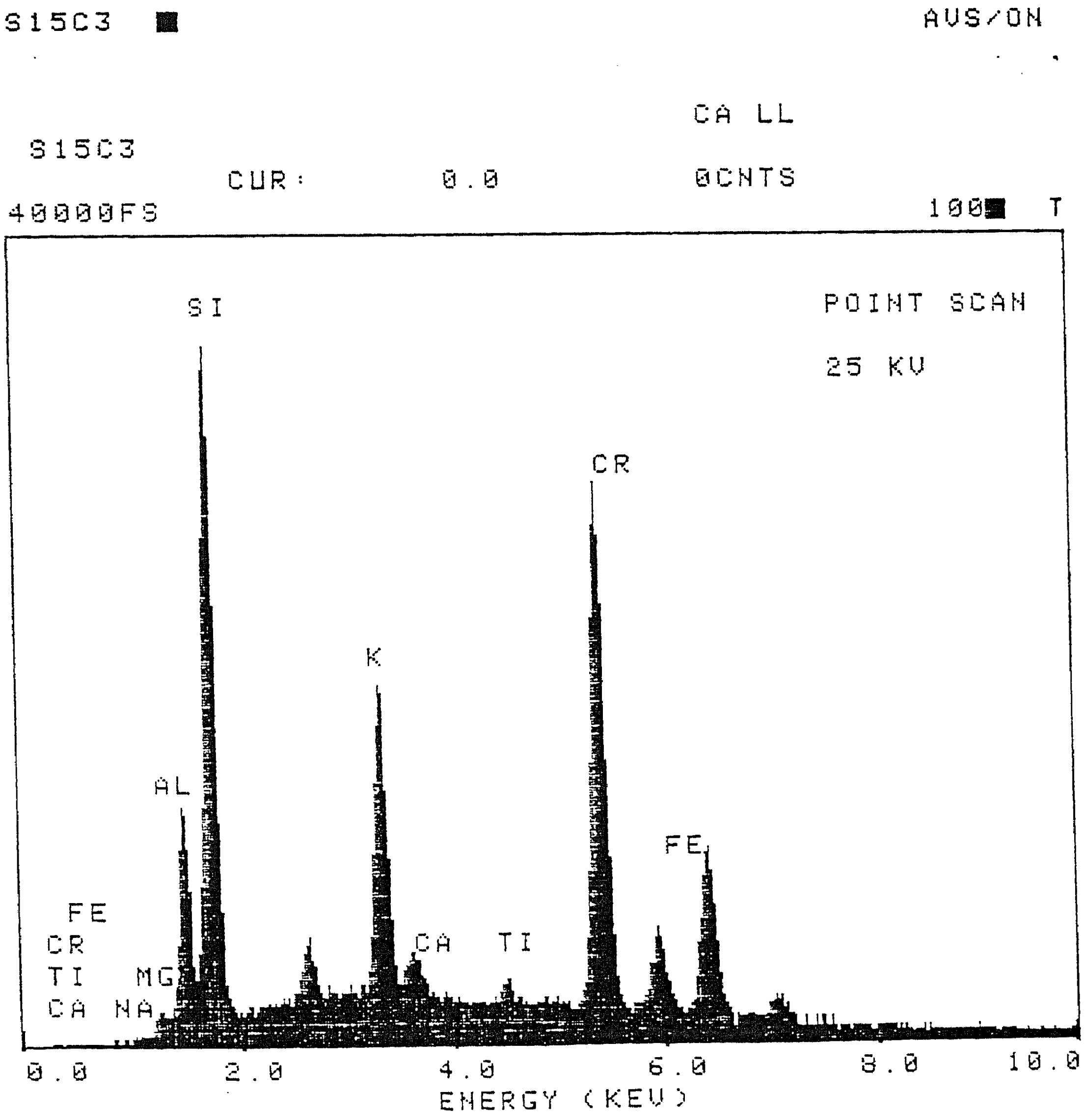

20-Oct-89 11:35

S15C4 ■ AUS/ON

CA LL

S15C4

CUR: 0.0 0CNTS

40000FS 100■ T

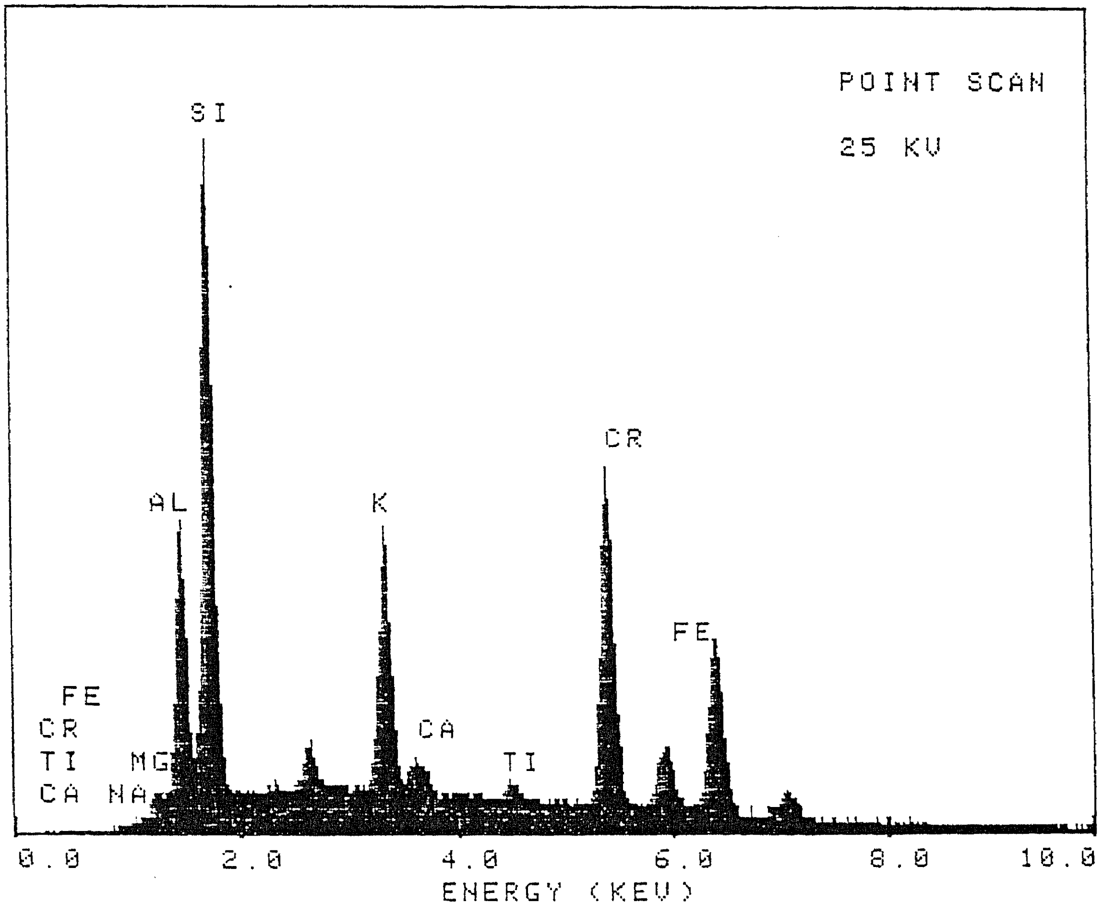

20-Oct-89 11:35

S15C5 ■ AVS/ON.

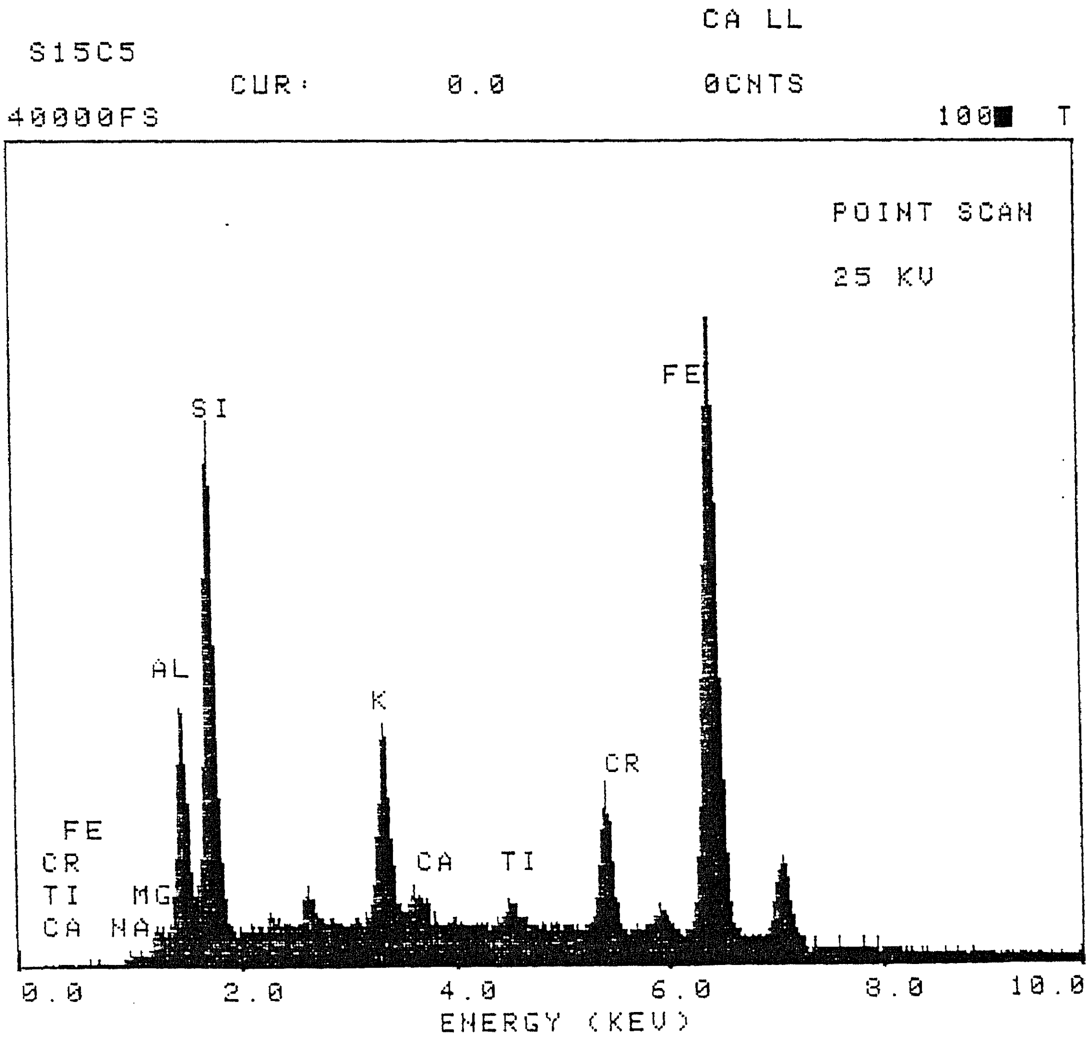

20-Oct-89 11:35

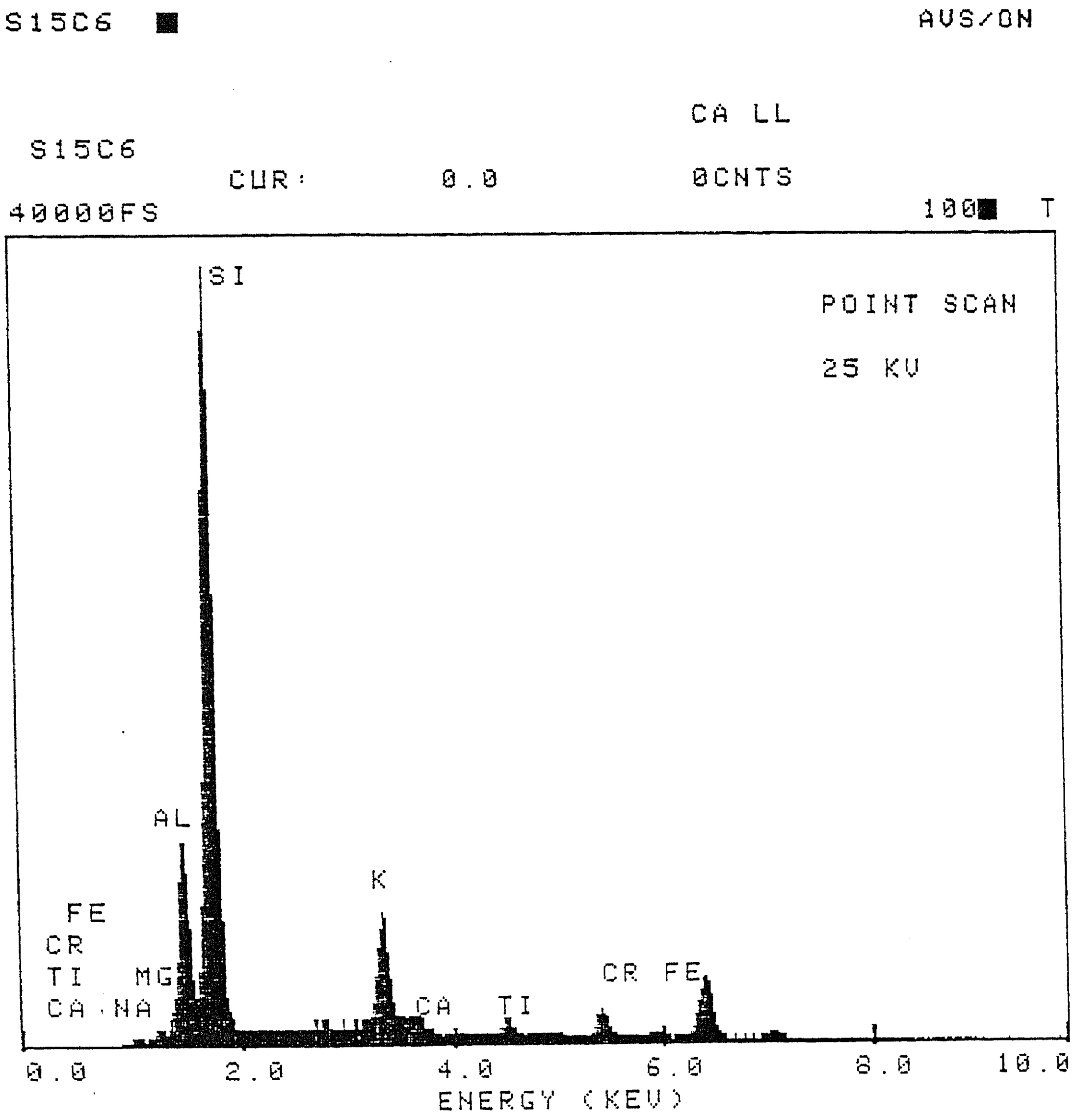

20-Oct-89 11:35

S15C7 ■ AVS/ON

CA LL

S15C7

CUR: 0.0 0CNTS

40000FS 100■ T

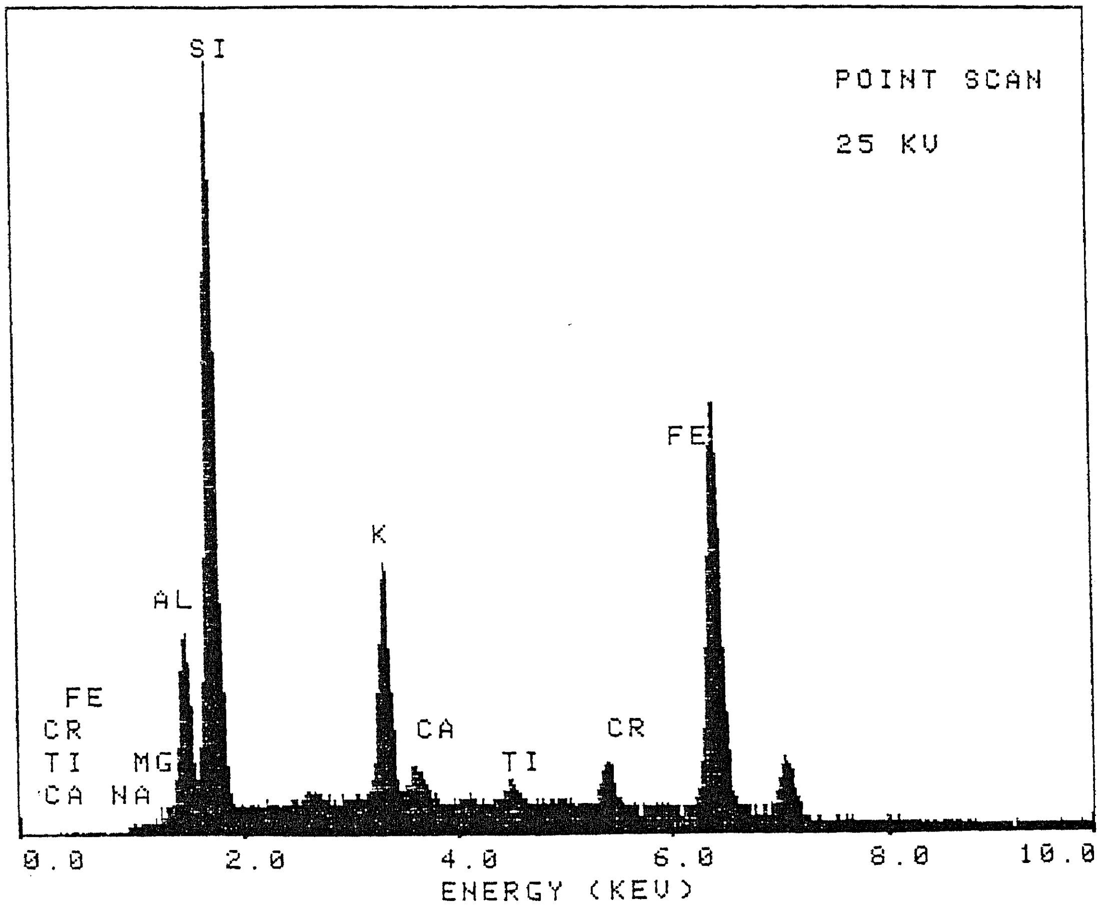

20-Oct-89 11:35

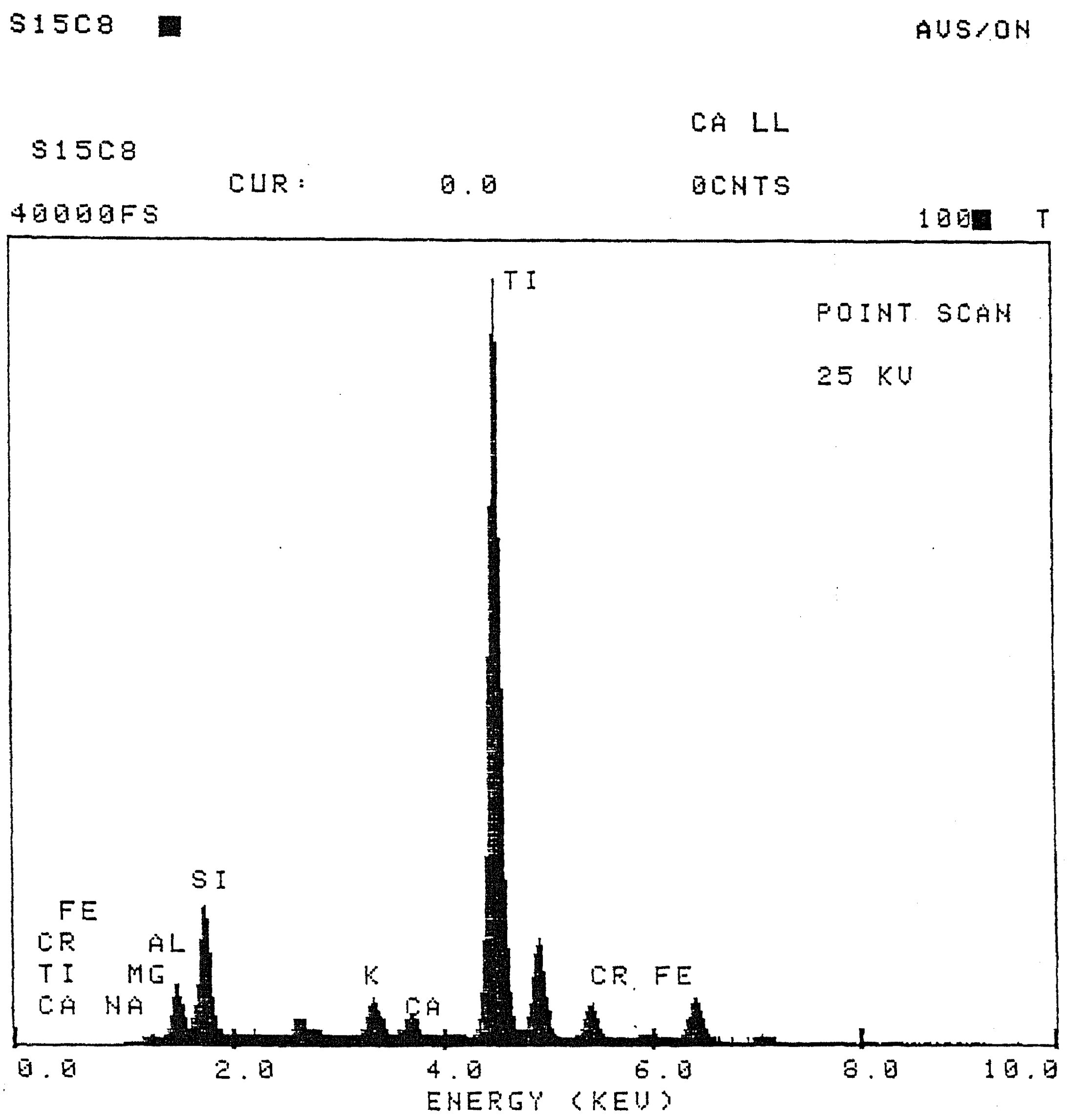

20-Oct-89 11:35

SEM IMAGES OF SAMPLE # Microwave 30 minutes Powder Sample

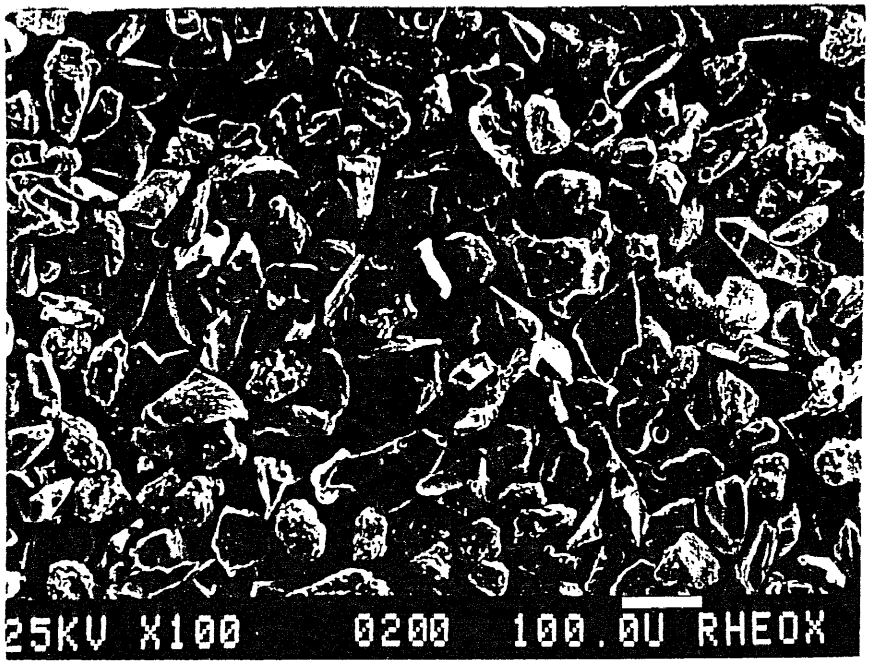

Figure 157

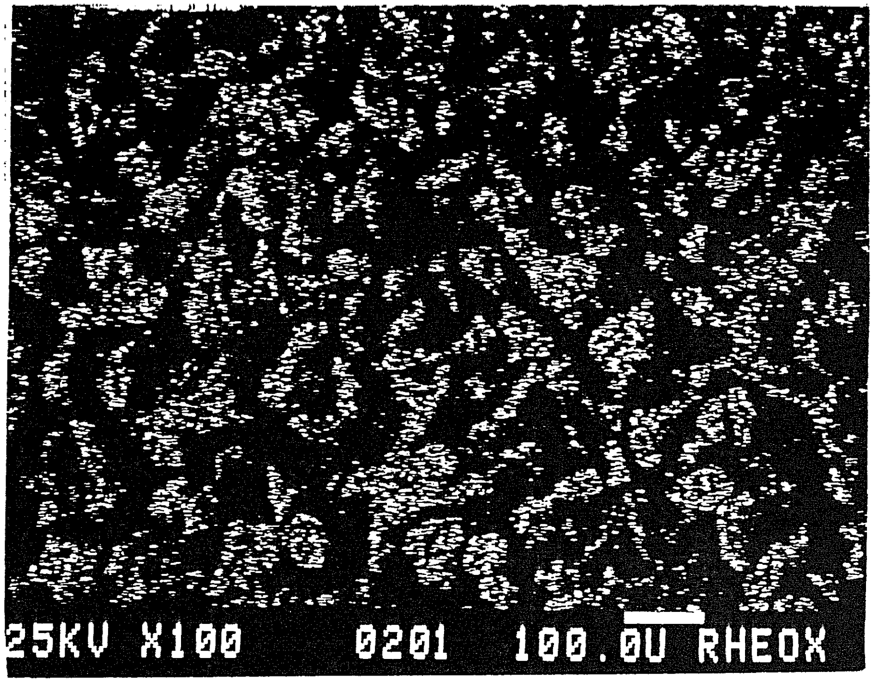

Figure 158 AL X-ray Image of Figure 157

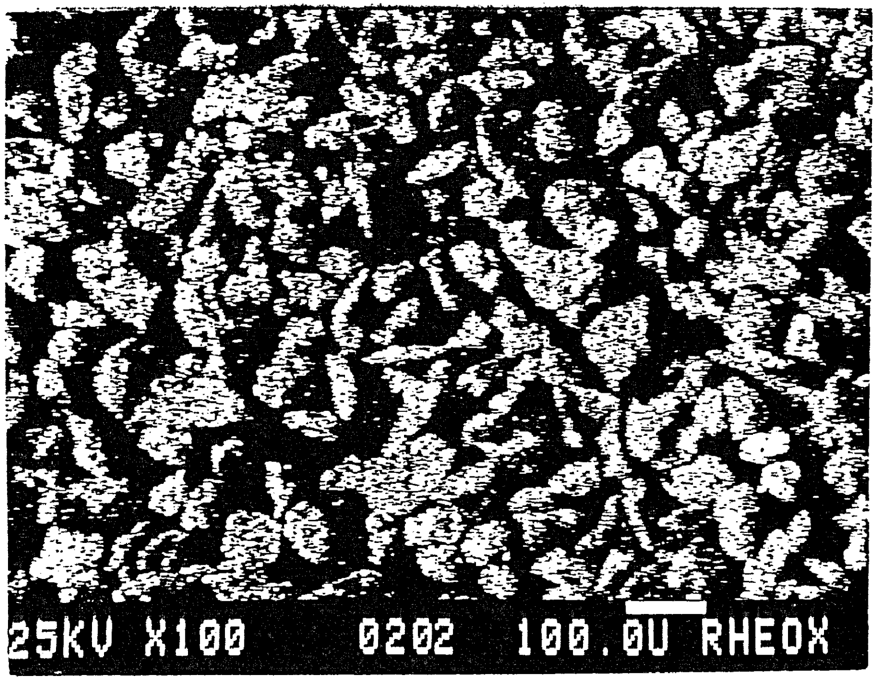

Figure 159 Si X-ray Image of Figure 157

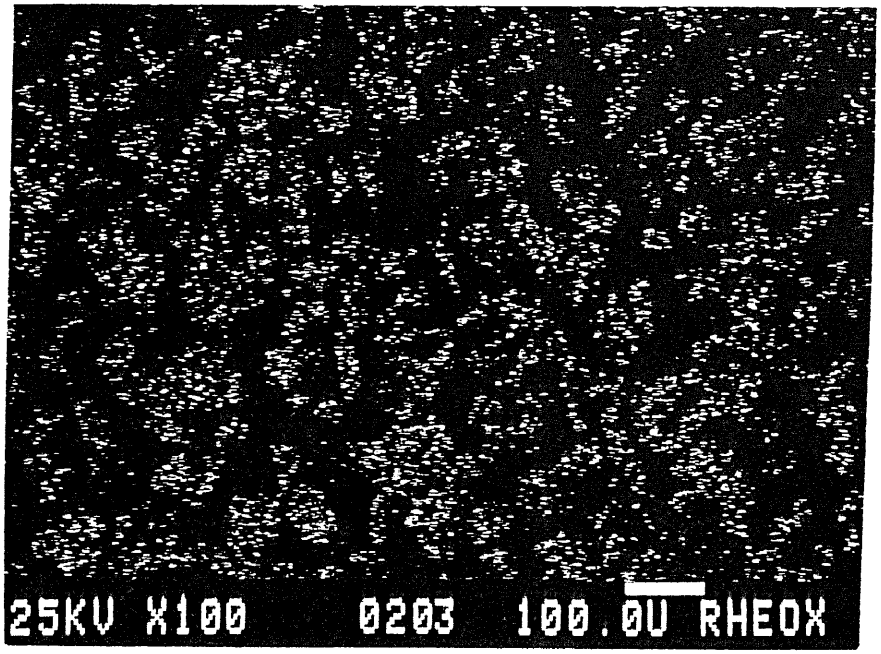

Figure 160 K X-ray Image of Figure 157

SEM IMAGES OF SAMPLE # Microwave 30 minutes Powder Sample

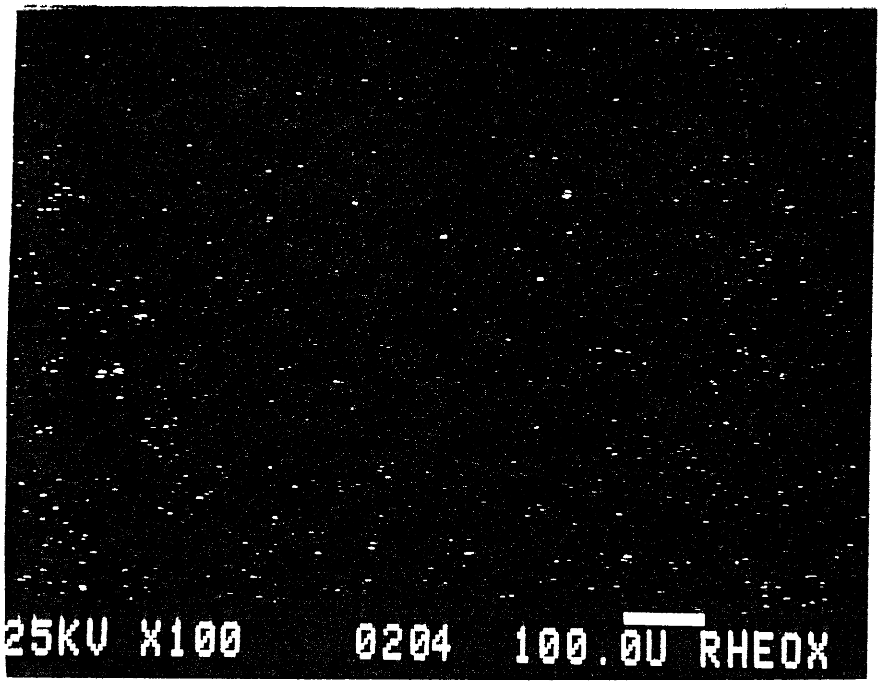

Figure 161 Ti X-Ray Image of Figure 157

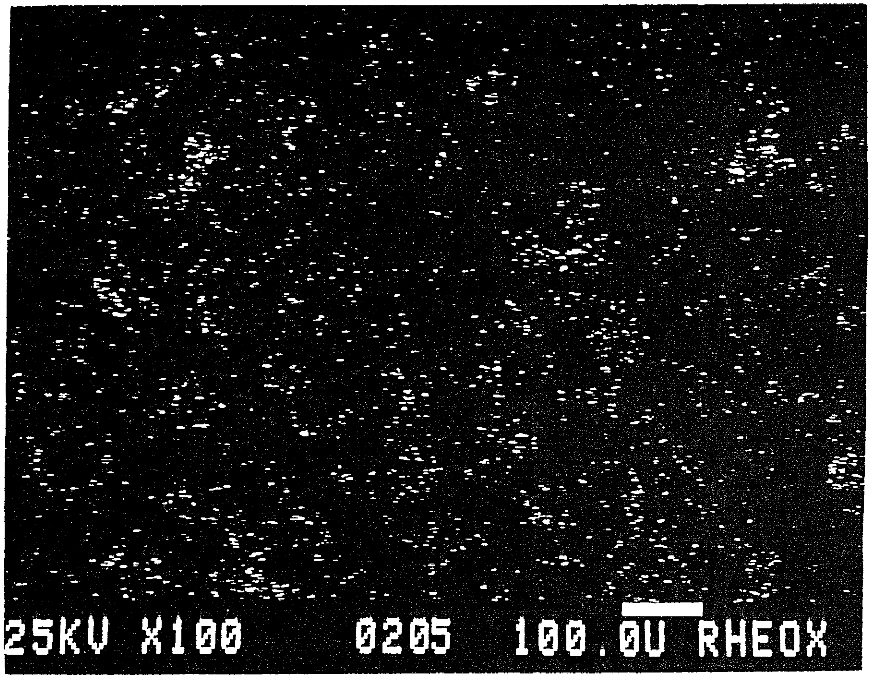

Figure 162 Cr X-Ray Image of Figure 157

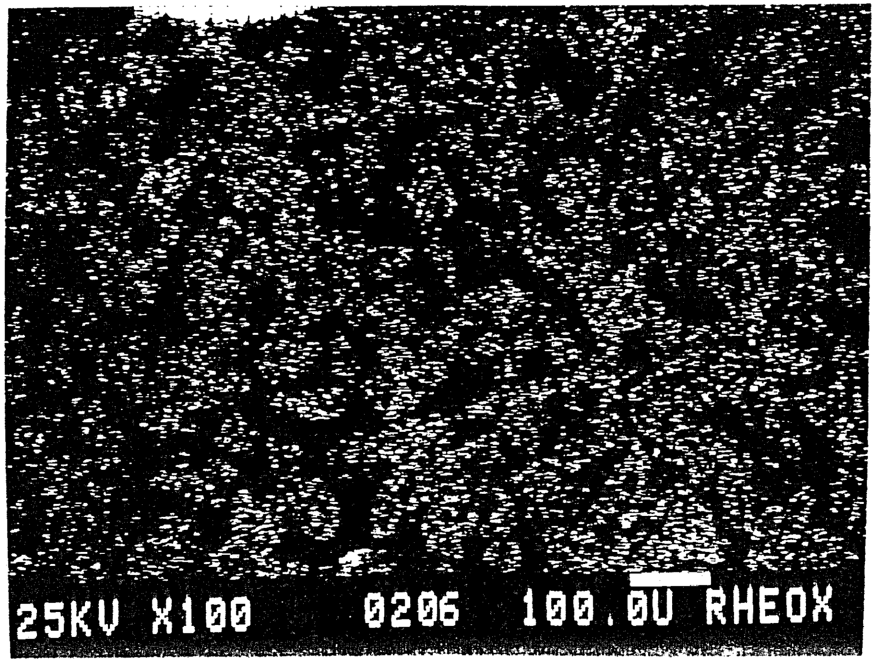

Figure 163 Fe X-Ray Image of Figure 157

SEM IMAGES OF SAMPLE # Microwave 30 minutes Powder Sample

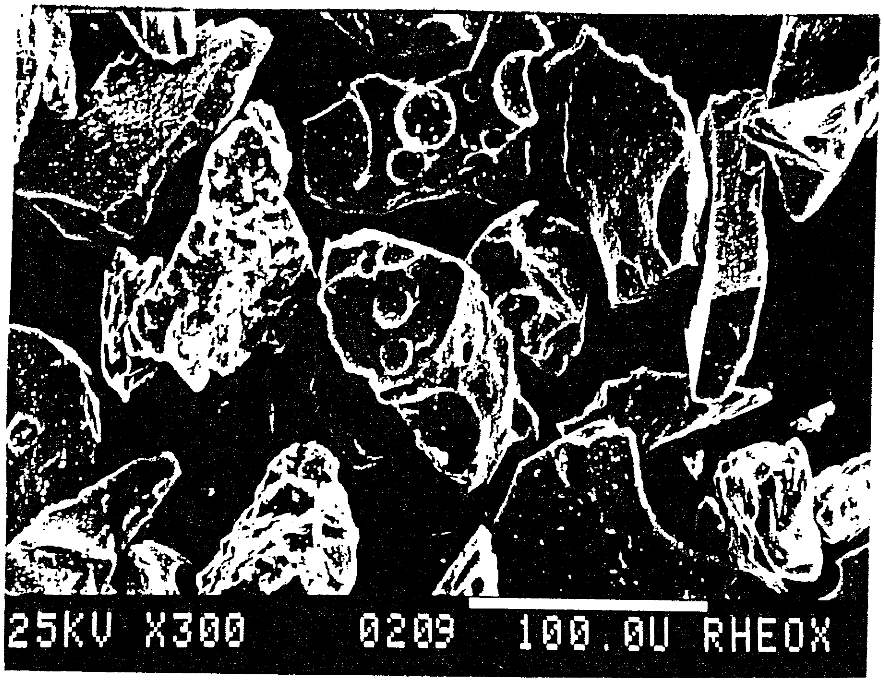

Figure 164

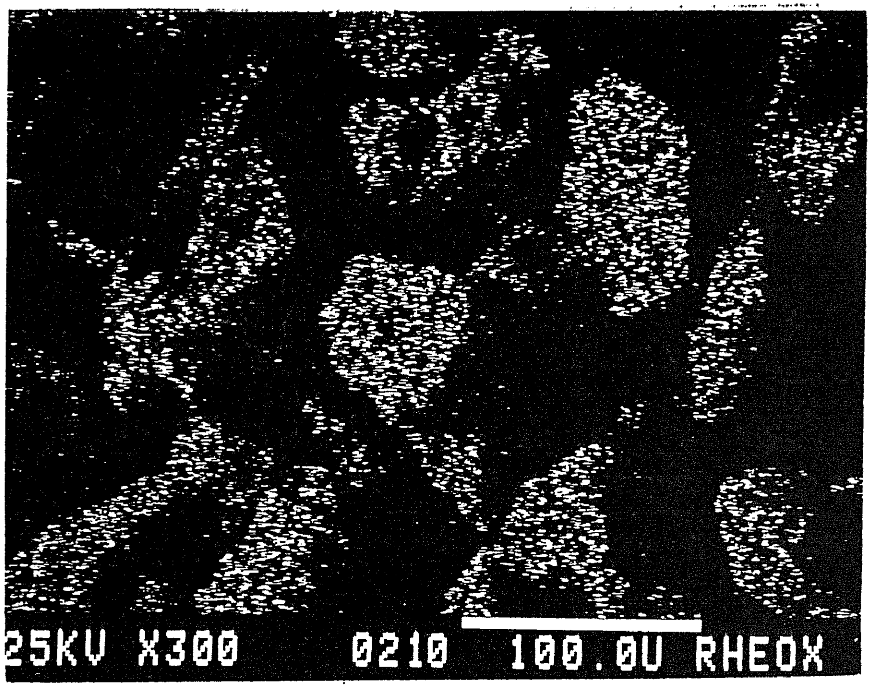

Figure 165 AL X-ray Image of Figure 164

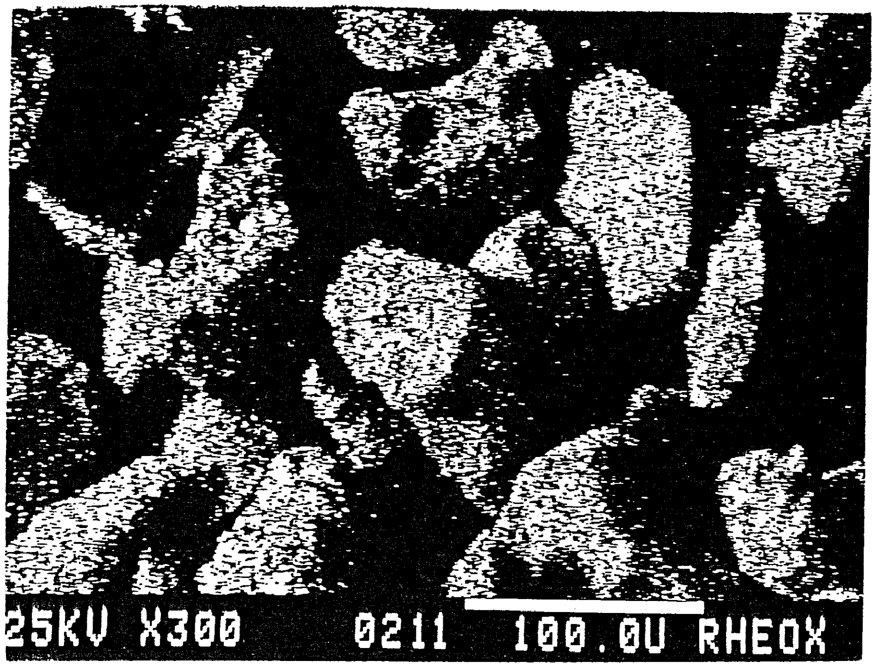

166 Si X-ray Image of Figure 164

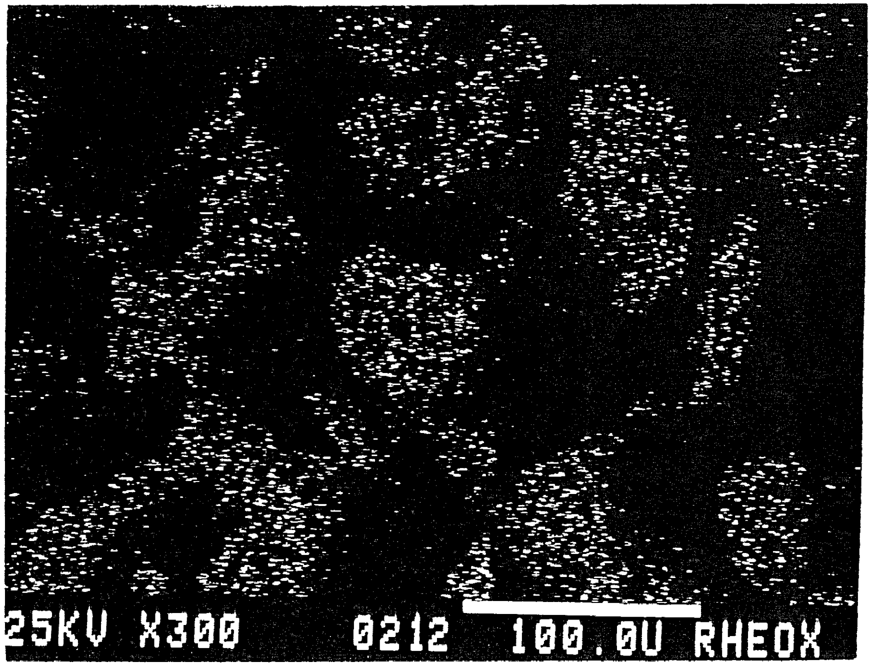

Figure 167 K X-ray Image of Figure 164

SEM IMAGES OF SAMPLE # Microwave 30 minutes Powder Sample

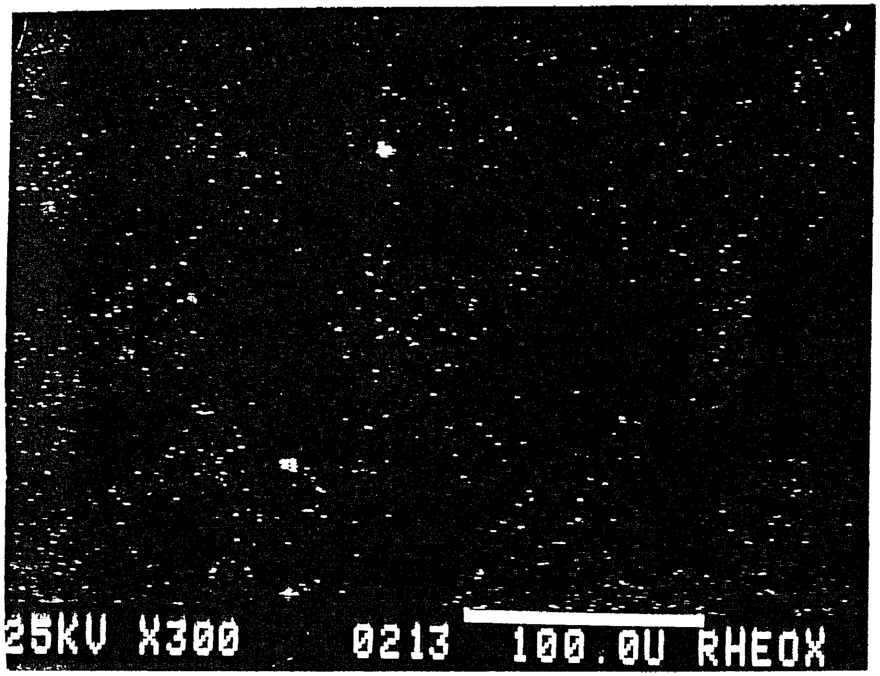

Figure 168 Ti X-Ray Image of Figure 164

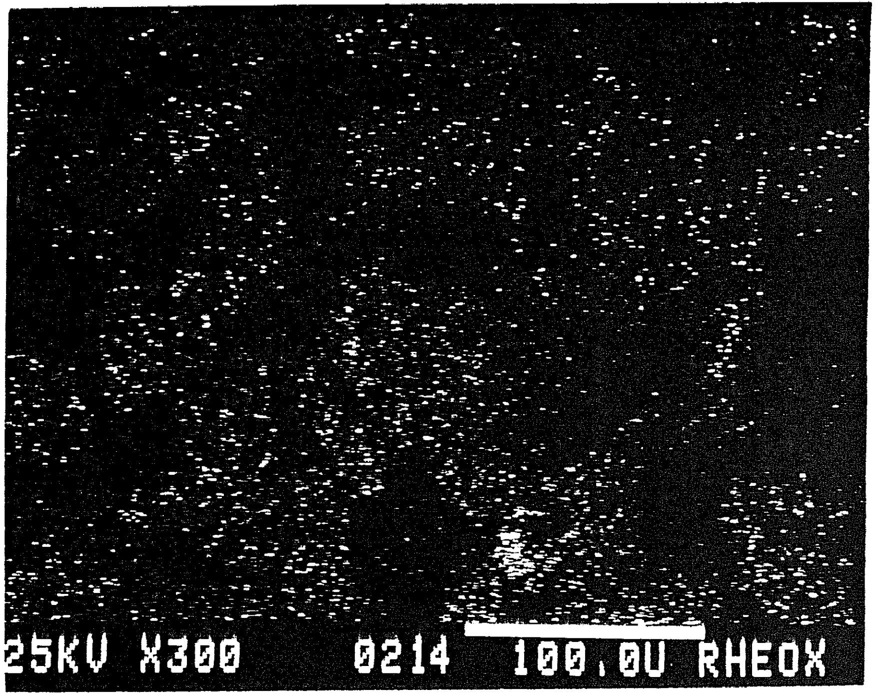

Figure 169 Cr X-Ray Image of Figure 164

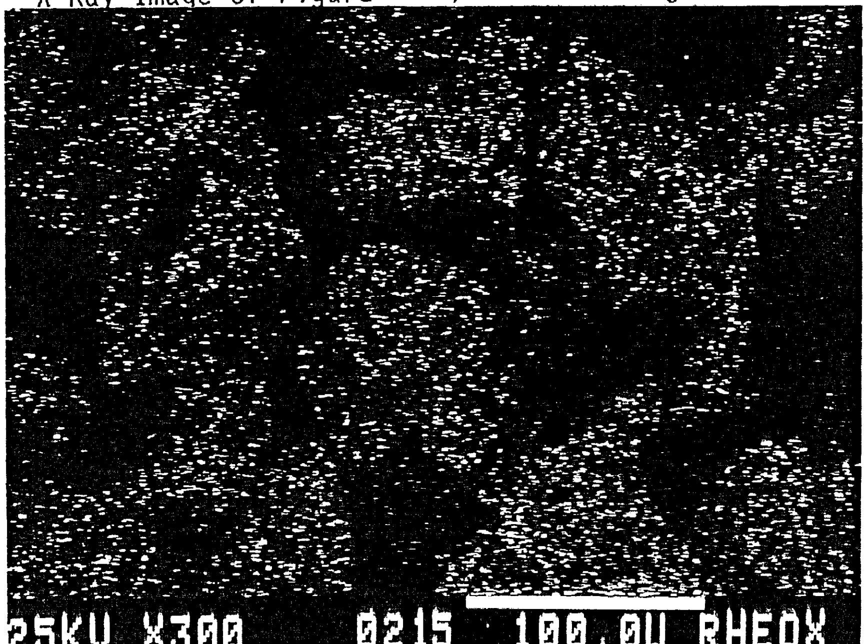

SEM IMAGES OF SAMPLE # Microwave 30 minutes Powder Sample

Figure 171

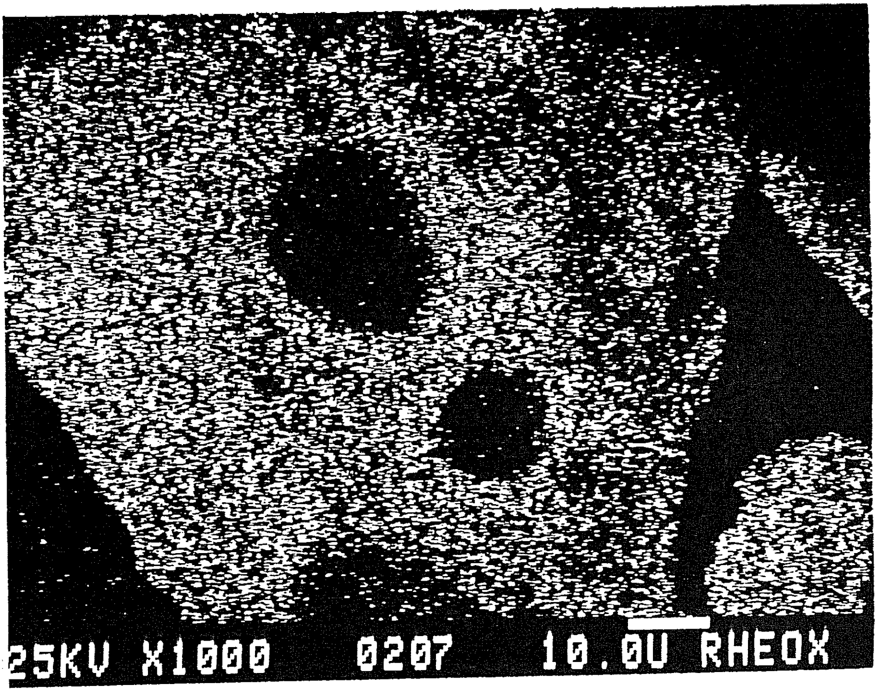

Figure 172 AL X-ray Image of Figure 171

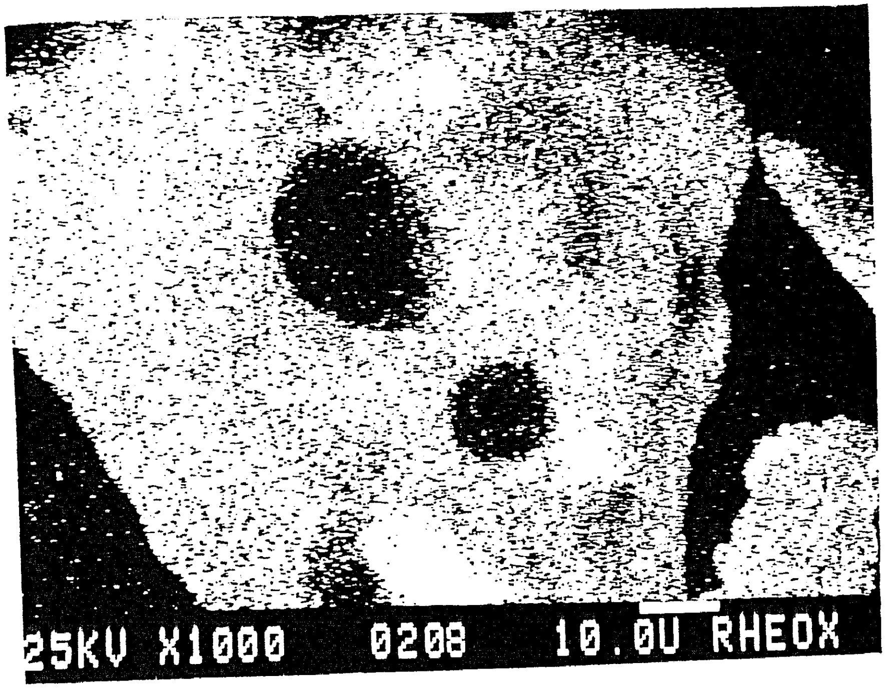

Figure 173 Si X-ray Image of Figure 171

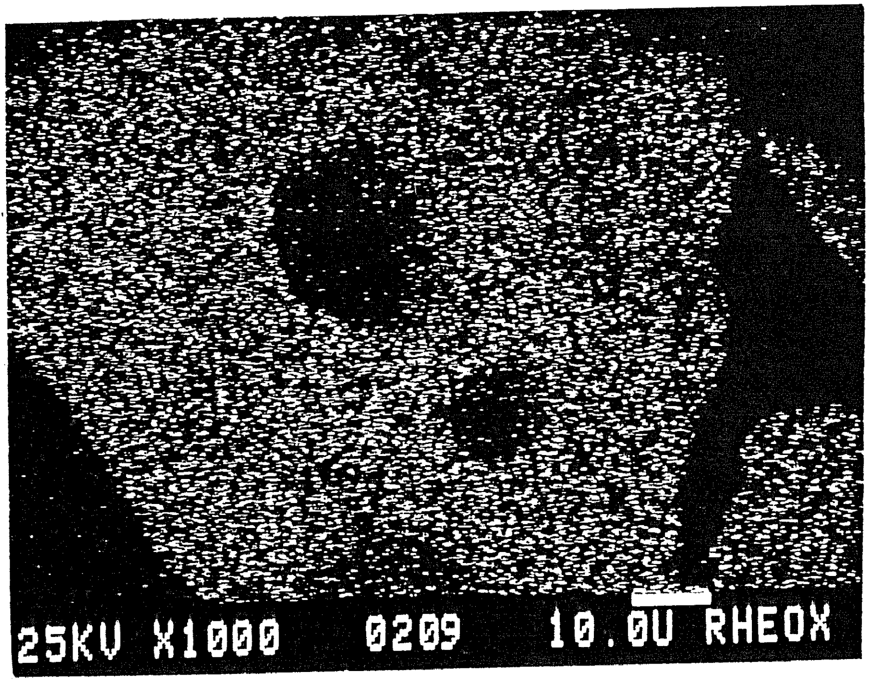

Figure 174 K X-ray Image of Figure 171

SEM IMAGES OF SAMPLE # Microwave 30 minutes Powder Sampl

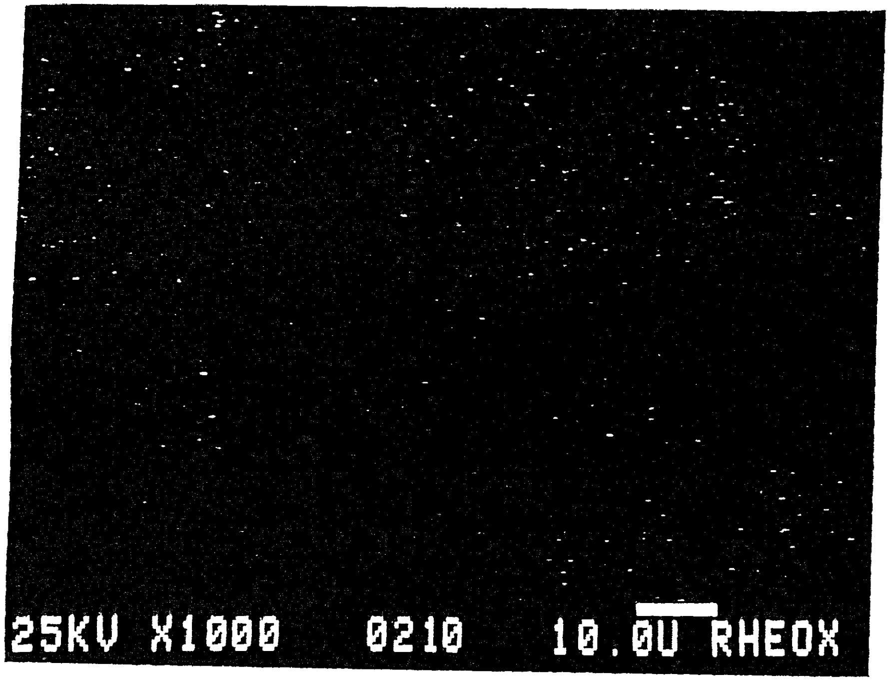

Figure 175 X-Ray Image of Figure 171

Figure 176 X-Ray Image of Figure 171

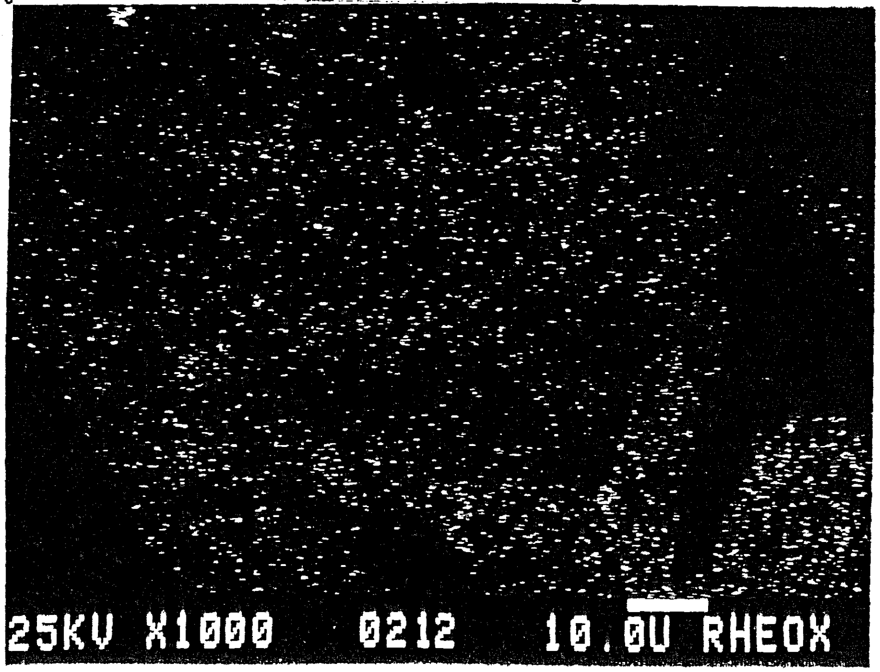

Figure 177 X-Ray Image of Figure 171

Figure 178

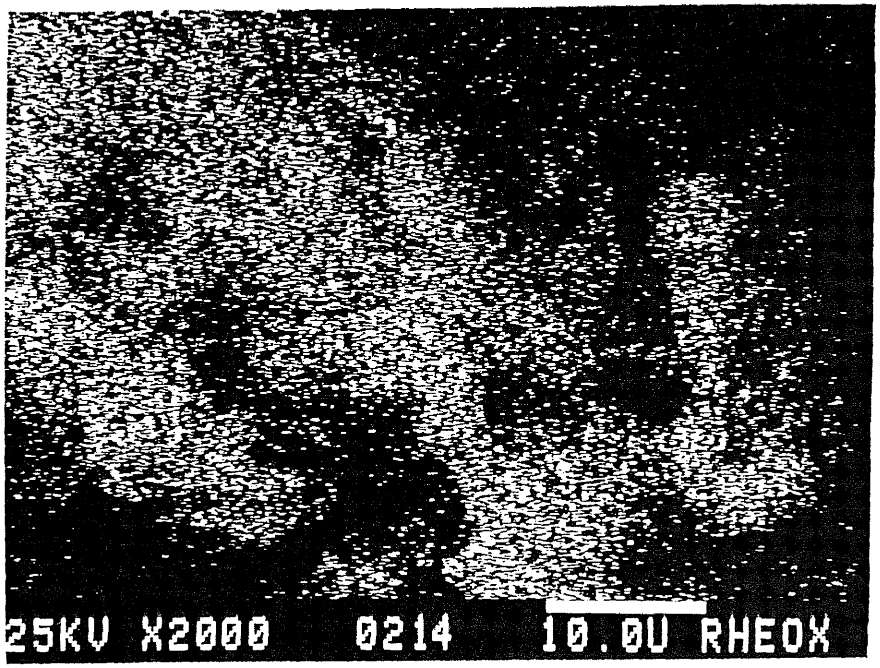

Figure 179 X-ray Image of Figure 178

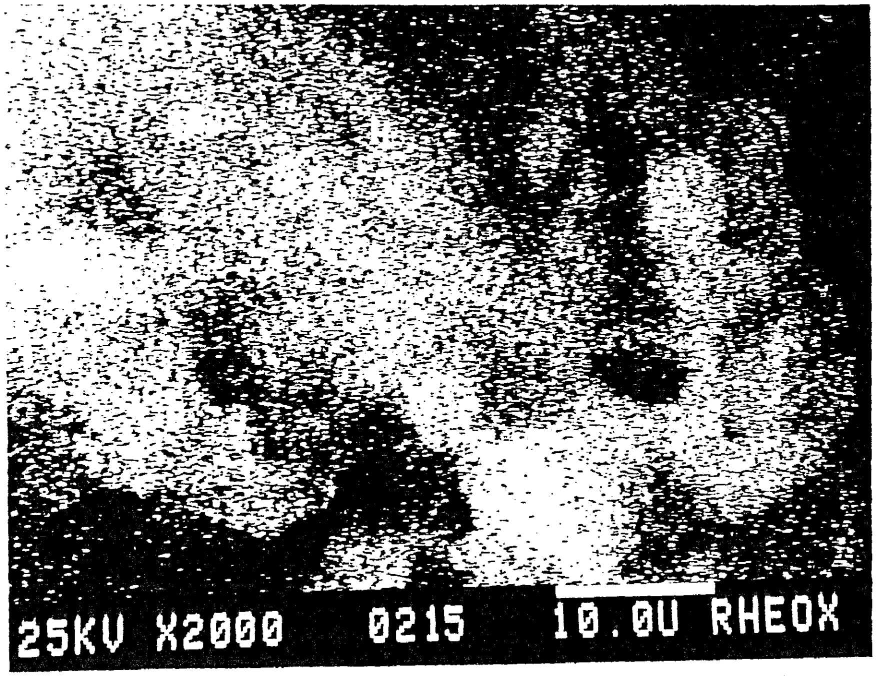

Figure 180 X-ray Image of Figure 178

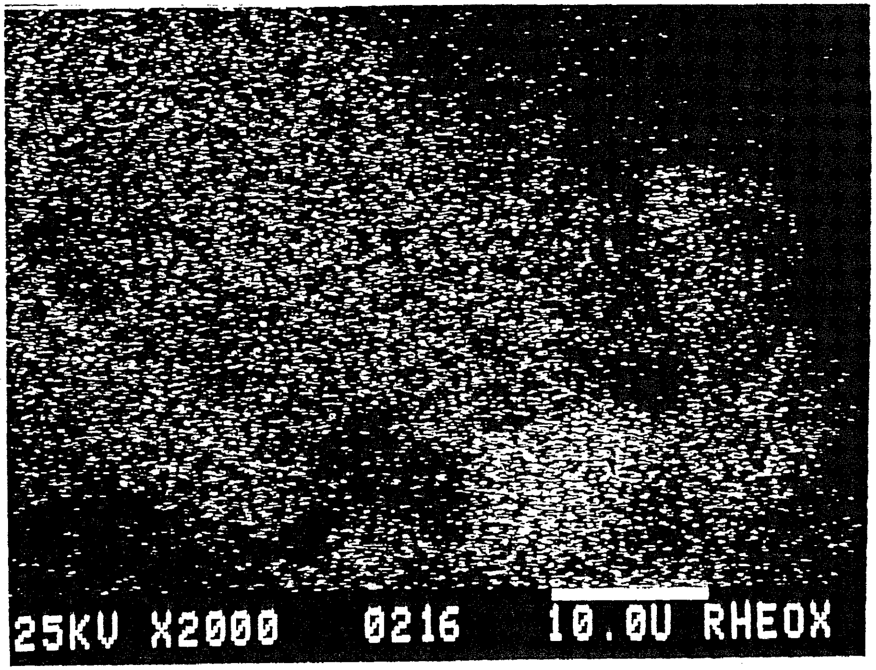

Figure 181 X-ray Image of Figure 178

SEM IMAGES OF SAMPLE # Microwave 30 minutes Powder Sample

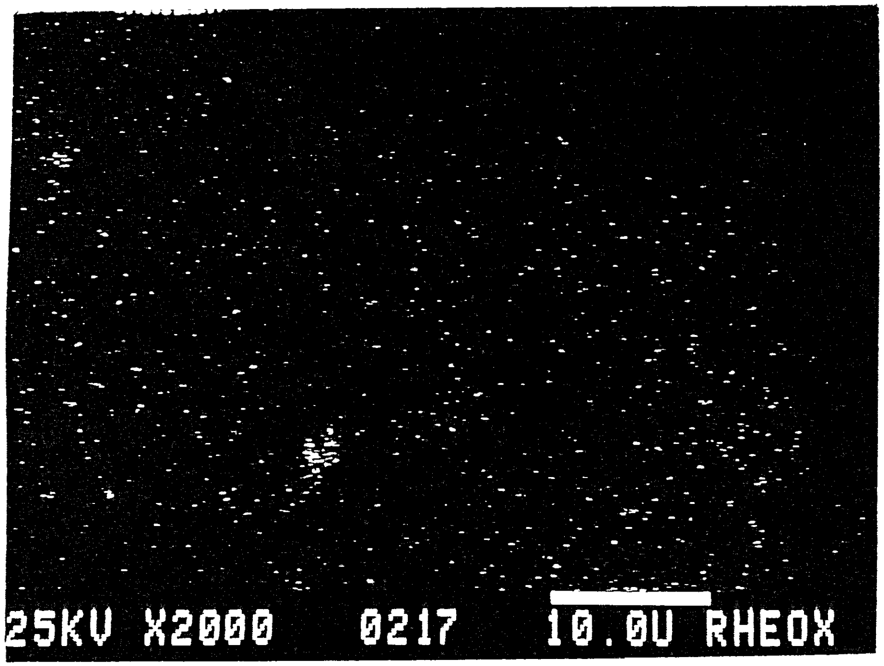

Figure 182 Ti X-Ray Image of Figure 178

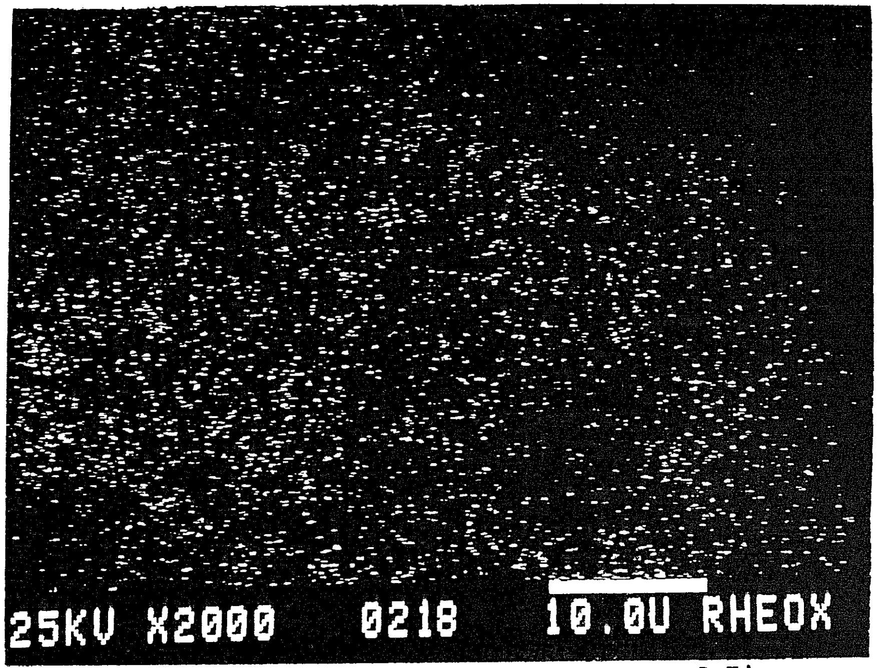

Figure 183 Cr X-Ray Image of Figure 178

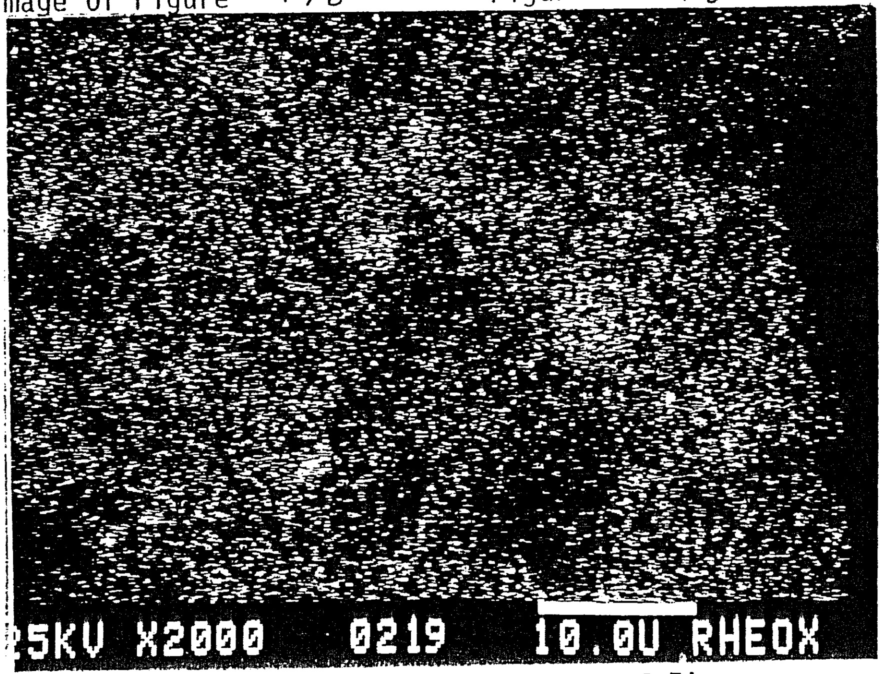

Figure 184 Fe X-Ray Image of Figure 178

S30H1 ■ AVS/ON

CA LL

S30H1

CUR: 0.0 0CNTS

40000FS 100■ T

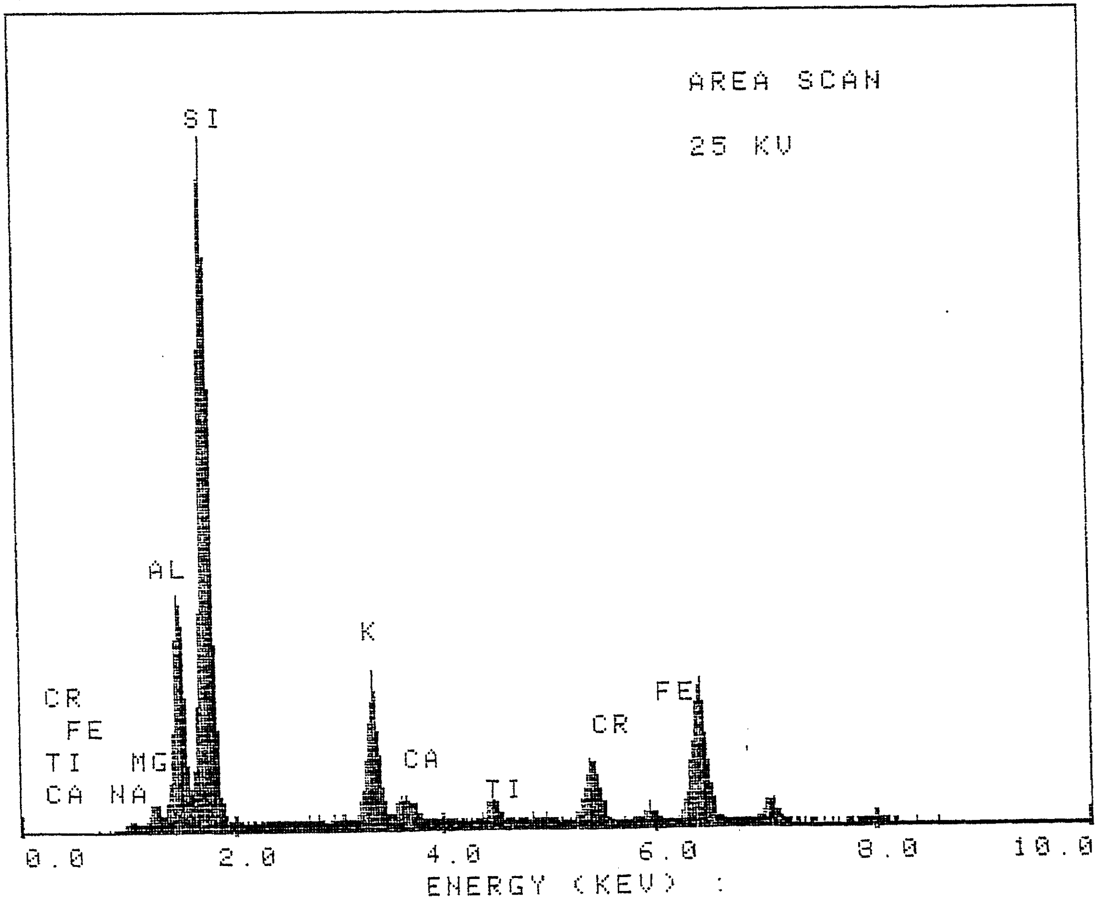

20-Oct-89 11:35

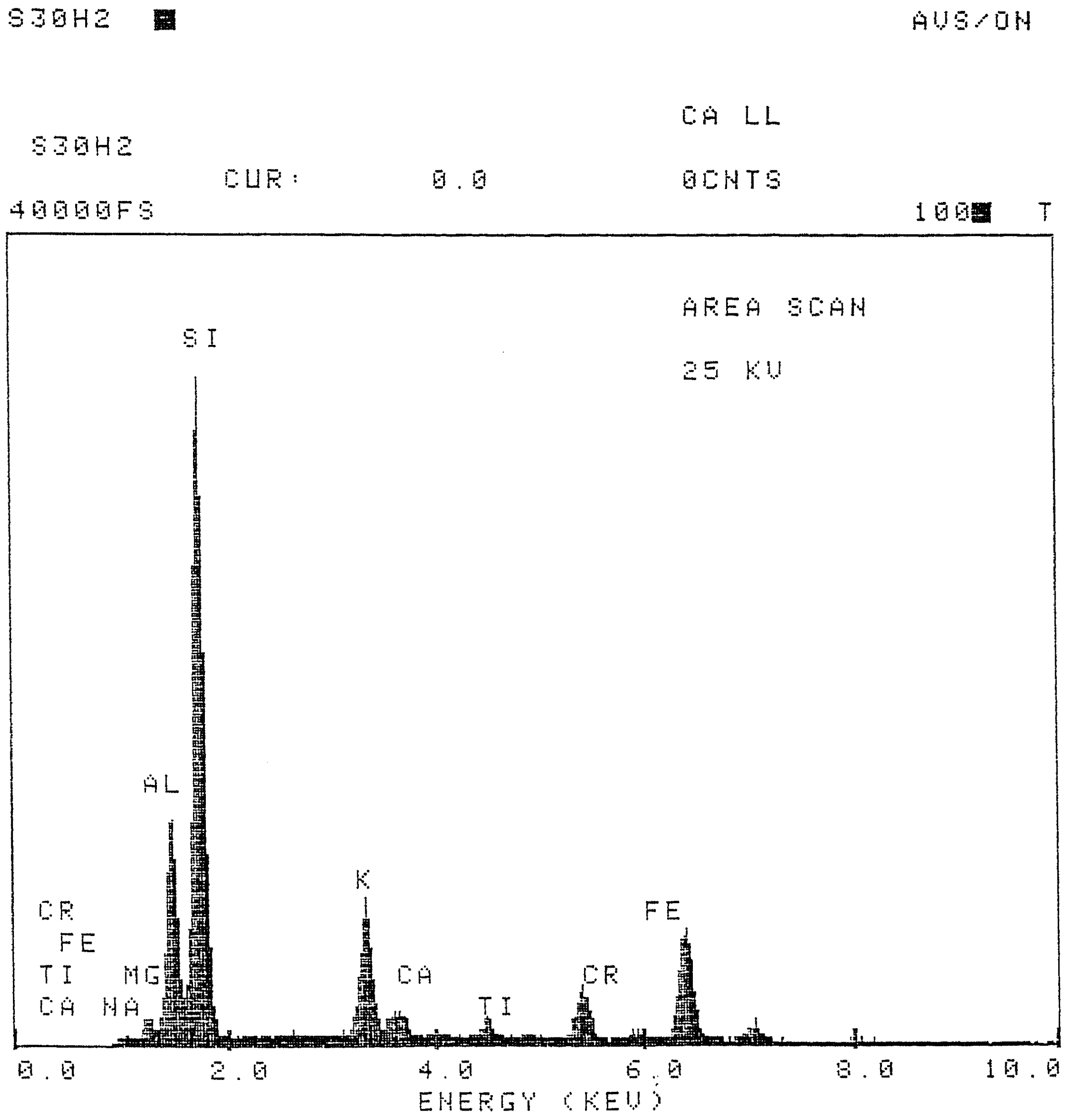

```
S30H2  ■                                          AVS/ON

                                        CA LL
 S30H2
         CUR:        0.0                0CNTS
40000FS                                           100■   T
```

20-Oct-89 11:35

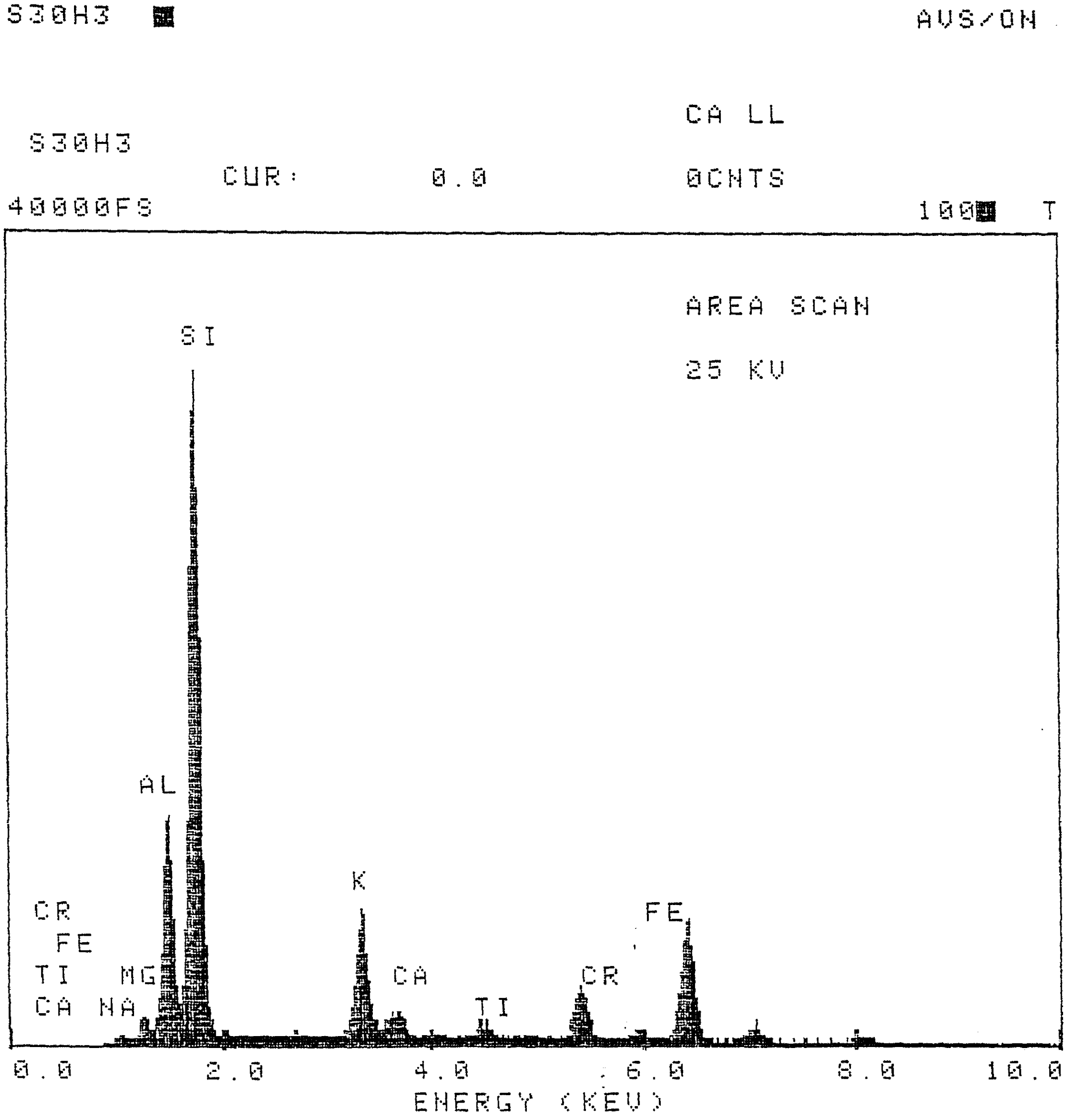

20-Oct-89 11:35

S30H4 ■ AVS/ON

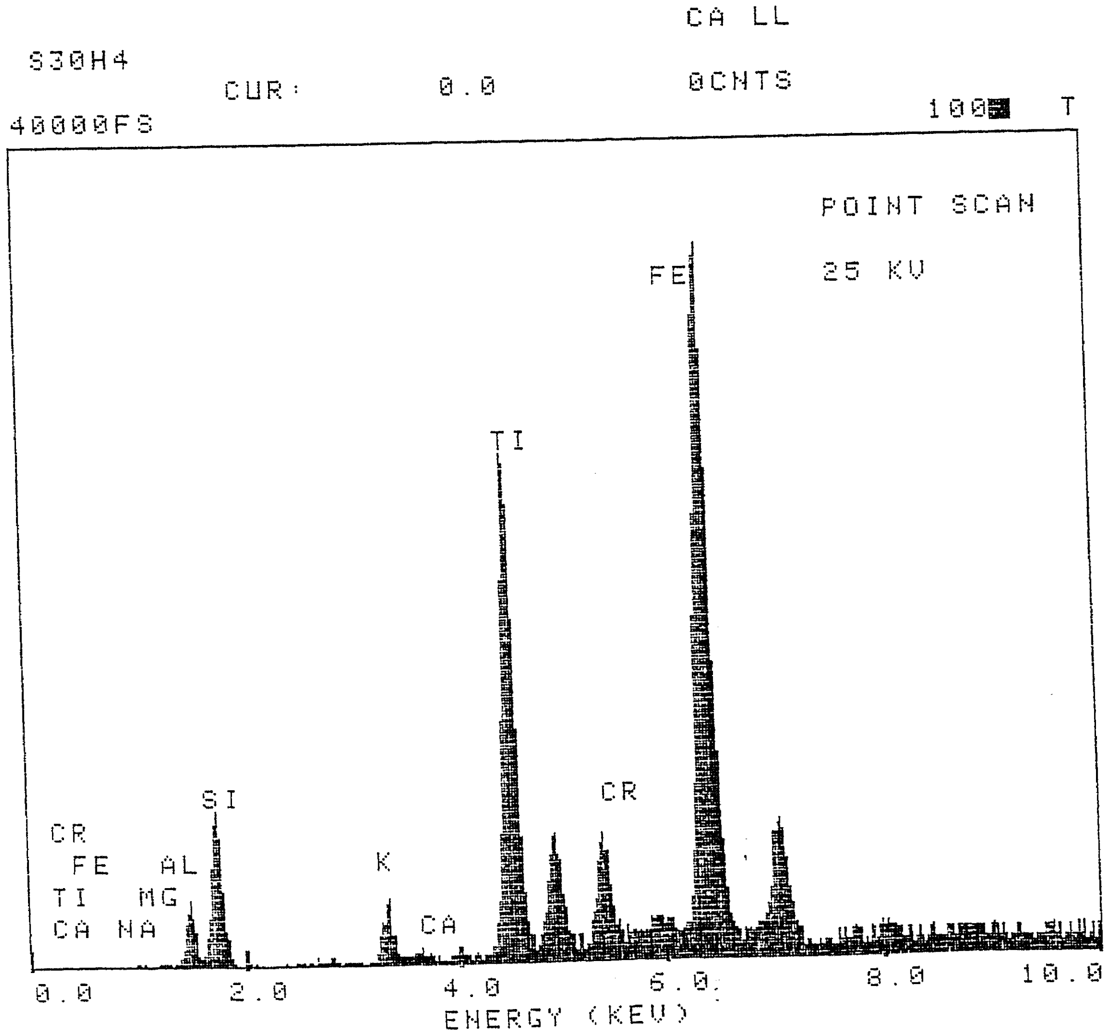

20-Oct-89 11:35

S30H5 ■ AVS/ON

CA LL

S30H5

CUR: 0.0 0CNTS

40000FS 100■ T

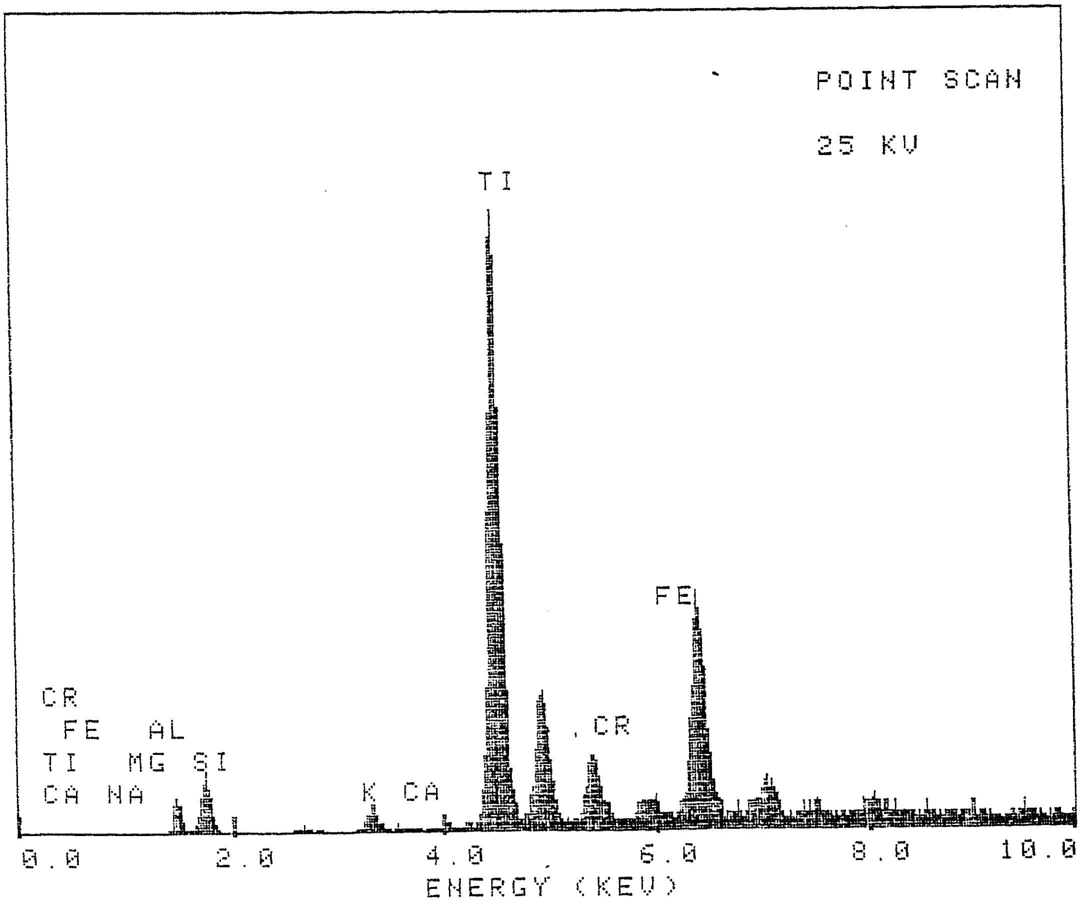

20-Oct-89 11:35

S30H6 ■ AVS/ON

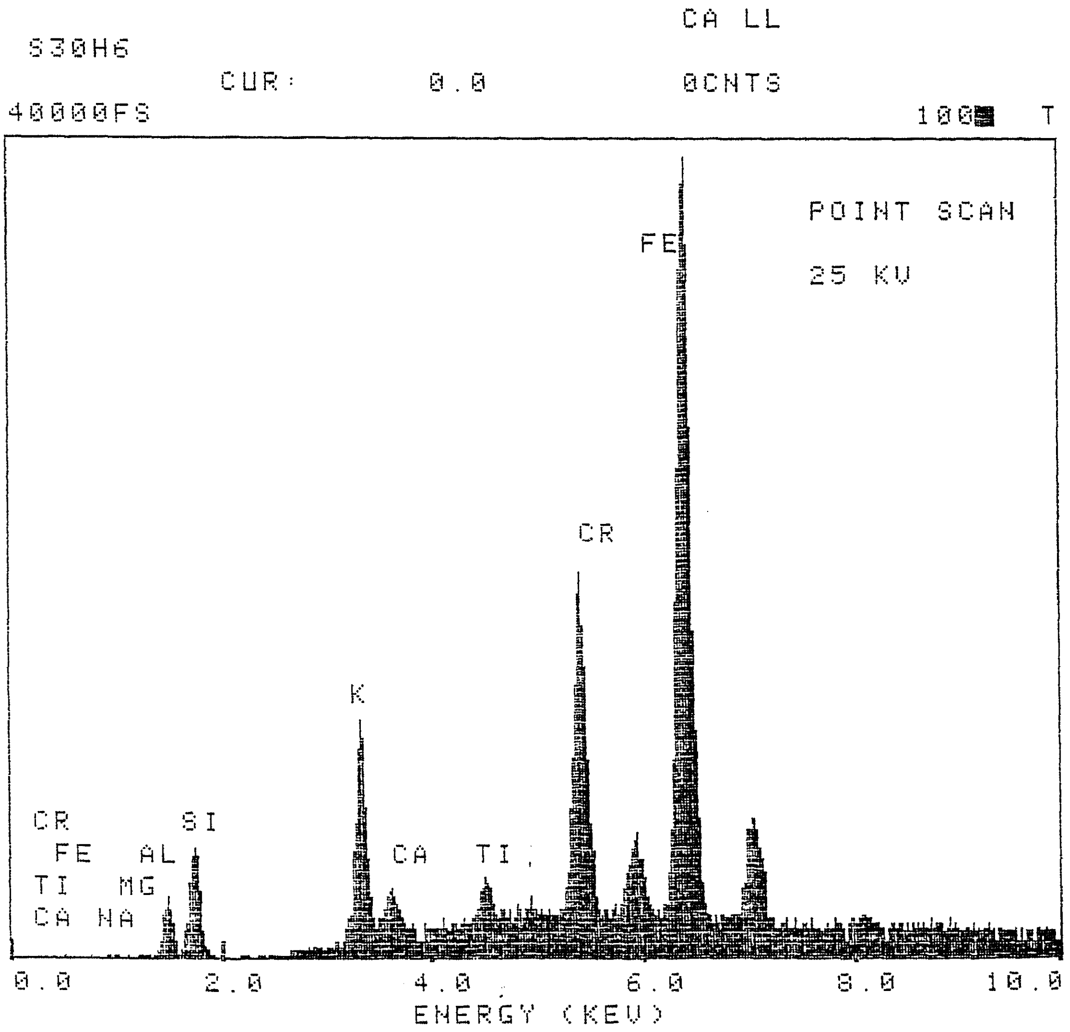

20-Oct-89 11:35

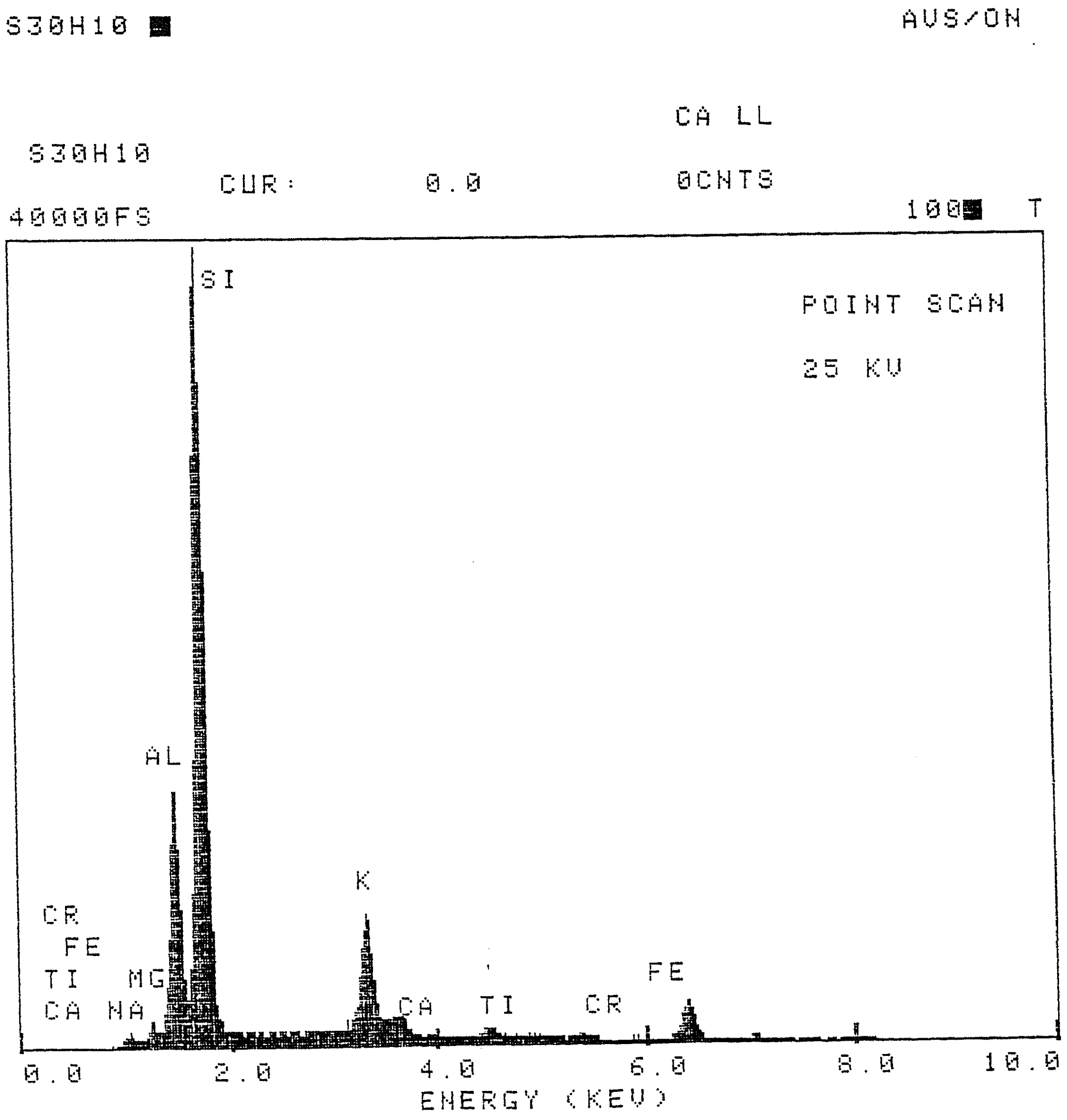

20-Oct-89 11:35

S30H11 ■ AVS/ON

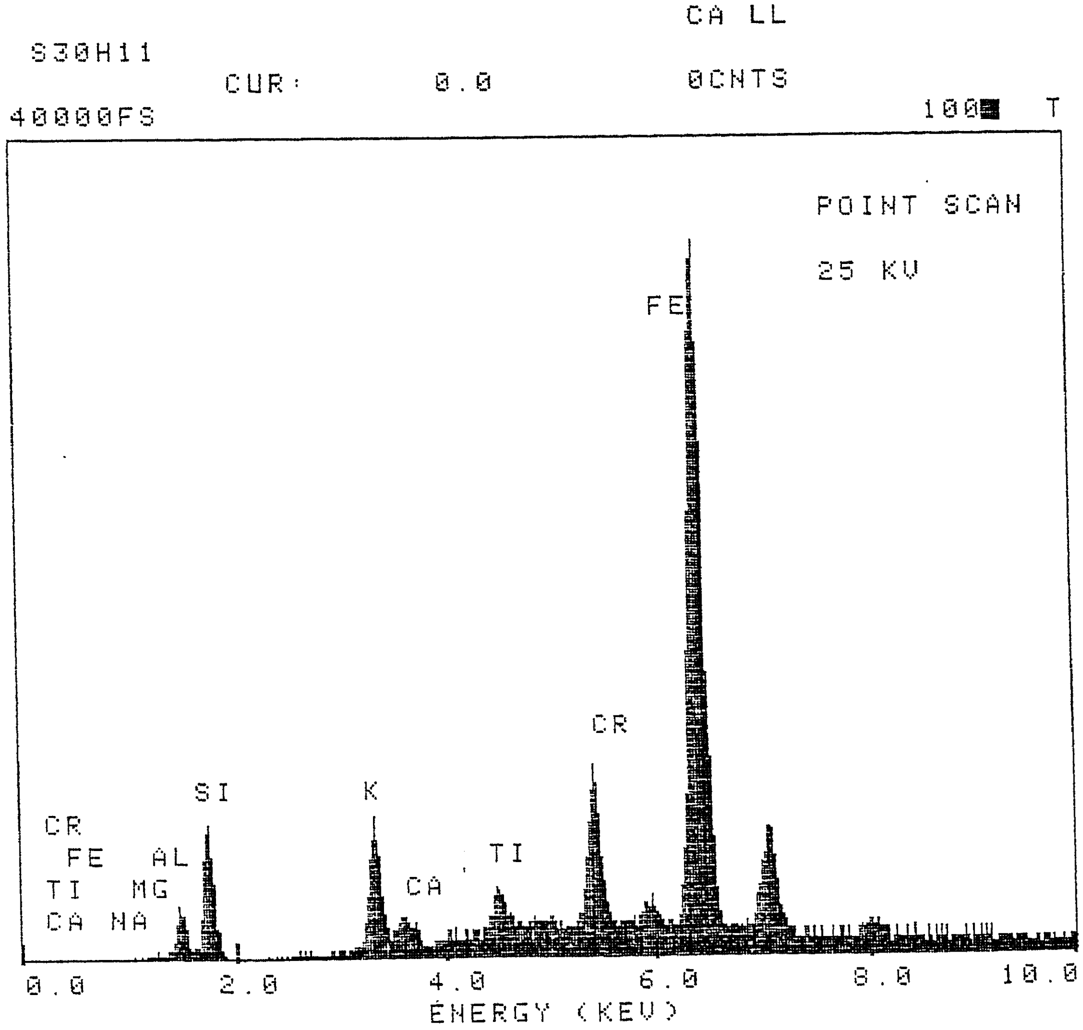

20-Oct-89 11:35

S30H12 ■ AVS/ON

CA LL

S30H12

CUR: 0.0 0CNTS

40000FS 100■ T

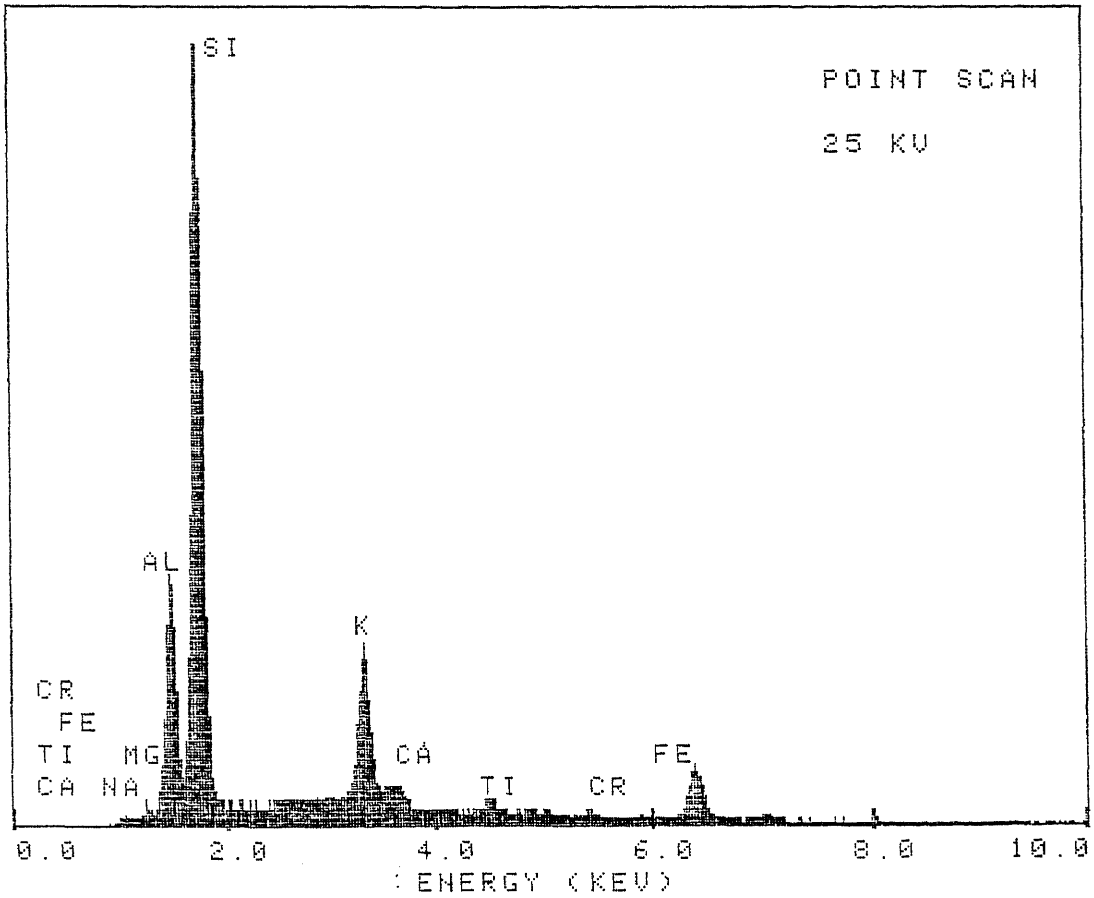

20-Oct-89 11:35

S30H13 ■ AVS/ON

CA LL

S30H13

CUR: 0.0 0CNTS

40000FS 100■ T

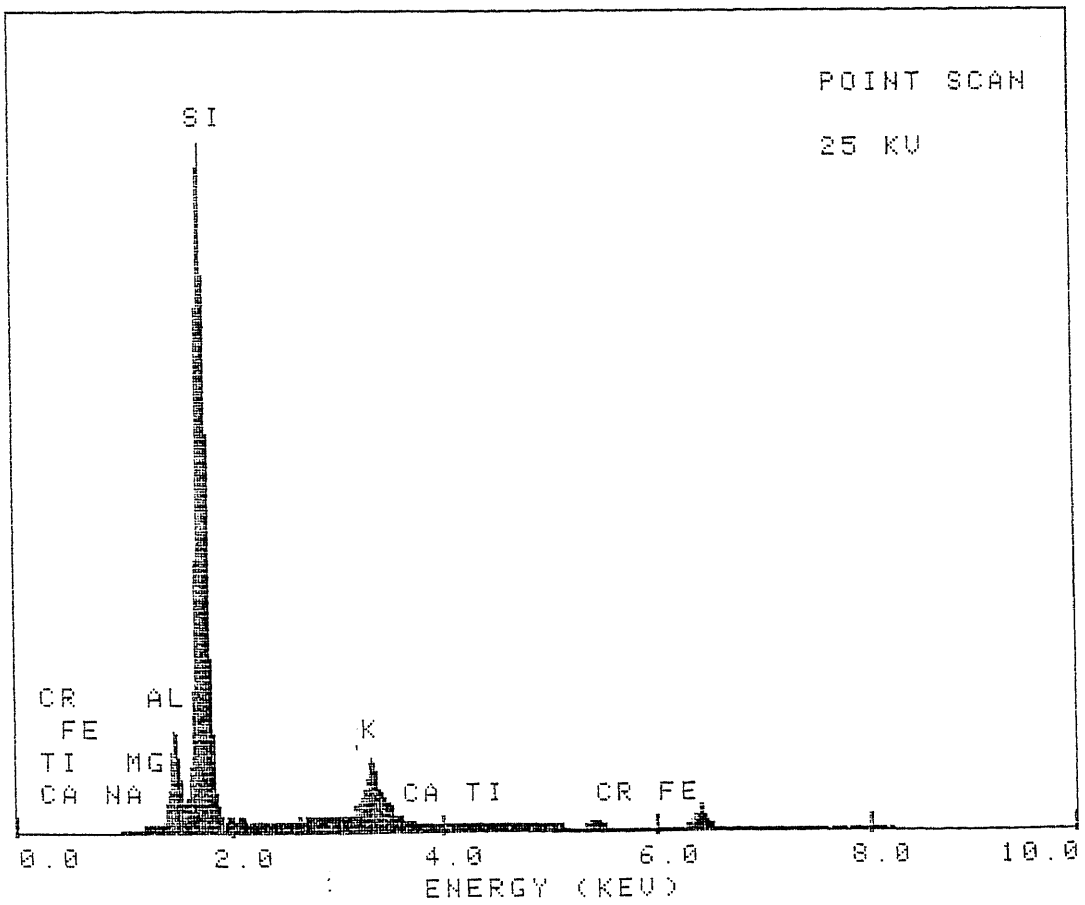

20-Oct-89 11:35

S30H14 ■ AVS/ON

CA LL

S30H14

CUR: 0.0 0CNTS

40000FS 100■ T

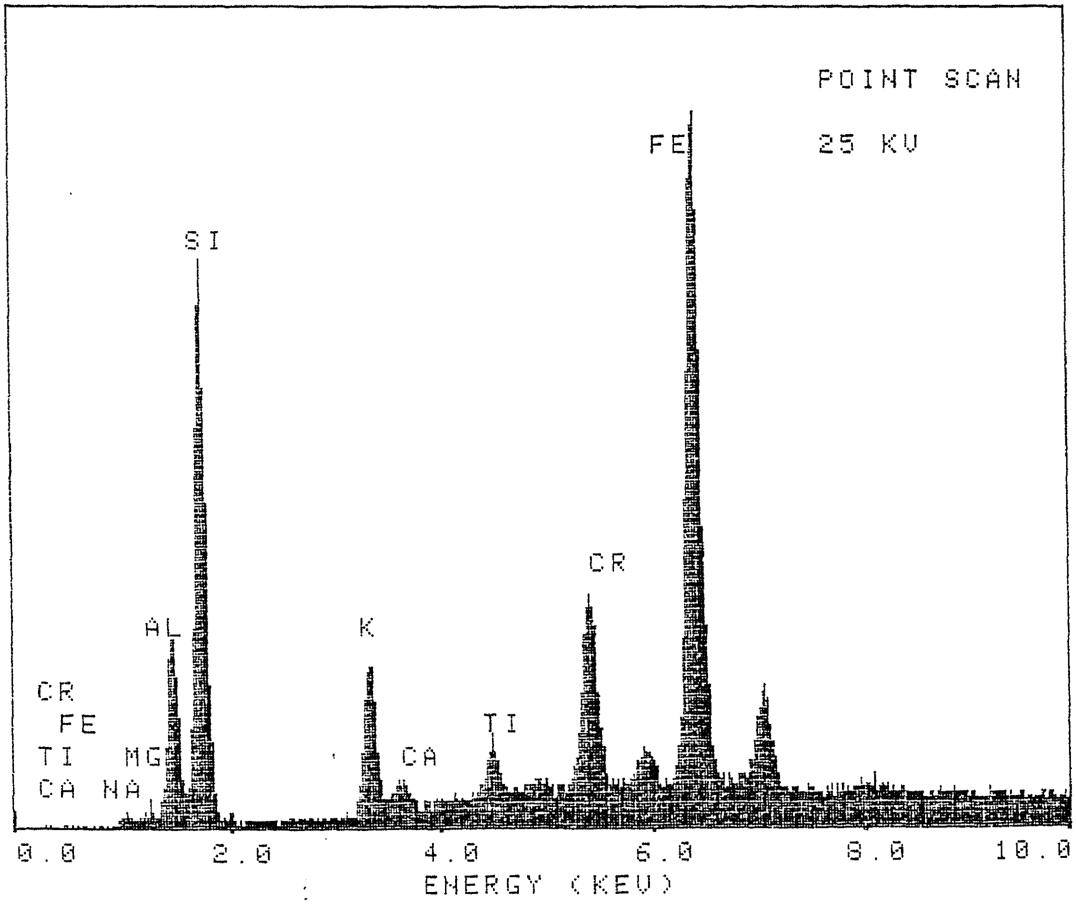

20-Oct-89 11:35

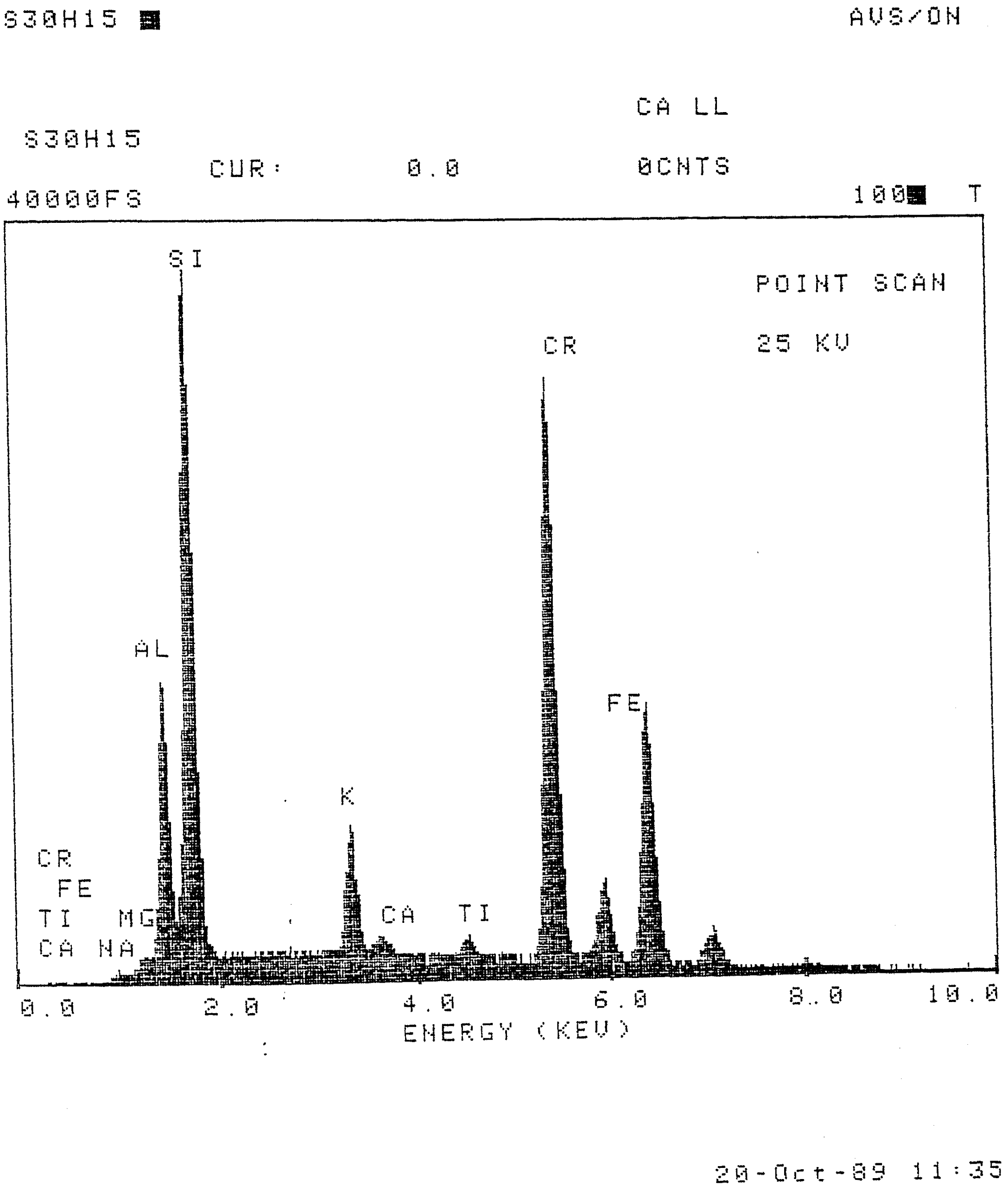
S30H15
AVS/ON
CA LL
S30H15
CUR: 0.0
0CNTS
40000FS
100 T
SI
POINT SCAN
25 KV
CR
AL
FE
K
CR
FE
TI
MG
CA
NA
CA
TI
0.0
2.0
4.0
6.0
8.0
10.0
ENERGY (KEV)
20-Oct-89 11:35

SEM IMAGES OF SAMPLE

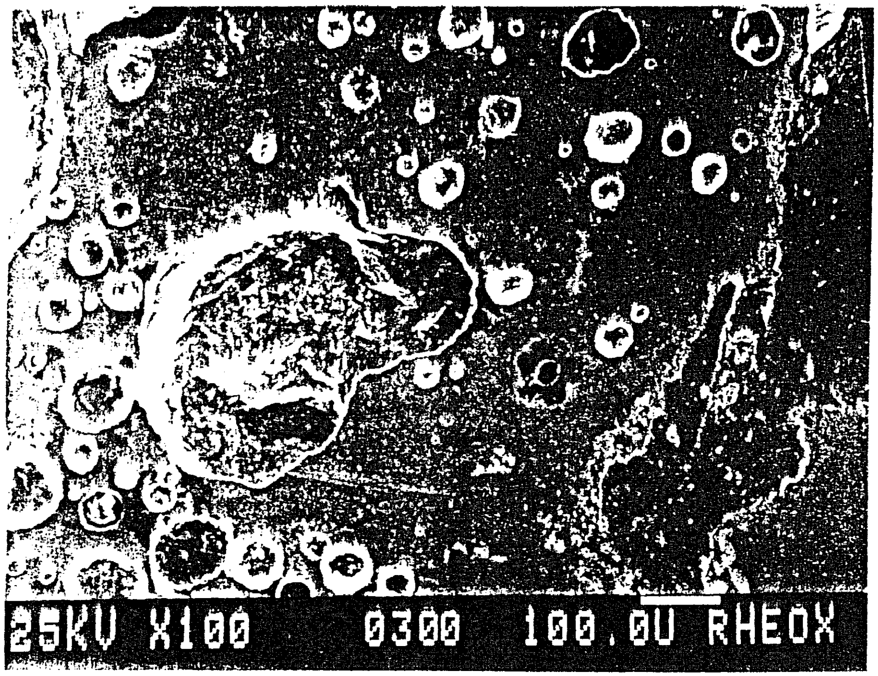

Figure 185

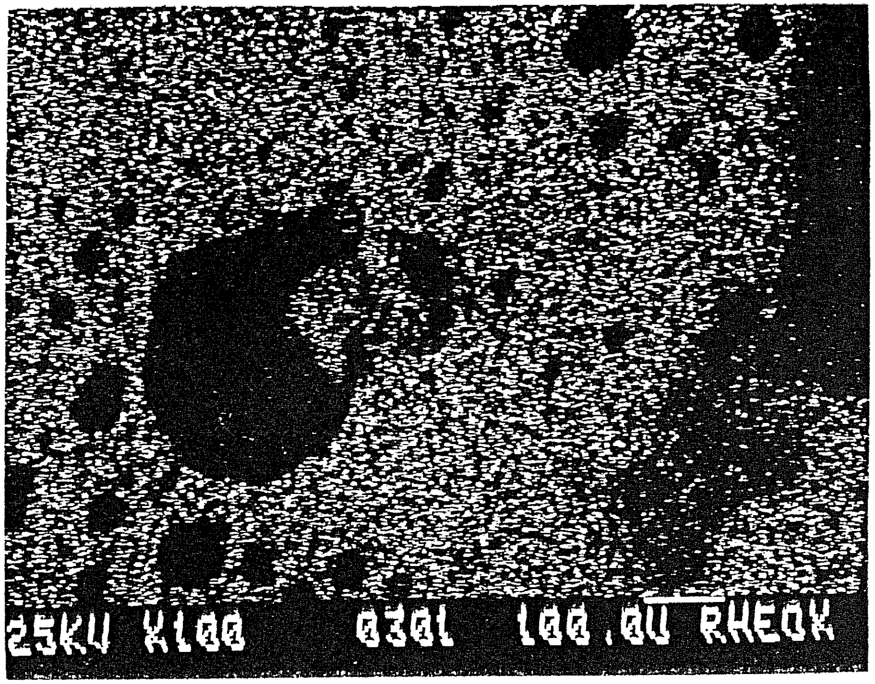

Figure 186 AL X-ray Image of Figure 185

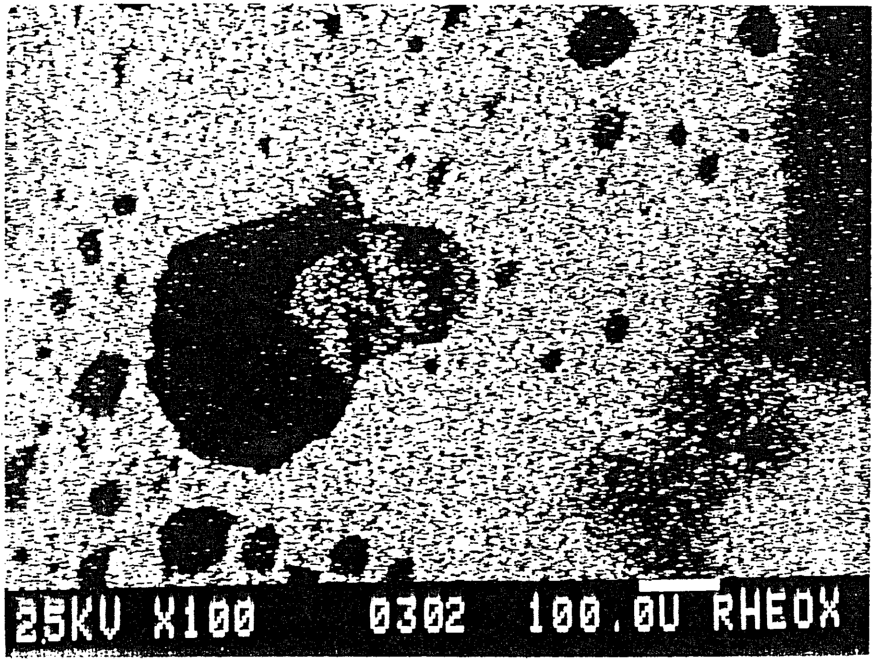

Figure 187 Si X-ray Image of Figure 185

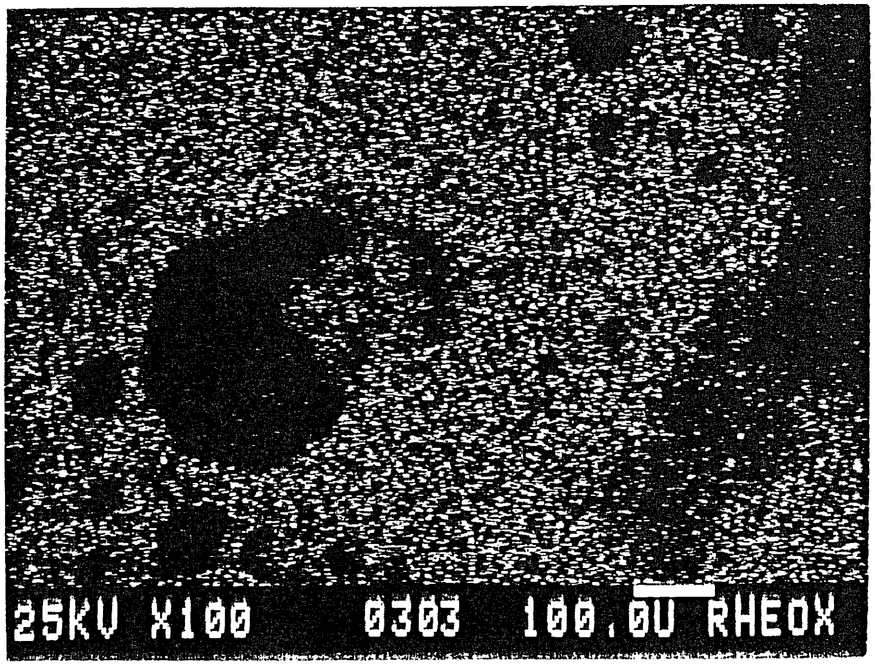

Figure 188 K X-ray Image of Figure 185

SEM IMAGES OF SAMPLE # Microwave 30 minutes Cross Section

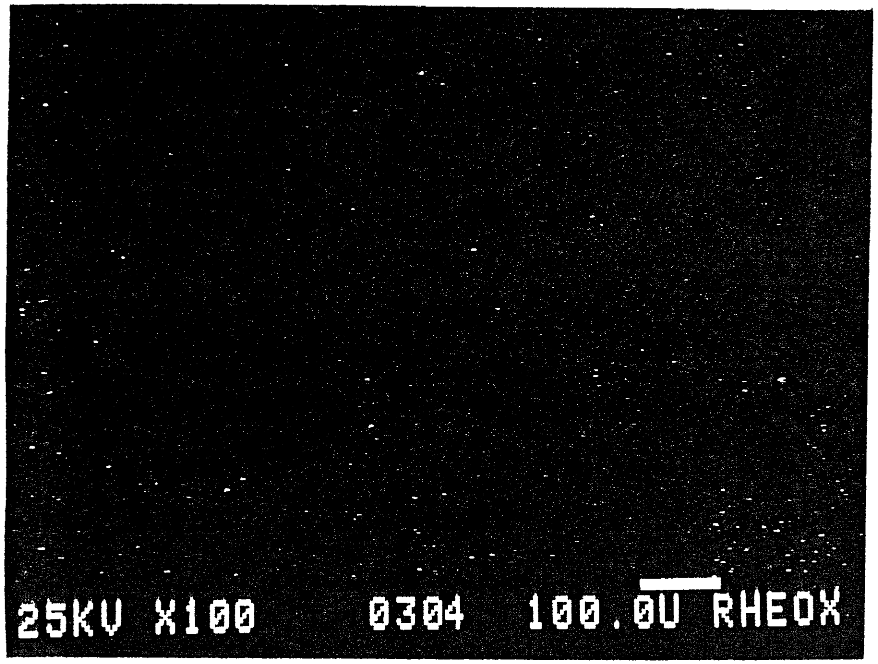

Figure 189 Ti X-Ray Image of Figure 185

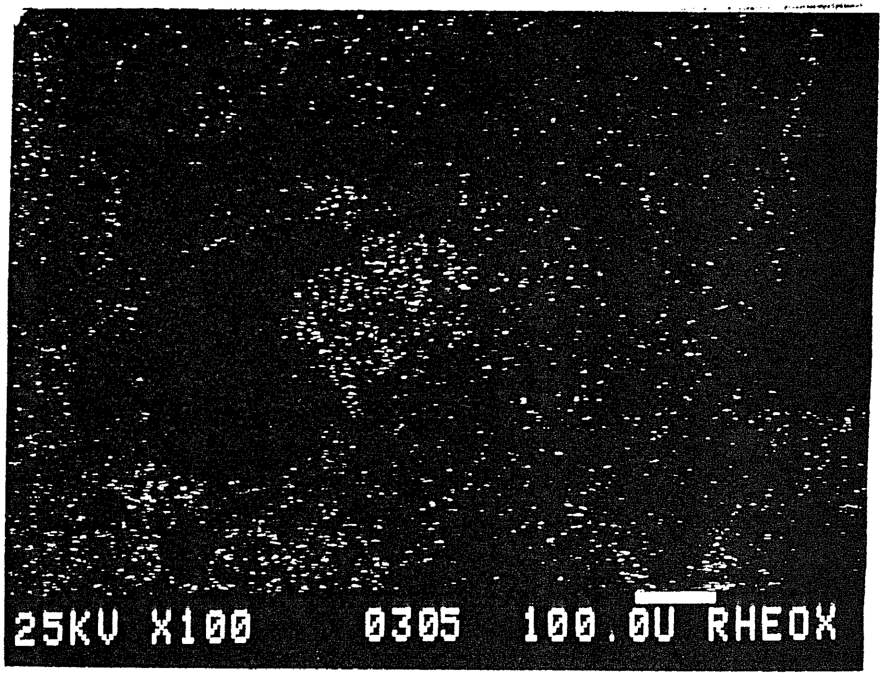

Figure 190 Cr X-Ray Image of Figure 185

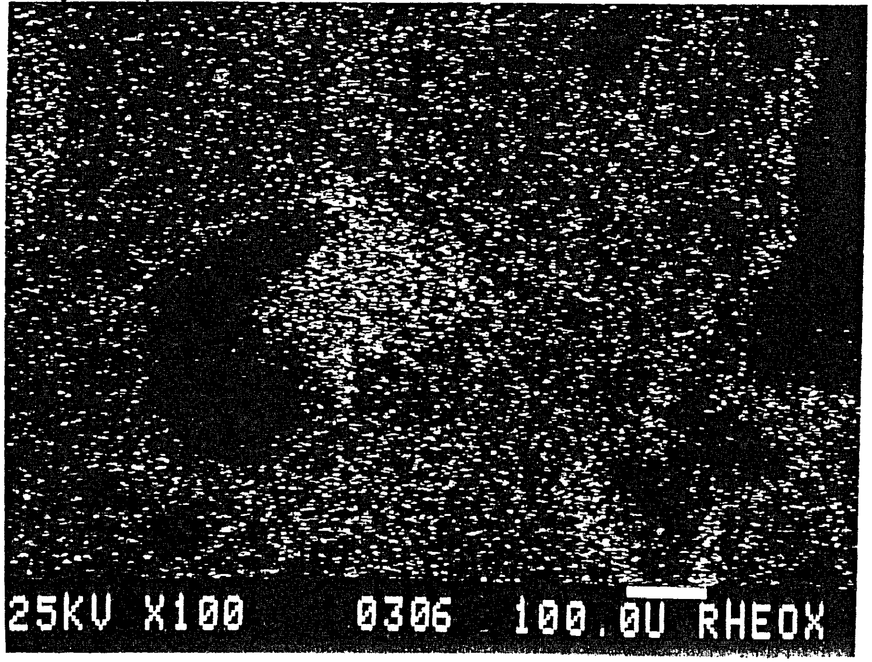

Figure 191 Fe X-Ray Image of Figure 185

SEM IMAGES OF SAMPLE # Microwave 30 minutes Cross Section

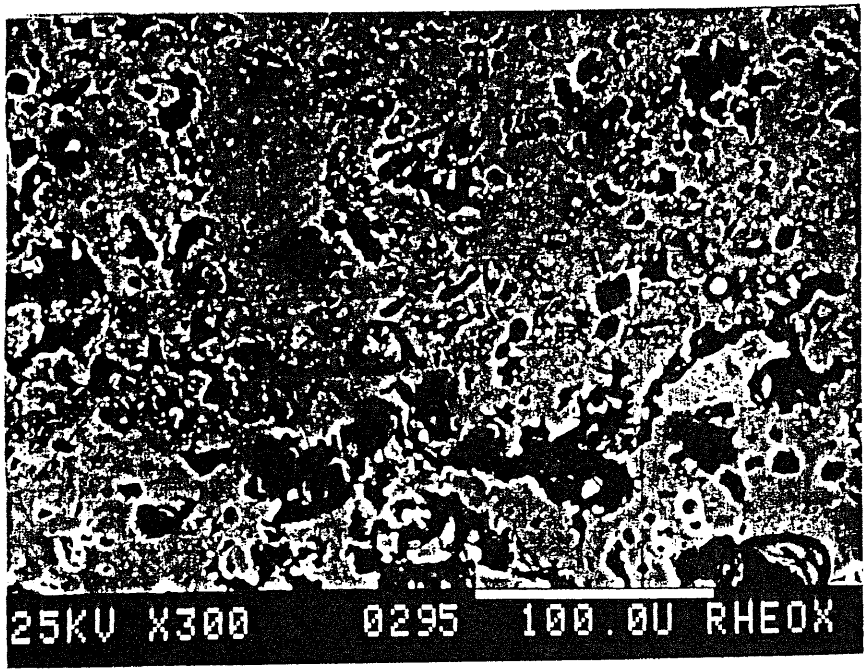

Figure 192

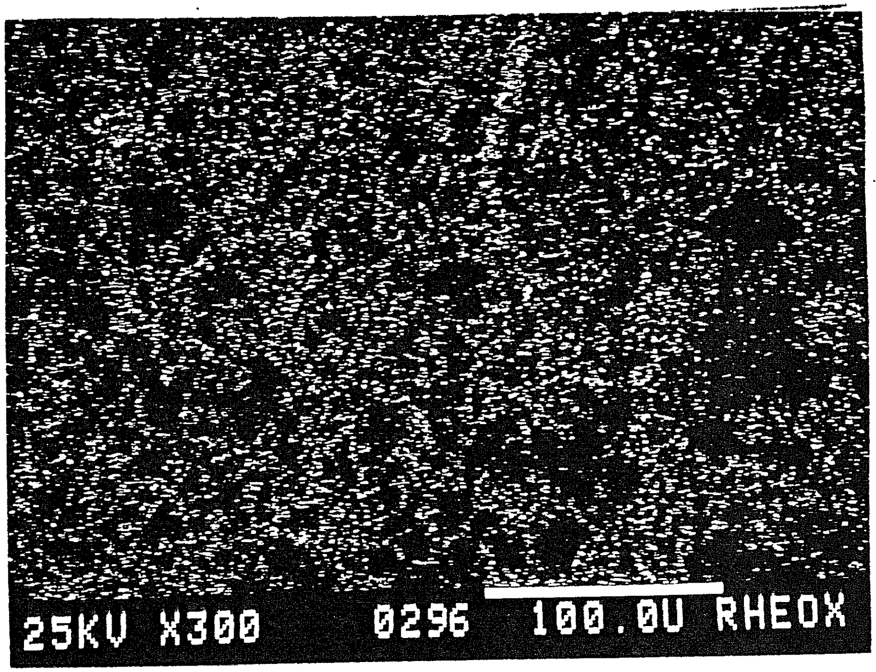

Figure 193 AL X-ray Image of Figure 192

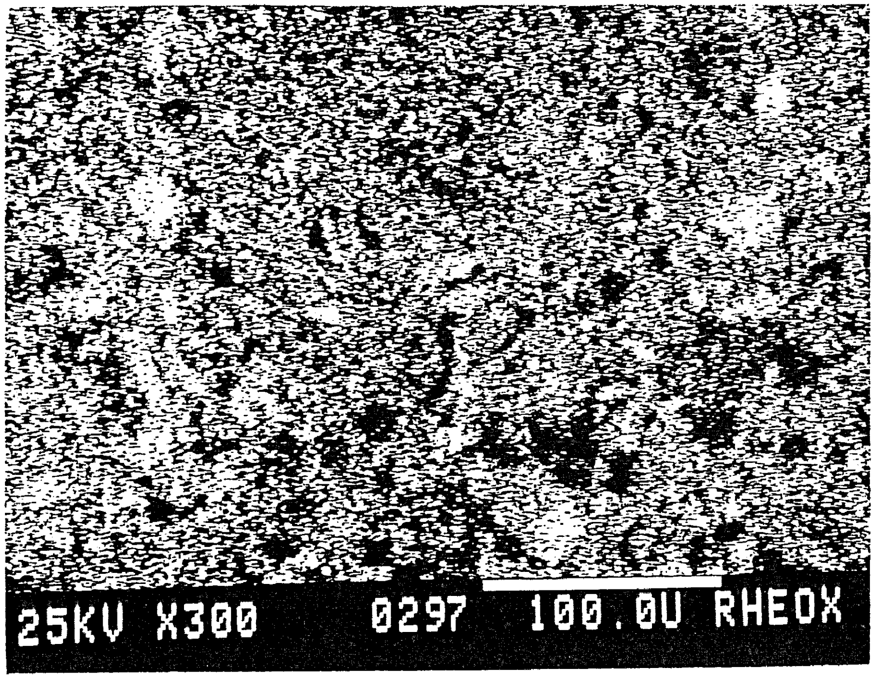

Figure 194 Si X-ray Image of Figure 192

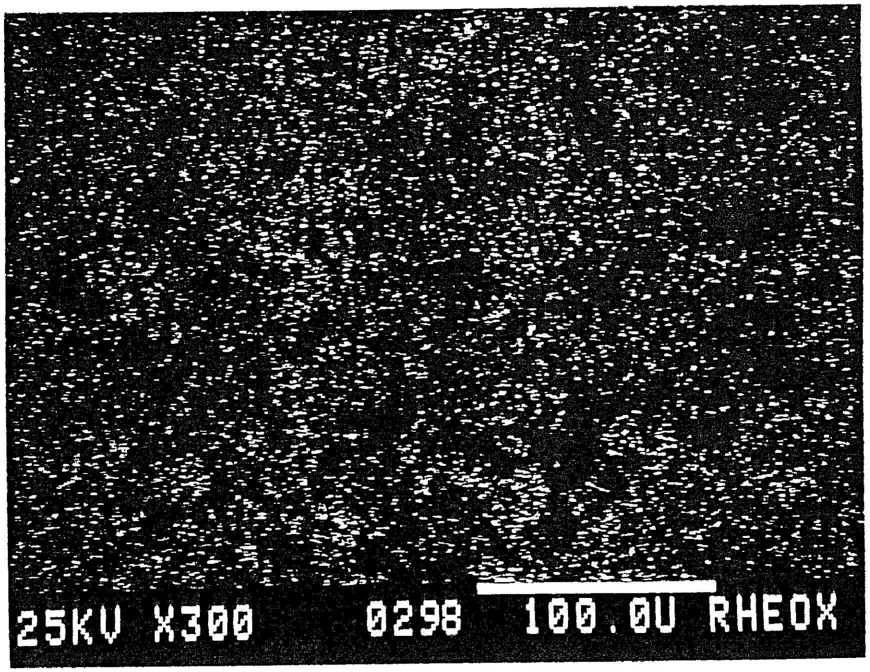

Figure 195 K X-ray Image of Figure 192

SEM IMAGES OF SAMPLE #

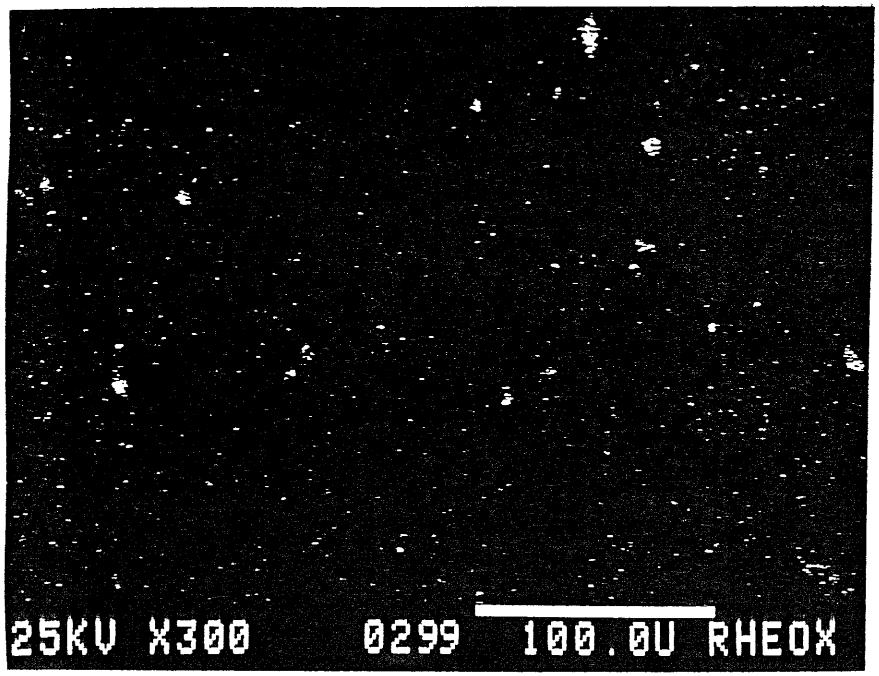

Figure 196 Ti X-Ray Image of Figure 192

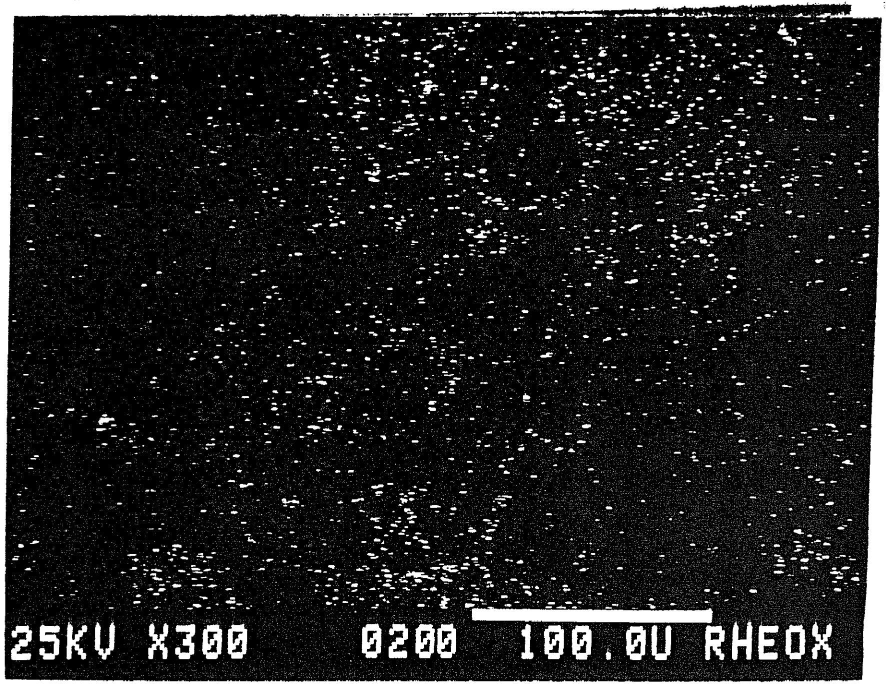

Figure 197 Cr X-Ray Image of Figure 192

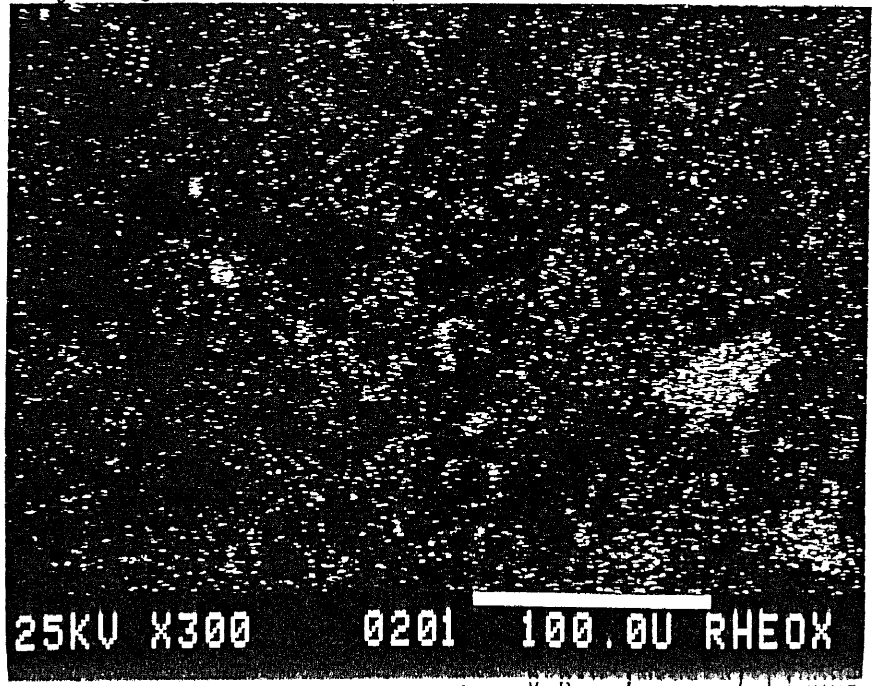

Figure 198 Fe X-Ray Image of Figure 192

SEM IMAGES OF SAMPLE # Microwave 30 minutes Cross Section

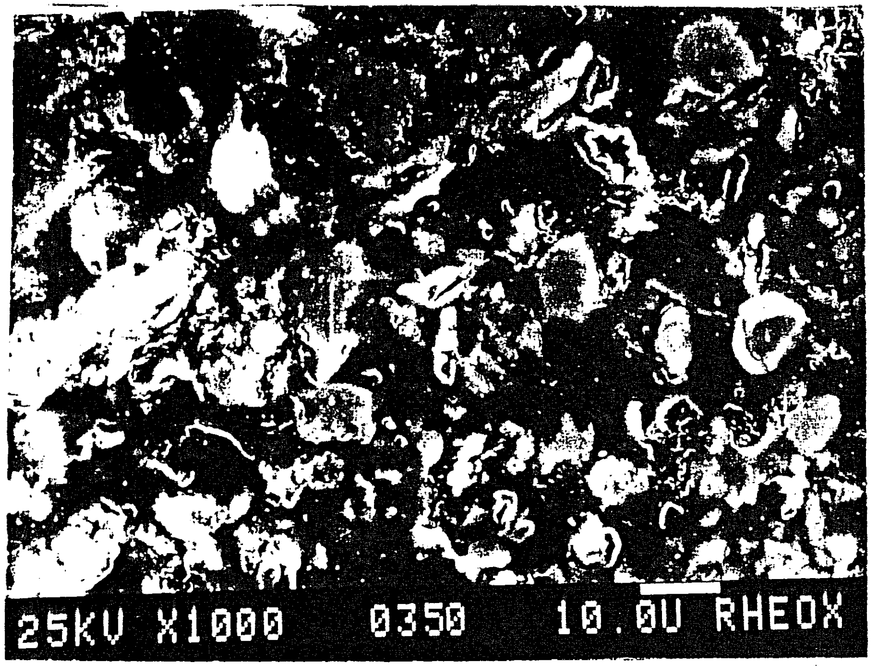

Figure 199

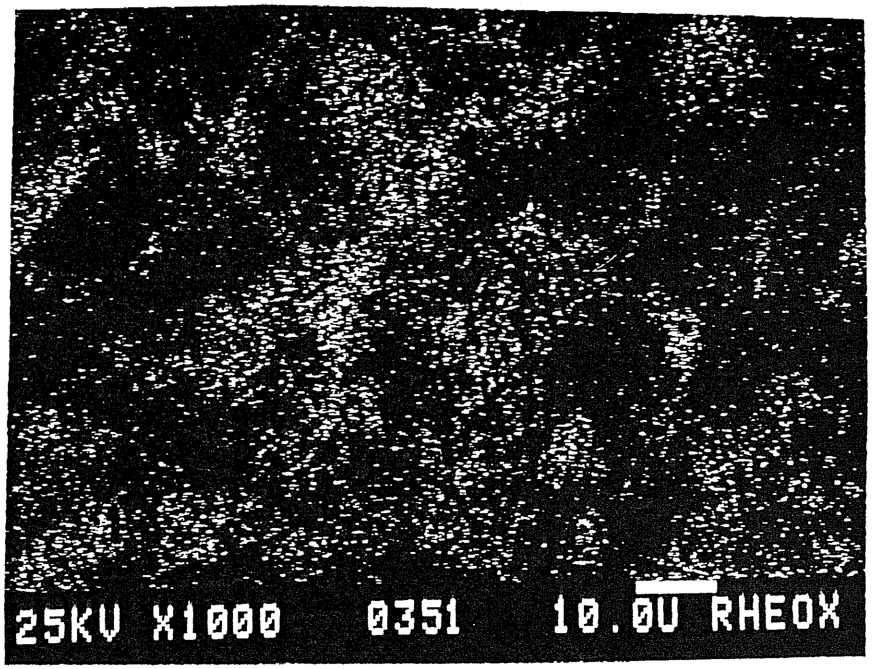

Figure 200 AL X-ray Image of Figure 199

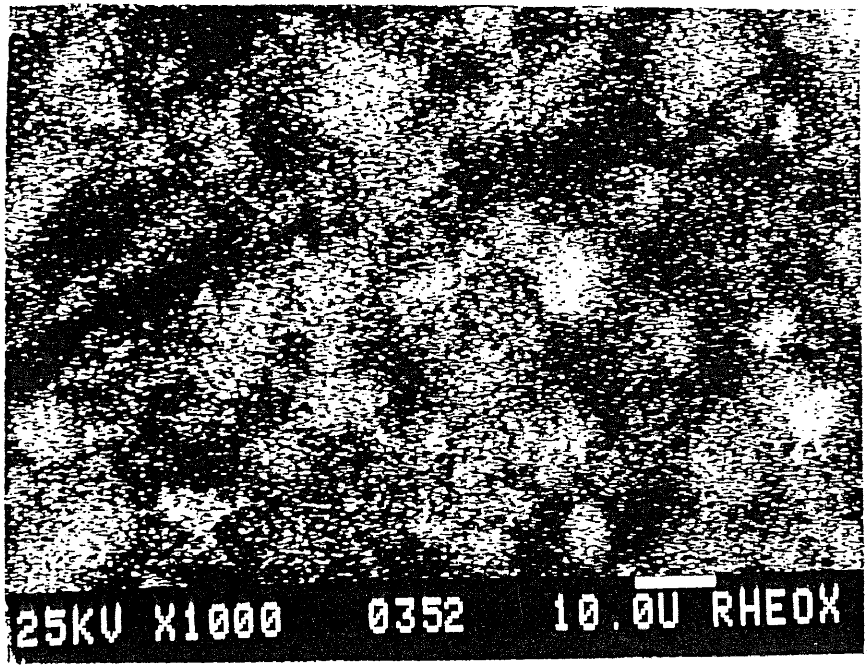

Figure 201 Si X-ray Image of Figure 199

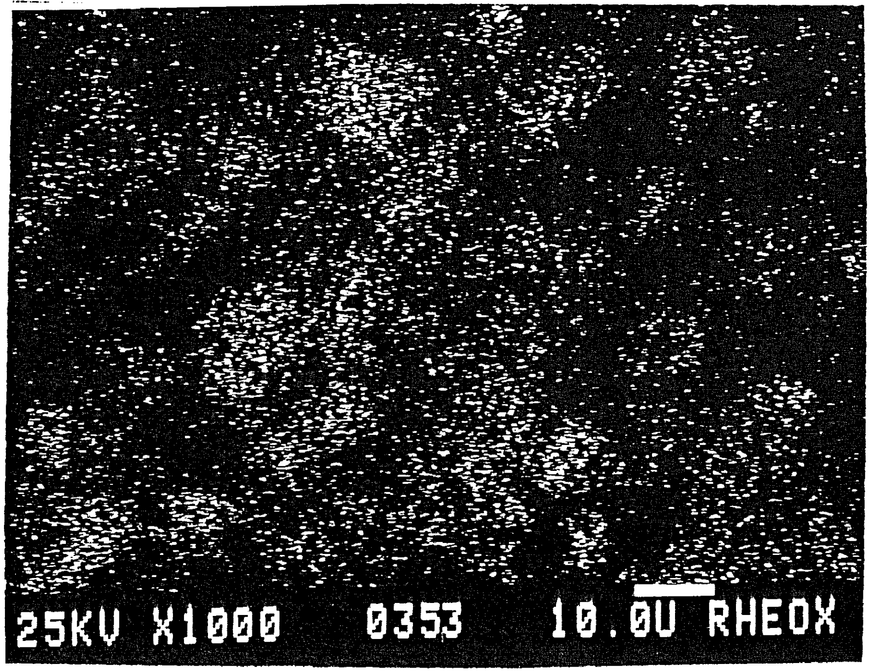

Figure 202 K X-ray Image of Figure 199

SEM IMAGES OF SAMPLE # Microwave 30 minutes Cross Section

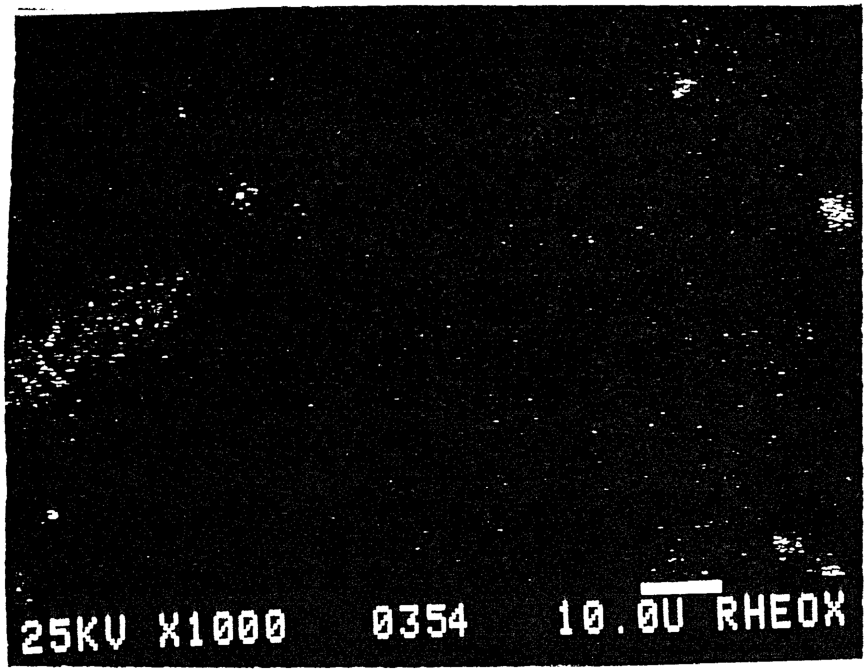

Figure 203 Ti X-Ray Image of Figure 199

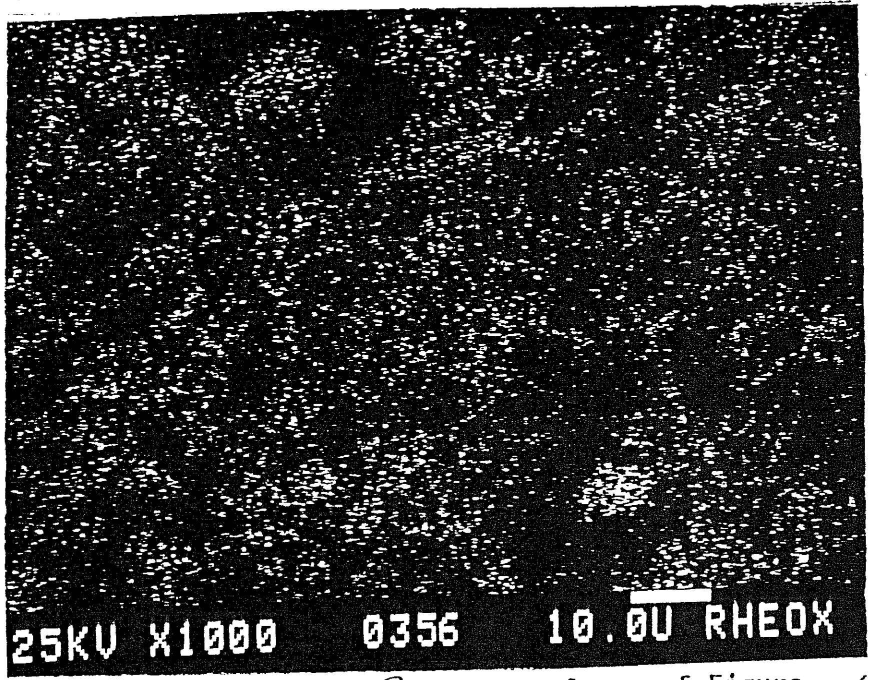

Figure 204 Cr X-Ray Image of Figure 199

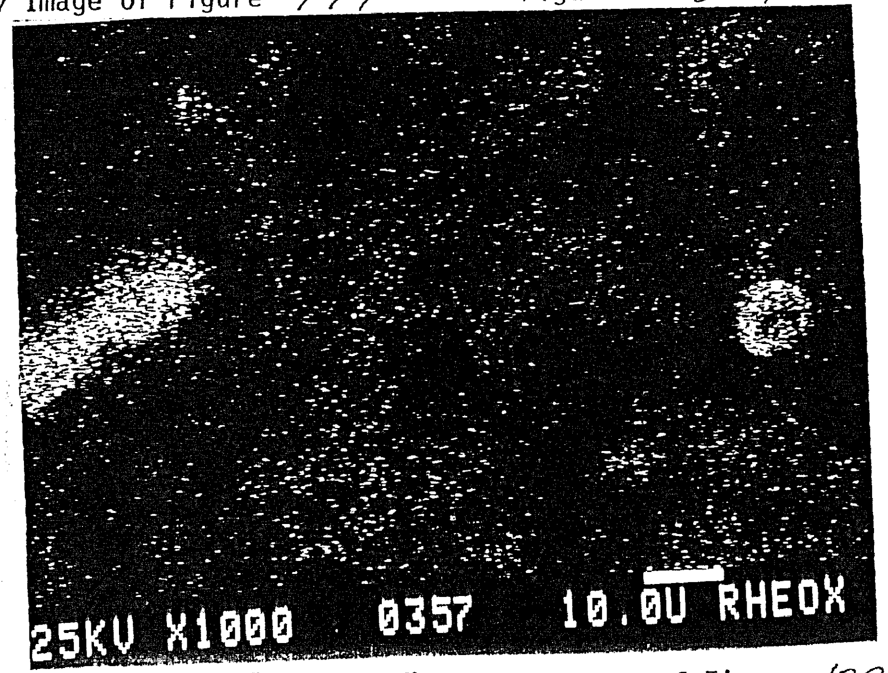

Figure 205 Fe X-Ray Image of Figure 199

SEM IMAGES OF SAMPLE # Microwave 30 minutes, cross section

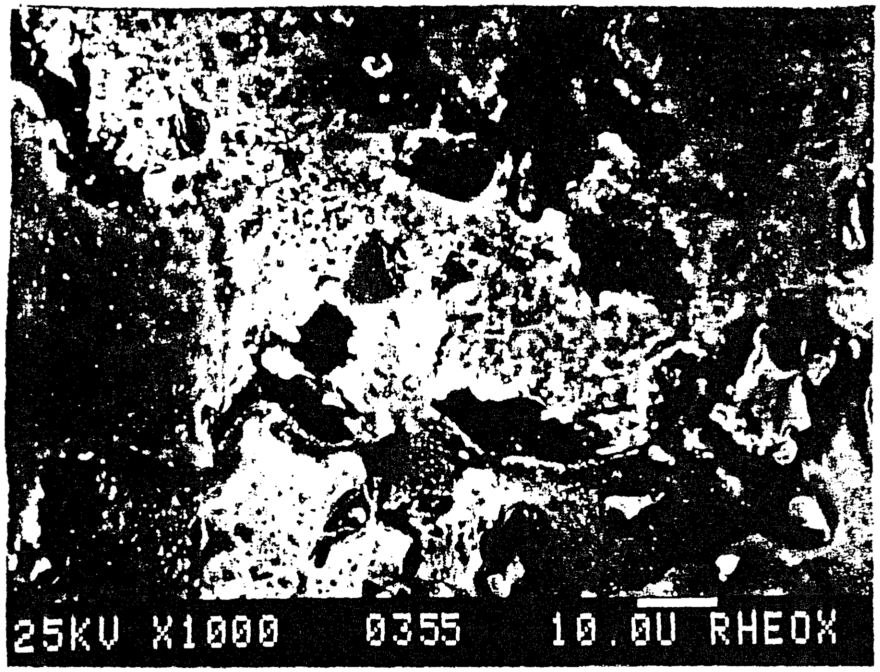

Figure 206

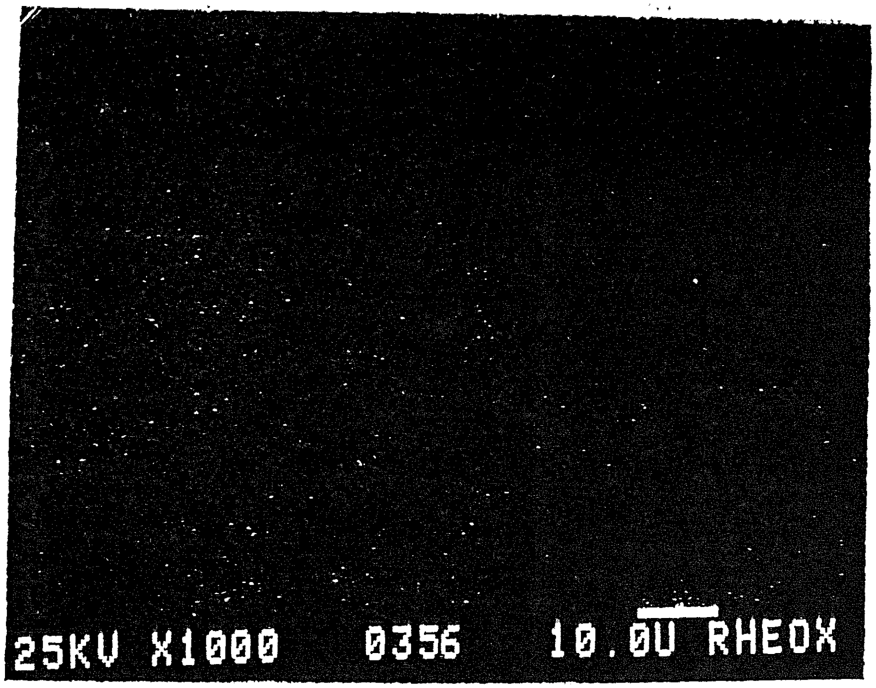

Figure 207 AL X-ray Image of Figure 206

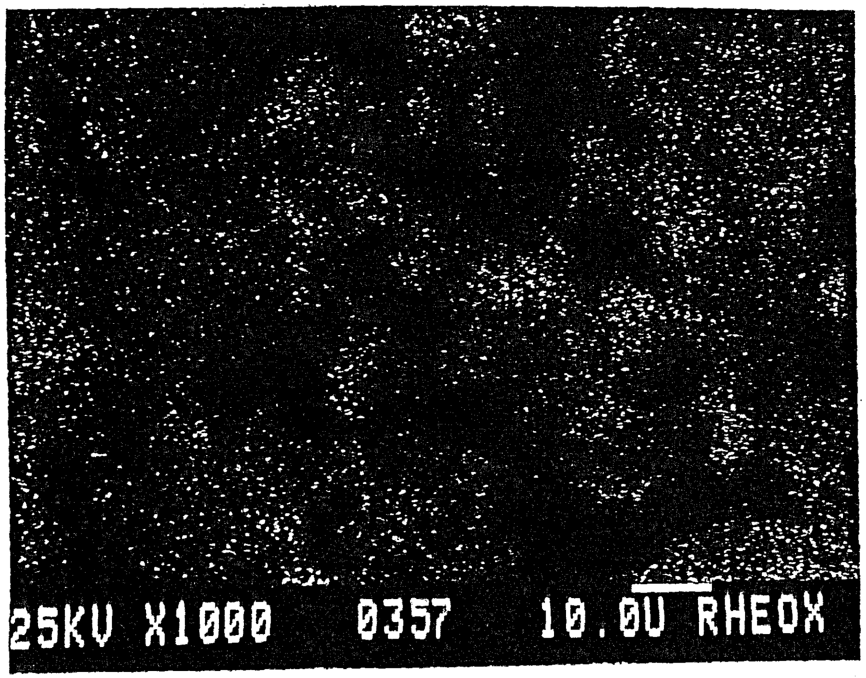

Figure 208 Si X-ray Image of Figure 206

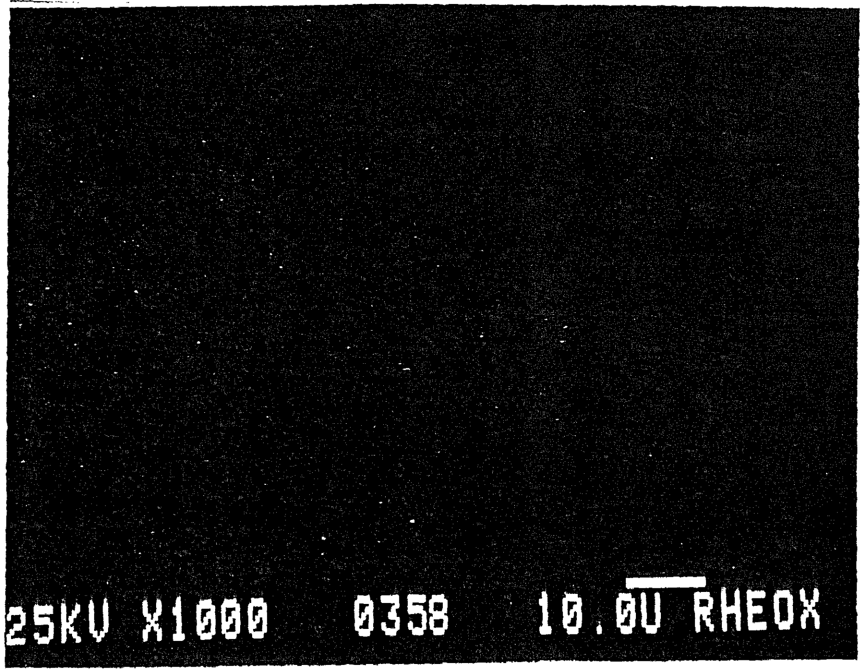

Figure 209 K X-ray Image of Figure 206

SEM IMAGES OF SAMPLE # Microwave 15 minutes Cross Section

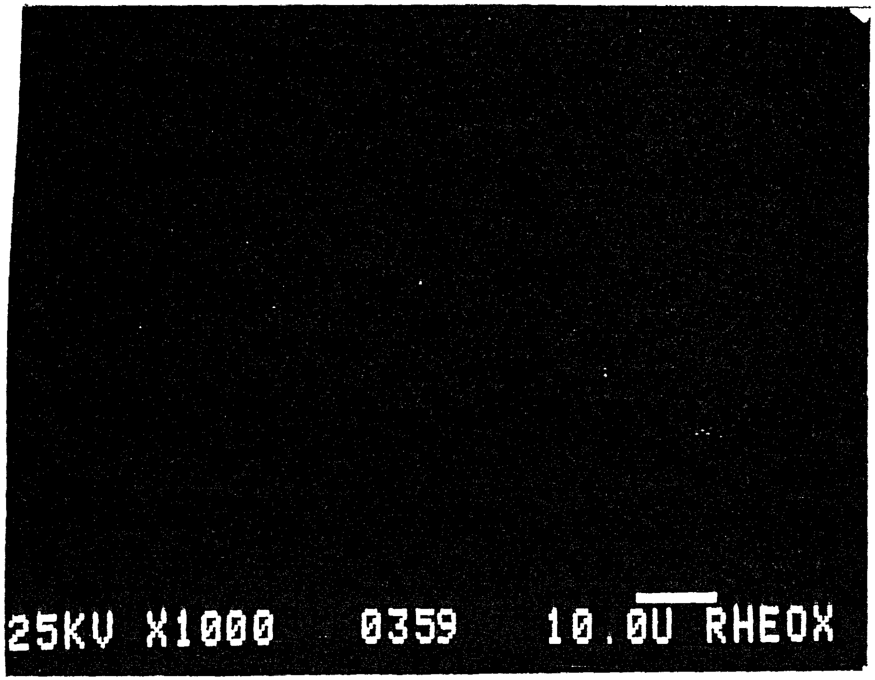

Figure 210 Ti X-Ray Image of Figure 206

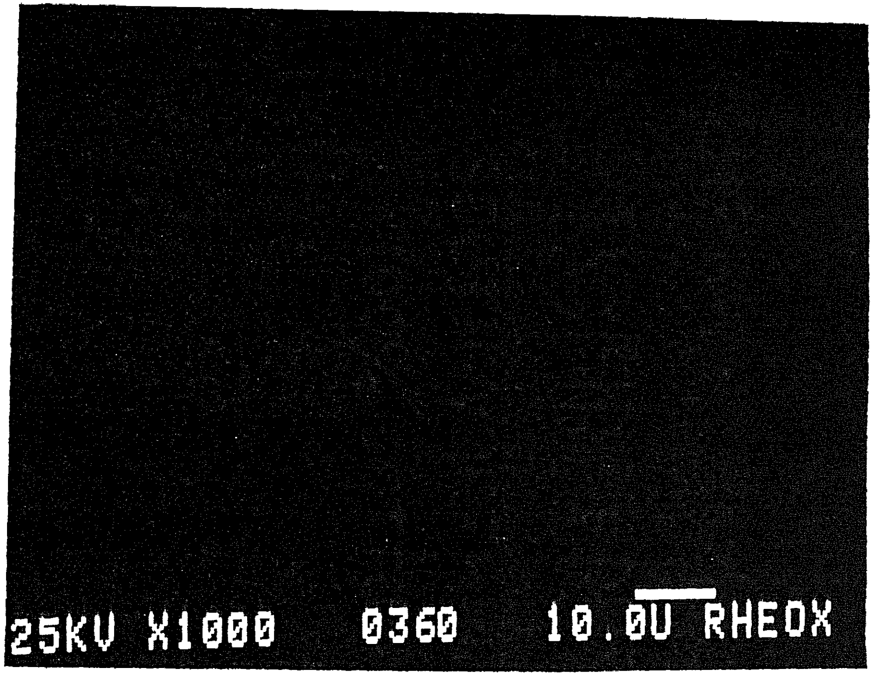

Figure 211 Cr X-Ray Image of Figure 206

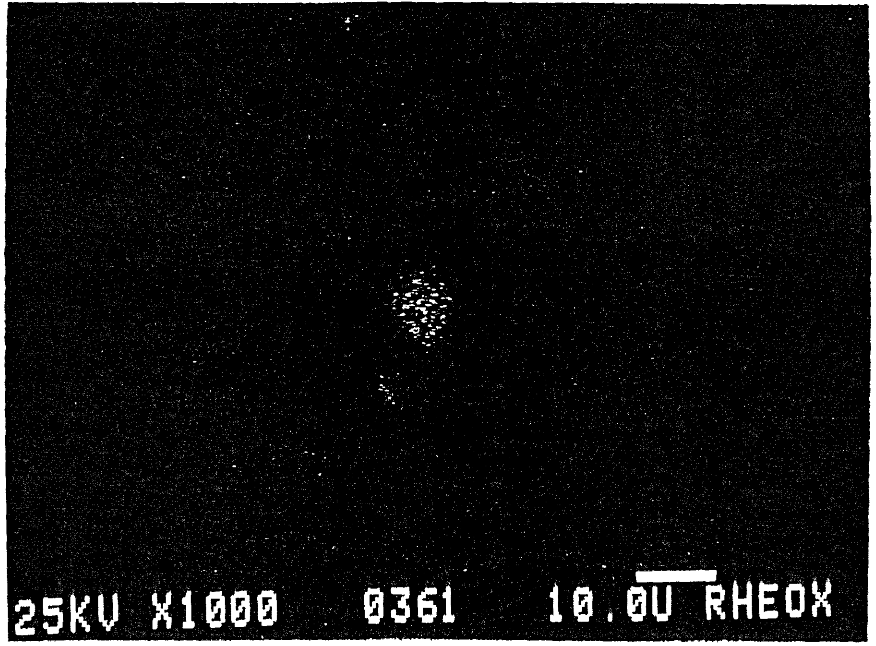

Figure 212 Fe. X-Ray Image of Figure 206

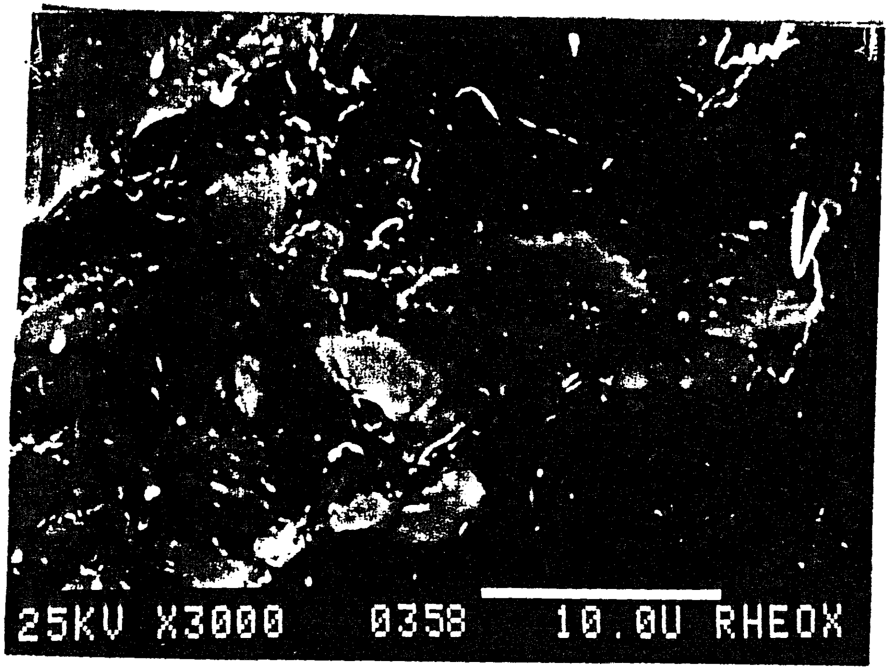

Figure 213

Line Profile Scan

AL →

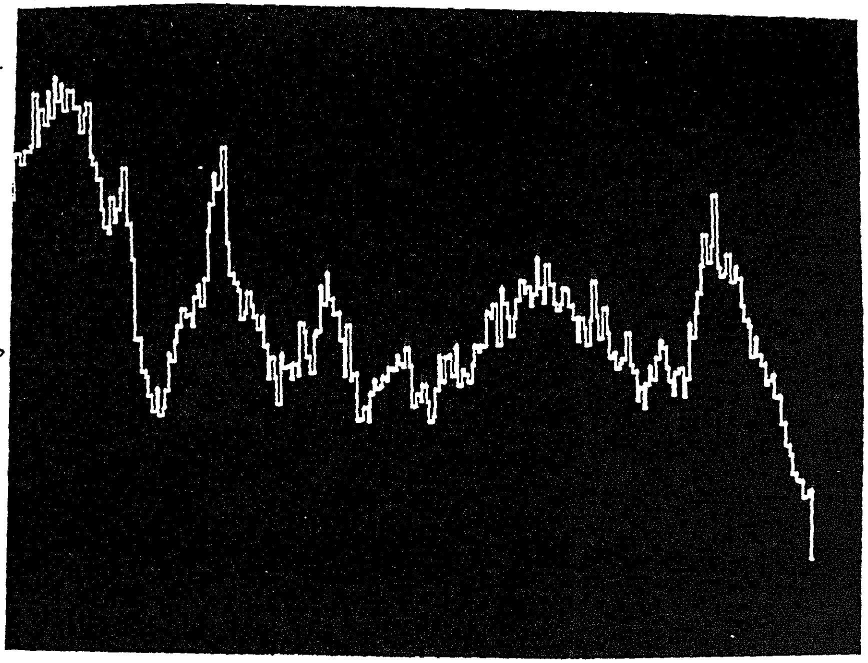

Figure 214

← Si

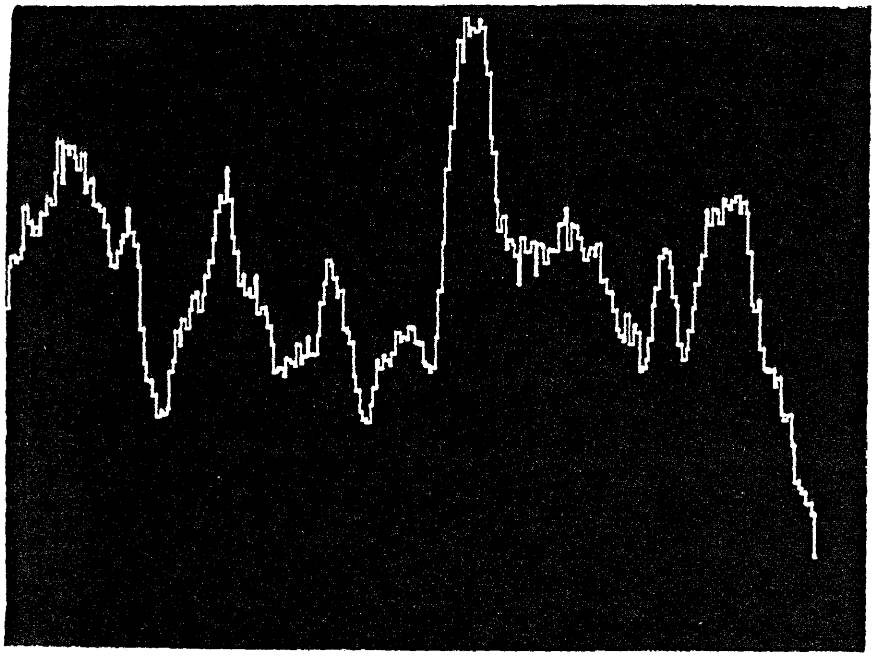

Figure 215

K →

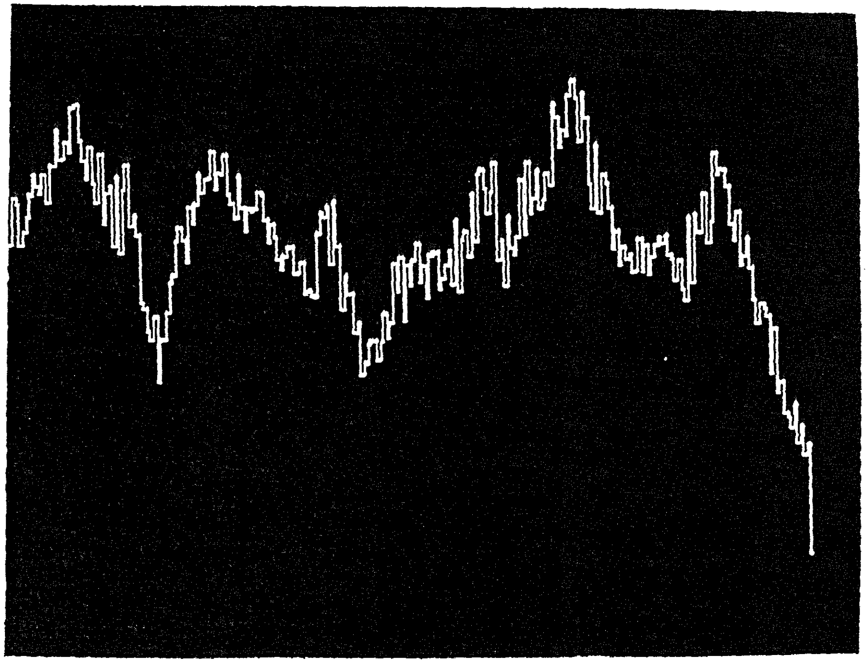

Figure 216

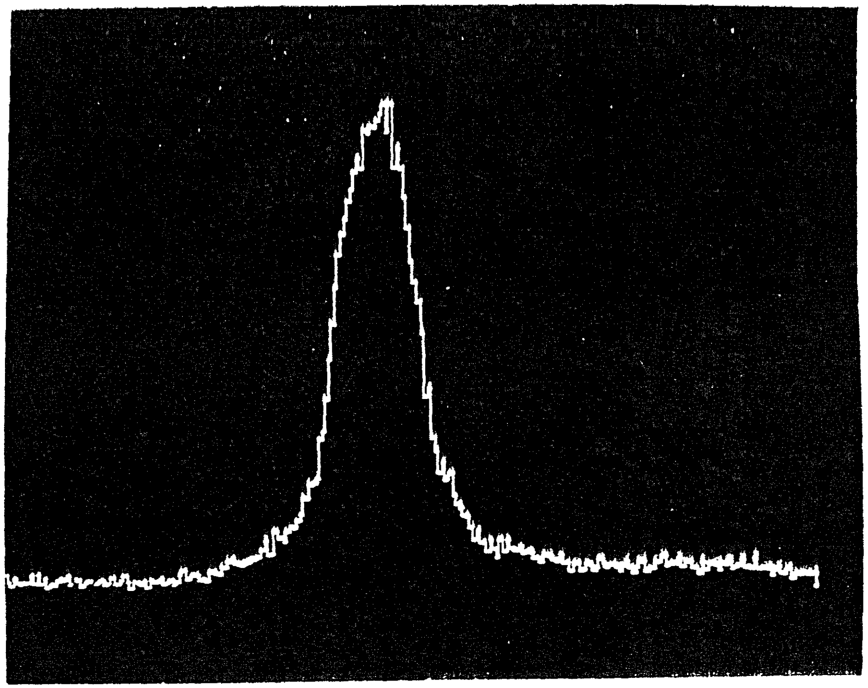
Ti ←

Figure 217 Line Profile Scan

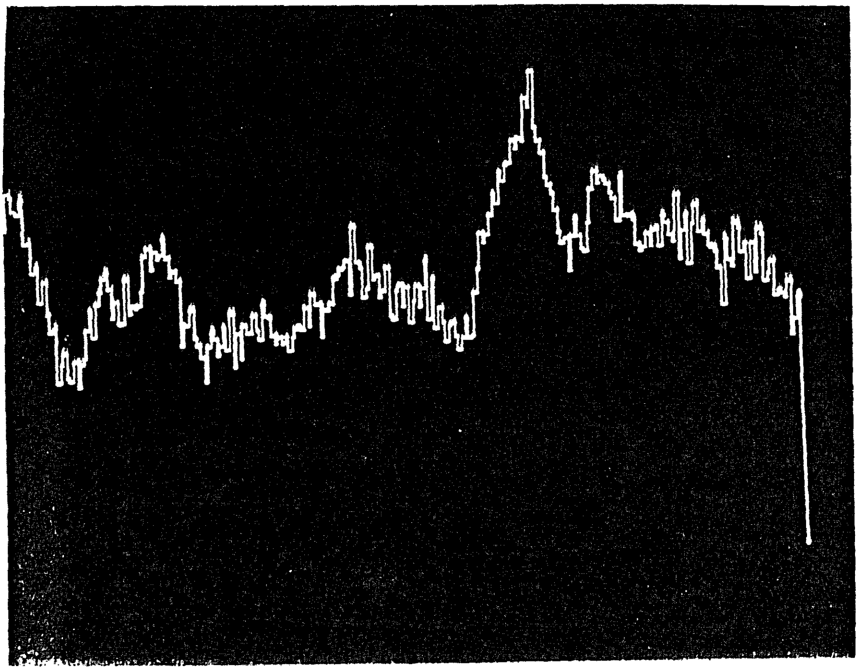
Figure 218

Cr ←

Fe →

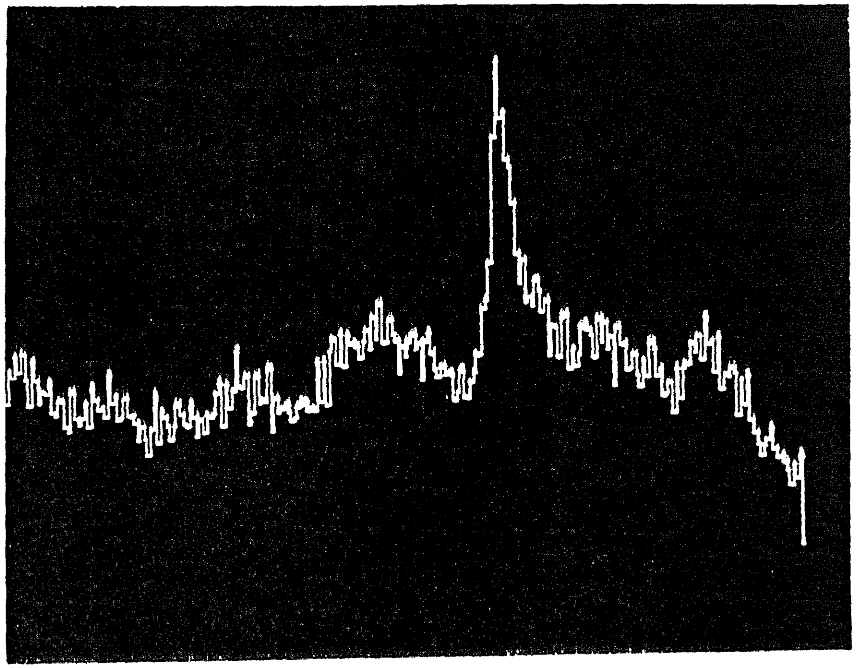
Figure 219

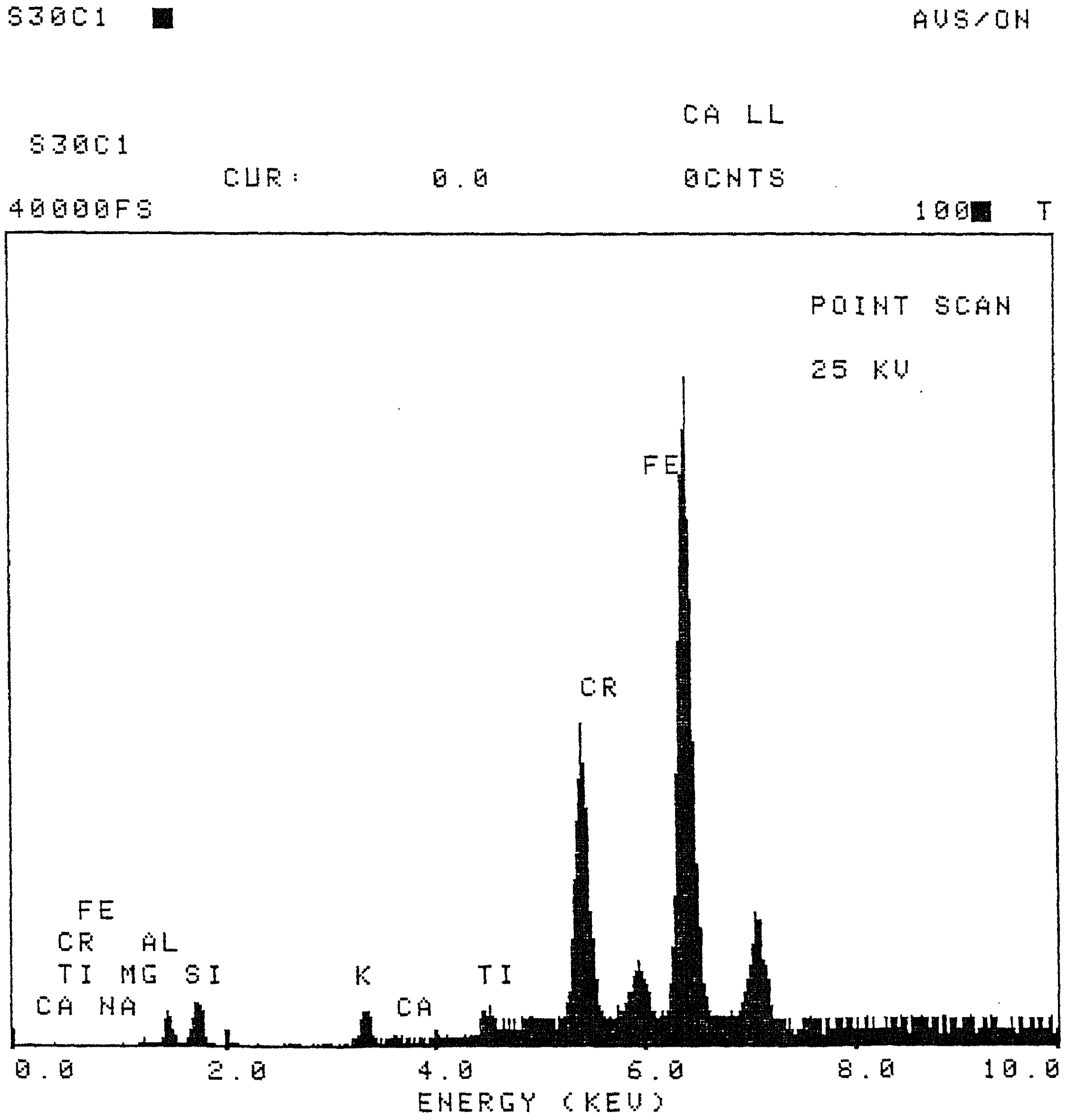

20-Oct-89 11:35

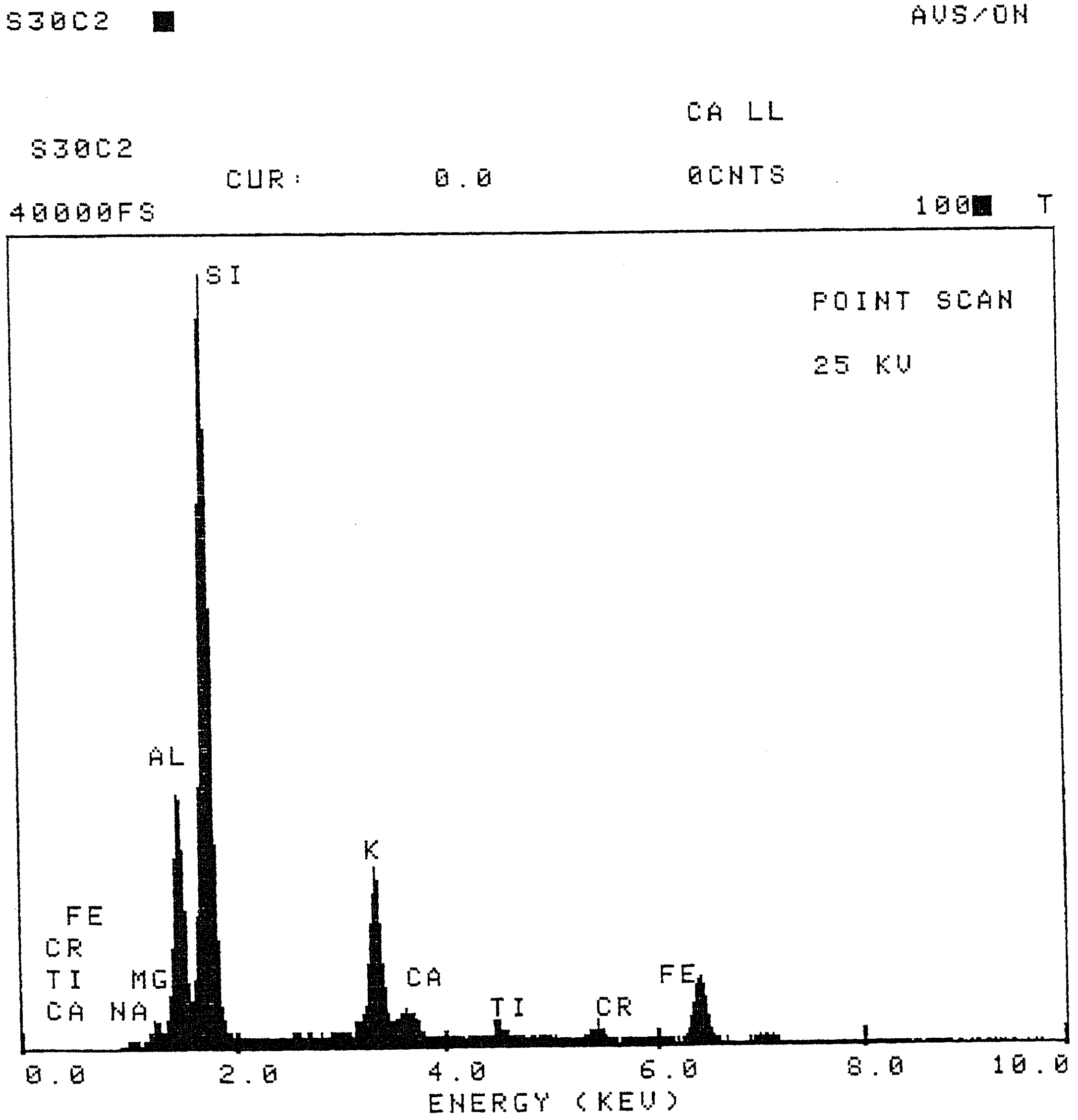

20-Oct-89 11:35

S30C3 ■ AVS/ON

CA LL

S30C3

CUR: 0.0 0CNTS

40000FS 100■ T

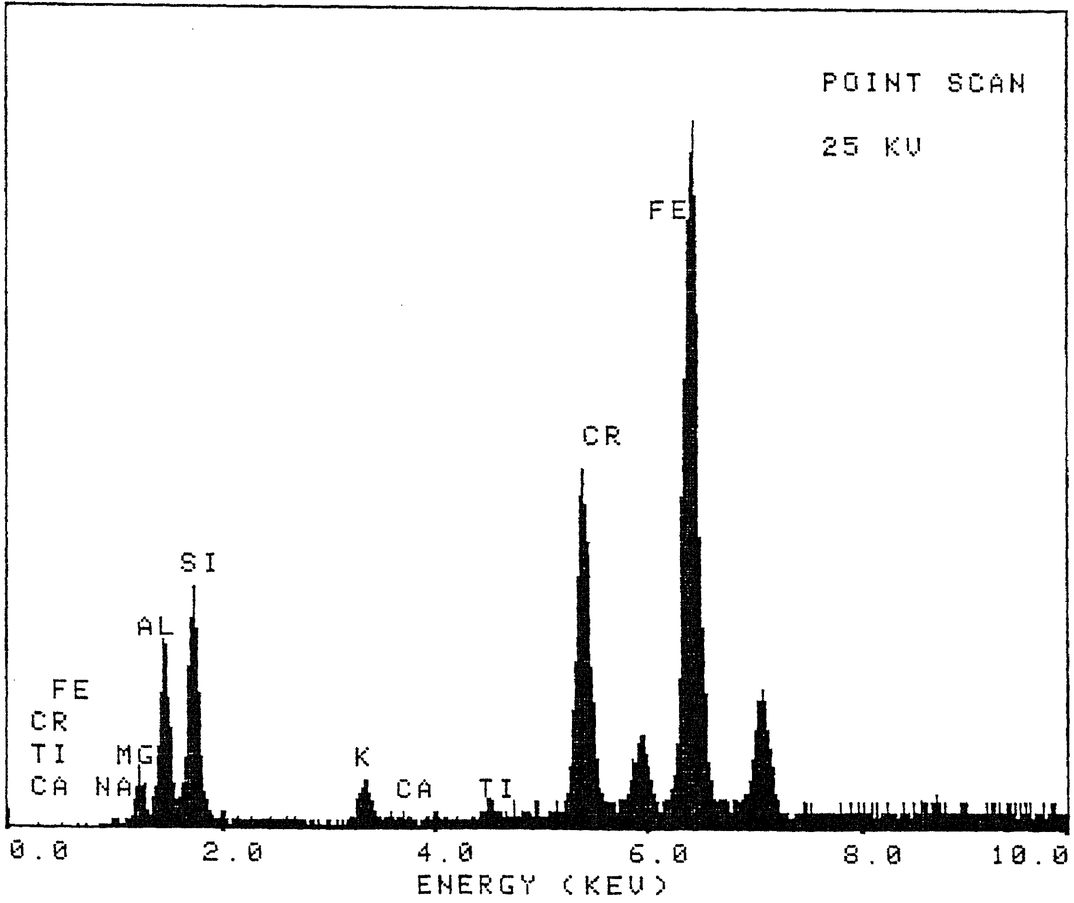

20-Oct-89 11:35

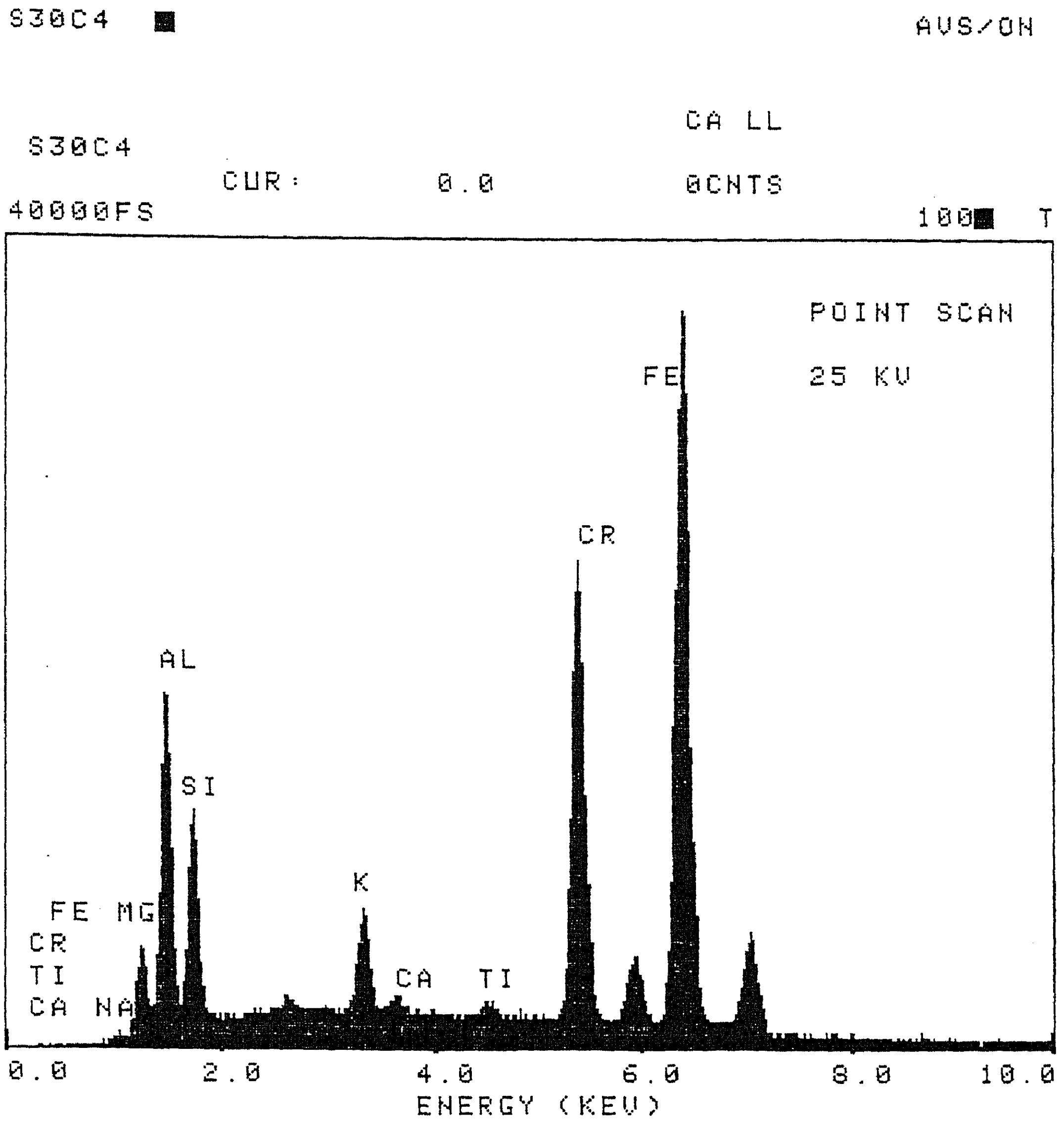

20-Oct-89 11:35

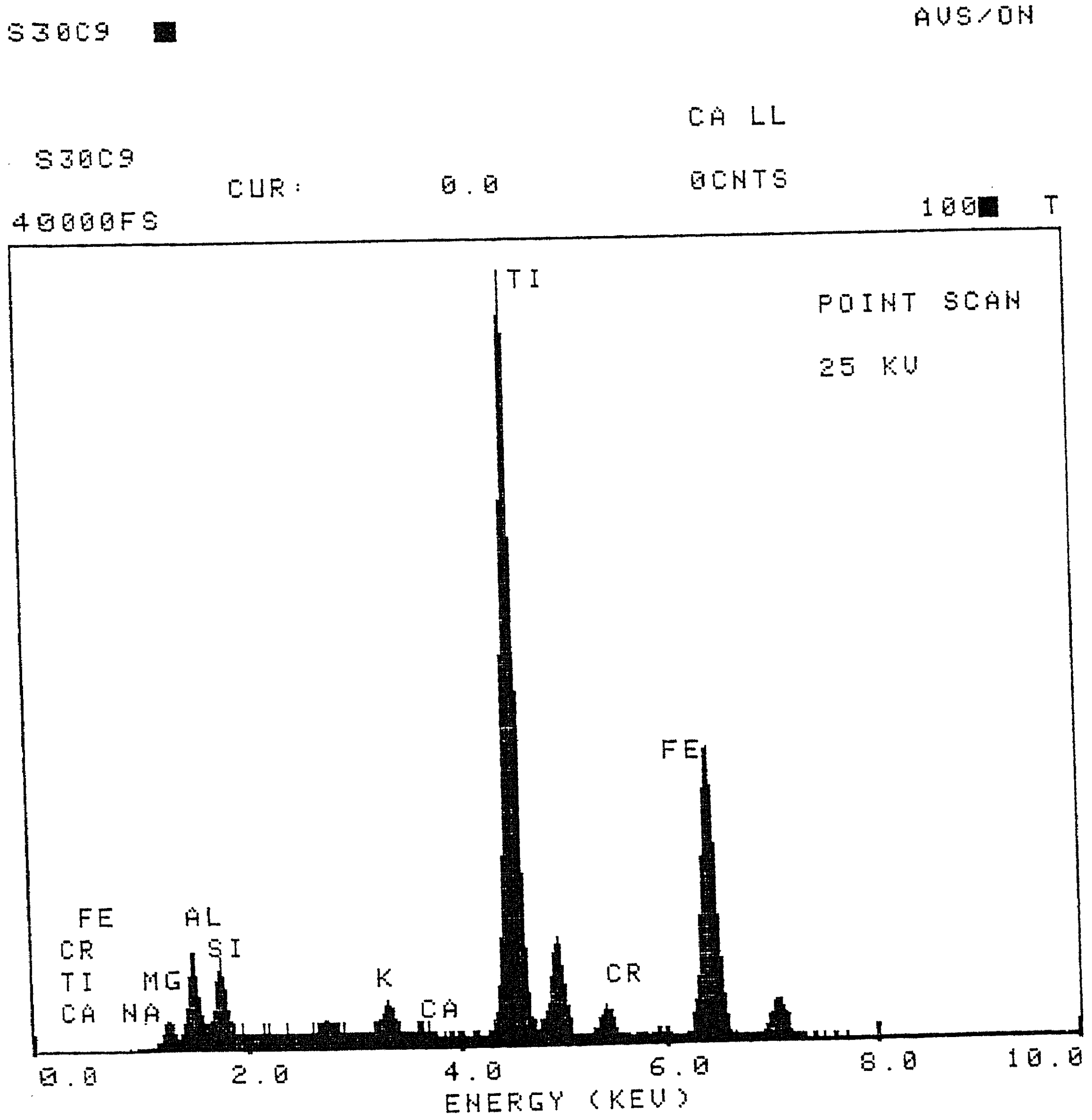

20-Oct-89 11:35

```
S30C11 ■                                        AVS/ON
                                           4006CPS TCR
                                              0CPS  TI
                                    CA LL
 S30C11
         CUR:      0.0              0CNTS
40000FS                                        100■  T
```

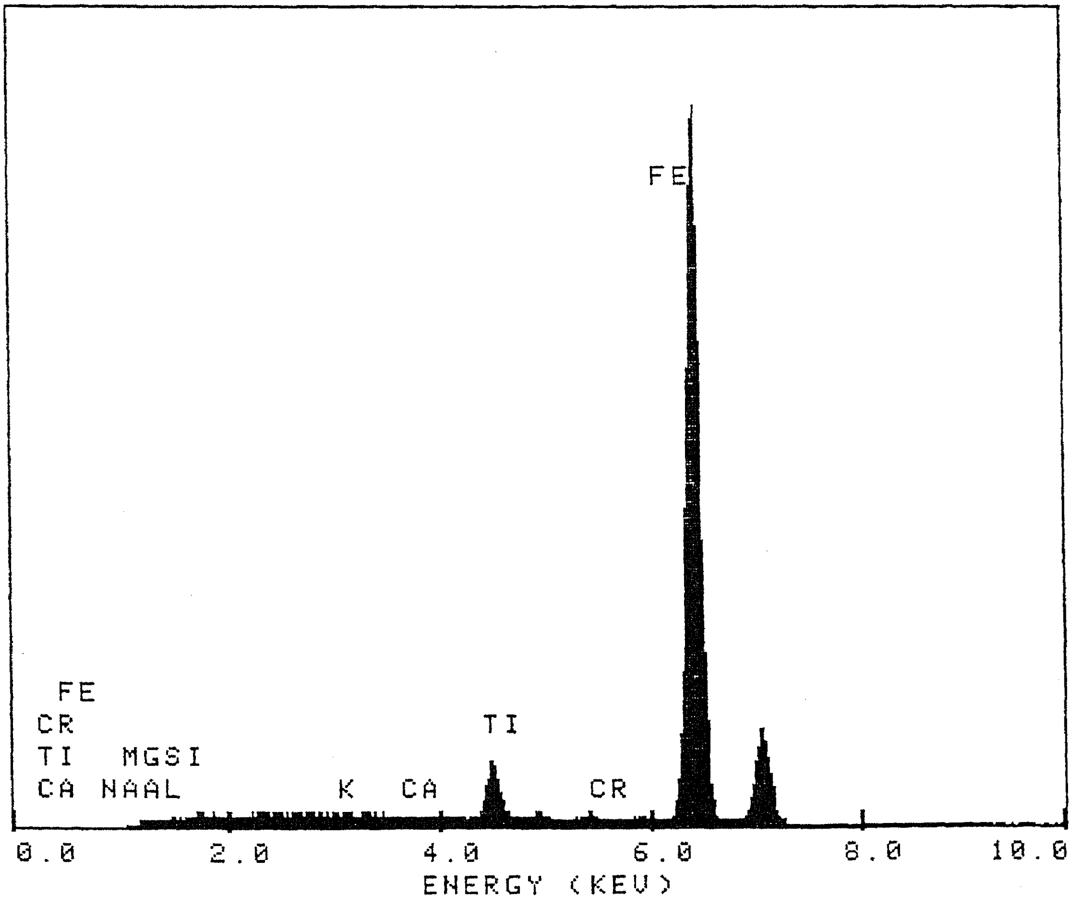

20-Oct-89 11:35

SEM IMAGES OF SAMPLE # Microwave 45 minutes Powder Sample

Figure 192

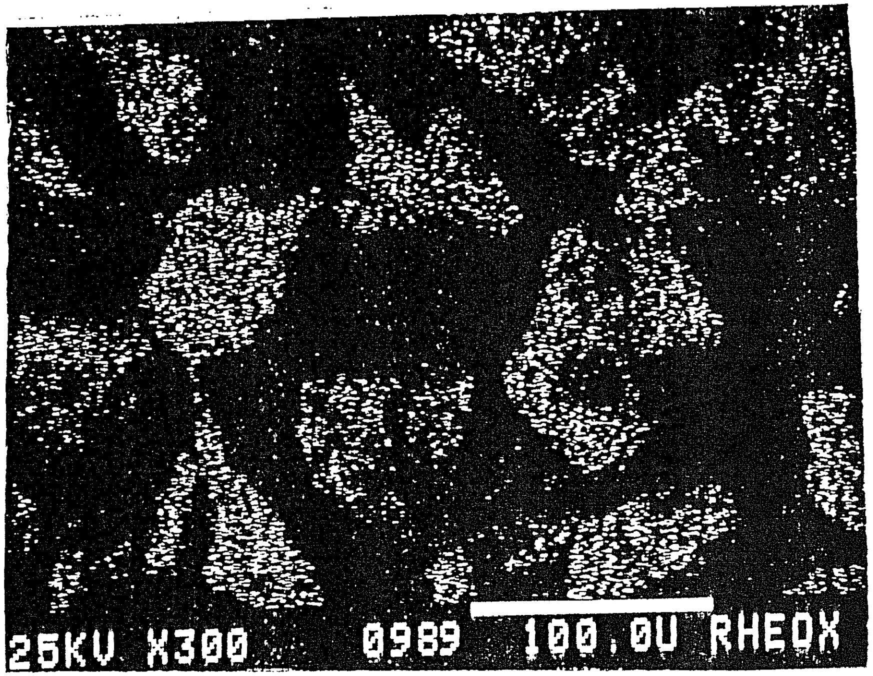

Figure 193 Al X-ray Image of Figure 192

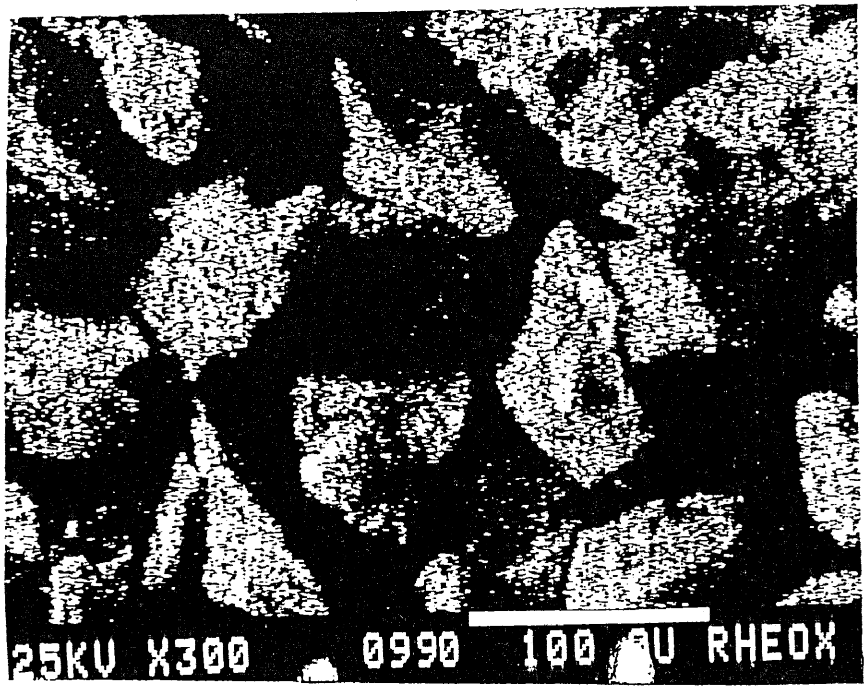

Figure 194 Si X-ray Image of Figure 192

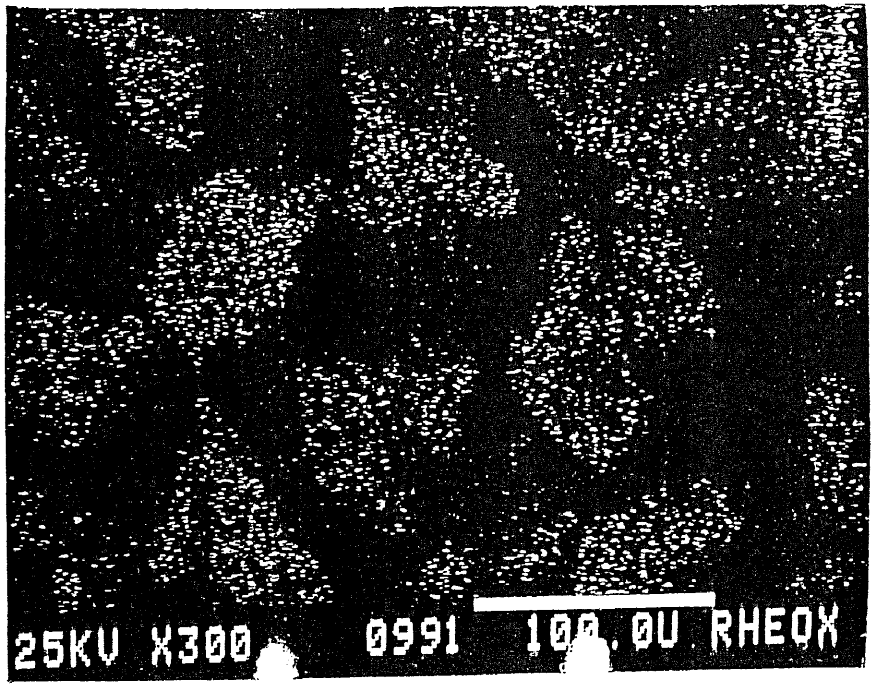

Figure 195 K X-ray Image of Figure 192

SEM IMAGES OF SAMPLE # Microwave At 5 minutes Powder Sample

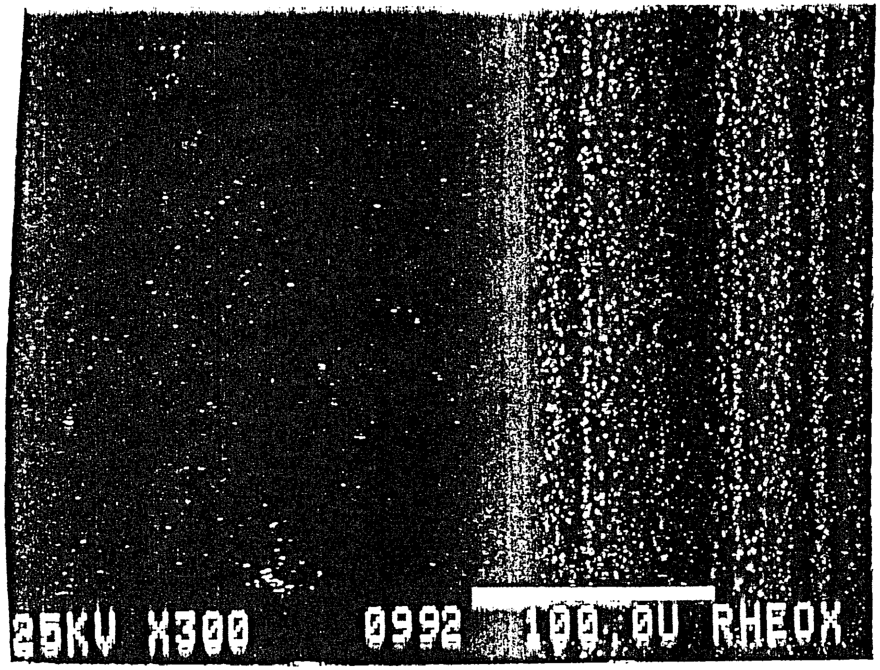

Figure 196 Ti X-Ray Image of Figure 192

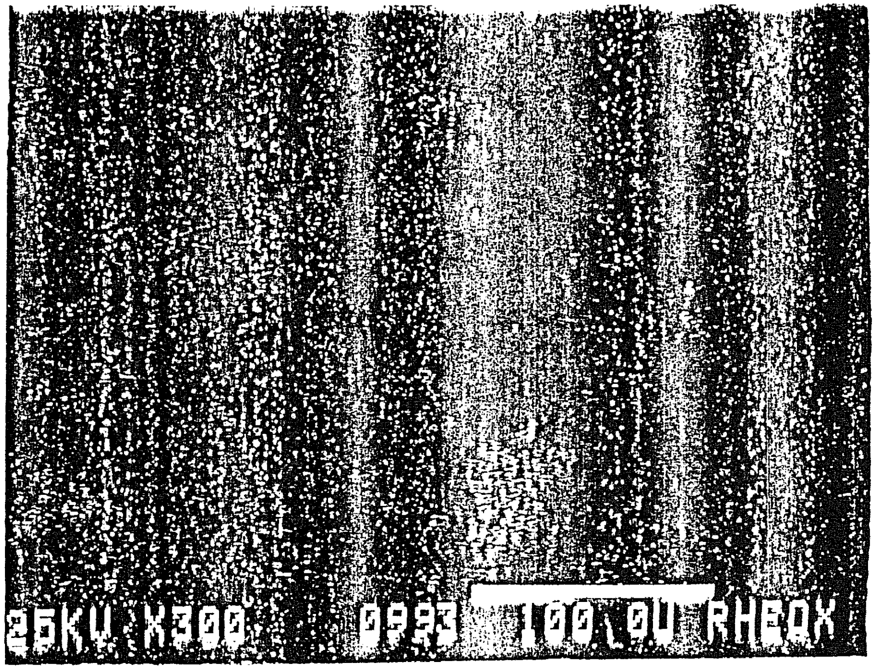

Figure 197 Cr X-Ray Image of Figure 192

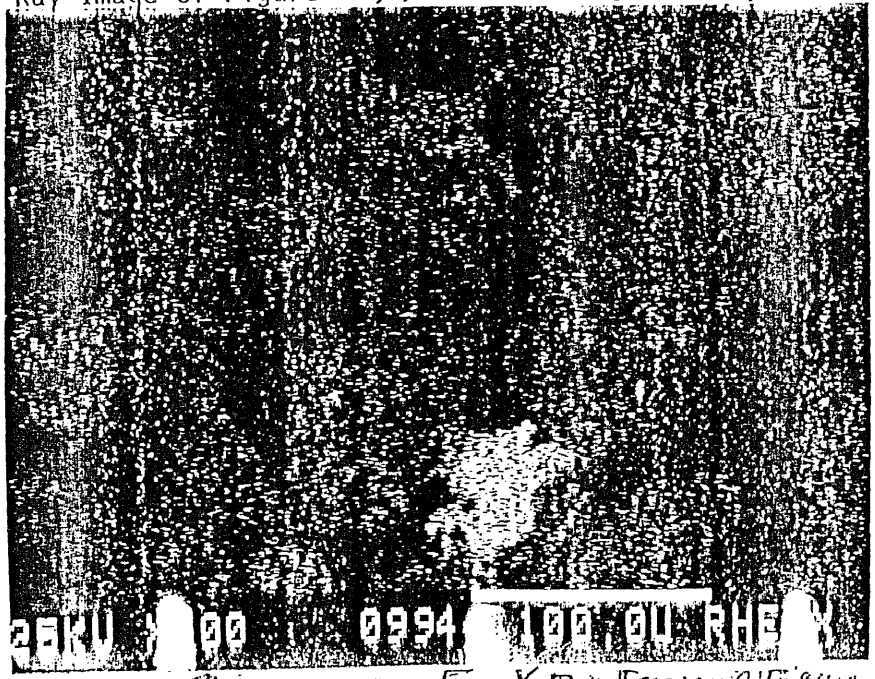

Figure 198 Fe X-Ray Image of Figure 192

Figure 199

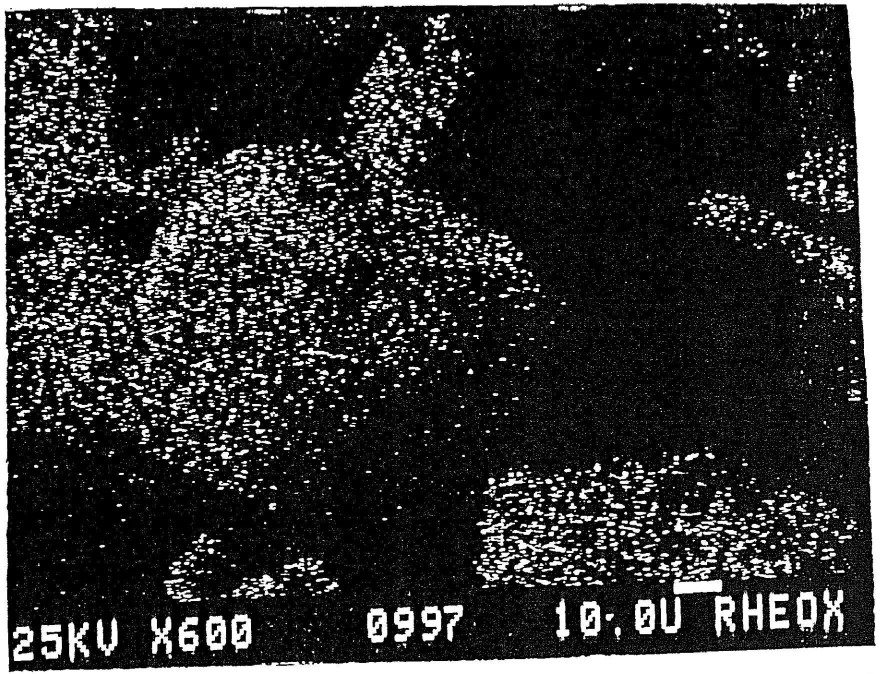

Figure 200 AL X-ray Image of Figure 199

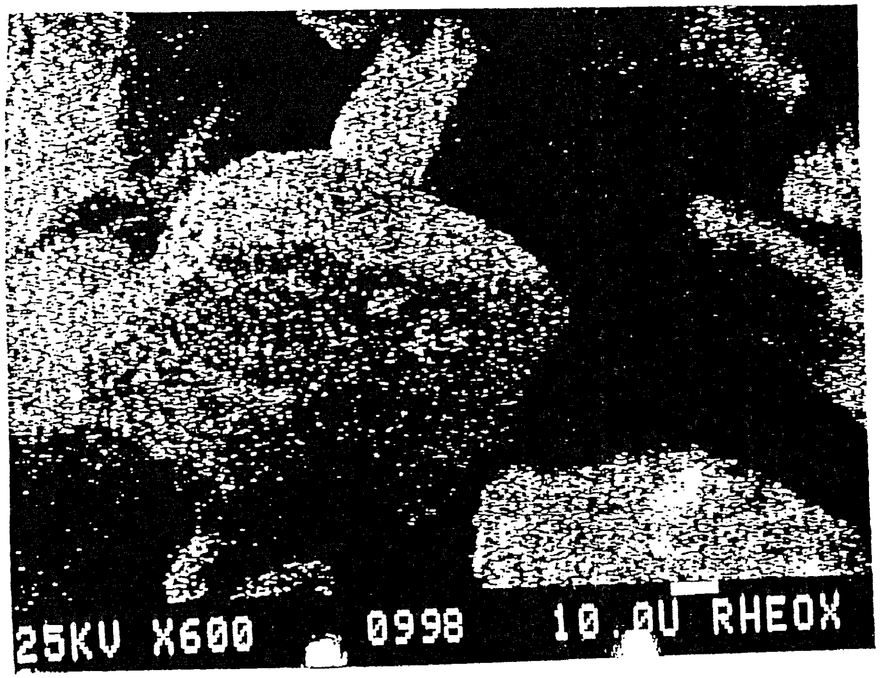

Figure 201 Si X-ray Image of Figure 199

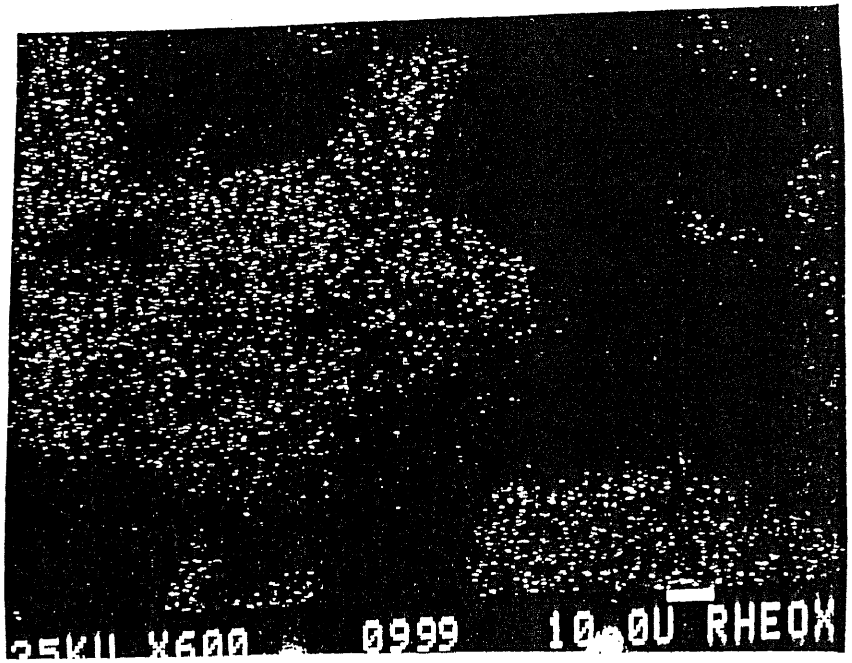

Figure 202 K X-ray Image of Figure 199

SEM IMAGES OF SAMPLE # Microwave 45 minutes Powder Sample

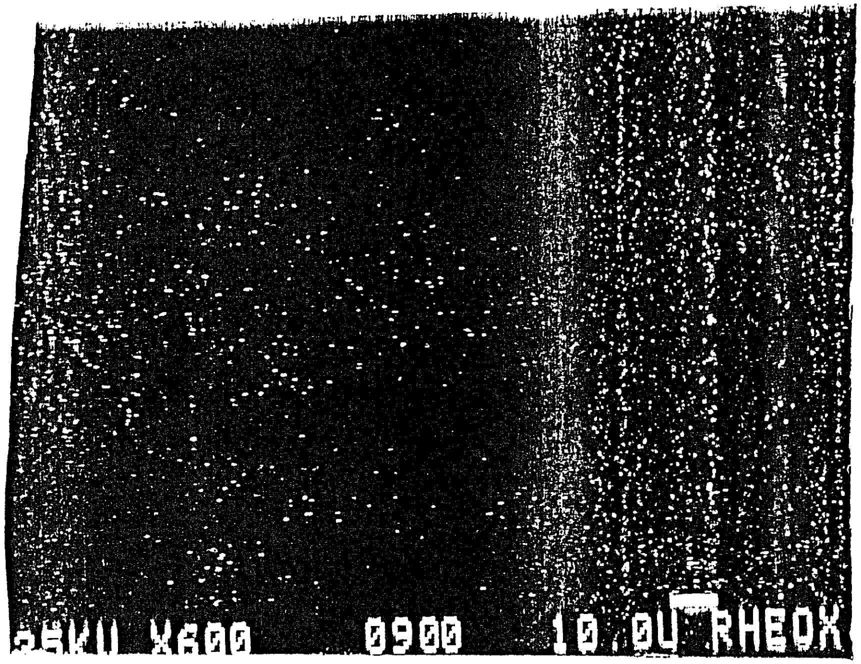

Figure 203 Ti X-Ray Image of Figure 199

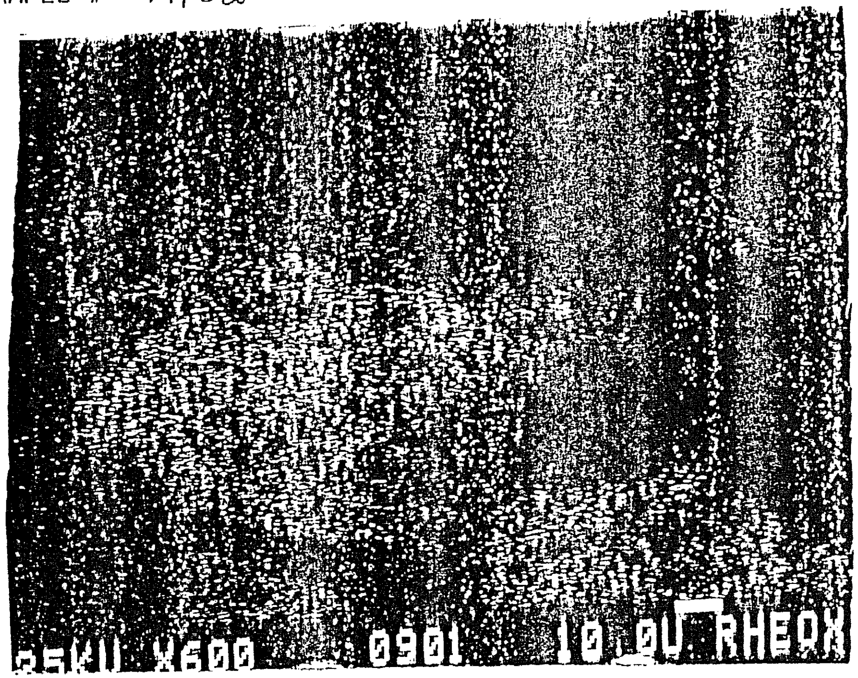

Figure 204 Cr X-Ray Image of Figure 199

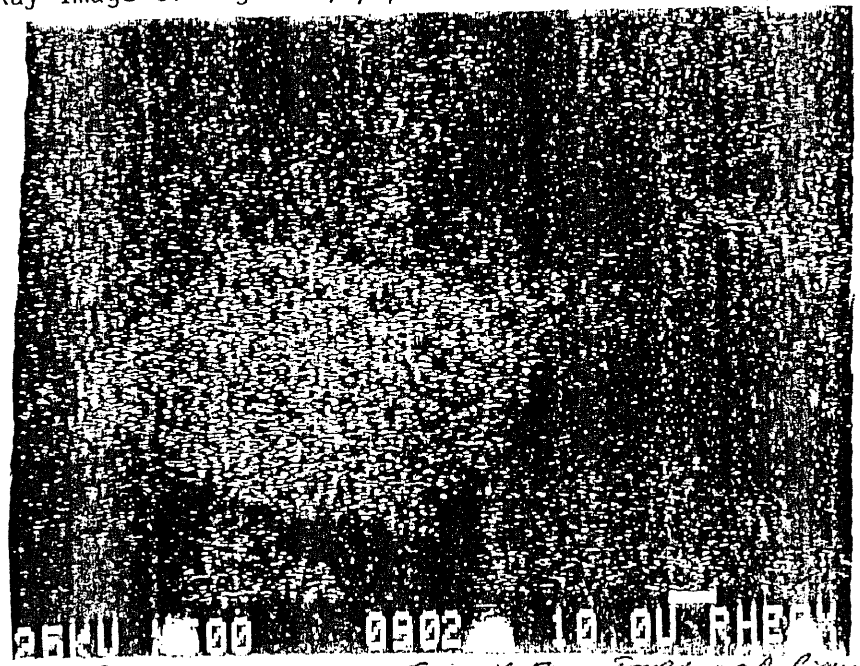

Figure 205 Fe - X-Ray Image of figure 199

S45H1 ■ AVS/ON

CA LL

S45H1

CUR: 0.0 0CNTS

40000FS 100■ T

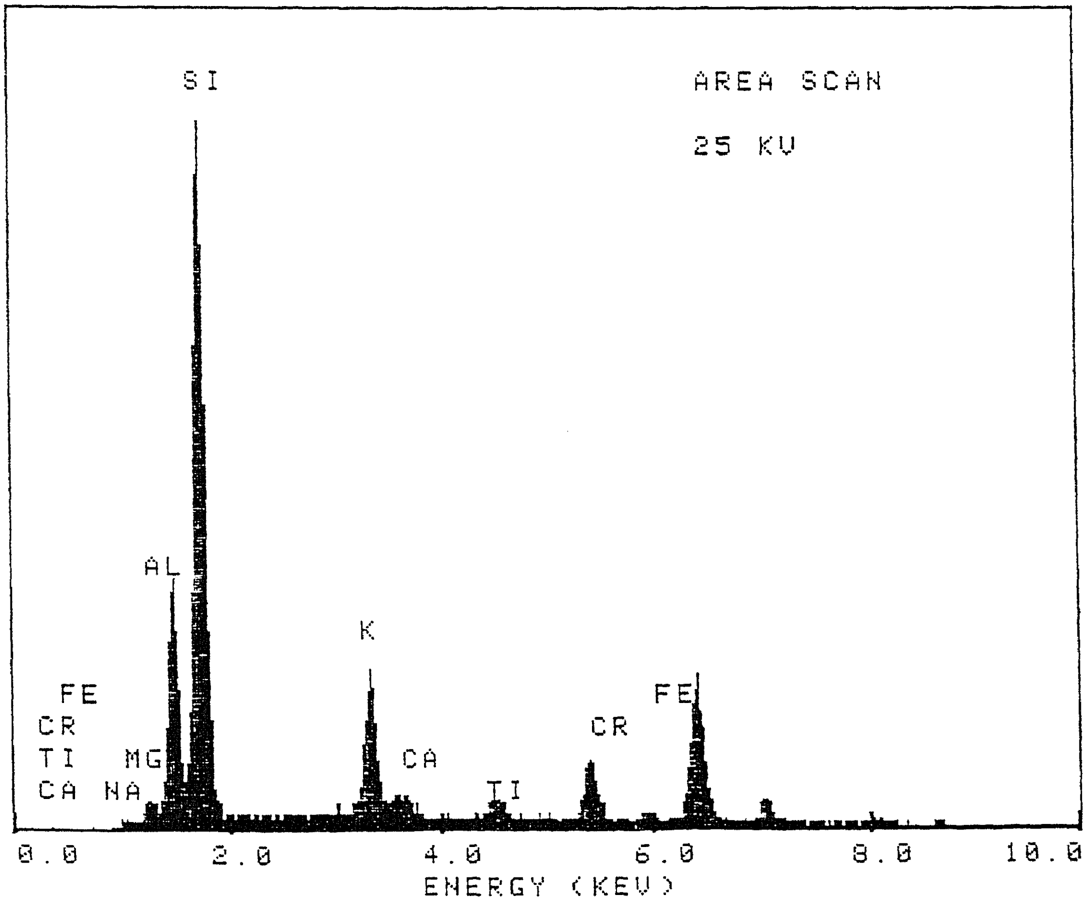

10-Nov-89 16:41

S45H2 ■ AVS/ON

CA LL

S45H2

CUR: 0.0 0CNTS

40000FS 100■ T

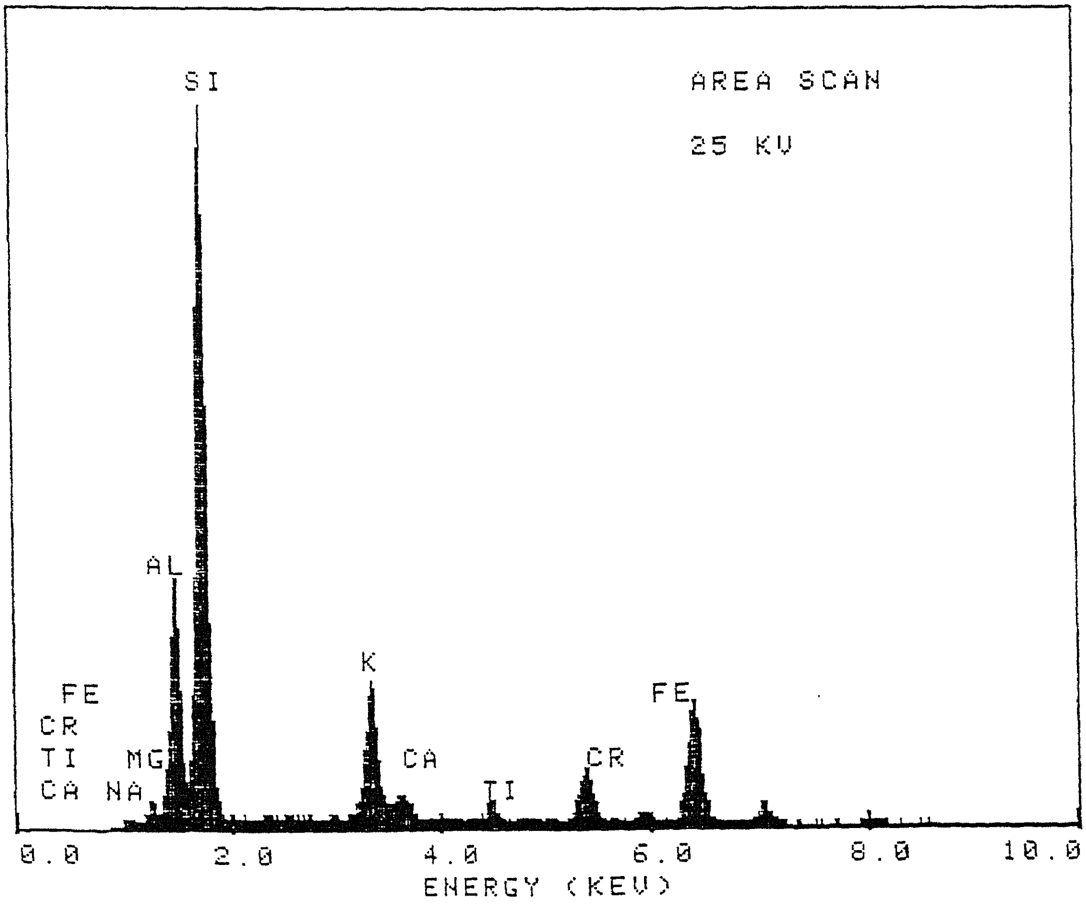

10-Nov-89 16:43

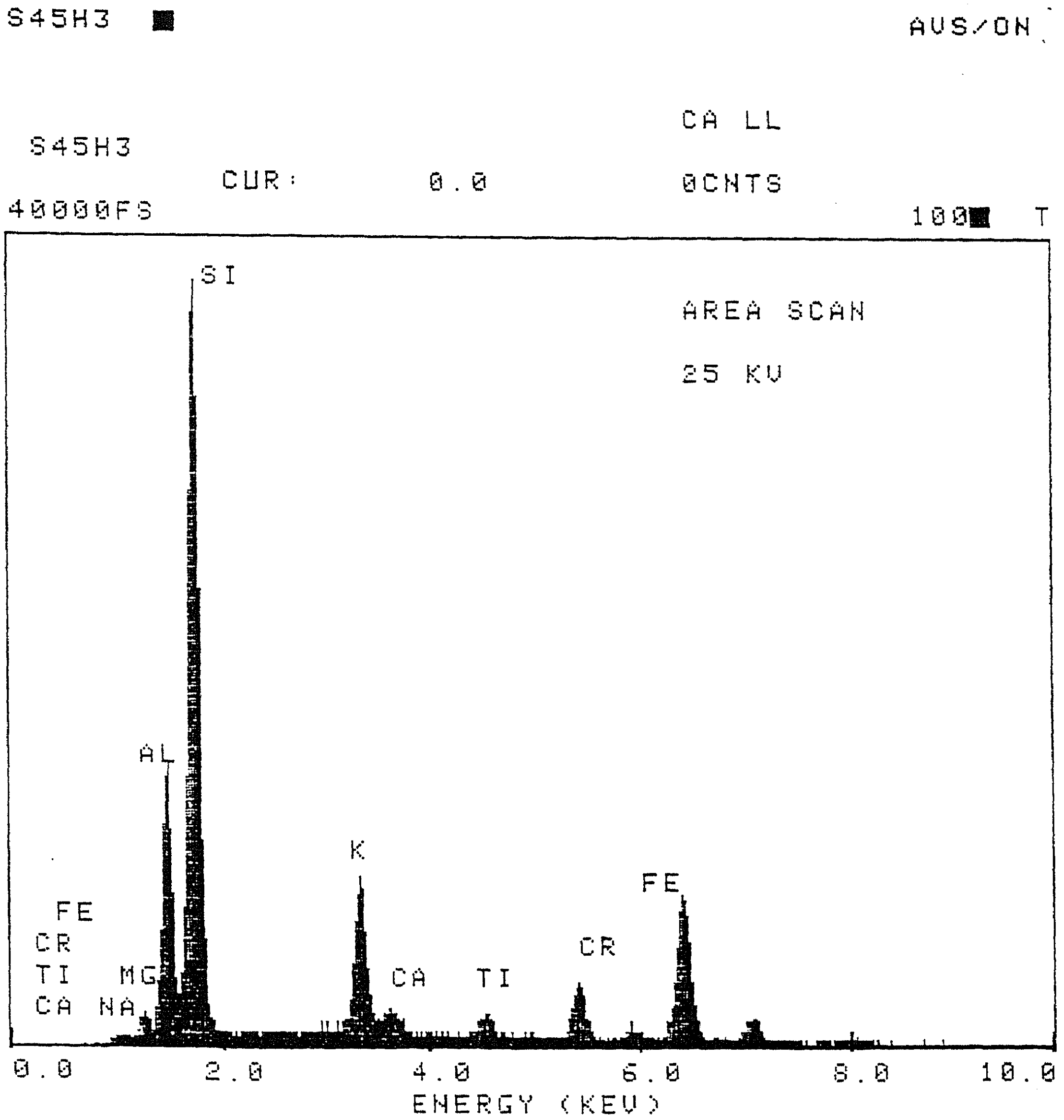

10-Nov-89 16:46

S45H4 ■ AVS/ON

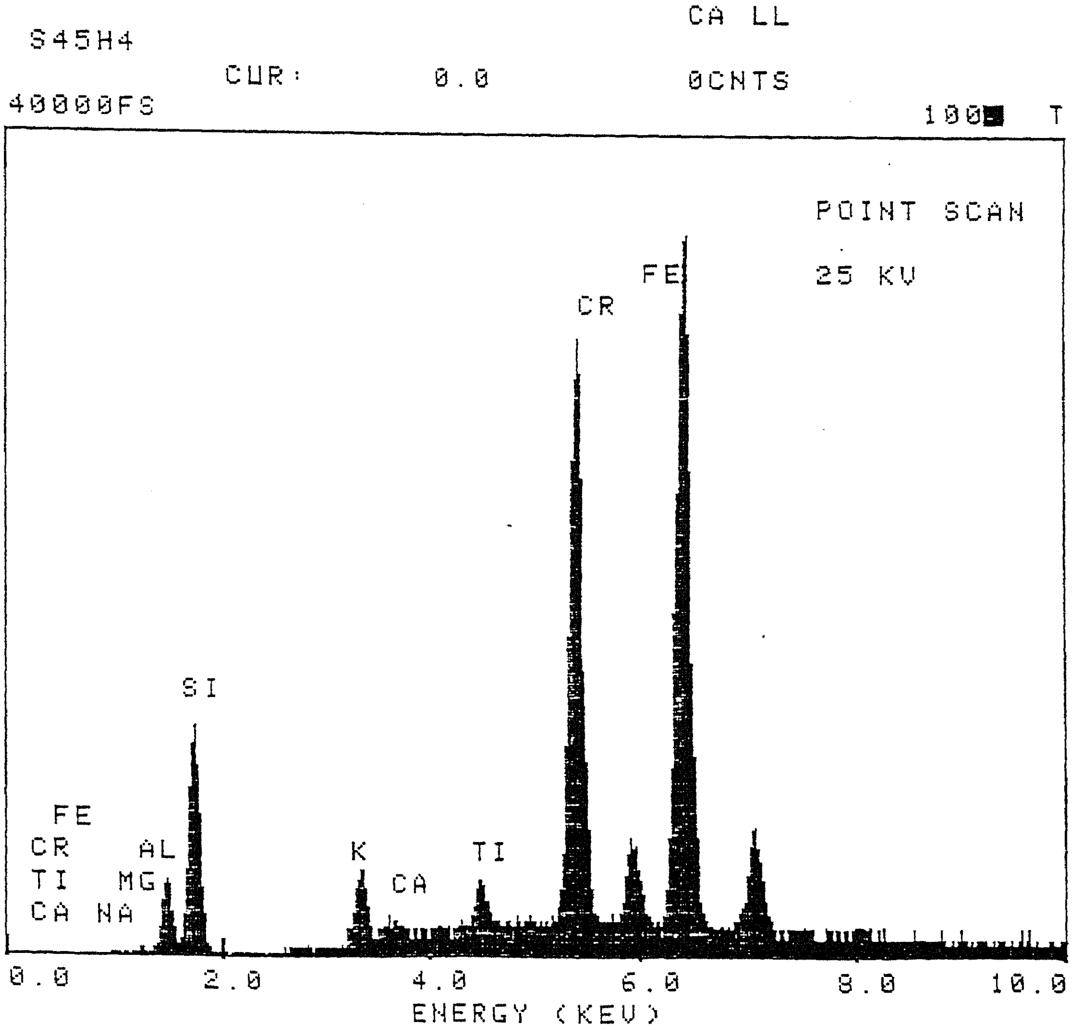

10-Nov-89 16:48

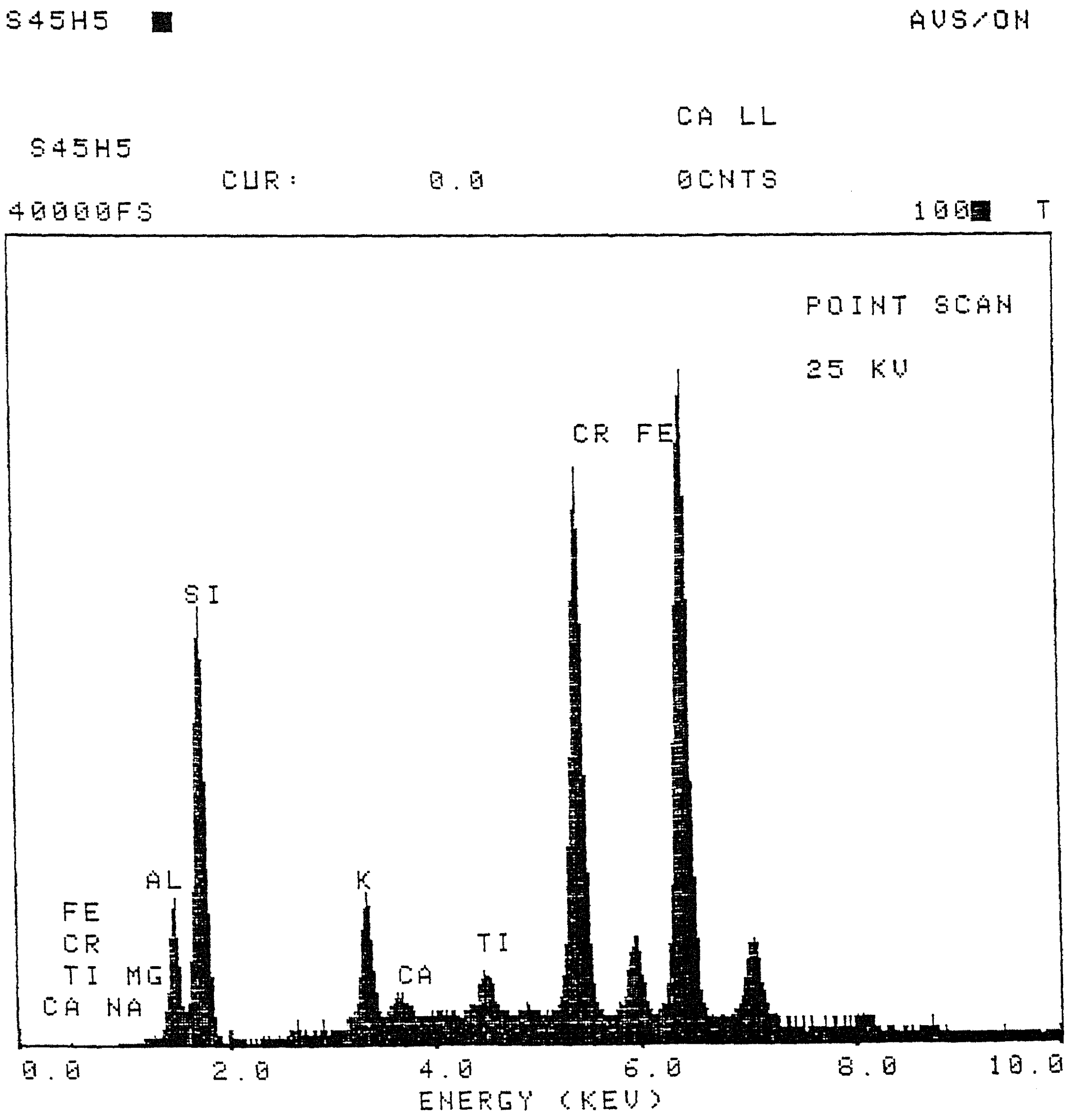

10-Nov-89 16:51

S45H6 ■ AVS/ON

CA LL

S45H6

CUR: 0.0 0CNTS

40000FS 100■ T

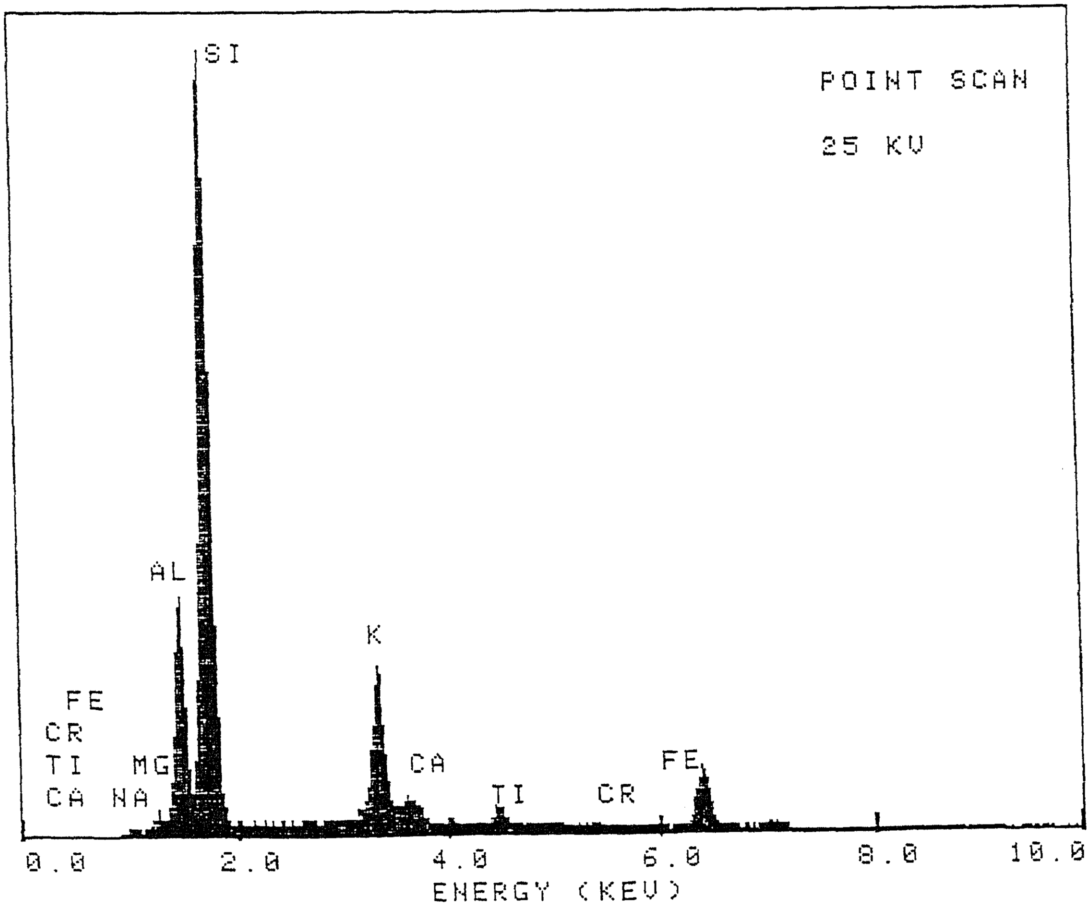

13-Nov-89 08:40

S45H7 ■ AVS/ON

CA LL

S45H7

CUR: 0.0 0CNTS

40000FS 100■ T

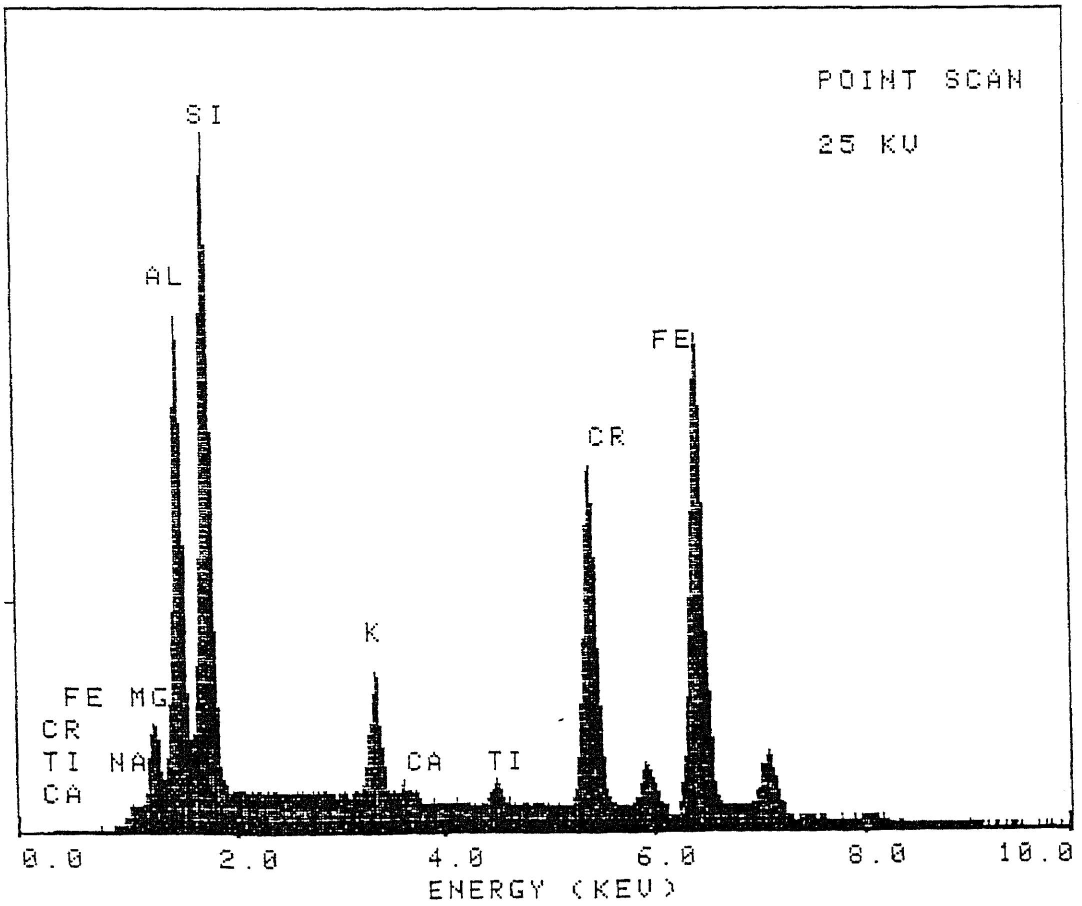

13-Nov-89 08:54

S45H8 ■ AVS/ON

CA LL

S45H8

CUR: 0.0 0CNTS

40000FS 100■ T

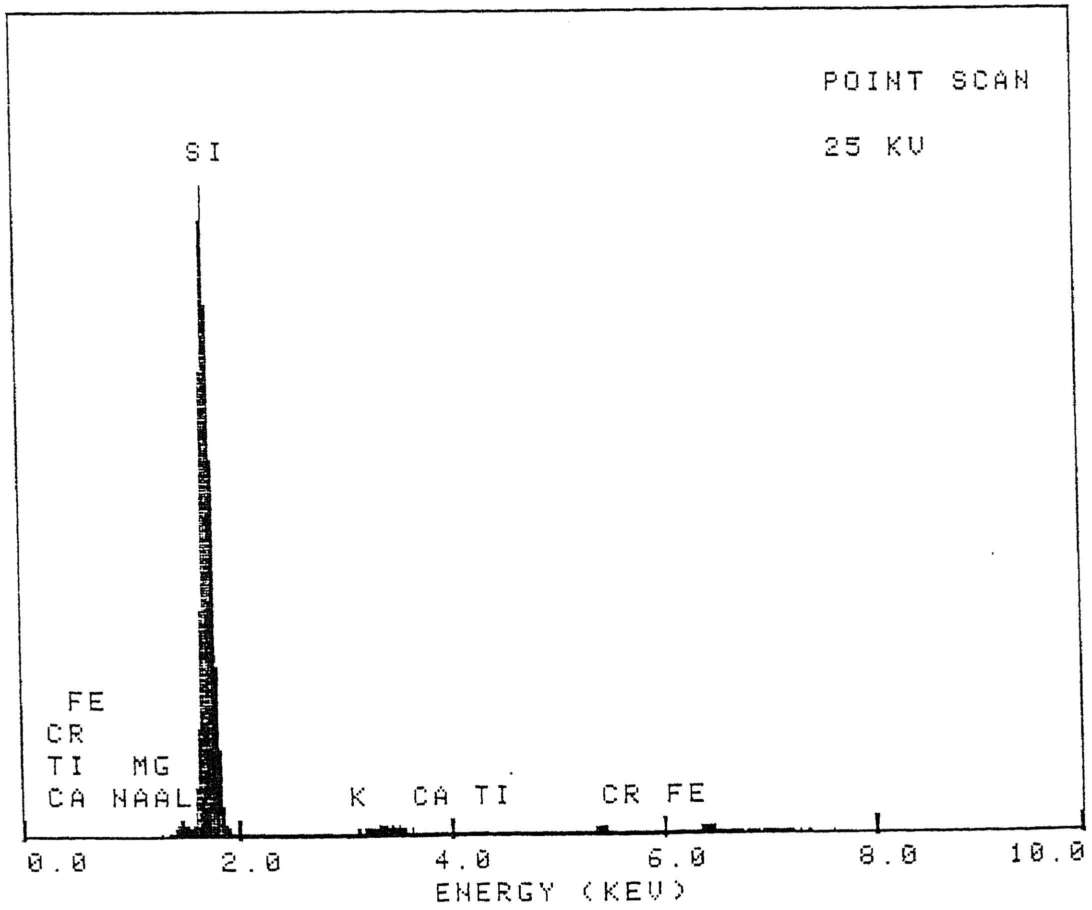

13-Nov-89 09:00

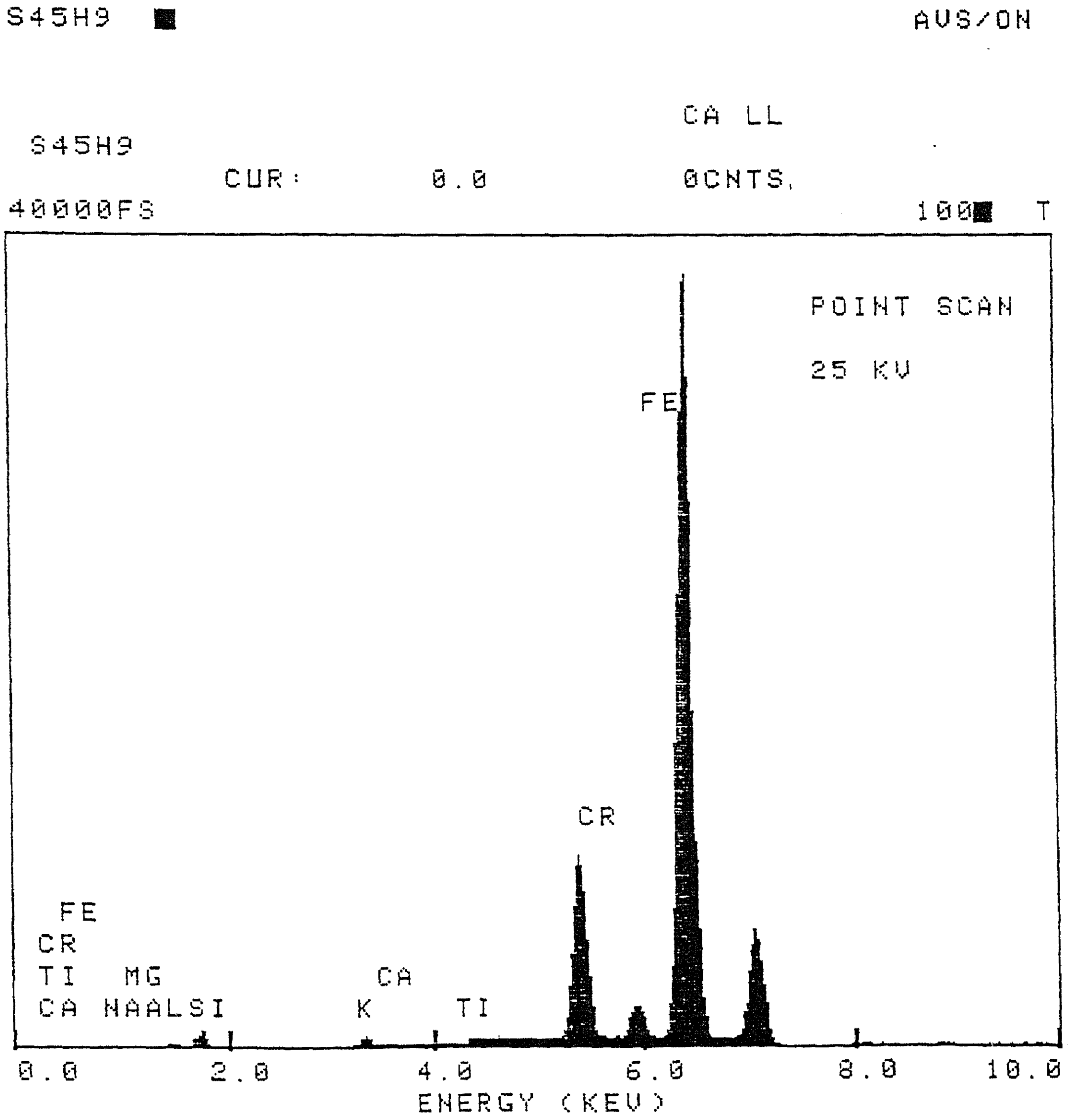

13-Nov-89 09:04

S45H10 ■ AVS/ON

CA LL

S45H10

CUR: 0.0 0CNTS

40000FS 100■ T

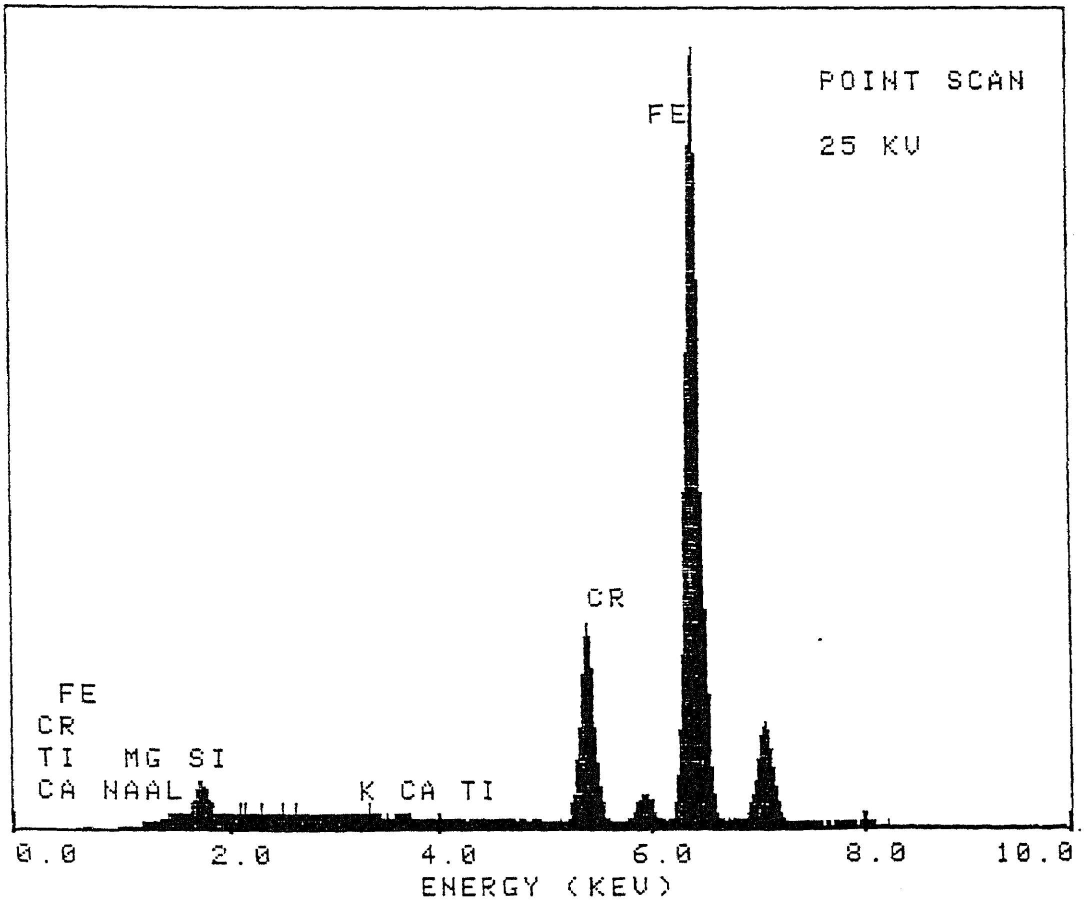

13-Nov-89 09:07

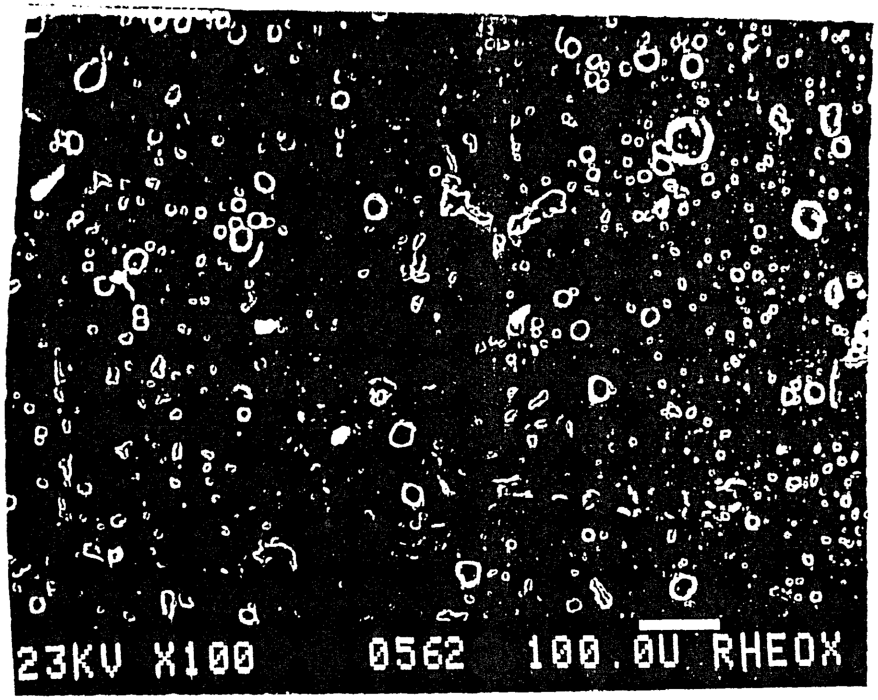

Figure 206

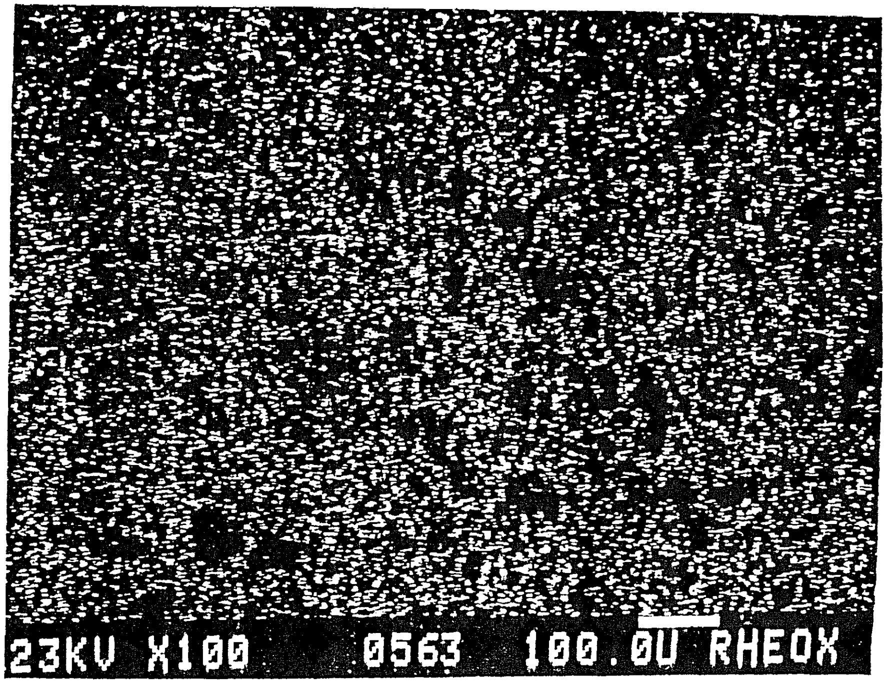

Figure 207 AL X-ray Image of Figure 206

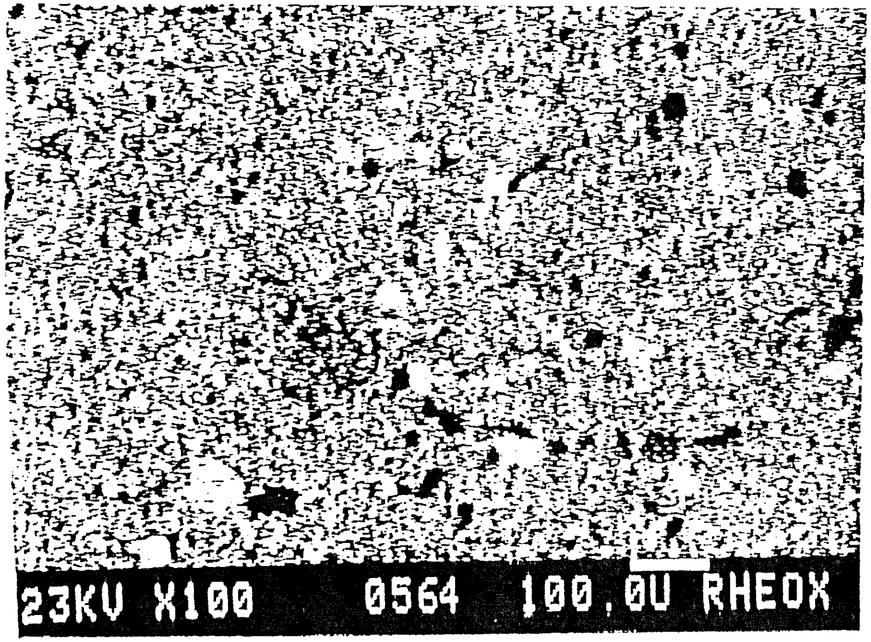

Figure 208 Si X-ray Image of Figure 206

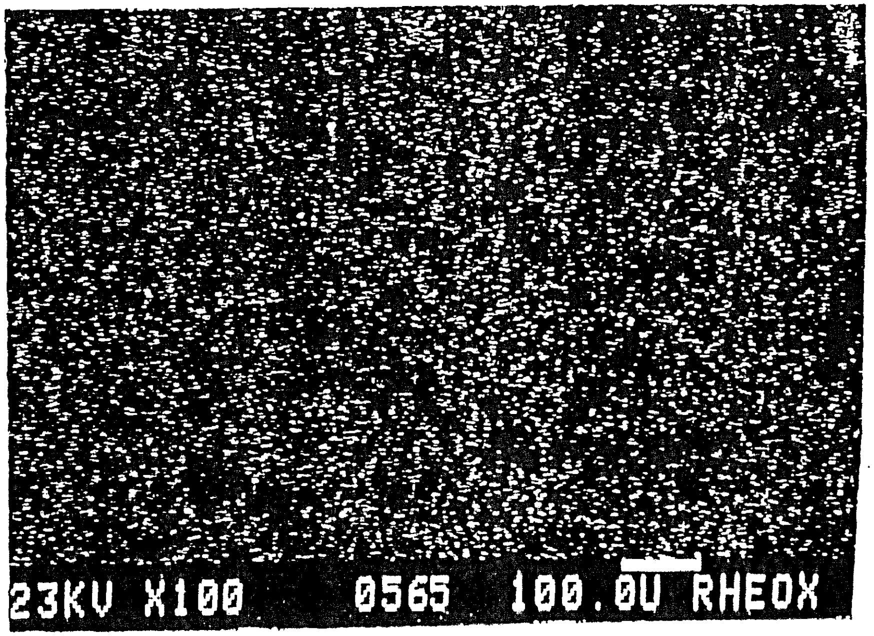

Figure 209 K X-ray Image of Figure 206

SEM IMAGES OF SAMPLE # Microwave 45 minutes Cross Section

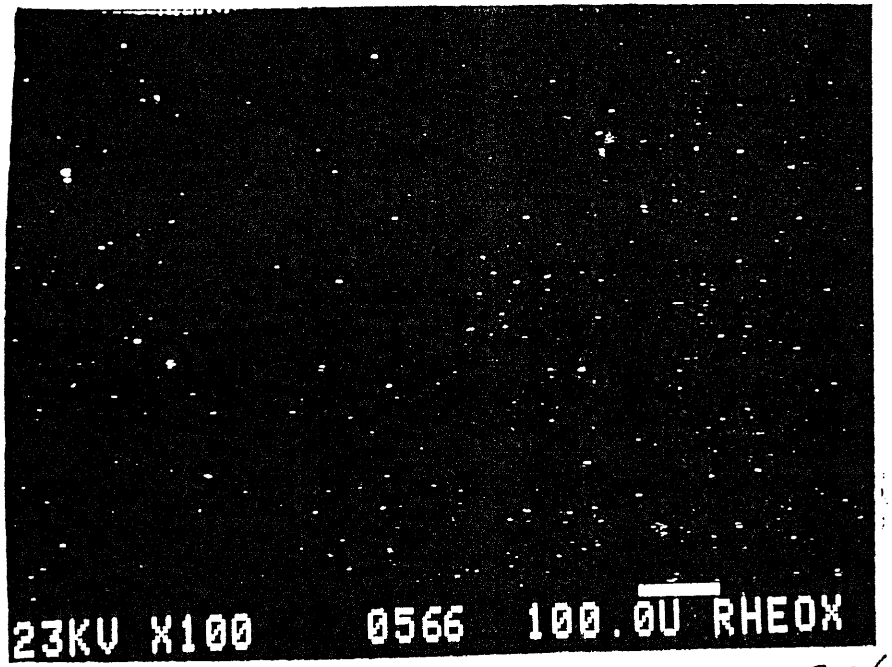

Figure 210 Ti X-Ray Image of Figure 206

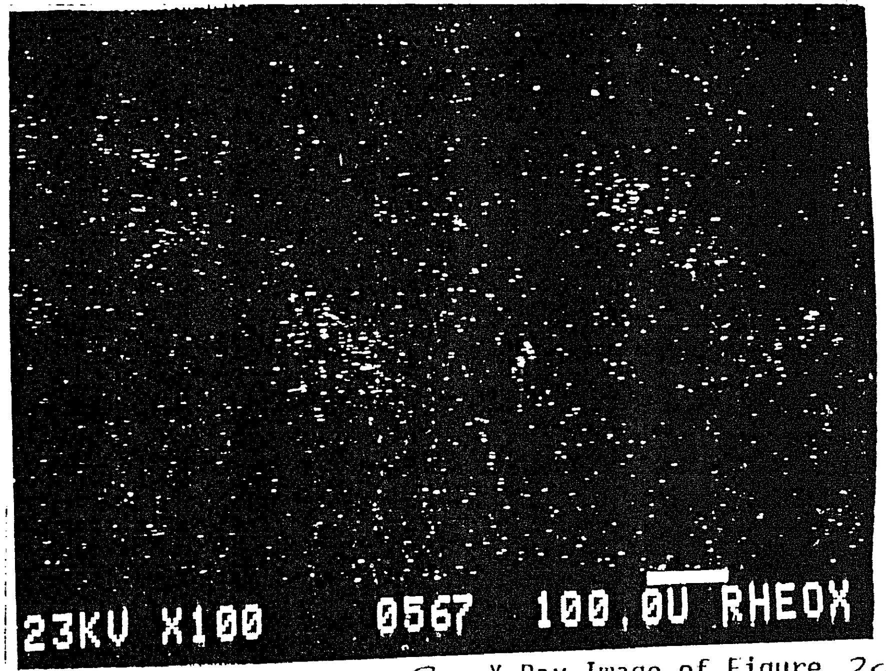

Figure 211 Cr X-Ray Image of Figure 20

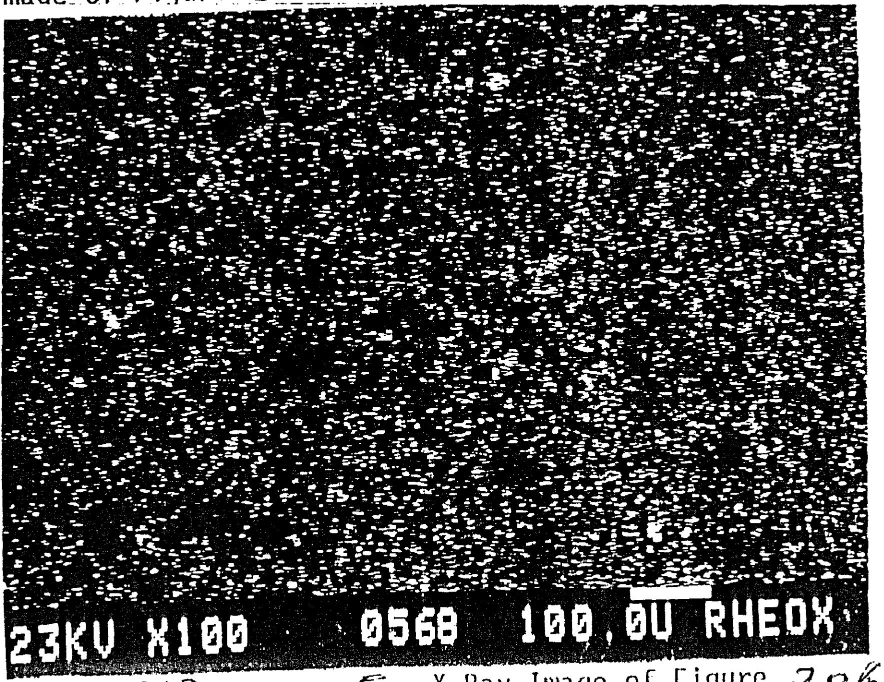

Figure 212 Fe X-Ray Image of Figure 206

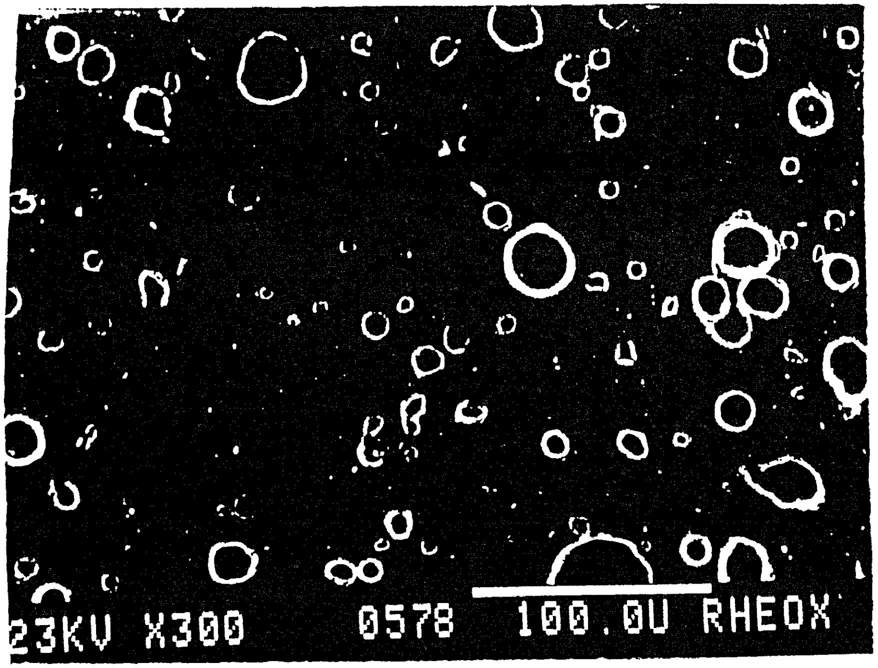

Figure 213

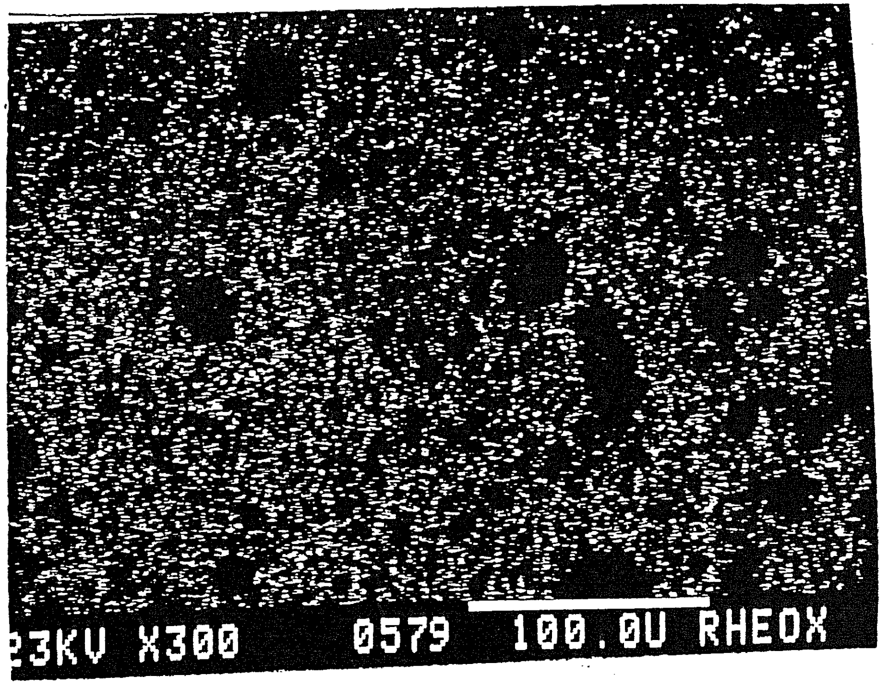

Figure 214 AL X-ray Image of Figure 213

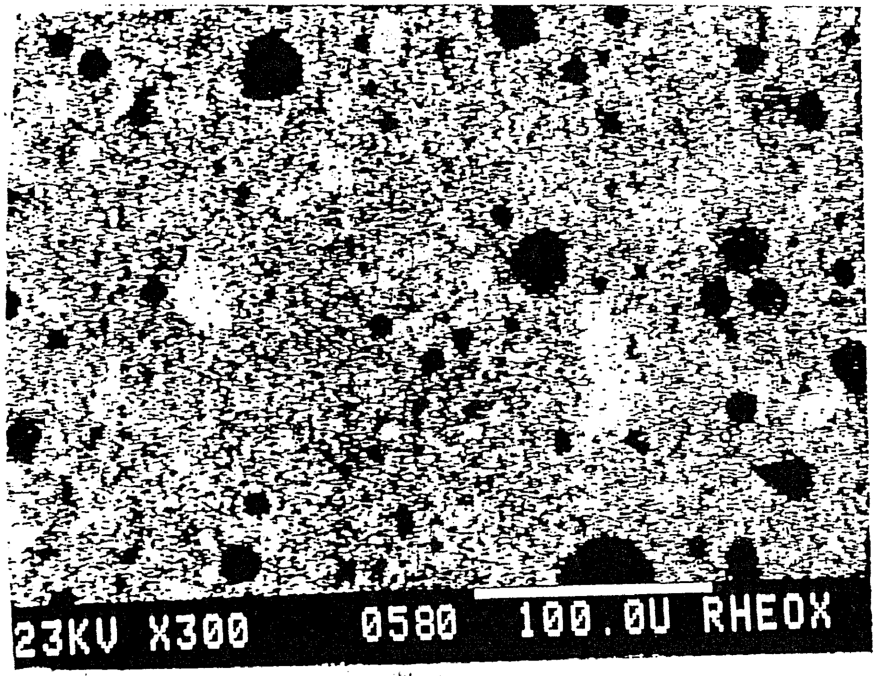

Figure 215 Si X-ray Image of Figure 213

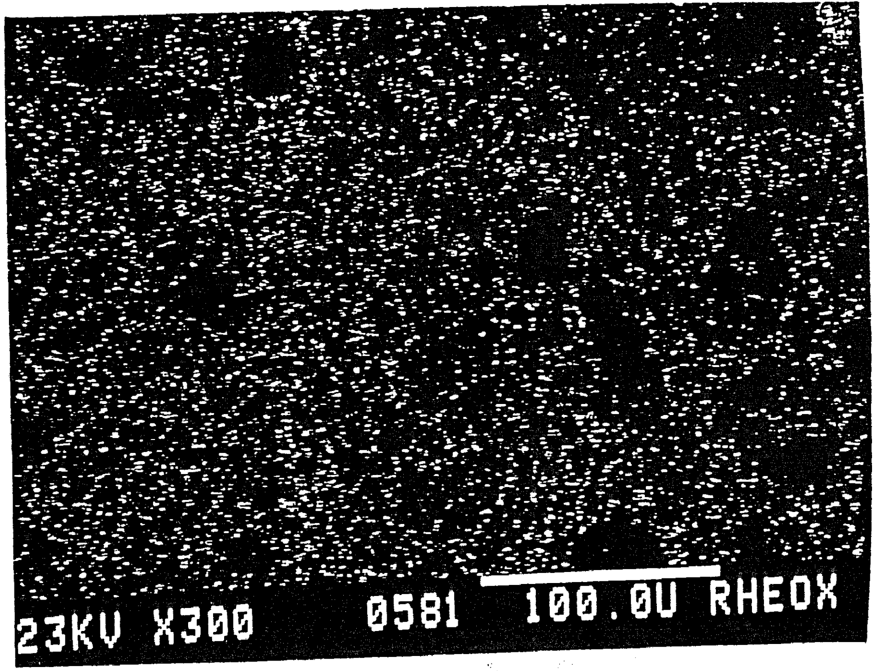

Figure 216 K X-ray Image of Figure 213

SEM IMAGES OF SAMPLE # Microwave 45 minutes Cross Section

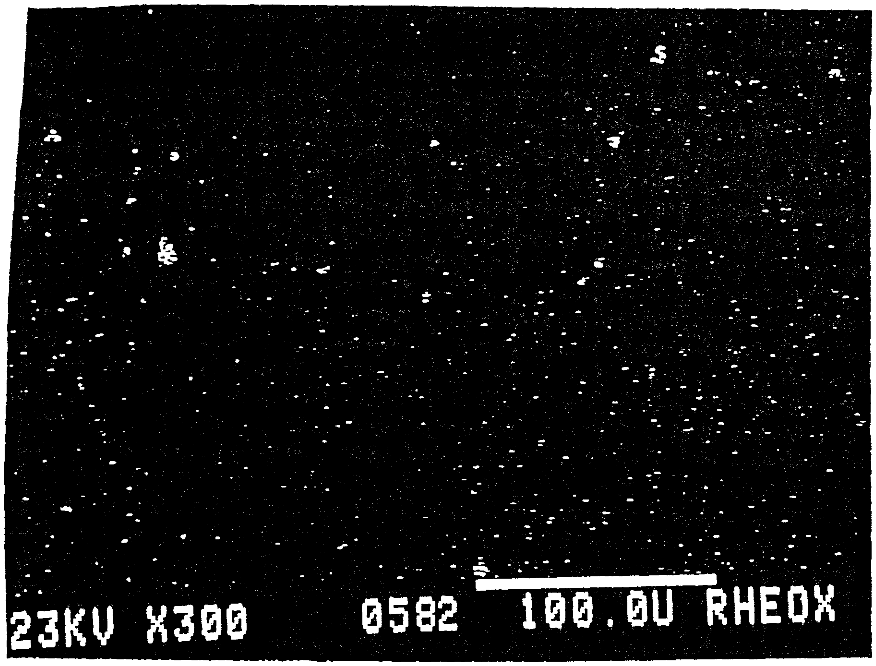

Figure 217 Ti X-Ray Image of Figure 213

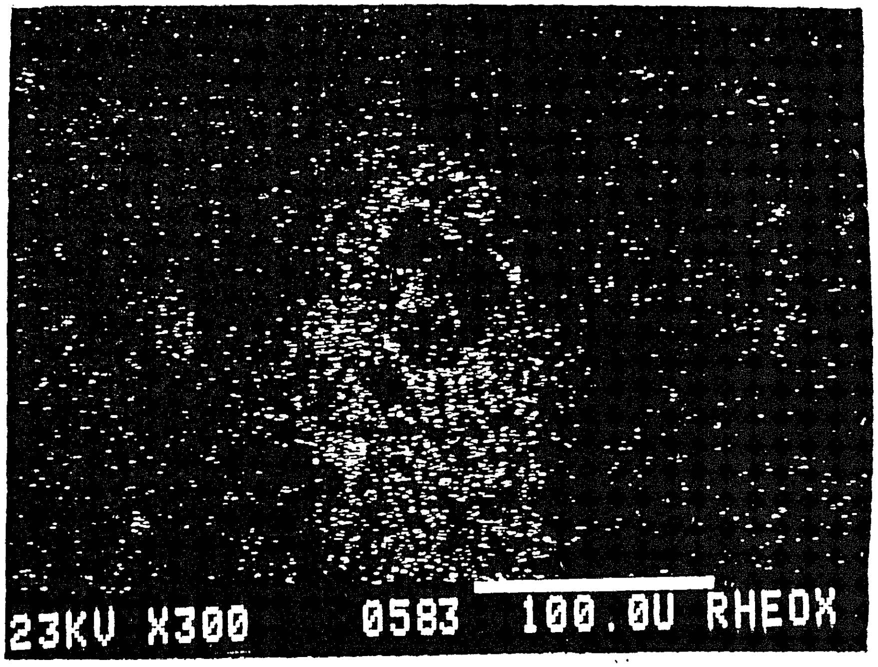

Figure 218 Cr X-Ray Image of Figure 213

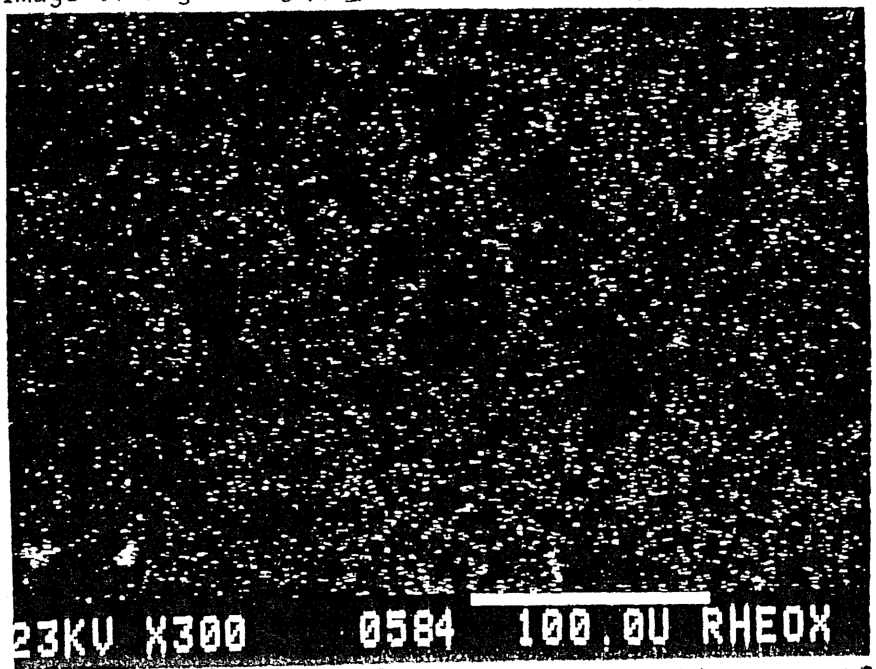

Figure 219 Fe X-Ray Image of Figure 213

Microwave 45 minutes Cross Section

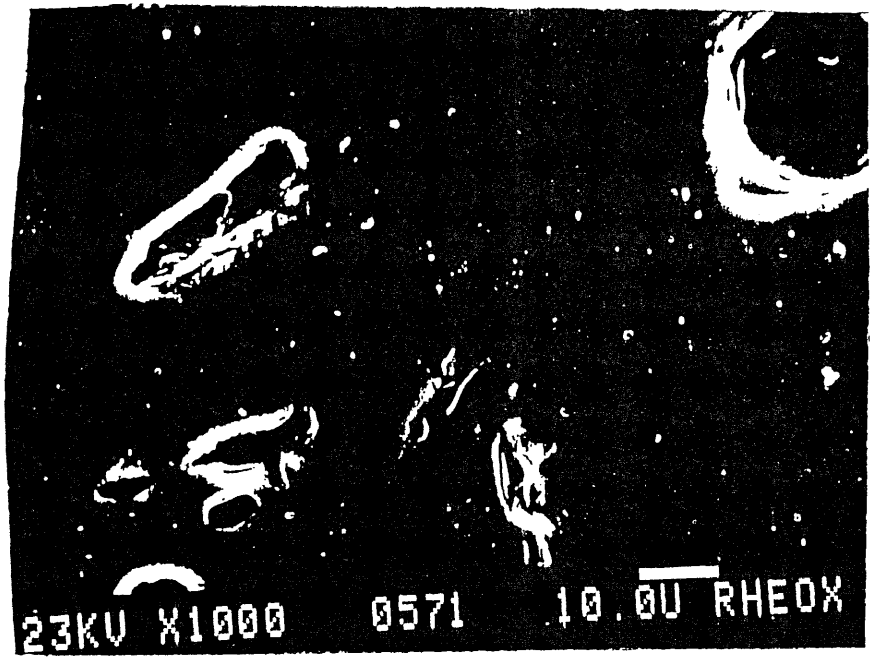

Figure 220

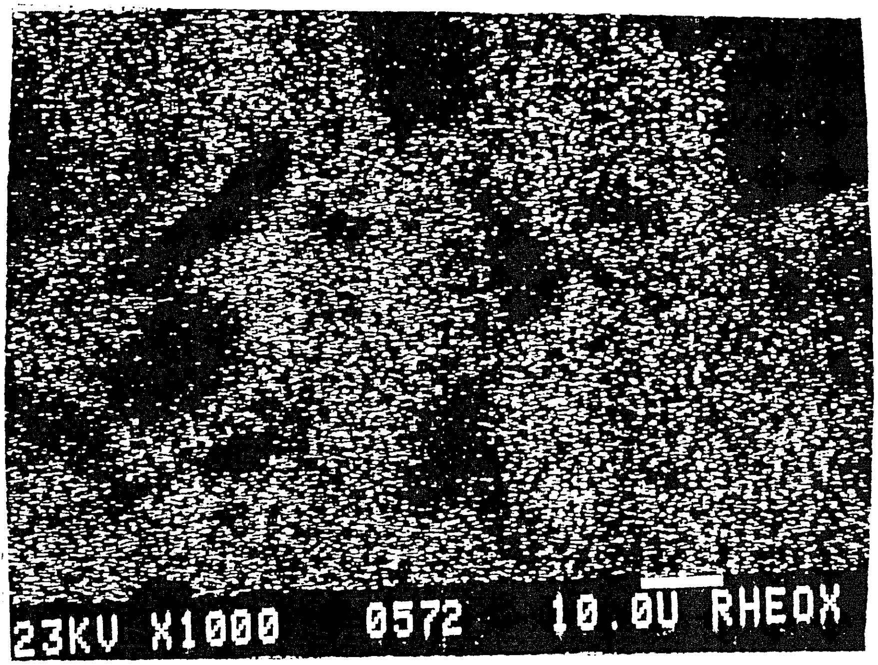

Figure 221 AL X-ray Image of Figure 220

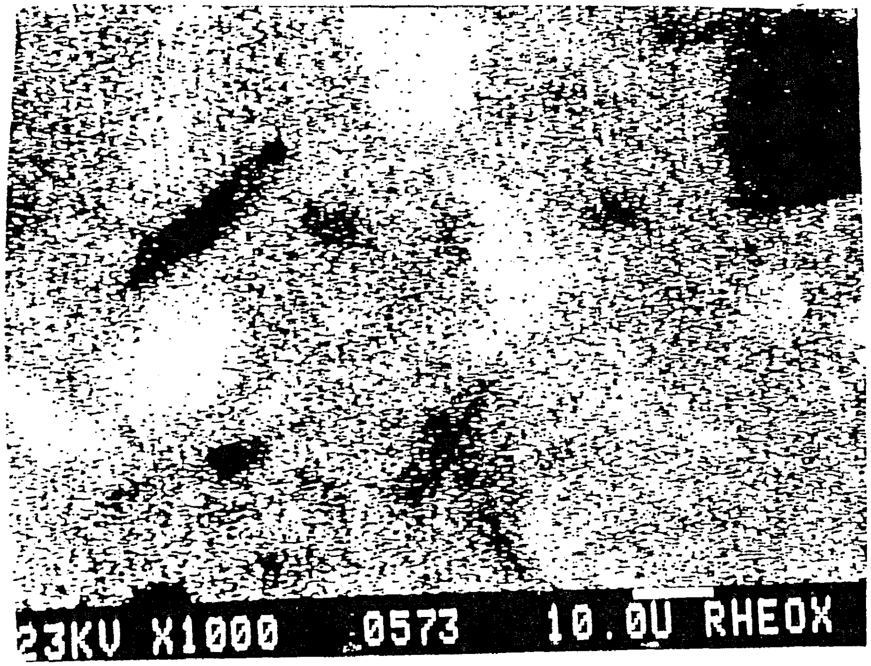

Figure 222 Si X-ray Image of Figure 220

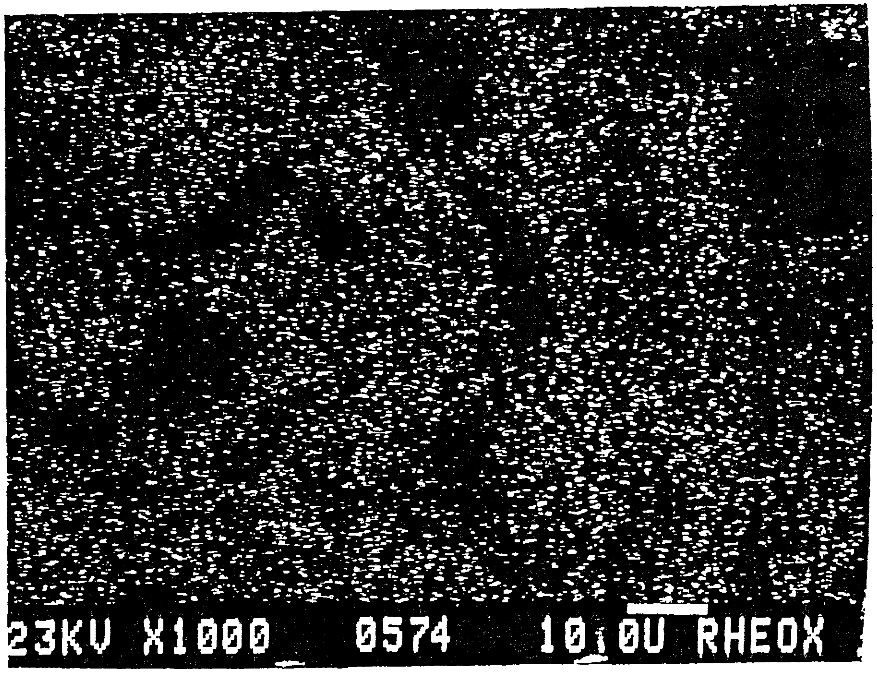

Figure 223 K X-ray Image of Figure 220

SEM IMAGES OF SAMPLE # Microwave 45 minutes Cross Section

Figure 224 Ti X-Ray Image of Figure 220

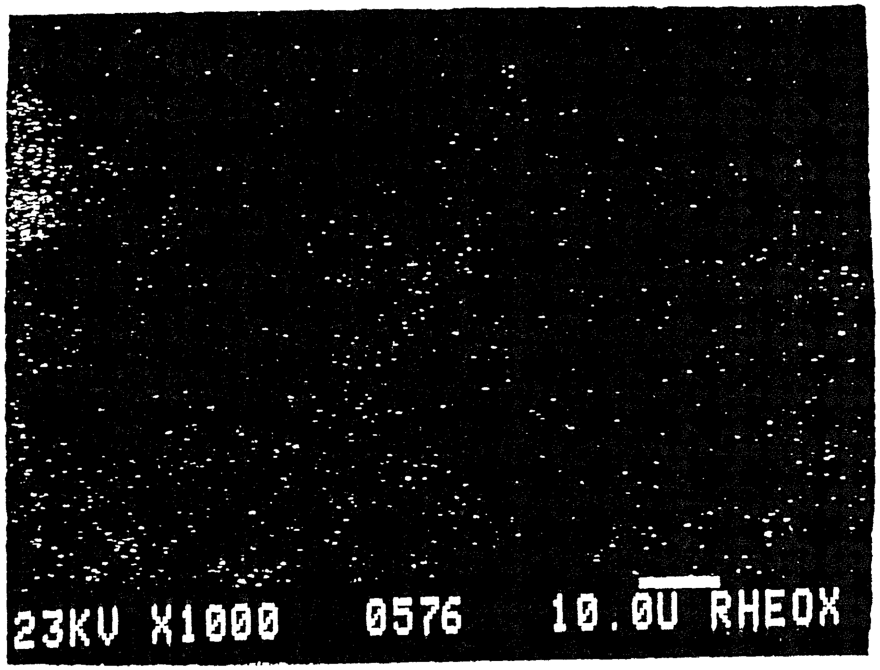

Figure 225 Cr X-Ray Image of Figure 220

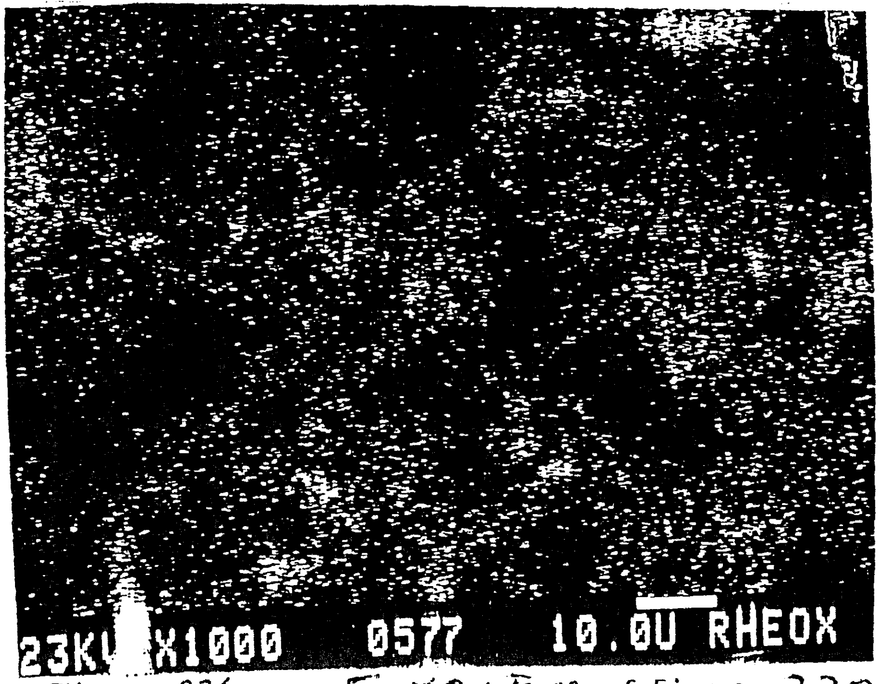

Figure 226 Fe X Ray Image of Figure 220

```
S45C1  ■                                                AVS/ON

                                          CA LL
 S45C1
          CUR:        0.0                 0CNTS
40000FS                                                 100■   T
```

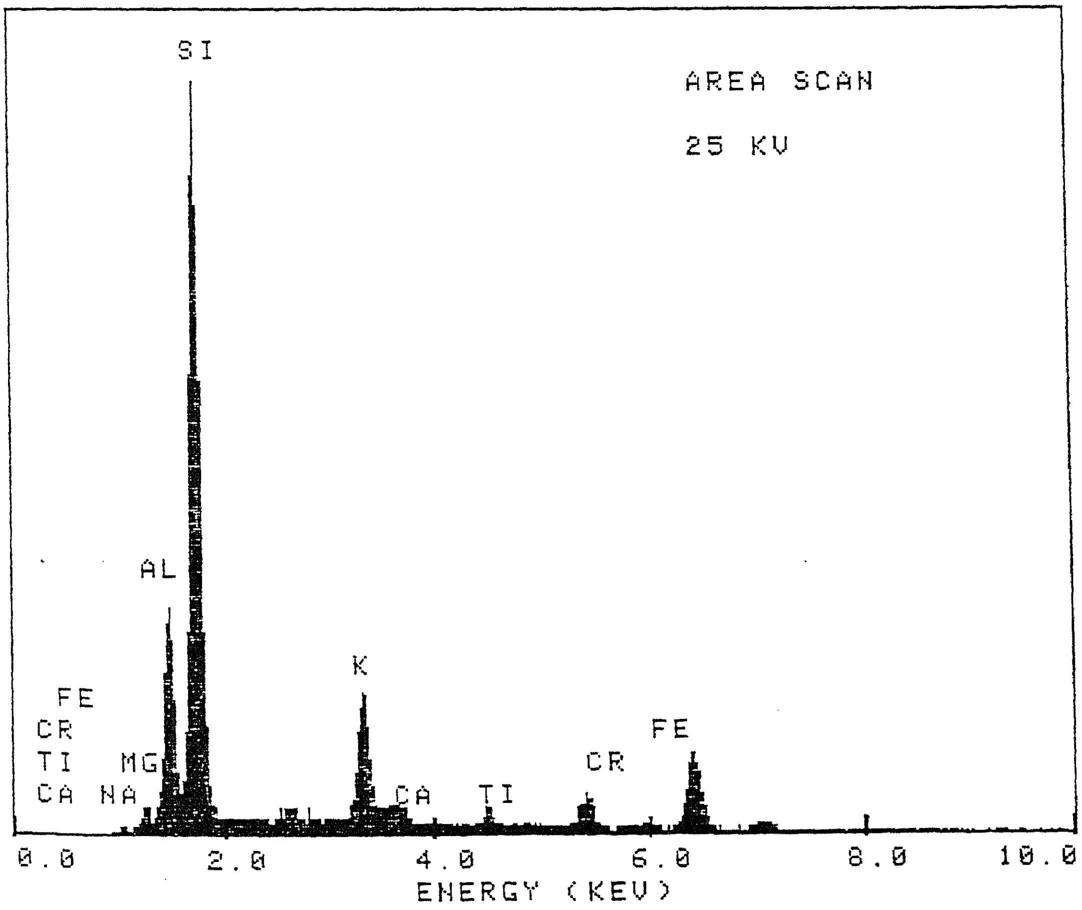

19-Nov-89 16:50

S45C2 ▪ AVS/ON

CA LL

S45C2

CUR: 0.0 0CNTS

40000FS 100▪ T

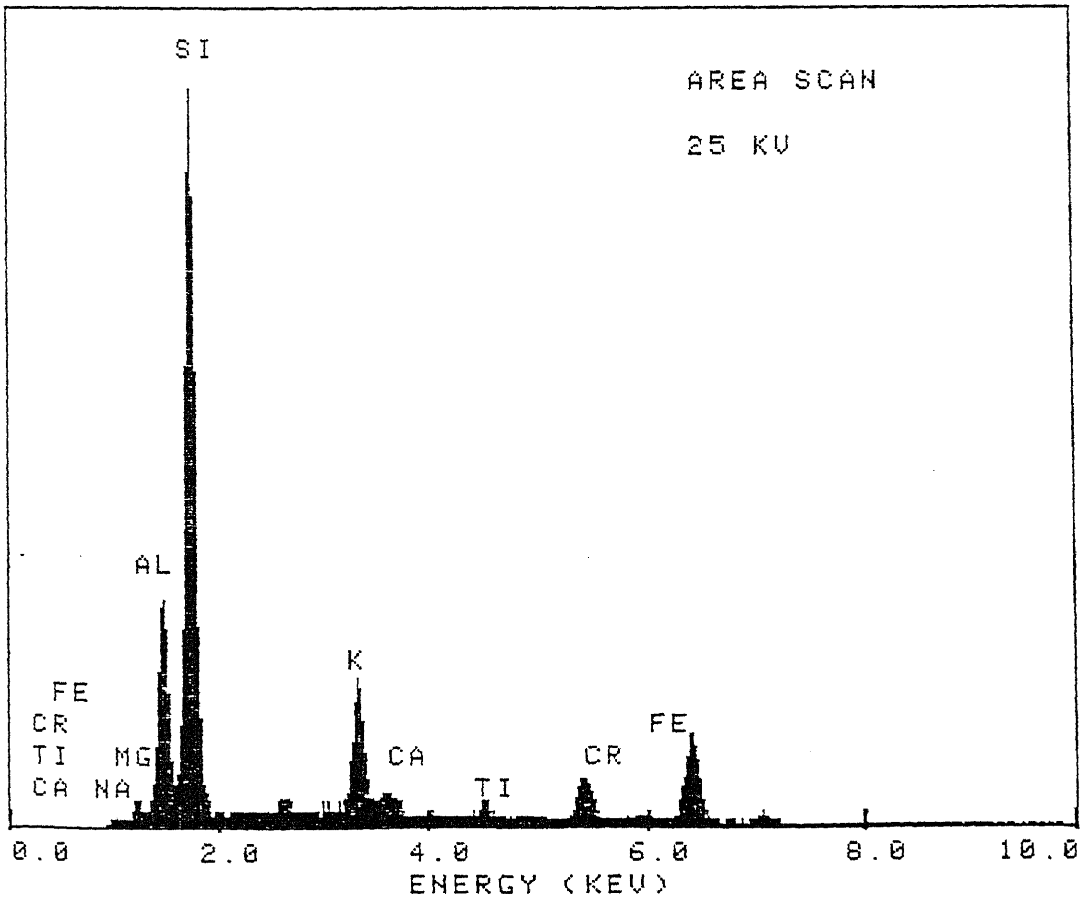

19-Nov-89 16:52

```
S45C3  ■                                                AVS/ON

                                          CA  LL
 S45C3
         CUR:         0.0                 0CNTS
40000FS                                                100■  T
```

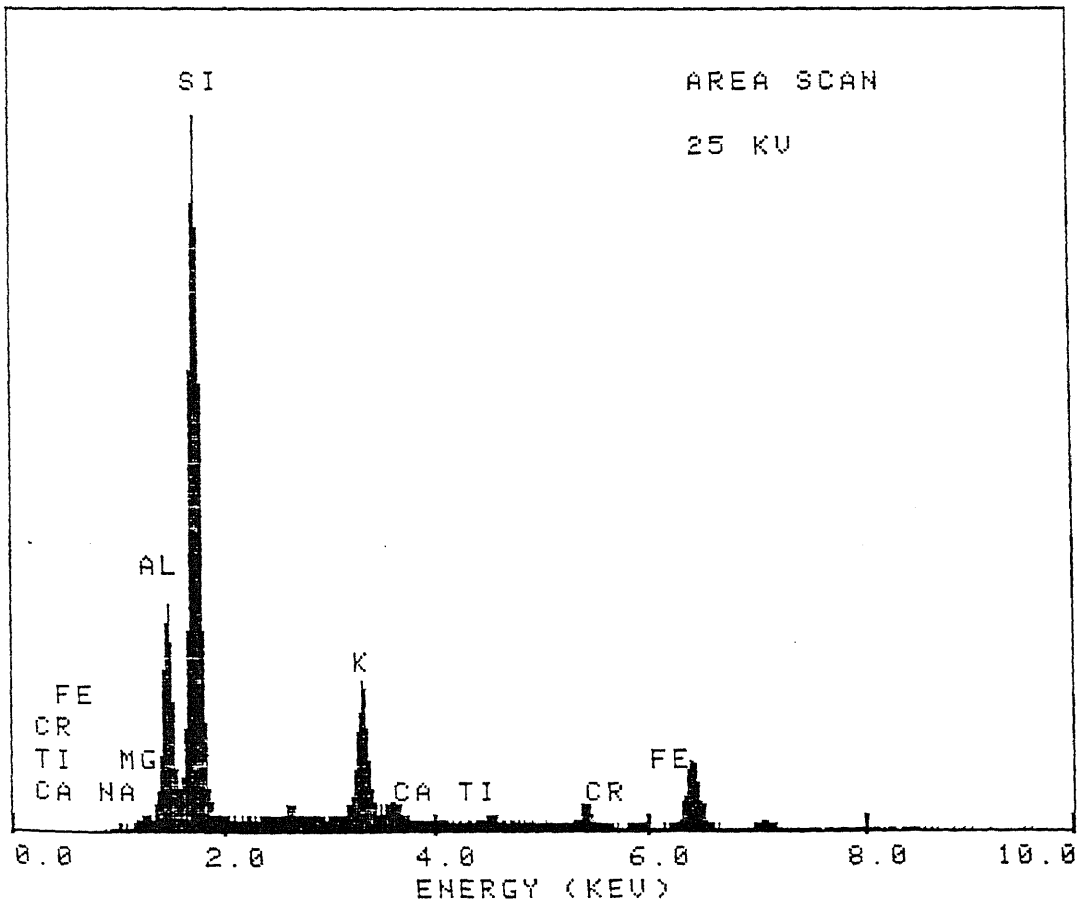

20-Nov-89 08:38

S45C4 ■ AVS/ON

CA LL

S45C4

CUR: 0.0 0CNTS

40000FS 100■ T

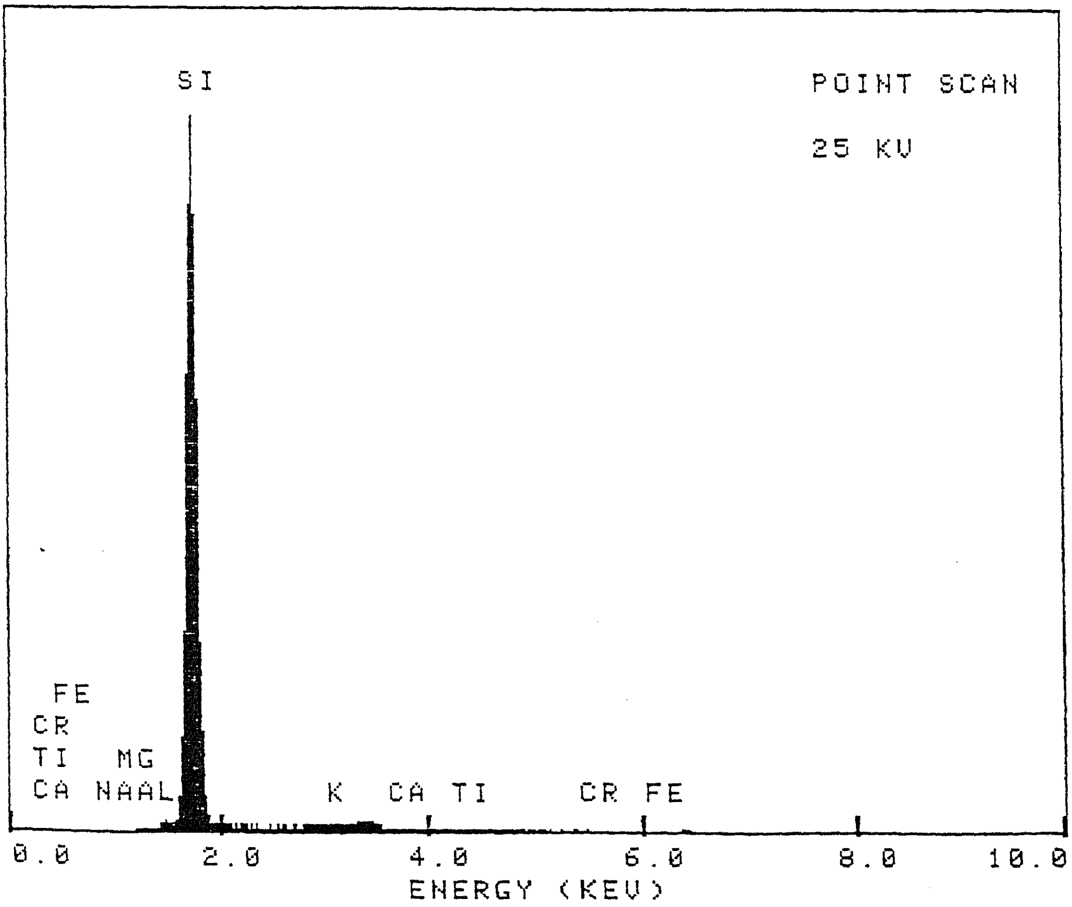

20-Nov-89 08:41

S45C5 ■ AVS/ON

CA LL

S45C5

CUR: 0.0 0CNTS

40000FS 100■ T

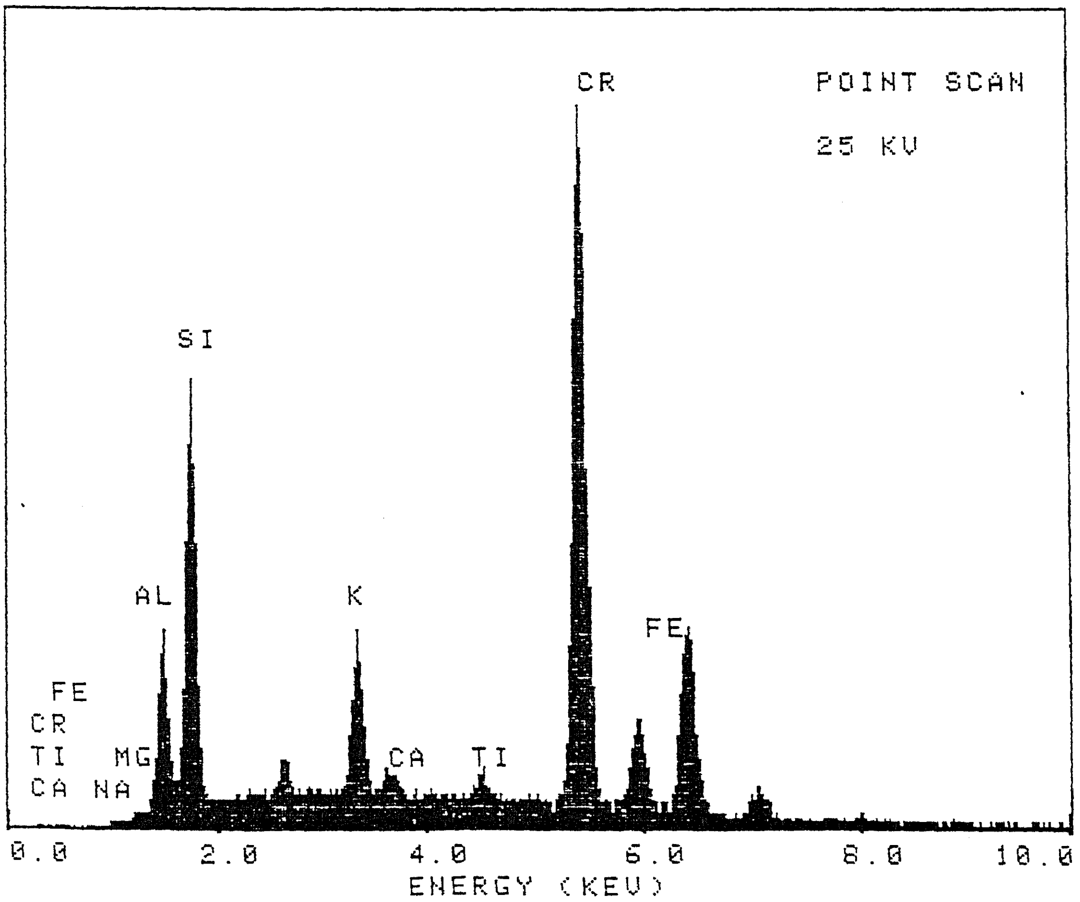

20-Nov-89 08:43

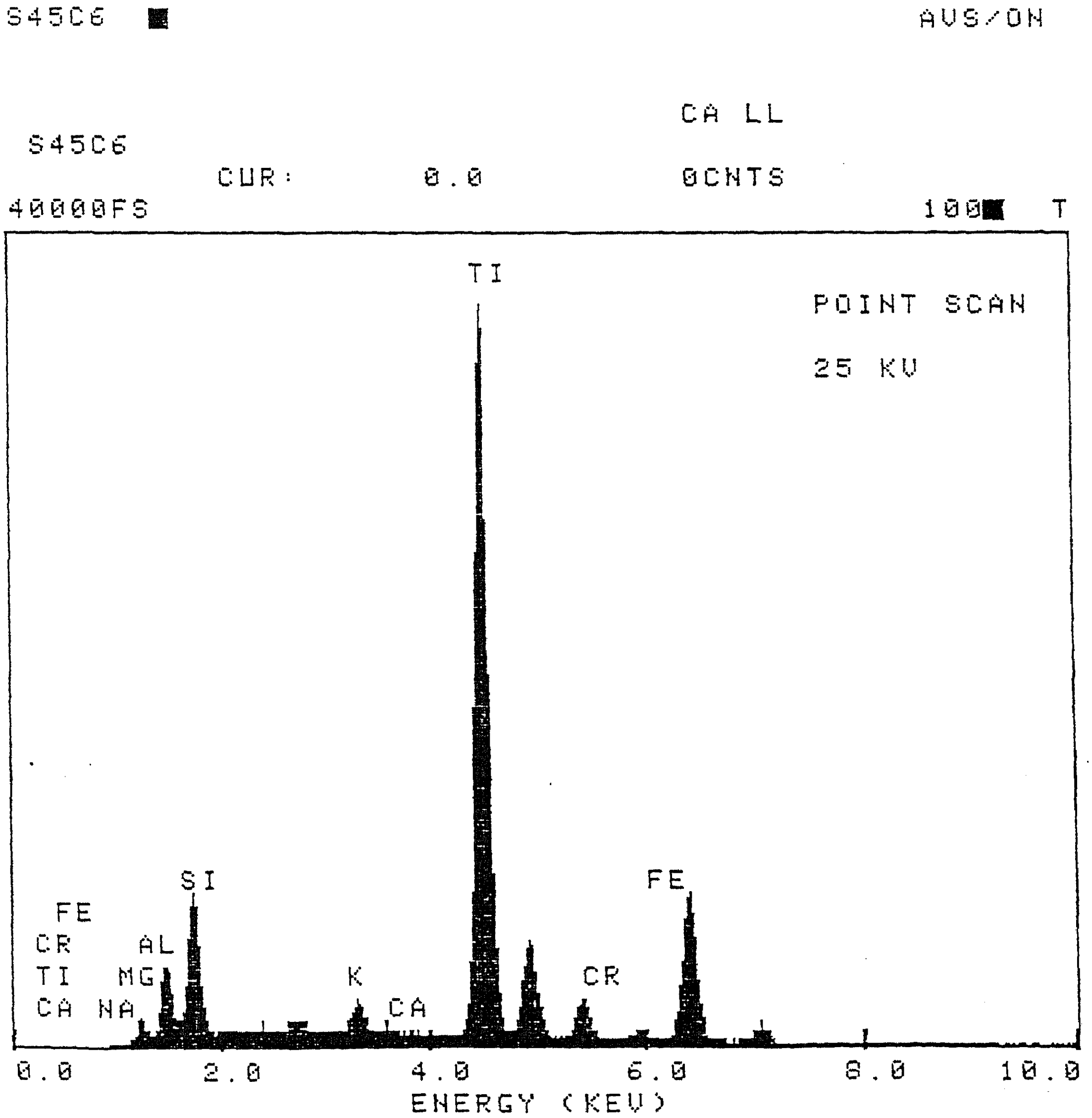

20-Nov-89 08:46

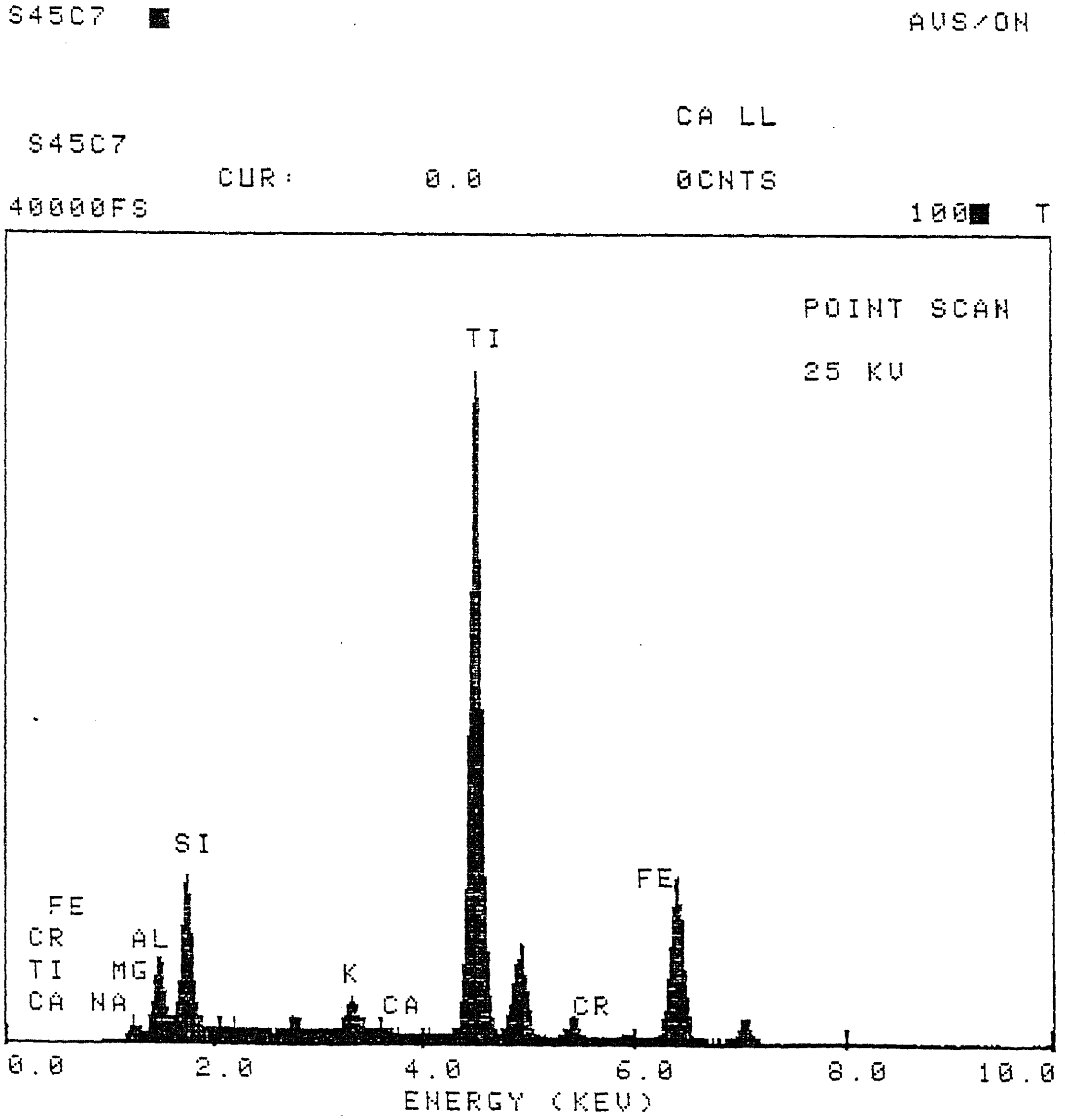

20-Nov-89 09:04

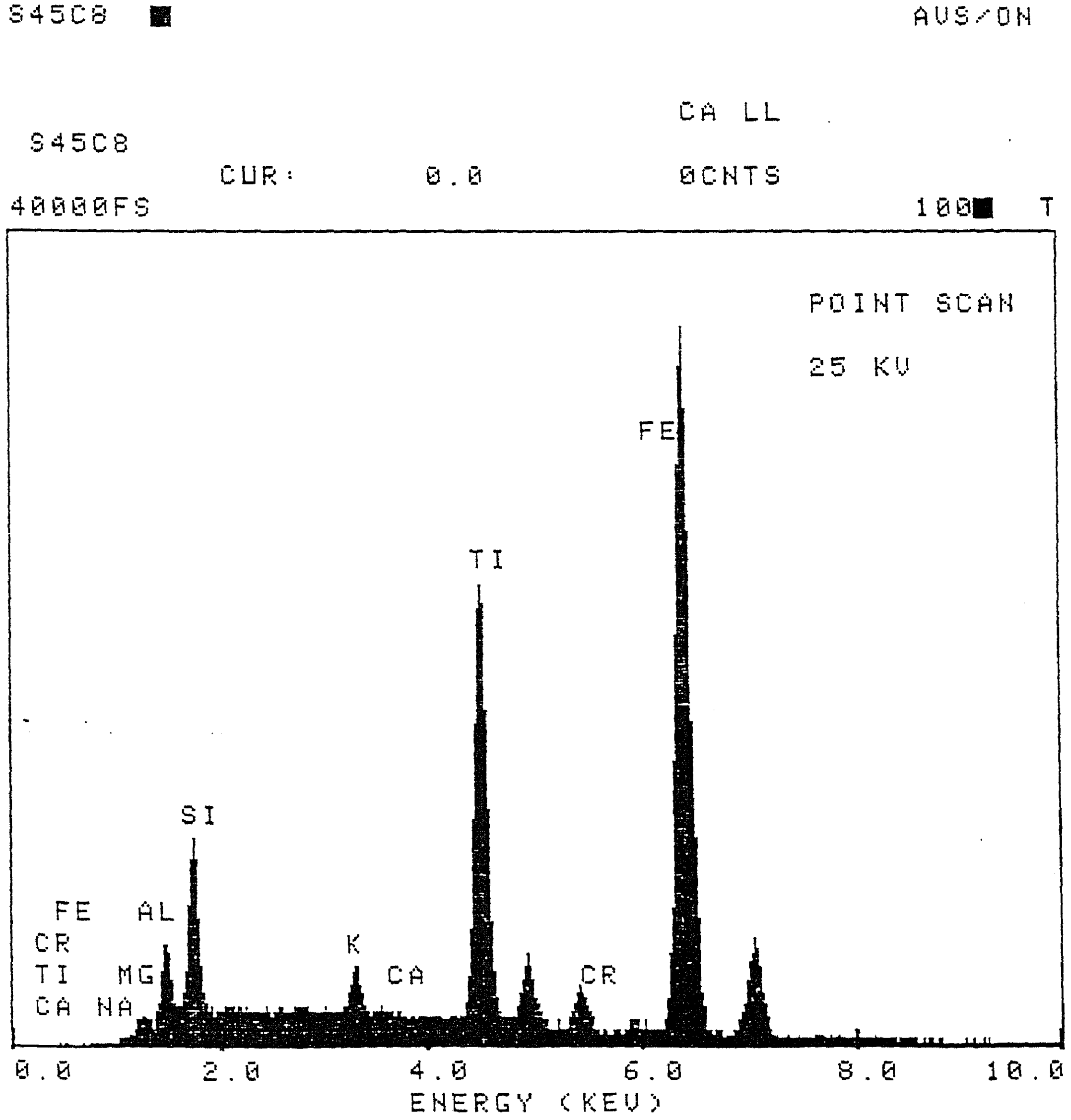

20-Nov-89 09:07

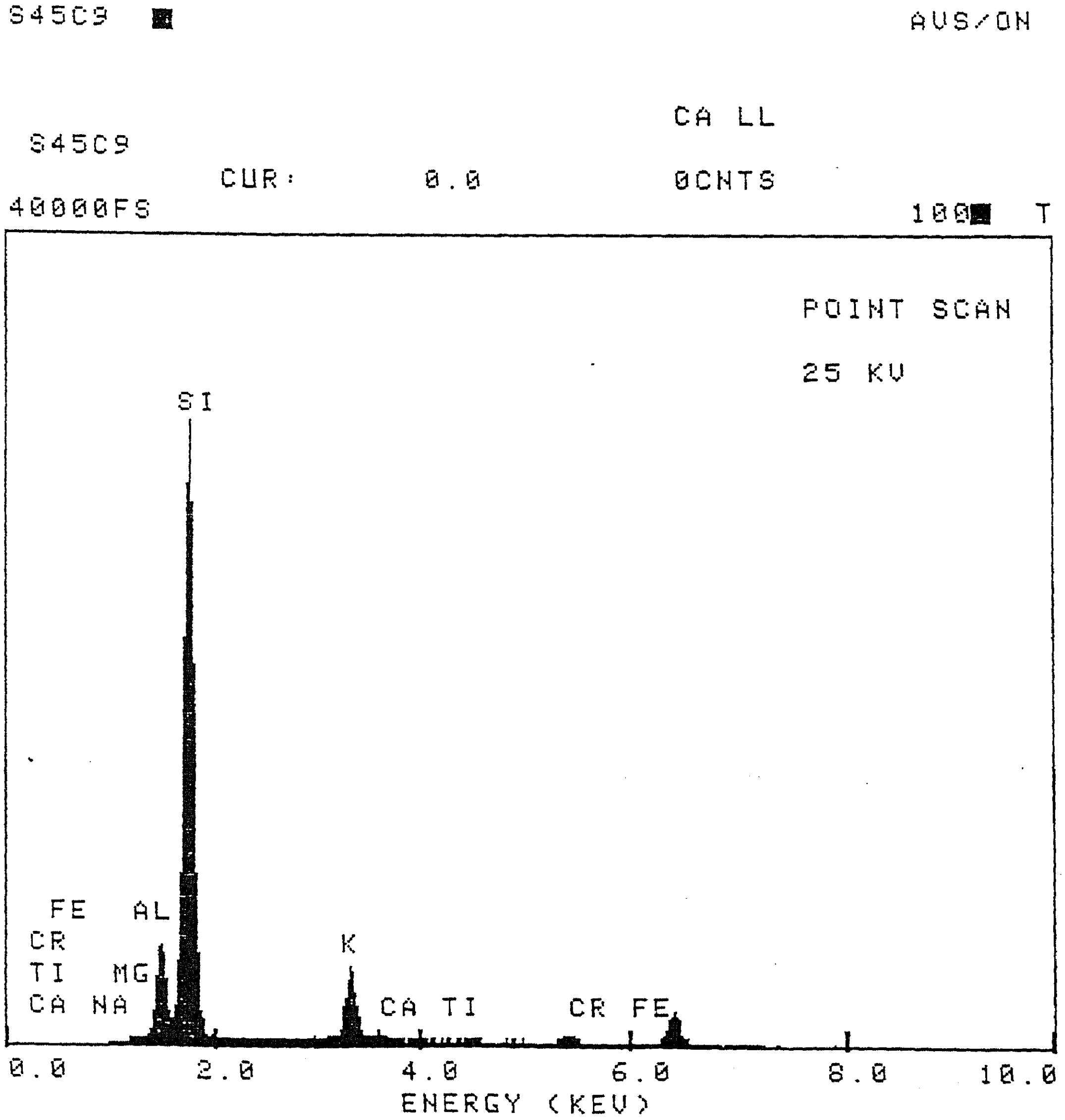

20-Nov-89 09:09

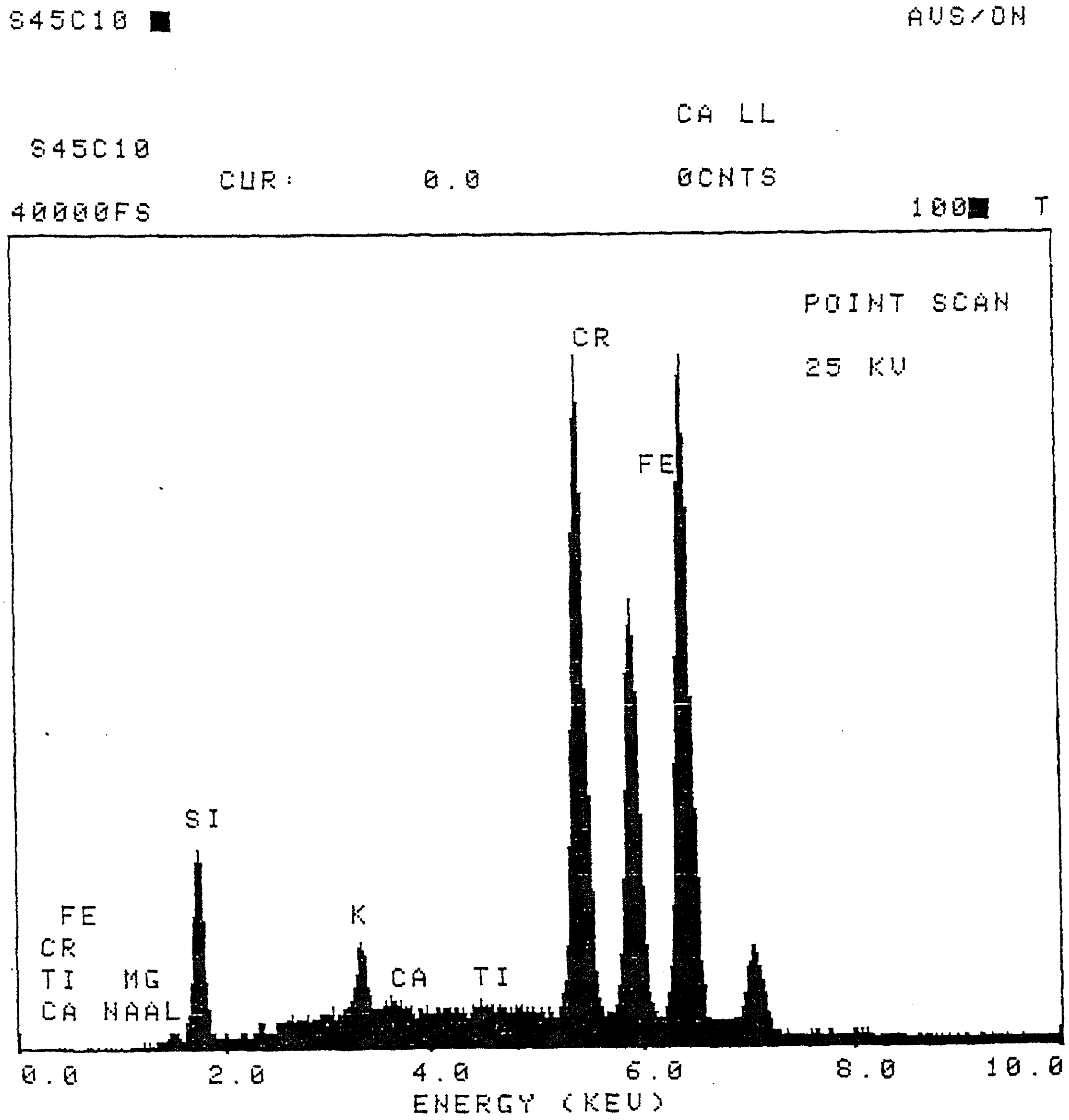

20-Nov-89 09:12

S45C11 ■ AVS/ON

CA LL

S45C11

CUR: 0.0 0CNTS

40000FS 100■ T

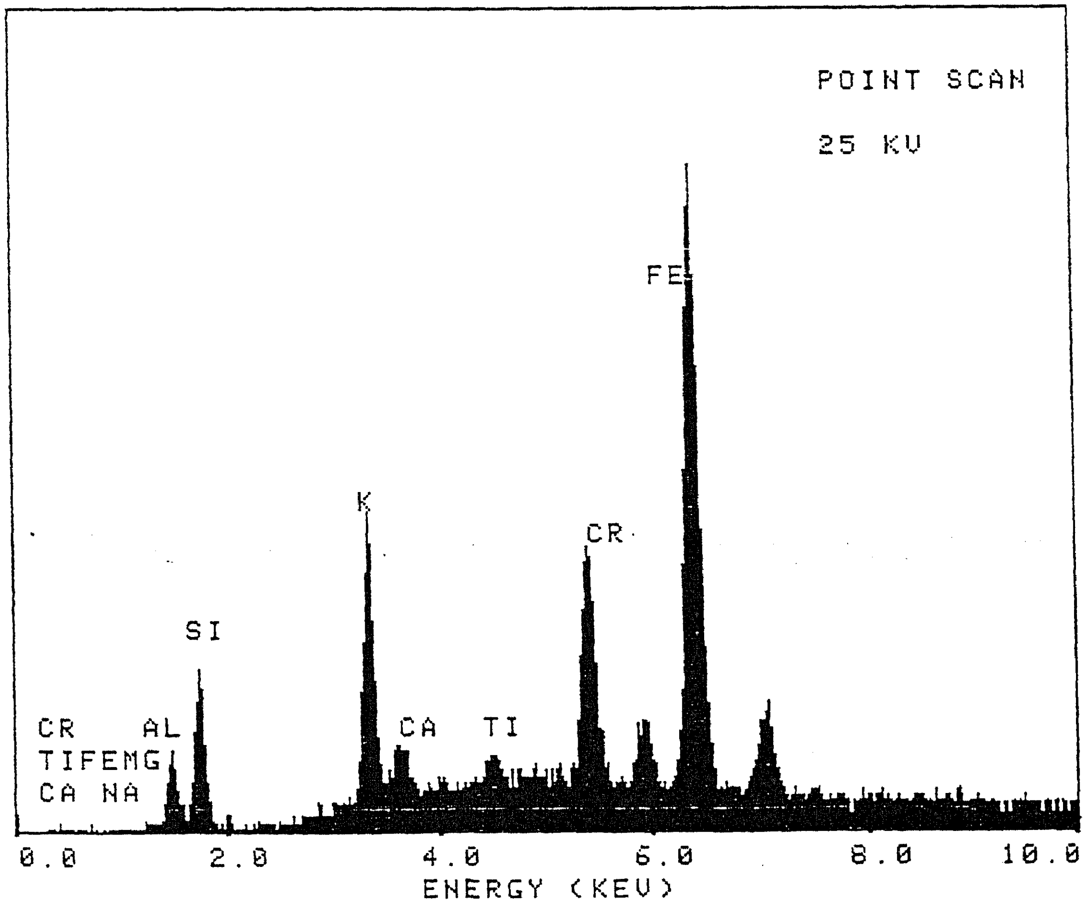

20-Nov-89 09:14

S45C12 ■ AVS/ON

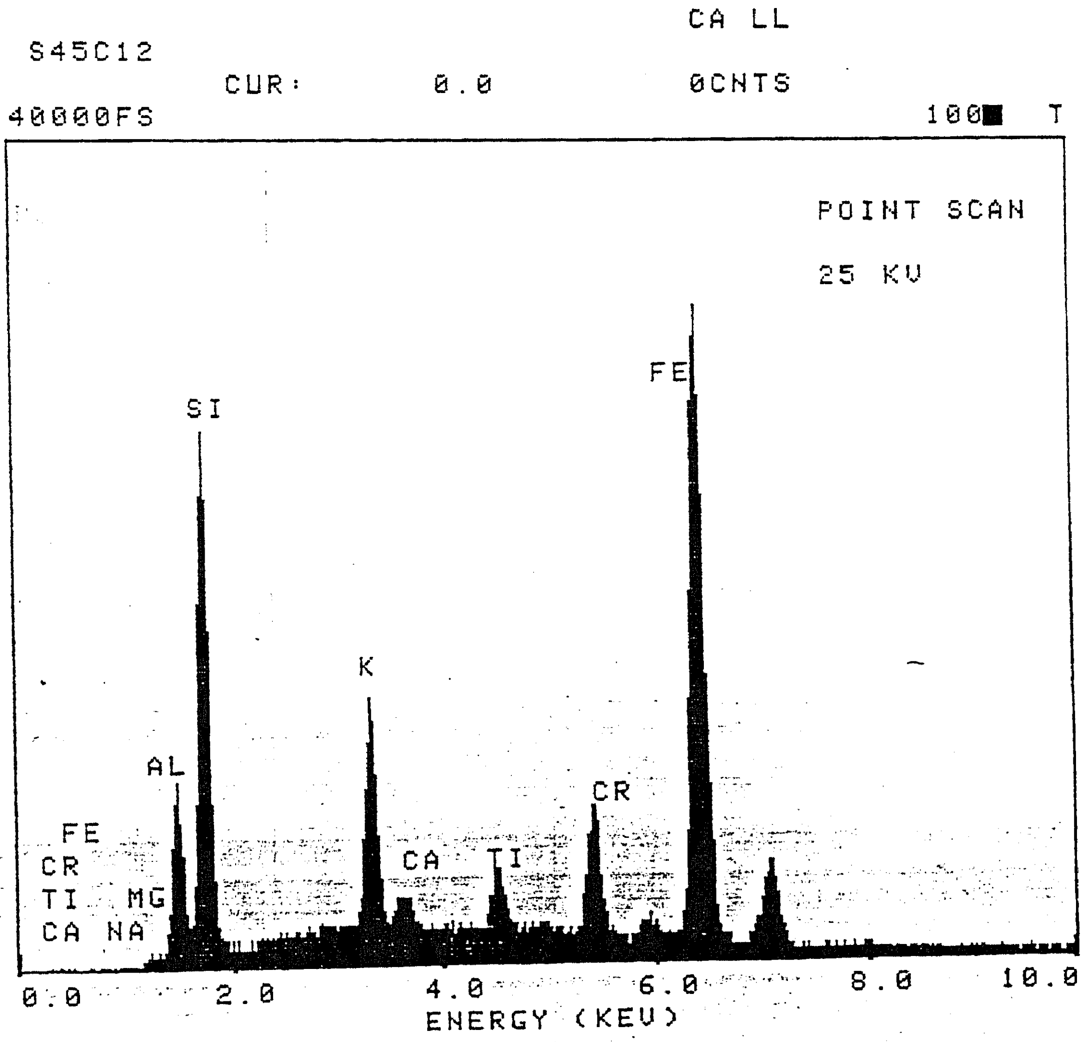

20-Nov-89 09:16

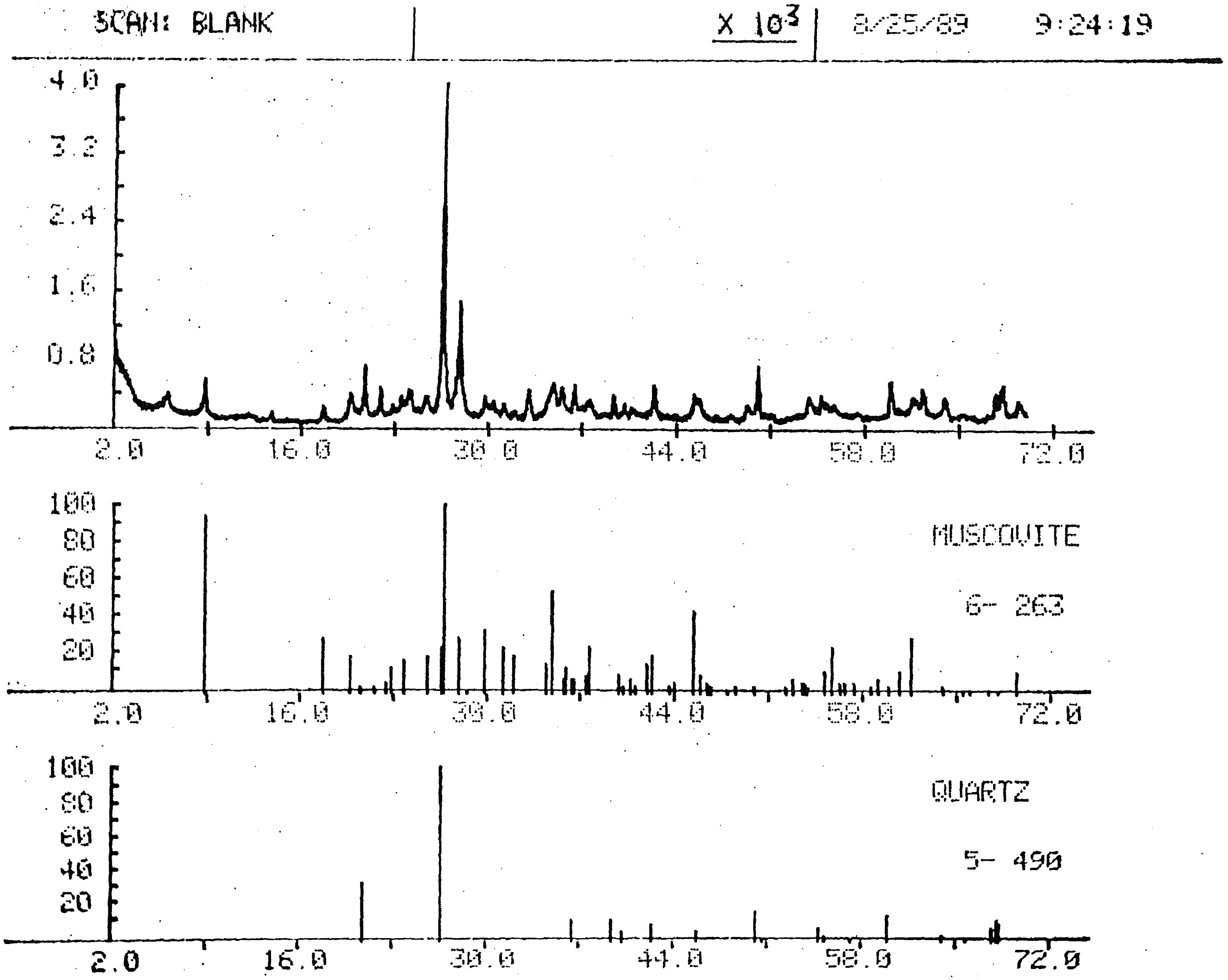
SCAN: BLANK
X 10^3
8/25/89
9:24:19
4.0
3.2
2.4
1.6
0.8
2.0
16.0
30.0
44.0
58.0
72.0
100
80
60
40
20
MUSCOVITE
6- 263
2.0
16.0
30.0
44.0
58.0
72.0
100
80
60
40
20
QUARTZ
5- 490
2.0
16.0
30.0
44.0
58.0
72.0

Figure 227

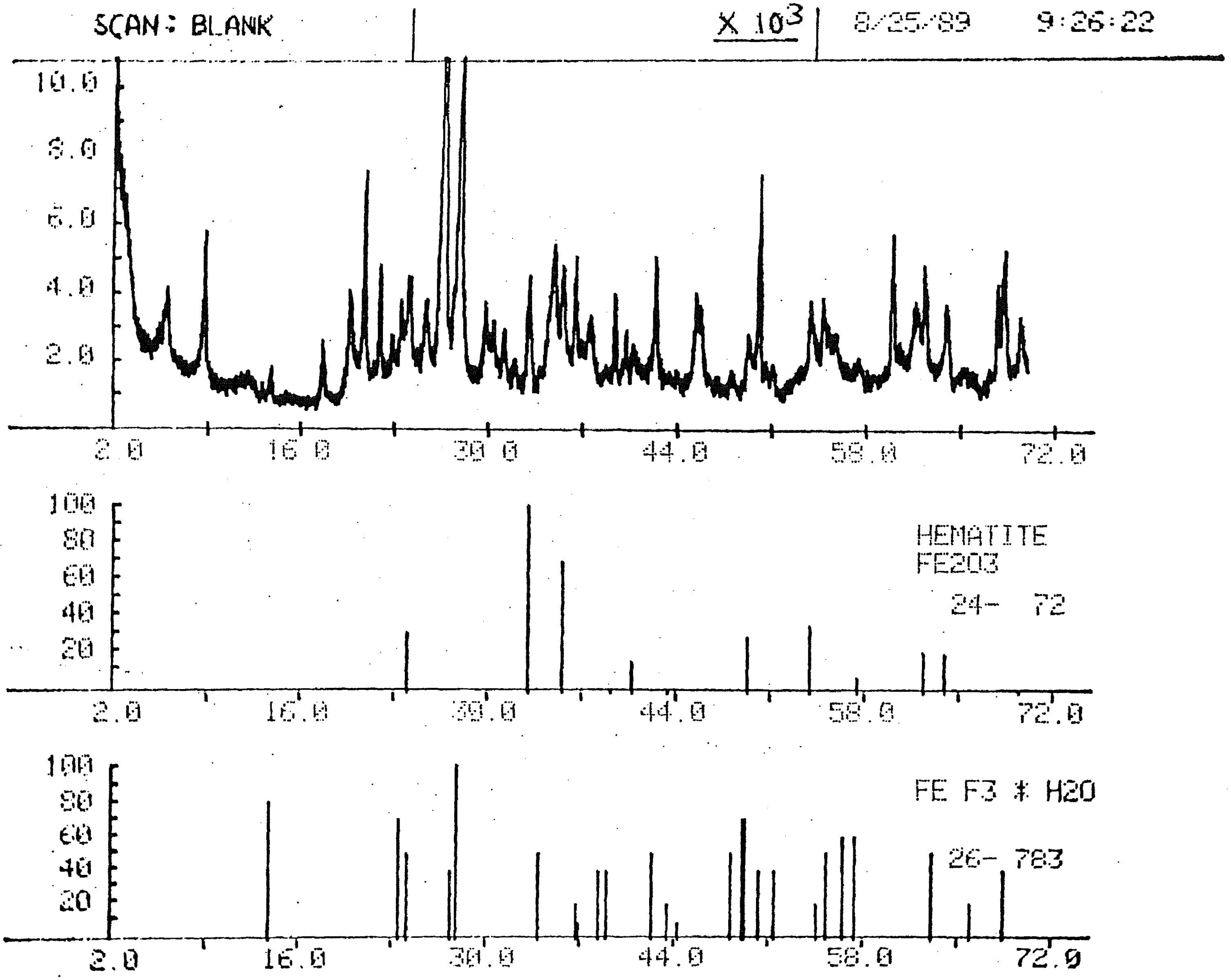
SCAN: BLANK
X 10³
8/25/89
9:26:22
10.0
8.0
6.0
4.0
2.0
2.0
16.0
30.0
44.0
58.0
72.0
100
80
60
40
20
HEMATITE
FE2O3
24- 72
2.0
16.0
30.0
44.0
58.0
72.0
100
80
60
40
20
FE F3 * H2O
26- 783
2.0
16.0
30.0
44.0
58.0
72.0

Figure 22B

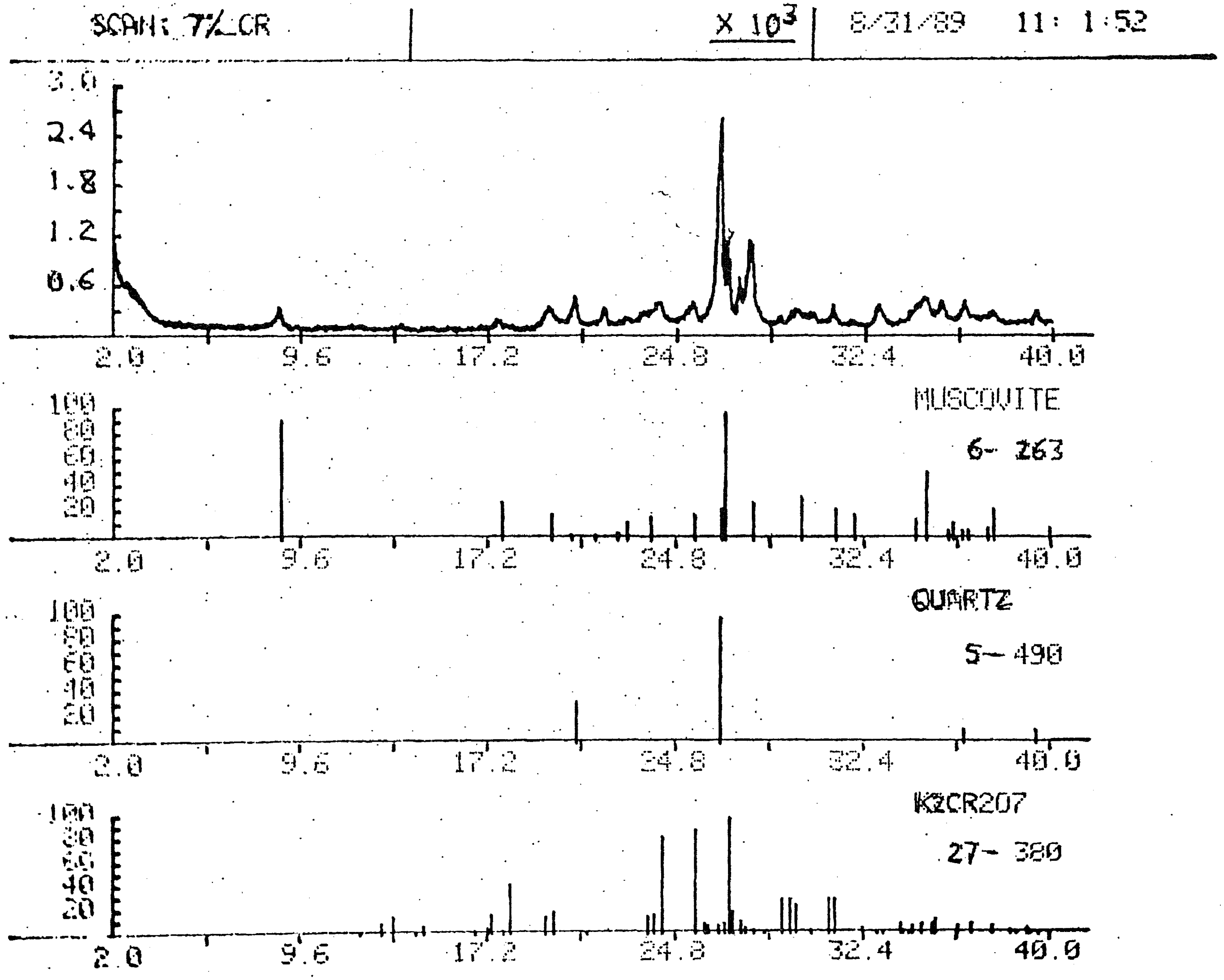
SCAN: 7% CR
X 10³
8/31/89 11: 1:52
3.0
2.4
1.8
1.2
0.6
2.0
9.6
17.2
24.8
32.4
40.0
MUSCOVITE
6- 263
100
80
60
40
20
QUARTZ
5- 490
K2CR207
27- 380

Figure 229

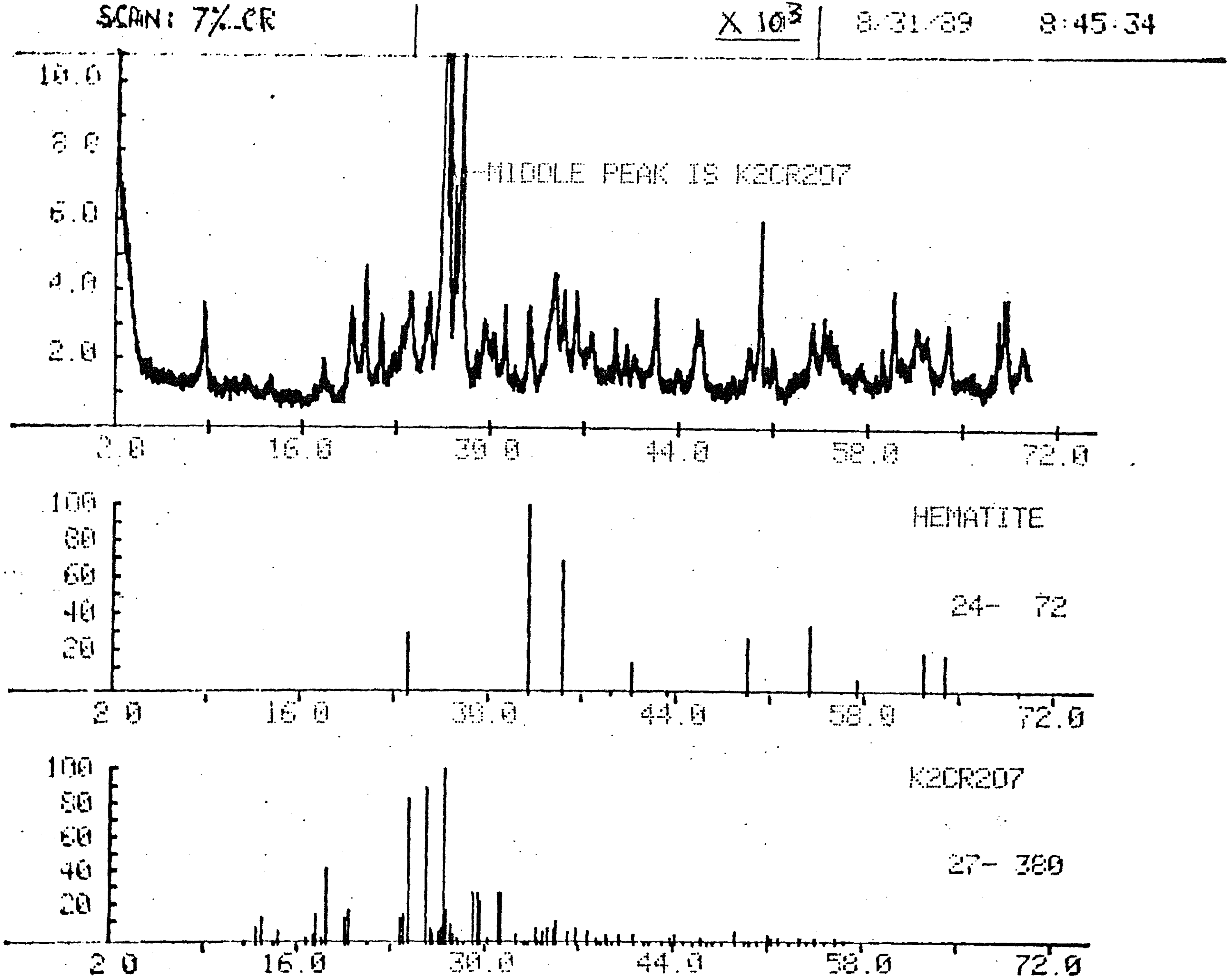
SCAN: 7%_CR
X 10³
8/31/89
8:45:34
MIDDLE PEAK IS K2CR2O7
10.0
8.0
6.0
4.0
2.0
2.0
16.0
30.0
44.0
58.0
72.0
HEMATITE
24- 72
100
80
60
40
20
2.0
16.0
30.0
44.0
58.0
72.0
K2CR2O7
27- 380
100
80
60
40
20
2.0
16.0
30.0
44.0
58.0
72.0

Figure 230

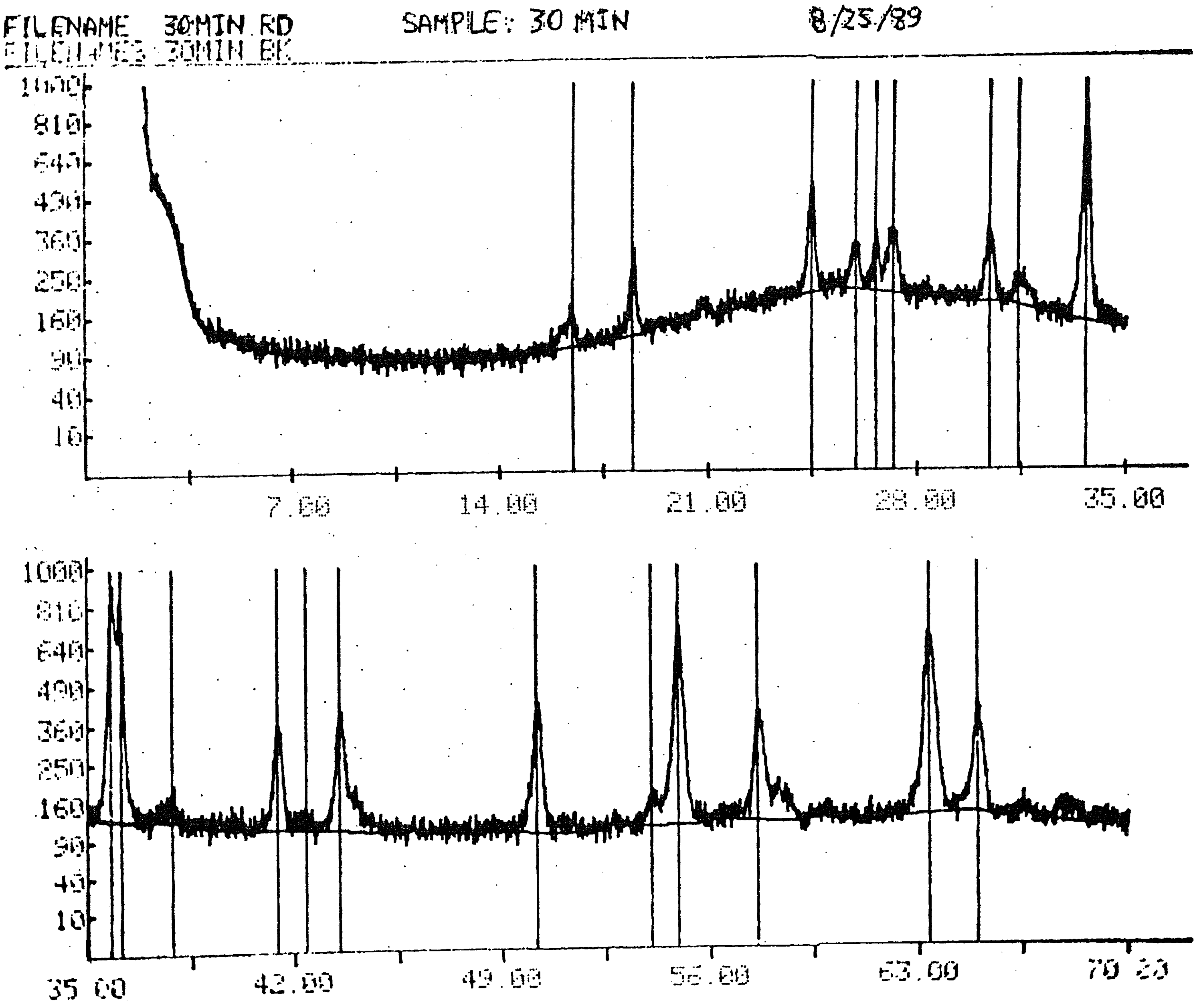

FILENAME 30MIN.RD
FILENAME2 30MIN.BK
SAMPLE: 30 MIN
8/25/89
1000
810
640
490
360
250
160
90
40
10
7.00
14.00
21.00
28.00
35.00
35.00
42.00
49.00
56.00
63.00
70.20

Figure 231

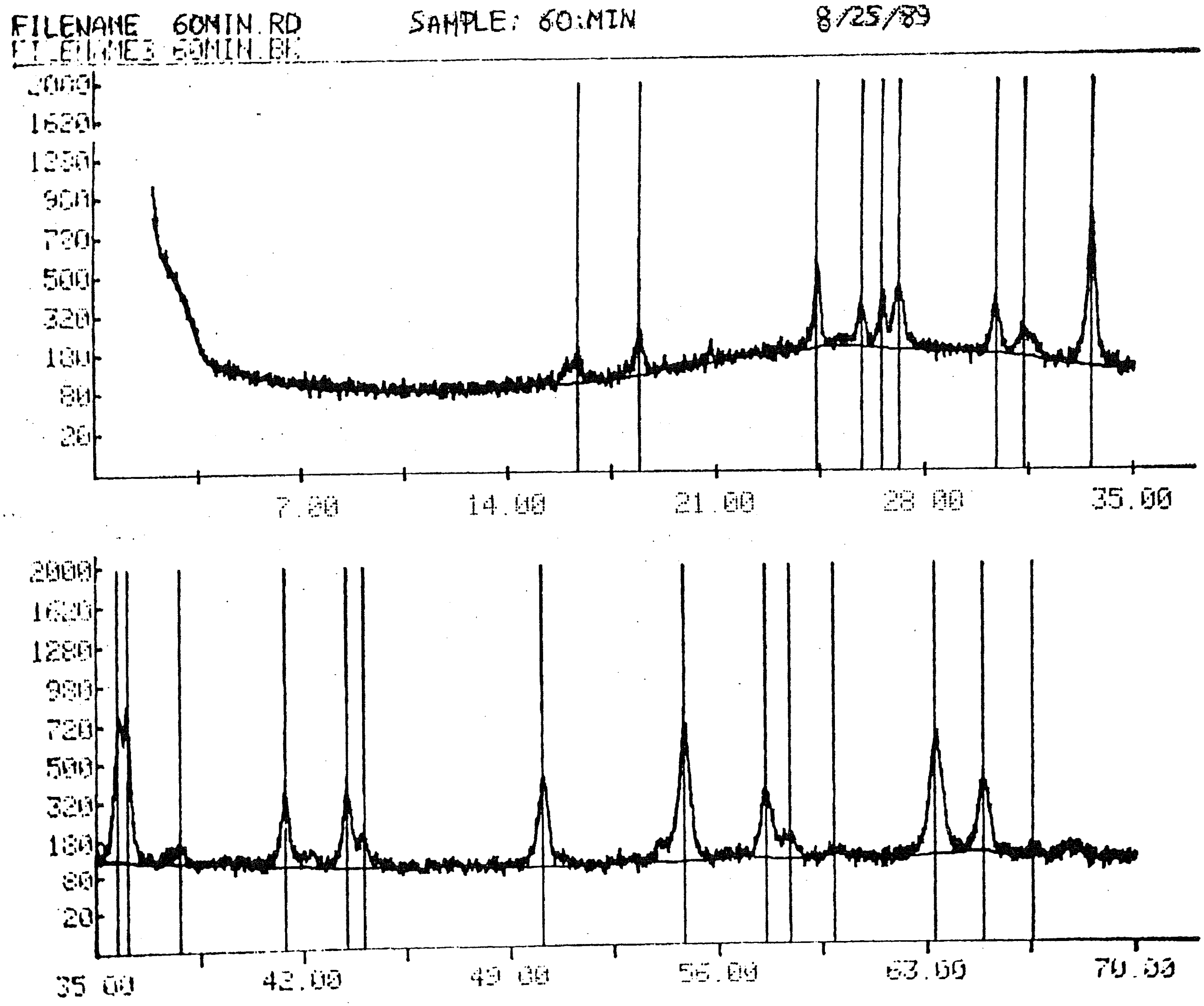
FILENAME 60MIN.RD
FILENAME3 60MIN.BK
SAMPLE: 60:MIN
8/25/89
2000
1620
1280
980
720
500
320
180
80
20
7.00
14.00
21.00
28.00
35.00
2000
1620
1280
980
720
500
320
180
80
20
35.00
42.00
49.00
56.00
63.00
70.00

Figure 232

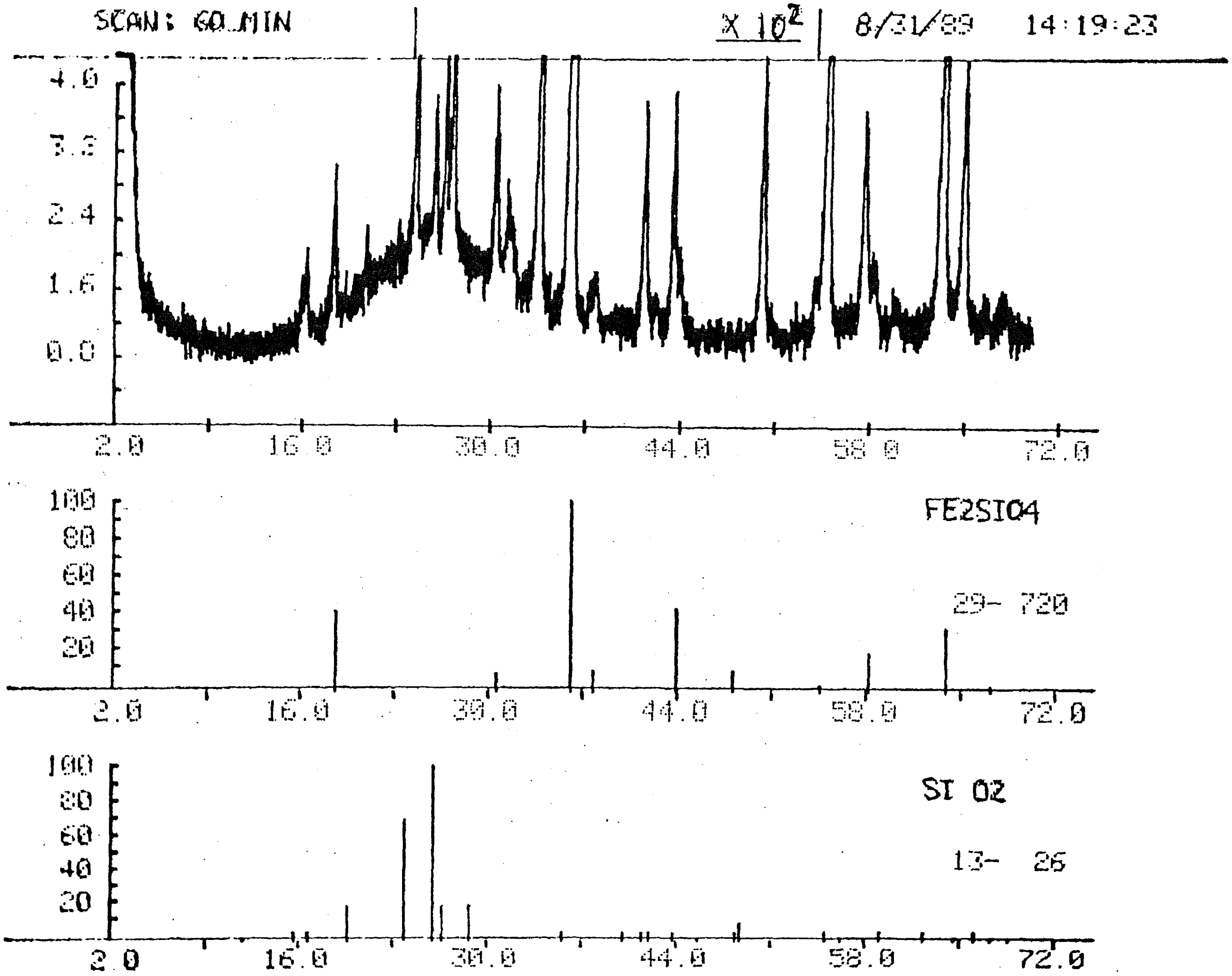
SCAN: 60.MIN
X 10^2
8/31/89 14:19:23
4.0
3.2
2.4
1.6
0.0
2.0
16.0
30.0
44.0
58.0
72.0
100
80
60
40
20
FE2SIO4
29- 720
2.0
16.0
30.0
44.0
58.0
72.0
100
80
60
40
20
SI O2
13- 26
2.0
16.0
30.0
44.0
58.0
72.0

Figure 233

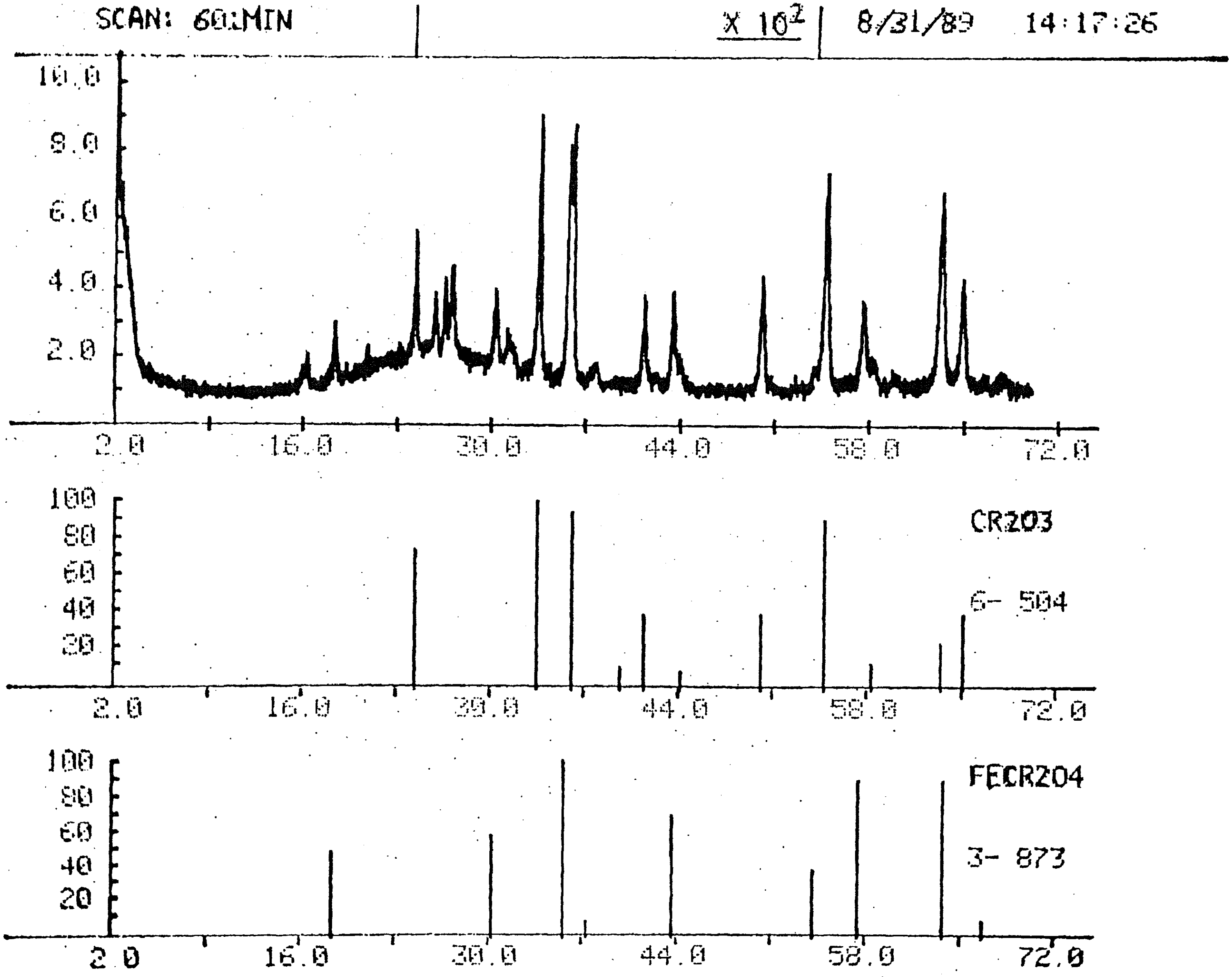
SCAN: 60:MIN
X 10^2
8/31/89
14:17:26
10.0
8.0
6.0
4.0
2.0
2.0
16.0
30.0
44.0
58.0
72.0
100
80
60
40
20
CR2O3
6- 504
2.0
16.0
30.0
44.0
58.0
72.0
100
80
60
40
20
FECR2O4
3- 873
2.0
16.0
30.0
44.0
58.0
72.0

Figure 234

```
29-720 Fe2SiO4                                               RHOMBIC      C
        2.484 (100)     2.058 ( 44)     4.754 ( 42)     LATTICE:  0
20 LINES IN PATTERN         PATTERN ACCESSED    9  TIMES        SPN:  65254
           4.754   42        1.889   11        1.255    6        0.950    3
           2.911   10        1.680    3        1.241    4        0.920    3
           2.484  100        1.584   21        1.188    4        0.863    2
           2.377   11        1.455   34        1.072    8        0.840    5
           2.058   44        1.391    3        1.029    3        0.796    2
```

```
24- 72   Fe2 O3                                                MIN-INORG     C
      2.703 (100)     2.519 ( 70)     1.697 ( 36)    LATTICE:  0
27 LINES IN PATTERN        PATTERN ACCESSED   13  TIMES       SPN:  14237
             3.687   32      1.697   36       1.260    4       0.961    3
             2.703  100      1.601    8       1.229    2       0.960    3
             2.519   70      1.487   22       1.191    3       0.952    2
             2.295    2      1.454   21       1.165    3       0.909    2
             2.208   17      1.351    2       1.142    4       0.879    2
             2.080    2      1.313    7       1.104    4       0.845    2
             1.843   30      1.308    4       1.057    4
```

```
 3- 873   Fe Cr2 O4                                          MIN-INORG      I
        2.519 (100)    1.600 ( 90)    1.460 ( 90)    LATTICE:  0
22 LINES IN PATTERN       PATTERN ACCESSED   11  TIMES      SPN:  14516
          4.819   50      1.600   90      1.160   20      0.931   30
          2.950   60      1.460   90      1.110   30      0.873   30
          2.519  100      1.400   10      1.100   60      0.850   60
          2.400   10      1.310   20      1.040   30      0.815   10
          2.069   70      1.260   50      0.979   20      0.805   40
          1.690   40      1.200   30      0.960   40
```

```
6- 504   .Cr2 O3                                       MIN-INORG     +
       2.666 (100)     2.480 ( 94)     1.672 ( 90)    LATTICE:  O
28 LINES IN PATTERN      PATTERN ACCESSED  20  TIMES       SPN:   7252
           3.633   74       1.672   90       1.173   14       0.896   14
           2.666  100       1.579   14       1.149   10       0.888    8
           2.480   94       1.465   25       1.124   10       0.866   25
           2.265   12       1.431   40       1.087   18       0.842    8
           2.176   40       1.296   20       1.042   16       0.833   12
           2.047   10       1.240   18       0.946   14       0.826   10
           1.815   40       1.210    8       0.937   12       0.798   16
```

```
3- 26    Si O2                                                INORGANIC
      3.419 (100)     3.719 ( 70)      4.499 ( 20)     LATTICE:  0
27 LINES IN PATTERN        PATTERN ACCESSED    4 TIMES        SPN: 36617
            7.460    2 S     3.109   20        1.879    5       1.441    2
            5.640    5       2.516    5        1.864   10       1.412    5
            5.278    5       2.246    5        1.667    5       1.389    2
            4.499   20       2.174    5        1.636    2       1.366    2
            3.719   70       2.148    5        1.589    2       1.321    2
            3.419  100       2.067    5        1.562    5       1.246    2
            3.331   20       1.987    2        1.489    5
```

```
5- 490    Si O2                                            MIN-INORG
      3.343 (100)      4.260 ( 34)      1.817 ( 17)     LATTICE:  0
40 LINES IN PATTERN          PATTERN ACCESSED   38  TIMES        SPN:   6600
          4.260   34       1.659    3       1.228    2        1.048    2
          3.343  100       1.608    1 S     1.200    5        1.044    2
          2.458   12       1.541   15       1.197    2        1.035    2
          2.282   12       1.453    3       1.184    4        1.015    2
          2.237    6       1.418    1 S     1.180    4        0.990    2
          2.128    9       1.382    7       1.153    2        0.987    2
          1.980    6       1.375   11       1.141    1 S      0.978    1 S
          1.817   17       1.372    9       1.114    1 S      0.976    1
          1.801    1 S     1.288    3       1.082    4        0.961    2
          1.672    7       1.256    4       1.064    1        0.928    1 S
```

```
- 263   K Al2 ( Si3 Al ) O10 ( O H, F )2                          MIN-INORG      +
      3.319 (100)      9.949 ( 94)      2.566 ( 54)      LATTICE:  0
¯8 LINES IN PATTERN          PATTERN ACCESSED  14  TIMES       SPN:  6603
           9.949   94         2.464    8       1.731    8      1.335   10
           4.969   30         2.450    8       1.710    6      1.321    4
           4.470   20         2.399   10       1.705    6      1.299    8
           4.301    4         2.383   25       1.699    4      1.292    6
           4.110    4         2.255   10       1.662   12      1.274    6
           3.949    6         2.236    4       1.646   25      1.267    4
           3.881   14         2.208    8       1.631    6      1.253    6
           3.730   18         2.190    4       1.620    6      1.246    8
           3.481   20         2.150   16       1.603    6      1.227    4
           3.340   25         2.132   20       1.573    4      1.221    6
           3.319  100         2.069    4       1.559    8      1.208    4
           3.189   30         2.053    6       1.541    4      1.200    4
           3.120    2         1.992   44       1.524   12      1.190    4
           2.986   34         1.972   10       1.504   30      1.183    4
           2.858   25         1.951    6       1.453    4      1.158    2
           2.789   20         1.941    4       1.424    2      1.130    2
           2.596   16         1.894    2       1.414    2      1.122    4
           2.566   54         1.872    4       1.388    2      1.117    4
           2.505    8         1.822    4       1.375    2
           2.492   14         1.746    4       1.352   12
```

```
19- 720   Fe2 Si O4                                          INORGANIC      C
        2.484 (100)     2.058 ( 44)     4.754 ( 42)     LATTICE:  0
20 LINES IN PATTERN        PATTERN ACCESSED    9  TIMES      SPN:  65254
          4.754   42       1.889   11        1.255    6        0.950    3
          2.911   10       1.680    3        1.241    4        0.920    3
          2.484  100       1.584   21        1.188    4        0.863    2
          2.377   11       1.455   34        1.072    8        0.840    5
          2.058   44       1.391    3        1.029    3        0.796    2
```

```
-5- 783    Fe F3 + H2 O                                        INORGANIC       I
       3.201 (100)      6.388 ( 80)      3.769 ( 70)      LATTICE:  0
26 LINES IN PATTERN          PATTERN ACCESSED    1  TIMES        SPN:    4333
           6.388    80        2.428    10        1.854    70        1.602    60
           3.769    70        2.340    40        1.846    70        1.472    50
           3.681    50        2.302    40        1.811    40        1.414    20
           3.250    40        2.132    50        1.774    40        1.369    40
           3.201   100        2.077    20        1.680    20        1.321    50
           2.639    50        2.043    10        1.659    50
           2.441    20        1.886    50        1.626    60
```

```
7- 380    K2 Cr2 O7                                                   MIN-INORG     ◆
      3.298 (100)     3.471 ( 90)     3.657 ( 84)    LATTICE:  0
 LINES IN PATTERN          PATTERN ACCESSED    6  TIMES        SPN:   6612
            7.311    2        3.350    8       2.604    8       1.990    2
            6.824   10        3.319   10       2.576   10       1.966    4
            6.600   16        3.298  100       2.544   10       1.948    2
            6.182    2        3.282   20       2.536   14       1.930    2
            6.038    8        3.241   12       2.474    8       1.905    2
            5.292    4        3.218    6       2.438   10       1.869    8
            5.131    6        3.183    4       2.383    8       1.843    2
            5.090   18        3.137    1 S     2.340    4       1.830    2
            4.952    4        3.063   30       2.325    2       1.811    2
            4.872   44        3.027   30       2.300    6       1.786    6
            4.521   16        3.005   25       2.292    4       1.777    4
            4.451   20        2.944    4       2.273    2       1.761    4
            4.171    2        2.878   30       2.247    6       1.736    1 S
            3.744   16        2.857   30       2.192    6       1.711    4
            3.708   18        2.758    6       2.152    2       1.696    2
            3.657   84        2.712    2       2.133    2       1.677    4
            3.471   90        2.693    2       2.088    2       1.658    2
            3.422   10        2.640   10       2.060    4       1.637    4
            3.407    8        2.633    4       2.047    6       1.621    2
            3.402    6        2.614    2       2.019    2
```